Synthesis of Artificial Receptor Motifs for Anion Binding and Organocatalysis

By

Michael Kinsella

A dissertation submitted to WIT for the degree of Doctor of Philosophy

October 2011

Based on research carried out under the supervision of

Principal supervisor: Dr. Claire Lennon

and

Co-supervisor: Dr. Patrick Duggan.

Pharmaceutical & Molecular Biotechnology Research Centre
Department of Chemical and Life Sciences,
Waterford Institute of Technology,
Waterford,
Ireland.

Declaration

I hereby declare that this thesis is my own work, in fulfilment of the requirements of Doctor of Philosophy degree. It is based on research carried out in the Department of Chemical and Life Sciences, Waterford Institute of Technology, Ireland.

_____

Michael Kinsella

_____

Date

Acknowledgements

Table of Contents

Abstract

The initial part of this works involves the evaluation of a related series of bisamides for rational correlation between anion complexation and organocatalysis: remarkable enhancement of hydrogen bonding to anions was observed along with significant increases in catalytic activity in the Morita-Baylis-Hillman reaction. In addition, X-ray crystallography showed a large degree of pre-organisation was observed in one receptor by incorporation of *bis*(trifluoromethyl)aniline groups along with a thioamide functionality. A novel bifunctional amide/*N*-acylsulfonamide within the series gave the best catalytic profile for the initial receptors/organocatalysts.

Following on from the initial work, a series of bifunctional hybrid (thio)urea/amide molecules were designed and also tested for their anion binding properties and catalytic activites. A urea/amide hybrid produced the highest binding constants while a thiourea/amide analogue gave optimal catalytic properties in the aforementioned reaction with yield of up to 79% obtained. Catalyst-substrate binding studies were undertaken for the most successful catalysts and a catalytic mechanism related to receptor/catalyst acidity was proposed.

Another major part of this work involved the design and screening of a range of simple *N*-aryl and *N*-heteroaryl pyrrolidine amide organocatalysts incorporating *N*-pyridyl and *N*-quinolinyl groups in the synthetically useful aldol reaction of isatin with acetone. The 'reverse amide' *N*-pyridyl pyrrolidinylmethyl amide catalysts proved highly catalytically active but gave disappointing enantioselectivities. However, an *N*-3-pyridyl prolinamide catalyst gave the aldol adduct in high yields and high enantioselectivity with up to 72% ee of the (*S*)-isomer. Conditions were optimised for this catalyst and in particular an additive screen identified a link between the pK_a of the acid additive and the yield and enantioselectivity. An *N*-acylsulfonamide prolinamide was also identified as a catalyst for this reaction giving the (*R*)-enantiomer in 68% ee.

Abbreviations

Ar	Aryl
BINAM	1,1′-Binaphthyl-2,2′-diamine
BINOL	1,1'-bi-2-naphthol
t-Bu	*tert*-Butyl
Bn	Benzyl
COSY	Correlated Spectroscopy
DABCO	1,4-diazabicyclo[2.2.2]octane
DBU	1,8-Diazabicyclo[5.4.0]undec-7-ene
DCC	1,3-Dicyclohexylcarbodiimide
dr	Diastereomeric ratio
DEPT	Distortionless Enhancement by Polarization Transfer
DMAP	4-Dimethylaminopyridine
DMF	*N,N*-Dimethylformamide
DMP	2,4-Dimethoxyphenyl
DMPU	1,3-Dimethyl-3,4,5,6-tetrahydropyrimidin-2(1H)-one
DPFGSE	Double Pulsed Field Gradient Spin-Echo
EDCI	1-Ethyl-3-(3-dimethylaminopropyl) carbodiimide
ee	Enantiomeric excess
ESI	Electrospray ionisation
Et	Ethyl
HMPA	Hexamethylphosphoramide
HPLC	High-Performance Liquid Chromatography
LC-MS	Liquid chromatography- mass spectroscopy
LUMO	Lowest Unoccupied Molecular Orbital
HMQC	Heteronuclear Multiple-Quantum Coherence
Me	Methyl
MTBE	Methyl *tert*-butyl ether
NMR	Nuclear magnetic resonance
NOESY	Nuclear Overhauser Enhancement Spectroscopy
Ph	Phenyl
rt	Room temperature

TADDOL	α,α,α',α'-tetraaryl-1,3-dioxlane-4,5-dimethanol
TBAF	Tetrabutylammonium fluoride
TBDMS	*tert*-Butyldimethylsilyl
TBDPS	*tert*-Butyldiphenylsilyl
TFA	Trifluoroacetic acid
THF	Tetrahydrofuran
TIPS	Triisopropylsilyl
TLC	Thin Layer chromatography
TMS	Trimethylsilyl
Ts	*p*-Tolylsulfonyl

1 Chapter 1

Designed Organic Molecules as Anion Receptors and Organocatalysts

1.1   Introduction

The recognition of anions is an ever-expanding field.[1,2] Many hosts incorporating functional groups such as indoles, pyrroles, sulfonamides, ureas and amides have been successful in selectively complexing a range of anionic guests *via* hydrogen bonding.[3-6] Often, these receptor molecules are designed with some degree of pre-organisation in mind, creating a cleft-like structure.[7,8] The use of metal-free organic molecules to catalyse reactions has also received intense interest.[9] The catalytic activity of several such organocatalysts involves coordination of groups such as those listed above *via* hydrogen bonding (H-bonding) to highly negative or anionic intermediates.[10-17] Considering a major objective of both receptor and organocatalyst design is the molecular recognition of anions, much can be gained from taking a cooperative view between both areas, giving rise to the potential of dual application of molecular receptors for anion recognition and organocatalysis.[18,19]

The focus of Chapter 2 of the thesis lies in the rational design of receptors for selective anion binding and catalysis, specifically reactions where H-bonding and electrophile activation play key mechanistic roles. Instead of the lengthy and potentially troublesome synthesis of transition state analogues for binding studies, we look to the binding characteristics of our target receptors with anions as a guide to catalytic mechanisms and in some cases, use anion binding properties as a mechanistic probe into organic reactions.

This review Chapter will present a separate review of the areas of anion recognition and organocatalysis giving a brief history, some key findings and more recent developments in each field. Finally, both themes will be brought together in a more detailed analysis of their interrelationships with a focus on design & application of receptor motifs as organocatalysts.

1.2   Acyclic Receptors for Anion Binding

This section will provide a general overview of anion binding including a consideration of the design parameters of simple anion receptors and comparison of their anion complexation abilities. It will focus on acyclic (non-macrocyclic) receptors for simple anions containing the secondary amide binding functionality such as diamidopyrroles and isophthalamides and also

urea and thiourea binding sites. A number of applications of anion binding will be described, including transport across cell membranes, anion sensors and organocatalysis, the latter forming an integral part of the work presented in Chapter 2.

The design of anion receptors is a quite challenging area. Anions tend to be larger than cations and therefore have a lower charge to radius ratio.[20] Anions may be sensitive to pH and become protonated under acidic conditions, thus losing their charge. Solvent effects can play a key role in controlling binding strength and selectivity. For example some solvents can form H-bonds to anions and an anion receptor must compete with the solvent for the binding site. Anions possess a wide range of geometries and a high degree of pre-organisation may be necessary to design effective anion receptors. Halides such as fluoride (F^-), chloride (Cl^-), bromide (Br^-) and iodide (I^-) are spherical in shape while linear anions include hydroxide (OH^-) and cyanide (CN^-). Carbonate (CO_3^{2-}) and nitrate (NO_3^{2-}) ions are trigonal planar in nature and phosphate (PO_4^{3-}), dihydrogen phosphate ($H_2PO_4^-$) and sulfate (SO_4^{2-}) are tetrahedral anions. Acetate (AcO^-) and benzoate (BzO^-) are examples of Y-shaped anions (Figure 1.1).
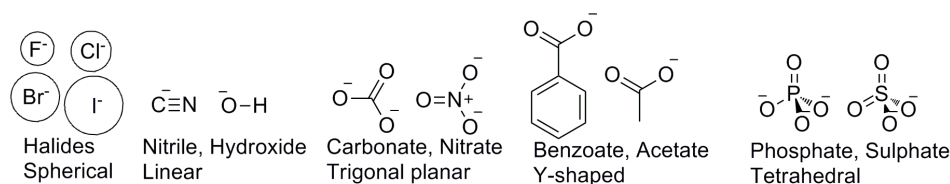
Figure 1.1: Variation of anion shapes showing examples of spherical, linear, trigonal planar, Y-shaped and tetrahedral anions.

Despite the 1968 development of the first synthetic anion receptor by Park and Simmons,[21] the coordination of anions was largely unexplored until approximately 30 years ago. It has since become a well studied area of supramolecular chemistry due to potential binding applications in the fields of biology, the environment and chemical processes.[21-23] Anion coordination chemistry was initially concerned with the design and synthesis of simple uncharged receptors which could complex anions in an organic environment.[24] More recently, the focus has shifted towards the selective anion binding in aqueous solvent conditions,[25] selective sensing of biologically significant anions *in vivo*,[26] detection of anionic pollutants at very low levels,[27] anion transport across cell membranes[28] and extraction and transport of specific anions against Hofmeister bias from aqueous to organic conditions.[29] Receptors may complex an anionic

3

guest through strong electrostatic interactions,[30] metal-anion complexation[31,32] or through weaker but more directional interactions including Lewis acid-base,[33] π-anion,[34] hydrophobic effects or hydrogen bonding (H-bonding),[35-37] the most common being through H-bonding. [2,23,38]

Hydrogen bonds are directional, therefore receptors with specific H-bond arrangements can distinguish between anions of different geometries in non-polar solvents.[20] Several hydrogen bonds can also be incorporated into a supramolecular structure to form a cleft with convergent H-bonding groups, capable of cooperative anion binding. Neutral receptors incorporating amide,[39] squaramide,[40,41] urea and thiourea,[3,42-46] pyrrole,[4,47,48] and indole[3,49] groups as H-bond donors have been reported to bind anions (Figure 1.2).
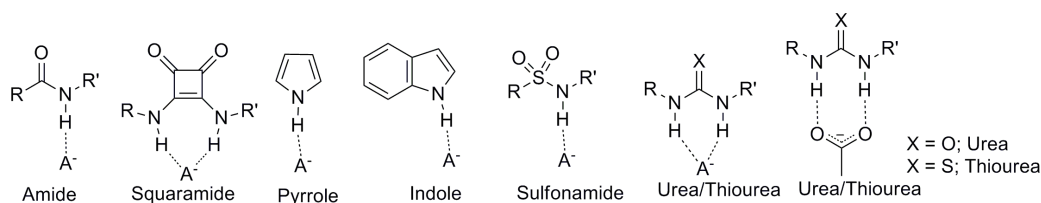
Figure 1.2: Some functional groups capable of H-bonding to anions including 6-membered and 8-membered chelated system which ureas and thioureas may form with anions.

In particular, secondary amides are commonly used in anion receptors as they act as efficient H-bond donors.[50] They can also act as H-bond acceptors leading to intramolecular H-bonding, self-association and disruption to anion binding. Despite this, they have been found to efficiently bind anions,[51] and neutral molecules such as barbiturates[52] and dicarboxylic acids.[53] Squaramides have been observed to bind halides and oxyanions with high binding strength.[41] Sulfonamide moieties have also been shown to be effective anion receptors, due to their highly acidic H-bond donating groups (Figure 1.2).[54] Pyrrole and indole based receptors can only act as H-bond donors and therefore, intramolecular H-bond formation which can inhibit anion binding is not possible (Figure 1.2). Ureas and thioureas are known to be very efficient anion receptors as both possess two N-H groups which can bind a single acceptor atom such as a halide anion forming a six-membered chelate ring or can also bind two adjacent oxygen atoms of an oxyanion producing an eight-membered ring system. A review of receptors containing the motifs described above will be presented in the following sections.

4

1.2.1 Isophthalamides and Analogues as Amide Based Anion Receptors

An isophthalamide unit consists of a 1,3-dicarboxamide attached to a benzene scaffold. It contains two complementary amide N-H groups arranged in a "cleft-like" structure capable of binding to anions. Inspired by the findings of Hamilton regarding the binding ability of isophthalamide receptors for neutral nucleotide bases,[55] barbiturates[52] and dicarboxylic acids,[53] Crabtree *et al.* designed a simple acyclic isophthalamide with minimal pre-organisation to bind halide anions in 1997 (Scheme 1.1b).[24] Previous to this, Hunter *et al.* had studied the conformations of isophthalamide and 2,6-pyridine-dicarboxamide units.[56] Using conformational studies and ^{1}H NMR NOESY experiments, they found that the *syn-anti* conformation was most stable for isophthalamides while *syn-syn* was optimal for the pyridyl diamide derivative (Scheme 1.1a). Alternative conformations were disfavoured in the case of the latter receptor due to repulsion between the pyridyl nitrogen and carbonyl oxygen atom.
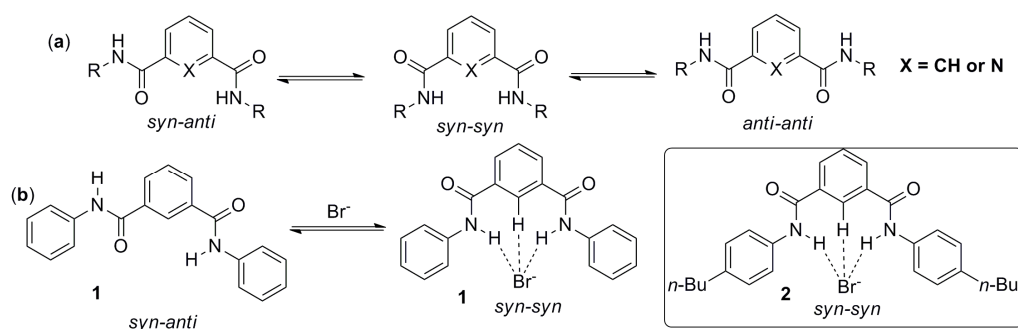
Scheme 1.1: (a) Possible conformations for isophthalamides and 2,6-pyridine-dicarboxamides. (b) Change in conformation of **1** from *syn-anti* to *syn-syn* conformation upon introduction of Br$^-$ anion.[51]

In accordance with the work of Hunter *et al.*[56] X-ray diffraction studies conducted by Crabtree *et al.* confirmed 1:1 complexation between [PPh$_4$]Br and both amide N-H groups of **1**. The conformation switched from the *syn-anti* preferred conformation in the absence of anionic guest to the *syn-syn* conformation for anion binding (Scheme 1.1). Due to poor solubility of the *N*-phenyl isophthalamide **1**, ^{1}H NMR spectroscopic titrations were carried out on the *N*-(*n*-butyl phenyl) derivative **2**, producing large downfield shifts of the N-H and aromatic C-H protons *ortho* to the amide groups consistent with H-bonding. Large association constants (K$_{ass}$ values) of 6.1 x 10^4 M^{-1} and 7.1 x 10^3 M^{-1} were obtained for **2** with Cl$^-$ and Br$^-$ respectively. Crabtree *et al.* later studied the effects of structural rigidity and H-bonding

functionality (amide vs sulfonamide) on the selectivity and binding efficiency to anions (Figure 1.3).[51]

1: Ar = Ph
2: Ar = p-(n-Bu)C_6H_4
3: Ar = 2,4,6-Me$_3C_6H_2$
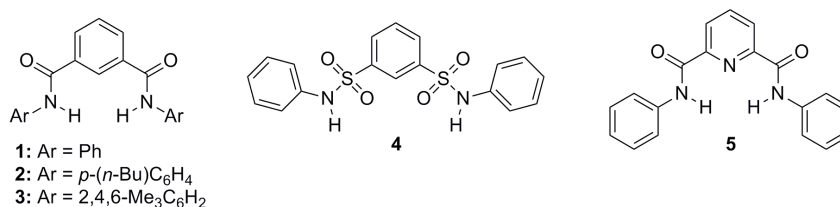
Figure 1.3: Receptors **1**-**5** analysed by Crabtree *et al.*[51]

^{1}H NMR spectroscopic titrations of **2**-**5** with Cl^{-}, Br^{-}, I[-], AcO[-] were indicative of a cleft-like H-bonding structure in all cases involving the amide or sulfonamide N-H, C-H *ortho* to both amide groups (present in **2**-**4**) and phenyl C-2 protons *ortho* to the N-H groups. K_{ass} values of the order of 10^4 M^{-1} were found for the most efficient isophthalamide receptor **2**, ascribed to the absence of rigid or bulky groups and the flexible nature of the host skeleton which could undertake slight conformational adjustments to accommodate anions of varying sizes. In the case of pyridyl diamide **5**, repulsion due to the lone pair on the nitrogen atom was a major factor when binding large anions such as Br^{-} and I[-] but less significant for smaller anions. A 1:1 binding stoichiometry was found for **2**, **3** & **5**.

Smith *et al.* incorporated a Lewis-acidic boronate group into neutral urea and amide based receptors producing a series of boronate ureas and a related *bis*(boronate-amide) incorporated into an isophthalamide structure (Figure 1.4).[7] High K_{ass} values up to 6 x 10^4 M^{-1} were obtained for the urea based receptors with AcO[-] in DMSO.[7] Incorporation of the boronate substituent into an isophthalamide produced **6**, where intramolecular coordination between the amide oxygen atom and Lewis acidic boronate substituent pre-organised the receptor to the *syn-syn* conformation. This receptor produced a K_{ass} value which was a factor of 10 greater than a related isophthalamide with AcO[-] in DMSO-d_6. The enhanced AcO[-] binding for the boronate ureas and amides was proposed to be due to intramolecular coordination, inducing a larger host dipole moment and increased surface potential at the urea and amide groups.
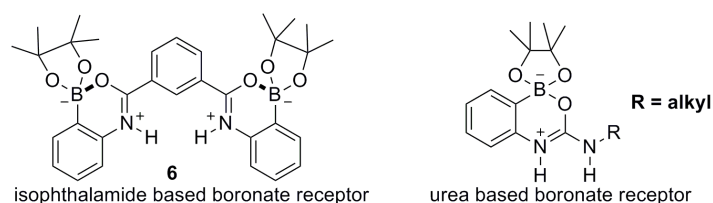
Figure 1.4: Smith's *bis*(boronate-amide) and urea receptors.[7]

In 2003, Gale *et al.* studied the F⁻ binding abilities of isophthalamides with enhanced N-H acidity due to an electron withdrawing 3-nitrophenyl **7** or 3,5-dinitrophenyl **8** group attached to the amide (Figure 1.5).[57] In both cases, the amide N-H signal disappeared, requiring the titration to be monitored through the isophthaloyl H-2 resonance. A complex ¹H NMR titration curve for **7** was suggestive of multiple equilibria while the H-2 resonance of **8** shifted upfield and plateaued upon the addition of 1 equivalent of F⁻. At higher F⁻ concentration, upfield shift continued, suggesting initial formation of a 1:1 or 2:2 receptor:F⁻ complex followed by a 1:2 receptor:F⁻ complex at higher concentrations of F⁻. X-ray crystal structure of the F⁻ complex of the dinitrophenyl derivative showed the formation of an unusual "2+2" double helix formed by two isophthalamides wrapping around two F⁻ anions *via* N-H⋯F⁻ H-bonds and potential π-π interactions between the nitroaromatic rings.
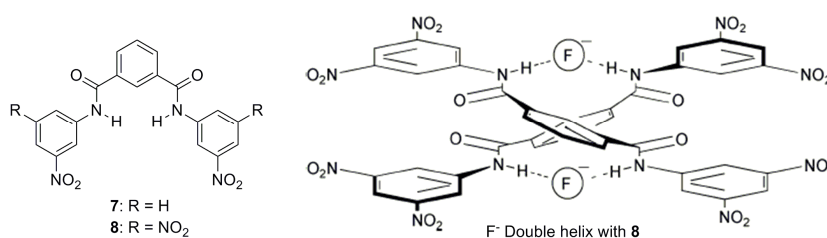
Figure 1.5: Structure of isophthalamide based receptors **7** & **8** developed by Gale *et al.*[57] Fluoride double helix with **8** also shown.

In 2005, the same group studied 1,3-dicarboxamido-9,10-anthraquinone derivatives where steric interactions between the amide in the 1-position and the anthraquinone oxygen in the 9-position twisted the amide out of the anthraquinone plane, forcing the *syn-syn* conformation to be disfavoured in the hope of favouring higher order receptor:anion complexes[58] (Figure 1.6). ¹H NMR spectroscopic titration data in DMSO-d_6/0.5% water for F⁻ could not be fitted to a 1:1 or 1:2 binding model in some cases. Br⁻ and hydrogen sulphate $H_2SO_4^{2-}$ were not significantly bound and only the most efficient chloro-substituted receptor **11** complexed Cl⁻.

$H_2PO_4^-$ was bound more strongly to the twisted methoxy isophthalamide **10** compared to the standard methoxy isophthalamide **9**, (K_{ass} = 214 M^{-1} vs 120 M^{-1}), which was ascribed to oxo-anion bridging between the amide groups in the anthraquinone derivatives. X-ray crystallography of the tetrabutylammonium fluoride complex of **12** revealed a 2:2 receptor:anion complex.
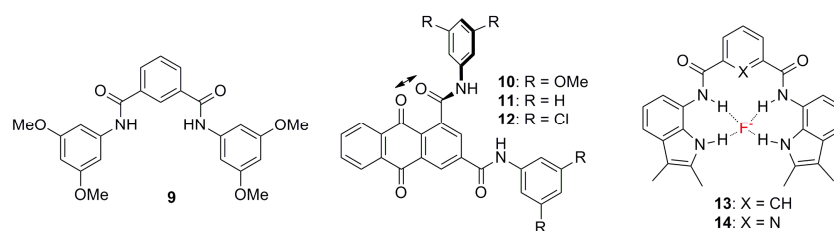
Figure 1.6: Structure of non-twisted & twisted isophthalamide analogues **9 & 10-12**.[58] Isopthhaloyl & pyridyl receptors **13** & **14** incorporating indole groups also shown.[59]

In 2007, Gale *et al.* examined isophthalamide and 2,6-dicarboxamidopyridyl derived receptors substituted with pendant indole groups (Figure 1.6).[59] X-ray crystallography confirmed that these receptors bound F$^-$ anions in a twisted conformation while Cl$^-$ lay above the plane of the complex. ^{1}H NMR spectroscopic titrations in DMSO-d_6 + 0.5% H_2O and DMSO-d_6 + 5% H_2O showed a high selectivity of the pyridyl receptor **14** for F$^-$, however a binding constant could not be measured for the isophthaloyl derivative **13**, possibly due to multiple binding stoichiometries.

In 2007, Gale *et al.* designed a pre-organised isophthalamide **16** capable of anion transport across membranes.[8] The incorporation of hydroxyl groups at the 4,6-positions of the isophthalamide forced it to assume the *syn-syn* conformation through intramolecular H-bonding (Figure 1.7). ^{1}H NMR spectroscopic titrations with Cl$^-$, Br$^-$ and I$^-$ in CD$_3$CN showed downfield shifts of the N-H and isophthaloyl H-2 proton, confirming cleft H-bonding interactions. This pre-organisation increased the K_{ass} value significantly; 5230 M^{-1} with Cl$^-$ for **16** compared to 195 M^{-1} with Cl$^-$ for **15**. Receptor **16** was also shown to be a potent transmembrane Cl$^-$ transporter. A methoxy substituted isophthalamide **17** did not bind appreciably to anions, possibly due to intramolecular H-bonding favouring the *anti-anti* conformation.
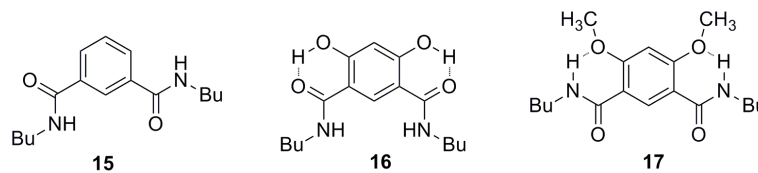
Figure 1.7: Transmembrane Cl⁻ receptors **15**-**17** synthesised by Gale *et al.* including the pre-organised **16**.

In further membrane transport work, the same group developed synthetic HCl receptors with a 2,6-dicarboxamidopyridyl core **19** or an isophthalamide core **20** incorporating two H-bonding sites and a basic imidazole ring (Figure 1.8) while **18** acted as a control receptor.[60] In the presence of one equivalent of HPF$_6$, **19** exhibited increased Cl⁻ binding compared to isophthaloyl derivative **20** in this acidic environment.
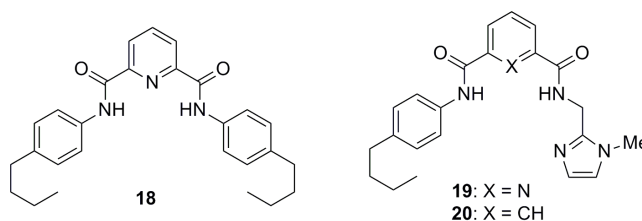
Figure 1.8: Imidazole & non-imidazole functionalised receptors/transporters **18-20** tested under acidic and neutral conditions by Gale *et al.*[60]

An additional strategy employed to enhance the overall binding properties of isophthalamides and 2,6-dicarboxamides has been the incorporation of additional thiourea groups into the structure. In 2008, Gunnlaugsson *et al.* developed a pre-organised *bis*-amidothiourea receptor **21** based on a pyridine-2,6-dicarboxamide skeleton (Figure 1.9). The coordination of biologically significant adenosine monophosphate (AMP) and adenosine diphosphate (ADP) in a 20% aqueous solution was accompanied by a colour change with K$_{ass}$ values of up to 4 x 10^5 M^{-1} reported along with selectivity for AMP and ADP over ATP.[61] In 2010 they developed a fluorescent anion sensor **22** based on a *bis*-quinoxaline amidothiourea receptor molecule (Figure 1.9).[62] Approximately equal K$_{ass}^{1:1}$ and K$_{ass}^{1:2}$ values from fluorescence titrations indicated both thiourea units bound one anion each. ^{1}H NMR spectroscopic titrations showed initial broadening of the amide N-H and aromatic protons with sharpening of signals following addition of 2 equiv AcO⁻ with no subsequent signal migration observed due to anion induced deprotonation of the thiourea N-H groups by the anion.

9
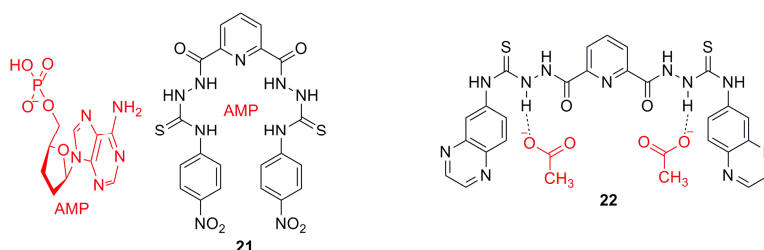
Figure 1.9: Gunnlaugsson's *bis*-amidothiourea receptor **21** with a pyridine skeleton binding to AMP anion.[61] The *bis*-quinoxaline receptor **22** binding 2 equivalents of AcO⁻ also shown.[62]

1.2.2 Amidopyrrole Bisamide based Anion Receptors

Using ^{1}H NMR spectroscopy, Gale *et al.* studied the anion binding abilities of an *n*-butyl derived amidopyrrole bisamide receptor **23** in CD$_3$CN while the phenyl analogue **24** was assessed in DMSO/0.5% H$_2$O (Figure 1.10).[63] Both receptors possessed similar binding affinities and were selective for oxyanions over F⁻, Cl⁻ or Br⁻. Crystals of **23** in the presence of excess tetrabutylammonium benzoate showed the BzO⁻ was held within the binding cleft by three H-bonds (Figure 1.10).[64] The same group subsequently incorporated chlorine atoms at the 3- and 4- positions of the pyrrole ring to increase N-H acidity[65] (**25** & **26**, Figure 1.10). ^{1}H NMR spectroscopic binding studies showed that addition of F⁻ caused an initial amide N-H downfield shift followed by an upfield migration between 1 and 2 equivalents, plateauing following addition of 2 equivalents of anion. X-ray crystallography confirmed this was due to deprotonation of the pyrrole N-H and this was also observed for BzO⁻ and H$_2$PO$_4$⁻. Titration of Cl⁻ with the acidic receptors **25** & **26** produced up to 15 fold increases in K$_{ass}$ values compared to the 3,4-phenyl substituted analogues **23** & **24**.

23: R$_1$ = *n*-Bu, R$_2$ = Ph
24: R$_1$ = Ph, R$_2$ = Ph
25: R$_1$ = *n*-Bu, R$_2$ = Cl
26: R$_2$ = Ph, R$_2$ = Cl
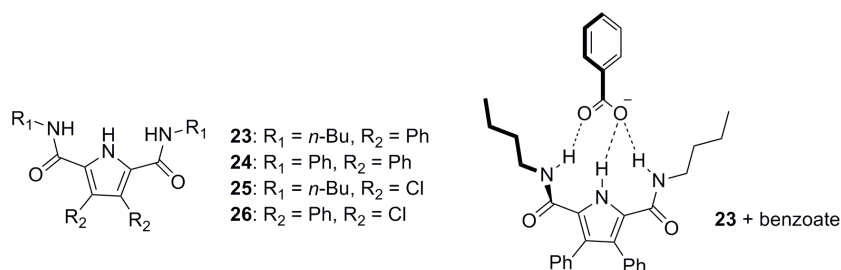
23 + benzoate

Figure 1.10: 2,5-Diamidopyrroles **23**-**26** studied by Gale.[63,65] Structure of **23** in presence of excess benzoate determined by X-ray diffraction.[64]

Gale *et al.* subsequently incorporated electron withdrawing groups into the amide side-groups of a diamidopyrrole[66] (**27** & **28** in Figure 1.11). ^{1}H NMR spectroscopic titrations of the 4-

nitrophenyl derivative **27** in DMSO-d_6/0.5% water produced K_{ass} values of 1245 M^{-1} for F$^-$, 39 M^{-1} for Cl$^-$ and 4150 M^{-1} for BzO$^-$ while the H$_2$PO$_4^-$ titration could not be fitted to a 1:1 model. Under the same conditions, 3,5-dinitrophenyl analogue **28** suffered deprotonation with BzO$^-$ and F$^-$. The first equivalent of anion was coordinated by the receptor, the second equivalent promoted deprotonation and the third equivalent of F$^-$ was bound by the deprotonated receptor. In 2005, Jurczak and Zielinski investigated similar 2,5-diamidopyrrole receptors and compared binding between an amide and thioamide derivative in this receptor motif (Figure 1.11).[4] Anion binding studies produced lower binding constants compared to the phenyl-substituted diamidopyrroles developed by Gale.[63] They reported anion binding strength differences for the amide and thioamide receptors; thioamides had stronger affinity towards BzO$^-$ and Cl$^-$ while amides were more selective towards H$_2$PO$_4^-$.
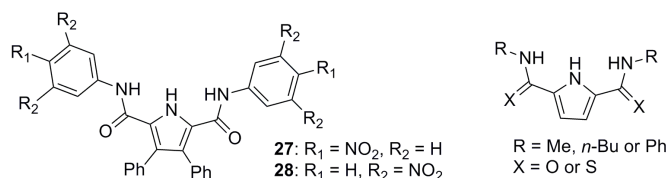
Figure 1.11: Structure of nitrophenyl derivatives of pyrrole-2,5-diamides studied by Gale *et al.*[66] Structure of amidopyrroles and thioamidopyrroles examined by Jurczak *et al.*[4] also shown.

In 2006, Gale *et al.* synthesised a number of 'naked-eye' colorimetric anion receptors which combined amidopyrroles with urea and thiourea groups (Figure 1.12). [67] X-ray crystal analysis and ^{1}H NMR spectroscopy showed that deprotonation occurred in the thiourea containing analogues with basic anions. The 2,5-diamidopyrroles **29-31** proved the most efficient anion receptors providing K_{ass} values of the order 15,000 M^{-1} in DMSO.
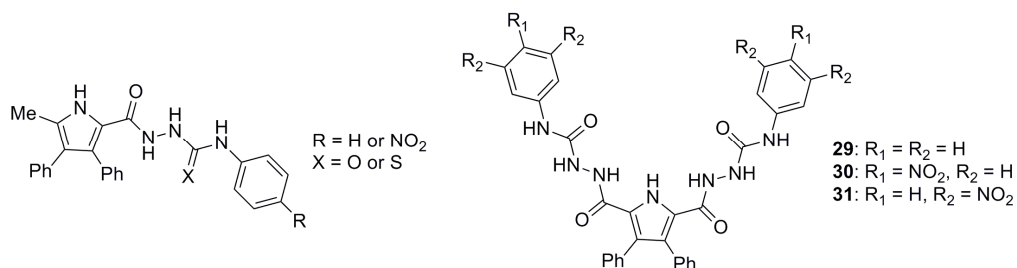
Figure 1.12: Structure of amidopyrrole thiourea receptors reported by Gale *et al.*[67]

Gale *et al.* later replaced the pyrrole group with a dipyrrolylmethane group which was expected to experience less strain, as the receptor can twist around the pyrrole-CR$_2$-pyrrole

group with less strain on the receptor compared to the twist of an amide bond in receptor **24** and they also now possessed four cooperative H-bond donating sites (Figure 1.13).[68] Compound **32** possessed exceptionally high affinity for $H_2PO_4^-$ with a K_{ass} in excess of 10^4 M^{-1} in DMSO-d_6/5% water. Receptor **33** in which the carbon between the two pyrrole rings was substituted with two methyl groups preferentially bound $H_2PO_4^-$ with a K_{ass} of 1092 M^{-1}.[69]
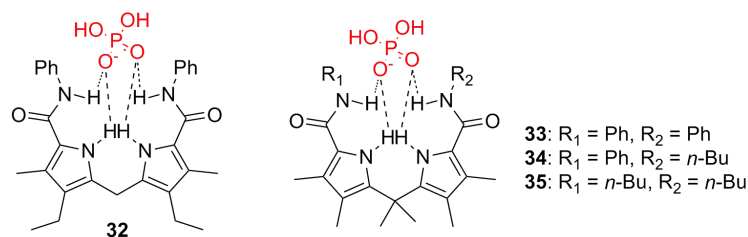
Figure 1.13: Structure of $H_2PO_4^-$ selective 2,2'-*bis*amidodipyrrolylmethanes developed by Gale *et al.*[68,69]

Cheng *et al.* evaluated a number of pyrrole bearing isophthaloyl and bisamide derived pyridyl receptors for their anion binding properties in DMSO-d_6 (Figure 1.14).[70] The binding to F^- was more efficient than to $H_2PO_4^-$ or AcO^- and was ascribed to anion basicity, size and shape effects. *N*-Boc protected receptors were found to be less efficient due to the bulky *tert*-butyl groups where the pre-organisation imparted by the pyridyl receptor was outweighed by the Boc group inhibiting formation of a cleft structure. DFT calculations confirmed the adoption of the *syn-syn* conformation by the isophthaloyl receptor upon introduction of anion.
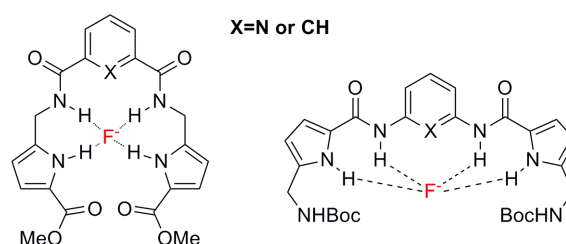
Figure 1.14: Structure of pyrrole derived receptors with selective binding to F^-.

1.2.3 Indole based Amide/Urea Receptors for Anion Binding

Indoles and indole-derived receptors are a more recent feature of anion coordination chemistry.[38] The indole group is more acidic than the pyrrole group and contains a single H-bond donor group which would be expected to form stronger H-bonds to anions.

In 2007, Pfeffer *et al.* developed indole receptors which also incorporated amide, urea and thiourea groups and ^{1}H NMR spectroscopic titrations with various anions were conducted monitoring all four N-H groups of the receptors **36**-**38** (Figure 1.15).[3] Deprotonation of the urea N-H and indole N-H groups occurred with F$^-$ for **36**-**38** while **36** & possessed strong AcO$^-$ binding and weaker Cl$^-$ and Br$^-$ binding through the urea groups with only minor binding observed to the indole and amide N-H groups. In the case of the larger receptor **38** with AcO$^-$, the amide and indole bound anion strongly following the addition of 1 equivalent of anion, at which point the large size could accommodate independent anion binding at these sites. K_{ass} values of approximately 7,900 M^{-1} were obtained for **38** with both AcO$^-$ and $H_2PO_4^-$ while lower values were observed for Cl$^-$ binding.
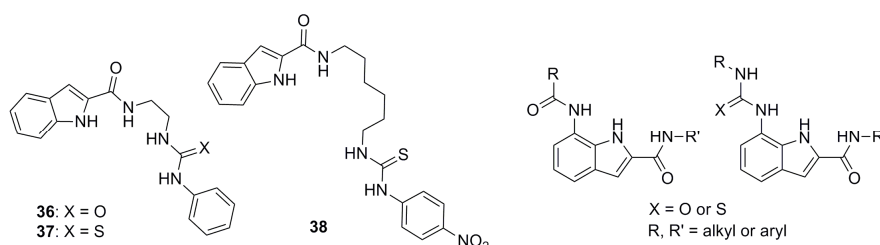
Figure 1.15: Structure of Indole urea and thiourea receptors studied by Pfeffer *et al.*[3] Gale & Albrecht's 2,7-functionalised indole receptors also shown.[71]

Gale and Albrecht synthesised a series of functionalised indoles with attached *bis*-amides and ureas in a similar cleft arrangement to an isophthalamide and found strongest binding for AcO$^-$ in wet DMSO (Figure 1.15).[71] Later X-ray crystallography studies confirmed adoption of a cleft conformation in the presence of anionic guest.[72] The amide functionalised indoles bound anions more weakly compared to the urea analogues while a thiourea derivative gave lower K_{ass} values due to steric effects with the S atom inhibiting the approach of anions.

Having recognised the minor role which the amide at the 2-position played in the coordination of anions evaluated in previous indole receptors, Gale *et al.* subsequently synthesised 1,3-diindolylurea and 1,3-diindolylthiourea based receptors (Figure 1.16).[49] The urea receptors exhibited a high affinity for oxoanions and a particular selectivity for $H_2PO_4^-$ ($K_{ass} > 10^4$ M^{-1} in presence of 0.5 % H_2O for oxoanions; 4790 M^{-1} in 10% H_2O for H_2PO_4). X-ray crystallography showed that the diindolylurea was bound to BzO$^-$ through four H-bonds incorporating all N-H groups (Figure 1.16). $H_2PO_4^-$ was bound to three diindolylthiourea

molecules by twelve H-bonds. Significantly lower K_{ass} values were observed for thioureas without selectivity, ascribed to steric effects from the large S atom.
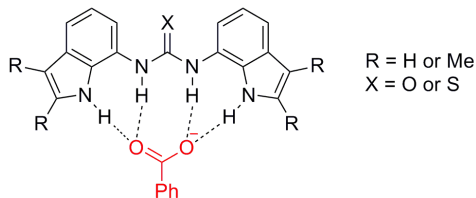
Figure 1.16: Structure of diindolylureas and diindolylthioureas binding to benzoate developed by Gale *et al.*[49]

Gale *et al.* later synthesised 2-amidoindole amide based receptors of varying acidity which were linked through 1,5-diaminopentane or 1,3-phenylenediamine groups[73] (Figure 1.17). ^{1}H NMR spectroscopic titrations in DMSO-d_6/0.5% H_2O preferentially bound oxoanions, in particular $H_2PO_4^-$, and in some cases, the negative steric effects of the NO_2 group outweighed its beneficial enhanced acidity effect. In some instances, 1:2 receptor: $H_2PO_4^-$ binding was observed due to binding to a dimerised $H_2PO_4^-$ anion pair, as evidenced by X-ray crystallography.
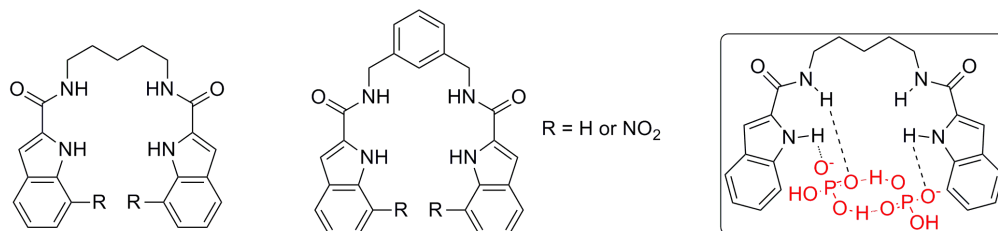
Figure 1.17: Structure of 2-amidoindole receptors and also a receptor binding to a H_2PO_4 dimer anion.[73]

Jurczak *et al.* reported a series of receptors combining 2,2-diindolylmethanes with urea functional groups to give highly efficient 7,7'-diureido-2,2'-diindolylmethanes **39**-**41** capable of binding anions in methanol[74] (Figure 1.18). K_{ass} values of up to 535 M^{-1} were calculated for the 1:1 binding with halides and oxyanions with approximate equivalent binding strength to the urea and indole protons. Receptor **40** bound the pyrophosphate anion with a 2:1 receptor:anion stoichiometry with $K_{ass}^{2:1}$ of 10,000 M^{-1} and $K_{ass}^{1:1}$ of 815 M^{-1}. X-ray crystallography of **41** bearing 4 indole subunits with $H_2PO_4^-$ showed that the receptor was deprotonated and in a 'bent sheet' conformation but there was no evidence of deprotonation in solution.

14
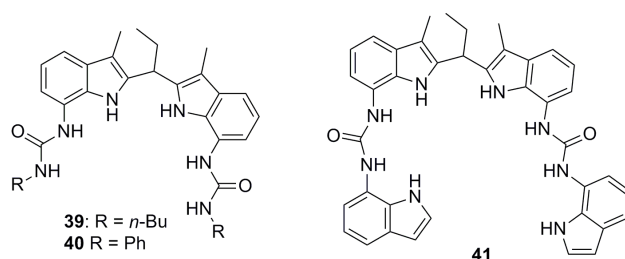
Figure 1.18: Structure of 7,7'-diureido-2,2'-diindolylmethane receptors developed by Jurczak *et al.*[74]

1.2.4　Urea and Thiourea based Anion Receptors

Ureas and thioureas are attractive building blocks for the design of anion receptors as they possess two N-H fragments which can bind a single anion e.g. a halide anion or two adjacent oxygen atoms of an oxyanion.[37,75] In 1992, Wilcox developed a urea receptor **42** capable of binding anions such as phosphonates, sulfates and carboxylates[76] while Kelly & Kim described **43** capable of binding to phosphonate and sulfonate anions (Figure 1.19).[77] Umezawa *et al.* synthesised acylic thiourea cleft receptors **44** & **45** containing a xanthene spacer which could selectively bind $H_2PO_4^-$ in DMSO-d_6 producing K_{ass} values up to 1.95 x 10^6 M^{-1} due to formation of four cooperative H-bonds. (Figure 1.19).[78] Reinhoudt *et al.* reported strong $H_2PO_4^-$ receptors containing two *ortho*-phenylenediamine based *bis*-ureas producing K_{ass} values up to 5 x 10^7 M^{-2} for **47** in a 1:2 receptor: $H_2PO_4^-$ stoichiometry (Figure 1.19).[79]
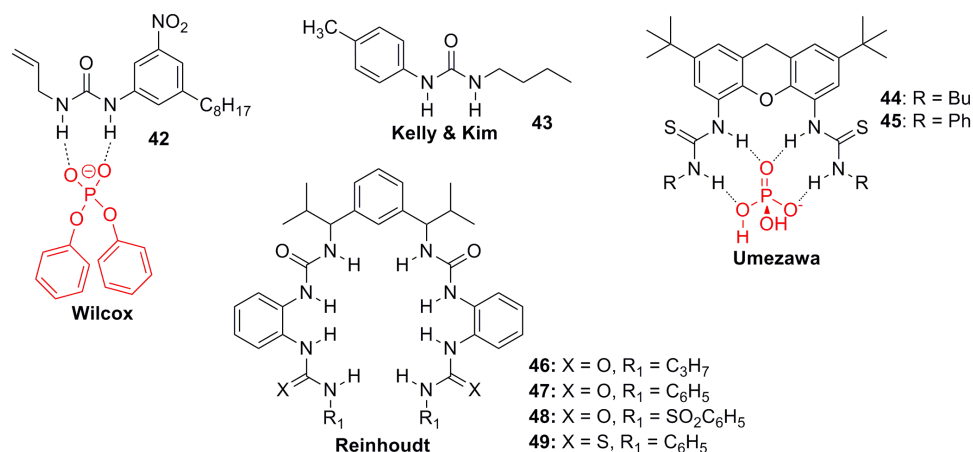
Figure 1.19: Structure of simple urea developed by Wilcox,[76] Kelly & Kim,[77] Umezawa's xanthene based receptor[78] and Reinhoudt's *ortho*-phenylenediamine receptor.[79]

15

The simple *p*-NO$_2$-containing *N*-arylthiourea receptor **50** studied by Kato *et al.* was selective for AcO$^-$ with binding in the order AcO$^-$ >> H$_2$PO$_4^-$ > Cl$^-$ > Br$^-$ > I$^-$ > SCN$^-$ > NO$_3^-$ > HSO$_4^-$ > ClO$_4^-$ in acetonitrile/1% H$_2$O solution (Figure 1.20).[80] A colour change with AcO$^-$ was ascribed to H-bonding rather than proton tranfer. In 2004, Fabbrizzi *et al.* demonstrated that the anion binding properties of (thio)urea receptors **51** & **52** was related to N-H acidity and anion basicity with deprotonation observed for basic anions such as F$^-$.[81,82] Gunnlaugsson *et al.* developed naphthalimide thiourea based receptors **53** & **54** which could bind AcO$^-$, H$_2$PO$_4^-$ & F$^-$ in aqueous solution with an accompanying colour change (Figure 1.21).[83] X-ray crystallography showed that the thiourea protons existed in the *anti*-conformation with intermolecular interactions between adjacent molecules. UV titrations in DMSO were consistent with anion complexation which required the *syn* orientation and K$_{ass}$ values of approx 10^4 – 10^5 M^{-1} for AcO$^-$, F$^-$ and H$_2$PO$_4^-$ were observed with stronger binding for **54**. Deprotonation was observed for F$^-$ accompanied by colour changes which could not be reversed upon addition of ethanol or water.
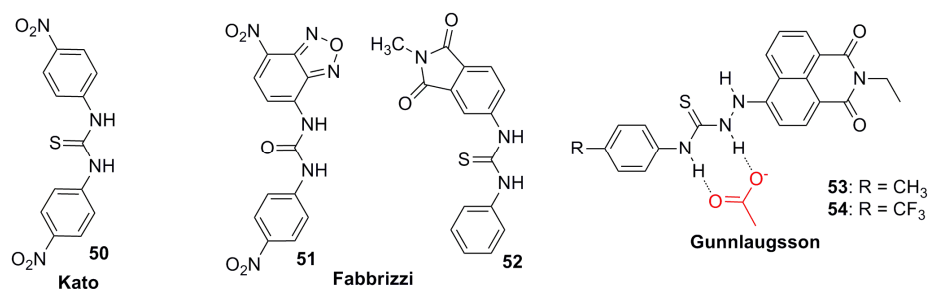
Figure 1.20: Structure of (thio)urea receptors studied by Kato *et al.*,[80] Fabbrizzi *et al.*[81,82] & Gunnlaugsson *et al.*[83]

In 2005, Gale *et al.* reported significantly enhanced anion binding constants from receptors containing simple *bis*-urea groups linked by a 1,2-phenylenediamine spacer[84] (Figure 1.21). ^{1}H NMR spectroscopic titrations in DMSO-d_6/0.5% water showed that the *bis*-urea receptor **57** was selective for carboxylate anions with K$_{ass}$ values of 3210 M^{-1} and 1330 M^{-1} for AcO$^-$ and BzO$^-$ respectively compared with 100-200 M^{-1} typical for non-urea based receptors **55** & **56**. X-ray crystallography confirmed that the **57** bound anions through four complementary H-bonds. Significant K$_{ass}$ improvements were obtained using a 4,5-dichloro-substituted central ring and a nitro group at the 2-position of the urea *N*-aryl rings **58**.[85] A *bis*-thiourea derivative **59** produced significantly lower K$_{ass}$ values, ascribed to the large S atom altering the shape of the binding site, hindering binding to the outer NH groups.

16
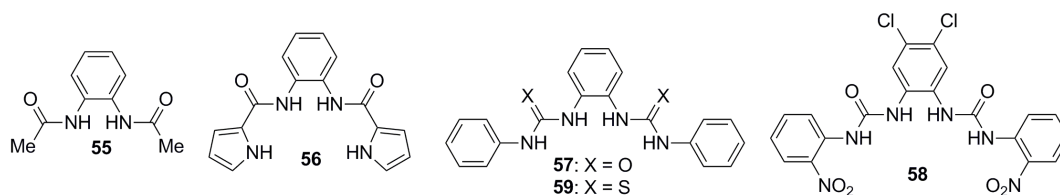
Figure 1.21: Structure of urea based receptor tested by Gale *et al.*[84]

In 2008, Gunnlaugsson *et al.* developed a number of diaryl-urea based receptors with an amide group at the *ortho*, *meta* or *para* position on one of the aryl rings attached to the urea, and electron withdrawing *para*-CF$_3$ group on the other aryl ring (**60-62**).[86] They also studied their thiourea counterparts (**63-65**) in 2010 (Figure 1.22).[42] The anion binding properties were studied using UV and ^{1}H NMR spectroscopic titrations in CH$_3$CN and DMSO-d_6. The *para*-amido substituted receptors **60** & **63** bound anion at the urea/thiourea site in a 1:1 stoichiometry followed by formation of a 1:2 species through binding interactions at the *para*-amide group with weak contributions from the aryl protons.[87] Thiourea binding was generally stronger than urea, *e.g.* AcO$^-$ K$_{ass}$ of 2 x 10^6 M^{-1} and 1.9 x 10^5 M^{-1} for **63** and **60** respectively. The *meta*-amido substituted urea **61** bound anions in 1:1, 1:2 and 2:1 stoichiometries with the anion bridged between two receptors while its thiourea analogue **64** produced cleaner 1:1 binding. The *ortho*-amido-substituted thiourea **65** facilitated the formation of 1:2 receptor:anion complexes while **62** gave pure 1:1 interactions.
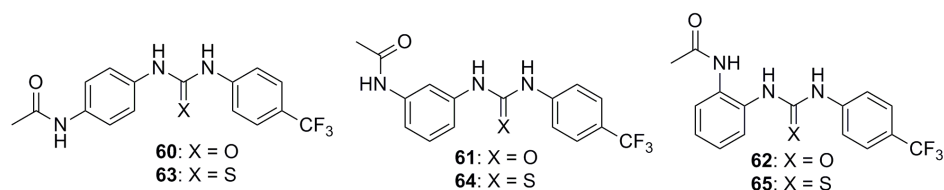
Figure 1.22: Structure of urea-amide and thiourea-amide receptors reported by Gunnlauggson *et al.*[42,86]

In 2009, Sargent *et al.* synthesised ureas containing alkyl ether groups to improve solubility and studied their binding abilities to a range of anionic guests by UV-Vis and ^{1}H NMR spectroscopic titration in CH$_3$CN (Figure 1.23).[88] They observed binding affinity in order of decreasing anion basicity (AcO$^-$ > BzO$^-$ > H$_2$PO$_4^-$ > NO$_2^-$ > NO$_3^-$) with K$_{ass}$ values of up to 5 x 10^5 M^{-1} for the optimal NO$_2$ substituted receptor **67** and with AcO$^-$ and lower values for receptor **66**.
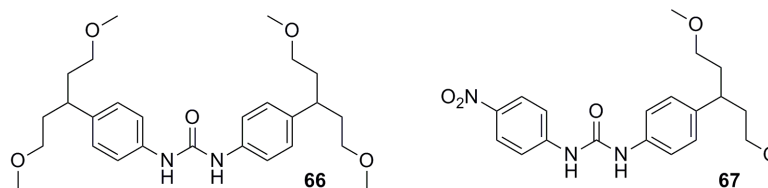
Figure 1.23: Structure of alkyl ether substituted urea receptors developed by Sargent *et al.*[88]

1.2.5   Sulfonamide based Anion Receptors

An efficient sulfonamide receptor **4** was reported together with the previously described isophthalamides **1**-**3** and pyridyl-2,6-dicarboxamide receptor **5** by Crabtree *et al.*[51] This receptor produced strong Cl$^-$ binding and moderate Br$^-$ binding with K_{ass} values of 20,000 M^{-1} and 4,600 M^{-1} obtained from fitting to a 1:1 model. An interesting anion binding stoichiometry was observed with F$^-$ and AcO$^-$. In the unbound state, **4** was proposed to exist in the *anti-anti* conformation and changed into its *syn-syn* conformation upon addition of up to 1 equivalent of F$^-$. It reverted back to an *anti-anti* conformation with further addition of anion facilitating the formation a 1:2 receptor:anion complex (Scheme 1.2).
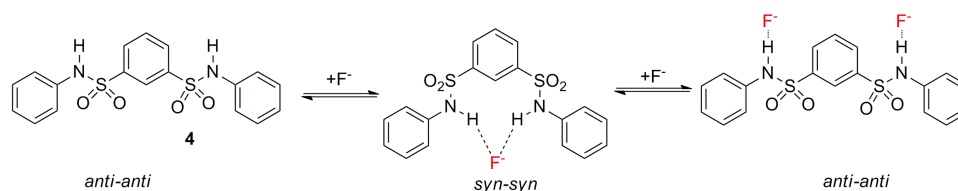
Scheme 1.2: Unbound sulfonamide receptor **4** in *anti-anti* conformation, change to *syn-syn* conformation up to 1 equiv of AcO$^-$ or F$^-$ and reverts back to *anti-anti* conformation for 1:2 binding to AcO$^-$ or F$^-$.[51]

Sulfonamide groups have been incorporated into a urea receptor reported by Gale *et al.* in 2008 (Figure 1.24).[89] Anion binding was monitored using ^{1}H NMR spectroscopy and specifically the urea N-H protons as the sulfonamide resonances were not visible. Upon addition of Cl$^-$, 1:1 complexes were formed with K_{ass} values of 7550 M^{-1} and >10^4 M^{-1} for **68** and **69** respectively. Upon addition 1 equivalent of AcO$^-$ or 2 equivalents of F$^-$, the urea N-H group shifted downfield and subsequently migrated upfield with further additions, due to deprotonation of the acidic sulfonamide N-H group and decomplexation effects.

18
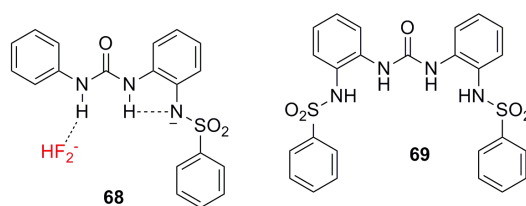
Figure 1.24: Ureas containing sulfonamide groups (**68** & **69**) observed to bind anions and become deprotonated upon addition of basic anions.[89]

In 2009, Kilburn *et al.* studied a number of acyclic and macrocyclic disulfonamide based receptors and tested them as anion receptors for Br^-, Cl^-, AcO^- and $H_2PO_4^-$ in CD_3CN by ^1H NMR spectroscopic titration (Figure 1.25).[90] For the acyclic receptors **70** & **71**, the sulfonamide protons broadened upon introduction of AcO^- with a downfield shift of the amide N-H signals observed. The ^1H NMR spectroscopic titration data provided evidence of dominant 1:1 binding however 1:2 binding was also present. This was explained by efficient binding of the first equivalent of AcO^- by both sulfonamide protons followed by binding of a second molecule of AcO^- separately, corresponding to a previous report of conformational change to accommodate binding of a second equivalent of anion by a disulfonamide receptor.[51] K_{ass} values from dominant 1:1 interactions with AcO^- were 36,000 M^{-1} and 11,000 M^{-1} for **70** & **71** respectively in CD_3CN. The macrocyclic receptors **72** & **73** exclusively formed 1:1 interactions with high binding constants in excess of 10^4 M^{-1} for AcO^- obtained. These efficient systems were also titrated in a more competitive system (CD_3CN/2% H_2O) and yielded 1:1 K_{ass} values less than 1000 M^{-1} for AcO^- with affinity in the order $AcO^- > H_2PO_4^- > Cl^- > Br^-$. Receptor **72** was the optimum macrocyclic receptor containing the similar urea sulfonamide arrangement.
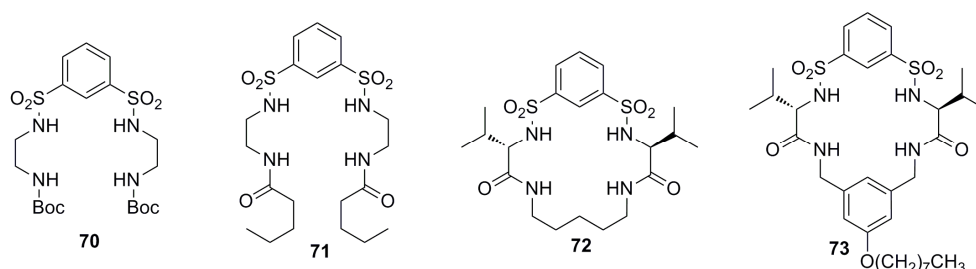
Figure 1.25: Structure of disulfonamide based acyclic and macrocyclic anion receptors synthesised by Kilburn *et al.*[90]

19

A number of simple pyrrole sulfonamide receptors developed by Huggins *et al.* were found to exist in the *syn* conformation optimal for binding based on NOESY experiments and molecular mechanics studies (Figure 1.26).[5] Anion binding titrations in dry $CDCl_3$ showed 1:1 receptor:anion binding for a range of anions with K_{ass} values up to 1768 M^{-1}. The sulfonamide N-H signals migrated further downfield compared to the pyrrole N-H protons and the *bis*-pyrrole disulfonamide receptors displayed most success. Further molecular modelling and ^{1}H NMR spectroscopic studies confirmed that no change in conformation occurred upon anion binding.
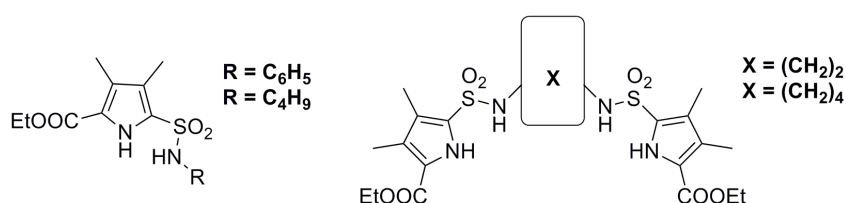
Figure 1.26: Structure of pyrrole sulfonamide receptors synthesised by Huggins *et al.*[5]

1.2.6   Squaramides as Anion Receptors

Squaramides are four-membered ring systems derived from squaric acid which can form up to four H-bonds; its carbonyl groups may act as H-bond acceptors while its N-H groups may act as H-bond donors. Similar to urea based receptors, squaramides are capable of binding anions in a bifurcated system with simultaneous bonding from both N-H groups to a single anion. In 2001, Costa *et al.* conducted a thermodynamic study probing the implications of binding of squaramides to carboxylates and observed that binding was exothermic in DMSO and chloroform.[91] In methanol, the association was endothermic but entropically driven as a result of breakage of solvent interactions and release of solvent molecules to the bulk phase. Costa *et al.* later reported a range of positively charged squaramide receptors which could bind SO_4^{2-} and $H_2PO_4^-$ in ethanol/water mixtures and they reported moderate SO_4^{2-} selectivity.[92]

In 2008, Muthyala *et al.* designed squaramide molecules bearing carbonyl groups which could effectively open and close the anion binding cleft as a result of intramolecular interactions, an application which was designed with anion transport in mind (Figure 1.27).[93] In non-polar solvents, virtually no Cl^- binding was observed owing to intramolecular H-bonding. In polar solvents, H-bonding was disrupted, allowing a conformational change to occur and Cl^-

binding to proceed. There was no Cl$^-$ binding of **74** & **75** observed in CHCl$_3$ while in CH$_3$CN, both receptors bound anion; with a 5-fold increase observed in K$_{ass}$ value for **75** as a result of chloro-substitution. The *meta*-isomer **76** bound anions in both polar and non-polar solvents with K$_{ass}$ values of up to 7.8 x 10^5 M^{-1} reported due to the lack of steric hindrance effects in **76** compared to **74** & **75**. Al-Sayah *et al.* later studied a thiourea and squaramide bipyridine containing receptor for binding AcO$^-$ in a number of solvents *via* ^{1}H NMR titration (Figure 1.27). In 1:1 CD$_3$CN: CDCl$_3$, thiourea **77** produced a K$_{ass}$ value of 5790 M^{-1} while the squaramide **78** bound AcO$^-$ with a K$_{ass}$ value of 7390 M^{-1}.
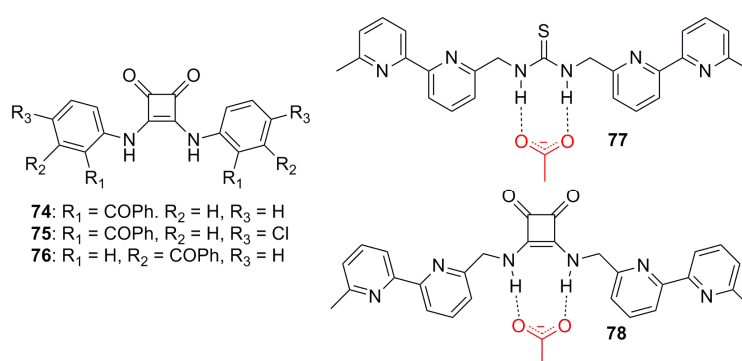
Figure 1.27: Squaramide receptors **74**-**76** developed by Muthyala *et al.*[93] Thiourea and squaramide receptors **77** & **78** studied by Al-Sayah *et al.* in 2010.[94]

In 2010, Taylor *et al.* reported a new synthetic procedure for the preparation of squaramide receptors and examined an acidic 4-nitroaniline derived squaramide **79** for its anion binding properties through UV spectroscopy.[40] Interestingly, substantial differences in UV spectra of **79** were observed in CH$_3$CN compared to DMSO, ascribed to deprotonation of one of the squaramide N-H groups in DMSO without the need to add any base. This deprotonation was more pronounced with increasing dilution. It was proposed that the H-bond accepting ability of DMSO promoted this equilibrium process which became unfavoured at higher concentrations of **79** due to self-association. Addition of basic anions such as AcO$^-$ and H$_2$PO$_4^-$ to a DMSO solution of **79** did not impart any spectral changes, further evidence of DMSO induced deprotonation. However, addition of tetrabutylammonium fluoride induced deprotonation of the second squaramide N-H group with an accompanying colour change. In acetonitrile, **79** existed in its neutral state with deprotonation induced upon addition of fluoride, acetate, dihydrogen phosphate and *p*-toluenesulfonate. Interestingly, **79** was observed to reprotonate upon addition of excess tetrabutylammonium tosylate following initial

deprotonation, an effect which was ascribed to the formation of a stable double H-bonded complex which was more stable than the protonated form of DMSO.
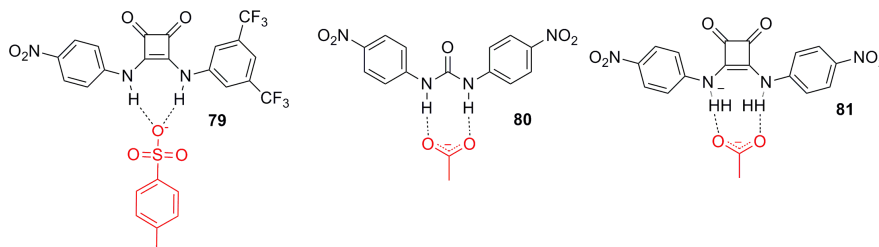
Figure 1.28: Acidic squaramide **79** which undergoes proton transfer events reported by Taylor *et al.*[40] Structure of urea **80** and corresponding squaramide **81** compared for their anion binding abilities by Fabbrizzi *et al.*[41]

Fabbrizzi *et al.* compared the anion binding properties of the squaramide receptor **81** possessing an electron withdrawing NO_2 group with a similar urea receptor **80** (Figure 1.28).[41,95] 1:1 complexes were observed in all cases through UV/Vis and ^{1}H NMR spectroscopy. In the case of squaramide **81**, bifurcated H-bond interactions involved the N-H and also closely located aryl C-H groups to give a total of four H-bonds. Complexes with halides were approximately 1 to 2 orders of magnitude more stable than in the case of urea **80** while both possessed approximately equal K_{ass} values for oxo-anions. For the most basic anions such as AcO^- and F^- with **81**, 1:1 H-bonding complexes were initially formed followed by N-H deprotonation. However, deprotonation did not occur for **80** with AcO^-, evidence of its lower acidity. Overall, they concluded that **81** was a more efficient halide receptor while both **80** & **81** functionalities possessed similar proclivities for oxyanions.

Amendola *et al.* conducted a thermodynamic study to compare the anion binding properties of urea **82**, squaramide **83** and sulfonamide **84**-**86** based receptors using spectrophotometric, isothermal titration calorimetry ITC and ^{1}H NMR titrations in CH_3CN (Figure 1.29).[95] The results showed that all receptors **82**-**86** formed 1:1 H-bond complexes to Br^- and Cl^- with **83** producing the strongest binding. The urea **82** and squaramide **83** formed extremely strong binding complexes with AcO^- while proton transfer effects were evident in the titrations of **84**, **85** & **86** with this anion. In the case of $H_2PO_4^-$, 1:1 and 1:2 receptor:anion interactions were observed. Potentiometric studies in H_2O/CH_3CN showed that the pK_a values of **83**, **84**, **85** & **86** were 10.9, 8.3, 8.3 & 4.3 respectively; highlighting the enhanced acidity of **86** and this was ascribed to the stabilizing effect of the *meta*-NO_2 groups on the negative charge formed

through receptor deprotonation. A pK_a value for **82** could not be calculated as this receptor did not deprotonate.
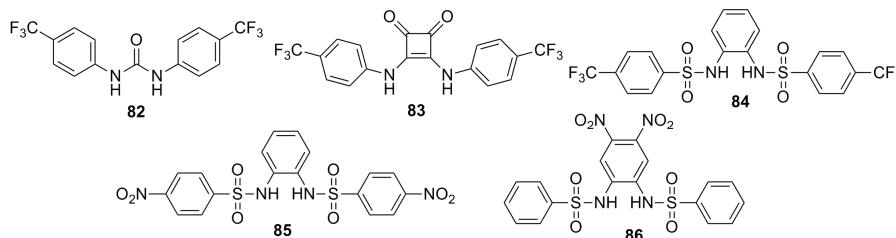
Figure 1.29: Urea **82**, squaramide **83** and sulfonamide **84**-**86** analysed in a thermodynamic study of anion binding.[95]

1.3   Organocatalysis

The synthesis of organic molecules has been a major scientific objective for over a century and plays a key role in the pharmaceutical industry as the majority of therapeutic drugs are small molecule organic compounds.[96] Organic synthesis is met by many challenges including cost of reagents, poor reaction efficiencies and environmental concerns. A major challenge for chiral pharmaceutical compounds in particular is the synthesis of single enantiomers.[9]

In order to overcome some of these challenges, catalysts have been employed. Traditionally, metal-based Lewis acidic catalysts have existed at the core of asymmetric enantioselective catalysis.[11,97] In many cases, their catalytic activity can be ascribed to a lowering of the lowest unoccupied molecular orbital energy as a result of catalyst coordination. The transfer of chirality from the catalyst to the product of a reaction can be brought about by chiral ligands surrounding the metal core. A general representation is shown in Figure 1.30 and a brief introduction and history into the development of metal-based catalysts will be presented below.
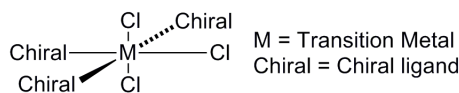
Figure 1.30: General representation of chiral transition metal based catalyst.

In 1968, Knowles *et al.* replaced the achiral triphenylphosphine ligands in a Rhodium complex which Wilkinson applied to the hydrogenation of alkenes with the chiral phosphine

23

ligands methylpropylphenylphosphine, creating the first asymmetric catalyst **87** which was employed in an asymmetric hydrogenation reaction to give product in 15% ee.[98] They later employed a cyclohexyl-*o*-anismethylphosphine (CAMP) ligand to create catalyst **88** capable of producing up to 90% ee in the hydrogenation of dehydroamino acids (Scheme 1.3).[98,99]
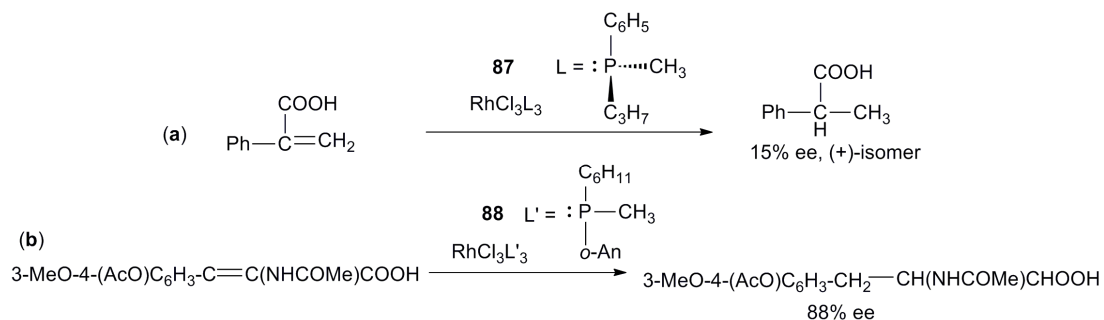
Scheme 1.3: (a) Hydrogenation reactions using chiral **87** to give 15% ee of hydrogenated product.[98] (b) Hydrogenation of dehydroamino acids using CAMP ligand **88** to give 88% ee reported by Knowles.[99]

Kagan & Dang bridged two mono-dentate phosphines to form the first chiral bidentate phosphine ligand and reported ee values up to 72% for the catalytic hydrogenation of a number of precursors of phenylalanine using a rhodium-DIOP (2,3-Isopropylidene-2,3-dihydroxy-1,4-*bis*(diphenylphosphino)butane) complex **89** (Scheme 1.4a).[100] A major breakthrough came when Knowles later reported that a rhodium complex **90** containing chiral phosphine DIPAMP ligands could enantioselectively catalyse the addition of H_2 to one face of a prochiral olefin substrate in up to 95% ee. This was used in 1983 on a commercial scale for the synthesis of *L*-DOPA (3,4-dihydroxy-*L*-phenylalanine) **91**, a drug for the treatment of Parkinson's disease.[101]
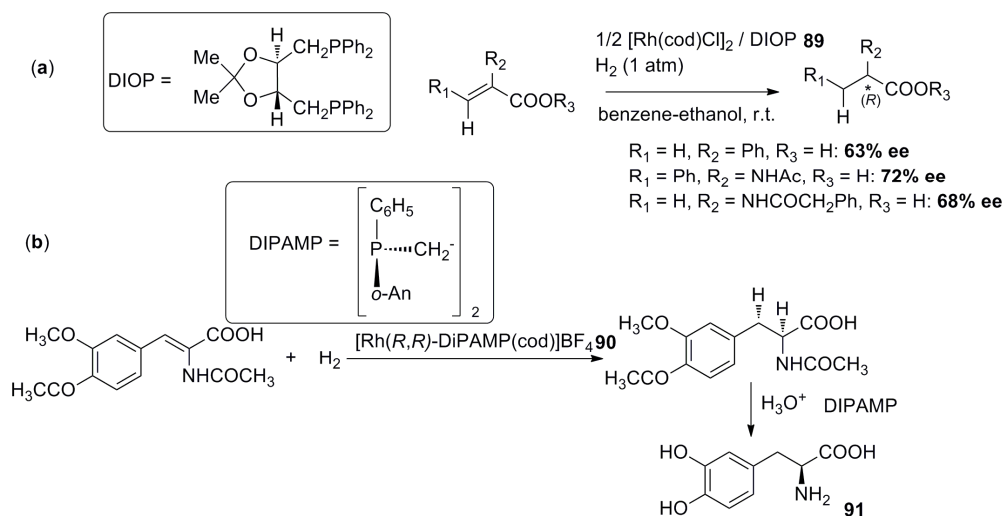
Scheme 1.4: (a) Kagan's rhodium DIOP catalyst **89** in enantioselective hydrogenation of phenylalanine precursors.[100] (b) DIPAMP catayst **90** which could enantioselectively catalyse hydrogenation of *L*-DOPA **91**.[101]

This work led to metal-based catalysts being extensively developed as catalysts for enantioselective synthesis.[102] So much so that Knowles and Noyori shared half of the 2001 Nobel prize in chemistry for their work on asymmetric catalytic hydrogenation with Sharpless for his work on asymmetric catalytic oxidation (Figure 1.31).[103]
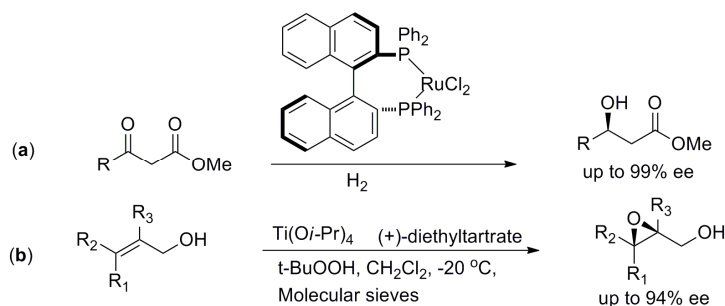
Figure 1.31: Asymmetric catalytic hydrogenation reaction conducted by Noyori *et al.* using (*R*)-BINAP catalyst. Asymmetric epoxidation developed by Sharpless also shown.[103]

While metal-based catalysis has been extensively studied and advances in ligand design have resulted in the development and application of a vast number of Lewis acidic metal-based catalysts, the use of such catalysts has some of the following disadvantages:

o Product inhibition can occur due to binding of reaction product with the catalyst.
o Metal catalysts may react with oxygen making the exclusion of air and moisture imperative, limiting functional group and solvent tolerance.

25

o   Catalyst disposal issues can exist surrounding their heavy metal content.

o   High cost makes catalyst recycling essential which is not always possible due to degradation.

In the last 15 years, the concept of designing more selective, robust, environmentally friendly and functional group tolerant catalysts has been explored. In natural systems, hydrogen extensively acts as a catalyst e.g. phosphodiesterase enzymes such as *staphylococcal nuclease* hydrolyses DNA 10^{16} times faster than the uncatalysed process through anionic transition state stabilisation.[104,105] Due to the success of enzymes in catalysing natural systems, the use of analogous small organic molecules as catalysts was considered promising.

Initial examples were reported by the Wiechert and Hajos groups, employing proline as an organocatalyst for the intramolecular aldol reaction of a triketone to give a chiral bicyclic enone, in the early 1970s (Scheme 1.5).[106,107] Hine *et al.* and also Kelly *et al.* also contributed significantly to the development of organocatalysts for epoxide ring opening and Diels-Alder reactions respectively.[108,109] Following these discoveries, the field remained dormant until an almost explosive growth in interest around 2000.[110,111] Since then, a significant number of organocatalysed carbon-carbon and carbon-heteroatom bond forming reactions (e.g. Diels Alder, 1,3-dipolar cycloaddition, direct aldol condensation, Mannich and Michael reactions)[112] have been reported producing high yields and enantioselectivies.[112]
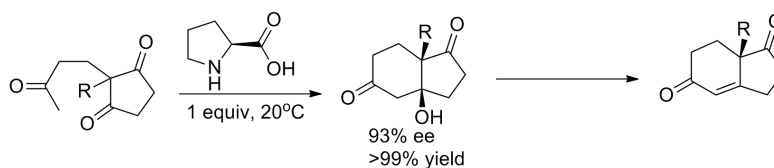
Scheme 1.5: Proline catalysed Robinson annulations reported at Hoffman-La Roche and Schering AG.[106,107]

There are a number of modes by which organocatalysts are known to operate and by which organocatalysts are classified and these include:

1.   Secondary amine catalysis *via* enamines,[113]
2.   Secondary amine catalysis *via* iminium ions,[113]
3.   Phase transfer catalysis,[114]

26

4. Nucleophilic and Brønsted base catalysis[115] and

5. Hydrogen bonding catalysis[11,116]

While H-bonding catalysis is classified separate from other modes, it may also act cooperatively in a number of examples of organocatalysis.

Secondary amine catalysis *via* enamines is an example of Lewis-basic catalysis while primary amines have also been shown to promote enamine based reactions.[117] An electron pair donor (Lewis base catalyst) increases the reaction rate through nucleophilic addition to a substrate acceptor atom which may enhance the nucleophilic character of the substrate, promoting its reaction. H-bonding interactions from the catalyst may simultaneously impart a cooperative effect through activation of an electrophilic substrate. A key example of enamine catalysis is in the proline-catalysed intramolecular aldol reaction (Robinson-type annulation) of a triketone to give a chiral bicyclic enone (Scheme 1.5)[106,107] The success of this system was ascribed to cooperative effects between H-bonding of the carboxylic acid group and the carbonyl electrophile, activating it towards enantioselective nucleophilic addition of the enamine nucleophile. Secondary amine catalysis *via* enamine has received significant interest following the report by List *et al.* of the proline catalysed intermolecular aldol reaction of aliphatic aldehydes with ketones (Scheme 1.6) and is detailed at length in Chapter 3.[118]

20-30 mol%
4:1 DMSO: acetone   96% ee; 97% yield   Proline/acetone enamine
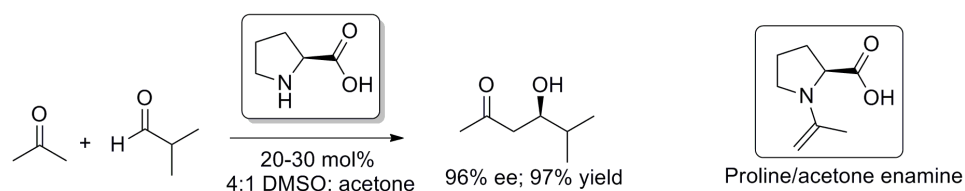
Scheme 1.6: Intermolecular aldol reaction catalysed by proline *via* enamine catalysis reported by List *et al.*[118]

Also central to the rapid growth in organocatalysis was the report of MacMillan *et al.* of the use of chiral secondary amines as catalysts to activate enals *via* the formation of an iminium ion in a Lewis basic catalytic process.[119] The iminium ion is formed through condensation of the chiral secondary amine with a carbonyl substrate, often enal (*α,β*-unsaturated aldehyde) molecules. The lowest unoccupied molecular orbital of the iminium ion species is lowered making it more reactive towards attack from a nucleophilic reactant molecule. This has been

applied to various cycloaddition and conjugate addition reactions.[115] In a cycloaddition reaction using MacMillan's catalyst **92**, the bulky dimethyl group forces the bulk portion of the iminium ion away while a possible π-interaction with the benzyl group imparts stability and gives high facial attack selectivity during attack on the alkene (Scheme 1.7).
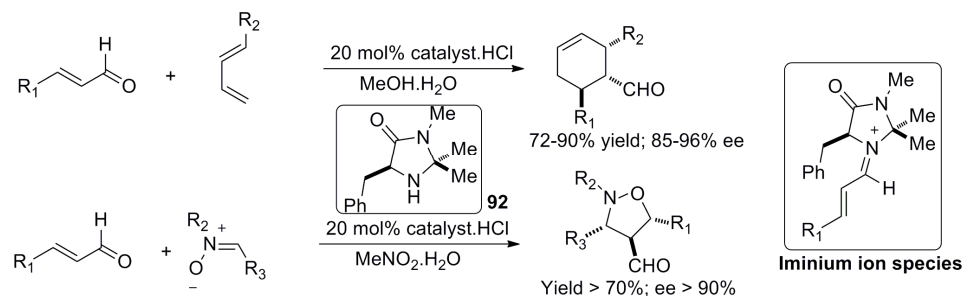
Scheme 1.7: Secondary amine catalysed [4+2] cycloaddition of enals and nitrones using iminium ion catalysis.[119]

As previously stated, both of these catalytic modes employ of Lewis base catalysis where a nucleophilic attack by the catalyst on a substrate activates it towards reaction with an electrophile (enamine catalysis) or nucleophiles (iminium ion catalysis). Scheme 1.8 contains a basic representation of each mode showing the mechanistic differences.
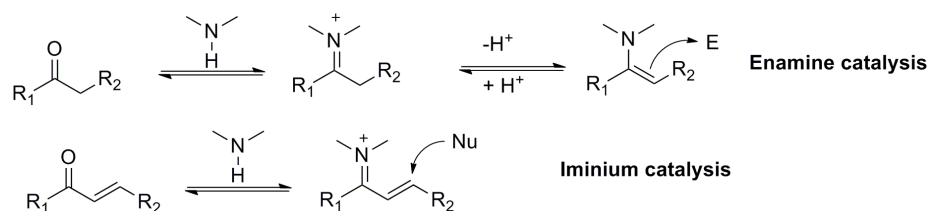
Scheme 1.8: Comparison of enamine and iminium catalysis.

Phase transfer organocatalysis (PTC) is an example of Lewis acidic catalysis. PTC is necessary when reactants exist in different phases due to substantially different solubility characteristics. The catalyst is designed to be soluble in both the organic and aqueous phase and has the ability to bind a reactant from one phase as an ion pair and shuttle it into the phase which contains the other reactant. PTC has had a major impact on enantioselective synthesis, in particular in for the synthesis of unnatural amino acid derivatives by asymmetric alkylation reactions.[120,121] For example, a number of authors applied chiral phase transfer catalysts under different conditions to an enantioselective alkylation of *tert*-butyl glycinate-benzophenone (Scheme 1.9). Lygo's Cinchona alkaloid catalyst **94** gave product in moderate yield and 94% ee in favour of (*S*)-isomer.[122] Corey *et al.* and O' Donnell *et al.* both used catalyst **95** to

produce similar yields of the order of 88% while Corey obtained 94% ee and O Donnell reported 91% ee, both favouring the (*S*)-product.[123,124] Corey *et al.* rationalised the origin of enantioselectivity based on the structure of the ion pair formed between the enolate of **93** and catalyst **95** upon transfer to the reactant phase. The alkyl halide was proposed to approach from one side only leading to the reported (*S*)-product. In 2003, Maruoka *et al.* applied a C_2-symmetric chiral quaternary ammonium salt **96** derived from (*S*)- or (*R*)-1,1'-bi-2-naphthol containing a 3,4,5-fluoro-substituted aromatic substitutent at the 3,3' position of one binaphthyl substituent.[125] Catalyst **96** resulted in a good yield and 99% ee in favour of the (*R*)-product (Scheme 1.9).
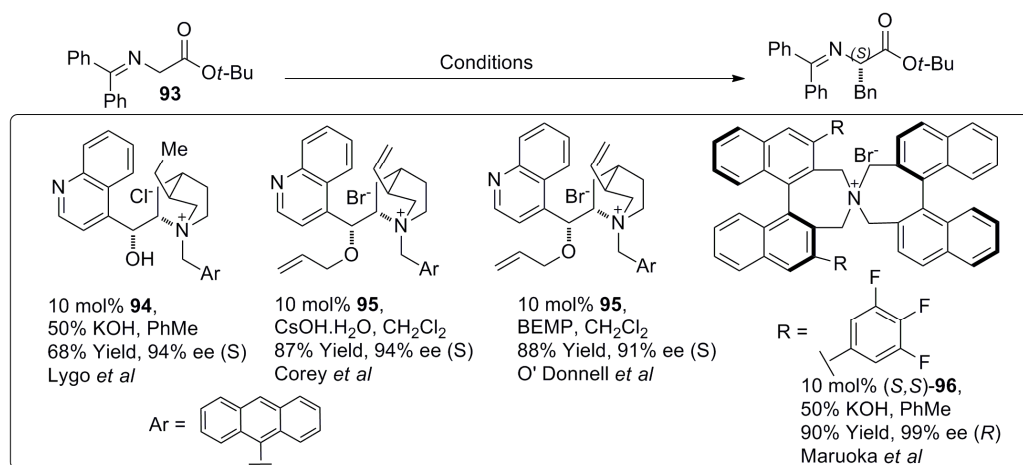
Scheme 1.9: Phase transfer catalysts **94-96** promoting alkylation of **93** conducted by various authors.[122-125]

Brønsted base catalysis is initiated when a basic catalyst partially deprotonates a reaction substrate which then undergoes reaction followed by product protonation to reform the base catalyst. This catalytic mode has played a significant role in the development of chiral organocatalysts.[115] As an example a cinchona alkaloid may act as a base to deprotonate substrates containing relatively acidic protons, e.g. malonates, thiols or a proton which is α to two carbonyl groups, forming an ion pair between the anion and protonated amine catalyst. This leads to a chiral environment around the anion and an enantioselective reaction with an electrophile can generate an enantioenriched product (Scheme 1.10).
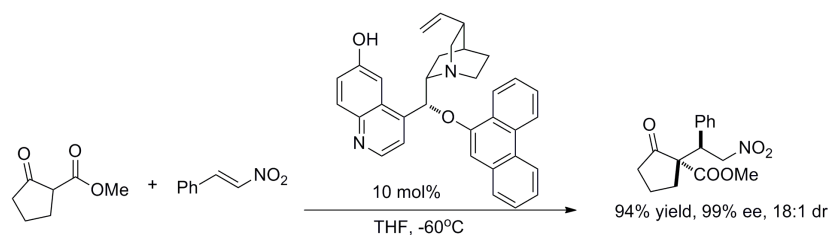
Scheme 1.10: Brønsted base catalysis in the cinchona alkaloid catalysed conjugate addition to nitroalkenes as reported by Deng et al.[126]

In the following section and for the remainder of the review, details of H-bonding as a mode of organocatalysis will be presented, as this underpins the work in Chapter 2.

1.3.1   H-Bonding Organocatalysts

Hydrogen bonding is a powerful technique for molecular recognition, carbonyl group activation and activation of many biologically important reactions. Significant research has also gone into the development of H-bonding catalysts including cinchona alkaloids, ureas, thioureas, and diols such as phosphoric acid and TADDOL (α,α,α',α'-tetraaryl-1,3-dioxlane-4,5-dimethanol) derivatives.[116,127] Such catalysts operate through electrophile activation in a similar way to Lewis acid activation; however H-bonding alone is used to enhance activation and chirality in the catalyst generates a chiral environment around the reaction electrophile or transition states.
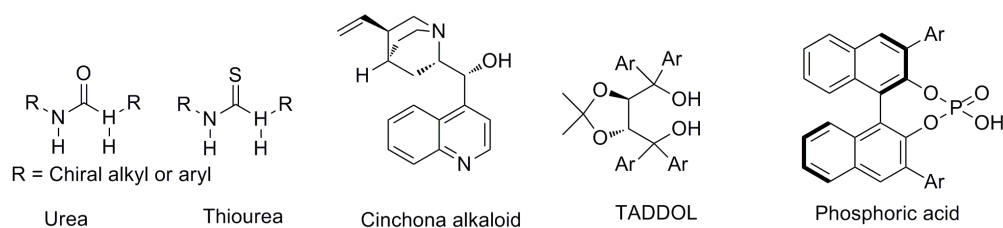
Figure 1.32: General representation of a number of types of H-bonding organocatalysts.

In general, H-bonding organocatalysts may enhance the rate of reaction by reducing the activation energy by stabilising the transition state (TS) through either H-bonding or proton transfer. The weaker forces involved in H-bonding organocatalysis compared to metal based Lewis acid catalysts may produce lower turnover frequencies but also facilitates greater control of binding selectivity resulting in product inhibition and catalyst air/moisture

30

sensitivity being less problematic in organocatalytic systems.[115] The main modes of H-bond activation of carbonyl compounds are single H-bonding and double H-bonding (Figure 1.33),[128] both of which activate the carbonyl exclusively through H-bond interactions from a H-bond donating group, e.g. amide or urea/thiourea functionality.
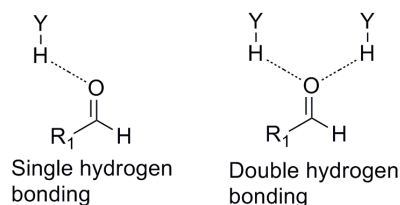
Figure 1.33: Modes of activation of a carbonyl group. [128]

The principal focus of this section on H-bonding organocatalysts places a particular emphasis on urea and thiourea catalysts and will finish with a linking of the use of receptors as organocatalysts where amide, urea and thiourea based receptors will be presented. However a short summary of the use of cinchona alkaloids, phosphoric acids and TADDOL based catalysts will first be presented.

Cinchona alkaloids are well known natural products isolated from the bark of evergreen trees which can act as bifunctional H-bond donor catalysts.[129] Their catalytic activity may be ascribed to the presence of the Lewis basic tertiary quinuclidine nitrogen and the Lewis acidic polar hydroxyl group capable of H-bonding to reaction substrates in a chiral environment. They also exist in pseudoenantiomeric forms such as cinchonidine and cinchonine while the secondary alcohol group at C-9 can be readily modified to include other H-bonding moieties (Scheme 1.11a). Cinchona alkaloids were first applied as bifunctional catalysts in the enantioselective conjugate addition of thiols to cycloalkenones where the catalyst was proposed to activate the thiol nucleophile by general base catalysis and the enone by H-bonding.[130] In addition, the OH group at the 9-position of the alkaloid bound to and stabilised the developing negative charge at the carbonyl oxygen in the reaction transition state. H-bonding to this chiral OH group promoted facial selectivity in the nucleophilic attack. Subsequently, cinchona alkaloids have been used as phase transfer catalysts but have also been exploited to impart enantioselectivity in a large number of organic reactions.[114] In 2005, Schaus employed cinchona alkaloid catalysts **97** & **98** to the addition of β-keto esters to

carbamate protected aromatic imines.[131] They obtained the products in excellent yields and in general, obtained high enantioselectivities in the range of 81-96% ee, however diastereoselectivity tended to be poor in some cases (Scheme 1.11b).
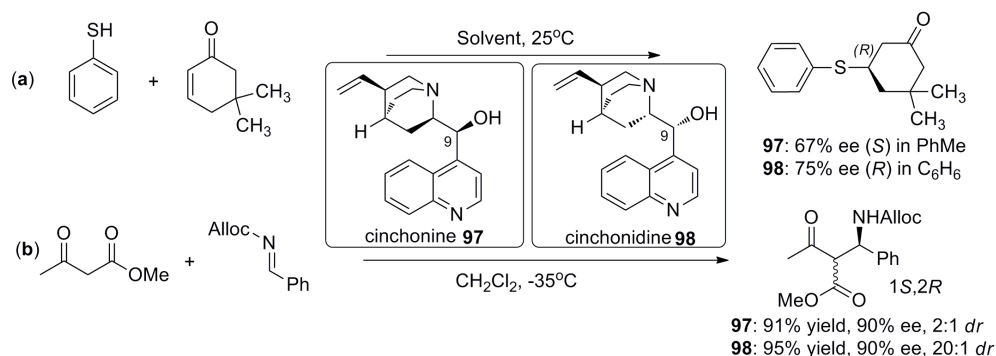
Scheme 1.11: (a) Cinchona alkaloid **97** & **98** catalysed conjugate addition of thiols to cycloalkenones reported by Wynberg *et al.*[130] (b) Application of catalysts **97** & **98** in addition of β-keto esters to protected imines.[131]

Diols including 1,1'-bi-2-naphthol (BINOL) and α,α,α',α'-tetraaryl-1,3-dioxlane-4,5-dimethanol (TADDOL) derivatives are useful for enantioselective Lewis-acid catalysed reactions. Diols were first reported as efficient H-bond donating organocatalysts by Hine *et al.* in 1985.[108] Schaus *et al.* reported that H8-BINOL derivatives **99** & **100** possessed very similar catalytic activities in the Morita-Baylis-Hillman (MBH) reaction of a number of aldehydes with cyclohexenone.[132] High yields and enantioselectivities were reported for cyclic alkyl aldehydes while aromatic aldehydes gave inferior results of the order 30-40% yield and 34-67% ee in favour of (*S*)-product. They proposed that the chiral Brønsted acid group promoted the conjugate addition step and remain H-bonded to the enolate for the aldehyde addition step, thereby imparting enantioselectivity.
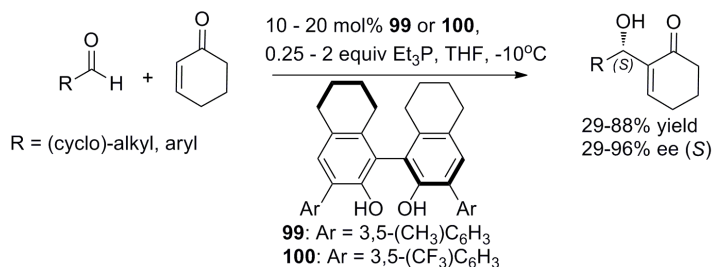
Scheme 1.12: Morita-Baylis-Hillman reaction of various aldehydes with cyclohexenone catalysed by BINOL derivatives **99** & **100** reported by Schaus *et al.*[132]

Rawal *et al.* reported TADDOL derivatives such as **101** were capable of enantioselectively catalysing the asymmetric hetero- Diels-Alder reaction of aminodienes with aldehydes to generate the dihydropyran product in high enantioselectivity.[133] The reported mode of action of TADDOL catalyst **101** involved H-bonding of the chiral alcohol to the aldehyde carbonyl group, creating a chiral environment.
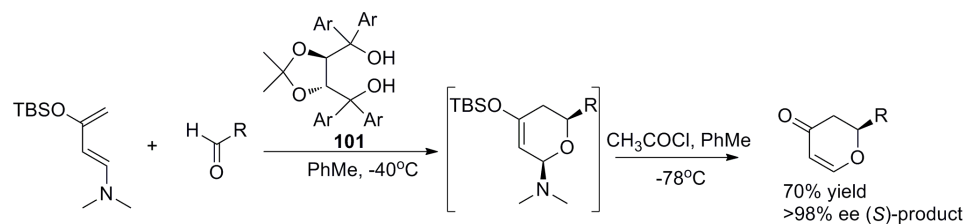
Scheme 1.13: TADDOL derivative reported by Rawal *et al.* to enantioselectively catalyse hetero-Diels Alder reaction.[133]

Phosphoric acids may participate in reasonably strong Brønsted acid catalysis. Akiyama *et al.* developed a chiral cyclic phosphoric acid diester **102** starting from (*R*)-BINOL and applied it to the Mannich type reaction of ketene silyl acetal **103** with an aldimine.[134] The aryl groups on the 3- and 3-positions proved essential for enantioselectivity; the 4-nitrophenyl substituted phosphoric acid catalyst **102** produced highest yields and enantioselectivities. The *β*-amino ester products were obtained favouring the *syn*-isomer with ee values up to 96% observed. The authors proposed that the reaction proceeded *via* an iminium salt generated from the aldimine and the Brønsted acid catalyst and the 3,3'-diaryl groups shielded the phosphate group, resulting in asymmetric induction. The same authors later applied a TADDOL-based phosphoric acid diester catalyst **104** to a similar Mannich reaction using **105** in place of ketene silyl acetal **103**.[135] The aryl substituents on the TADDOL strongly affected catalytic performance and use of the 4-(trifluoromethyl)phenyl group in the catalyst proved essential.
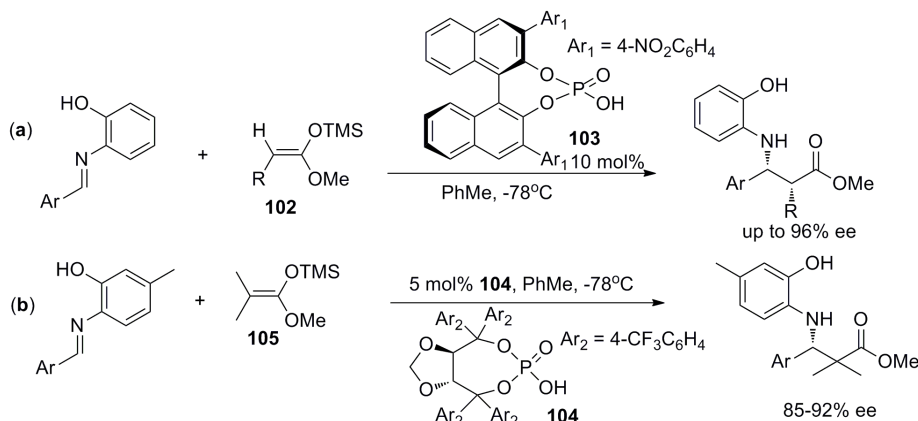
Scheme 1.14: (a) Mannich reaction using BINOL derived phosphoric catalyst **103** reported by Akiyama *et al.*[134] (b) Use of a TADDOL-derived phosphoric acid catalyst **104** in a similar reaction.[135]

1.3.2 Evolution of Urea based H-Bonding Organocatalysts

Pioneering work using H-bonding in catalysis was conducted by Hine *et al.*[136] They confirmed that 1,8 biphenylenediol **106** could form strong H-bonds from both OH groups to the oxygen atom of Lewis basic substrates, e.g. 1,2,6,-trimethyl-4-pyridone **107** and hexamethyl phosphoramide (HMPA) **108** through X-ray crystallography (Scheme 1.15a).[136] This H-bonding interaction promoted the aminolysis of phenyl glycidyl ether **109** with diethylamine in butanone with similar catalytic activity to what would be expected from a phenol 600 times as acidic (Scheme 1.15b).[108] This showed that general acid catalysis by metal free diprotic acids was a valid strategy on which to design organocatalysts.[137]
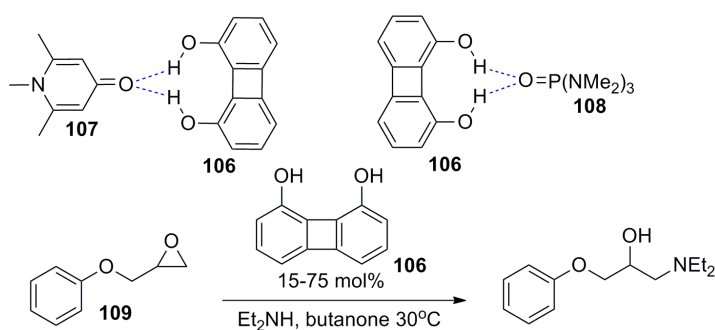
Scheme 1.15: (a) H-bonding of 1,8-biphenylenediol **106** to Lewis basic 1,2,6-trimethyl-4-pyridone **107** and HMPA **108**.[136] (b) Aminolysis of **109** in butanone promoted by biphenylenediol **106.**[108]

Kelly *et al.* used biphenylene diol **110** derivatives as catalysts in the Diels-Alder reaction of cyclopentadiene and *α,β*-unsaturated aldehydes (Scheme 1.16).[109] They suggested that the mechanism involved dienophile activation through double H-bond donation by the catalyst.
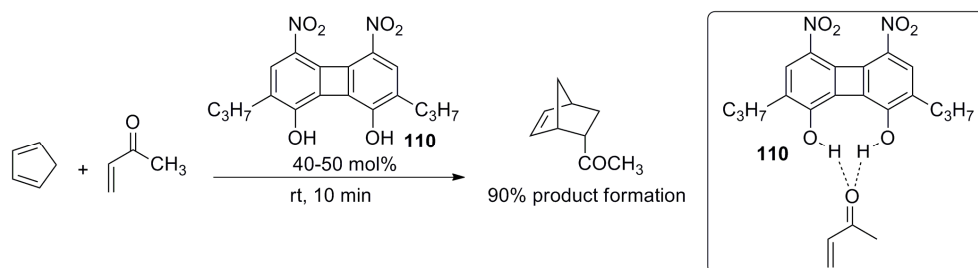
Scheme 1.16: Double hydrogen bond donation of **110** to the dienophile catalysed the Diels-Alder reaction.[109]

Etter *et al.* found that a diaryl urea with electron withdrawing substituents **111** formed co-crystals with proton acceptors such as carbonyl compounds *via* two H-bonds between the urea and carbonyl group (Figure 1.34).[138,139] Jorgensen used this theory to explain the rate acceleration observed in Diels-Alder reactions and Claisen rearrangements through a dual hydration model.[140]
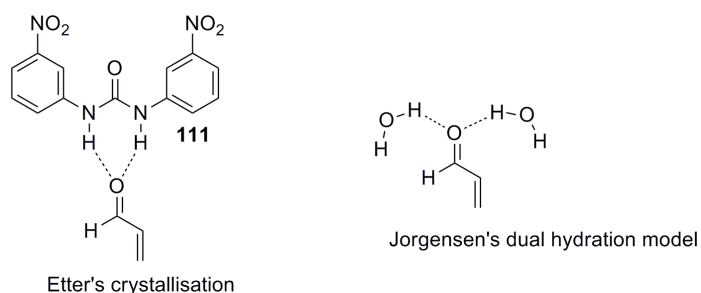
Figure 1.34: Diaryl urea **111** crystallised with a carbonyl compound reported by Etter *et al.*[139,141] Jorgensen's explanation for rate enhacement for Diels-Alder reactions and Claisen rearrangements in the presence of water.[140]

A progression from biphenylene diols was the development of urea based catalysts. Curran & Kuo designed a urea Lewis acid catalyst **112** for the allylation reaction of α-(phenylseleno)-sulfoxide **113** with allyltributylstannane **114** (Scheme 1.17).[142] In order to aid synthesis and solubility, a trifluoromethyl group and an octyl ester were introduced on to the urea aromatic rings. Using 1 equivalent urea catalyst, up to 80% yield and 7:1 *trans:cis* ratio was obtained. The increase in *trans/cis* ratio was explained by the intermediate sulfoxide radical H-bonding to **112**.
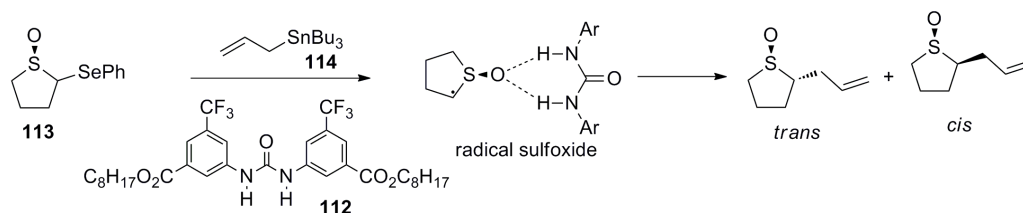
Scheme 1.17: Curran's diarylurea catalyst **112** in the acceleration of the allylation of phenylseleno sulfoxides.[142]

Curran observed a 4-fold rate enhancement in the presence of 1 equivalent of **112** for the Claisen rearrangement reaction of 6-phenyl allyl vinyl ether **115** at 100 °C.[143] The rate of rearrangement of 6-methoxy allyl vinyl ether at 80 °C increased by a factor of 22 using of 1 equivalent of **112** while use of *N,N*-dimethylurea resulted in a loss of catalytic effect (Scheme 1.18). DMSO enhanced the rate of the uncatalysed reaction slightly but hindered the accelerating effect of the catalyst.
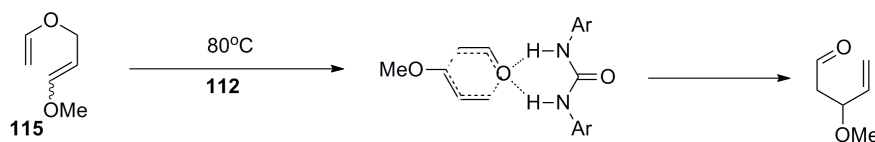
Scheme 1.18: Acceleration of the Claisen rearrangement of **115** using diaryl urea catalyst **112**.

Schreiner & Wittkopp subsequently used urea and thiourea based catalysts in the Diels-Alder reaction of cyclopentadiene and α,β unsaturated carbonyl compounds.[144] The thiourea motif was also investigated as a replacement for the urea group due to its enhanced organic solvent solubility, their ease of preparation and because the thiocarbonyl group is known to be a weaker H-bond acceptor, leading to less self-association.[144] The introduction of electron withdrawing non H-bonding CF_3 substituents in the *meta*-position of the aryl ring was proposed to increase the catalytic ability by generating a more rigid conformation due to H-bonds between the sulphur atoms and *ortho*-protons based on computational modelling (Scheme 1.19). For the reaction of *N*-acyloxazolidinone **116** and cyclopentadiene, using 25 mol% of thiourea catalyst **117** (Scheme 1.19), the reaction proceeded at a much lower temperature and in higher yield with improved diastereomeric ratio (*dr*). Rate enhancement was proposed to be due to coordination of **117** to a lone pair located on the Lewis-basic centre of **116** *via* H-bonding lowering the LUMO energy of the conjugated system. Schreiner's

36

catalyst **117** has since been used by many others as a template for catalysis of a number of organic reactions.[145-147]
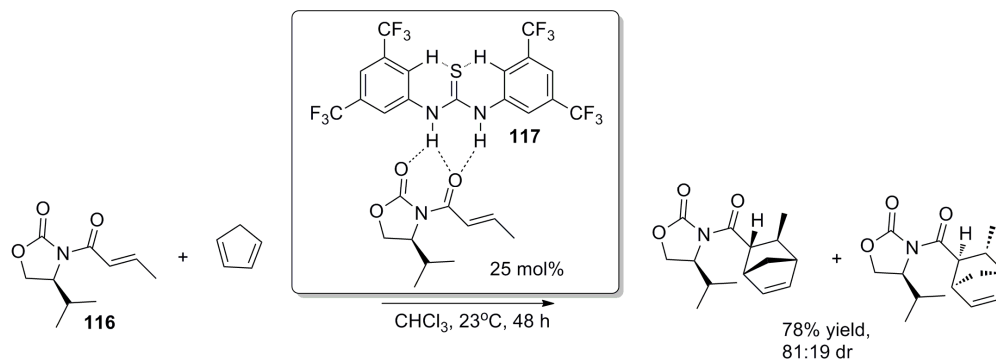
Scheme 1.19: Catalysis of Diels-Alder reaction using Schreiner's thiourea **117**. Attractive S-H intramolecular interaction of thiourea catalyst giving it structural rigidity.[144]

1.3.3 3,5-*bis*(Trifluoromethyl)phenyl based (Thio)urea Catalysts

Takemoto reasoned that the N-H bonds of ureas would also activate the nitrone group *via* H-bonding. They evaluated the addition of trimethylsilylcyanide and ketene silyl acetals (nucleophiles) to various nitrones and obtained the corresponding hydroxyamines in good yields in the presence of urea based catalysts.[146] A correlation was observed between the N-H acidity on amides, ureas and thioureas and their catalytic abilities; Schreiner's thiourea catalyst **117** produced optimum yields.[144,148] Rate enhancement based on H-bonding interactions between the catalyst and nitrone was confirmed by ^{1}H and ^{13}C NMR spectroscopic studies. Scheme 1.20 details the reaction and the proposed mode of catalysis by binding to nitrone and activation towards nucleophilic attack.
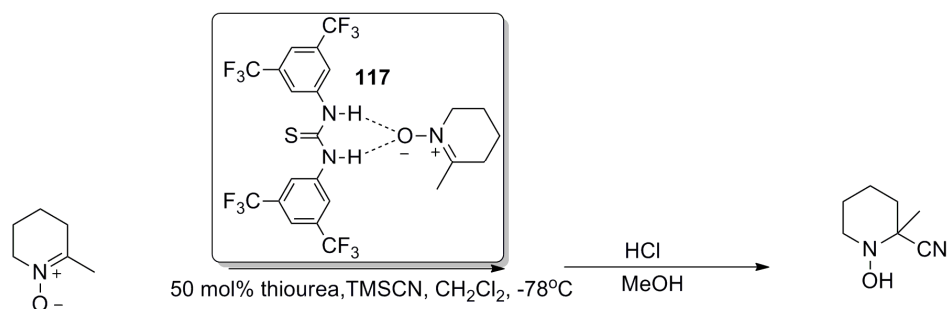
Scheme 1.20: Reaction of 6-methyl-3,4,5-tetrahydropyridine with TMSCN[146] with suggested activation of **117** mechanism of nitrones also shown (H-bonding activation).[146]

Nagasawa *et al.* investigated the acceleration of the hetero-Michael reaction of α,β-unsaturated carbonyl compounds and found optimal results using thiourea **117** and its urea analogue **118**.[149] The reaction of pyrrolidine with γ-crotonolactone **119** produced a 24 fold increase in reaction rate using thiourea catalyst **117**.
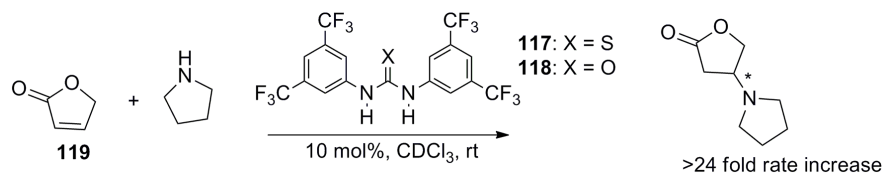
Figure 1.35: Hetero-Michael addition of pyrrolidine to lactone **119** using catalysts **117** & **118**.[149]

In 2004, Connon & Maher successfully applied catalysts **117** & **118** and also a range of Lewis acidic diarylureas catalysts in the DABCO (1,4-diazabicyclo[2.2.2]octane) promoted Morita-Baylis-Hillman (MBH) reaction of benzaldehyde and methyl acrylate (Scheme 1.21).[145] Interestingly, they found that thiourea **117** was inferior to the urea **118** while both were more efficient than water or methanol additives. The authors proposed that rate enhancement was a result of aldehyde electrophile activation or H-bonding to the enol transition state of the reaction (betaine intermediate) through a Zimmerman-Traxler type transition state for the addition of the enolate anion to the aldehyde. The allylic alcohol product was obtained in up to 88% yield and the most efficient diarylurea catalyst could be recycled without loss of activity.
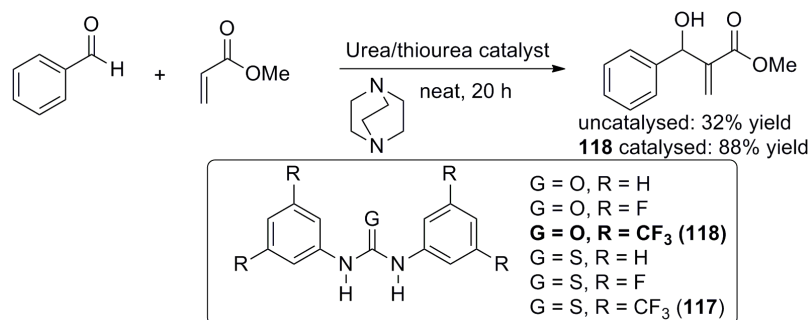
Scheme 1.21: Baylis Hillman reaction of benzaldehyde and methyl acrylate using urea & thiourea catalysts with most successful diaryl urea catalyst **118** highlighted in bold.[145]

Also in 2004, Sohtome *et al.*[147] investigated **117** and **118** in the DABCO catalysed MBH reaction of cyclohexenone with benzaldehyde and obtained a 50 fold increase in product formation compared to the uncatalysed process. ^{1}H NMR spectroscopic studies showed that

117 interacted with both starting materials and these findings aided the development of a chiral variant which will be detailed in the next section.

Schreiner *et al.* successfully applied **117** to a number of reactions and these will be now be discussed together. In 2006, they reported that the rates of acetalization reactions of a number of aliphatic and aromatic carbonyl compounds were highly increased with turnover frequencies of the order of 600 h^{-1} using this catalyst (Scheme 1.22a).[13] The reactions of acid sensitive silyl protected alcohols were also effected and catalyst loading could be reduced to 0.01 mol% without loss in activity. Mechanistic investigations pointed towards catalysis by **117** of the heterolysis of the orthoester followed by stabilisation of a number of oxyanion intermediates. They subsequently demonstrated the ability of this catalyst to coordinate negatively charged intermediates in the addition of amines, thiophenol and alcohols to epoxides where a cooperative effect with water was observed (Scheme 1.22b).[150] Later, the same catalyst was employed in a cooperative Brønsted acid type organocatalysis in the regioselective alcoholysis of styrene oxides (Scheme 1.22c).[151] It was envisaged that water could compete with the nucleophile and as a result, mandelic acid was used as a mild acid alternative additive. Under these conditions, high yields and regioselectivites were obtained for aliphatic, sterically hindered and unsaturated alcohols with styrene oxide.

In 2007, Schreiner and Kotke applied urea **117** to tetrahydropyranylation (THP-protection) of hydroxyl groups in a variety of phenols, sterically hindered alcohols and particularly acid-sensitive reactants such as aldol products, hydroxyl esters, acetals and silyl-protected alcohols (Scheme 1.22d).[152] THP-protection would facilitate the use of these compounds in further synthetic processes. DFT (density functional theory) calculations suggested that the catalyst aided in formation of the nucleophiles (RO$^-$) and stabilised the oxyanion developing in the reaction transition state through double H-bonding.
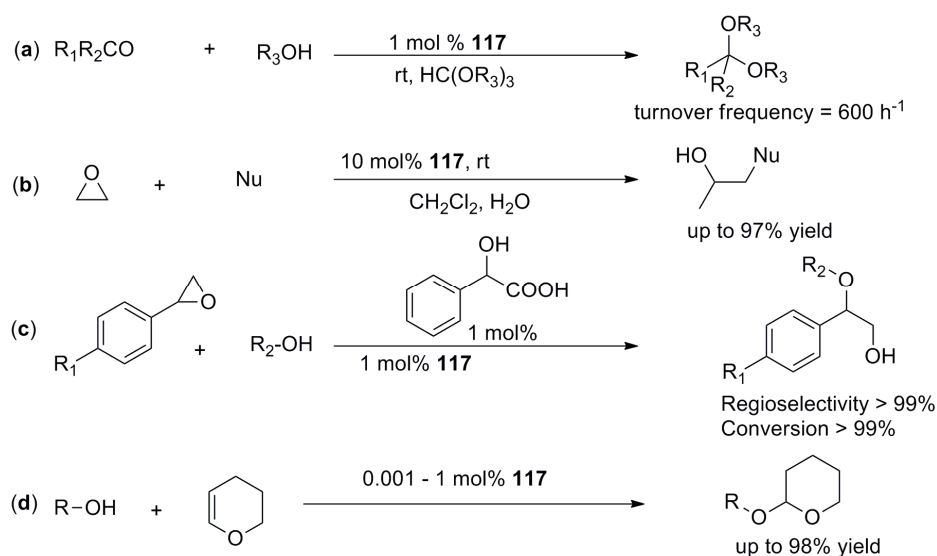
Scheme 1.22: (a) Thiourea catalysed acetalization reaction.[13] (b) Coperative organocatalysis of thiourea **117** with water in addition of amines, thiols and phenols to epoxides.[150] (c) Alcoholysis of styrene oxides promoted by thiourea catalyst **124**.[151] (d) THP-protection of hydroxyl containing groups including acid-labile alcohols.[152]

Philp *et al.* used molecular modelling studies to rationally design a H-bond donating catalyst for the DMAP (dimethylaminopyridine) catalysed MBH reaction of cyclohexenone and 4-fluorobenzaldehyde (Scheme 1.23).[12] Using molecular modelling studies, they designed catalysts consisting of two thioureas separated by either an *m*-xylyl or *o*-xylyl bridge and predicted that these catalysts could bind the electrophilic aldehyde and also the enolate intermediate from the reaction of DABCO with cyclohexenone. These interactions activated the aldehyde and enolate intermediate and held them in close proximity thereby promoting their reaction and resulting in enhanced yields and rates compared to the Schreiner and Sohtome's catalysts.[144,147]
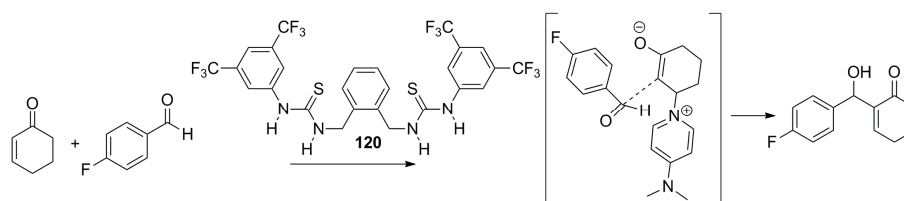
Scheme 1.23: Philp's most successful bifunctional thiourea catalyst **120** capable of binding the enolate anion and aldehyde simultaneously.[12]

In 2008, Connon *et al.* used computational techniques to assess the stabilities of complexes between (thio)urea molecules and a number of electrophiles which incorporated a Lewis-basic

functionality in an attempt to design new more acidic (thio)urea catalysts.[153] This approach focused on the interaction between the catalyst and electrophile, without taking account of the reaction intermediates, but served as a rapid matching of potential catalysts with reaction substrates. A number of catalysts were screened for their interaction with an oxirane group for an addition reaction to epoxides. An *N*-tosyl analogue of **117** proved highly catalytically active but had poor stability. The corresponding urea **121** was also highly catalytically active in the addition of 1,2-dimethylindole to an oxirane with a 71% yield of product obtained (Scheme 1.24). A substrate scope investigation showed that the acidic urea was an efficient organocatalyst for many styrene oxides and indole derivatives including aniline nucleophiles.
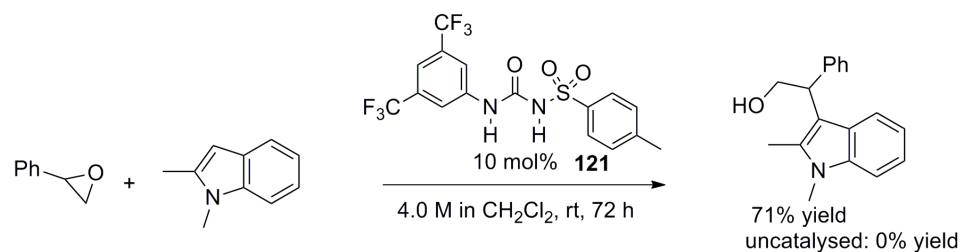
Scheme 1.24: Connon's addition of 1,2-dimethylindole to an epoxide catalysed by **121**.[153]

In 2009, Lattanzi *et al.* studied catalysts **117**, **118** and also two alternative H-bond donating catalysts in the oxidation of sulfides with *tert*-butyl hydroperoxide (TBHP).[154] Catalyst **117** was found to be most active giving the sulfoxide product in high yield in many cases. The origin of catalysis was proposed to be double H-bonding between **117** and an oxygen atom of TBHP, enhancing its electrophilicity and making it more susceptible to nucleophilic attack by the sulfide (Scheme 1.25).
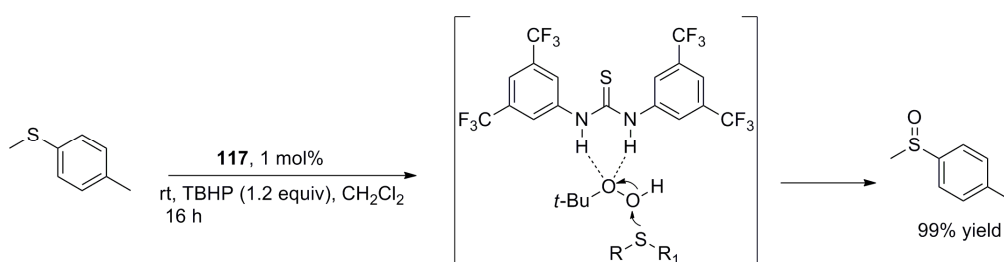
Scheme 1.25: Suggested activation of TBHP by thiourea catalyst **117**.[154]

41

1.3.4 Chiral Urea and Thiourea Catalysts

In this section, some key examples of chiral (thio)urea H-bonding organocatalysis will be presented, however it is not designed as a comprehensive review of this field. Jacobsen's group began the development of chiral urea and thiourea based catalysts.[116] In 1998 they reported an asymmetric Strecker reaction of *N*-allyl aldimines with Schiff base urea catalysts and found moderate to high enantioselectivities of 70-91% ee of product (Scheme 1.27).[155]
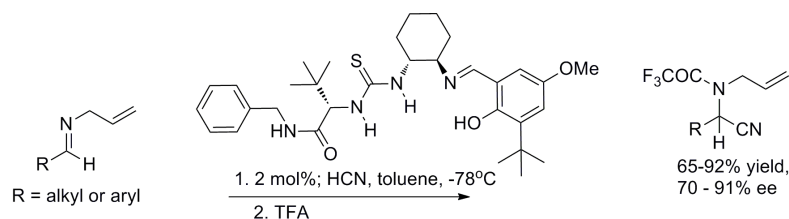
Scheme 1.26: Asymmetric Strecker reaction of *N*-allyl aldimines with Schiff-base thiourea catalyst.[155]

In 2003, Takemoto *et al.* reported seminal findings on the use of bifunctional urea and thiourea catalysts to promote a Michael addition reaction.[156] They postulated that a basic, nucleophile-activating group in a chiral thiourea catalyst along with nitroolefin electrophile activation through H-bonding to both oxygen atoms might allow a synergistic interaction between the functional groups and control their approach stereoselectively leading to an efficient bifunctional catalyst **122** for the Michael reaction of diethyl malonate with *β*-nitrostyrene. Product was obtained in 86% yield and up to 93% ee in favour of the (*S*)-isomer, while reduced ee values were observed in competitive polar solvents (Scheme 1.27). Papai *et al.* later conducted theoretical studies on the enantioselective Michael addition reaction catalysed by thiourea based bifunctional organocatalysts and postulated an alternative mechanism.[157] This mechanism was consistent with the dual activation principle of Takemoto, however electrophile activation was proposed to occur through interaction with the protonated amino group of the catalyst rather than the H-bond donors of thiourea. The key intermediate was the catalyst-nucleophile ion pair while the acidic groups along with the protonated amine were determined to stabilise the transition state in a chiral environment leading to stereoselectivity in the reaction.
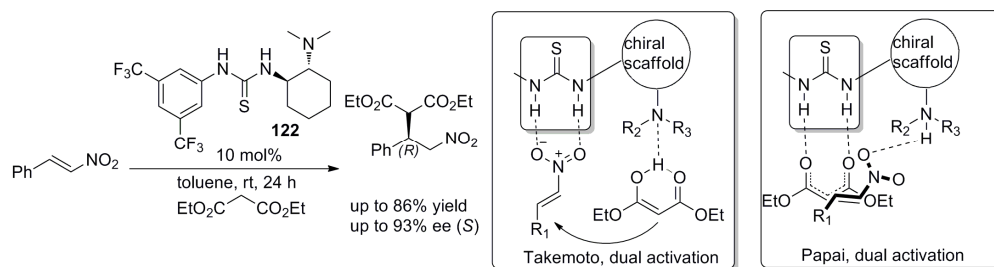
Scheme 1.27: Reaction of diethylmalonate with β-nitrostyrene catalysed by bifunctional thiourea catalyst **122**.[156] Dual activation models proposed by Takemoto *et al.* and Papai *et al.* also shown.

They subsequently successfully applied bifunctional thiourea **122** in the enantioselective addition of malononitrile to α,β-unsaturated imides and in the *aza*-Henry reaction to give high enantioselectivies of the nitroamine product.[158,159] Catalysis in the latter reaction was due to activation of the nitro group which favoured the formation of the nucleophilic nitronate anion (Scheme 1.28).
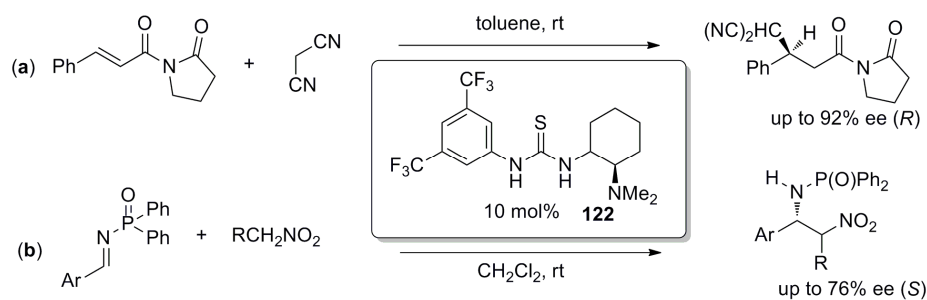
Scheme 1.28: (a) Use of bifunctional **122** in Michael reaction with α,β unsaturated imide. (b) Henry reaction (reaction of nitroalkanes to imines) catalysed by **122**.[158,159]

Wang *et al.* reported a novel binaphthyl catalyst **123** containing a thiourea and tertiary amine group for the MBH reaction.[160] They proposed that the catalyst would H-bond to and activate the carbonyl functionality of the α,β-unsaturated system, facilitating the Michael addition of the catalyst tertiary amine group to the β-position of the substrate while the chiral scaffold could impart stereochemical control on the reaction. In the reaction of cyclohexenone with 3-phenylpropionaldehyde, catalyst **123** gave product in up to 84% yield and 94% ee in favour of the (*R*)-enantiomer (Figure 1.36a). Acetonitrile as solvent at 0 °C produced optimal results producing yields of 63-84% and 80-94% ee for aliphatic aldehydes with cyclohexenone. In further work, they applied catalyst **123** to the Michael reaction of a 1,3-diketone to

43

nitroolefins, observing low catalyst loading (down to 1 mol%) was sufficient for the reaction giving moderate yields of 78-92% and up to 97% ee (Figure 1.36b).[161]
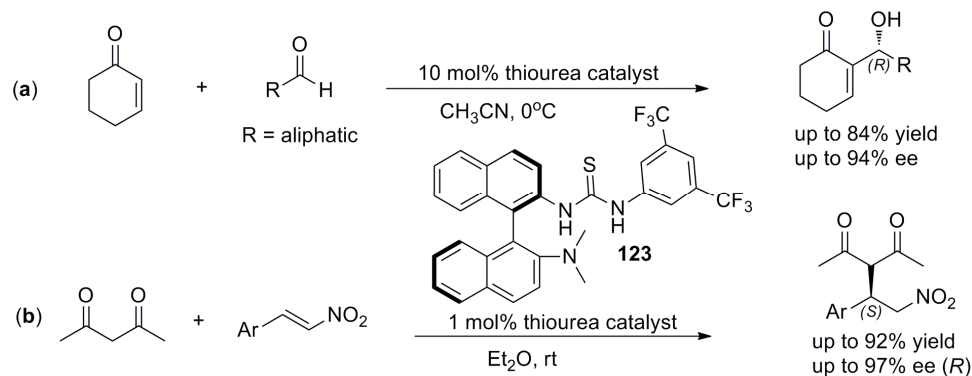
Figure 1.36: (a) MBH reaction of cyclohexenone with aldehydes catalysed by bifunctional thiourea **123**.[160] (b) Michael addition of 2,4-pentanedione to *trans-β*-nitrostyrene catalysed by **123** also shown.[161]

Tsogoeva *et al.* synthesised a bifunctional catalyst **124** consisting of a thiourea group and also a primary amino group attached to a chiral backbone and used it in the Michael addition of acetone to aromatic nitroolefins in toluene producing up to 92% ee of product (Scheme 1.29).[162,163] They proposed that the primary amino group would activate acetone through enamine formation while the thiourea group would H-bond and activate the nitroolefin. DFT calculations showed one oxygen of the nitro group was involved with H-bonding with the thiourea and steric effects resulted in preferential formation of the (*R*)-product.
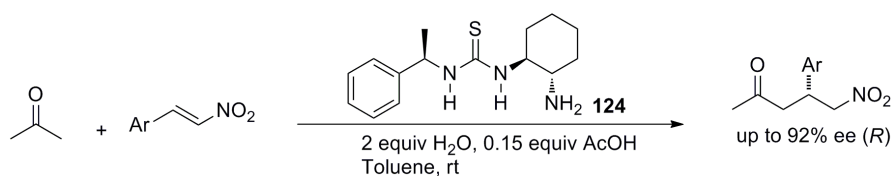
Scheme 1.29: Bifunctional thiourea **124** catalysed Michael addition of acetone to aromatic nitroolefins reported by Tsogoeva.[162]

Sohtome *et al.* investigated the asymmetric Baylis-Hillman reaction using a *bis*-thiourea type catalyst **125** containing two urea/thiourea moieties connected through a 1,2-cyclohexanediamine chiral group.[147] Catalyst **125** produced a 72 fold increase in product formation with 33% ee for the reaction of benzaldehyde and cyclohexenone and they also found success with a number of aromatic and aliphatic aldehydes (Scheme 1.30a). ^{1}H NMR spectroscopic studies were used to postulate a dual activation mode where two thiourea functionalities could co-ordinate to the carbonyl groups of the aldehyde and the enolate.[10] The

R substituent on the aldehyde favoured an *anti* relationship to avoid disrupting thiourea – enolate H-bonding. In addition, carbonyl activation of the enolate **A** led to rapid elimination of the tertiary amine catalyst, currently considered to be the rate determining step based on mechanistic reports for the Baylis-Hillman reaction.[164]
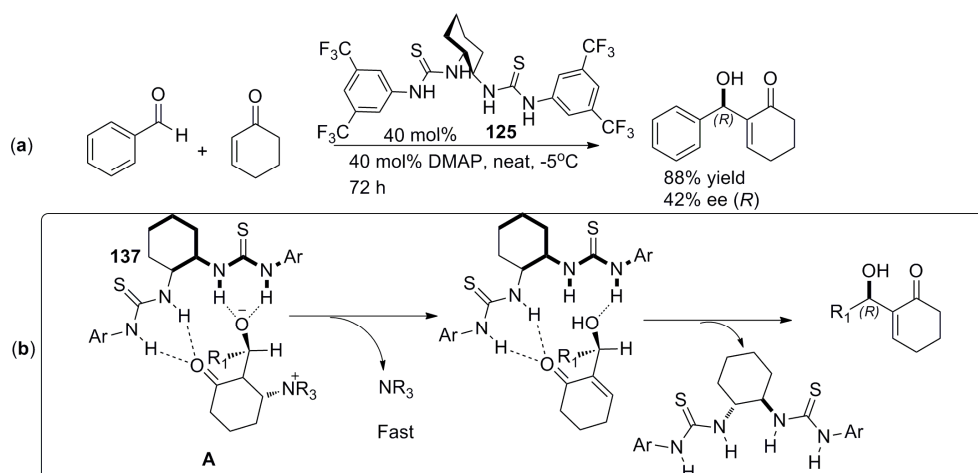
Scheme 1.30: MBH reaction catalysed by *bis*-thiourea chiral catalyst **125** with proposed transition state in (b).[10]

Berkessel *et al.* applied a number of *bis*-thioureas derived from isophoronediamine (IPDA) with a 5,5-dimethyl-1,3-diaminocyclohexane chiral spacer group as catalysts in the MBH reaction of cyclohexenone with cyclohexanecarboxaldehyde.[165] Under optimal neat reaction conditions, *bis*-thiourea **126** produced 90% yield and 91% ee in favour of the (*R*)-product in the presence of tetramethylated isophoronediamine (TMIPDA) (Scheme 1.31).
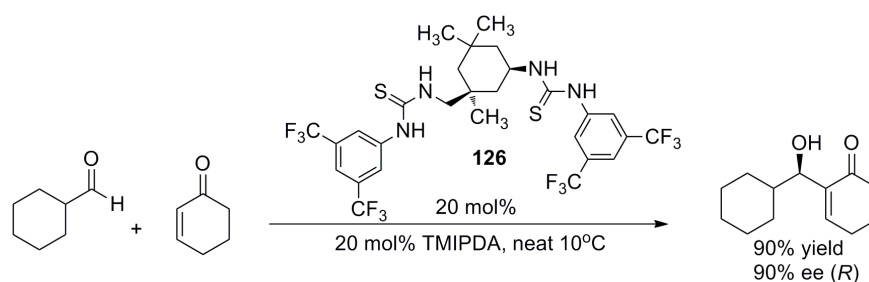
Scheme 1.31: Baylis-Hillman reaction catalysed by *bis*-thiourea catalyst **126**.[165]

Wu *et al.* developed a range of chiral phosphinothiourea organocatalysts derived from *trans*-2-amino-1-(diphenylphosphino)cyclohexane including **127** for the enantioselective MBH reaction of methyl vinyl ketone with a number of aldehydes and the product was obtained in

up to 75% yield and 94% ee.[166] A transition state model where the thiourea H-bonds to the aldehyde carbonyl while the chiral cyclohexyl scaffold forces the phosphinoyl associated enolate to attack the carbonyl from the *si* face to give the (*R*)-product was proposed (Scheme 1.32).
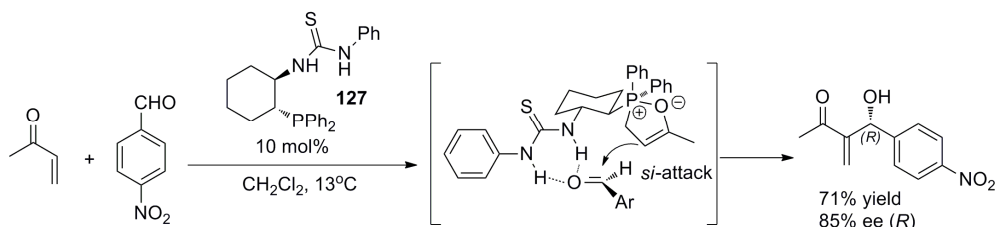
Scheme 1.32: Baylis-Hillman reaction of 4-nitrobenzaldehyde with methyl vinyl ketone catalysed by phosphinothiourea **127**. Proposed transition state leading to (*R*)-product also shown.[166]

Wang *et al.* reported a range of bifunctional amine thiourea catalysts with multiple H-bond donating sites including **128** for the enantioselective direct Michael addition of nitroethane with *β*-nitrostyrene.[167] Product was obtained in 87% yield, 83% ee in favour of the 2*R*,3*R* product and 73:27 *syn:anti* ratio at -30°C (Scheme 1.33).
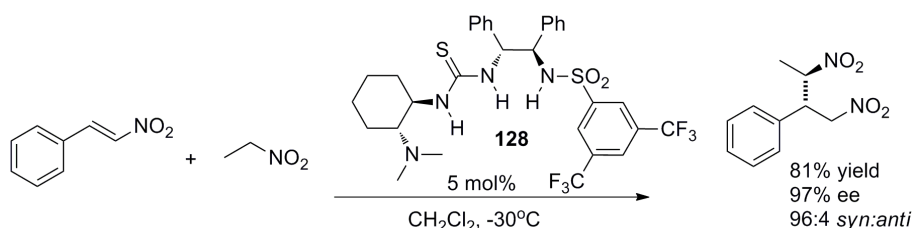
Scheme 1.33: Wang's asymmetric Michael reaction of nitroethane & *β*-nitrostyrene catalysed by bifunctional catalyst **128**.[167]

In 2008, the groups of Connon *et al.* and Song *et al.* reported thiourea functionalised cinchona alkaloid catalyst **129** for the methanolysis of cyclic anhydrides (Scheme 1.34).[168,169] In both cases, dilute conditions were necessary to achieve high enatioselectivities. Connon *et al.* found MTBE methyl *tert*-butyl ether to be optimal as solvent while Song used dioxane. Song *et al.* later reported an analogous sulfonamide derivative **130** which was also efficient in less dilute conditions.[170] It was proposed that activation of the anhydride electrophile through H-bonding and promotion of attack at a single anhydride carbonyl group through general base catalysis from the chiral quinuclidine base. These activations in a chiral environment were suggested to stereoselectively enhance reaction rate.
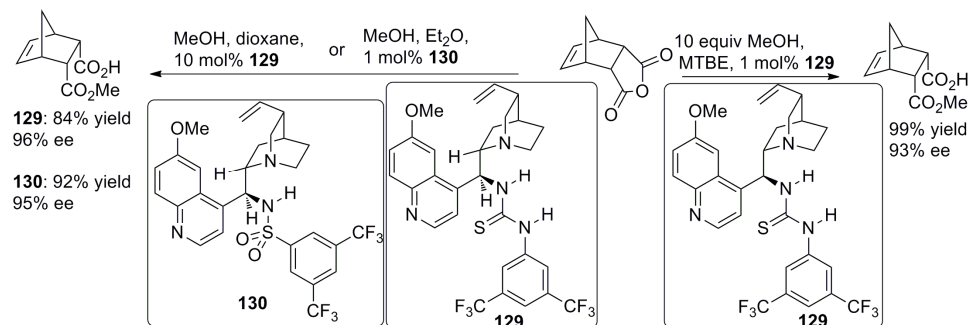
Scheme 1.34: Successful application of thiourea and sulfonamide functionalised cinchona alkaloids **129** & **130** in desymmetrization reactions.[168-170]

In 2011, Connon *et al.* developed a cinchona alkaloid based organocatalyst **131** with a urea group substituted at the C-5' position to examine the distance between the nucleophile- and electrophile activating groups on the bifunctional catalyst.[171] These catalysts were successfully applied to the 1,2-addition of nitromethane to trifluoromethylketones in up to 90% ee for trifluoracetophenone (Scheme 1.35).
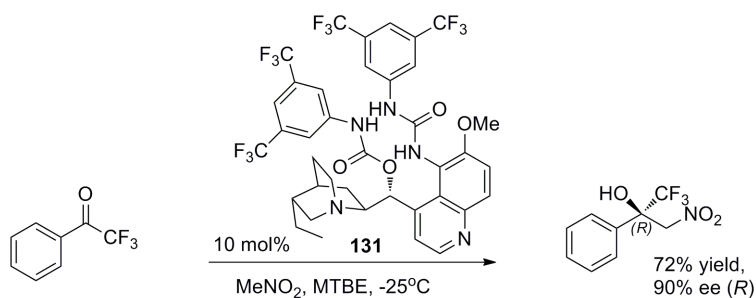
Scheme 1.35: C-5' substituted cinchona alkaloid catalyst **131** in the Henry reaction involving trifluoroacetophenone.[171]

1.4   The Application of Acyclic Receptors in Organocatalysis

A common theme arising from organocatalysis has shown that complexation and activation of neutral functional groups such as carbonyl groups with H-bond donors has resulted in catalytic activity.[144] While this viewpoint acknowledges the significance of stabilisation of developing negative charge and groups with partial charges, it does not consider potential relationships between anion recognition and organocatalysis. Over the last number of years, the strong relationship which exists between anion receptors and organocatalysts for reactions which

contain anionic transition states has come to the fore. The concept of application of specifically designed anion receptors as organocatalysts will be discussed in this section.

Enzyme catalysis commonly relies upon preferential H-bonding complexation and stabilisation of transition states over starting materials and products.[172] Therefore, successful artificial enzymes (organocatalysts) must be complementary to the electrostatic and spatial features of transition state structures. Hamilton *et al.* reported the acceleration of a phosphoryl-transfer reaction with an artificial H-bonding receptor.[172] Their previously successful *bis*-amide receptor **132** synthesised from isophthaloyl dichloride and 2,6-diaminopyridine[173] was deemed suitable to bind the planar-trigonal intermediate and also possibly activate the starting material P=O towards nucleophilic attack. A 10-fold acceleration in reaction rate in the aminolysis of phosphorodiamidic chloride with *n*-butylamine was observed (Scheme 1.36) while no starting material or product binding was observed.

Proposed transition state binding
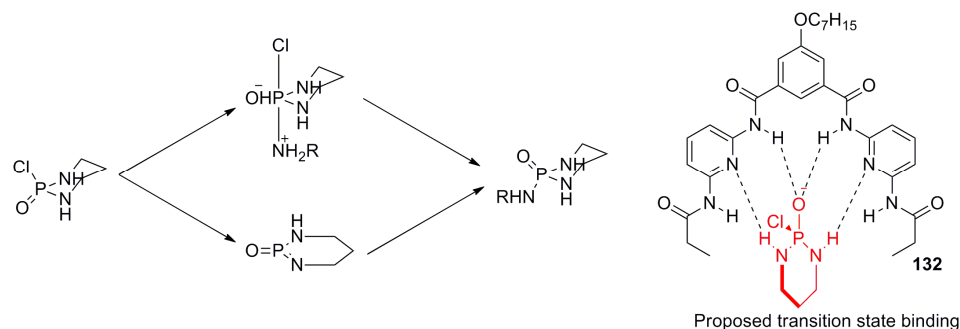
Scheme 1.36: Phosphoryl transfer catalysed by isophthalamide derived receptor **132**. Proposed catalyst:intermediate binding also shown.[172]

In 1991, Hamilton *et al.* used synthetic receptors to increase the rate of the intramolecular Diels-Alder reaction of disubstituted *N*-furfurylfumaramide derivatives through selective binding to different structures on the reaction pathway (Scheme 1.37).[174] A previously successful dicarboxylic acid *bis*-amide based receptor derived from terephthaloyl dichloride and 6-amino-2-picoline caused a 10 fold decrease in rate of reaction due to complexation and stabilization of the starting material, increasing the activation energy.[53] Selective complexation of the transition state was achieved by integrating aminopicoline groups into an isophthaloyl motif **133** resulting in a 30-fold increase in reaction rate (Scheme 1.37a). The same group utilised a H-bonding receptor **134** based on staphylococcus nuclease enzyme in

the acceleration of phosphodiester cleavage in 1992.[105] The receptor derived from dimethyl isophthalate and guanidium hydrochloride bound phosphodiester **135** with a K_{ass} value of 5 x10^4 M^{-1} in acetonitrile (Scheme 1.37b). This receptor also increased the rate of release of 4-nitrophenol in the intramolecular cleavage reaction of phosphodiester by a factor of 700, comparable to phosphodiesterase performance.[105]
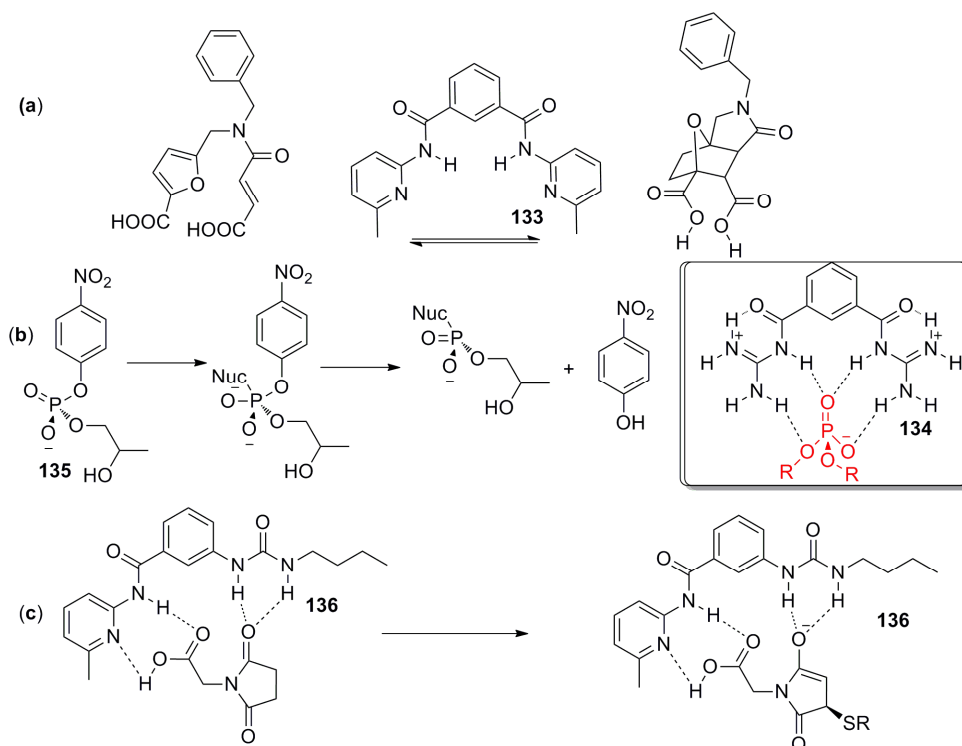
Scheme 1.37: (a) Intramolecular Diels-Alder reaction catalysed by isophthaloyl catalyst **133**.[174] (b) Intramolecular cleavage reaction of **135** increased 700 fold with enzyme mimic **134**.[105] (c) Anion binding receptor **136** resulted in accelerated 1,4 addition of a thiol to a maleimide.[14]

Hamilton *et al.* used an anion binding strategy to stabilise an oxyanion transition state, thus accelerating the 1,4 addition of a thiol to a maleimide in 1997.[14] The build up of negative charge on the carbonyl oxygen in the enol transition state was stabilised by H-bonding to a urea group on catalyst **136** while the carboxylic acid group formed H-bonds with the aminopyridine motif, resulting in transition state stabilisation and rate enhancement (Scheme 1.37c). When an amide was substituted in place of the urea, weaker substrate binding and catalytic activity was observed, consistent with less efficient H-bonding of an amide.

Crabtree *et al.* found a 6-fold increase in the rate of imine formation in the presence of a sulfonamide catalyst **137**.[17] The rate determining nucleophilic attack on the carbonyl by the amine has an anionic transition state which was suggested to be more tightly bound to the sulfonamide catalyst compared to the starting aldehyde or the product. Based on previous anion binding results for this catalyst,[51] they suggested that a two point H-bonding interaction of the convergent sulfonamide groups with the anionic transition state was responsible for catalysis (Scheme 1.38a). With the known anion binding ability of the *bis*-sulfonamide receptor motif in mind, Brenner *et al.* studied a number of chiral bifunctional sulfonamide catalysts including **138** for conjugate addition reactions of 1,3-dicarbonyl compounds with *β*-nitrostyrene (Scheme 1.38b).[175] The optimum catalyst **138** containing a 3,5-*bis*(trifluoromethyl)aniline ring and a chiral amine group catalysed the reaction of diethyl malonate and *β*-nitrostyrene to give product in up to 68% yield and 70% ee. ^{1}H NMR spectroscopic studies confirmed H-bonding interactions of the *N*-aryl sulfonamide with *β*-nitrostyrene while a correlation was observed between N-H acidity and enantioselectivity.
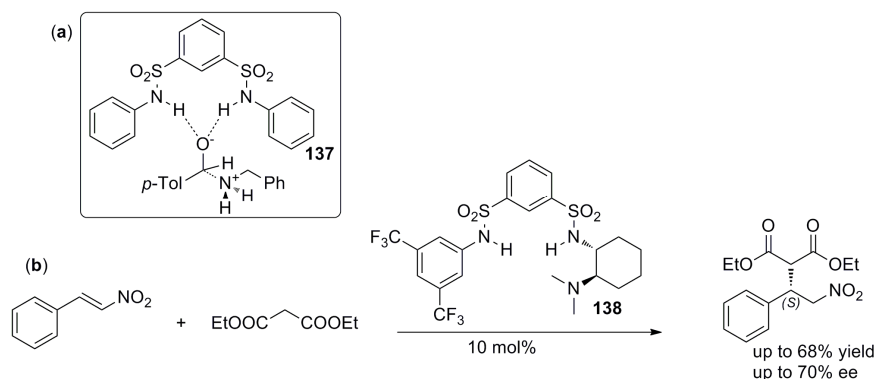
Scheme 1.38: (a) Proposed binding of Crabtree's disulfonamide **137** to transition state of aldehyde imination reaction.[17] (b) Brenner's reaction of *β*-nitrostyrene with diethyl malonate catalysed by *bis*-sulfonamide **138**.[175]

In 2006, Gong *et al.* reported a catalytic system based on original findings by Hamilton *et al.* that an amide **139** derived from the 2-aminopyridine group could bind to a carboxyl group.[53] Gong *et al.* successfully used (*S*)-prolinamide catalysts containing an aminopyridine moiety for the aldol reaction of acetone and phenylglycoxylic acid to produce a high yield of product in up to 98% ee (Scheme 1.39).[176] Experimental and theoretical studies showed the importance of the H-bonding between the optimal catalyst **139** and the keto and carboxyl

groups of the keto acid substrate, resulting in activation towards attack by the nucleophilic enamine.
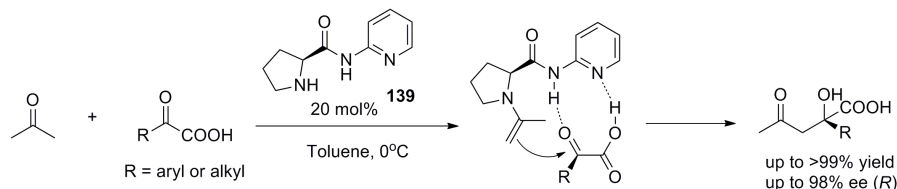
Scheme 1.39: Reaction of phenylglycoxylic acid with acetone catalysed by prolinamide catalyst **139**.[176]

Moran *et al.* studied the binding interactions between a number of thiourea derivatives with triphenylarsine oxide, an oxyanion hole mimic capable of strong substrate binding.[177] In particular, incorporation of the 3,5-*bis*(trifluoromethyl)phenyl group into the thiourea structure led to a significant enhancement in binding strength. They reported significant catalysis using both the Schreiner thiourea catalyst **117** and also a receptor **140** containing triflamide moieties in the Diels-Alder reaction of methyl vinyl ketone with cyclopentadiene (Scheme 1.40).
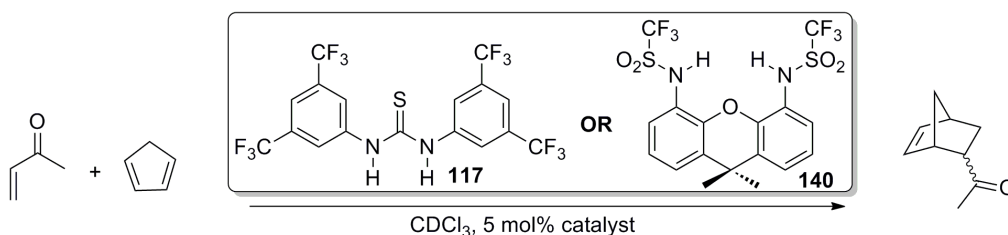
Scheme 1.40: Diels-Alder reaction catalysed by successful triphenylarsine oxide receptors **117** & **140**.[177]

As detailed in previous sections, squaramides have been found to be efficient anion receptors. Squaramides and (thio)ureas are rigid structures, however the former possess a larger disatance between the two N-H groups. Squaramides have been shown to bind anions through the N-H groups and cations through its acceptor oxygen atoms and recently, they have also been applied as organocatalysts. The first reports of squaramides as bifunctional organocatalysts came in 2008 when Rawal *et al.* reported that these easily synthesised, modular catalysts enantioselectively catalysed the conjugate addition of 2,4-pentanedione to β-nitrostyrene.[178] The optimal (-)cinchonine substituted derivative **141** was applied to the addition of activated methylenes to nitroalkenes providing yields of the order 65-98%, 77-99% ee and up to 1:50 d.r (Scheme 1.41a). The mode of catalysis was proposed to be similar

to that of Takemoto *et al.* (Scheme 1.27)[156] where the rigid squaramide pocket provided a well-defined chiral pocket.
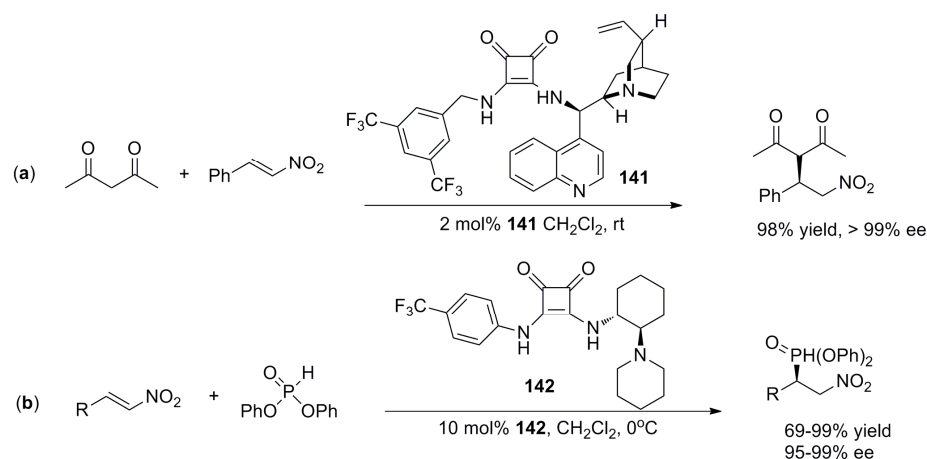
Scheme 1.41: (a) Squaramide **141** catalysed conjugate addition of 2,4-pentanedione and β-nitrostyrene to give high yields and ee values. (b) Michael addition of diphenyl phosphite to nitroalkenes catalysed by **142**.

Rawal *et al.* subsequently reported a new squaramide **142** derived from 1,2-diaminocyclohexane (Scheme 1.41b).[179] They successfully applied this catalyst to the Michael addition of diphenylphosphite to nitroalkenes with results which exceeded that of chiral thioureas. The same group later reported an enantioselective Friedel-Crafts reaction of indoles with arylsulfonylimines using bifunctional chiral squaramide catalyst **143** and obtained product in up to 99% ee using 2.5 mol% loading.[180]
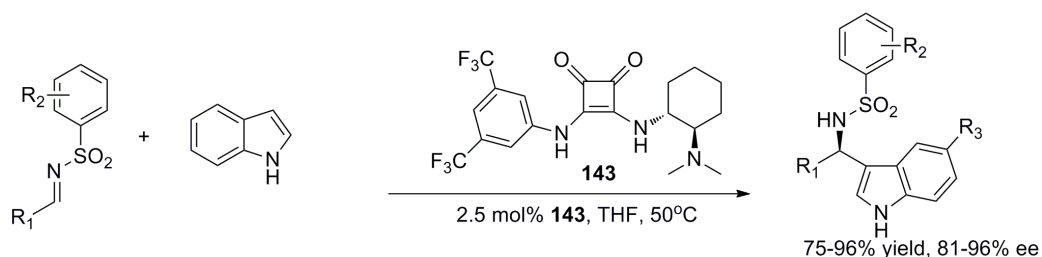
Scheme 1.42: Friedel-Crafts reaction of indoles with *N*-sulfonylimines catalysed by chiral squaramide **143**.

In 2011, Wu *et al.* synthesised a squaramide analogue **144** of their urea/phosphine catalyst containing a tertiary phosphine as a chiral bifunctional catalyst for the intramolecular MBH reaction and the MBH adducts were obtained in high yields and high enantioselectivity up to 93%.[181] The authors proposed a transition state **A** where the nucleophilic phosphine attacks the β-position of the Michael acceptor generating an enolate while the electrophillic

squaramide activates the aldehyde group through oxygen atom H-bonding. The chiral cyclohexyl scaffold forces the phosphinoyl bound enolate to attack the carbonyl from the *si*-face to form the (*S*)-product.
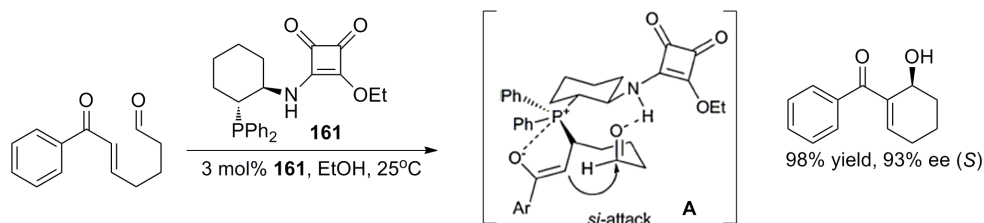
Scheme 1.43: Intramolecular MBH reaction catalysed by phosphine-squaramide **161**. Proposed transition state also shown.[181]

1.5   Conclusions

This Chapter has detailed the close interplay which exists between anion recognition and organocatalysis. Chapter 2 will describe experimental work conducted which probes this relationship further by synthesising compounds suitable for binding anions and acting as organocatalysts using molecular recognition techniques to probe the relationship between strong anion binding and organocatalytic activity.

2 Chapter 2

Synthesis and ^{1}H NMR Spectroscopic Binding Studies towards Rational Design of a Series of Electron-Withdrawing Diamide Receptors/Organocatalysts

2.1 Background

In recent years, the coordination of anions via hydrogen bonding (H-bonding) has become a significant and well studied area of supramolecular chemistry due to the many roles which anions play in biological processes, medicine, catalysis and the environment.[22,23,182] As detailed in Chapter 1, a considerable amount of work has been undertaken to design selective anion receptors.[22,182]

Secondary amides are commonly used as anion receptors as they act as H-bond donors.[50] They can also act as H-bond acceptors, which can have a disruptive effect on their binding properties.[4] Despite this, they have been found to bind efficiently to anions such as halides and oxyanions[51] and additionally neutral molecules such as barbiturates[52] and dicarboxylic acids.[53] Thioamides also bind anions well but have less of a tendency to act as H-bond acceptors due to their higher acidity. Sulphur has a lower electronegativity and a larger atomic radius compared to oxygen which makes thioamides less likely to self-associate and they have also been studied for their anion coordination properties.[4,182] Additionally, there have been a number of other motifs reported as anion receptors including pyrroles,[4,47,48] indoles[3,49] and sulfonamides.[5,54] Ureas and thioureas are also efficient anion receptors which can form two cooperative H-bonds to anions.[37]

2.2 Scope of Project

The objective of this project was to rationally design, synthesise and test a series of simple, minimally pre-organised amide-based receptors for anion coordination and organocatalysis. Organocatalysis involves catalysis of synthetic reactions using small organic metal-free organic molecules and has attracted much interest over the last number of years.[9,115] The mode of action of H-bonding organocatalysts in particular involves coordination of H-bond donating groups to highly negative or anionic species.[10-14,17,19] Considering a major objective of both receptor and organocatalyst design is the molecular recognition of anions, much can be gained from taking a cooperative view between both areas. This would lead to the development of molecules with dual application; anion recognition and organocatalysis. In this case, instead of the troublesome synthesis of transition state analogues for binding studies, binding

characteristics with anions could be used to predict their applicability as organocatalysts. The DABCO promoted Morita-Baylis-Hillman (MBH) reaction of benzaldehyde with methyl acrylate was chosen as a reaction to test this dual approach. In the next section, a short introduction to the MBH reaction studied will be presented and will include current mechanistic understanding in order to place the design of receptors/catalysts in context.

2.3   Morita-Baylis-Hillman (MBH) Reaction

The Morita-Baylis-Hillman reaction was first reported in 1968 by Morita using a tertiary phosphine catalyst[183] while A. B. Baylis and M. E. D. Hillman reported the tertiary amine catalysed version in 1972.[184] It involves the reaction of activated alkenes e,g, α,β-unsaturated esters, amides, nitriles and ketones typically with aldehydes, ketones or imines catalysed by a bicyclic amine such as DABCO or quinuclidine to give multifunctional products (Scheme 2.1).[184] A new carbon–carbon bond is formed between the α-carbon of activated olefin component and carbon electrophiles. This reaction combines the aldol and Michael reactions in a single pot to convert two relatively simple molecules into a highly functionalised product. One of the challenges associated with the reaction has been slow reaction rates (up to a number of days) and limited substrate scope.[185] Physical methods of rate enhancement (microwave, ultrasound, high pressure) are troublesome and expensive, therefore a number of authors have developed organocatalysts to accelerate this highly useful reaction.[10,12,145,147]

EWG = COR, CN, COOR or CHO
X = O or N,
R = aryl, alkyl, heteroaryl
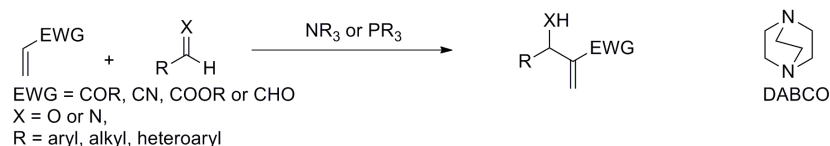
Scheme 2.1: General representation of a Baylis-Hillman reaction.

2.3.1   Mechanism of MBH Reaction

The first generally accepted MBH reaction mechanism, based on rate, pressure dependence and kinetic isotope effect data, was proposed by Hill & Isaacs in 1990.[185,186] It proceeds through a Michael-initiated addition-elimination sequence and is shown in Scheme 2.2 using methyl acrylate (as the activated olefin) and benzaldehyde (as the electrophile) with DABCO as the tertiary amine catalyst.
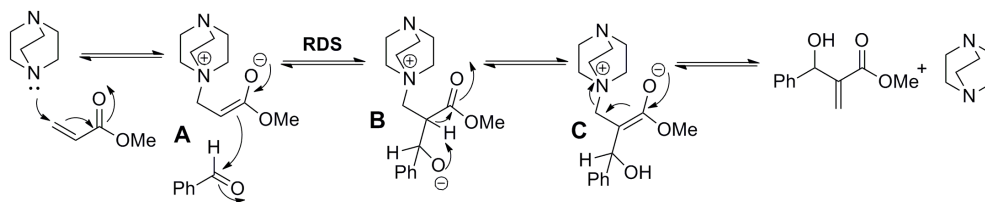
Scheme 2.2: Mechanism of the MBH reaction as postulated by Hill & Isaacs.[186]

The first step in the cycle involves the reversible Michael-type nucleophilic addition of the tertiary amine Lewis basic catalyst to the acrylate producing a Zwitterionic enolate intermediate **A**. This intermediate is thought to possess enhanced nucleophilic reactivity at the C-2 position facilitating aldol-like nucleophilic attack on the aldehyde giving a second Zwitterionic intermediate **B**. Following prototropic rearrangement from the α-carbon atom to the β-alkoxide, intermediate **C** is formed and β-elimination releases the product and tertiary amine catalyst.[186] The authors reported that this α-proton cleavage did not constitute the rate-determining step (RDS) of the process.[186] Therefore, they concluded that the addition of the enolate **A** to the aldehyde was the RDS. This mechanism has been supported by Coelho *et al.* through structural characterisation of each of the intermediates using electrospray ionisation with mass spectrometry.[187]

Based on this mechanism, rate increase in the presence of protic solvents/additives could arise due to aldehyde activation by H-bonding.[188] However, such H-bonding to the aldehyde may compete with the enolate **A**, a better H-bond acceptor and this latter interaction could stabilise and deactivate **A** causing a decrease in reaction rate. A number of observations were reported which contrasted with the Hill & Isaacs mechanism. A dioxanone was formed as a side product (Scheme 2.3) and Aggarwal *et al.* reported an autocatalytic effect of the reaction product in the absence of protic additives due to the product acting as a H-bond donor promoting the reaction (Scheme 2.4).[189] These observations which could not be explained by the original Hill & Isaacs mechanism, resulting in further mechanistic investigations being later conducted.

In 2005, McQuade *et al.* demonstrated that the kinetics of the MBH reaction were second order in aldehyde and first order in DABCO and acrylate in both polar and non-polar

solvents.[190] In the absence of protic additives, they proposed that the reaction begins with the combination of the acrylate and the Lewis base with subsequent addition to the aldehyde as previously proposed. The next step involves reaction with a second equivalent of aldehyde to form a hemiacetal conjugate base **C** which undergoes the rate-determining deprotonation followed by a number of steps to form the product (Scheme 2.3).[190] In the presence of polar solvents, they suggested that all of the ionic transition states were stabilised, enhancing reaction rates.
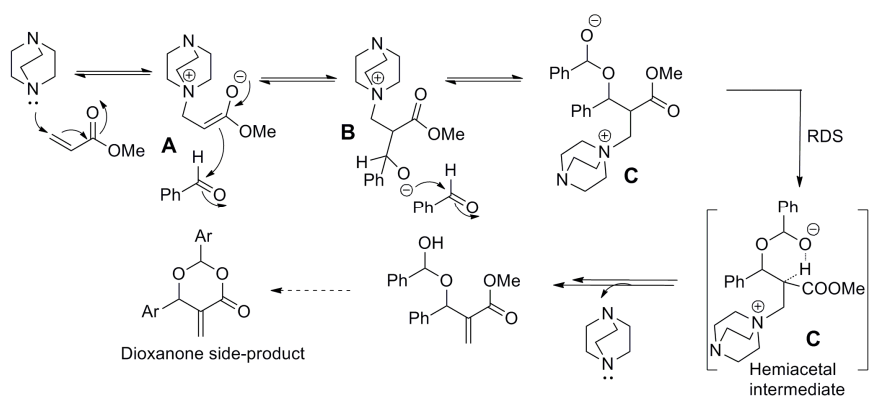
Scheme 2.3: McQuade's proposed mechanism of the MBH reaction.[190]

Sunoj *et al.* used DFT calculations to confirm that the RDS of the MBH reaction was the intramolecular proton transfer step in the Zwitterionic intermediate generated from addition of the enolate to the aldehyde (**B** in Scheme 2.3) under polar aprotic conditions.[191] Calculations which included water molecules showed a lowering of the activation barrier and it was suggested that in a polar protic solvent, the proton transfer in the transition state could be facilitated through a relay type mechanism. Electrostatic stabilisation of the Zwitterionic transition states was suggested to enhance the reaction in polar solvents.[192,193]

In 2005, Aggarwal *et al.* reported that in the initial phase of the reaction in the absence of H-bond donors, the RDS is the proton transfer step of the reaction.[189] As the reaction proceeds, autocatalysis is thought to occur. The effective autocatalysis of the proton transfer step can be considered by a model involving a six-membered proton transfer from the product R–OH to the alkoxide with simultaneous deprotonation of the α-hydrogen and elimination to give the MBH adduct (Scheme 2.4). In the latter stages of the reaction when a significant quantity of the polar MBH adduct is present, they proposed that the RDS is the addition of the enolate to

the aldehyde, contrary to McQuade's proposal that the loss of the proton in the α-position is the RDS in the presence of a protic species throughout the reaction.[194]
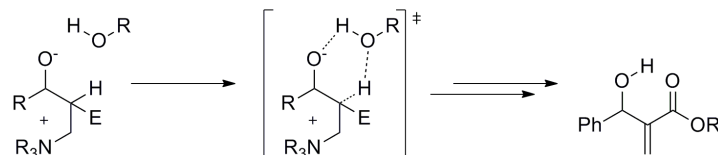
Scheme 2.4: Autocatalytic influence of the MBH product (ROH) promoting the proton transfer step proposed by Aggarwal *et al.*[189]

In 2007, Aggarwal conducted further mechanistic studies on the MBH reaction using computational methods and confirmed that the reaction is second order with respect to aldehyde at initial stages (up to approximately 20% conversion), consistent with previous results of McQuade *et al.*[164,189] In the absence of protic additives, the reaction is initiated by Michael addition of the amine to the acrylate to form the enolate **A**. This enolate adds to the aldehyde to from **B** which adds to another molecule of aldehyde to give **C** (Scheme 2.5). This hemiacetal betaine molecule undergoes intramolecular proton transfer through a six-membered transition state **TS C-D**. Elimination of the amine yields the hemiacetal **E** which decomposes into product and aldehyde or may cyclise in a small number of cases to form dioxanone. They suggested that deprotonation of the α-position was the RDS occurring through transition state **C-D**.
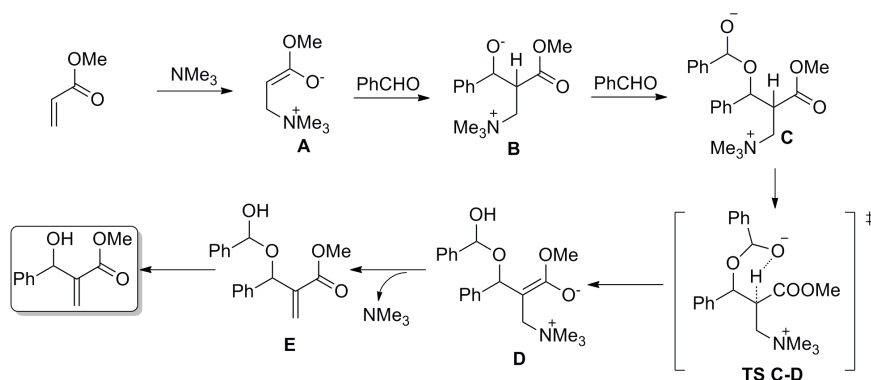
Scheme 2.5: Mechanism of MBH reaction in absence of protic species proposed by Aggarwal *et al.*[164]

In the presence of alcohol or a protic additive, H-bonding of **A** & **B** with methanol **A-MeOH** & **B-MeOH** stabilises these intermediates making their synthesis more thermodynamically favourable compared to the system without protic additives. Methanol allows **B-MeOH** to

undergo a concerted proton transfer via **TS B-C MeOH** to give **C-MeOH** which can decompose into the product and amine catalyst (Scheme 2.6).
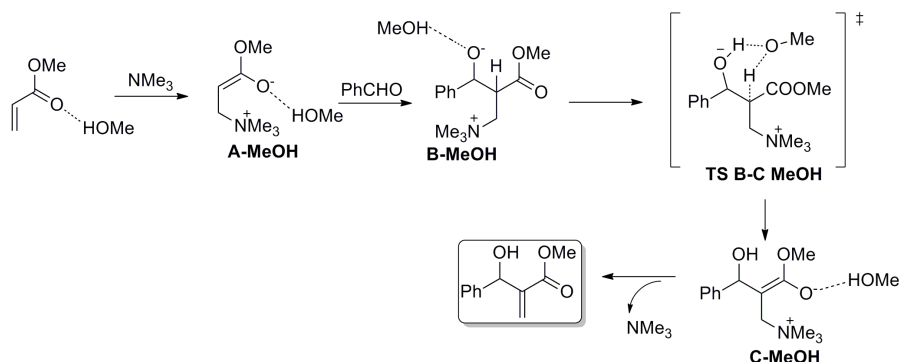
Scheme 2.6: Mechanism of MBH reaction in presence of protic additive proposed by Aggarwal *et al.*[164]

Kappe and Cantillo have since conducted computational and experimental investigations into the DABCO promoted MBH reaction of benzaldehyde and methyl acrylate in 2010.[195] Their data supported the results of McQuade and Aggarwal and suggested that the methanol catalysed proton transfer mechanism reported by Aggarwal was similar in energy to the case where a second molecule of aldehyde promotes this step. Therefore, depending on the amount of protic species and the progress of the reaction, both catalytic pathways are feasible.

As described in Chapter 1, the use of *bis*-aryl ureas and thioureas as H-bonding catalysts in the MBH reaction has been explored by a number of authors such as Sohtome *et al.*[10,147] and Connon *et al.*[145] The presence of the 3,5-*bis*(trifluoromethyl)phenyl group was found to be key to high reactivity and enantioselectivity. It was postulated that incorporating 3,5-*bis*(trifluoromethyl)phenyl groups into secondary amide receptors may lead to organocatalysts employing binding effects and therefore may exhibit a catalytic effect on the MBH reaction (Scheme 2.7).[10,145,147] The receptors/catalysts could bind to the anionic intermediates activating their reaction with the aldehyde, thus catalysing the reaction. This would be particularly relevant if one takes into account Aggarwal's proposal that the RDS is the addition of the enolate to the aldehyde in the latter stages of the reaction when autocatalysis can enhance the proton transfer step. H-bond receptors of reasonably high acidity were also expected to aid in the proton transfer step which has been determined to be the RDS both in the presence and absence of protic additives by McQuade.[194] This step was expected be

enhanced by acidic H-bonding receptors in a similar way to the methanol catalysed pathway previously described by Aggarwal *et al.*[164] and the *bis*-thiourea catalysed MBH reaction reported by Sohtome *et al.*[10] In both of these cases, the proton transfer step was enhanced through H-bonding.
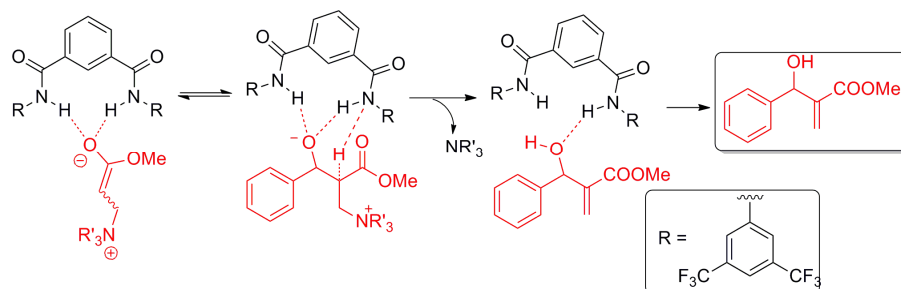
Scheme 2.7: Proposed binding of isophthalamide based receptors to enolate[189,196] and also potential carbonyl activation of a later Zwitterionic transition state promoting elimination of the tertiary amine similar to Sohtome *et al.*[10]

In addition, by using anion binding properties as a probe into potential catalytic activity, one may expect a correlation between the anion binding ability of receptors and their catalytic activity. In particular, in order for this study to be valid, the investigation of binding to anions of various shapes and sizes and in particularly oxyanions would be essential.

2.4   Receptor/Catalyst Design

Receptor design was inspired by the previous work of Crabtree,[24,51] Hamilton,[53] Jurczak[4] and Gale[8] on the design of simple acyclic and macrocyclic secondary amide and thioamide receptors for the binding of anions and netural hosts. For example, as mentioned in Chapter 1 Crabtree used a relatively simple aromatic isophthalamide to bind anionic species such as Cl⁻ and Br⁻ while X-ray crystallography of an isophthalamide/Br⁻ complex confirmed H-bonding interactions from both amide N-H groups of **1** to the halide in the *syn-syn* conformation with additional potential interactions from nearby aryl protons enhancing binding (Figure 2.1).[24] They subsequently designed successful receptors bearing pyridyl and sulfonamide groups with conformational changes accommodating anion binding in some cases.[51]
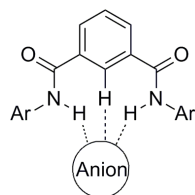
Figure 2.1: Isophthalamide group binding to an anion through complementary H-bonding with N-H groups.[51]

A series of H-bond donating receptors/organocatalysts **145**-**151** were designed incorporating acidic functionalities (Figure 2.2). In order to synthesise these receptors, the well known receptor building blocks of isophthalic acid and 2,6-pyridinedicarboxylic acid would be used and coupled with a series of CF_3-derived arylanilines. The *n*-butyl aniline receptor **145** was used as a control receptor to compare the binding performance of the rationally designed receptors. The 4-trifluoromethylphenyl group would be incorporated into the diamide structure to form **146** while the 3,5-*bis*(trifluoromethyl)phenyl group would be integrated into the structure of **147**-**151**. In addition to the isophthaloyl motif, receptor **148** based on a 1,3-pyridine dicarboxamide skeleton would also be considered. Thioamides are stronger acids than amides[4] and are less likely to self-associate; therefore **149** was expected to be a more efficient anion binding receptor compared to **147**.[197] Receptor **150** contained an additional nitro group at the 5-position of the central isophthaloyl ring in order to further enhance acidity over **147**.
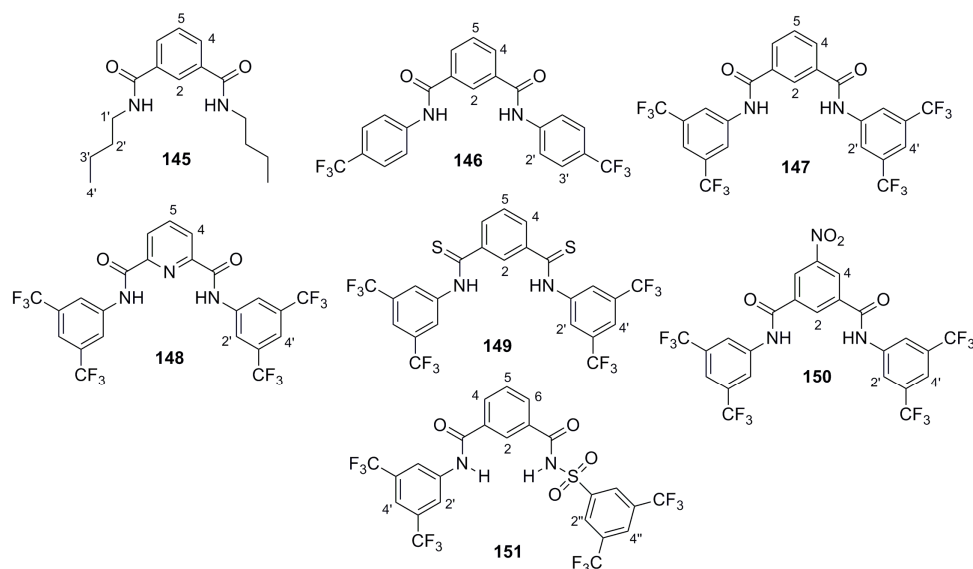
Figure 2.2: Structure of diamide based receptors designed for anion binding with potential catalytic activity.

Receptor **151** consisted of an unsymmetrical isophthaloyl skeleton bearing an amide group with a second *N*-acyl sulfonamide group. The N-H group adjacent to the sulfonyl group was expected to possess acidity comparable to a carboxylic acid,[198,199] making it highly favourable towards anion binding and participation in a proton shuttling event in the MBH reaction.

The receptors **145**-**151** would be first evaluated with a series of anions to potentially predict catalytic effect. The anions to be evaluated in this study were spherical halides (bromide and chloride) and Y-shaped oxyanions (acetate and benzoate) which were commercially available as tetra-*n*-butylammonium salts. These anions were chosen to represent varying anion sizes and topologies and to give good indications of receptor selectivity and catalytic potential. Br^- is larger, possesses a lower charge density and was expected to be more difficult to complex compared to Cl^-. The study of both Br^- and Cl^- could give an indication of the ability of the receptor to bind anionic species of varying sizes, useful when considering reaction intermediate size for the design of receptors as organocatalysts. AcO^- and BzO^- may H-bond to receptors through both oxygen atoms in a cooperative system. Such oxyanions can be considered structurally similar to many anionic reaction transition states and the ability of **146**-**151** to bind oxyanions could provide some indication of their ability as H-bond donating organocatalysts in reactions possessing anionic transition states.[19]

^{1}H NMR spectroscopy is widely used for the investigation of molecular interaction[200,201] and can be used to determine binding strength and stoichiometry. ^{1}H NMR spectroscopic titration can be used to determine binding constants K_{ass}, a measure of the strength of anion binding. For this analysis, the concentration of the receptor remains constant while the change in chemical shift of one or more of its proton signals are monitored upon addition of a known quantity of anionic guest. The resulting data from a series of additions can be fitted to WINEQNMR[202] mathematical model in order to calculate K_{ass} values. ^{1}H NMR spectroscopic titrations provide binding information at an atomic level including location of binding site and evidence of the bifurcated binding cleft. The JOB plot or method of continuous variation is commonly used to determine binding stoichiometry.[200,201,203] It involves use of equimolar solutions of substrate and ligand to prepare solutions containing varying mole fractions of receptor. The chemical shift of a proton which varies with the degree of complex formation is

plotted against the mole fraction of receptor. The maxima from such plots represent the mole fraction ratio of the receptor:anion complex.

2.5 Synthesis of Diamide Receptors 145-151

A number of different synthetic approaches were adopted for the synthesis of receptors **145-151**. The reaction of the appropriate acid dichloride with the respective amine produced the corresponding secondary amides **145**-**148** (Scheme 2.8a). High Resolution Mass Spectrometry (HRMS) confirmed all new compounds, details can be found in Chapter 6.
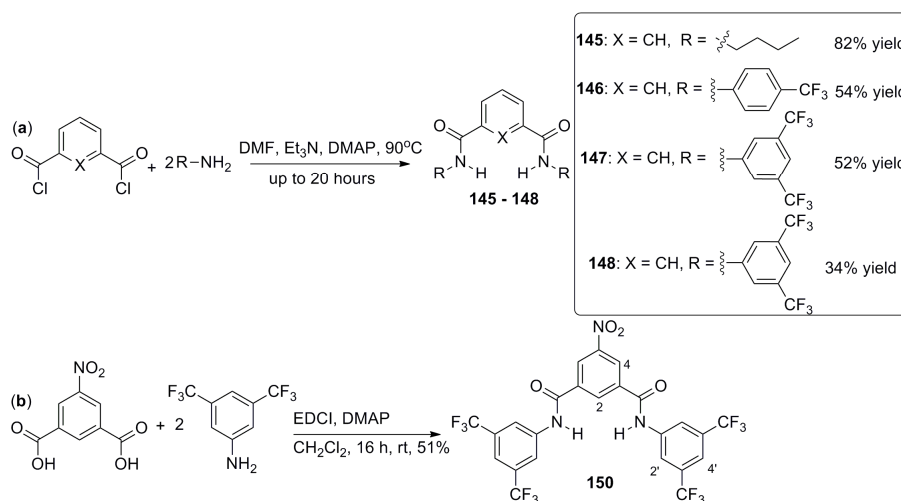
Scheme 2.8: (a) Synthesis of receptors **145-149** from reaction of acid chloride with the appropriate amine.[204] (b) EDCI coupling of 5-nitroisophthalic acid with 3,5-*bis*(trifluoromethyl)aniline to form **150.**

Receptor **145** was synthesised according to a previously published procedure[204] in relatively high yield followed by recrystallisation with diethyl ether and petroleum ether. ^{1}H & ^{13}C NMR spectroscopy and LC-MS data confirmed the structure of the product and all data corresponded to previous characterisation reports.[204] For the synthesis of **146**, isophthaloyl dichloride was reacted with 2 equivalents of 4-(trifluoromethyl)aniline in DMF in the presence of triethylamine and DMAP.[17] Following 20 hours stirring at 90°C with reaction monitoring by thin-layer chromatography (TLC), the mixture was added to water and an extractive work-up was employed. Flash chromatography gave **146** as a white solid in 54% yield. Key ^{1}H NMR spectroscopic resonances included the amide N-H signals at 9.17 ppm, isophthaloyl ring protons H-2 (triplet), H-4 (doublet) and H-5 (triplet) at 8.53, 7.76 and 7.69

ppm respectively. The 4-(trifluoromethyl)phenyl ring contained two sets of doublets, H-4' at 8.15 ppm and H-3' at 7.97 ppm. LC-MS analysis gave the MH$^+$ ion at m/z 453 and HRMS also confirmed the product.

Initial attempts at the synthesis of **147** from the reaction of isophthaloyl dichloride with 3,5-*bis*(trifluoromethyl)aniline were carried using dichloromethane and chloroform as solvent at 25°C but proved unsuccessful presumably due to the slow reaction rate. The synthesis of **147** was achieved in DMF as solvent at 75-80 °C for 20 hours. The reaction mixture was subsequently added to water and following extractive work-up and purification by flash chromatography, **147** was obtained in 52% yield. The product identity was confirmed by LC-MS showing an ion at m/z 589 and ^{1}H & ^{13}C NMR spectroscopy. Key ^{1}H NMR spectroscopic resonances included the amide N-H signal at 9.33 ppm, isophthaloyl ring protons at 8.58 ppm, 8.19 ppm and 7.73 ppm corresponding to H-2, H-4 & H-5 respectively. Additional ^{1}H NMR spectroscopic signals of the 3,5-*bis*(trifluoromethyl)aryl ring included the H-2' and H-4' signals at 8.38 ppm and 7.77 ppm.

Receptor **148** was synthesised by reaction of 3,5-*bis*(trifluoromethyl)aniline with pyridine-2,6-dicarboxylchloride in the presence of triethylamine and DMAP in DMF with stirring at 75-80°C for 18 hours. Water was subsequently added and following extractive work-up and purification by trituration with ethyl acetate, **148** was obtained in 34% yield. LC-MS and ^{1}H & ^{13}C NMR spectroscopy confirmed the product. LC-MS analysis provided a peak at m/z 590 corresponding to the MH$^+$ ion. ^{1}H NMR spectroscopic analysis produced a peak at 10.51 ppm due to the amide N-H groups and also peaks at 8.50 ppm & 8.29 ppm corresponding to H-4 & H-5 respectively. Peaks at 8.60 ppm and 7.62 ppm resulted from the H-2' and H-4' signals of the 3,5-*bis*(trifluoromethyl)phenyl group respectively.

Receptor **147** was converted into its thioamide counterpart **149** using Lawesson's reagent (Scheme 2.9).[205,206] The amide **147** and 2.7 equivalents of Lawesson's reagent were heated to reflux for 16 hours in dry toluene. Upon reaction completion determined by TLC, direct flash chromatography of crude reaction mixture gave the yellow solid thioamide product **149** in 96% yield. The identity of the product was confirmed by an LC-MS peak at m/z 621

corresponding to the MH$^+$ ion and ^{1}H & ^{13}C NMR spectroscopy. Key ^{1}H NMR spectroscopic resonances included the thioamide N-H signal at 10.77 ppm, isophthaloyl ring H-2, H-4 & H-5 signals at 8.36 ppm, 8.04 ppm and 7.57 ppm respectively and 3,5-*bis*(trifluoromethyl)phenyl ring signals at 8.53 & 7.91 ppm for H-2' and H-4'. A ^{13}C NMR spectroscopic signal at 200 ppm was ascribed to the C=S group.
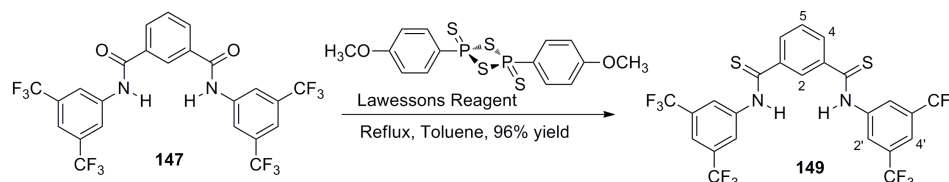
Scheme 2.9: Synthesis of thioamide **149** through reaction of **147** with Lawessons reagent. [205,206]

Receptor **150** was synthesised through 1-ethyl-3-(3-dimethylaminopropyl)carbodiimide (EDCI) coupling of 5-nitroisophthalic acid with 3,5-*bis*(trifluoromethyl)aniline in the presence of DMAP (Scheme 2.8b). Following room temperature stirring for 16 hours and aqueous extraction,[207] the product was purified by flash chromatography to give the white solid product in 51% yield. The identity of the product was verified by LC-MS with a peak at m/z 634 due to MH$^+$ and ^{1}H & ^{13}C NMR spectroscopy. Key ^{1}H NMR spectroscopic signals included the amide N-H signals at 9.53 ppm with H-2 and *ortho* H-4 isophthaloyl ring protons at 8.94 & 8.99 ppm respectively. Peaks at 8.38 & 7.81 ppm were assigned to H-2' & H-4' respectively.

In order to increase the acidity of the N-H bond further an unsymmetrical isophthaloyl skeleton bearing an amide group and an *N*-acyl sulfonamide **151** was proposed. The N-H group adjacent to the sulfonyl group was expected to possess increased acidity, making it more favourable towards anion binding. Such groups are known to possess equivalent acidity to a carboxylic acid,[198,199] although the former may possess additional conformational properties due to the bulky sulfonyl group. Acidic 3,5-*bis*(trifluoromethyl)phenyl groups were also incorporated into the aryl portion of the sulfonamide. This was expected to further increase N-H acidity also potentially impart conformational or rigidifying effects similar to those reported by Schreiner for their acidic thiourea **124**.[127,144]

The first steps towards synthesis of **151** involved coupling of the acid group of commercially available monomethyl isophthalate to 3,5-*bis*(trifluoromethyl)aniline using EDCI and DMAP in dichloromethane. The corresponding ester/amide hybrid intermediate **152** was obtained following aqueous work-up and chromatographic purification in 92% yield (Scheme 2.10). LC-MS analysis produced an ion at m/z 392 for the MH$^+$ ion and the structure of the compound was also confirmed by ^{1}H & ^{13}C NMR spectroscopy. Key ^{1}H NMR spectroscopic resonances included the single amide N-H signal at 8.32 ppm and also the central ring isophthaloyl protons H-2, H-6, H-4 & H-5 at 8.51, 8.26, 8.17 & 7.64 ppm respectively. The 3,5-*bis*(trifluoromethyl)phenyl ring protons H-2' and H-4' were present at 8.23 & 7.68 ppm respectively while the methoxy protons present at 3.98 ppm also confirmed the amide/ester product. This ester/amide hybrid **152** was hydrolysed using NaOH in hot methanol to the corresponding acid/amide **153**. After heating to reflux for 1 hour, the reaction mixture was diluted with water, acidified to pH 3 and filtered to give **9** as a white solid in 77% yield (Scheme 2.10). LC-MS analysis of this acid produced an MH$^+$ ion at m/z 378 while ^{1}H & ^{13}C NMR spectroscopy were used to confirm the acid product. Key ^{1}H NMR spectroscopic peaks were the COOH broad signal at 13.3 ppm with all other aromatic peaks present corresponding to the expected pattern based on peak assignment of **153**.
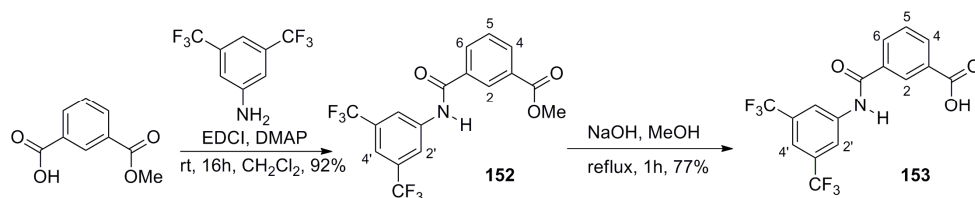
Scheme 2.10: Reaction of monomethyl isophthalate with 3,5-*bis*(trifluoromethyl)aniline creating ester/amide **152** followed by hydrolysis to acid/amide **153** using NaOH in methanol.

Commercially available 3,5-*bis*(trifluoromethyl)benzene sulfonyl chloride was added to a mixture containing DMF, triethylamine and aqueous ammonia. After 16 hours stirring at room temperature, the mixture was diluted with water and the pH was reduced to pH 2 using concentrated HCl. The primary sulfonamide **154** was recovered in 98% yield following filtration of the acidic reaction mixture (Scheme 2.11). GC-MS analysis produced a peak at m/z 293 corresponding to M$^+$ ion while ^{1}H & ^{13}C NMR spectroscopic analysis were used to confirm the identity and purity of product and COSY analysis aided ^{1}H NMR spectroscopic

peak assignment. A COSY interaction was observed between the singlet at 8.46 ppm (H-4)
and 8.40 ppm (H-2) and the broad signal at 7.79 ppm was assigned to the NH$_2$ group.
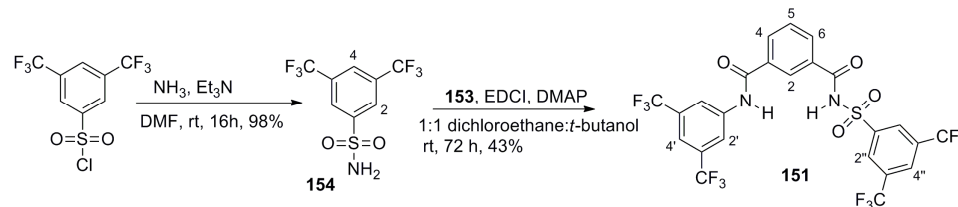
Scheme 2.11: Synthesis of bifunctional amide/*N*-sulfonlyated amide **151** from acid **153** and sulfonamide **154**.

Sulfonamide **154** was coupled to acid **153** in the presence of EDCI and DMAP. Initial
attempts at coupling in dichloromethane were unsuccessful and as a result, a method used by
Berkessel was adapted (Scheme 2.11).[208] Acid **153** (1.4 equiv) was dissolved in a 1:1 mix of
dichloroethane:*t*-butanol and to this was added DMAP (4.3 equiv), EDCI (3.6 equiv) and
sulfonamide **154** (1 equiv). This reaction was stirred for 72 hours, and subsequently treated
with Amberlyst 15 anion exchange resin. After filtration through a plug of silica gel, washing
with ethyl acetate, solvent removal *in vacuo* and chromatographic purification, **151** was
obtained in 43% yield. LC-MS produced an (M-H)$^-$ ion at m/z 651. Key ^{1}H NMR
spectroscopic peaks included the amide N-H peak at 9.37 ppm, isophthaloyl H-2, H-4, H-5 &
H-6 peaks at 8.61, 7.96, 7.39 & 8.13 ppm respectively. The sulfonyl N-H proton was not
visible by ^{1}H NMR spectroscopy.

2.6   ^{1}H NMR Spectroscopic Binding Studies of 145-151

The binding interactions of receptors **145-151** with anions were investigated using ^{1}H NMR
spectroscopic titration with Br$^-$, Cl$^-$, AcO$^-$ and BzO$^-$ as tetra-*n*-butylammonium salts.

2.6.1   Preliminary Binding in CDCl$_3$

^{1}H NMR spectroscopic titrations were carried out with **145** in relatively non-competitive
CDCl$_3$[209] with Br$^-$, Cl$^-$ and AcO$^-$ anions.[200] Each titration was conducted using a 1 mM
receptor solution of **145** and a 20 mM anion solution which was prepared using the 1 mM
receptor solution as diluent. Therefore, the receptor concentration was assumed to remain
constant throughout the analysis. The ^{1}H NMR spectrum was recorded for the initial solution

without anion and following the addition of each aliquot of anion. The titrations were continued until 10 equivalents of anion had been added to the initial 500 µL receptor solution to give a final volume of 1 mL. A titration curve of amide chemical shift (ppm) versus ratio anion:receptor was constructed for each anion shown in Figure 2.3.
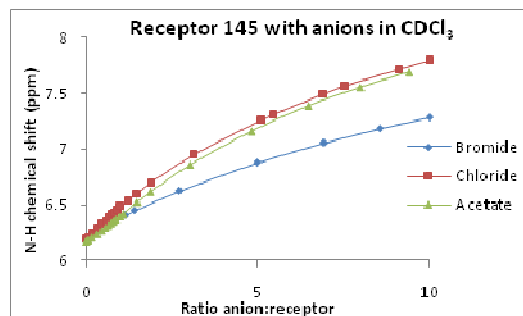
Figure 2.3: Initial ^{1}H NMR spectroscopic titrations of **145** with various anions conducted in CDCl₃.

H-bonding was observed to all anions as indicated by a significant downfield migration of the amide N-H peak of up to 1.5 ppm in some cases. The titration curves did not possess a distinct inflexion point or plateau region, rather a constant increase in chemical shift with added anion, indicative of relatively weak binding.[200] Cl⁻ appeared to be bound most strongly, followed by AcO⁻ while significantly weaker binding to Br⁻ was observed. This may have been due to the favourable size of the former anions.[51,210]

A number of the newly designed anion receptors were initially examined for their binding properties to Br⁻ in CDCl₃ (Table 2.1). This resulted in significant ^{1}H NMR signal downfield migration of the amide N-H proton of up to 2.9 ppm in some cases followed by a sudden levelling of the curve, indicative of tight association.[200] It was observed however that solubility was an issue in CDCl₃, therefore binding constants were not calculated for these titrations. The largest downfield migration occurred for receptor **147** followed by **149** while **150** produced a surprisingly small downfield migration following addition of 1 equiv Br⁻. This study offered a preliminary indication of the efficacy of these compounds as anion receptors.

Table 2.1: Preliminary binding of receptors **145** & **147-150** to TBA Br$^-$ in CDCl$_3$.

Receptor	Initial N-H δ (ppm)	Receptor + 1 equiv TBA Br$^-$ δ (ppm)
145	6.19	6.39
147	8.25	11.20
148	8.30	8.80
149	9.54	12.25
150	8.43	8.84

2.6.2   Binding Studies in CD$_3$CN

Due to the poor receptor solubility in CDCl$_3$, alternative NMR solvents were considered including CD$_3$OD, CD$_3$CN, D$_2$O and DMSO-d_6. Of these solvents, CD$_3$CN was chosen for further binding studies as it was expected to be least competitive[211] and all receptors were soluble in CD$_3$CN. ^{1}H NMR spectroscopic titrations for receptors **145**-**151** with Br$^-$, Cl$^-$, AcO$^-$ and BzO$^-$ were conducted in CD$_3$CN to collect binding data and subsequently determine the K$_{ass}$ value for the complexes.[200] The receptor amide N-H proton was monitored while the isophthaloyl H-2 and H-2' protons were monitored in cases where the amide N-H signal broadened or disappeared. K$_{ass}$ values for the CD$_3$CN titrations were calculated from receptor concentration, anion concentration and ^{1}H NMR chemical shift values using non-linear curve fitting in the WINEQNMR program.[202]
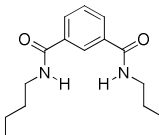
In the following section, results of binding studies for each individual receptor with a range of different anions in CD$_3$CN will be presented along with a brief description of the binding event. In each case, ^{1}H NMR spectroscopic results were initially fitted to a 1:1 model but where a poor fit was obtained, multiple stoichiometries were considered and data fitted to these models with the aim of obtaining a good fit. A summary and comparison between the receptors and their binding ability to different anions will be given at the end of this section.

Receptor 145

The binding results for the control receptor **145** with anions in CD$_3$CN are summarised in Table 2.2 and Figure 2.5 contains binding curves for the amide N-H group. Overall, binding strength decreased in the order of AcO$^-$ > BzO$^-$ > Cl$^-$ > Br$^-$. In the case of Cl$^-$, AcO$^-$ and BzO$^-$,

relatively sharp binding curves were observed while Br$^-$ titration curves resembled an exponential curve, further evidence of weak binding.[200]

Table 2.2: Summary of K_{ass} values for amide N-H of receptor **145** with anions in CD$_3$CN fitted to a 1:1 model.[202]

Structure	K_{ass} (M^{-1}) [% error]	Anion
	80 [4.1]	Br$^-$
	260 [5.6]	Cl$^-$
	920 [2.5]	AcO$^-$
	650 [3.0]	BzO$^-$
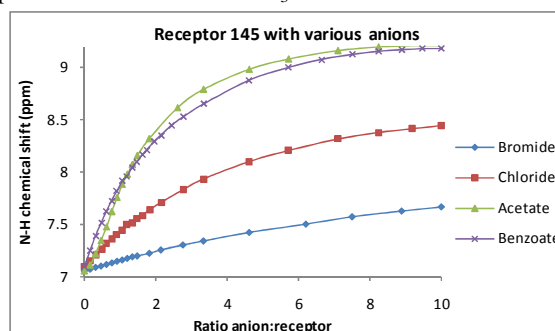
Figure 2.4: Titration curves showing migration of amide N-H signals of **145** upon addition of anions in CD$_3$CN.
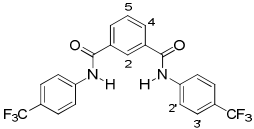
The spherical Cl$^-$ anion was more strongly bound than Br$^-$ producing a K_{ass} value of 260 M^{-1} for Cl$^-$ compared to 80 M^{-1} for Br$^-$. This enhancement was ascribed to the smaller size and higher charge density of the Cl$^-$ anion facilitating efficient binding in the isophthaloyl cleft while Br$^-$ may have been less favourable.[51,210] Titration of **145** with AcO$^-$ & BzO$^-$ produced a slightly sharper plateau of chemical shift migration, indicating stronger binding for these anions compared to the halides. The titration curves of BzO$^-$ and AcO$^-$ also displayed slight curvature for a number of initial additions of anion where the rate of change of chemical shift was low. This was ascribed to a desolvation effect where the anion needed to displace a solvent molecule from the binding site, similar to that previously seen by Gale *et al.*[44] and Fabbrizzi *et al.*[82] This may also have been accompanied by a slight conformational change upon introduction of anion which preceded efficient binding in the cleft structure. K_{ass} values of 650 M^{-1} and 920 M^{-1} were obtained for BzO$^-$ and AcO$^-$ respectively.

Receptor 146

Receptor **146** was derived from 4-trifluoromethylaniline coupled to an isophthaloyl substructure and possessed potentially increased N-H binding capability due to the inductive effect of the CF$_3$ groups on 4-(trifluoromethyl)phenyl rings enhancing acidity and H-bonding potential. Titration with all anions resulted in a significant downfield migration of the amide N-H, H-2 and H-2' signals (atom labels in Table 2.3), suggesting binding in a cleft-like

manner. The binding curves of the H-2 and H-2' protons followed a similar profile to the amide N-H group with sharp levelling of the plot following the addition of 1 equiv anion (Figure 2.5a). The degree of chemical shift migration decreased in the order amide N-H > H-2 > H-2' with amide N-H chemical shift changes of up to 3.4 ppm for BzO^- and 3.2 ppm for AcO^-. K_{ass} values were calculated based on the amide N-H signal and titration with Br^- and Cl^- showed a large increase in anion binding strength compared to the control receptor **145** for all anions. This was exemplified by a 34-fold increase in Cl^- binding; 8,900 M^{-1} for **146** vs 260 M^{-1} for **145** (Table 2.3).

Table 2.3: Summary of K_{ass} values for amide N-H of receptor **146** with anions in CD_3CN fitted to a 1:1 model.[202]

Structure	K_{ass} (M^{-1}) [% error]	Anion
	700 [1.3]	Br^-
	8,900 [3.6]	Cl^-
	4,900 [14.9]	AcO^-
	12,100 [2.7]	BzO^-
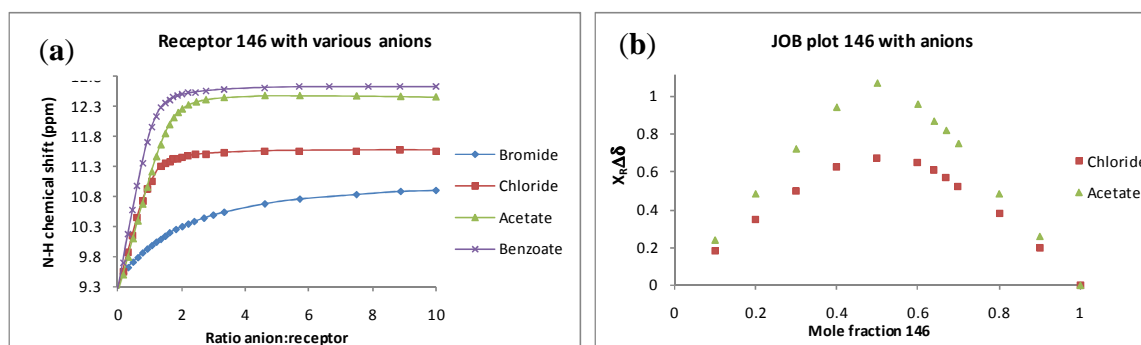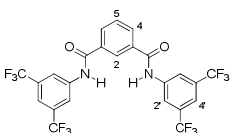
Figure 2.5: (a) Titration curves showing migration of amide N-H signals of **146** upon addition of anions in CD_3CN. (b) JOB plot of **146** with Cl^- and AcO^- in CD_3CN confirming 1:1 stoichiometry.

Strong binding was also observed to BzO^- and AcO^-. These titrations produced K_{ass} values up to 12,100 M^{-1} for BzO^- and 4,900 M^{-1} for AcO^-. Receptor **146** appeared relatively selective for BzO^- with binding strength of the order $BzO^- > Cl^- > AcO^- > Br^-$. It must be noted that ^1H NMR based determinations of K_{ass} are reliable for association constants in the range $10 - 10^4$ M^{-1} and as a result, high K_{ass} values can only treated as an estimation.[201] JOB plot analysis indicated 1:1 binding stoichiometry in all cases (Figure 2.5b).

Receptor 147

Receptor **147** possessing 3,5-*bis*(trifluoromethyl)phenyl rings was expected to possess increased N-H acidity and superior anion binding performance compared to **145** & **146**. It was also considered that the 3,5-*bis*(trifluoromethyl)phenyl groups may impart a rigidifying effect on the molecule in a similar way to that reported for an analogous thiourea with the 3,5-*bis*(trifluoromethyl)phenyl functionality.[144] Titration of **147** with Br⁻ resulted in downfield migration of approximately 1.9 ppm for the N-H chemical shift upon addition of 1 – 2 equivalents of Br⁻ and beyond this point, the chemical shift change plateaued (Figure 2.6a) Similar chemical shift change patterns for H-2 and H-2' indicated binding in a cleft structure. An association constant of 4700 M^{-1} was calculated for this titration when fitted to a 1:1 model; a 56 fold increase compared to the control receptor **145** (Table 2.4). Titration with Cl⁻ produced an amide N-H downfield shift of 2.4 ppm followed by a sharp inflexion point. This translated to a K_{ass} value of 10,800 M^{-1} when fitted to a 1:1 model corresponding to a 41 fold increase compared to **145**.

Table 2.4: Summary of K_{ass} values for amide N-H of receptor **147** with anions in CD_3CN fitted to a 1:1 model.[202]

Structure	K_{ass} (M^{-1}) [% error]	Anion
	4,700 [0.7]	Br-
	10,800 [12.6]	Cl-
	14,300 [17.1]	AcO-
	19,200 [12.0]	BzO-

Figure 2.6: (a) Titration curves showing migration of amide N-H signals of **147** upon addition of anions in CD_3CN. (b) JOB plot of **147** with Br⁻, Cl⁻ & AcO⁻ in CD_3CN confirming 1:1 stoichiometry.

Binding studies of **147** with AcO⁻ and BzO⁻ produced titration curves consistent with extremely tight 1:1 receptor:anion stoichiometry with amide N-H migrations of 3.52 and 3.70 ppm respectively.[200] WINEQNMR fitting to 1:1 binding systems was used to calculate K_{ass}

values of 14,300 M^{-1} and 19,200 M^{-1} for AcO^- and BzO^- corresponding to 15 fold and 30 fold increases respectively. Preferential binding was observed of the order $BzO^- > AcO^- > Cl^- > Br^-$ and JOB plot analysis indicated 1:1 receptor:anion binding in all cases (Figure 2.6b). Figure 2.7 contains an example of a stack plot of ^{1}H NMR spectra for titration of receptor **147** with AcO^- showing the migration of the ^{1}H NMR spectroscopic resonances with increasing AcO^- addition up to 1 equivalent anion after which the chemical shifts became effectively constant.
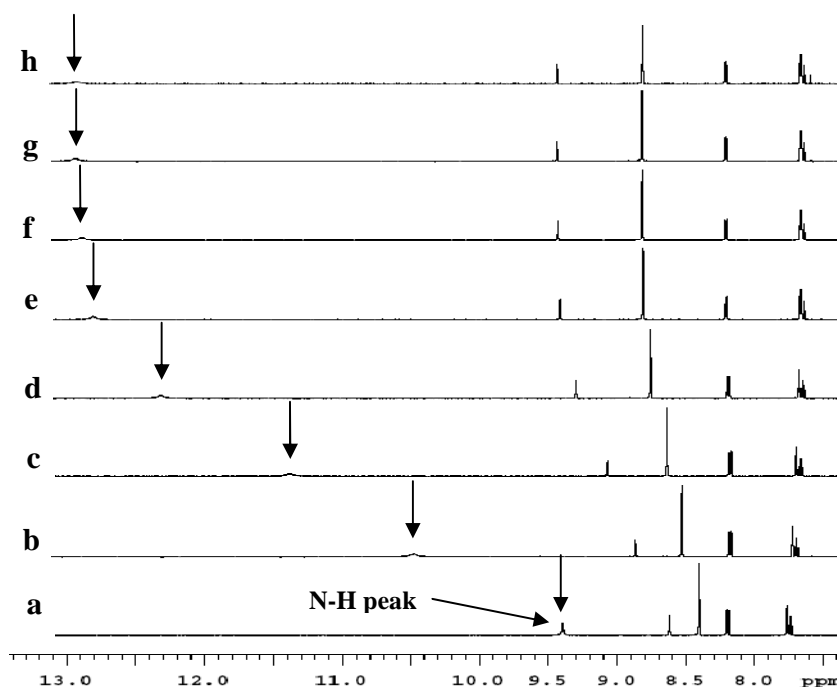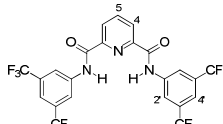
Figure 2.7: Stack plot of ^{1}H NMR spectra for titration of receptor **147** with AcO^- in CD_3CN. a = T_0, b = $T_0 + 0.3$ eq, c = $T_0 + 0.6$ eq, d = $T_0 + 0.9$ eq, e = $T_0 + 1.2$ eq, f = $T_0 + 1.5$ eq, g = $T_0 + 2.6$ eq, h = $T_0 + 6.7$ eq.

Receptor 148

The pyridine 1,3 dicarboxamide arrangement has been incorporated into a number of receptors studied by Crabtree *et al.*,[51] Jurczak *et al.*[4] and Gale *et al.*[44] As previously described, 1,3-pyridyl-diamide compounds may preferentially exist in the *syn-syn* conformation, optimal for efficient binding.[56] As a result, **148** was expected to bind anions efficiently due to the acidic 3,5-*bis*(trifluoromethyl)phenyl groups and its preference for the *syn-syn* conformation. Table 2.5 contains a summary of the anion binding constants. Titration of **148** with Br^- produced a weak titration curve characteristic of weak binding (Figure 2.8a) with a moderate increase in chemical shift of 1.2 ppm and a K_{ass} value of 290 M^{-1}, a 16-fold decrease in K_{ass} compared to

its isophthaloyl analogue **147** (Table 2.5). This was ascribed to the beneficial effects of conformational pre-organisation negated by repulsion of the pyridyl lone pair electrons and anionic guest, a feature which was particularly pronounced for large the Br⁻ anion.[51] The pyridyl nitrogen is also known to be sterically more bulky than an aromatic C-H bond and this may influence its Br⁻ binding efficiency.[212] Crabtree found their 1,3-pyridyl-diamide receptor to be most successful for small anions where electrostatic repulsion is minimised but ineffective for binding larger anions.[17] Titration of **148** with Cl⁻ afforded more efficient binding with a K_{ass} value of 3,800 M⁻¹, a factor of 3 lower than **147** with Cl⁻ but a 13 fold increase over the control **145**. Electrostatic repulsion resulting from the pyridyl nitrogen was also suggested to hinder Cl⁻ binding.

Table 2.5: Summary of K_{ass} values for amide N-H of receptor **148** with anions in CD_3CN fitted to a 1:1 model.[202]

Structure	K_{ass} (M⁻¹) [% error]	Anion
	290 [1.3]	Br⁻
	3,800 [2.2]	Cl⁻
	8,700 10.9]	AcO⁻
	3,800 [6.0]	BzO⁻

Figure 2.8: (a) Titration curves showing migration of amide N-H signals of **148** upon addition of anions in CD_3CN. (b) JOB plot of **148** with Cl⁻ & AcO⁻ in CD_3CN.
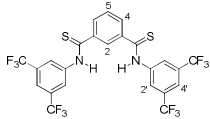
Titration of **148** with AcO⁻ and BzO⁻ displayed moderate binding. Amide N-H chemical shift changes of approximately 2.30 ppm were observed for both of these anions corresponding to K_{ass} values of 8,700 M⁻¹ and 3,800 M⁻¹ for AcO⁻ and BzO⁻ binding respectively when fitted to 1:1 models. The H-2' signals were also shifted during the titration and interestingly, the initial shift of this signal was an upfield migration until the addition of approximately 0.5 equiv AcO⁻ or 1 equiv BzO⁻ followed by a downfield shift for the remainder of the titration. This may be a result of conformational changes to accommodate the Y-shaped anions. Overall, the

binding curves and K_{ass} values indicated that **148** preferentially bound AcO⁻ with binding affinity in the order AcO⁻ > BzO⁻, Cl⁻ > Br⁻ (Table 2.5). JOB plots were used to investigate binding stoichiometry and in the the maxima observed at approximately 0.7 mole fraction receptor suggested 2:1 receptor: anion stoichiometry (Figure 2.8b). However, the titrations of **148** with anions produced a very poor fit to 2:1 stoichiometry but appeared to fit the 1:1 model most efficiently. The apparent 2:1 stoichiometry may be due to slight solubility issues encountered with **148** at the concentration at which JOB plot analysis was conducted.

Receptor 149

The thioamide derivative **149** was expected to be more acidic than the corresponding amide **147,** less prone to self-association[4] and was therefore predicted to possess enhanced anion binding properties. Soon after this work was complete, Moran *et al.* reported binding studies using **149**[177] with triphenylarsine oxide in CDCl$_3$ and calculated a K_{ass} of 1 x 10^5 M^{-1}. However, there have been no complete binding studies reported on this receptor with anions. In addition, **149** was the only compound from this series which Moran *et al.* investigated. See Table 2.6 below for a summary of the K_{ass} values calculated for receptor **149** with Br⁻, Cl⁻, AcO⁻ and BzO⁻. Titration of **149** with Br⁻ & Cl⁻ yielded titration curves suggesting relatively strong binding with migration of chemical shift values downfield of 1.65 ppm and 2.4 ppm for Br⁻ and Cl⁻ corresponding to K_{ass} values of 5,900 M^{-1} and 17,500 M^{-1} respectively (Figure 2.9a). This represented a 66-fold increase in K_{ass} for **149** binding Cl⁻ binding compared to the control receptor **145** and both Br⁻ and Cl⁻ binding constants were higher than those found with the amide analogue **147**. This clearly showed that substitution of the amide with thioamide gave significant enhancement in anion binding properties. Titration curves for **149** with Br⁻ and Cl⁻ are shown in Figure 2.9 and JOB plot analysis of these anions confirmed 1:1 binding interactions however ion the case of Br⁻, minor 2:1 receptor:anion interactions may also be present (Figure 2.9b).

Table 2.6: Summary of K_{ass} values for thioamide N-H of receptor **149** with anions in CD_3CN fitted to a 1:1 model.[202]

Structure	K_{ass} (M^{-1}) [% error]	Anion
	5,900 [12.0]	Br^-
	17,500 [12.4]	Cl^-
	$-^a$	AcO^-
	$-^a$	BzO^-

^{a}Proton transfer prevented the calculation of an accurate association constant.
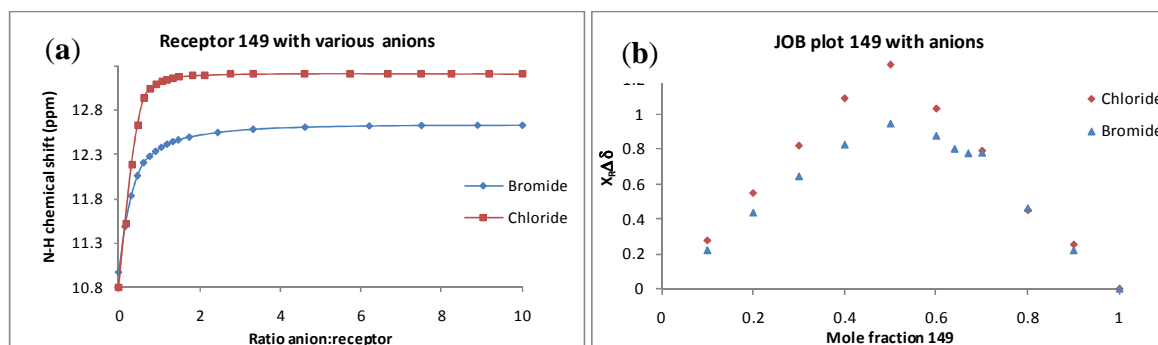
Figure 2.9: (a) Titration curves showing migration of thioamide N-H signals of **149** upon addition of Br^- & Cl^- in CD_3CN. (b) JOB plot of **149** with Br^- & Cl^- in CD_3CN confirming 1:1 stoichiometry.

Titration of **149** with AcO^- and BzO^- produced unusual titration curves (Figure 2.10). Upon initial addition of AcO^- anion to the receptor solution, the thioamide N-H signal disappeared and the titration was subsequently monitored using the isophthaloyl H-2 proton *ortho* to both thioamide groups. Initially, a minor upfield shift of this resonance was observed followed by a significant downfield migration, with a second minor upfield shift upon addition of 1 equiv AcO^-. This was followed by a final significant downfield migration. This phenomenon was ascribed to initial desolvation of the receptor,[44] followed by strong H-bonding to the anion, indicated by the downfield shift. The minor upfield shift at 1 equiv anion may have been due to two factors. Because of the increased acidity of the thioamide N-H, proton transfer from the receptor to the carboxylate or changing complex stoichiometries could account for this chemical shift perturbation. In either case, a subsequent conformational change could allow for further binding events resulting in migration downfield of H-2 over the remaining course of the titration.
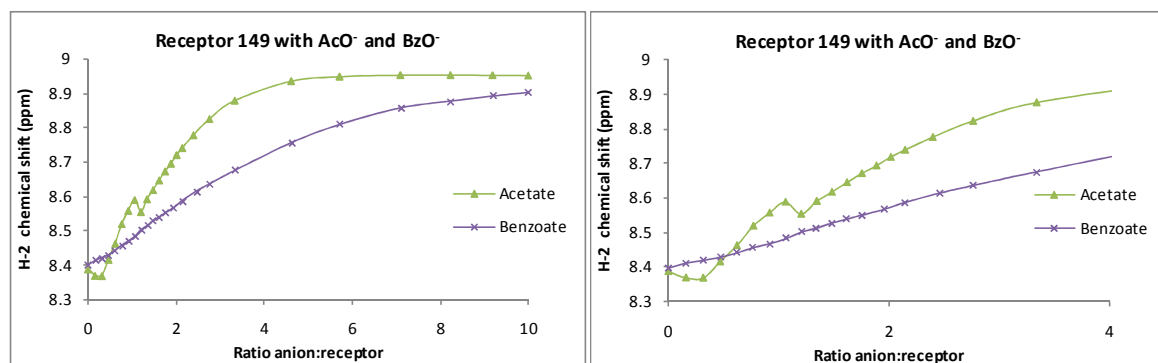
Figure 2.10: Titration curves showing migration of isophthaloyl H-2 signal of **149** upon addition of AcO⁻ & BzO⁻ in CD₃CN.
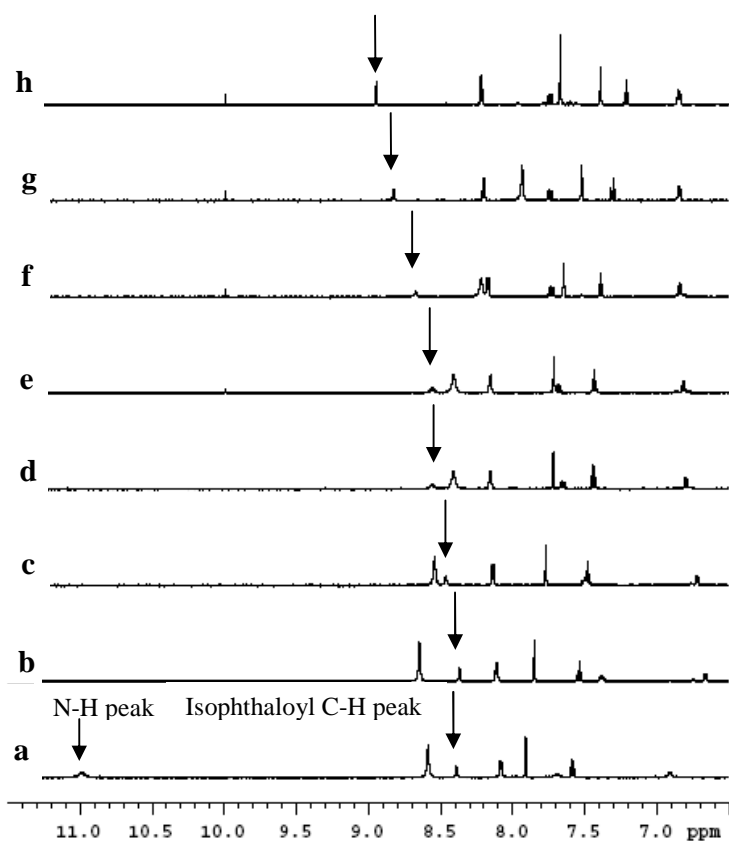
Figure 2.11: Representative stack plot for titration of **149** with AcO⁻ in CD₃CN showing initial upfield shift of isophthaloyl C-H and subsequent downfield shift. a = T_0, b = T_0 + 0.3 eq, c = T_0 + 0.6 eq, d = T_0 + 0.9 eq, e = T_0 + 1.2 eq, f = T_0 + 1.75 eq, g = T_0 + 2.75 eq, h = T_0 + 5.7 eq.

Similar effects were previously observed by Gale *et al.;*[66] upon coordination of 1 equivalent of a nitrophenyl derivative of a pyrrole 2,5-diamide **28** to F⁻, apparent deprotonation and further coordination of the deprotonated receptor to anion occurred (Figure 2.12). Conformational

78

change post 1:1 complexation followed by additional anion binding has also previously been reported by Crabtree *et al.*[51] and Gale *et al.*[44]
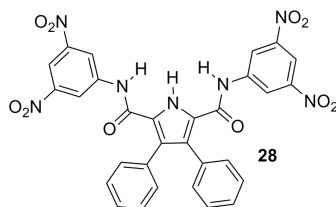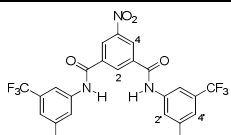
Figure 2.12: Structure of **28** which appeared to deprotonate during titration with fluoride.[66]

As shown by the titration curves and binding constants, **149** was most selective for Cl⁻ yielding a K_{ass} in excess of 10^4 M^{-1}. The occurrence of conformational changes and/or proton transfer events with AcO⁻ and BzO⁻ prevented the calculation of K_{ass} values for these anionic guests.[4] However, despite proton transfer events, the receptor was observed to bind these anions in a manner possibly facilitated by conformational change and including binding to acidic isophthaloyl C-H groups such as H-2.[44] JOB plots of **149** with AcO⁻ and BzO⁻ produced abnormal profiles due to the assumed proton transfer events and therefore binding stoichiometry could not be reliably assessed.

Receptor 150

Receptor **150** possessed a highly electron withdrawing NO_2 group *meta* to the amide groups in the isophthaloyl core which was expected to further enhance the acidity of the amide N-H groups along with 3,5-*bis*(trifluoromethyl)phenyl groups. Receptor **150** was initially titrated with Br⁻ and Cl⁻ and in both cases, a titration curve indicative of tight 1:1 binding with amide N-H downfield migrations of 1.9 ppm and 2.5 ppm was observed over the course of the titrations (Figure 2.13a). K_{ass} values of 6,100 M^{-1} and 11,100 M^{-1} were obtained for Br⁻ and Cl⁻ respectively (Table 2.7). This represented a 73-fold increase in Br⁻ binding strength compared to **145** and a 1.3-fold increase compared to **147**.

Table 2.7: Summary of K_{ass} values for amide N-H of receptor **150** with anions in CD$_3$CN fitted to a 1:1 model.[202]

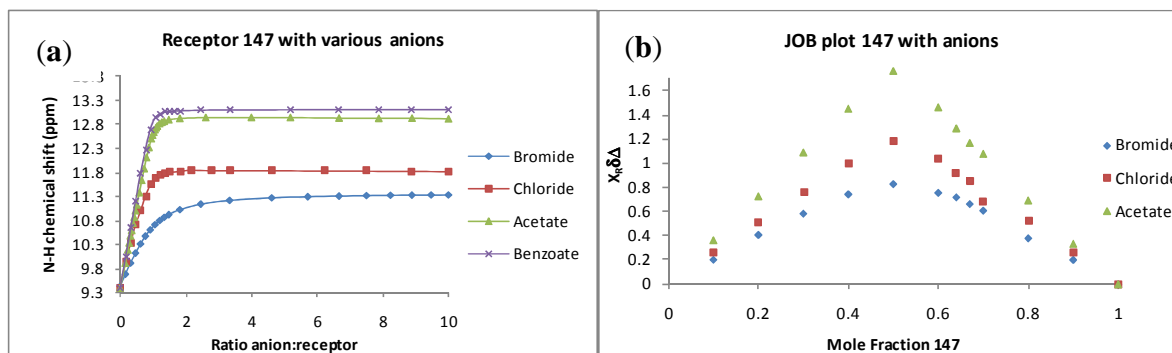| Structure	K_{ass} (M^{-1}) [% error]	Anion
	6,100 [2.1]	Br$^-$
	11,100 [6.8]	Cl$^-$
	16,600 [8.9]	AcO$^-$
	21,000 [12.0]	BzO$^-$
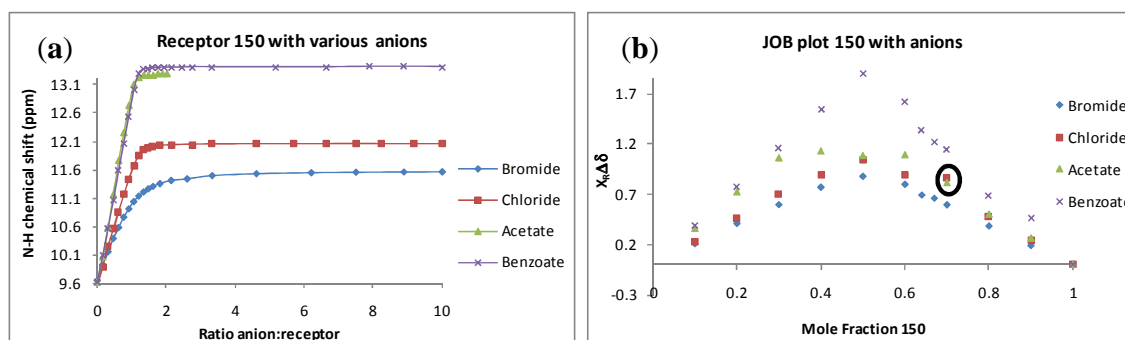
Figure 2.13: (a) Titration curves showing migration of amide N-H signals of **150** upon addition of anions in CD$_3$CN. (b) JOB plot of **150** with Br$^-$, Cl$^-$, AcO$^-$ & BzO$^-$ in CD$_3$CN confirming 1:1 stoichiometry with minor 2:1 receptor:anion species for Cl$^-$ & AcO$^-$.
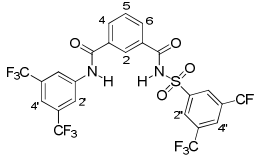
Titration of **150** with AcO$^-$ and BzO$^-$ also produced titration curves indicative of tight binding with large amide N-H chemical shift downfield migrations of 3.70 ppm and 3.80 ppm respectively over the course of the titration. In the case of AcO$^-$, the amide N-H signal broadened and disappeared following the addition of 2 equiv anion and the titration was subsequently monitored using the isophthaloyl H-2 peak. Despite the N-H disappearance, it was still possible to calculate K_{ass} values using this resonance. K_{ass} values of 16,600 M^{-1} and 21,000 M^{-1} were observed for AcO$^-$ and BzO$^-$ respectively, corresponding to an 18-fold and 32-fold increase in AcO$^-$ and BzO$^-$ binding respectively compared to **145** and significantly increased compared to **148**, displaying the beneficial effects of an additional NO$_2$ group in the isophthalamide structure.

As shown by the titration curves and binding constants, **150** bound BzO$^-$ most efficiently followed by AcO$^-$, Cl$^-$ and Br$^-$ while the H-2 and H-2' protons possessed similarly shaped binding curves to the amide N-H. JOB plot analysis of anions with **150** indicated exclusive 1:1 binding for Br$^-$ and BzO$^-$ binding while dominant 1:1 binding with additional minor 2:1 receptor:anion interactions were observed with Cl$^-$ and AcO$^-$ indicated by a small shoulder on the JOB plot at 0.65 mole fraction receptor (Figure 2.13b).

80

Receptor 151

Of the initial series of diamide based anion receptors, **151** was the only bifunctional molecule evaluated. It was designed to enhance acidity through incorporation of an *N*-acyl sulfonamide functionality, creating a hybrid amide/*N*-acyl-sulfonamide receptor. The behaviour of this acidic receptor **151** was examined through ^{1}H NMR spectroscopic titration with anions and the K_{ass} values are summarised in Table 2.8. The highly acidic sulfonamide N-H group was not visible by ^{1}H NMR spectroscopy, therefore the titration was monitored using the amide N-H and isophthaloyl H-2 peaks. Titration with Br$^-$ resulted in downfield migration of 0.3 ppm and 0.075 ppm for these signals and the almost exponential binding curves produced without detectable plateau were indicative of modest binding (Figure 2.14a). Similar shapes of curves were obtained for the amide N-H and isophthaloyl H-2 signals, suggesting involvement of both these groups in binding Br$^-$. Additionally, monitoring of the other receptor proton signals showed an almost linear downfield shift of the H-2' and H-4 signals with addition of anion. A number of other proton signals including H-2'', H-4'' and H-4' experienced a significant binding curve change following the addition of 2 equiv Br$^-$, suggestive of a conformational change. Similar binding curves were observed in the case of Cl$^-$ binding, although the shape of amide N-H and isophthaloyl H-2 signals and the larger chemical shift changes of 0.57 ppm and 0.19 ppm for these signals were indicative of stronger binding (Figure 2.14b).

Table 2.8: Summary of K_{ass} values for amide N-H of receptor **151** with anions in CD$_3$CN.[202]

Structure	K_{ass} (M^{-1}) [% error]	Anion
	$K_{ass}^{1:1}$ 900 [0.1] $K_{ass}^{2:1}$ 6,100 [0.1]	Br$^-$
	$K_{ass}^{1:1}$ 4,000 [0.1] $K_{ass}^{2:1}$ 3,700 [0.1]	Cl$^-$
	-^{a}	AcO$^-$
	-^{a}	BzO$^-$

^{a}Deprotonation prevented the calculation of an accurate K_{ass} value and could not be fitted to a binding model.
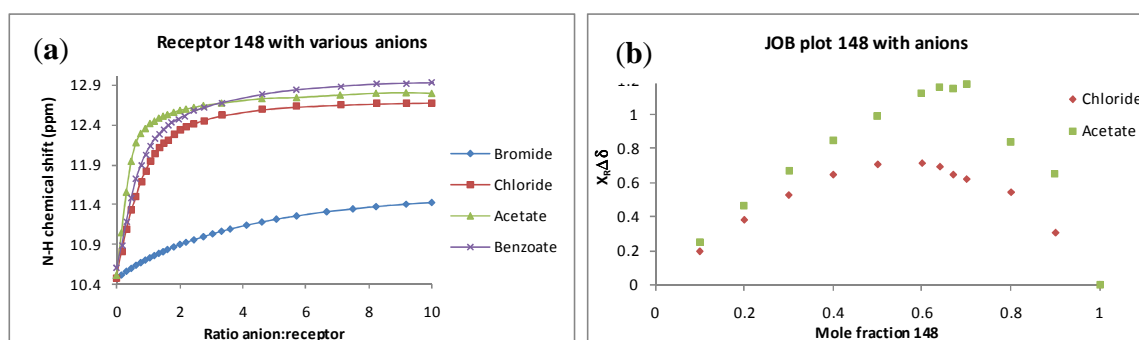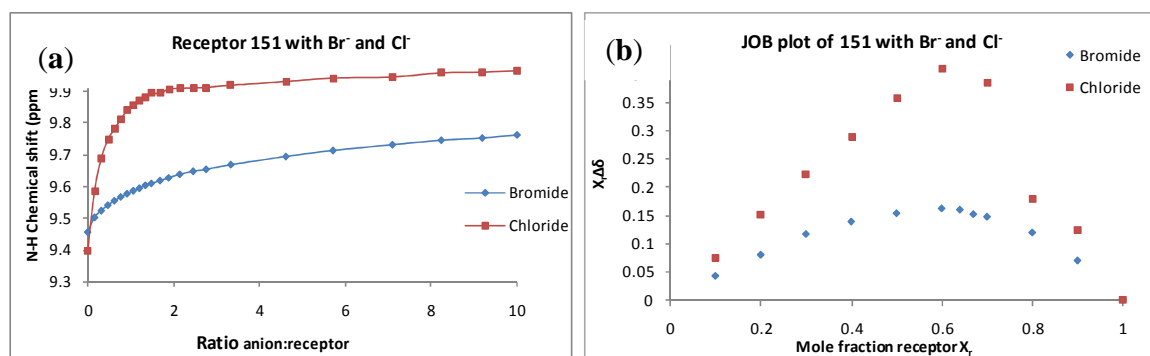
Figure 2.14: (a) Titration curves showing migration of amide N-H signals of **151** upon addition of Br$^-$ & Cl$^-$ in CD$_3$CN. (b) JOB plot of **151** with Br$^-$ & Cl$^-$ in CD$_3$CN confirming 2:1 receptor:anion stoichiometry.

Titrations of **151** with Br$^-$ and Cl$^-$ could not be fit to an exclusive 1:1 model but produced an excellent fit to a 1:1 and 2:1 receptor:anion system and JOB plot analysis for **151**:Br$^-$ and **151**:Cl$^-$ displayed maxima at approximately 0.67 mole fraction receptor, confirming 2:1 receptor:anion stoichiometries (Figure 2.14b). The K$_{ass}$ for 1:1 and 2:1 receptor:anion binding to Br$^-$ were 900 M^{-1} and 6,100 M^{-1} respectively (Table 2.8). The strong K$_{ass}^{2:1}$ for Br$^-$ was ascribed to its large size facilitating binding to two separate receptor molecules at opposite sides of the anion. Receptor **151** with Cl$^-$ produced K$_{ass}$ values of 4,000 M^{-1} and 3,700 M^{-1} for 1:1 and 2:1 receptor anion association respectively. To compare with Br$^-$ binding, the higher 1:1 value may have been due to the proclivity of the smaller Cl$^-$ anion to bind a receptor in the 1:1 stoichiometry while the smaller K$_{ass}^{2:1}$ may have been due to the small Cl$^-$ anion less favourable towards accomodating two receptor molecules simultaneously. Similar binding stoichiometries have also been previously reported.[57,74,213] Coles *et al.* observed a 2:1 receptor:anion complex for their *bis*-4-nitroaniline derived isophthalamide with a hexafluorophosphate anion.[57] Jurczak *et al.* found that their 7,7'-diureido-2,2'-diindolylmethane receptor bound the pyrophosphate anion in a 2:1 receptor:anion stoichiometry.[74] Gunnlaugsson *et al.* also observed this stoichiometry for their thiourea functionalised [3]polynorbornyl receptors with the dihydrogen pyrophosphate anion.[213]

During the titrations of **151** with AcO$^-$ and BzO$^-$, proton transfer effects were observed representing deprotonation of the *N*-acylsulfonamide. When monitoring the titration using the amide N-H proton, addition of up to 0.5 equiv anion caused a downfield shift. Upon addition of a further 0.5 equiv anion, an upfield shift occurred with an almost linear downfield

migration upon further additions (Figure 2.15). Furthermore, the isophthaloyl H-2, H-2'', H-4' & H-4'' protons broadened significantly up to the addition of 1 equiv of anion but subsequently sharpened. This was ascribed to an overall equilibrium process involving binding of the first 0.5 equiv anion followed by deprotonation of the highly acidic sulfonyl N-H group. This equilibrium process may account for the broadened signals up to 1 equiv anion with the equilibrium driven to a single complexed species by addition of further anion. A conformational change may have occurred following the addition of 1 equivalent of anion, allowing the amide N-H to further bind anionic species with no isophthaloyl H-2 involvement (Figure 2.15). A similar trend involving deprotonation was observed for sulfonamide functionalised urea compounds[89] with evidence of conformational change allowing further binding events post 1:1 binding reported by Crabtree *et al.*[24,51] and Kilburn *et al.*[90] for disulfonamide receptors.
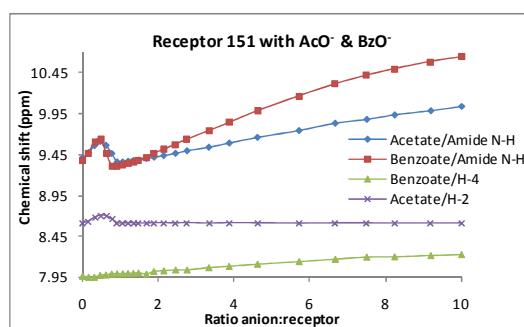
Figure 2.15: Titration curves showing migration of amide N-H signals of **151** upon addition of AcO⁻ & BzO⁻ in CD$_3$CN. Titration curves for H-4 with BzO⁻ and H-2 with AcO⁻ also shown.

2.6.3 Binding in Competitive Solvent

The working range of K_{ass} values which can be accurately quantified using ^{1}H NMR spectroscopic data is from approximately $10 – 10^4 \, M^{-1}$ and values which lie outside this range may suffer relatively large margins of error due to poor fit.[202] Therefore titrations for receptors **146**, **147**, **149** & **150** with Cl⁻, AcO⁻ and BzO⁻ anions were repeated in DMSO-d_6. Solvent is known to play a key role in the solution stability of anion complexes; the higher the solvent polarity, the higher the anion desolvation energy and therefore the lower the stability of the H-bonding complex.[82] A more competitive solvent environment would further facilitate the direct comparison the binding performance of the receptors. DMSO is a highly polar, aprotic solvent which displays a high solvation ability towards cations. The oxygen atom of DMSO is

quite basic and may act as a H-bond acceptor causing it to compete with anions for the H-bond donating receptor N-H groups.

Table 2.9: Summary of K_{ass} values for amide N-H of receptors **146**, **147**, **149** & **150** with Cl⁻, AcO⁻ & BzO⁻ in DMSO-d_6.[202] Percentage errors are included in parentheses.

Receptor	Chloride [% error]	Acetate [% error]	Benzoate [% error]
146	100 [8.43]	480 [2.7]	160 [3.1]
147	120 [4.8]	1,370 [7.5]	720 [2.1]
149	80 [5.3]	2,700ᵃ [6.4]	2,540ᵃ [4.3]
150	100 [0.2]	5,200ᵃ [1.0]	800 [5.7]

ᵃCalculated based on isophthaloyl H-2 proton.
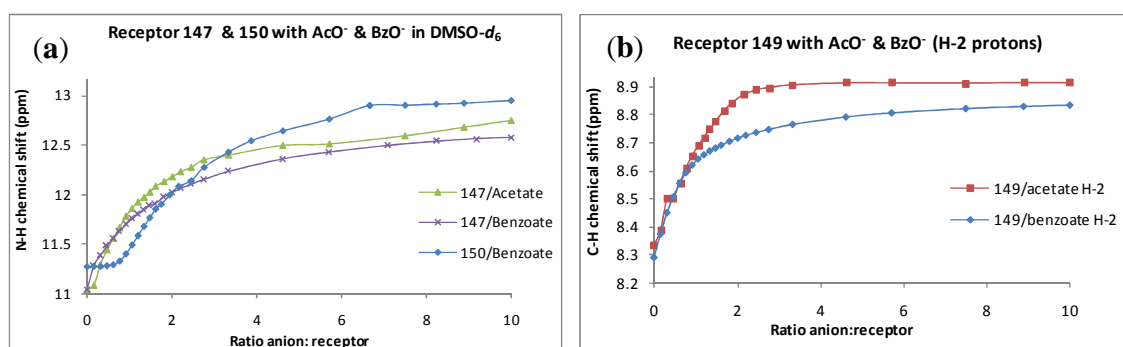
Figure 2.16: (a) Titration curves showing migration of amide N-H signals of **147** upon addition of AcO⁻ & **150** upon addition of BzO⁻ in DMSO-d_6. (b) Binding curves of H-2 proton for **149** with AcO⁻ & BzO⁻ in DMSO-d_6.

As expected, significantly reduced K_{ass} values were observed for titrations in DMSO-d_6 for titrations in DMSO-d_6 (Table 2.9). Receptors **146**, **147**, **149** & **150** were observed to bind Cl⁻ with $K_{ass}^{1:1}$ values of the order of 100 M⁻¹ with moderate (thio)amide N-H chemical shift downfield migrations of approximately 0.2 ppm. For AcO⁻ titrations, **146** & **147** gave K_{ass} values of 480 M⁻¹ and 1,370 M⁻¹ respectively with binding interactions through the amide N-H, isophthaloyl H-2 & aryl H-2' observed (Figure 2.16a).

The thioamide N-H signal of **149** disappeared during the titration with AcO⁻ and BzO⁻; as a result, the isophthaloyl H-2 proton was used to calculate K_{ass} values for both of these titrations. This resonance moved downfield upon addition of AcO⁻ but underwent a slight upfield migration at 0.5 equiv AcO⁻ while a similar upfield migration was observed at 1 equiv AcO⁻ in CD₃CN (Figure 2.16b). These anomalies may be due to proton transfer events as previously described for **149** with acetate in CD₃CN or slight conformational changes upon addition of anion. It is interesting to note that behaviour of the N-H signals of thioamide **149**

84

with AcO⁻ differed in DMSO-d_6 and CD$_3$CN. In DMSO-d_6, the thioamide N-H signal broadened and migrated upfield until 1.3 equivalents anion had been added, followed by N-H disappearance of this signal; in CD$_3$CN, the N-H signal disappeared immediately upon addition of 0.15 equiv AcO⁻. This may be due to DMSO-d_6 competing with AcO⁻ for the binding sites of **149**, therefore the effects of the basic AcO⁻ anion may be minimized in this solvent up to a larger concentration of anion. There were no detectable upfield migrations in binding curves for the H-2 signal of **150** in DMSO-d_6 or CD$_3$CN with AcO⁻. It was possible to calculate K$_{ass}$ values of 2,700 M^{-1} & 5,200 M^{-1} for **149** & **150** with AcO⁻ respectively.

Titrations of **146**, **147** & **150** with BzO⁻ produced K$_{ass}$ values of 160 M^{-1}, 720 M^{-1} and 800 M^{-1} respectively with binding interactions through the amide N-H, isophthaloyl H-2 & aryl H-2' observed. Interestingly, **149** appeared to bind most strongly to BzO⁻ compared to **146**, **147** & **150**. This may be due to proton transfer from the acidic N-H group of **149** to the BzO⁻ anion as indicated by broadening and subsequent loss of the amide N-H signal after addition of 1 equiv anion. As a result, the H-2 proton was used to calculate K$_{ass}$ and this produced a downfield chemical shift of 0.55 ppm and K$_{ass}$ value of 2,540 M^{-1}.

To compare the binding strengths and selectivities in CD$_3$CN to those in DMSO-d_6, **146**, **147** & **150** preferentially bound BzO⁻ in CD$_3$CN but were more selective for AcO⁻ in DMSO-d_6. Proton transfer of **149** in the presence of AcO⁻ or BzO⁻ in CD$_3$CN prevented the calculation of K$_{ass}$ values for these titrations, however it was possible to obtain K$_{ass}$ values for titrations with these anions in DMSO-d_6 through fitting of data from the H-2 resonance to a 1:1 model. It appeared that proton transfer effects were less pronounced in DMSO-d6, requiring more anion to shift the equilibrium towards the deprotonated state. This feature may be due to the improved solvation of AcO⁻ in DMSO-d_6 and also stronger solvent binding to the receptor, moderating the effects of basic AcO⁻ and preventing significant proton transfer in DMSO-d_6.

2.6.4 Summary of Binding Studies of 145-151

To summarise, binding studies were carried out on the diamide and thioamide receptors **145-151** with Br⁻, Cl⁻, AcO⁻ and BzO⁻ in CD$_3$CN. A general trend observed in all systems was that in the case of halides, Cl⁻ was bound more strongly than Br⁻, presumably due to its smaller

size and increased charge density. Oxyanions AcO⁻ and BzO⁻ were generally bound more strongly than Cl⁻ and this may be a reflection of the ability of Y-shaped oxyanions to H-bond to receptors from both oxygen atoms, creating stronger complexes.

Table 2.10: Summary of binding constants K_{ass} (M^{-1}) in CD_3CN calculated using WINEQNMR

Receptor	Bromide	Chloride	Acetate	Benzoate
145	80	260	920	650
146	700	8,900	4,900	12,100
147	4,700	10,800	14,300	19,200
148	290	3,800	8,700	3,800
149	5,900	17,500	-ᵃ	-ᵃ
150	6,100	11,100	16,600	21,000
151	$K_{ass}^{1:1}$ 900 $K_{ass}^{2:1}$ 6,100	$K_{ass}^{1:1}$ 4,000 $K_{ass}^{2:1}$ 3,700	-ᵃ	-ᵃ

ᵃProton transfer prevented the calculation of an accurate association constant.

In all cases, the newly designed receptors **146**-**151** produced significantly enhanced K_{ass} values compared to control receptor **145**, for example a 66-fold increase in Cl⁻ binding was observed for thioamide **149** compared to **145**. In general, binding was also observed through the H-2 and H-2' signals indicated by the shape of the titration curves observed for these protons. This suggests that the diamide receptors bind anions with cooperative H-bonding from both amide N-H groups and also a number of C-H groups in close proximity to the binding site. In cases where K_{ass} values in excess of 10^4 M^{-1} was observed, titrations were repeated in DMSO-d_6 and in general, reduced binding efficiencies were noted in this solvent been due to the increased polarity and competitive nature of this solvent medium.

The highly acidic thioamide **149** and nitro-substituted **150** appeared to be the most successful anion receptors producing the highest K_{ass} values; in particular **150** bound AcO⁻ and BzO⁻ with K_{ass} values of 16,000 M^{-1} and 21,000 M^{-1} respectively in CD_3CN. Receptor **151** bound halides with multiple stoichiometries confirmed by JOB plot analysis and successful fitting of these systems to a model involving simultaneous 1:1 and 2:1 receptor: halide interactions.

Possible receptor proton transfer was observed in the titration of thioamide **149** and amide/*N*-acyl sulfonamide hybrid **151** with AcO⁻ and BzO⁻. These proton transfer events did not allow a direct prediction of catalytic activity from binding studies but did point to strong binding

events possibly with multiple stoichiometries and potential interactions during the proton shuttling step which is now considered as part of the RDS of the MBH reaction. It must also be considered here that species which bind anions too strongly may have a negative impact on reaction catalysis through catalyst binding and inhibition.

2.7 Conformational Analysis in Solid and Liquid State

Conformational studies were undertaken for a number of receptors in the absence and presence of anionic guests. Several attempts at crystal growth for some receptors including slow evaporation and vapour diffusion using a number of solvents failed, however success was achieved in the case of thioamide **149**. X-ray diffraction grade crystals of **149** were grown through slow evaporation of a chloroform/methanol mixture at room temperature and X-ray crystallography revealed a crystallographic twofold axis through the centre of the molecule (Figure 2.17).[214] The two nitrogen atoms were twisted in opposite directions out of the plane to minimise steric conflict and enable H-bonding to a neighbouring sulphur atom. Receptor **149** existed in the solid state in its *syn-syn* conformation, possibly due to internal interactions between the polarized C-H bonds (H-7) *ortho* to the CF_3 groups and the Lewis basic sulphur atom.[148]
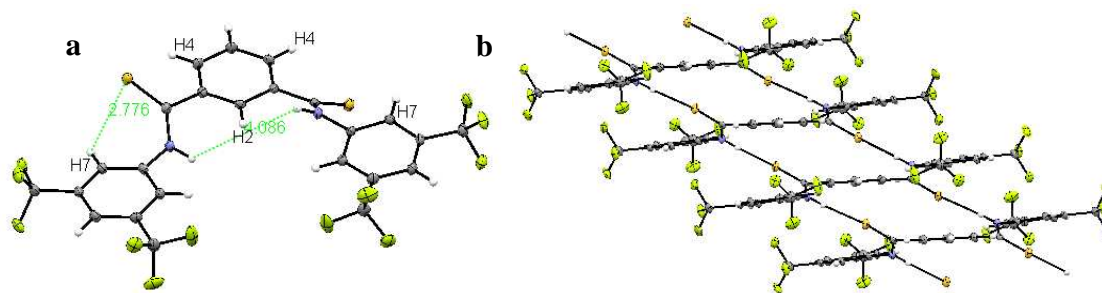
Figure 2.17: (a) X-ray crystal structure of thioamide **149** showing measurements between a number of atoms. (b) Crystal packing diagram of **149** showing intramolecular H-bonding between the sulphur atom and N-H group of a neighbouring molecule.

^{1}H NMR spectroscopy also somewhat supported the apparent favoured *syn-syn* conformation of **149** in the liquid state. The chemical shift of the H-7 (H-2') proton lay further downfield in the case of thioamide **149** (δ = 8.53 ppm for **149**; δ = 8.38 ppm for **147**) relative to other receptors, suggesting possible H-bonding interactions. Moreover, the H-2 proton *ortho* to both thioamide moieties was further upfield for **149** compared to the corresponding proton on **147**.

87

This is in agreement with previously reported similar systems in which isophthaloyl H-2 existed most upfield for an isophthalamide in the *syn-syn* conformation.[8] Therefore, it was likely that **149** existed in a number of possible conformations with the equilibrium lying potentially towards *syn-syn* conformation (Scheme 2.12).
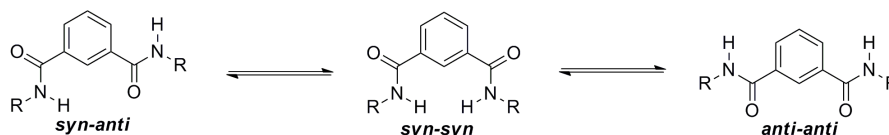
Scheme 2.12: Potential conformations of isophthalamide receptors.

A 2D NOESY NMR spectroscopy study of **149** in CD$_3$CN demonstrated through space interactions between H-4 & H-5, N-H & H-2, N-H & H-2' and also between N-H & H-4 indicating an equilibrium existed between the potential conformations. These latter NOE interactions were absent in a solution of **149** containing 1 equiv Cl$^-$, suggesting that the *syn-syn* conformation dominated in the presence of anion (Figure 2.18a & b). A 1D-NOE dpfgse experiment of **149** in the presence of Cl$^-$ identified neighbouring protons within 5 Å and found interactions between the N-H and H-2 and a weaker interaction between N-H and H-2' (Figure 2.18c) without NOE effects between the thioamide N-H and H-4, confirming *syn-syn* conformation.
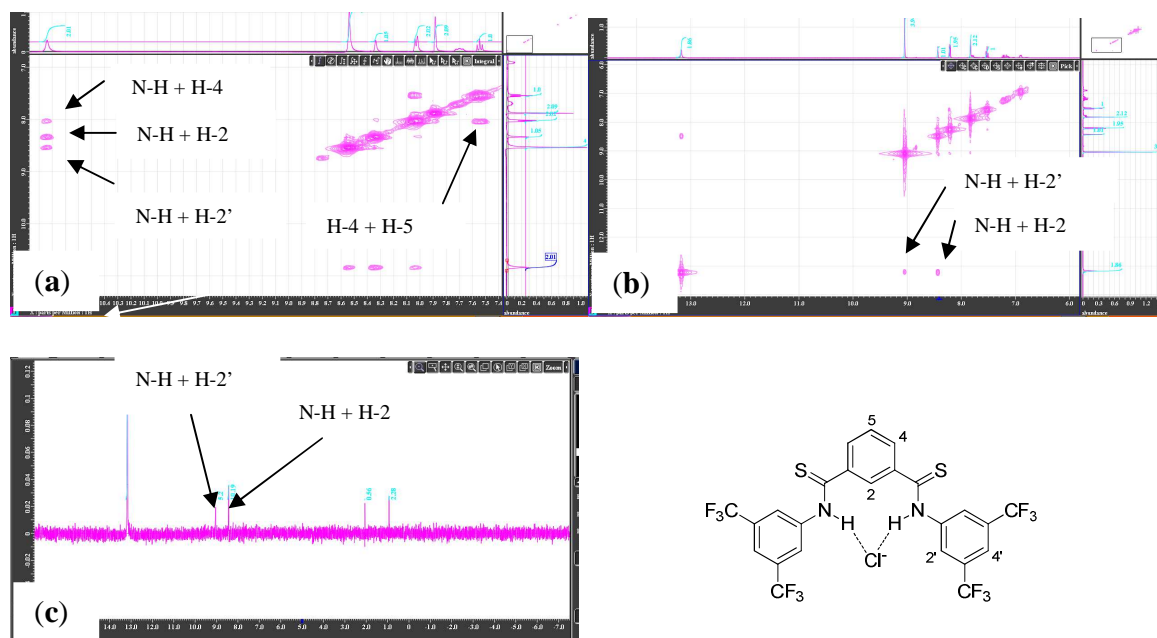
Figure 2.18: 2D NOESY of (a) **149**, (b) **149** + 1 equivalent TBACl$^-$ in CD$_3$CN. (c) 1D NOE of **149** + 1 equiv TBACl in CD$_3$CN.

Crystals of suitable quality for X-ray diffraction could not be obtained for the other receptors, therefore some conformational studies were conducted in solution using NMR spectroscopy. A 2D NOESY study of **147** in CD$_3$CN showed NOE correlations between the amide N-H group and H-2, H-2' and also weak interactions with H-4 (Figure 2.19a). In the absence of anionic guest, the amide N-H resonance of **150** was broad and it was difficult to observe NOE effects with this signal. In the presence of 1 equiv Cl$^-$, the amide N-H appeared sharp and NOE interactions were observed between this group and the isophthaloyl H-2, supporting *syn-syn* conformation. Other NOE interactions were difficult to decipher due to overlap of the H-2' and H-4 signals in the presence of Cl$^-$ (Figure 2.19b).
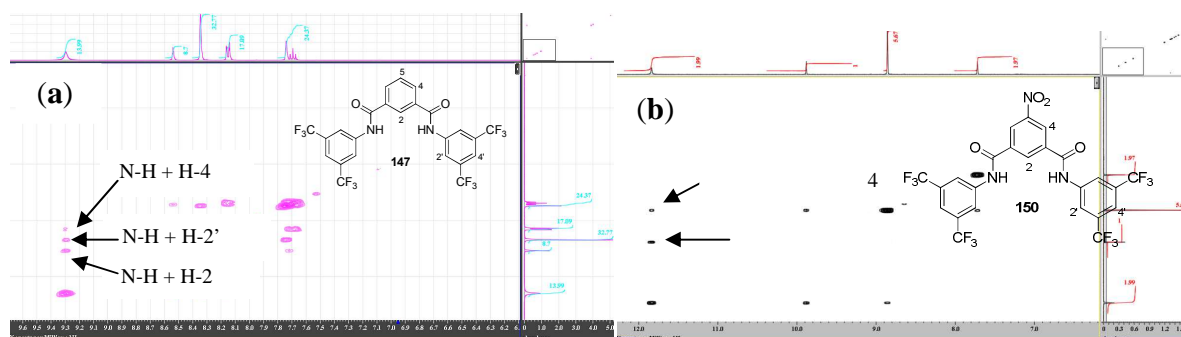
Figure 2.19: (a) 2D NOE of receptor **147** in CD$_3$CN.(b) 2D NOESY spectrum of **150** in the presence of 1 equiv Cl$^-$ in CD$_3$CN

Conformational analysis of **151** via NOE spectroscopy unveiled through space interactions between the amide N-H and H-2, H-2' and H-4 signals, demonstrating equilibration between the *syn* and also the *anti*-conformations for the amide portion of the *N*-acyl sulfonamide. In the presence of 2.3 equivalents Br$^-$ or 0.4 equiv AcO$^-$, the amide N-H displayed NOE effects with the isophthaloyl H-2 and H-2' while no effects with H-4 were observed (Figure 2.22). This was further evidence that the amide existed in its *syn*-conformation prior to proton transfer effects.

89
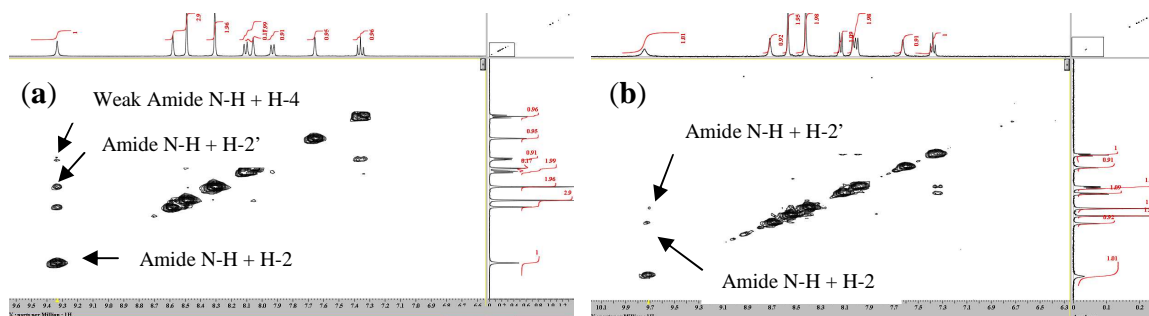
Figure 2.20: (a) 2D NOESY spectrum of **151** in CD$_3$CN. (b) 2D NOESY spectrum of **151** in the presence of 2.3 equiv Br$^-$ in CD$_3$CN.

To conclude, X-ray crystallography confirmed that **149** existed in the *syn-syn* conformation in the solid state and therefore possessed a degree of pre-organisation towards binding anions. In the liquid state, NMR spectroscopic evidence suggested that the conformations of **149** and a number of other receptors existed in equilibrium while the *syn-syn* conformation appeared to dominate in the presence of 1 equiv anion, optimal for binding anionic guests.

2.8   Screening of 145-151 for Catalytic Activity

The reaction studied in this work was the DABCO promoted MBH reaction of benzaldehyde with methyl acrylate. Preliminary reactions were conducted in the presence of 50 µL acetonitrile in order to assess the performance of thioamide **149** & nitro-substituted **150** at 20 mol% catalyst loadings. The reaction was carried out using 1 equiv benzaldehyde and DABCO, 3 equiv of methyl acrylate and 20 mol% receptor. Each reaction was stirred at room temperature for 20 hours and following aqueous work-up and purification by flash chromatography, the product **155** was isolated and confirmed using GC-MS and ^{1}H & ^{13}C NMR spectroscopy. A peak at m/z 192 was observed by GC-MS corresponding to the M$^+$ ion of the MBH adduct with additional fragment ions at m/z 175, 160, 132, 105 & 77. Key ^{1}H NMR spectroscopic resonances included the OH peak at 3.01 ppm and the doublet at 5.57 ppm due to the C_H_-OH proton. Aromatic signals in the range of 7.24-7.40 ppm, a methoxy group at 3.72 ppm and vinyl protons at 5.83 & 6.35 ppm served as further evidence of the desired MBH product.

145: X = CH; G = O; Y = H;   R = *n*Bu
146: X = CH; G = O; Y = H;   R = 4-(CF$_3$)C$_6$H$_4$
147: X = CH; G = O; Y = H;   R = 3,5-(CF$_3$)$_2$C$_6$H$_3$
148: X = N; G = O; Y = H;   R = 3,5-(CF$_3$)$_2$C$_6$H$_3$
149: X = CH; G = S; Y = H;   R = 3,5-(CF$_3$)$_2$C$_6$H$_3$
150: X = CH; G = O; Y = NO$_2$; R = 3,5-(CF$_3$)$_2$C$_6$H$_3$
151: X = CH; G = O; Y = H; R = 3,5-(CF$_3$)$_2$C$_6$H$_3$; R' = SO$_2$3,5-(CF$_3$)$_2$C$_6$H$_3$
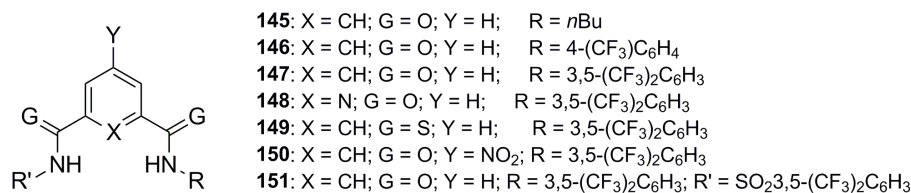
Figure 2.21: Structure of receptors/catalysts **145**-**151** tested in the MBH reaction.

The uncatalysed reaction produced a yield of 51% in acetonitrile while the **150**-catalysed reaction provided product **155** in 53% (Scheme 2.13). The **149**-catalysed reaction produced a yield of 66% and these results indicated a relatively minor catalytic effect of these anion receptors in solution, possibly due to solvent competition for the receptor binding sites or a dilution effect where the presence of the H-bond donating receptors was negated by the dilute conditions employed.
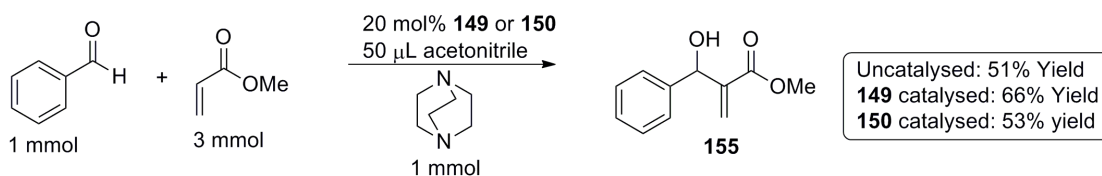
Scheme 2.13: Preliminary catalysis of DABCO promoted MBH reaction of benzaldehyde (1 equiv) and methyl acrylate (3 equiv) in the presence of 50 µL acetonitrile using 20 mol% **149** or **150**.

As a result of the poor performance in acetonitrile, receptors **145**-**151** were tested for their catalytic effects under neat reaction conditions (Table 2.11). The uncatalysed reaction produced a yield of 34% while the use of 20 mol% of the simple aliphatic non-acidic isophthalamide **145** gave a 10% yield improvement. The product yield obtained from **146**, **147** & **149** increased with increasing acidity of the amide N-H ranging from 50% yield for the 4-trifluoromethylphenyl substituted isophthalamide catalyst **146** to 71% for the 3,5-*bis*(trifluoromethyl)phenyl substituted thioamide **149**. The *p*-nitro substituted acidic receptor **150** yielded disappointing results with 51% isolated yield while the hybrid amide/*N*-acyl sulfonamide **151** gave a yield of 76%.

Table 2.11: Catalysis of Baylis-Hillman reaction of benzaldehyde and methyl acrylate using **145-151** as H-bond donating organocatalysts.[a]

Receptor	Yield [%][a]	k_{obs} x 10^{-2} [h^{-1}][b]	k_{rel}	k_{rel} Lit[145]
Uncatalysed	34	0.82	1.0	1.0
145[c]	44	0.77	0.9	1.7
146[c]	50	0.55	0.7	1.2
147	68	2.38	2.9	5.2
148[d]	-[d]	-[d]	-[d]	-[d]
149	71	2.5	3.1	5.4
150	51	2.68	3.3	5.8
151	76	3.19	3.9	6.9

[a]Reagents and conditions: benzaldehyde (1 equiv), DABCO (1 equiv), methyl acrylate (3 equiv), catalyst **145-151** (20 mol%), r.t., 20 h. Isolated yield. [b]Initial rates, 10 equiv methyl acrylate used; (E)-stilbene used as an internal standard for ^{1}H NMR spectroscopy. [c]Poor solubility in kinetic experiment. [d]Not determined due to complete insolubility of catalyst in these conditions.

The kinetics of the uncatalysed and **145**-**151** catalysed reactions were monitored by ^{1}H NMR spectroscopy using a method previously described by Connon & Maher.[145] The reaction was conducted under pseudo-first order conditions with respect to benzaldehyde using E-stilbene as an internal standard. Initially, a small sample was taken, diluted in CDCl$_3$ and immediately analysed by ^{1}H NMR spectroscopy. Samples were subsequently taken at a number of intervals over 8 hours. The ratio of benzaldehyde: E-stilbene was calculated at each time point and the rate constant was determined from the slope of a graph of –Log$_e$[benzaldehyde] versus time (Table 2.11 & Figure 2.22). A slightly lower initial rate constant was observed for **145** & **146** compared to the uncatalysed process, possibly due to poor solubility of these catalysts in the reaction media. The rate constant for the uncatalysed reaction was determined to be 0.82 x 10^{-2} h^{-1} following 3 replicates, significantly higher than the 0.46 x 10^{-2} h^{-1} value previously observed by Connon and Maher for this reaction.[145] This was discussed with the external examiner at the *viva-voce* and the difference was ascribed to experimental technique for sample collection, specifically evaporation of methyl acrylate throughout the reaction, causing a decrease in dilution and increased reaction rate. It was noted that the use of a more thoroughly sealed reaction vessel could inhibit this evaporation. When the rates of the organocatalysed reactions are compared to Connon & Maher's uncatalysed reaction rate, a more pronounced catalytic effect is observed (Table 2.11). Based on this uncatalysed rate

constant, all catalysts display positive catalytic effects. Catalyst **147** generated a 2.9 fold increase in initial rate constant compared to the uncatalysed process while the thioamide **149** gave a 3.1 fold increase, matching the trend of the increasing yields from **149** compared to **147** (71% vs 68% yield for **149** vs **147**).

The yield from the **150**-catalysed reaction was 51% while an initial rate constant of 2.68×10^{-2} h^{-1} was observed, representing a faster rate compared to the more successful, higher yielding catalysts **147** & **149**. This was ascribed to possible strong binding of one of the several anionic species involved in the reaction cycle causing product inhibition, supported by previous anion binding studies showing very strong binding interactions for AcO^- even in highly competitive media ($K_{ass} = 16,600$ M^{-1} in CD_3CN, $K_{ass} = 5,200$ M^{-1} in DMSO-d_6). Receptor **151** was deemed to be the most successful catalyst from **145**-**151**; this catalyst produced a 3.9 fold increase in rate constant over the uncatalysed system and also gave the highest isolated yield. It may be envisaged that **151** would possess sufficient acidity to protonate DABCO, leading to catalyst quenching. However, given the significant yield and rate enhancements observed, this was deemed not to occur, instead high catalyst acidity may have favoured proton transfer between the starting material and catalyst, thus enhancing the rate.
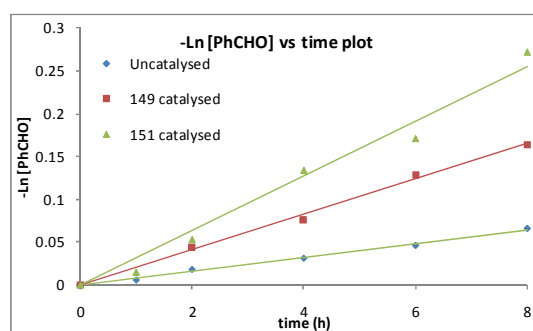
Figure 2.22: Kinetic plots and least square fits of –Ln[PhCHO] vs time for receptor **149** & **151** catalysed Baylis-Hillman reaction. The uncatalysed reaction is also shown.

In order to probe high catalytic activity of **151**, a more acidic *bis-N*-acyl sulfonamide was considered (receptor **156**) which would possess two highly acidic sulfonamide N-H groups in an isophthaloyl scaffold. Receptor **156** was synthesised from commercially available isophthalic acid. A number of different reactant ratios were investigated for this synthesis and the successful system comprised of 1 equiv of isophthalic acid, 2.5 equiv primary sulfonamide

154, 5 equiv EDCI and 3.5 equiv DMAP in 50:50 dichloroethane: *t*-butanol (Scheme 2.14). After treatment with Amberlyst 15 anion exchange resin and ethyl acetate, the mixture was filtered through a plug of silica gel and solvent removed *in vacuo*. Chromatographic purification provided **156** in 61% yield. LC-MS analysis in negative mode produced an ion at m/z 715 corresponding to the M-H ion while ^{1}H & ^{13}C NMR spectroscopy were used to verify the product. Key ^{1}H NMR spectroscopic peaks included the isophthaloyl H-2 proton at 8.49 ppm, the H-2' signal as a singlet integrating for 4 protons at 8.38 ppm, the H-4' signal at 8.19 ppm, a doublet at 7.86 ppm corresponding to H-4 and a triplet at 7.24 due to H-5.
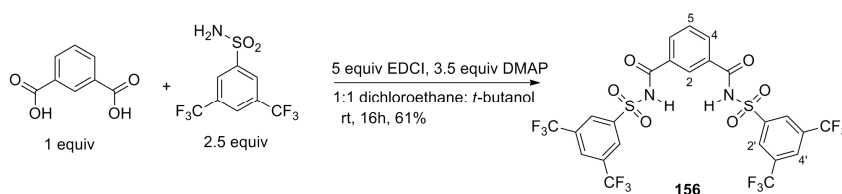
Scheme 2.14: Synthesis of *bis-N*-sulfonylated amide receptor **156**.

Due to the high level of success obtained with the hybrid amide/N-acyl sulfonamide catalyst **151** in the MBH reaction, a preliminary investigation into the catalytic activity of **156** was conducted and produced a disappointing yield of 48%. Due to its poor catalytic properties, **156** was not assessed for its anion binding properties.

2.8.1   Variation of Base in the MBH reaction using Catalyst 151

Having determined the hybrid amide/*N*-acyl sulfonamide **151** to be the optimal catalyst, the nucleophilic base was varied in order to investigate the effects of this species on the catalytic performance. In the reaction of methyl acrylate with benzaldehyde, DBU (1,8-diazabicycloundec-7-ene), PPh₃ (triphenylphosphine) and DMAP were evaluated and provided inferior yields compared to DABCO (Table 2.12).

Table 2.12: MBH reaction of benzaldehyde with methyl acrylate catalysed by **151** with varying base.
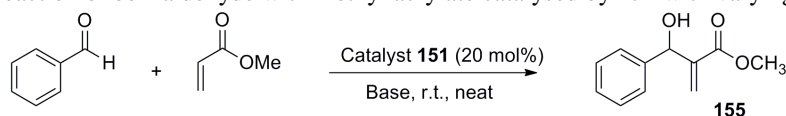
Base	mol% 151	Time (h)	Yield %[a]
DABCO	-	20	34
DABCO	20	20	76
DMAP	-	20	8
DMAP	20	20	41
DBU	-	20	33
DBU	20	20	34
PPh$_3$	-	20	trace
PPh$_3$	20	20	trace

[a]Isolated yield after flash chromatography.

2.8.2 Variation of Substrates in the MBH reaction using Catalyst 151

Having verified DABCO to be the optimum base, the aldehyde component was varied. Various activated and deactivated aldehydes were evaluated in the **151** catalysed MBH reaction with methyl acrylate and compared to the uncatalysed reaction. In all of the **151** catalysed reactions, yield improvement was observed in particular for electron donating 2-methoxybenzaldehyde and 4-methoxybenzaldehyde where a 9.2 fold and 4.8-fold increase product yield was noted (Table 2.13). Reactions of methyl- and nitro-substituted benzaldehydes catalysed by **151** produced smaller yield enhancements. Finally, reactions of a number of Michael acceptors with benzaldehyde were investigated including *tert*-butyl acrylate and 2-cyclohexenone. The uncatalysed reaction with *tert*-butyl acrylate produced significantly lower yields compared to methyl acrylate while a 7-fold increase in product yield was obtained in the presence of catalyst **151** (Table 2.13). A 15-fold increase in product yield was obtained for the reaction of cylohexenone with benzaldehyde.

Table 2.13: DABCO promoted MBH reaction using a variety of substrates catalysed by **151**.
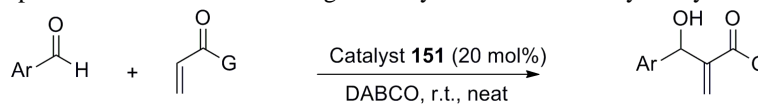
Ar	G	mol% 151	Time (h)	Yield %[a]
C_6H_5	OMe	-	20	34
C_6H_5	OMe	20	20	76
o-$O_2NC_6H_4$	OMe	-	1	79
o-$O_2NC_6H_4$	OMe	20	1	86
o-MeC_6H_4	OMe	-	42	6
o-MeC_6H_4	OMe	20	42	22
o-$MeOC_6H_4$	OMe	-	72	6
o-$MeOC_6H_4$	OMe	20	72	55
p-FC_6H_4	OMe	-	42	69
p-FC_6H_4	OMe	20	42	82
p-MeC_6H_4	OMe	-	36	19
p-MeC_6H_4	OMe	20	36	38
p-$MeOC_6H_4$	OMe	-	96	4
p-$MeOC_6H_4$	OMe	20	96	19
C_6H_5	O-tBu	-	20	4
C_6H_5	O-tBu	20	20	28
C_6H_5	(cyclohexenone)	-	38	4
C_6H_5	(cyclohexenone)	20	38	59

[a]Isolated yield after flash chromatography

A correlation was observed between the yield from the both the uncatalysed and **151**-catalysed reactions and the electronic nature of the benzaldehyde substitutuent. In the case of the *para*-substituted benzaldehyde derivatives, the MBH adduct yield increased as the electron withdrawing nature of the substituent increased. This was as expected due to electron withdrawing groups making the aldehyde carbonyl more electrophilic. The recyclability of **151** was investigated the DABCO promoted MBH reaction of benzaldehyde with methyl acrylate. In each case, the catalyst was recovered following chromatographic purification and re-used with less than 5% reduction in catalytic activity after 3 cycles.

2.8.3   Investigation into Catalytic Mechanism

It is proposed that the catalytic activity of the anion receptors **145**-**151** in the MBH reaction may in part be due to their ability to coordinate anionic species through acidic N-H groups with additional interactions also possible from acidic C-H groups in the cleft. In general, the

increase in N-H polarisation through the use of electron withdrawing functional groups led to enhanced catalytic activity, consistent with the previously described anion binding studies. For the strong oxyanion receptor **150**, catalyst inhibition may have lead to the high reaction rate and low yield. Pre-organisation of **149** into its *syn-syn* conformation may have contributed to its catalytic success.

Furthermore, a number of receptors which underwent proton transfer effects with basic AcO⁻ and BzO⁻ anions were highly successful MBH catalysts, perhaps indicative of a cooperative effect, particularly in light of reported mechanistic studies highlighting the rate-determining nature of the proton transfer step as opposed to the Michael addition step.[164] The acidic receptors may have acted as a proton shuttle promoting this step in combination with aldehyde activation or anionic intermediate binding. In an attempt to investigate binding between the catalyst and reaction starting materials, a ^{1}H NMR spectroscopy binding study of a number of catalysts with MBH components and adduct was undertaken and the results compared to the chemical shift changes in the presence of 1 equivalent AcO⁻.

2.8.4   Substrate & Product Binding Studies to Catalysts 149-151

^{1}H NMR spectroscopic binding studies of **151** in the presence of 1 equivalent of reactants or MBH product revealed minor chemical shift changes (Table 2.14). The amide N-H signal migrated upfield for methyl acrylate which may be suggestive of a proton transfer effect to the acrylate, possibly activating it towards nucleophilic attack. A slight upfield amide N-H migration was also observed upon addition of **155**, suggesting no product inhibition occurred. The minor downfield shift observed for benzaldehyde was suggestive of minimal binding and activation.

Table 2.14: Binding study of **151** with reactants and MBH product by ^{1}H NMR spectroscopy in CD$_3$CN.

	Δδ (Amide N-H)	Δδ (H-2)	Δδ (H-2'')	Δδ (H-2')
151 + benzaldehyde	0.0072	-0.0004	-0.0004	0.0016
151 + methyl acrylate	-0.0112	-0.0008	-0.0026	0.0032
151 + MBH adduct **155**	-0.0048	0.0001	0.0014	0.0034
151 + 1 equiv acetate	-0.0498	0.0038	-0.0379	0.0188

Thioamide **149** produced a 71% yield and binding studies showed a broadening and considerable downfield migration of 0.19 ppm and 0.16 ppm of the thioamide N-H groups upon addition of 1 equivalent of benzaldehyde and **155** respectively (Table 2.15). As expected, smaller downfield migrations of the order 0.002 ppm were observed for the H-2' protons while the isophthaloyl signals appeared to move slightly upfield. A smaller thioamide N-H downfield migration was observed following addition of methyl acrylate of approximately 0.02 ppm with H-2' and H-2 downfield shifts of 0.009 ppm. Therefore it appeared that **149** bound strongly to benzaldehyde and MBH product but not to methyl acrylate, suggesting that benzaldehyde activation and product inhibition may have occurred.

Table 2.15: Binding study of **149** with reactants and MBH product monitored by ^{1}H NMR spectroscopy

	Δδ (Thioamide N-H)	Δδ (H-2')	Δδ (H-2)
149 + benzaldehyde	0.1855[a]	0.0023	-0.0025
149 + methyl acrylate	0.0162	0.0009	0.0009
149 + MBH adduct **155**	0.1624[a]	0.0034	-0.0014
149+ 1 equiv acetate	-[b]	0.0266	0.1818

[a]Significant peak broadening observed. [b]Peak disappeared

Binding of **150** with the reactants and MBH product produced smaller chemical shift migrations compared to **149** with downfield shifts of 0.025 ppm and 0.014 ppm for the amide N-H proton with benzaldehyde and MBH adduct respectively (Table 2.16). Similar to **149**, acrylate binding was significantly weaker compared to benzaldehyde or **155** interactions. It may be considered that while **150** had weaker binding strengths to the neutral reactants and product compared to **149**, the former may have bound anionic intermediates more strongly, leading to inhibition. This theory is supported by the strong anion binding results observed for **150** with carboxylates.

Table 2.16: Binding study of **150** with reactants and MBH product monitored by ^{1}H NMR spectroscopy.

	Δδ (Amide N-H)	Δδ (H-2)
150 + benzaldehyde	0.0254	0.012
150 + methyl acrylate	0.0083	0.0063
150+ MBH adduct **155**	0.0135	0.0068
150 + 1 equiv acetate	3.486	0.5763

The role of the anion binding sites in catalysis for **147** & **151** was further investigated through ^{1}H NMR spectroscopic kinetic experiments in the presence of 1 equivalent of tetra-*n*-butyl

ammonium benzoate. Under these conditions, substantial reduction in rate constants was observed. In the case of **147**, an initial rate constant of 0.45 h^{-1} was obtained in the presence of BzO$^-$, 81% lower than the value of 2.38 h^{-1} without added anion. In addition, **151** with BzO$^-$ gave a rate constant of 1.17 h^{-1}, 63% reduced compared to that without BzO$^-$. This was ascribed to competition between the anionic reaction intermediates and BzO$^-$ for the H-bonding sites of these catalysts. Therefore, it was proposed that binding of negatively charged reaction intermediates had a significant catalytic effect through anionic intermediate stabilisation promoting the reaction. In the presence of BzO$^-$, the H-bond donating groups were unavailable for transition state binding or proton shuttling, both of which may promote the MBH reaction.

A catalytic mechanism is postulated in an attempt to rationalise the successful catalytic results of **151** (Scheme 2.15). It is proposed that electrophile activation does not play a significant role due to the small chemical shift migrations of **151** in the presence of 1 equivalent of benzaldehyde. Rather, it is more likely that the negatively charged betaine intermediate **A** generated from conjugate addition of the tertiary amine catalyst to methyl acrylate was bound by **151**. Aldol addition to the aldehyde then generated Zwitterionic **B**. H-bonding interactions between the sulfonamide N-H group and the *β*-alkoxide anion may have activated intermediate towards a rate determining proton transfer *via* the catalyst *N*-acyl sulfonamide group. This transition state may act as a proton shuttle, facilitating proton migration, elimination of the tertiary amine base and enhancing the reaction rate.[164,189,194,195] Similar H-bond interactions promoting the proton transfer have previously described for protic additives such as methanol[164] and a *bis*-thiourea organocatalyst.[10]
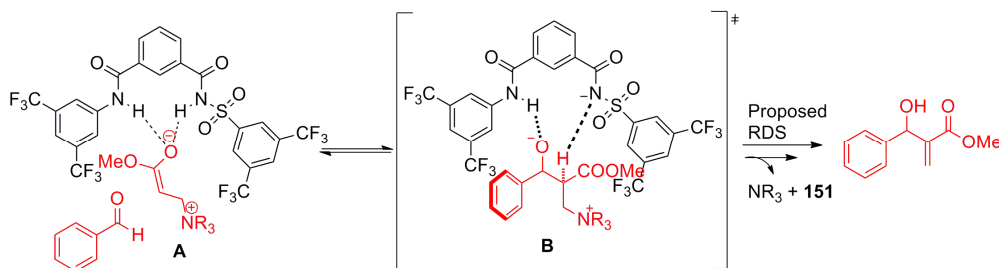
Scheme 2.15: Postulated mode of action of **151** in MBH reaction with cyclic transition state **B** proposed.

2.9 Further Bifunctional Receptors

Having tested a range of bisamide and thioamide based receptors **145**-**150** and a bifunctional hybrid amide/*N*-acyl sulfonamide **151** for anion binding properties and catalysis and also having confirmed a correlation between their anion coordination properties and catalytic activity, alternative urea based bifunctional receptors were considered (Figure 2.24).

2.9.1 Bifunctional Receptor Design
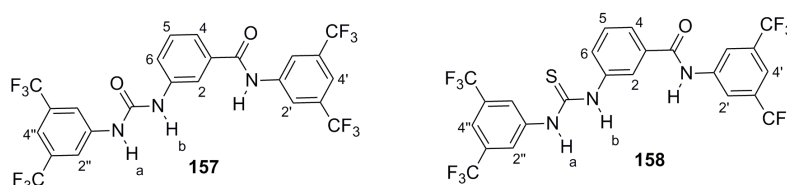
Figure 2.24: Structure of phase 2 acidic bifunctional receptors **157** & **158**.

Urea and thiourea groups have been applied as receptors for anionic species[79-84,86,215] and have also been extensively used as H-bond donating organocatalysts.[10,12,145,147] As previously described, isophthalamide receptors incorporating 3,5-*bis*(trifluoromethyl)phenyl groups as part of the amide moiety led to significant improvements in anion binding abilities and catalysis in the MBH reaction. It was considered that other receptors could be further optimised through inclusion of 3,5-*bis*(trifluoromethyl)phenyl rings into a bifunctional receptor consisting of a (thio)urea group and an amide motif with applications as anion receptors and H-bond donating organocatalysts for the MBH reaction. As detailed in Chapter 1, Hamilton *et al.* successfully applied a urea/amide hybrid receptor containing an oxyanion hole in the addition of a thiol to a maleimide.[14] Through ^{1}H NMR spectroscopic binding studies, they confirmed that the catalyst operated through cooperative H-bonding to the anionic transition state from the urea and aminopyridine functionalities, stabilising the developing negative charge over the course of the reaction and producing a rate enhancement.

It was envisaged that a bifunctional (thio)urea/amide hybrid could be suitably pre-organised towards binding a number of the anionic intermediates in the MBH reaction. It was also hoped that such a hybrid molecule may enhance the proton transfer step of the MBH reaction

mechanism by acting as a proton shuttle. In addition, based on previous reports by Schreiner *et al.*, the thiourea analogue **158** was expected to possess enhanced rigidity due to interactions between the sulphur atoms and H-2'' proton in the *ortho*-position of the 3,5-*bis*(trifluoromethyl)phenyl ring which could improve binding ability and catalytic activity.

2.9.2   Synthesis of Bifunctional Receptors 157 & 158

The EDCI mediated coupling of 3,5-*bis*(trifluoromethyl)aniline with 3-nitrobenzoic acid at room temperature was conducted and following extractive work-up, the product was recrystallised from dichloromethane to give **159** in 92% yield (Scheme 2.16). The product's structure was confirmed by LC-MS and ^{1}H & ^{13}C NMR spectroscopy. LC-MS analysis produced a MH$^+$ peak at m/z 378 while key ^{1}H NMR spectroscopic peaks included the amide N-H signal at 9.38 ppm; relevant COSY interactions and peak assignments are given in Table 2.17. The singlet integrating for 2 protons at 8.31 ppm was ascribed to H-2' while the singlet at 7.75 ppm was assigned to H-4'.
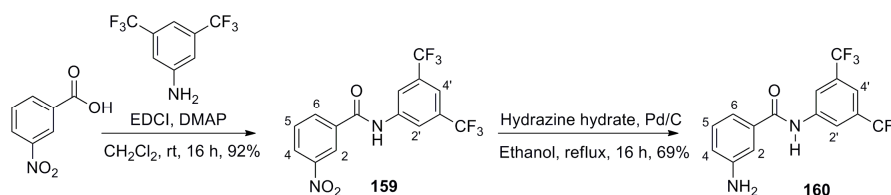
Scheme 2.16: Synthesis of **159** & **160** through EDCI coupling of 3-nitrobenzoic acid with 3,5-*bis*(trifluoromethyl)aniline followed by reduction using hydrazine hydrate.

Table 2.17: List of COSY interactions and ^{1}H NMR assignents of nitro/amide hybrid intermediate **159**.

Structure	Proton	δ (ppm)	Correlated With δ (ppm)	Correlated proton
	H-4	8.37-8.41 (m, 1H)	7.74 (m, 1H)	H-5
	H-6	8.27-8.31 (m, 1H)	7.74 (m, 1H)	H-5
	H-2	8.73-8.75 (m, 1H)	8.37-8.41 (m, 1H)	H-4
	H-2	8.73-8.75 (m, 1H)	8.27-8.31 (m, 1H)	H-6

The reduction of the aryl NO$_2$ group to an aryl NH$_2$ group was successfully achieved through reaction of **159** with hydrazine monohydrate in ethanol using a catalytic quantity of 10% palladium on carbon (Scheme 2.16). After 16 hours of reflux, the mixture was filtered through a plug of silica gel and aqueous work-up conducted.[44] Flash chromatography eluted the product in 69% yield while LC-MS and ^{1}H & ^{13}C NMR spectroscopy confirmed the successful reduction. An LC-MS signal at m/z 348 corresponded to the MH$^+$ ion and key ^{1}H
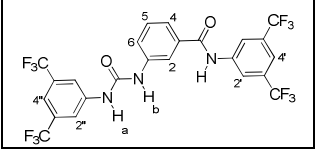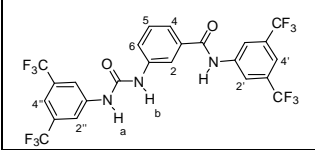
NMR spectroscopic resonances confirming the synthesis included the broad NH_2 signal at 4.40 ppm, the amide N-H at 9.03 ppm and H-2' and H-4' signals at 8.34 ppm and 7.73 ppm respectively. The H-2 proton occurred at 7.19 ppm while H-4, H-5 & H-6 were observed at 6.84-6.89 ppm, 7.24 ppm and 7.20-7.24 ppm respectively.

The final step in the synthesis involved reaction of intermediate **160** with 3,5-*bis*(trifluoromethyl)isocyanate and 3,5-*bis*(trifluoromethyl)isothiocyanate to give urea/amide hybrid **157** and thiourea/amide hybrid **158** respectively (Scheme 2.17). Receptor **157** was obtained in 98% yield following room temperature stirring for 24 hours and chromatographic purification. An LC-MS peak at m/z 604 corresponded to the MH^+ ion. Key ^{1}H NMR spectroscopic peaks included the amide N-H group at 10.83 ppm, urea N-H_a and N-H_b peaks at 9.48 & 9.27 ppm and H-2' and H-4' signals at 8.51 ppm and 7.78 ppm respectively. The H-2'' and H-4'' signals appeared at 8.15 ppm and 7.62 ppm respectively while the H-2, H-4, H-5, & H-6 signals occurred at 8.09 ppm, 7.65 ppm, 7.49 ppm and 7.71 ppm respectively. COSY & NOESY ^{1}H NMR interactions aided peak assignment and are given in Table 2.18.
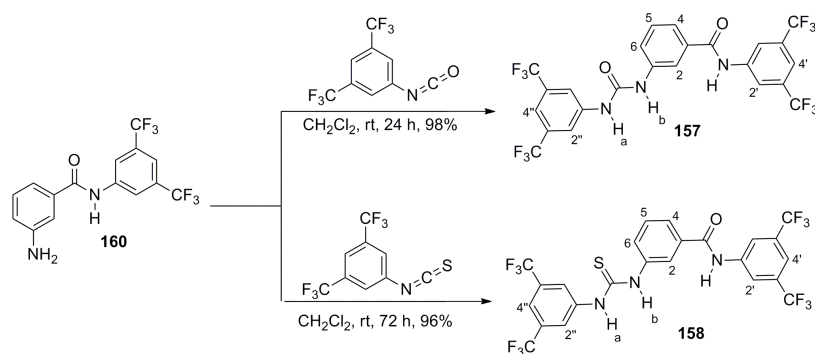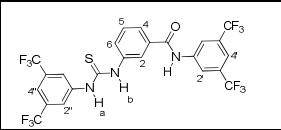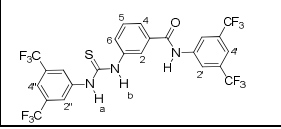
Scheme 2.17: Synthesis of urea/amide hybrid **157** and thiourea/amide hybrid **158**.

Table 2.18: List of COSY and NOESY interactions and ^{1}H NMR spectroscopic peak assignments of **157**.

Structure	Proton	δ (ppm)	Correlated With δ (ppm)	Correlated proton
COSY interactions	H-2'	8.51 (s, 2H)	7.78 (s, 1H)	H-4'
	H-2''	8.15 (s, 2H)	7.62 (s, 1H)	H-4''
	H-4	7.65 (d, J = 7.63 Hz, 1H)	7.49 (t, J = 7.63 Hz, 1H)	H-5
	H-6	7.71 (d, J = 7.63 Hz, 1H)	7.49 (t, J = 7.63 Hz, 1H)	H-5
	Amide N-H	10.83 (s, 1H)	8.51 (s, 2H)	H-2'
	Amide N-H	10.83 (s, 1H)	8.09 (s, 1H)	H-2
NOESY interactions	Amide N-H	10.83 (s, 1H)	7.65 (d, J = 7.63 Hz, 1H)	H-4
	Amide N-H	10.83 (s, 1H)	8.09 (s, 1H)	H-2
	Amide N-H	10.83 (s, 1H)	8.51 (s, 2H)	H-2'
	N-H$_a$	9.48 (s, 1H)	9.27 (s, 1H)	N-H$_b$
	N-H$_a$	9.48 (s, 1H)	8.15 (s, 2H)	H-2''
	N-H$_b$	9.27 (s, 1H)	7.71 (d, J = 7.63 Hz, 1H)	H-6
	H-2'	8.51 (s, 2H)	7.78 (s, 1H)	H-4'
	H-2''	8.15 (s, 2H)	7.62 (s, 1H)	H-4''

The thiourea/amide hybrid **158** was obtained in 96% yield following chromatographic purification. LC-MS analysis produced a peak at m/z 620 corresponding to the MH[+] signal and ^{1}H & ^{13}C NMR spectroscopy were used to characterise the product. Key ^{1}H NMR spectroscopic resonances included an amide N-H peak at 9.19 ppm and two thiourea N-H peaks at 8.77 and 8.69 ppm. In addition to these signals there were also H-2'' & H-4'' signals at 8.14 & 7.79 ppm and H-2' & H-4' peaks at 8.34 & 7.75 ppm respectively. The central ring H-2, H-4, H-5 & H-6 protons were observed at 8.01 ppm, 7.68 ppm, 7.58 ppm & 7.83 ppm respectively while a ^{13}C NMR spectroscopic signal at 180 ppm was ascribed to the C=S group. COSY and NOESY interactions aided peak assignment and are shown in Table 2.19.

Table 2.19: List of COSY and NOESY interactions and ^{1}H NMR spectroscopy peak assignments of **158**.

Structure	Proton	δ (ppm)	Correlated With δ (ppm)	Correlated proton
COSY interactions	H-2'	8.34 (s, 2H)	7.75 (s, 1H)	H-4'
	H-2''	8.14 (s, 2H)	7.79 (s, 1H)	H-4''
	H-4	7.68 (d, J = 7.63 Hz, 1H)	7.58 (t, J = 7.63 Hz 1H)	H-5
	H-6	7.83 (d, J = 7.63 Hz, 1H)	7.58 (t, J = 7.63 Hz 1H)	H-5
NOESY interactions	Amide N-H	9.19 (s, 1H)	8.34 (s, 2H)	H-2'
	Amide N-H	9.19 (s, 1H)	8.01 (s, 1H)	H-2
	Amide N-H	9.19 (s, 1H)	7.68 (d, J = 7.63 Hz, 1H)	H-4
	N-H$_b$	8.77(s, 1H)	8.01 (s, 1H)	H-2
	N-H$_a$	8.69 (s, 1H)	8.14 (s, 2H)	H-2''
	H-2'	8.34 (s, 2H)	7.75 (s, 1H)	H-4'
	H-2''	8.14 (s, 2H)	7.79 (s, 1H)	H-4''

2.9.3   Binding Studies on Phase 2 Receptors 157 & 158

The anion binding properties of **157** & **158** were investigated using ^{1}H NMR spectroscopic titrations with Br$^-$, Cl$^-$, AcO$^-$ and BzO$^-$ as tetra-*n*-butylammonium salts in CD$_3$CN, monitoring all three N-H signals. K$_{ass}$ values were determined for each N-H group using WINEQNMR.[202]

Receptor 157

Receptor **157** contained both an amide N-H group and a urea moiety and was therefore expected to bind through either cooperative multi-point interaction in a cleft-like system or possibly through separate binding events at the urea and amide groups. The electron-withdrawing 3,5-*bis*(trifluoromethyl)phenyl groups in the structure would bring enhanced acidity, strengthening the binding interactions. Titrations of urea/amide hybrid **157** with Br$^-$ in CD$_3$CN produced typical expected N-H$_a$ & N-H$_b$ binding curves while the shape of the amide N-H binding curve was indicative of significantly weaker binding (Figure 2.25a). K$_{ass}$ values calculated for each of these protons were fitted to a 1:1 model (Table 2.20). Downfield chemical shift changes of 2.50 ppm, 1.98 ppm and 0.30 ppm were observed corresponding to urea N-H$_a$ & N-H$_b$ and amide N-H while K$_{ass}$ values of 2,800 M^{-1} & 2,700 M^{-1} and 140 M^{-1} were obtained respectively. This clearly shows the higher anion binding proclivity of ureas compared to amides.
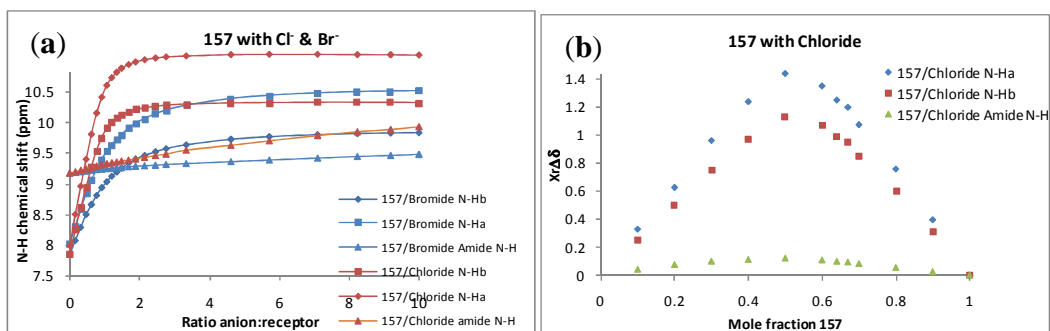
Figure 2.25: (a) Titration curves for **157** with Br- and Cl- in CD$_3$CN for urea N-H$_a$ & N-H$_b$ groups and also the amide N-H. (b) JOB plot for **157** with Cl- in CD$_3$CN confirming 1:1 stoichiometry for all N-H protons.

As observed for previous receptors, Cl- was bound with a considerably larger K$_{ass}$ compared to Br- and this was also evident from the shape of the binding curves. Chemical shift changes of 3.11 ppm, 2.48 ppm & 0.77 ppm were observed for urea N-H$_a$, urea N-H$_b$ and amide N-H protons resulting in K$_{ass}$ values of 15,300 M^{-1}, 16,800 M^{-1} & 100 M^{-1} respectively (Table 2.20). Interestingly, the amide N-H K$_{ass}$ for **157** with Cl- was lower than with Br-, opposite to the selectivity previously observed for diamide receptors **145**-**151**. This may be ascribed to predominant anion binding at the urea site with additional possible cooperative interactions with the amide N-H group, an effect which may be more pronounced for Br- due to its larger size. JOB plot analysis of **157** with Br- and Cl- were plotted for each N-H group and were indicative of 1:1 binding in all cases (Figure 2.25b).

Table 2.20: Binding constants for both urea N-H protons and also amide N-H group with % errors for **157** with anions determined in CD$_3$CN.

Structure	K$_{ass}$ urea N-H$_a$/M^{-1} [% error]	K$_{ass}$ urea N-H$_b$/M^{-1} [% error]	K$_{ass}$ Amide N-H/ M^{-1} [% error]	Anion
	2,800 [1.5%]	2,700 [1.5%]	140 [9.5%]	Br-
	15,300 [2.0%]	16,800 [1.0%]	100 [6.7%]	Cl-
	17,800 [12.8%]	24,400 [6.7%]	550 [22.0%]	AcO-
	16,100 [14.0%]	12,800 [23.6%]	280 [17.0%]	BzO-

^{1}H NMR spectroscopic titration curves for **157** with AcO- and BzO- in CD$_3$CN were indicative of very tight binding with a large downfield chemical shift migration of the urea protons of 4.5-4.9 ppm followed by a sharp inflexion point at a ratio of 1:1 receptor:anion. Particularly high binding was observed for urea N-H$_a$ and N-H$_b$ protons binding AcO- with K$_{ass}$ values of 17,800 M^{-1} & 24,400 M^{-1} respectively (Table 2.20). Slightly weaker urea N-H K$_{ass}$ values

were observed with BzO⁻; 16,100 M⁻¹ & 12,800 M⁻¹ for urea N-H$_a$ & N-H$_b$ respectively. The amide N-H proton migrated linearly downfield for approximately 0.7 ppm up to the addition of 1 equiv anion, followed by a decrease in slope to a less steep profile. K$_{ass}$ values for amide N-H binding of 550 M⁻¹ and 280 M⁻¹ were calculated for AcO⁻ and BzO⁻ respectively when fitted to a 1:1 model.
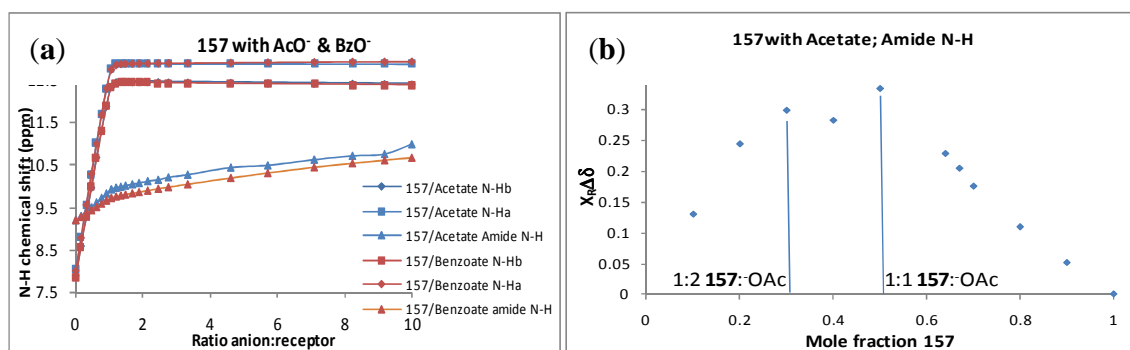
Figure 2.26: Titration curves for **157** with AcO⁻ and BzO⁻ in CD₃CN for urea N-H$_a$ & N-H$_b$ and amide N-H signals. (b) JOB plot of amide N-H proton of **157** with AcO⁻ showing 1:2 receptor:AcO⁻ and also 1:1 binding.
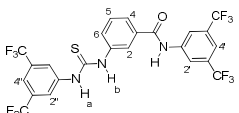
JOB plot analysis revealed 1:1 binding for the urea N-H$_a$ and N-H$_b$ protons in all cases while the amide N-H protons were bound in alternative stoichiometries. The amide N-H JOB plot of **157** with BzO⁻ disclosed a 1:2 receptor anion stoichiometry with a plot maximum at approx 0.3 – 0.4 mole fraction of **157**. In the case of AcO⁻, two maxima were observed, one at 0.5 mole fraction **157** and another at approximately 0.3 – 0.4 mole fraction **157** corresponding to both 1:1 and 1:2 **157**:AcO⁻ binding (Figure 2.26b). This may be due to initial 1:1 binding up to the addition of 1 equiv AcO⁻ followed by a 1:2 **157**:anion complex formation where the amide N-H could bind to an anion and also form cooperative binding to an anion coordinated by the urea N-H groups. The ability of **157** to simultaneously coordinate two anionic species could facilitate dual enhancement through binding of the betaine intermediate and the aldehyde carbonyl group, activating these species and positioning them in close proximity for reaction.

Receptor 158

Thiourea/amide hybrid receptor **158** was also tested for its anion binding ability in CD₃CN. ¹H NMR spectroscopic titrations with Br⁻ produced titration curves which were indicative of relatively weak binding with less sharp inflexion points (Figure 2.27a). Chemical shift

106

changes of 2.0-2.6 ppm for both thiourea N-H protons and approximately 0.4 ppm for amide N-H were observed while K_{ass} values of thiourea N-H_a and N-H_b groups were of the order of 1600-1700 M^{-1} with a considerably weaker K_{ass} of 190 M^{-1} observed for the amide N-H (Table 2.21). JOB plot analysis of this binding interaction showed 1:1 **158**:Br^- interaction. Binding of **158** with Cl^- was considerably stronger indicated by K_{ass} values of the order of 12,800-15,130 M^{-1} and binding curves which were characteristic of strong binding systems (Table 2.21 & Figure 2.27a). A K_{ass} value of 185 M^{-1} was found for the amide N-H binding Cl^-, slightly lower than the binding to Br^- possibly due to the smaller Cl^- anion less effective at forming cooperative H-bonds to all three N-H groups. Interestingly, the binding curves for thiourea N-H_a & N-H_b contained a slight perturbation at 1 equivalent Cl^-, this may be due to a conformational change upon saturation of the receptor with Cl^- although there is no further evidence of this. JOB plot analysis of **158** with Br^- and Cl^- plotted for each N-H group was indicative of 1:1 binding in all cases (Figure 2.27b).

Table 2.21: Binding constants for both thiourea N-H protons and also amide N-H group of **158** with % errors in parentheses.

Structure	K_{ass} N-H_b/M^{-1} [% error]	K_{ass} N-H_a/M^{-1} [% error]	K_{ass} Amide N-H/ M^{-1} [% error]	Anion
	1,610 [1.3]	1,730 [1.4]	190 [11.9]	Br^-
	12,800 [2.0]	15,130 [1.8]	185 [12.5]	Cl^-
	-[a]	-[a]	-[a]	AcO^-
	-[a]	- No fit	160 [9.9]	BzO^-

[a]Peak disappearance preventing calculation of K_{ass}
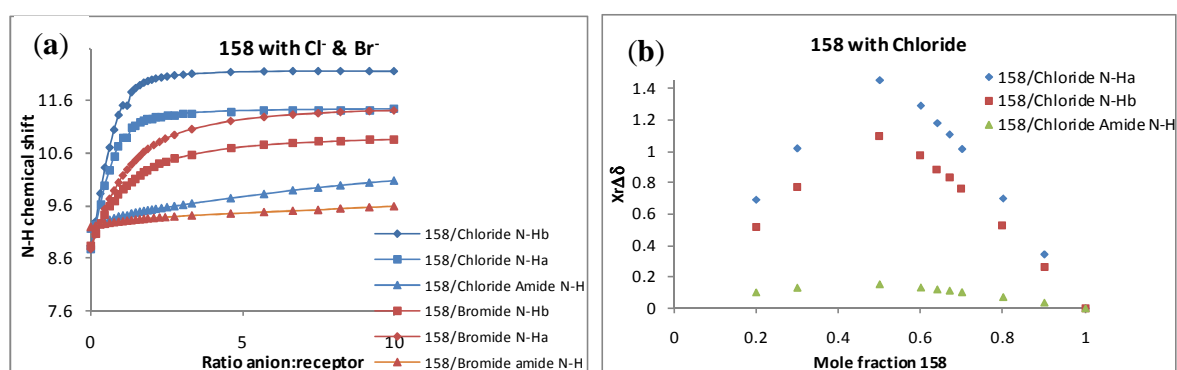
Figure 2.27: (a) Titration curves for **158** with Br^- and Cl^- in CD_3CN plotted for both thiourea N-H groups and also the amide N-H. (b) JOB plot for **158** with Cl^- in CD_3CN confirming 1:1 stoichiometry for all N-H protons.

Titration of **158** with BzO⁻ and AcO⁻ produced interesting observations. Upon addition of a small quantity of AcO⁻, severe N-H broadening followed by peak disappearance was observed for all N-H signals and as a result, the titration was monitored using aromatic H-2, H-2' and H-2'' signals. The binding curve for the H-2' signal close to the amide was indicative of weak binding with an almost linear downfield migration throughout the titration and only slight curvature present at approximately 1 equiv AcO⁻ (Figure 2.28).

The H-2'' signal adjacent to the thiourea group migrated linearly downfield up to the addition of 1 equiv AcO⁻ and after this point, there is evidence of a shift in equilibrium towards the suggested N-H proton transfer event indicated by the H-2'' migration upfield (Figure 2.28). A similar but less severe effect was also observed for the H-2 signal located between the amide and thiourea binding sites with JOB plot confirming dominant 1:1 **158**:AcO⁻ interactions. Overall, this behaviour may be attributed to proton transfer from the thiourea N-H group to the basic AcO⁻ anion with an associated conformational change and further weak binding through the H-2' proton close to the amide group. Similar binding profiles were observed previously with a urea/sulfonamide receptor for basic anions by Gale *et al.*[89] where the first equivalent of AcO⁻ bound to the receptor deshielding the urea N-H groups and further additions promoted sulfonamide deprotonation and an upfield shift of the urea N-H resonance. Fabbrizzi *et al.* reported a downfield shift of aromatic C-H groups adjacent to acidic urea protons during the addition of the first equiv of an anion followed by N-H deprtonation resulting in electron density delocalisation leading to nuclear shielding and an upfield shift of the aromatic C-H protons in close proximity to the urea.[45]
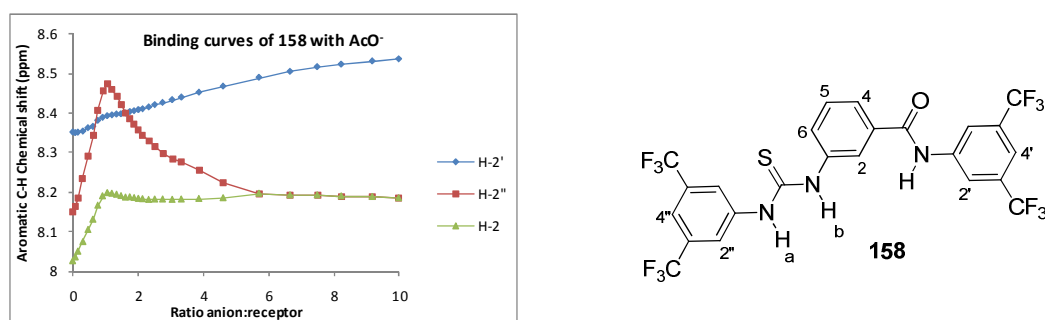
Figure 2.28: Titration curves showing migration of H-2, H-2' & H-2'' signals of **158** upon addition of AcO⁻ in CD₃CN

Titration of **158** with BzO⁻ was also accompanied by severe broadening of all N-H signals and disappearance of the thiourea N-H$_b$ resonance, therefore the titration was tracked using the remaining amide N-H group and thiourea N-H$_a$ groups. The thiourea N-H$_a$ shifted significantly downfield for approximately 4.8 ppm upon addition of 1 equiv BzO⁻ followed by a sudden plateau without change in chemical shift for the remainder of the titration. The amide N-H binding curve migrated significantly downfield with the initial additions of BzO⁻ followed by a less severe downfield migration with addition of further anion, indicative of weak binding (Figure 2.29a). The H-2' proton adjacent to the amide group migrated downfield throughout the titration while both the H-2 and H-2'' migrated downfield with addition of the first equiv BzO⁻ followed by an upfield shift for the remainder of the titration in a similar manner to that observed with AcO⁻ (Figure 2.29b). This suggested weak binding to the H-2' but stronger binding to H-2 & H-2'' binding of the BzO⁻ to the thiourea N-H followed by equilibrium lying towards N-H group proton transfer upon further BzO⁻ addition. WINEQNMR produced a very poor fit for H-2 and H-2'' of **158** binding AcO⁻ and BzO⁻ however a reasonable fit was obtained for the H-2' proton adjacent to the amide N-H group producing low K$_{ass}$ values of 105 M⁻¹ and 325 M⁻¹ for AcO⁻ and BzO⁻ titrations respectively.
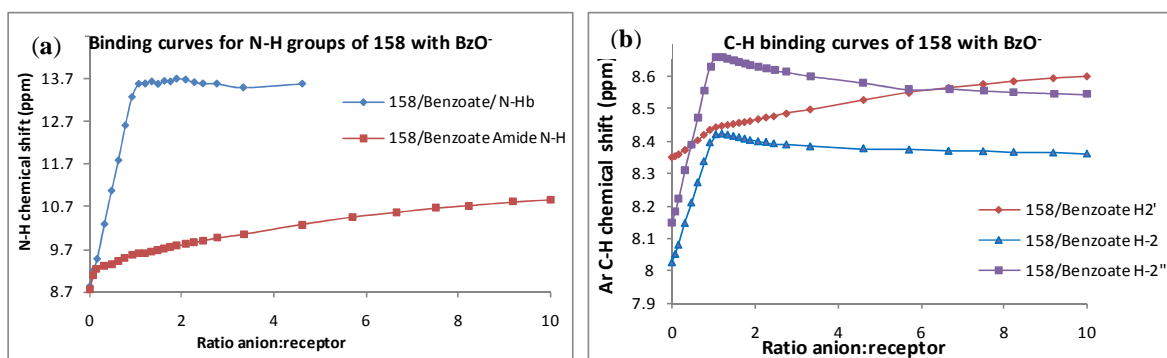
Figure 2.29: ¹H NMR spectroscopic titration curves of (a) N-H protons with increasing addition of BzO⁻ in CD₃CN. (b) Aromatic C-H titration curves for H-2, H-2' and H-2'' with increasing addition of BzO⁻ in CD₃CN.
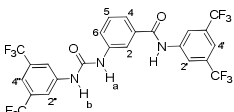
2.9.4 Binding of 157 & 158 in Competitive Solvent

Due to the relatively large error often associated with K$_{ass}$ values in excess of 10^4 M⁻¹ calculated from ¹H NMR spectroscopic data, titrations which produced high K$_{ass}$ values in CD₃CN were repeated in DMSO-d_6. Binding of **157** with Cl⁻ in DMSO-d_6 produced binding

curves characteristic of weak binding and significantly smaller chemical shift migrations of the order 0.4 -0.7 ppm compared to those in CD_3CN where downfield migrations of approximately 2.5-3.1 ppm were observed. K_{ass} values of 100 M^{-1} for the urea $N-H_a$ & $N-H_b$ groups and 65 M^{-1} for the amide N-H were obtained (Table 2.22), significantly reduced compared to those in CD_3CN.

^1H NMR spectroscopic titrations of **157** with BzO^- produced chemical shift downfield migrations of the amide and urea $N-H_a$ & $N-H_b$ signals of the order 0.12 ppm, 3.8 ppm & 3.3 ppm respectively with titration curves indicative of weak binding to the amide N-H signal but stronger interactions to the both urea N-H signals. K_{ass} values of 5,300 M^{-1} and 140 M^{-1} were calculated for both urea N-H protons and the amide N-H respectively. Binding titrations of **157** with AcO^- in DMSO-d_6 produced large chemical shift downfield migrations for the urea $N-H_a$ and $N-H_b$ signals of 3.9 ppm & 3.5 ppm respectively and a smaller migration for the amide N-H group of 0.19 ppm (Figure 2.30a). Acetate K_{ass} values of 18,000 M^{-1} and 15,000 M^{-1} were obtained for the urea $N-H_b$ and $N-H_a$ protons respectively while the amide N-H with AcO^- binding could not be fitted to a 1:1 model. These extremely high K_{ass} values in competitive DMSO-d_6 values represent a high level of selectivity of this receptor for AcO^-. Furthermore, the K_{ass} values in this solvent only slightly decreased compared to those obtained in the less competitive CD_3CN. This strong binding to anionic species in a competitive environment may have implications for anionic transition state binding in the MBH reaction.

Table 2.22: K_{ass} values for N-H groups of urea/amide **157** with anions in DMSO-d_6. % errors are given in parentheses.

Structure	K_{ass} Urea $N-H_a$/M^{-1} [% error]	K_{ass} Urea $N-H_b$/M^{-1} [% error]	K_{ass} Amide N-H /M^{-1} [% error]	Anion
	100 [4.0%]	100 [4.0%]	65 [2.0%]	Cl^-
	15,000 [5.9%]	18,000 [3.2%]	No fit	AcO^-
	5,300 [3.5%]	5,300 [3.0%]	140 [9.0%]	BzO^-
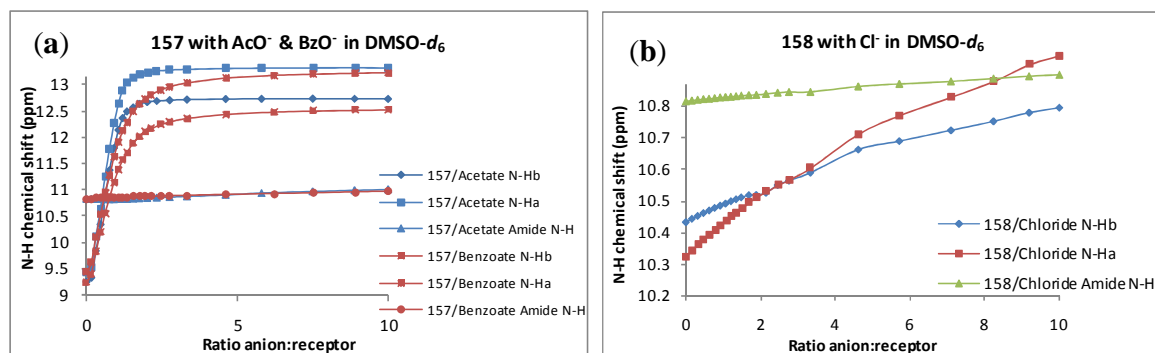
Figure 2.30: (a) Titration curves showing migration of urea & amide N-H signals of **157** upon addition of AcO⁻ & BzO⁻ in DMSO-d_6. (b) Titration curves of urea & amide N-H signals of **158** upon addition of Cl⁻ in DMSO-d_6.

For titration of **158** with Cl⁻ in DMSO-d_6, relatively small N-H chemical shift downfield migrations were observed with binding curves characteristic of weak binding systems (Figure 2.30a). In this titration, 1:1 K_{ass} values of 60 M⁻¹, 75 M⁻¹ & 40 M⁻¹ were obtained for the N-H_b, N-H_a and amide N-H groups respectively. For titrations with AcO⁻ and BzO⁻, the thiourea N-H resonances disappeared and the titrations were monitored using the amide N-H and aromatic C-H signals. In each case, the amide N-H peak was shifted upfield upon addition of the first equivalent anion followed by a linear downfield migration. It is proposed that this was due to the equilibrium favouring thiourea proton transfer following addition of the first equivalent of AcO⁻ or BzO⁻ followed by a conformational change allowing further binding to the amide N-H group, further indicated by severe broadening of many aromatic C-H signals throughout the titration.

To compare with similar titrations in CD₃CN, proton transfer effects were also observed with binding curve perturbations at 1 equiv AcO⁻ or BzO⁻, however these effects appeared less pronounced in the case of DMSO-d_6 shown by the amide N-H signal remaining visible throughout the titration. K_{ass} values for H-2' with AcO⁻ & BzO⁻ of 355 M⁻¹ and 315 M⁻¹ were calculated respectively but it was not possible to measure K_{ass} values for the H-2 or H-2'' protons due to severe peak broadening and signal overlap, presumably as a result of conformational change over the course of the titration.

Table 2.23: N-H K_{ass} values of thiourea/amide **158** with anions in DMSO-d_6. % errors are given in parentheses.

Structure	K_{ass} N-Hb/M^{-1} [% error]	K_{ass} N-Ha/M^{-1} [% error]	K_{ass} Amide N-H/ M^{-1} [% error]	Anion
	60 [16.6%]	75 [7.0%]	40 [15.0%]	Cl$^-$
	-^{a}	-^{a}	No fit	AcO$^-$
	-^{a}	-^{a}	No fit	BzO$^-$

^{a}Peak disappeared preventing calculation of K_{ass}.
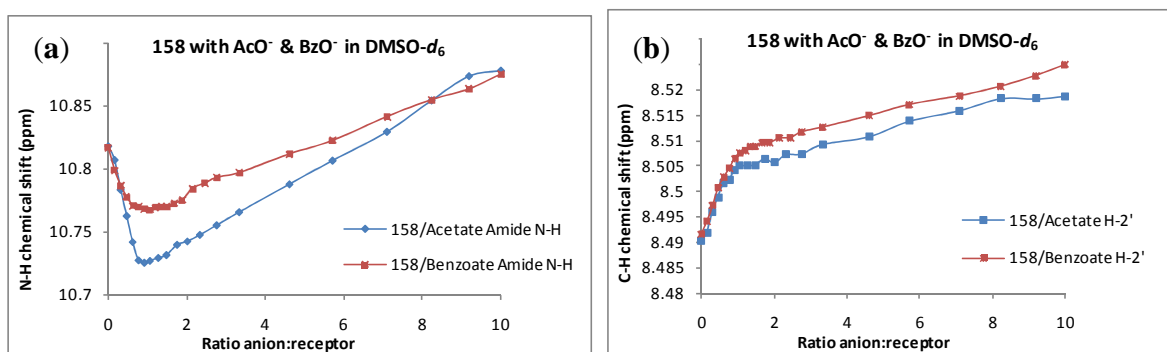
Figure 2.31: (a) ^{1}H NMR spectroscopic titration curves showing migration of amide N-H signals of **158** upon addition of AcO$^-$ or BzO$^-$ in DMSO-d_6 (b) Titration curves showing migration of H-2' signals of **158** upon addition of AcO$^-$ or BzO$^-$ in DMSO-d_6.

2.10   X-Ray Diffraction & Conformational Studies of 157 & 158

Several attempts at crystal growth of **157** & **158** individually and in the presence of AcO$^-$ and BzO$^-$ were undertaken including slow evaporation and vapour diffusion. Diffraction grade crystals of **158** were obtained following recrystallisation from acetonitrile.[216] X-ray diffraction revealed that **158** crystallised into monoclinic P2$_1$/c space group with Z' = 8 (Figure 2.32). Two molecules were arranged with intermolecular H-bond formation from the C=S group of one molecule to the amide N-H of a neighbouring molecule. All 3 aromatic rings were twisted in separate planes while both thiourea N-H groups pointed in the same direction, optimal for cooperative H-bonding to anionic guests. Additionally, it is reasonable to propose that the thiourea portion of the molecule formed a binding cleft involving the H-2 and H-2'' C-H groups as both of these atoms lay within 3 Å of the thiourea N-H.

112
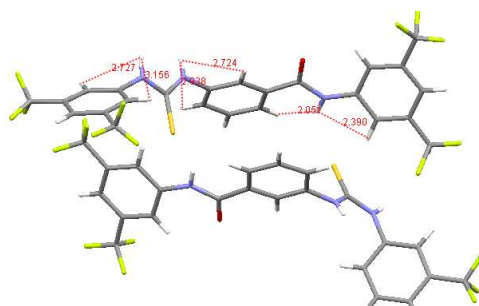
Figure 2.32: X-Ray crystal structure of **158** showing some distances between atoms and the conformation for intermolecular H-bonding.

The conformation of **158** in solution phase was assessed through 2D NOESY analysis in CD$_3$CN. In the absence of anion, NOE interactions were observed between the amide N-H and H-2, H-2' and H-4 protons, the latter interaction suggesting a *syn-anti* equilibration of conformation was occurring. NOE interactions between N-H$_b$ and H-2, N-H$_a$ and H-2'' were also detected (Figure 2.33a). In the presence of 1 equiv Cl$^-$ NOE interactions were observed between H-2 and the amide N-H, thiourea N-H$_a$ and H-2'' signals. There were also interactions between N-H$_b$ and H-2'' while significantly, there was no detectable interaction between the amide N-H and H-4 in the presence of Cl$^-$ (Figure 2.33b). This suggests that a conformational change may have occurred in the presence of Cl$^-$ which forced the amide N-H to project away from H-4 and into a *syn*-conformation for binding. This change in conformation should facilitate cooperative H-bonding from the urea and amide groups to the anion; however amide N-H binding was weak as evidenced from the ^{1}H NMR spectroscopic titrations and K$_{ass}$ values.
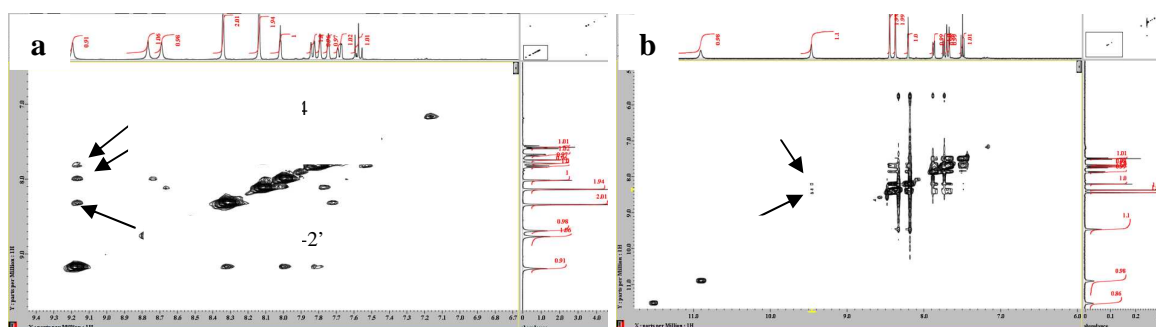
Figure 2.33: (a) 2D NOESY spectrum of **158** in CD$_3$CN. (b) 2D NOESY spectrum of **158** in the presence of 1 equiv Cl$^-$ in CD$_3$CN.

113

Conformational studies of **157** were also conducted through NOE experiments in the absence and presence of Cl$^-$. For a solution of pure receptor, NOE interactions were observed between the amide N-H and H-2, N-H$_b$, H-2' and also H-4, suggesting that the amide N-H equilibrated between the *syn* & *anti* conformations with respect to the urea N-H groups. This latter interaction was also visible in the presence of 1 equivalent Cl$^-$, a result which was in contradistinction to **158** with Cl$^-$. This may be due to conformational differences between **157** & **158** when binding Cl$^-$ and further evidence came from JOB plot analysis. Pure 1:1 stoichiometries were obtained for the H-2', H-2'' and H-2 signals of **13** with Cl$^-$. More complex Cl$^-$ binding to the H-2', H-2'' and H-2 protons of **157** gave rise to apparent maximum values at 0.33 mol fraction **157**, indicative of 1:2 receptor **157**: Cl$^-$ interactions. Therefore, it seems plausible that **157** bound two Cl$^-$ anions, one at the urea and another at the amide N-H site with the adjacent C-H groups interacting weakly in both binding processes.

The binding studies of **157** & **158** to anions of varying size and geometry in CD$_3$CN and DMSO-d_6 suggested that **157** & **158** should be efficient organocatalysts for reactions consisting of anionic transition states. In CD$_3$CN, extremely strong anion binding predominantly through the (thio)urea N-H group was observed to Cl$^-$, AcO$^-$ and BzO$^-$ with less efficient to Br$^-$. Minor cooperative binding effects were also observed from the amide N-H to bromide as previously discussed. Interestingly, 1:2 receptor: anion interactions were also observed for the amide N-H proton with carboxylate anions, therefore 1 equivalent of anion could bind to the amide N-H group and urea N-H simultaneously.

The urea/amide hybrid **157** appeared to bind halides stronger than the thiourea/amide **158** in CD$_3$CN. In the case of AcO$^-$ and BzO$^-$, strong binding was observed for **157** while **158** produced proton transfer effects. As previously stated, this could be considered to have a beneficial effect on the proton transfer step of the MBH reaction. In the case of **157** with AcO$^-$ and BzO$^-$, 1:1 and 1:2 receptor:anion stoichiometries were observed from the JOB plot of the amide N-H signal indicating that it could bind to more than one oxyanion species. This was expected to be beneficial to catalytic activity. In addition, **157** possessed a high level of selectivity for AcO$^-$ in polar competitive DMSO-d_6 with K$_{ass}$ values in excess of 10^4 M^{-1}. This selectivity and strong binding was also considered beneficial for catalytic activity in the highly polar methyl acrylate reaction medium.

2.11   Screening of 157 & 158 for Catalytic Activity

In order to probe the catalytic properties of bifunctional receptors **157** & **158** and compare them to the previously described catalysts **145-151**, they were tested in the DABCO promoted MBH reaction of benzaldehyde with methyl acrylate using the same procedure as described in earlier sections. Catalytic yields and rate constants were calculated and compared to the uncatalysed reaction using the initial rate conditions (Table 2.24 & Figure 2.34).

The urea/amide hybrid catalyst **157** produced a somewhat disappointing yield of 66%, lower than expected considering that the isophthalamide **147** produced a yield of 68%. However, **157** produced the highest initial rate constant of all the anion receptors analysed with a 7.2 fold increase in rate constant over the uncatalysed reaction (Figure 2.34). A number of additional bands were observed by TLC in the **158** catalysed reaction, many of which were in close proximity and co-eluting with the product. Several attempts were made to isolate the product by flash chromatography and preparative TLC, however all efforts proved unsuccessful. The yield was determined following construction of a calibration curve on HPLC with UV detection at 260 nm using a freshly synthesised purified batch of **155** as standard and a 79% yield was calculated. Receptor **158** was observed to enhance the reaction rate to by a factor of 5.5 compared to the uncatalysed reaction. In comparison, Sohtome *et al.* reported a 50-fold increase in reaction rate compared to the uncatalysed reaction for the *bis*-thiourea catalysed MBH reaction of cyclohexenone with benzaldehyde.[147]

Table 2.24: Catalysis of Baylis-Hillman reaction of benzaldehyde and methyl acrylate using **157** & **158** as H-bond donating organocatalysts.
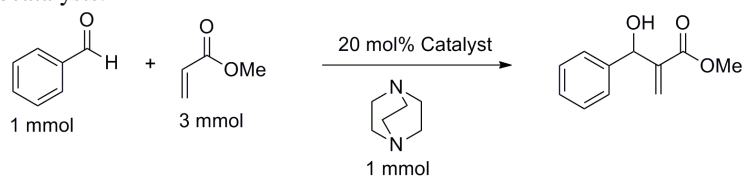
Receptor	Yield [%][a]	k_{obs} x 10^{-2} [h^{-1}][b]	k_{rel}
Uncatalysed	34	0.82	1
157	66	5.9	7.2
158[c]	79[c]	4.5	5.5

[a]Reagents and conditions: benzaldehyde (1 equiv), DABCO (1 equiv), methyl acrylate (3 equiv), catalyst **12** or **13** (20 mol%), r.t., 20 h. Isolated yields unless otherwise stated [b]Initial rates, 10 equiv methyl acrylate used; (*E*)-stilbene used as an internal standard for ^{1}H NMR spectroscopy. [c]Yield determined from HPLC calibration curve.
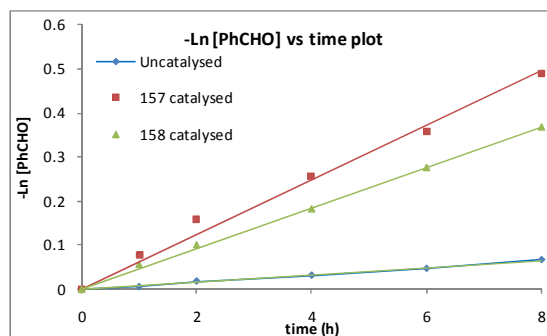
Figure 2.34: Kinetic plots and least square fits of –Ln[PhCHO] vs time for **157** & **158** catalysed Baylis-Hillman reaction of benzaldehyde with methyl acrylate. The uncatalysed reaction is also shown.

Due to the previously observed high proclivity of **157** for acetate anions even in a highly polar DMSO-d_6 environment, it was possible that it could bind and stabilise the anionic reaction intermediates to such an extent that they became less reactive and inhibited the catalytic cycle, thus a lower yield than expected based on kinetic data was observed. In addition, product binding may lead to inhibition of the reaction. It is possible that due to the higher acidity of **158** and given its tendency for proton transfer in the presence of AcO⁻ or BzO⁻, it may have acted as an anion receptor binding to and stabilising the intermediates while also aiding proton transfer by acting as a proton shuttle, thereby enhancing this important step.

In the case of **158**, the 79% yield determined by HPLC represented the highest catalytic yield of all receptors tested. However, due to formation of multiple side products and/or catalyst degradation, purification proved difficult. A number of conditions were screened for their effects on side-product formation. The use of alternative bases, aldehydes or Michael acceptors and reduced reaction temperatures gave no decrease in side product formation. A stability study on a solution of **158** both in the presence and absence of DABCO in CD₃CN showed no catalyst degradation at ambient temperature after 20 hours. Therefore the additional peaks may have been due to catalyst degradation under the conditions of the MBH reaction.

2.11.1 Investigation into Catalytic Mechanism

To investigate the binding properties of **158** to the MBH reactants and adduct, a ^{1}H NMR spectroscopic binding study was conducted in CD_3CN (Table 2.25). Addition of 1 equivalent of benzaldehyde to a solution of **158** in CD_3CN produced downfield migrations of 0.036 and 0.084 ppm for the thiourea N-H$_a$ and N-H$_b$ protons respectively while a change of 0.050 ppm occurred for the amide N-H. The H-2'' and H-2' protons were also moderately shifted downfield with changes of 0.008 and 0.002 ppm respectively. The thiourea N-H$_a$, N-H$_b$ and amide N-H signals broadened and shifted significantly downfield upon addition of 1 equivalent of methyl acrylate with chemical shift changes of 0.47, 0.31 & 0.26 ppm respectively. The H-2'' and H-2 signals were also shifted downfield by 0.021 and 0.01 ppm respectively.

Addition of 1 equivalent of methyl acrylate imparted the largest downfield chemical shift change to the amide N-H group which migrated 0.038 ppm downfield. Overall, these results suggest strong binding between **158** and methyl acrylate with significantly weaker binding to benzaldehyde and **155**. From these results, it is possible to suggest that **158** may impart several effects. Methyl acrylate binding and activation could occur at the thiourea N-H group. Upon reaction with DABCO, thiourea N-H protons may bind to the betaine group while the amide N-H may bind and activate benzaldehyde, thus positioning these molecules in close proximity.

Table 2.25: Binding study of **158** with reactants and MBH product monitored by ^{1}H NMR spectroscopy.

	Δδ (N-H$_b$)	Δδ (N-H$_a$)	Δδ (Amide N-H)	Δδ (H-2')	Δδ (H-2'')	Δδ (H-2)
158 + benzaldehyde	0.036	0.0837	0.0499	0.001	0.0077	0.0018
158 + methyl acrylate	0.3299[b]	0.4724[b]	0.2639[b]	0.001	0.021	0.009
158 + MBH adduct **155**	0.0134	0.0285	0.0382	0	0.0038	0.0021
158 + acetate	-[c]	-[c]	-[c]	0.041	0.3248	0.1709

[a]All analyses were conducted using 10 mM of **158** in CD_3CN with addition of 1 equivalent of each reactant/product. [b]Broad peak. [c]signal disappeared.

Therefore, a dual catalytic system is proposed for **158** (Scheme 2.18) via the simultaneous coordination of the betaine intermediate and benzaldehyde to the N-H groups of **158**. This may stabilise the betaine intermediate **A**, promoting its formation and also position it in close

proximity to the electrophilic aldehyde. Following the nucleophilic addition of the betaine to the aldehyde, the resulting Zwitterionic intermediate **B** is also expected to bind to the catalyst, causing carbonyl activation and rapid elimination of the tertiary amine catalyst in a similar mechanism to that described by Sohtome for their chiral *bis*-thiourea catalyst.[164]

An alternative catalytic activity model may be linked to the apparent proton transfer potential of **158**. As suggested in the ^{1}H NMR spectroscopic binding studies, **158** may undergo proton transfer in the presence of AcO[-] or BzO[-]. It may also be considered that intermediate **B2** generated following addition of the enolate to the aldehyde interacts with the thiourea N-H protons, thus facilitating formation of a six-membered cyclic transition state which could aid in the rate-limiting proton transfer step acting as a proton shuttle (Scheme 2.18).[164]
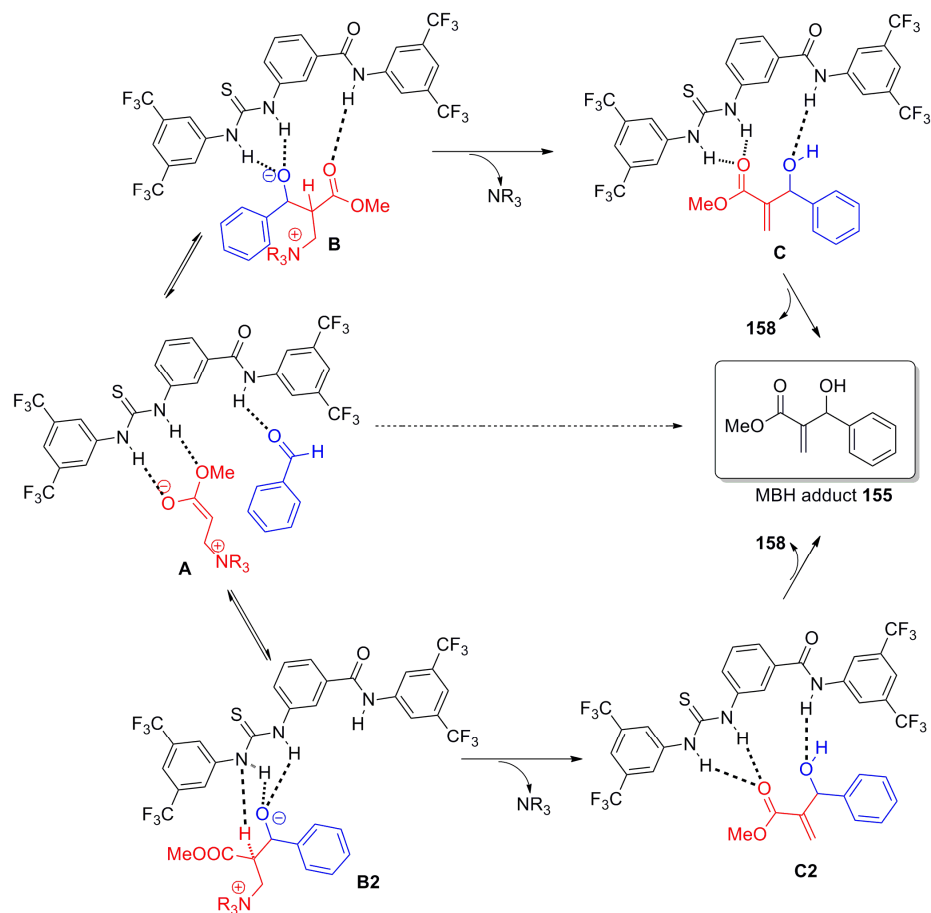
Scheme 2.18: Two proposed modes of action of **158** in the DABCO promoted MBH reaction of benzaldehyde with methyl acrylate.

118

2.12 Conclusions

The aim of this work was to synthesise a series of acidic monofunctional and bifunctional amide receptors and test their ability to act as anion receptors. It was envisaged that a study of the anion binding performance of these receptors would give a good indication of their catalytic activity in reactions possessing anionic transition states. Therefore, this method was used as an alternative approach to the synthesis of reaction transition state analogues in order to probe the catalytic activity a series of receptors.

The anion binding properties of a number of isophthalamide receptors and a hybrid amide/*N*-acylsulfonamide were assessed for Br⁻, Cl⁻, AcO⁻ and BzO⁻ through ^{1}H NMR spectroscopic titration in CD_3CN. In general, increasing acidity resulted in stronger binding while in the case of some of the more acidic receptors, proton transfer effects were observed with basic oxyanions. In a number of cases, K_{ass} values in excess of 10^4 M^{-1} were obtained and these systems were re-analysed in the more polar DMSO-d_6. In this environment, the acidic receptors appeared to possess a degree of selectivity for acetate, which may indicate the successful coordination of similar species in the highly polar MBH reaction conditions where an excess of methyl acrylate was used. Proton transfer effects were also noted in DMSO-d_6 but appeared less pronounced compared to those in CD_3CN.

The catalytic properties of **145**-**151** were studied in the DABCO promoted MBH reaction of benzaldehyde with methyl acrylate and yield and initial rate constant enhancements were observed with yields of up to 76% and up to a 3.9-fold increase in initial rate constant for receptor **151**. This catalyst was also successful for a number of alternative MBH substrates and could be conveniently recycled three times with insignificant loss of catalytic activity. There was correlation between reaction yield and acetate K_{ass} for receptors **145**, **146** & **147**, this relationship was more difficult to directly assess for the more acidic receptors due to proton transfer effects. However, this relationship may not be accurate due to the significant differences between the pK_a values of the anions studied and the likely pK_a values of the MBH reaction intermediates. In the case of the acidic receptors **149** & **151**, binding events and proton transfer effects were apparent, offering key mechanistic insights.

Based on the success of **145**-**151**, bifunctional **157** & **158** incorporating urea or thiourea groups were synthesised, tested for their anion binding properties through ^{1}H NMR spectroscopic titration in both CD$_3$CN and DMSO-d_6. For **157**, very strong binding was observed to Cl⁻, AcO⁻ and BzO⁻ and as a result, binding titrations were repeated in DMSO-d_6. In this medium, **157** displayed a remarkable level of selectivity for AcO⁻ however when this receptor was studied for its catalytic properties, high initial reaction rates but disappointing yields were obtained.

Receptor **158** underwent strong halide binding and proton transfer phenomena by AcO⁻ and BzO⁻ in CD$_3$CN and DMSO-d_6 and when tested as an organocatalyst, produced a high yield of 79%. Based on previous literature investigations into the MBH reaction mechanism, a rationale for the high catalytic of **151** and **158** was proposed involving anion binding and proton transfer and shuttling effects. Overall, this work showed that a cooperative view can be taken between the ability of a receptor to bind anions and to act as an organocatalyst while the anion binding properties can be used to predict catalytic activity and as a mechanistic probe.

3 Chapter 3

Proline and Proline Derivatives as Organocatalysts in the Direct Asymmetric Aldol Reaction

3.1 Introduction

Chapter 1 and 2 detailed the design and testing of a number of compounds with dual applicability to bind anions and act as organocatalysts, investigating the relationship between the anion binding ability of a H-bond donating receptor and its efficiency as a H-bond donating organocatalyst. The work reported in this Chapter and in Chapter 4 details the design and application of chiral iminium-based H-bond donating organocatalysts in synthetic organic reactions. In the design of chiral H-bonding organocatalysts based on molecular recongition, a number of factors must be considered including the structure of the reaction transition states and intermediates and how catalytic activity and enantioselective induction could be achieved using chiral organocatalysts.

This Chapter in particular contains a review of literature surrounding proline and proline derived organocatalysts in the stereoselective intermolecular aldol reaction of ketones with aldehydes and ketones with ketones. The various design techniques which have been applied to proline and proline based derivatives will be reviewed for their effect on the yield and enantioselectivity. Common modifications reported include incorporation of various H-bond donating functional groups, use of *bis*-substituted and bifunctional catalysts, use of various additives including acids and water and also the use of a range of reaction solvents. For consistency purposes and also to enable direct comparison of catalytic performance, two reactions which are most often used to examine the catalytic performance of new organocatalysts will be considered. These are the reactions of acetone with 4-nitrobenzaldehyde and also cyclohexanone with 4-nitrobenzaldehyde while other substrates will also be referred to but not dealt with in as much detail due to the breadth of the subject area. Additionally, the successful application of proline catalysts in intermolecular aldol reaction towards the synthesis of oxindole biological targets will be considered.

3.2 Aldol Reaction

The aldol reaction involves the reaction of an enolisable carbonyl compound (pro-nucleophile) with another carbonyl compound (an electrophile) or also possibly with itself to produce a β-hydroxy carbonyl compound. Frequently, the product undergoes dehydration to produce an

α,β-unsaturated carbonyl compound in an overall reaction known as an aldol condensation. The aldol reaction was first described by Kane *et al.* in 1838,[217] and later reported by Wurtz *et al.* in 1872.[218] It is extremely useful reaction due to the formation of new C-C bonds along with the potential generation of a new chiral centre (Scheme 3.1).
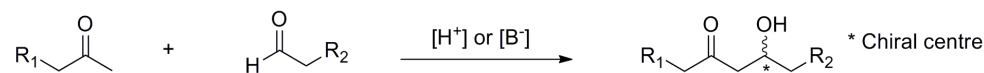
Scheme 3.1: General scheme showing the direct intermolecular asymmetric aldol reaction

A number of biochemical systems, e.g. aldolase enzymes[219] and catalytic antibodies[220] have been reported to enantioselectively catalyse aldol reactions.[221] The aldol reaction is effected in biological systems using either aldolase I or aldolase II enzymes (Scheme 3.2). Type I aldolases are found in animals and plants and operate through an enamine mechanism. The enzyme **A** activates the donor by forming a Schiff base enamine intermediate **B** at the active site. This activated donor adds stereoselectively to the acceptor electrophile to give an iminium adduct **C**. Subsequent hydrolysis releases the substrate from the enzyme. Type II aldolases are generally found in bacteria and fungi and contain a Zn^{2+} cofactor at the active site which activates the aldol donor. This activation has the effect of acidifying the α-proton, allowing a zinc enolate to form **B2**. Hydrogen bonding to the carbonyl of the acceptor activates it towards attack from the enolate and subsequent protonation and decomplexation releases the aldol product (Scheme 3.2).

The promotion of the aldol reaction has also been achieved using organocatalysts, a process which does not suffer the drawback of limited substrate scope commonly observed in enzymatic systems. Chemists have focused on the development of small molecule catalysts which mirror the aldolase enzymes in terms of catalytic activity and selectivity and surpass them in terms of substrate scope. The vast majority of organocatalysts function in a similar way to type I aldolases (enamine mechanism), confirming the success that can be achieved using natural systems as a starting point for catalyst design.
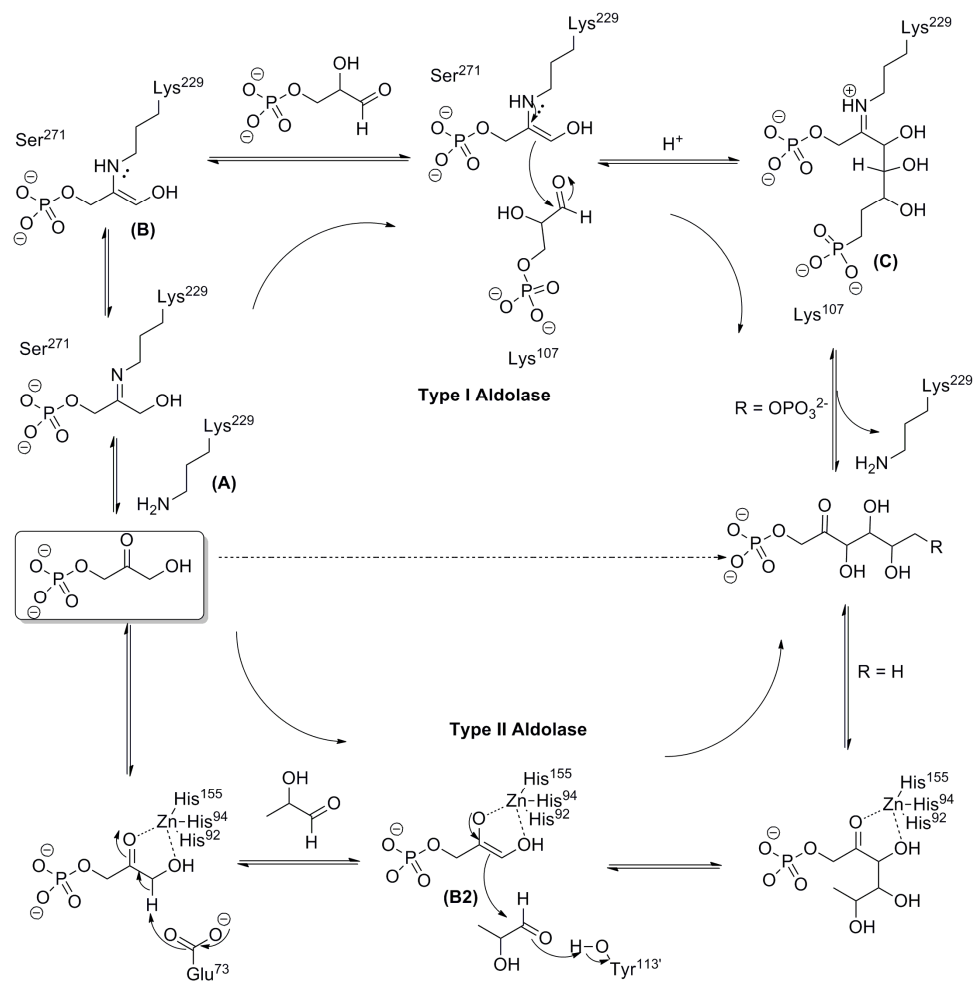
Scheme 3.2: Mechanism of type I and type II aldolases for aldol reaction.[222]

3.3 Development of Proline as Organocatalyst for Aldol Reaction

In the early 1970s, the first organocatalytic enantioselective aldol reaction was reported simultaneously by two separate industrial research groups, the group of Hajos and Parrish at Hoffman-La-Roche and Eder, Sauer and Wiechert at Schering AG.[106,107] The amino acid proline was used to catalyse an intramolecular asymmetric aldol cyclization reaction (Robinson-type annulation) of a triketone to give a chiral bicyclic enone (Scheme 3.3). Both groups found that the yield and enantioselectivity was improved using (*S*)-proline as catalyst and this method was later used to enantioselectively synthesise useful intermediates of progesterone and other steroids.[223,224]

124
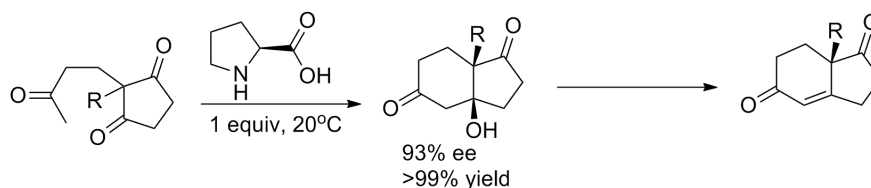
Scheme 3.3: Proline catalysed Robinson annulations reported by groups at Hoffman-La-Roche and Schering AG.[106,107]

Despite this early 1970's breakthrough, it was approximately 25 years before the full potential of this reaction was examined. In 2003, List *et al.* reported 6-enolexo aldolisations using (*S*)-proline as a catalyst with a number of dialdehydes to give *trans*-1,2-disubstituted cyclohexanes in high yield, enantio and diastereoselectivity (Scheme 3.4a).[225,226] The mechanism of action of (*S*)-proline was explained by transition state models for enolendo and enolexo aldolization reactions (Scheme 3.4b & c), thus providing a highly selective route to the intramolecular aldol adducts.
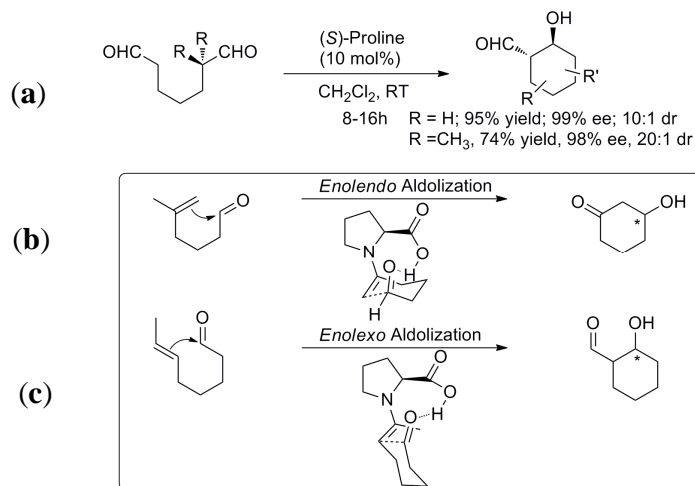
Scheme 3.4: (a) Intermolecular aldol reaction conducted by List *et al.*[225] (b) Proposed transition state for enolendo aldolization similar to that conducted by industrial groups at Hoffman-La-Roche and Schering.[106,107] (c) Proposed transition state for enolexo aldolization conducted by List *et al.*[225]

Proline has been applied as an organocatalyst for a multitude of reactions due to its low cost, availability in both enantiomeric forms and it because it boasts a carboxyl group and an amino group which may act as an acid or base similar to many enzymatic systems. Examples of successful proline-catalysed reactions include the intramolecular and intermolecular aldol reaction, Mannich reaction, Michael reaction and Baylis-Hillman reaction.[227] The remainder of this literature review details the use of proline and pyrrolidine based secondary amine

catalysts in the enantioselective intermolecular ketone:aldehyde aldol reaction. It will focus on variation of catalyst structure and detail developments of a range of structural motifs based around the pyrrolidine ring including an analysis of the advantages of each variation. The effects of reaction conditions such as temperatures, additives and solvents will also be considered. Finally, a general overview of the ketone:ketone aldol reaction will be presented followed by a more detailed analysis of the synthesis of oxindole natural products through ketone:ketone aldol reactions involving isatin derivatives.

3.4 Intermolecular Ketone:Aldehyde Aldol Reactions

3.4.1 (*S*)-Proline as an Aldol Organocatalyst

There are many reports of the use of (*S*)-proline as a catalyst in the intermolecular aldol reaction of ketones with aldehydes.[228] In 2000, using the activity of class I aldolase enzymes as a model system, List *et al.* reported the first intermolecular proline catalysed direct aldol reaction (Scheme 3.5a).[118] They obtained high ee values for the reaction of aliphatic and branched aldehydes with ketones; unbranched aldehydes gave low yields and ee values. In all cases, a large excess of ketone was used to minimize side reactions such as aldehyde self-condensation or oxazolidinone formation **161** from reaction of proline with the aldehyde. Both the pyrrolidine ring and carboxylate motifs were essential for efficient reaction catalysis and they later synthesised (*S*)-ipsenol **162**, a sex pheromone of the bark beetle (Scheme 3.5b).[229]
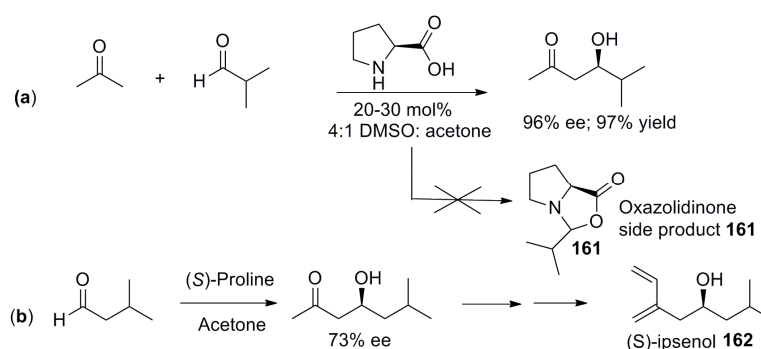
Scheme 3.5: (a) Most successful aldol reaction of isobutyraldehyde with acetone catalysed by (*S*)-proline conducted by List *et al.*[118] (b) Later synthesis of (*S*)-ipsenol which used (*S*)-proline as a major catalyst as part of the the synthetic route.[229]

Later, List *et al.* successfully applied hydroxyacetone as a donor in the proline catalysed direct aldol reaction using similar conditions.[230] This reaction was subsequently adapted by Peng *et al.* for the synthesis of brassinolide **163**, a steroidal plant growth inhibitor.[231]
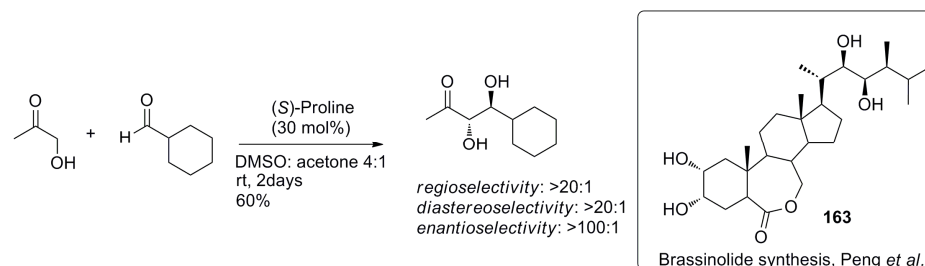
Scheme 3.6: Reaction of hydroxyacetone with cyclohexanecarboxaldehyde catalysed by (*S*)-proline studied by List *et al.*[230] This reaction was later modified to synthesise brassinolide **163** by Peng *et al.* in 2003.[231]

In 2001, Barbas *et al.* used proline as a catalyst in the reaction of a number of cyclic and acyclic ketones with aliphatic and aromatic aldehydes and obtained aldol products with high regio-, diastereo- and enantioselectivities in many cases.[232] Initially, they tested the reaction of acetone with 4-nitrobenzaldehyde using a number of amino acid catalysts (Scheme 3.7). The results showed the necessity of a five-membered cyclic secondary amine structure and an acidic proton in the catalyst structure. The 5,5-dimethyl thiazolidinium-4-carboxylate (DMTC) catalyst **164** gave product in 86% ee and 66% yield; 10% higher ee when compared to proline. Reaction with varying ketone donors and aliphatic and aromatic aldehydes showed that (*S*)-proline and catalyst **164** had similar activities. It was proposed that the formation of the kinetic enamine was rate limiting resulting in the exclusive formation of the linear product.
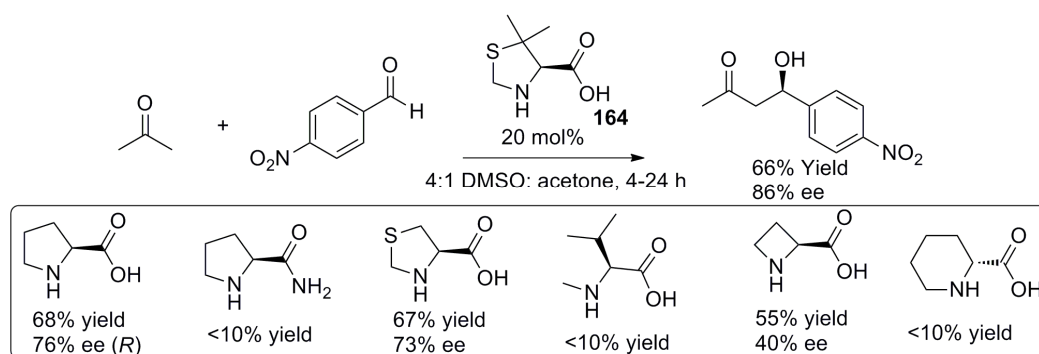
Scheme 3.7: Reaction of 4-nitrobenzaldehyde with acetone catalysed by amino acids reported by Barbas *et al.*[232] with most successful catalyst **164** also shown.

Casas *et al.* extended the scope of the (*S*)-proline catalysed aldol reaction to cyclic ketones.[233] They obtained aldol products in moderate yields but high enantioselectivity of 95-99% in the reaction of cyclic ketones with formaledehyde (Scheme 3.8).

Yield = 47%
ee = >99%
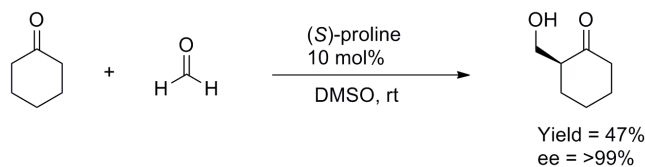
Scheme 3.8: Reaction of formaldehyde with cyclic ketones catalysed by (*S*)-proline. [233]

In 2006, Pihko *et al.* investigated the effects of various additives to the proline catalysed ketone:aldehyde aldol reaction and found the reactions were tolerant to low levels of tertiary amine bases or weak acids but not to strong acids.[234] Water as an additive had a positive effect on reactions where a stoichiometric ratio of ketone to aldehyde was used. The reaction of a number of ketones e.g. 4-thianone with a range of aldehydes gave high yields and excellent enantio- and diastereoselectivities using these additives (Scheme 3.9).

R	Yield	*Anti:syn*	ee
Ph	60	>20:1	98
i-Pr	50	15:1	95
4-NO$_2$Ph	45	20:1	99
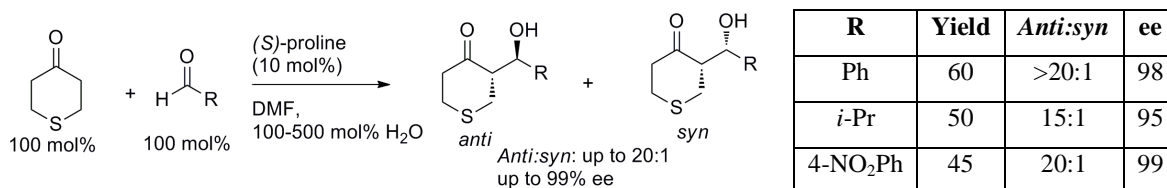
Scheme 3.9: Reaction of thianone with aldehydes giving products in high diastereo and enantioselectivities studied by Pihko *et al.*[234]

3.4.2   Mechanism of the Proline Catalysed Intermolecular Aldol Reaction

Based on type I aldolase enzyme (Scheme 3.2), List *et al.* proposed a similar mechanism for the proline catalysed aldol reaction in 2000 (Scheme 3.10) basing their proposal presented in earlier findings which successfully demonstrated the use of Aldolase Antibody 38C2 in aldol cyclodehydrations. The reaction is proposed to be initialized with the rate determining formation of the enamine **A**. H-bonding of the aldehyde to the catalyst carboxylic acid group is proposed to make it more susceptible to nucleophilic attack of the enamine, producing intermediate **B**. This nucleophilic addition step is expected to possess high enantiofacial selectivity due to a hydrogen bonded network. Hydrolysis of the iminium ion **C** releases the aldol product and the catalyst. The addition step in the mechanism to form **B** is proposed to have a similar activation energy barrier as the enamine formation step and therefore, in certain

instances, this addition can be the rate-determining-step (RDS).[235] Blackmond *et al.* conducted a kinetic study on the aldol reaction of 2-chlorobenzaldehyde with acetone, verified the enamine mechanism of List and proposed that the RDS was the addition of the enamine to the aldehyde.[236] Additionally, List *et al.* obtained crystal structures for proline ketone derived enamines, supporting this mechanism.[237]
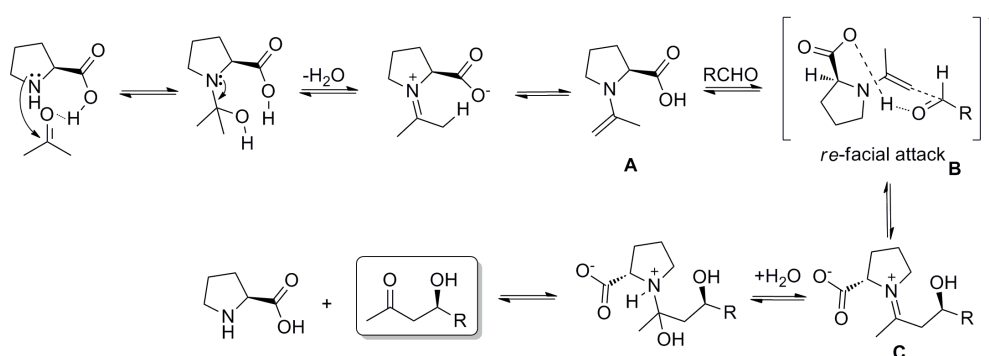
Scheme 3.10: Mechanism of the aldol reaction of acetone and aldehydes as proposed by List *et al.*[118]

In 2007, an alternative mechanism was proposed by Seebach *et al.* (Scheme 3.11).[238] This work proposed that two oxazolidinones, previously considered to be side-products, are involved in the catalytic cycle. The mechanism is proposed to begin by formation of the oxazolidinone **A** through condensation of proline with the aldol donor. This is followed by a proposed regioselective formation of enamine **B** either by E2 elimination or through a 2-step iminium formation and intramolecular proton transfer process. Enamine **B** is then suggested to undergo a *trans*-addition to an electrophile to generate oxazolidinone **C** and hydrolysis of **C** is expected to produce the aldol product. In contrast to the List-Houk model, the key activation step is a γ-lactonization step and not activation of the aldol acceptor by H-bonding to the catalyst. This mechanism has not been widely accepted due to a number of questions surrounding it, mainly based on facial selectivity and mode of action for catalysts which do not possess free carboxylic acid groups for oxazolidinone formation.
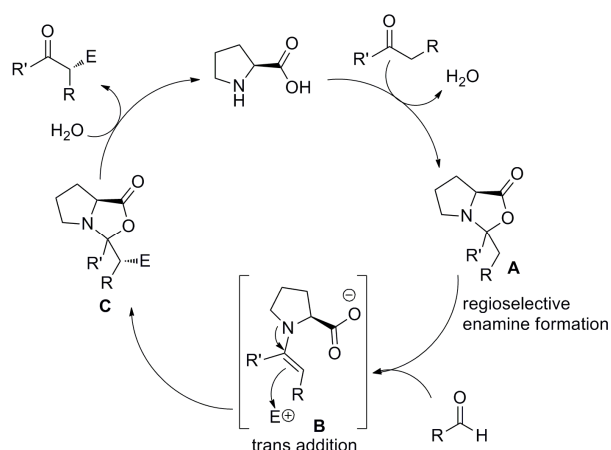
Scheme 3.11: Mechanism of aldol reaction as proposed by Seebach *et al.*[238]

In 2007, Armstrong *et al.* conducted kinetic and spectroscopic studies of the proline catalysed reaction of 2-chlorobenzaldehyde with acetone and proposed that water has two conflicting roles.[239] It is proposed to suppress the aldol reaction rate by shifting the equilibrium from **B** back towards enamine **A** while it simultaneously increases the total catalyst concentration within the reaction cycle due to suppression of off-cycle processes such as oxazolidinone formation (Scheme 3.12). In the absence of water, deactivation due to oxazolidinone formation was thought to be more pronounced, resulting in a lower yield than expected for a given concentration of proline.

Desired Pathway, potentially suppressed by H_2O

Off-cycle reaction of proline with aldehyde; also suppressed by H_2O, resulting in less proline being consumed here and more available for the desired reaction.
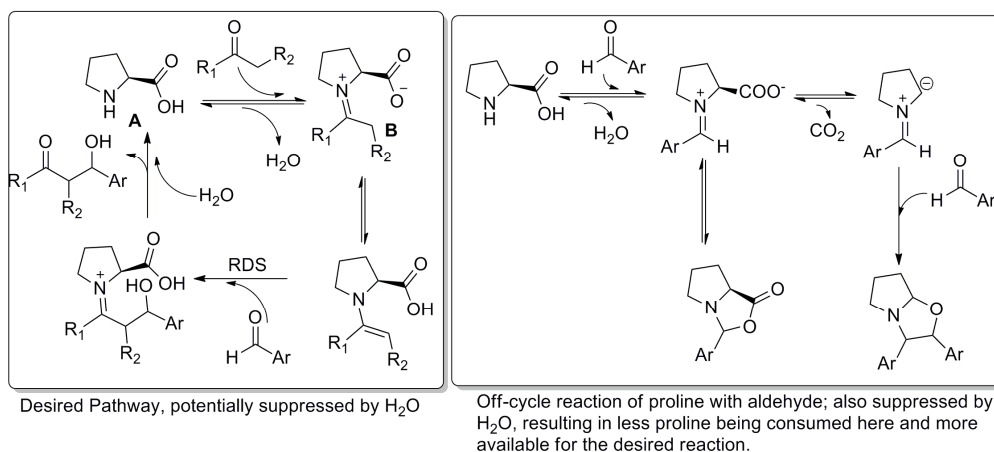
Scheme 3.12: Armstrong's proposed catalytic cycle for proline catalysed aldol reaction in the presence of water.[239]

In 2011, Penhoat *et al.* considered that addition of a Lewis acid into a proline catalysed aldol reaction in the presence of water without pre-mixing of reagents would create a dual catalytic

system; analogous to class II aldolases with a zinc co-factor and also by enamine activation through the proline moiety similar to class I aldolases.[240] Water compatible Lewis acids such as $ZnCl_2$, $FeCl_3$, $HgCl_2$ and $CuCl_2$ were studied in the reaction of cyclohexanone and 4-nitrobenzaldehyde (Scheme 3.13). In many cases, a reduction in side products such as 1-oxapyrrolylzidine **165**, higher ee values and enhanced diastereoselectivites were observed. The optimum proline: $ZnCl_2$ ratio was 2:1 and the authors postulated a zinc catalytic complex as shown in Scheme 3.13. A substrate study showed significant yield and enantioselectivity enhancements; one key example was a 77% improvement in ee using the zinc additive in the reaction of benzaldehyde with cyclohexanone.
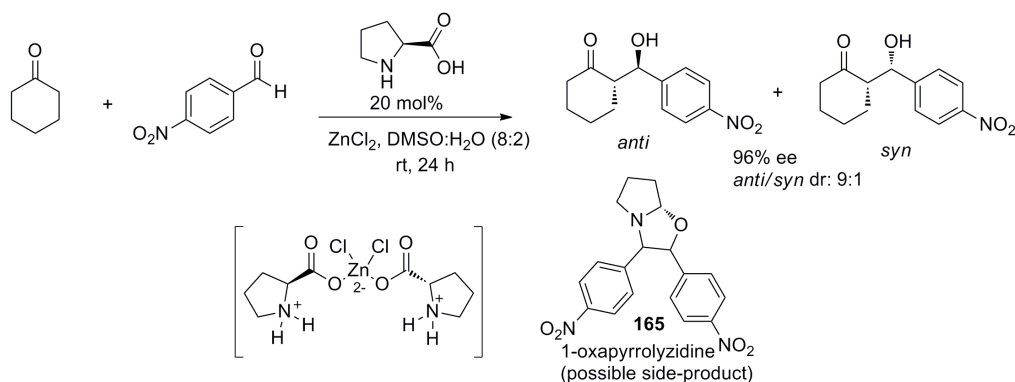
Scheme 3.13: Reaction of cyclohexanone with 4-nitrobenzaldehyde catalysed by a mixture of (*S*)-proline and $ZnCl_2$ Lewis acid additive reported by Penhoat *et al*.[240]

3.4.3 Substituted Proline Catalysts

The use of proline as a chiral catalyst for the aldol reaction was quite a milestone for organocatalysis, however it had some limitations including the formation of by-products leading to diminished yields in some cases e.g. self condensation of the aldehyde and formation of an oxazolidinone byproduct as mentioned in the previous section.[241] Additionally, often an excess of ketone is required to prevent aldehyde dimerization, minimize side-reactions and push equilibrium towards product but this is a significant disadvantage when using of larger, non-volatile ketones. In many cases, a high catalyst loading of 10-30 mol% is necessary and the poor solubility of proline in organic solvents proved troublesome often leading to extended reaction times. These disadvantages have resulted in a number of substituted proline derivatives being investigated. Common structural modifications include increasing the hydrophobicity thereby improving organic solvent solubility, substitution of the

carboxylic acid group for other H-bond donating functionalties and incorporation of additional stereocentres and bulky groups to the pyrrolidine ring to enhance enantioselectivity. Initially, pyrrolidine ring substituted proline derivatives will be discussed followed by other carboxyl derivatives.

3.4.4   Pyrrolidine Ring-Substituted Proline Derivatives

Ring-substituted proline derivatives include hydroxyproline and its derivatives, substituted with more bulky groups such as phenoxy and silyloxy groups (Figure 3.1). Incorporation of a hydroxyl group at the 4-position of the pyrrolidine ring provides an additional chiral non-covalent binding site which may exist in the *cis* or *trans* configuration with respect to the carboxyl group. This moiety may H-bond to the substrate or transition states, thereby enhancing reaction rates and influencing the stereochemistry of the reaction. Use of a hydrophobic silyloxy or phenoxy groups may sequester aldol transition states from water, resulting in enhanced catalyst solubility in the organic reactants. Furthermore, the oxygen atom of these derivatives may H-bond to the substrate, enhancing reaction rate. Pyrrolidine ring-substituted proline catalysts will now be discussed and their activity compared for the reaction of 4-nitrobenzaldehyde with acetone with the details summarised in Scheme 3.14 and Table 3.1.
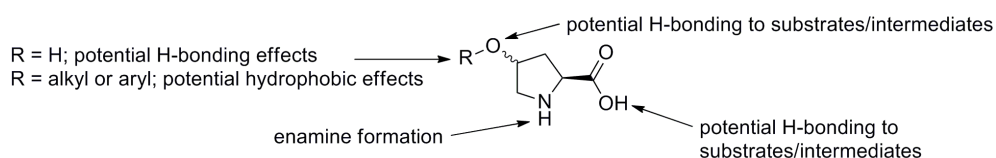
Figure 3.1: General structure of a pyrrolidine ring substituted catalyst showing potential points of interaction with substrates.

The initial catalyst screen for the asymmetric aldol reaction of 4-nitrobenzaldehyde with acetone reported by List *et al.* found that *trans*-4-hydroxy-(*S*)-proline produced an 85% yield with 78% ee compared to the 68% yield and 76% ee for (*S*)-proline. (Scheme 3.14).[118] The *cis*-diastereomer yielded the opposite enantiomer in 62% ee and lower yield and 62% ee while a number of other 4-substituted hydroxy proline derivatives proved inferior to (*S*)-proline (Scheme 3.14).
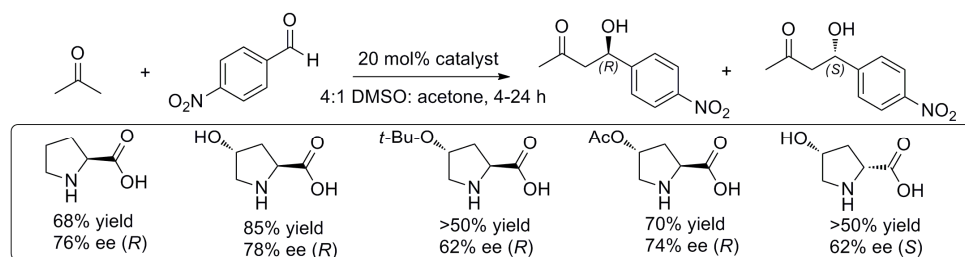
Scheme 3.14: Reaction of 4-nitrobenzaldehyde with acetone catalysed by4-substituted proline catalysts.[118]

Other similar modifications to the pyrrolidine ring have resulted in improvements in yield, enantioselectivity, purification conditions and solubility. For example, Fache & Piva applied a polyfluorohydroxyproline catalyst **166** using benzenetrifluoride as solvent in the same reaction, allowing direct chromatographic purification producing 72% yield and 73% ee (entries 1 & 2, Table 3.1).[242] Subsequently, Shen *et al.* incorporated a (*β*-naphthalenyl)methoxy group into the structure to form (4*R*)-4-(β-naphthalenyl)methoxy-(*S*)-proline **167** (entry 3, Table 3.1).[243] The improved solubility allowed the reaction to occure in neat acetone, however low temperatures were necessary to obtain high ee values with moderate reaction yields.

Table 3.1: Reaction of 4-nitrobenzaldehyde with acetone catalysed by 4-substituted proline catalysts.

Entry	Catalyst	Loading (mol%)	Temp (°C)	Solvent	Additive	% Yield	ee	Config
1[242]		25	rt	4:1 benzenetrifluoride: acetone; 48 h	-	58	63	*R*
2[242]	**166**	25	rt	4:1 benzenetrifluoride: acetone; 24 h	-	72	73	*R*
3[243]	**167**	5	-25	Acetone	-	41	86	*R*
4[244]	**168**	10	rt	DMF	Et$_3$N	71	90	*R*
5[245]	**169**	10	rt	Water (0.13 mL)	Water	63	67	*R*

133

Kokotos and Bellis prepared and tested a number of proline deroved catalysts substituted at the 4-position and found much improved enantioselectivities using (2*S*,4*R*)-4-camphorsulfonyloxyproline catalyst **168** as an alternative to proline. In addition, their catalysts could be used at lower catalyst loadings (entry 4, Table 3.1).[244] In 2006, Hayashi *et al.* reported the aldol reaction of a number of aromatic aldehydes with ketones in the presence of water using 4-*tert*-butyldimethylsiloxyproline (entry 5, Table 3.1).[245] The level of water had little effect on the reaction outcome; however, use of an organic solvent in combination with water caused a significant reduction in diastereoselectivity. The success of the siloxyproline catalyst under the optimum conditions was suggested to be linked to solubility causing it to form a distinct organic phase with the aldehyde and ketone reactants and catalyst loading was reduced to 1 mol% without loss of ee. The authors also studied the reaction of cyclohexanone with benzaldehyde using **169** and other similar catalysts and obtained moderate yields, high ee values and good diastereoselectivities of the *anti*-product in many cases (Scheme 3.15). The reaction with cyclohexanone produced higher enantioselectivities compared to the use of acetone as the aldol donor and this trend has also been observed for many proline derivatives.[221]
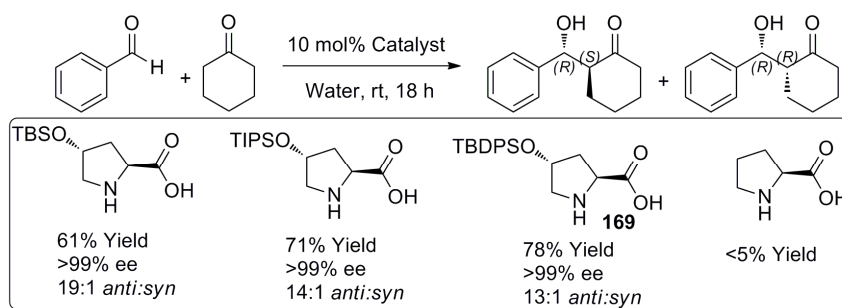
Scheme 3.15: Aldol reaction of benzaldehyde with cyclohexanone using the silyl-protected proline derivative in water without organic solvent reported by Hayashi *et al.* [245]

3.4.5   Prolinamide based Catalysts

Further attempts to enhance the aldol reaction while avoiding the drawbacks of proline led to the development of *N*-acyl proline derivatives such as prolinamides (Figure 3.2). Initially, the simple primary prolinamide **170** failed to be a successful organocatalyst (Scheme 3.7),[118] however further research showed it along with other *N*-acyl substituents could be successfully applied in a vast array of aldol reactions.[221] These derivatives allowed fine-tuning of catalytic

properties with improved activities and enantioselectivities compared to (*S*)-proline with up to 99% ee reported in some cases.[246] Prolinamides are easily prepared from proline by reaction with an appropriate amine and the amide NH group can be acidic enough to activate electrophiles.
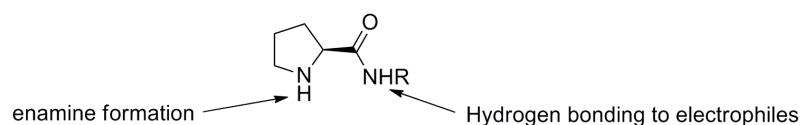
Figure 3.2: General structure of a prolinamide showing potential points of interaction with substrates.

In 2007, Gong *et al.* found that one of the best performing chiral prolinamide catalyst to be the previously unsuccessful (*S*)-prolinamide in the aldol reaction of trifluoroacetaldehyde ethyl hemiacetal **171** with a range of ketones or aldehydes (Scheme 3.16a).[247] (*S*)-prolinamide **170** was found to induce diastereo- and enantioselectivity of up to 90:10 dr and 88% ee respectively, considerably better than (*S*)-proline (35% ee) or its methyl ester (13% ee). Dodda *et al.* used catalyst **170** in the intermolecular aldol reaction of ketones and diethyl formylphosphonate to give the corresponding secondary α-hydroxyphosphonates (Scheme 3.16b) with high enantio- and diastereoselectivities.[248]
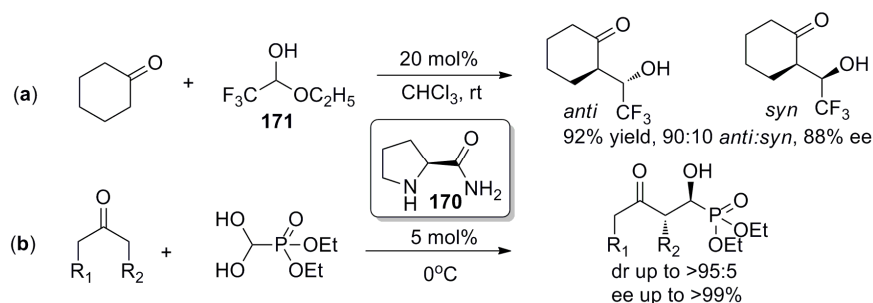
Scheme 3.16: (a) Reaction of trifluoroacetaldehyde ethyl hemiacetal **171** with cyclohexanone catalysed by primary prolinamide catalyst **170** studied by Gong *et al.*[247] (b) Reaction of ketones with diethyl formylphosphonate undertaken by Dodda *et al.*[248]

A variety of other prolinamide catalysts have been designed and applied in the intermolecular aldol reaction. This section will focus on the reaction of 4-nitrobenzaldehyde with acetone with a summary in Table 3.2 & Table 3.3. In 2003, Gong *et al.* successfully applied terminal hydroxyl bearing (*S*)-prolinamide derivatives such as catalyst **172** in this reaction.[249] These catalysts were capable of a second H-bonding effect through the OH group and they observed increased yields and enantioselectivities (entry 1, Table 3.2). Temperature had a dramatic

effect on ee while a substrate scope study for a number of aldehydes gave good yields and high enantioselectivites in many cases. Further work by the Gong group in 2004 showed that catalyst efficiency was affected by the H-bonding abilities of the amide N-H with electron deficient *N*-aryl prolinamides more effective in the reaction than *N*-alkyl analogues (entry 2, Table 3.2). A substrate scope study of a number of aldehydes with acetone and 2-butanone gave good yields and enantioselectivities up to 93% and 99% ee respectively.

Table 3.2: Reaction of 4-nitrobenzaldehyde with acetone catalysed by prolinamide catalysts

Entry	Catalyst		Loading (mol%)	Temp (°C)	Solvent	% Yield	ee	Config
1[249]	**172**		20	25	Neat acetone	89	69	*R*
			20	-25	Neat acetone	66	93	*R*
2[250]		R = *t*-Bu	20	25	Neat acetone	55	15	*R*
		R = 4-CF$_3$Ph	20	25	Neat acetone	88	45	*R*
3[251]	**173**		20	0-4	4:1 acetone:water	60	56 16[a]	*R* *R*
4[252]		R = C$_6$H$_{11}$	20	rt	Neat acetone	53	15	*R*
		R = COOEt	2	-25	Neat acetone	62	99	*R*
5[246]		R = Ph	5	-40	Neat acetone	78	85	*R*
		R = *i*-Bu	10	-40	Neat acetone	70	99	*R*

[a]non-protonated catalyst gave 16% ee.

In 2005 and also in a later report in 2006, Chimni *et al.* used a protonated chiral phenylethylamine prolinamide **173** for the aldol reaction in water (entry 3, Table 3.2).[251,253] A transition state involving a 6-membered cyclic structure with activation and orientation of the aldehyde by the amide N-H was proposed (Figure 3.3a). The hydrophobic interaction of the aromatic groups of the catalyst and the aldehyde were deemed to have a considerable effect on the catalytic ability. The extra flexibility associated with a benzyl amine derived prolinamide **175** catalyst afforded significantly higher activity compared to the more rigid aniline analogue

174, however a decrease in enantioselectivity of almost 50% was observed. The enhanced reactivity was ascribed to increased access to the catalytic enamine when substituted with an *N*-benzyl group compared to the more rigid *N*-phenyl substituted prolinamide (Figure 3.3b). Catalysts derived from alkyl amines with increasing chain lengths gave improved enantioselectivity with chain length due to increased hydrophobic interactions.
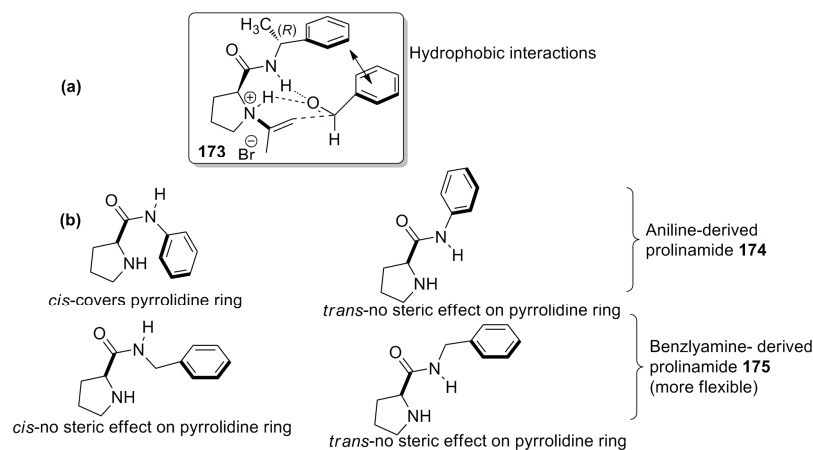
Figure 3.3: (a) Proposed transition state for phenylethylamine derived prolinamide catalysed aldol reaction.[251] (b) Diagram illustrating origin of reactivity and enantioselectivity differences between aniline and benzyl amine derived prolinamide catalysts in aldol reaction.[253]

In 2005, the Gong group found that more acidic prolinamide catalysts provided enhanced reactivity and enantioselectivity compared to less acidic analogues.[252] The (*R*)-configuration of the *α*- and *β*-carbons of catalysts with electron withdrawing ester groups was found to be optimal for generation of high enantioselectivity (entry 4, Table 3.2). A substrate scope study found that the reaction of a number of aldehydes with acetone and butanone produced high yield and enantioselectivities up to 99% in favour of the (*R*)-enantiomer of *α*-hydroxyketone product. For cyclic ketones, they found both high enantio- and diastereoselectivity for the *anti*-aldol product. Mechanistic studies through DFT calculations suggested aldehyde activation through H-bonding to both the amide N-H and hydroxyl protons in a cooperative system (Figure 3.4).
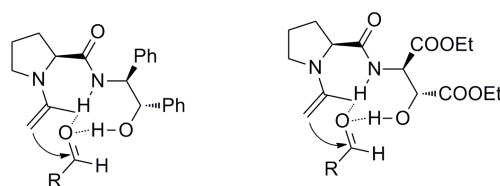
Figure 3.4: Proposed transition states for aldol reactions catalysed by prolinamides with a terminal OH group.[252]

137

Singh *et al.* also reported a number of aminoalcohol catalysts incorporating a *gem*-diphenyl group at the *β*-carbon in the reaction of acetone with aliphatic and aromatic aldehydes.[246] They obtained excellent enantioselectivities up to 99% using 5-10 mol% of catalyst (entry 5, Table 3.2) and a transition state based on DFT calculations was used to explain the enantioselectivity (Figure 3.5). The aldehyde was proposed to form H-bonds to the OH and NH groups of the catalyst which favoured reaction at the *re* face (**A**) The *si* face was unfavoured due to steric interactions between the alkyl or aryl portion of the aldehyde and the catalyst OH group (**B**). The *gem*-diphenyl group restricted the conformation, increased the H-bond donor capabilities of the OH group and improved solubility.

Favoured transition state **A**   unfavoured transition state **B**
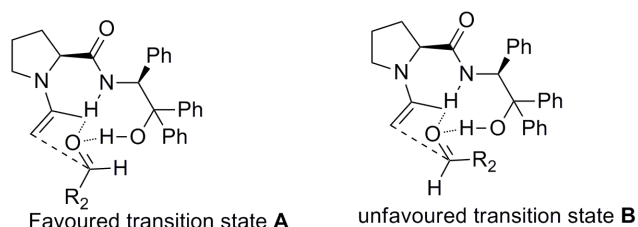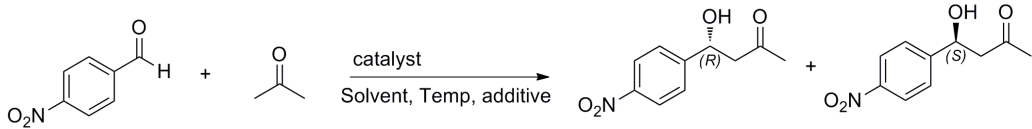
Figure 3.5: The proposed origin of enantioselectivity due to repulsion of the aldehyde with the catalyst bulky group is shown in the unfavoured transition state.[246]
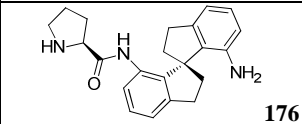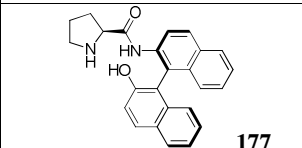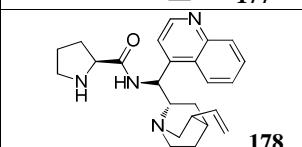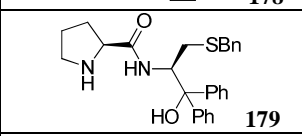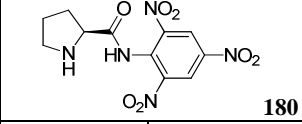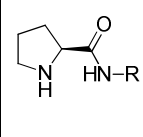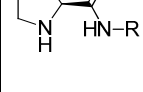
Zhou *et al.* reported a highly active prolinamide spiro-derivative **176** that could be used at 1 mol% loading and in a short reaction time of 4.5 hours at -25°C. Product was obtained in good yield but moderate enantioselectivity (entry 1, Table 3.3).[254] They also applied this catalyst to the reaction of a number of aliphatic and aromatic aldehydes with acetone and obtained product in up to 87% yield and 76% ee.

In 2007, Lattanzi *et al.* synthesised catalyst **177** comprising a prolinamide group with a binaphthyl ring system possessing axial chirality.[255,256] The most efficient catalyst reported incorporated (*S*)-NOBIN (2-amino-2'-hydroxy-1,1'-binaphthyl) ligands as the amide portion (entry 2, Table 3.3) used with 1.1 equiv water in 200 µL dioxane. They suggested that the amide N-H and OH of NOBIN activate the electrophile by H-bonding and the new bond is formed by attack of the enamine from its *Re* face onto the *Re* face of the aldehyde similar to that previously reported by Gong *et al.*[249]

In 2008, Xiao *et al.* reported the successful catalyst **178** based on the combination of proline with cinchona alkaloids providing a large chiral backbone and one tertiary quinuclidine nitrogen which could form an ion pair with acid additive and in turn act as a H-bond donor.[257] The optimum system involved using acetic acid or perchloric acid as additive in a ratio of 2:1 acid: catalyst (entry 3, Table 3.3). The scope of the catalyst was extended to aliphatic and aromatic aldehydes with acetone and 2-butanone.

Table 3.3: Reaction of 4-nitrobenzaldehyde with acetone catalysed by prolinamide catalysts.

Entry	Catalyst		Loading (mol%)	Temp (°C)	Solvent	Additive	% Yield	ee	Config
1[258]	**176**		1	-25	Neat acetone	-	82	55	*R*
2[255,256]	**177**		5	4	200 μL dioxane	1.1 equiv H$_2$O	77	80	*R*
3[257]	**178**		10	-30	Neat acetone	20 mol% AcOH	85	90	*R*
4[258]	**179**		10	-15	Neat acetone	-	40	64	*R*
5[259]	**180**		20	rt	HMPA	30 equiv H$_2$O	90	85	*R*
6[260]		R = C$_6$F$_5$ **181**	20	3	DMF	10 mol% TFA	80	90	*R*
		R = 3,5-(NO$_2$)$_2$C$_6$H$_3$ **182**	20	3	DMF	10 mol% TFA	78	72	*R*

In 2008, Schwab *et al.* studied the performance of cysteine-derived prolinamide catalysts.[258] The presence of a *gem*-diphenyl group was necessary for high enantioselectivity while temperature and solvent also played significant roles. The most successful *gem*-diphenyl cysteine catalyst **179** gave moderate yield and enantioselectivity in the reaction of 4-

nitrobenzaldehyde with acetone (entry 4, Table 3.3) and produced good yields and enantioselectivies of 82-94% in a substrate scope study of acetone with aldehydes.

A number of authors subsequently reported successful prolinamide based catalysts bearing electron withdrawing phenyl groups, highlighting the relationship between catalyst N-H acidity and enantioselectivity. Shirai *et al.* studied the electronic properties of prolinamide catalysts and found catalyst **180** which possessed NO_2 groups at the 2-, 4- & 6-positions of the *N*-aryl ring to be optimal in HMPA (hexamethylphosphoramide) solvent in the presence of H_2O (entry 5, Table 3.3).[259] It should be noted that they obtained a similar level of success for a perflouorophenyl prolinamide analogue. In 2009, Moorthy *et al.* found this latter perflouorophenyl prolinamide **181** to be optimal amongst a range of nitro- and methyl-substituted aromatic prolinamides.[260] In general, steric hindrance from the catalyst aryl ring reduced the product yield but successful enantioselectivity results for the sterically hindered 3,5-dinitrophenyl substituted catalyst **182** confirmed that N-H acidity was a dominant effect. In many cases, enantio- and diastereoselectivites were in of the order of 90%, (entry 6, Table 3.3). X-ray crystal analysis of catalyst **182** showed the 3,5-dinitrophenyl ring was almost co-planar with the amide while the perfluorophenyl ring was twisted by approximately 76° in another plane. The enhanced flexibility of the latter catalyst **181** was proposed to allow more effective H-bonding of the electrophile and the amide N-H while weak C-H···F, π-π interactions between the catalyst and substrate were also proposed to aid the transition state structure.

Many of the previously described prolinamide catalysts have also been applied in the enantioselective aldol reaction of 4-nitrobenzaldehyde with cyclohexanone. A summary of a number of previously discussed prolinamide catalysts which have been used for this reaction is given in Scheme 3.17. All catalysts favoured the *anti*-conformation with the (*R*)-configuration at the C-C bond formation site. Of these examples, Moorthy's perfluorophenyl prolinamide catalyst provided the best results with an 88% yield, 98:2 diastereomeric ratio (*dr*) of 98:2 in favour of *anti*-product in an 88% yield.[260]
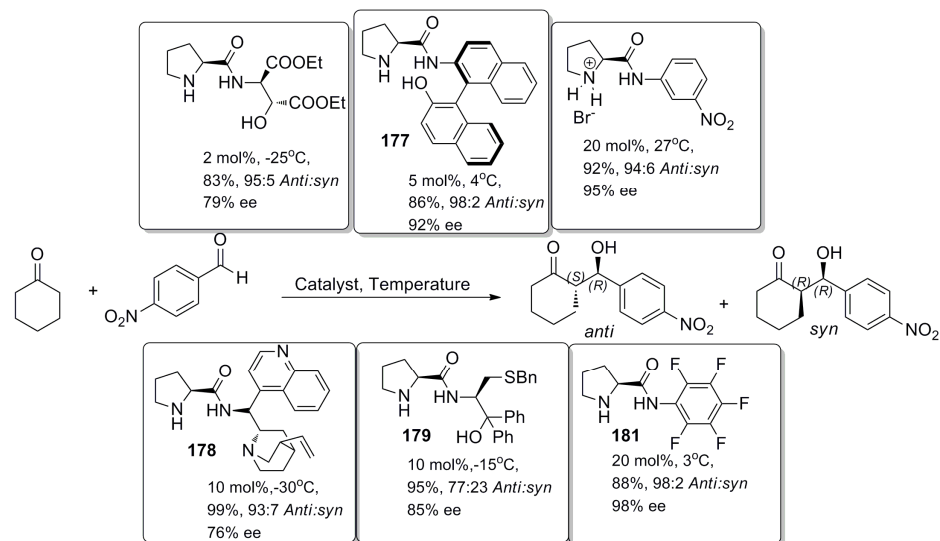
Scheme 3.17: Enantioselective reaction of 4-nitrobenzaldehyde with cyclohexanone catalysed by prolinamide catalysts.

3.4.6 Pyrrolidine Ring Substituted Prolinamides

As described in a previous section, the scope and capabilities of proline as a catalyst have been extended by synthesizing pyrrolidine ring substituted derivatives including *trans*-hydroxyprolines and this is also true of prolinamides (Figure 3.6). There has been significant reports of the use of hydroxy- and other pyrrolidine ring substituted derivatives of prolinamides for the aldol reaction and some of the more relevant ones will be discussed in this section. The use of pyrrolidine ring-substituted prolinamide catalysts in the reaction of 4-nitrobenzaldehyde with acetone will be summarised in Table 3.4 while Table 3.5 summarises their use in the reaction of cyclohexanone with 4-nitrobenzaldehyde.
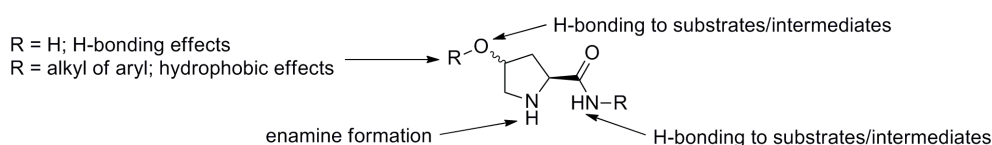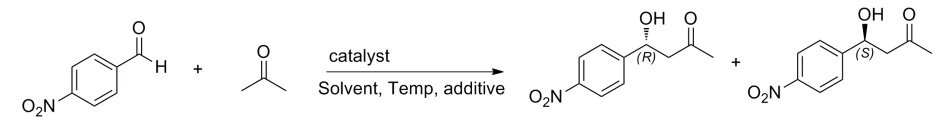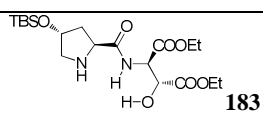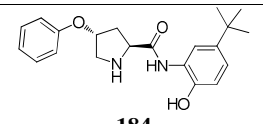
Figure 3.6: General structure of a pyrrolidine ring-substituted prolinamide showing potential points of interaction with substrates.

Gong *et al.* tested a number of pyrrolidine ring-substituted prolinamide catalysts in the aldol reaction using 1 mol% catalyst loading in water.[261] For the reaction of acetone with 4-nitrobenzaldehyde, they found trans-TBS ether pyrrolidine ring substituted amino alcohol **183** containing a chiral diester group at the amide moiety to be optimal producing the aldol

product in good yield and 71% ee (entry 1, Table 3.4). Catalyst **183** was also applied in the reaction of cyclohexanone with 4-nitrobenzaldehyde and gave a higher yield, 94% ee and 99:1 *anti*:*syn* (entry 1, Table 3.5). The reaction was found to occur under biphasic basic conditions with product enantioselectivity strongly influenced by the balance between the hydrophilic and hydrophobic nature of the catalyst and substrate. The electron withdrawing ester groups increased the H-bonding ability of the catalyst and also its hydrophilicity which was counteracted by the *trans*-hydrophobic siloxy group at the 4-position of the pyrrolidine ring.

Table 3.4: Reaction of 4-nitrobenzaldehyde with acetone catalysed by pyrrolidine ring-substituted prolinamide catalysts.

Entry	Catalyst	Loading (mol%)	Temp (°C)	Solvent	Additive	% Yield	ee	Config
1[261]	**183**	1	25	0.5 mL H_2O	-	85	71	*R*
2[262]	**184**	10	rt	0.4 mL H_2O	10 mol% TFA	90	80	*R*

Fu *et al.* incorporated a phenoxy group at the 4-position of the pyrrolidine ring and additional hydroxyl group at the 2-position of the *N*-aryl ring coupled to the prolinamide moiety to create the successful catalyst **184** for the reaction of actone with 4-nitrobenzaldehyde (entry 2, Table 3.4).[262] They observed higher selectivity in the reaction of cyclohexanone with 4-nitrobenzaldehyde which gave product in high yield, 94% ee and 99:1 dr in favour of the *anti*-product (entry 2, Table 3.5). They proposed that the hydrophobic phenyl ring of the phenoxy group would exclude water from the transition states, improve solubility in organic solvents and bring the reactants closer together.[263]

Table 3.5: Reaction of 4-nitrobenzaldehyde with cyclohexanone catalysed by pyrrolidine ring-substituted prolinamide catalysts.
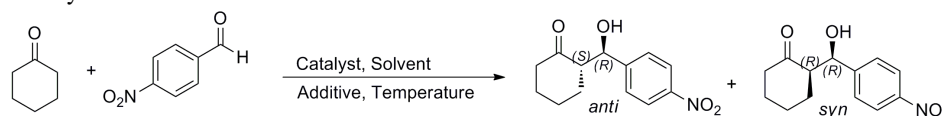
Entry	Catalyst	Loading (mol%)	Temp (°C)	Solvent	Additive	Anti:syn	% Yield	ee	Config
1[261]	183	1	25	0.2 mL H$_2$O	-	>99:1	99	94	R
2[262]	184	10	rt	0.4 mL H$_2$O	10 mol% TFA	99:1	99	94	R
3[264]	185	5	-10	0.2 mL dry MeOH	-	89:11	43	96	R
4[265]	186	10	rt	1 mL H$_2$O	10 mol% DBSA	96:4	90	98	R

In 2009, Takeshita *et al.* designed prolinamide catalyst **185** containing one covalent site (secondary amine for enamine formation) and 3 non-covalent binding sites; a hydroxyl group at the 4-position, amide N-H and terminal hydroxyl group (entry 3, Table 3.5).[264] Despite the failure of the hydroxyl group at the 4-position to bind the substrate, the other extra non-covalent sites were proven to have a significant catalytic effect, as observed from the reaction of cyclohexanone with 4-nitrobenzaldehyde using 2.5 mol% catalyst loading at -25°C (entry 3, Table 3.5). They also applied their *trans*-4-hydroxy-2-prolinamide alcohol catalysts in the aldol reaction of aldehydes and cyclic and acyclic ketones producing up to 99% ee and high diastereoselectivites.

Luo *et al.* used 4-substituted chiral prolinamide catalysts with surfactant Brønsted acids to form a colloidal dispersion in water, allowing the aldol reaction to proceed within micelles.[265] DBSA (*p*-dodecyl benzenesulfonic acid) along with chiral aminopyridine based prolinamide catalyst **186** were found to be optimal for the reaction of cyclohexanone with 4-nitrobenzaldehyde in water (entry 4, Table 3.5). Varying catalytic properties from different 2-, 3-, and 4- aminopyridine derived prolinamides were ascribed to pK$_a$ differences and spatial

effects. A substrate scope examining a number of 4-substituted cyclohexanone derivatives and aromatic aldehydes gave product in high yield, diastereo and enantioselectivities.

3.4.7 Proline Thioamides

Prolinethioamides share the same structural benefits with prolinamide catalysts, i.e. interactions from the (thio)amide N-H group, convenient structural modification, however, the thioamide group is potentially more efficient towards electrophile activation as a result of its increased acidity (Figure 3.7). A number of prolinethioamide catalysts will be discussed and summarised in Table 3.6 & Table 3.7 for the reaction of acetone and 4-nitrobenzaldehyde and cyclohexanone with 4-nitrobenzaldehyde respectively.
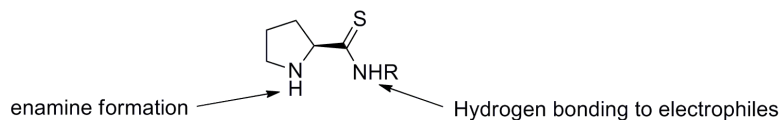
Figure 3.7: General structure of prolinthioamide catalyst showing potential points of interaction with substrates.

In 2006, Gryko and Lipinski in tested (*S*)-prolinethioamides with varying acidities and steric properties and also analysed a number of diastereomeric prolinethioamides derived from *α*-phenyl amines.[266] The latter catalysts proved optimal producing higher ee values than proline in the reaction of 4-nitrobenzaldehyde with acetone (entry 1, Table 3.6). Later, the same group found that prolinethiomide **187** in its TFA salt form gave improved efficiencies. A reduction in catalyst loading gave improved yields as a competing side reaction was minimized. They also observed that at the TFA salt of the successful prolinethioamide **187** catalyst was equally efficient in alternative solvents and neat acetone (entry 2, Table 3.6). The choice of acid was also investigated and it was found that salts derived from acids stronger than TFA led to recovery of starting material while highest yields were obtained from acids with pK_a of approximately 1.3 (entry 3, Table 3.6). This catalyst was also successfully applied to the reaction of 4-nitrobenzaldehyde with cyclohexanone (entry 1, Table 3.7). The authors proposed a similar mechanism to proline through a metal-free Zimmerman-Traxler type transition state while it was proposed that the thioamide formed stronger H-bonds to the aldehyde compared to the acid of proline.

144

Table 3.6: Reaction of 4-nitrobenzaldehyde with acetone catalysed by prolinethioamide catalysts.
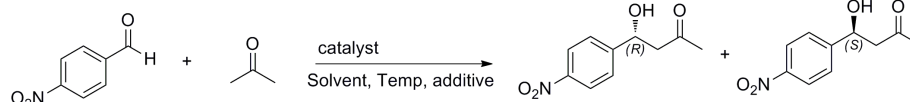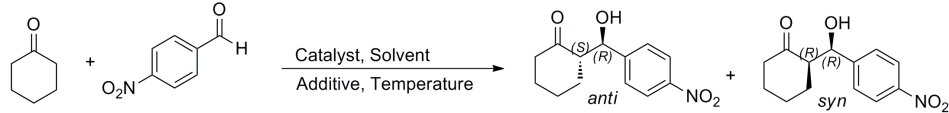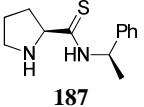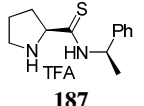
Entry	Catalyst	Loading (mol%)	Temp (°C)	Solvent	Additive	% Yield	ee	Config
1[266,267]	**187**	20	4	Neat acetone	-	62	84	*R*
		10	4	Neat acetone	-	68	44	*R*
2[267]	**187**	2.5	4	Neat acetone	TFA	81	94	*R*
		10	4	DMF	TFA	71	96	*R*
		10	4	THF	TFA	76	94	*R*
3[267]	**187**	2.5	4	acetone	F_2CHCO_2H	95	92	*R*
		2.5	4	acetone	Cl_2CHCO_2H	99	93	*R*
4[268]	**188**	0.2	0	water	2 mol% PhCOOH	92	95	*R*

Using their most efficient catalyst **187**, the same authors considered water as a solvent for the aldol reaction of cyclohexanone with 4-nitrobenzaldehyde and obtained 96% yield, 94% ee and 90:10 dr in favour of the *anti* product, an improvement over the reaction in neat cyclohexanone.[269] Salts were found to increase the hydrophobic effect by electrostriction of water, decreasing the solubility of non-polar species and promoting their association. The use of salting-out brine allowed the reduction of ketone excess to 1.2 equiv without detrimentally affecting the yields and stereoselectivities (entry 2, Table 3.7).

In 2010, Li *et al.* evaluated a number of prolinethioamide catalysts in aqueous reaction media.[268,270] Their most efficient catalyst **188** was a prolinethioamide with a terminal hydroxyl group and was successfully applied to the reaction of acetone and also cyclohexanone with 4-nitrobenzaldehyde with benzoic acid additive in water (entry 4, Table 3.6 & entry 3, Table 3.7). The catalyst was proposed to create a hydrophobic pocket for the reaction while H-bonding from the thioamide activated the electrophile.

Table 3.7: Reaction of 4-nitrobenzaldehyde with cyclohexanone catalysed by prolinethioamide catalysts.

Entry	Catalyst	Loading (mol%)	Temp (°C)	Solvent	Additive	*Anti:syn*	% Yield	ee	Config
1[267]	**187**	10	4	NMP	TFA	95:5	88	90	*R*
2[269]	**187**	5	rt	2 mL H_2O	-	95:5	96	94	*R*
		10	4	Neat ketone	-	77:13	82	86	*R*
		5	rt	2 mL H_2O	Sat NaCl	>95:5	90	92	*R*
6[268]	**188**	0.2	0	water	2 mol% PhCOOH	97:3	90	97	*R*

3.4.8 *Bis*-Prolinamide Catalysts

An improvement of catalytic activity without sacrificing enantioselectivity of was observed by incorporation of an additional proline amide group into the catalyst structure. In particular, when the molecule consists of two prolinamide units linked through a chiral spacer, there exists potential opportunity for further improved enantioselectivities (Figure 3.8).
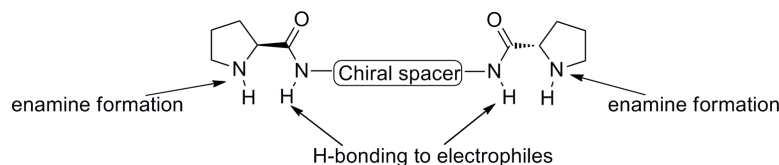
Figure 3.8: General structure of *bis*-prolinamide catalyst showing potential points of interaction with substrates.

A C_2-symmetric *bis*-prolinamide catalyst **189** was reported by Zhao *et al.* in 2005 and used in the aldol reaction of 4-nitrobenzaldehyde with acetone (entry 1, Table 3.8).[271] Their catalyst can be viewed as substitution of the hydroxyl group in Gong's phenyl substituted amino alcohol catalyst (entry 1, Table 3.2) with an additional prolinamide moiety capable of strong H-bonding to the electrophile.

Table 3.8: Reaction of 4-nitrobenzaldehyde with acetone catalysed by *bis*-prolinamide catalysts.
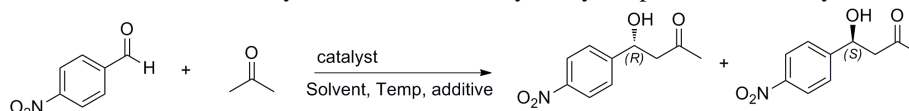
Entry	Catalyst	Loading (mol%)	Temp (°C)	Solvent	Additive	% Yield	ee	Config
1[271]	**189**	10	-35	Anhydrous acetone	-	88	98	*R*
2[272-274]	**190**	10	0	DMF:H$_2$O 1:1	-	99	79	*R*
		10	-20	DMF:H$_2$O 1:1	20 mol% PhCOOH	94	86	*R*
		5	0	2 equiv ketone	10 mol% PhCOOH	86	74	*R*
3[275]	**191**	10	2	1:1 acetone: H$_2$O	20 mol% stearic acid	100	58	*R*
4[276]	**192**	10	-40	3 mL toluene	10 mol% AcOH	83	93	*R*

In 2006, Najera *et al.* reported a C$_2$-symmetric catalyst **190** derived from 1,1'-binaphthyl-2,2'-diamine ((S_a)-BINAM) coupled to two (*S*)-prolinamide units for the reaction of 4-nitrobenzaldehyde with acetone (entry 2, Table 3.8).[272] They also studied a number of aldehyde and ketone substrates and obtained product in high yield up to 99%, good diastereoselectivity up to 10:1 dr and up to 96% ee (entry 2, Table 3.9). They later discovered that in general, the rate of reaction catalysed by **190** increased with decreasing pK$_a$ acid additive without loss of enantioselectivity (entry 2, Table 3.8).[273] Substrate scope studies produced high yields up to 99% and enantio-, diastereo- and regioselectivitites were obtained (99% ee, 100% dr and >50:1) in reasonable reaction times using of benzoic acid additive (entry 2, Table 3.9). In 2008, Using ESI-MS, they found evidence that benzoic acid promoted the enamine formation at each proline sub-unit.[274]

Table 3.9: Reaction of 4-nitrobenzaldehyde with cyclohexanone catalysed by *bis*-prolinamide catalysts.
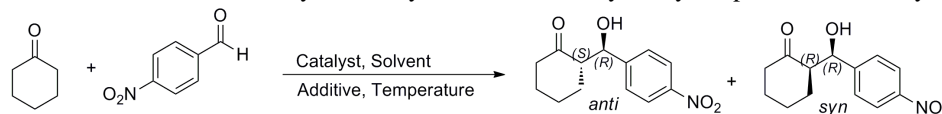
Entry	Catalyst	Loading (mol%)	Temp (°C)	Solvent	Additive	*Anti:syn*	% Yield	ee	Config
1	**189**	10	Rt	CH$_2$Cl$_2$	-	97:3	78	93	*R*
2[272-274]	**190**	10	0	DMF:H$_2$O 1:1	-	10:1	98	93	*R*
		10	-20	DMF:H$_2$O 1:1	20 mol% PhCOOH	99:1	99	97	*R*
		5	0	2 equiv ketone	10 mol% PhCOOH	96:4	85	90	*R*
3[275]	**191**	10	2	0.8 mL H$_2$O	20 mol% stearic acid	99:1	80	93	*R*
4[276]	**192**	10	-40	3 mL toluene	10 mol% AcOH	98:2	90	95	*R*

Benaglia *et al.* later reported a number of binaphthyl catalysts including catalyst **191** for the aldol reaction of acetone (entry 3, Table 3.8) with cyclohexanone with 4-nitrobenzaldehyde (entry 3, Table 3.8) in water using stearic acid as additive.[275] In general, the catalysts performed more successfully in water than in organic solvent due to proposed hydrophobic effects. In the same year, the Shi group also investigated BINAM derived catalysts in the aldol reaction.[276] Using 10 mol% AcOH as additive, the reaction of 4-nitrobenzaldehyde with acetone produced high yields and up to 93% ee (entry 4, Table 3.8) while the reaction with cyclohexanone gave 90% yield, 95% ee and 98:2 *dr* (entry 4, Table 3.9).

3.4.9 Bifunctional Prolinamide Catalysts

Bifunctional prolinamide catalysts contain a prolinamide group and an additional functionality capable of H-bonding or interacting with the substrate or reaction transition states. Some examples have been mentioned earlier in Table 3.4 & Table 3.5 in the context of prolinamides

148

functionalised with a second hydroxyl group. The *bis*-prolinamides described in the previous section 3.4.8 are symmetrical while the catalysts detailed in this section are non-symmetrical in nature (Figure 3.9). Prolinamides containing an additional functionality which may also cooperatively interact with aldol reaction substrates are potentially advantageous in terms of yield and enantioselectivity; specific examples summarised in Table 3.10 & Table 3.11.
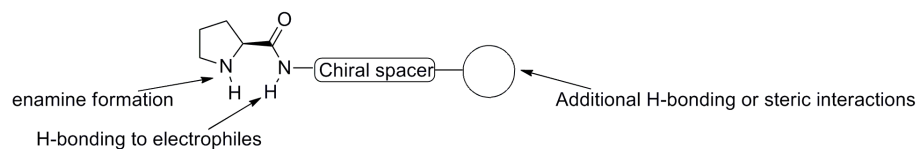
Figure 3.9: General structure of Bifunctional prolinamide catalyst showing potential interaction with substrates

Xiao *et al.* applied a number of unsymmetrical bisamide catalysts linked by a chiral cyclohexane ring.[277,278] They observed a strong dependence on the 'non-pyrrolidine' amide N-H pK_a for efficient catalyst performance and used an electron withdrawing groups to enhance this in the reaction of acetone with 4-nitrobenzaldehyde in combination with 40 mol% AcOH (entry 1, Table 3.10).[278] The bifunctional catalyst **193** combining an *N*-acyl-4-methylphenyl group with a prolinamide showed enhanced catalytic ability in the reaction using tetrahydro-4*H*-pyran-4-one with substantially improved results compared use of (*S*)-proline.[234] In addition, catalyst **193** efficiently catalysed the reaction of cyclohexanone with aromatic aldehydes (entry 1, Table 3.11).

In 2006, Benaglia *et al.* used a bifunctional C$_1$-symmetric binaphthyl amino derivative **194** in the reaction of 4-nitrobenzaldehyde with acetone giving product in 92% yield and 90% ee (entry 2, Table 3.10).[279] Use of 3 equivalents water had a positive effect on both reaction yield and ee but had no effect on diastereoselectivity when cyclohexanone was used (entry 2, Table 3.11). The Guillena group used a non-symmetric BINAM-(*S*)-prolinamide sulfonamide catalyst **195** in the aldol reaction of 4-nitrobenzaldehyde with acetone (entry 3, Table 3.10).[280] The sulfonamide N-H moiety was suggested to H-bond and activate the electrophile.[198,199,281] For the reaction of cyclohexanone with 4-nitrobenzaldehde, reactant conversion of 99% was observed with 98% ee and 99/1 dr using 5 mol% catalyst **195** under the optimal conditions at 0°C (entry 3, Table 3.11).

Table 3.10: Reaction of 4-nitrobenzaldehyde with acetone catalysed by bifunctional prolinamide catalysts.

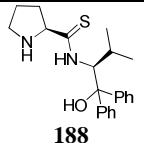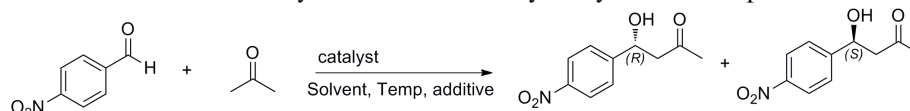| Entry	Catalyst	Loading (mol%)	Temp (°C)	Solvent	Additive	% Yield	ee	Config
1[278]	193	20	-40	THF	40 mol% AcOH	57	77	*R*
2[279]	194	10	-27	5 mol equiv DMF in acetone	-	92	90	*R*
3[280]	195	5	0	Neat ketone	5 mol% PhCOOH, 7 equiv H_2O	88	86	*R*
4[282]	197	1	Rt	Brine	1 mol% Dinitrophenol	96	94	*R*
5[283]	198	10	-20	Toluene	4-nitrobenzoic acid	95	97	*R*

A number of camphor containing prolinamide-thiourea catalysts were reported by Chen *et al.* in 2008.[284] The optimum catalyst **196** with 20 mol% DBSA in H_2O produced a high yield of 95%, diastereoselectivity of 96/4 and 99% ee from the reaction of cyclohexanone with 4-nitrobenzaldehyde (entry 4, Table 3.11). A substrate scope study with a number of arylaldehydes gave products in high diastero and enantioselectivities in most cases. The authors proposed that the reactants and catalysts were forced into close proximity due to hydrophobic interactions and H-bonding between the catalyst thiourea and amide protons with the aldol acceptor in the transition state allowing *si* enamine attack to the aldehyde carbonyl group.

Table 3.11: Reaction of 4-nitrobenzaldehyde with cyclohexanone catalysed by bifunctional prolinamide catalysts.
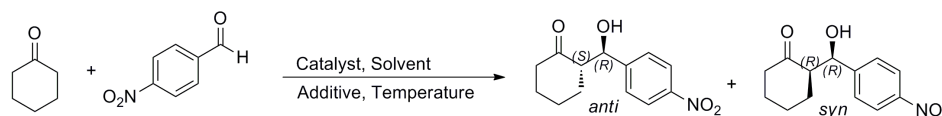
Entry	Catalyst	Loading (mol%)	Temp (°C)	Solvent	Additive	Anti:syn	% Yield	ee	Config
1[277]	193	20	-25	1:1 CHCl$_3$: ketone	20 mol% AcOH	96:4	89	92	R
2[279]	194	10	-27	3 mol equiv H$_2$O in acetone	-	>98:2	91	95	R
3[280]	195	5	0	Neat ketone	5 mol% PhCOOH, 7 equiv H$_2$O	99:1	99	98	R
4[284]	196	20	Rt	1 mL H$_2$O	20 mol% DBSA	96:4	95	99	R
5[282]	197	1	Rt	Brine	1 mol% Dinitrophenol	79:21	84	93	R
6[283]	198	10	-20	Toluene	4-nitrobenzoic acid	97:3	100	99	R

In 2009, Da *et al.* studied bifunctional prolinamide catalysts including catalyst **197** for the direct aldol reaction of ketones with aldehydes in brine.[282] Reactions without acid additives or including additives with very low pK$_a$ values such as TFA and 2,4,6-trinitrophenol produced unsatisfactory enantioselectivies and yield; however 2,4-dinitrophenol was identified as the optimum additive. Replacement of water with brine as reaction solvent produced a considerable improvement in selectivity. The authors tested a range of arylaldehydes with cyclohexanone and acetone and obtained high enantio- and diastereoselectivities under the optimised conditions (entry 4, Table 3.10 & entry 5, Table 3.11).

151

They proposed a transition state model based on electrophile activation as a result of H-bonding from the amide and tertiary ammonium salt (Figure 3.10). The enamine formed from the pyrrolidine with acetone was prosed to attack the aldehyde from its *Re*-face, producing an excess of the *R*-product.
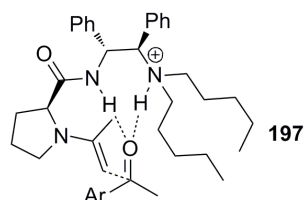
Figure 3.10: Proposed transition state showing binding of aldehyde to catalyst **197** studied by Da *et al.*[282]

In 2011, Kokotos *et al.* reported a number of successful bifunctional prolinamides containing thiourea groups in the aldol reaction of acetone and cyclohexanone with 4-nitrobenzaldehyde.[283] Acid additives with medium acidity were found to be most successful to enhance the reaction with 4-nitrobenzoic acid being the optimal additive (entry 5, Table 3.10 & entry 6, Table 3.11) while water as additive decreased reaction yields and stereoselectivities. A transition state model was proposed where the amide and thiourea groups formed H-bonds to the aldehyde influencing its reaction with the aldehyde leading to good enantioselectivities while a similar model was proposed in the presence of 4-nitrobenzoic acid which was proposed to form H-bonds to the catalyst thiourea and electrophilic aldehyde (Figure 3.11).
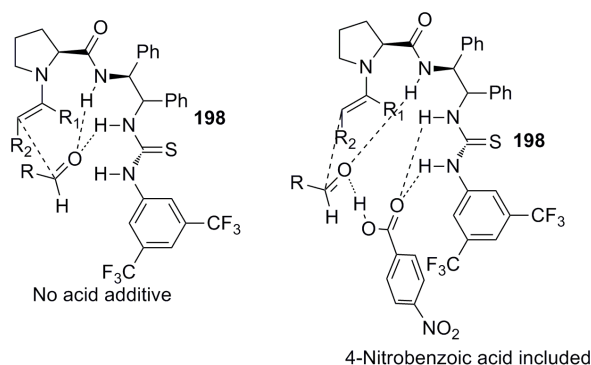
Figure 3.11: Proposed transition state models for thiourea-prolinamide catalysts.[283]

3.4.10 Proline-Derived *N*-acyl Sulfonamides

The use of proline and prolinamide derivatives as organocatalysts has been extensive.[228] The replacement of the hydroxyl group of (*S*)-proline with a sulfonamide has also been evaluated to generate catalysts of similar acidity to proline (Figure 3.12).[199] The use of this group allowed substantial changes in catalyst pK_a to be made without completely altering the backbone structure of the catalyst and also provided improved solubility compared to proline.
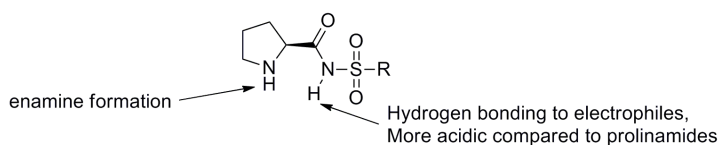
Figure 3.12: General structure proline derived *N*-acyl sulfonamide proline amide catalysts showing potential sites of interaction with substrates.

Berkessel *et al.* reported the first proline derived *N*-acyl sulfonamide organocatalyst in 2004 and varied the steric and electronic effects of the *N*-sulfonyl group creatong catalysts **199** & **200**.[198] They observed significantly improved results in the reaction of 4-nitrobenzaldehyde with acetone in polar aprotic DMSO (entries 1-2, Table 3.12). They explained the mechanism of action using a similar model to (*S*)-proline catalysis,[241] where the acidic N-H proton forms H-bonds with the reactants. Improved shielding of one of the enantiopic faces of the aldehyde by the sulfonyl aryl ring and also possibly stronger H-bonding compared to proline was proposed to explain the superior enantioselectivity.

In 2005, the Ley group used proline derived *N*-acylsulfonamide catalysts for the reaction of acetone and cyclohexanone with 4-nitrobenzaldehyde, observing dichloromethane to be the optimum solvent.[199] A number of ketones were examined for their reaction with 4-nitrobenzaldehyde using 20 mol% of *N*-acylsulfonamide catalysts and excellent enantioselectivities were observed, however, relatively poor *anti:syn* ratios were reported in the case of cyclic ketones (entry 3, Table 3.12 and entry 1, Table 3.13).[199] These catalysts gave significantly improved results compared to (*S*)-proline. The low *N*-acyl sulfonamide N-H pK_a was suggested to facilitate strong H-bonding of the N-H proton to the electrophile, producing a more tightly bound transition state and higher ee values.

153

Table 3.12: Reaction of 4-nitrobenzaldehyde with acetone catalysed by proline sulfonamide catalysts.
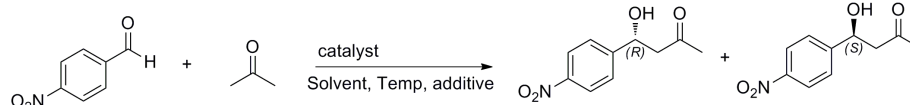
Entry	Catalyst		Loading (mol%)	Temp (°C)	Solvent	Additive	% Yield	ee	Config
1[198]	**199**		10	Rt	DMSO	-	91	95	*R*
2[198]	**200**		30	Rt	DMSO	-	73	98	*R*
3[199]	**(catalyst)**	R = CH₃	20	20	CH₂Cl₂	-	78	79	*R*
		R = Ph	20	20	CH₂Cl₂	-	49	84	*R*
4[285]	**201**		20	Rt	DMF	Et₃N	63	90	*R*

Later in 2005, Kokotos *et al.* studied proline derived *N*-acyl sulfonamide catalysts including some pyrrolidine ring 4-substituted derivatives[285] in the reaction of 4-nitrobenzaldehyde with acetone. A hydroxyproline derived *N*-acyl sulfonamide catalyst **201** was the most successful catalyst using 1 equivalent of triethylamine and acetone as a co-solvent (entry 4, Table 3.12). In 2006, Wang *et al.* synthesised a number of chiral dendritic *N*-acyl sulfonamides and studied their activity in the reaction of cyclohexanone with 4-nitrobenzaldehyde in water (entry 2, Table 3.13).[286] They proposed that their catalyst **202** bearing hydrophobic polyether dendritic groups enhanced the reaction in water through the hydrophobic effect.

In 2009, Fu *et al.* synthesised a range of 4-*tert*-butyldimethylsiloxy pyrrolidine ring substituted *N*-acylsulfonamides as catalysts in the aldol reaction of 4-nitrobenzaldehyde with neat cyclohexanone (entry 3, Table 3.13).[262] The authors ascribed the success of their catalysts to the hydrophobic effect of the TBS ether group. A detailed substrate scope gave successful results for cyclohexanone with a range of aldehydes and producing excellent yields, enantio and diastereoselectivities in many cases. Hua *et al.* considered a novel proline derived *N*-acylsulfonamide catalyst **203** similar in structure to Berkessel's and Ley's catalyst, however it contained a non-polar group at the *para-* position of the aromatic ring of the sulfonamide to improve solubility.[287] They obtained high yields, enantio and diastereoselectivities in the aldol reaction of cyclohexanone with 4-nitrobenzaldehyde (entry 4, Table 3.13). They later

successfully conducted this reaction in an industrially useful solvent 2-methyl-tetrahydrofuran and also under neat reaction conditions (entry 4, Table 3.13).[288] The Hua catalyst **203** gave improved performance over other catalysts tested, its success ascribed to high solubility in non-polar solvents.

Table 3.13: Reaction of 4-nitrobenzaldehyde with cyclohexanone catalysed by proline derived *N*-acyl sulfonamide catalysts.

Entry	Catalyst		Loading (mol%)	Temp (°C)	Solvent	Additive	*Anti:syn*	% Yield	ee	Config
1[267]		R = CH$_3$	20	20	CH$_2$Cl$_2$	-	51:29	80	78	*R*
		R = Ph	20	20	CH$_2$Cl$_2$	-	53:35	88	90	*R*
2[286]	**202**		5	Rt	1 mL H$_2$O	-	99:1	99	99	*R*
3[262]			3	Rt	0.5 mL H$_2$O	-	97:3	>99	99	*R*
4[287,288]	**203**		20	4	C$_2$H$_4$Cl$_2$	1 equiv H$_2$O	>99:1	95	99	*R*
			2	Rt	Neat	1 equiv H$_2$O	>99:1	96	96	*R*
			20	Rt	2-Me-THF	1 equiv H$_2$O	30:1	85	94	*R*

3.5 Intermolecular Ketone:Ketone Aldol Reactions

The number and variety of aldol acceptors is quite extraordinary however the number of aldol donors remains more limited. Ketones are known to be less reactive than aldehydes and may have less steric discrimination compared to an aldehyde. Despite these challenges, there has been significant progress on this type of aldol reaction driven by the valuable nature of the aldol adducts as building blocks for biologically active compounds.[228,289]

In 2005, Wen *et al.* were the first to report an enantioselective aldol addition of methyl ketones such as acetone to aryl ketones containing CF$_3$ groups catalysed by (*S*)-proline (Scheme 3.18).[290] They used acetone in large excess, therefore acting as the solvent and the

nucleophilic source in combination with 10 mol% (*S*)-proline to give the product in moderate enantioselectivity (Scheme 3.18).
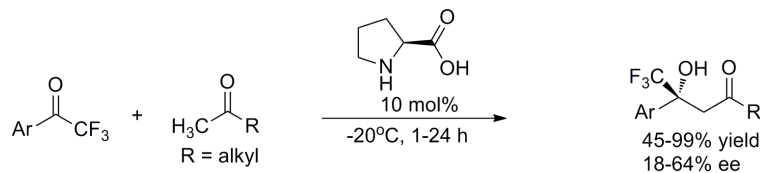
Scheme 3.18: Reaction of 1-aryl-2,2,2-trifluoroethanones with methyl ketones catalysed by (*S*)-proline reported by Wen *et al.*[290]

In 2006, Gong *et al.* reported a catalytic system for the reaction of α-keto acids with acetone Scheme 3.19.[176] This work was based on original findings by Hamilton *et al.* that the prolinamide catalyst **139** derived from 2-aminopyridine group was a highly efficient artificial molecular recognition receptor which could bind strongly to a carboxyl group.[53] Gong *et al.* developed a number of relatively simple (*S*)-prolinamide catalysts containing the aminopyridine moiety and found the catalyst **139** derived from proline with 2-aminopyridine to be optimal producing high yield and up to 98% ee. Experimental investigations showed the importance of the H-bonding interactions between the 2-pyridyl prolinamide catalyst and the both the keto and carboxyl groups of the keto-acid substrate. These H-bonding interactions activated the keto functionality for controlled attack by the closely located enamine nucleophile to form the product in high ee.
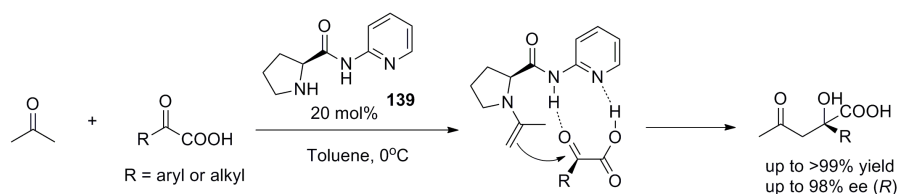
Scheme 3.19: Reaction of α-keto acids with acetone catalysed by a 2-pyridyl prolinamide catalyst **139**.[176,291]

Feng *et al.* used a C$_2$-symmetric *bis*-prolinamide catalyst **189** for the reaction of α-keto esters with acetone.[292] The chiral tertiary alcohol product was obtained in high yield and up to 94% ee (Scheme 3.20). The authors also tested this reaction using the mono-prolinamide equivalent of their catalyst and obtained a yield of 32% and 11% ee, confirming the importance of the cooperative effects of the two pyrrolidine amide units.[251] Theoretical calculations showed that one pyrrole ring was involved in enamine formation while the α-keto ester H-bonded with the

second amide and protonated pyrrolidine amine group in the presence of an acid. As a result, the *Re* face was more prone to nucleophilic attack, resulting in stereoselective catalysis as shown in the proposed transiton states in Scheme 3.20.
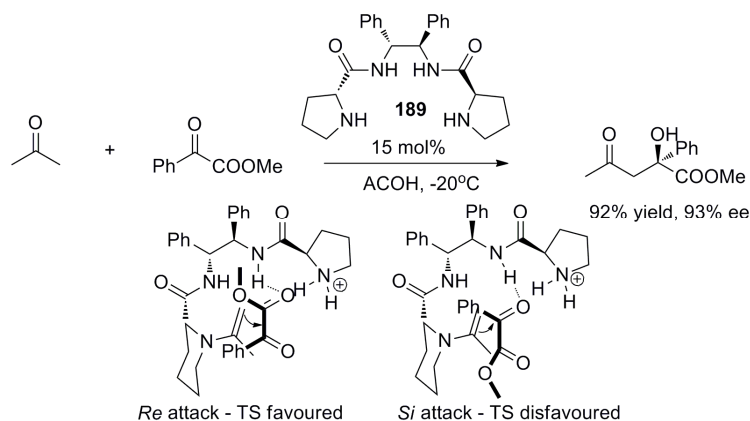
Scheme 3.20: Asymmetric aldol reaction of α-keto esters with acetone using *bis*-prolinamide catalyst **189**.[292] Proposed transition states leading to enantioselectivity of the catalyst obtained based on theoretical calculations by the authors.

In 2011, Nakamura applied their previously successful *N*-(heteroarenesulfonyl)prolinamide catalysts for the reaction of 2,2,2-trifluoro-1-phenylethanone with acetone and determined the *N*-(8-quinolinesulfonyl)prolinamide catalyst **204** to be optimal (Scheme 3.21).[293] The product was obtained in 92% yield and 89% ee. This catalyst was also efficient using a range of fluoroalkyl ketones and trichloroalkyl ketones with acetone. The authors proposed that the transition state leading to the (*R*)-product was disfavoured due to steric repulsion between the trifluoromethyl groups and the 8-quinolyl groups (Scheme 3.21).
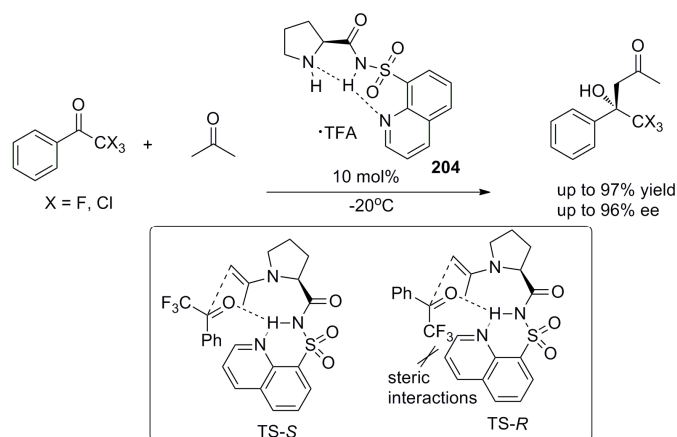
Scheme 3.21: Reaction of trihaloketones with acetone catalysed by optimum *N*-(8-quinolinesulfonyl)prolinamide catalyst **204**. Transition states proposed to explain preference for (*S*)-product also shown.[293]

157

3.5.1　Ketone: Ketone Aldol Reactions towards Natural Products

The enantioselective synthesis of natural products is of continuing interest. Compounds based on the indole substructure appear in many natural products and drug molecules. For example, oxindoles, which possess a carbonyl group at the 2-position of the 5-membered ring and a quaternary carbon centre at the 3-position of this ring (Figure 3.13) are present in many biologically active alkaloids and pharmacological agents.[294-300] Structure-activity relationships have shown the absolute configuration and substitution pattern at the C-3 position control the biological activities of these groups,[301] creating a need to develop methods to enantioselectively synthesise these compounds.
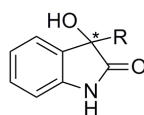
3-substituted-3-hydroxyindoline-2-ones

Figure 3.13: General structure of 3-substituted-3-hydroxyindoline-2-ones.

Oxindoles are present in convolutamydines A-E, maremycin, dioxibrassinine and 3-cycloalkanone-3-hydroxy-2-oxindoles (Figure 3.14).[294-300,302-305] One other notable example is 3-acetonyl-3-hydroxyoxindole which has been shown to be a chemical inducer of systemic acquired resistance, an inducible defence mechanism against microbial pathogen attack in tobacco plants against the tobacco mosaic virus.[306] The potential applications of oxindoles has led to much interest in their synthesis.[307-311] The aldol addition of ketones to substituted and unsubstituted isatins would appear to be a simple and route towards these important biological compounds.[312-315] This method can be rather challenging due to the relatively poor electrophilicity of ketones for the aldol reaction.[313,316,317]

Convolutamydine A-E
A: R = CH$_2$COCH$_3$
B: R = CH$_2$CH$_2$Cl
C: R = CH$_3$
D: R = CH=CH$_2$
E: R = CH$_2$CH$_2$OH

maremycin
R = ""OH
R = —OH

dioxibrassinine

3-cycloalkanone-3-hydroxy-2-oxindoles
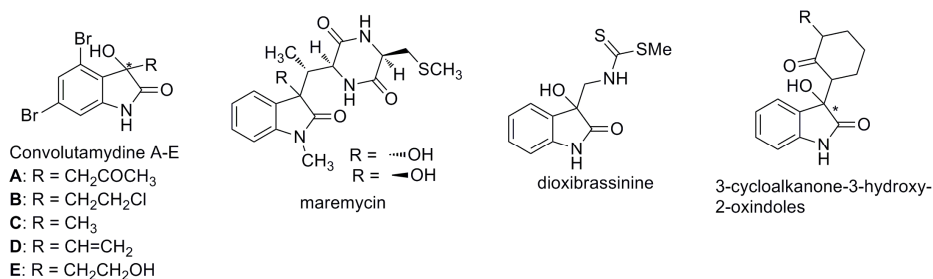
Figure 3.14: Structure of some biologically active compounds based on 3-substituted-3-hydroxyindolin-2-one substructure.

In 2005, Tomasini *et al.* reported the first enantioselective addition of isatin and *N*-alkylated isatins to acetone using organocatalysis.[318] In the reaction of isatin with acetone, they tested a library of prolinamide based dipeptides and found the optimal dipeptide H-D-Pro-L-β3-hPhg-OBn catalyst **205** gave the (*R*)-aldol product in 73% ee at -15 °C, much improved compared to (*S*)-proline which produced 33% ee of (*S*)-product. They also reported ee of the order of 73-77% for a number of substituted isatin derivatives with acetone (Scheme 3.22). Interestingly, a degree of enantiomeric enrichment was observed during chromatographic purification.
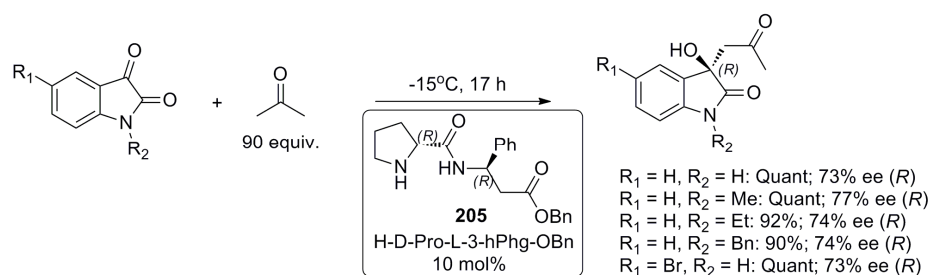
Scheme 3.22: Reaction of isatins with acetone catalysed by optimum proline dipeptide catalyst **205** reported by Tomasini *et al.*[318]

Chen *et al.* evaluated the (*S*)-proline catalysed reaction of several isatins with acetone, observed faster reactions and higher ee values where *N*-substituted isatins were used and postulated a mechanism to account for the relatively poor ee values for the reaction with unsubstituted isatin (Scheme 3.23).[313] Isatin may exist in a more active form **A'**, which facilitates intramolecular H-bond formation between the carbonyl oxygen and enol hydrogen atom. Meanwhile, enamine formation occurs with proline and acetone to form **D** which would combine with **A'** *via* transition state **E**. In this transition state, H-bonding between **A'** and the carboxylic acid of enamine **D** is proposed to ensure that reaction occurs at only one face of the pyrrolidine ring while this H-bonding also lowers the reaction energy barrier through charge stabilisation. Based on this proposed mechanism, the intermolecular H-bond in **A'** would hinder this H-bonding. In the case of *N*-substituted isatins, tautomerisation and intramolecular H-bond formation is not possible and in the comparable transition state **E**, the proline carboxylic acid group binds tightly to both carbonyl groups of the isatin, resulting in much higher ee compared to unsubstituted isatin.
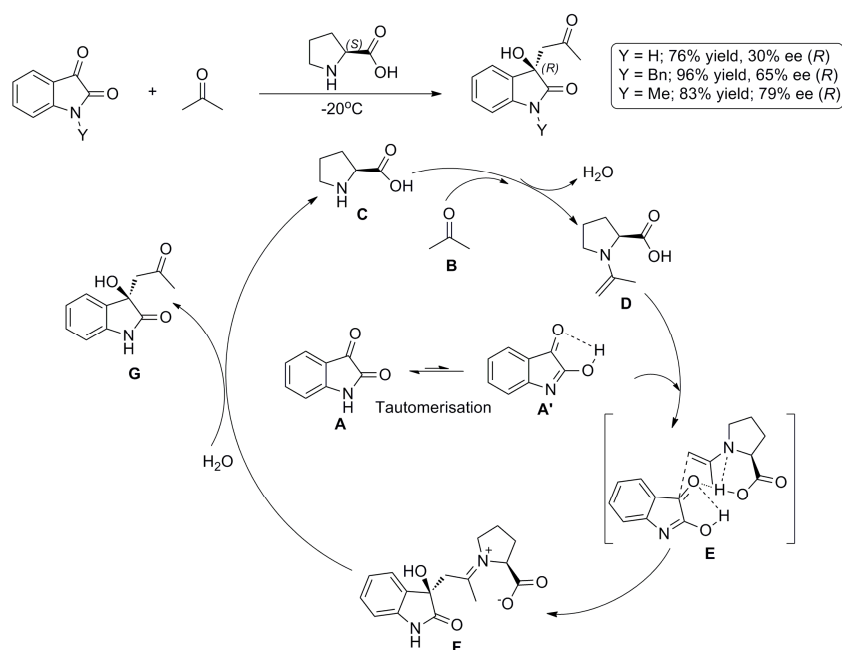
Scheme 3.23: Mechanism of (*S*)-proline catalysed aldol reaction of isatin with acetone as proposed by Chen *et al.*[313]

In 2006, Tomasini *et al.* reported the synthesis of (*R*)-Convolutamydine A through the reaction of 4,6-dibromoisatin with acetone catalysed by (*R*)-proline and also a number of dipeptide prolinamide organocatalysts (Table 3.14).[312] The (*R*)-proline catalysed reaction was very sensitive to temperature producing 3.5% ee of (*R*)-product at room temperature compared to 55% ee of (*S*)-product at -20°C, the opposite configuration compared to when unsubstituted isatin was used as the aldol substrate. The reaction was less efficient in anhydrous acetone suggesting involvement of water in the mechanism. Their previously determined optimum catalyst **205** for the reaction of isatin with acetone[318] was also found to be optimal for the synthesis of (*R*)-Convolutamydine A. The product was obtained in 97% ee through initial removal of catalyst by filtration followed by recrystallisation (entry 2, Table 3.14).

Table 3.14: Reaction of 4,6-dibromoisatin with isatin catalysed by (S)-proline and prolinamide dipeptide studied by Tomasini *et al.*[312]
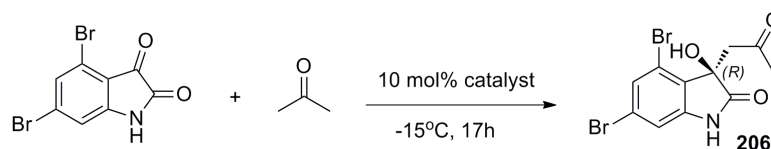
Entry	Catalyst	Yield	ee	Config
1[319]		86	55	S
2[319]		Quant	68	R
		50[a]	97[a]	R

[a]After recrystallisation.

Xiao *et al.* tested a range of (S)-proline derived bifunctional bisamide catalysts for the reaction of isatin with acetone and 2-butanone.[314] Their most successful catalyst **207** resulted in product **208** with an ee of 88% for the reaction using acetone, 20 mol% AcOH and 10 mol% catalyst loading at -50°C. High ee values were also obtained using catalyst **207** with a number of other substrates (Scheme 3.24). They confirmed the product had the (S)-configuration through X-ray crystallography. Based on this, they suggested a possible transition state model where the catalyst controlled the enamine geometry and also orientation of the isatin substrate with both amide N-H groups involved in binding the substrate (Scheme 3.24).

R = Y = H, R' = CH₃; -50°C; 99% yield, 88% ee, (S)
R = H, Y = Bn, R' = CH₃; -45°C; 99% yield, 87% ee (config not given)
R = H, Y = H, R' = CH₂CH₃; -20°C; 98% yield, 80% ee, regioselectivity 9:1 (config not given)
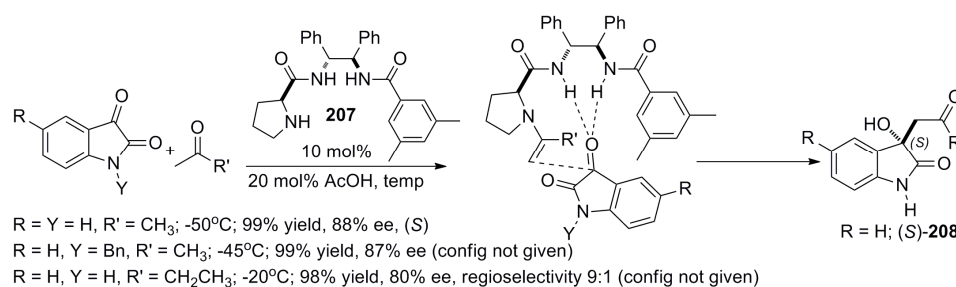
Scheme 3.24: Reaction of isatin with acetone using bifunctional bisamide catalyst **207**. Their proposed transition state is also shown.[314]

In 2008, Nakamura *et al.* reported the enantioselective synthesis of (R)-Convolutamydine A using a novel sulfonyl prolinamide organocatalyst **209** and in 2009, they also reported the synthesis of (R)-Convolutamydines B and E using the same catalyst.[320,321] The TFA salt of *N*-(2-thienylsulfonyl)prolinamide catalyst **209** in the presence of 10 equivalents H₂O was found to be optimal in the reaction of 4,6-dibromoisatin with acetone to obtained (R)-

Convolutamydine A (Scheme 3.25a).[320] Catalyst loading could be reduced to 0.5 mol% without significant loss of enantioselectivity. For the reaction of unsubstituted and substituted isatins with acetone, good yields and high enantioselectivites were obtained in all cases. They subsequently applied this catalyst to the reaction of isatin derivatives with acetaldehyde followed by reduction to give Convolutamydine B and E (Scheme 3.25b). The authors postulated that intramolecular hydrogen bonding between the amide N-H and the sulfur heteroatom as the mode of activation, such an interaction leading to two potential transition states (Scheme 3.25c). The *syn-trans* transition state was proposed to be disfavoured due to steric interactions between the Br substituents and the catalyst thienyl ring, thus preferentially giving the *anti-trans* transition state, leading to high product ee.
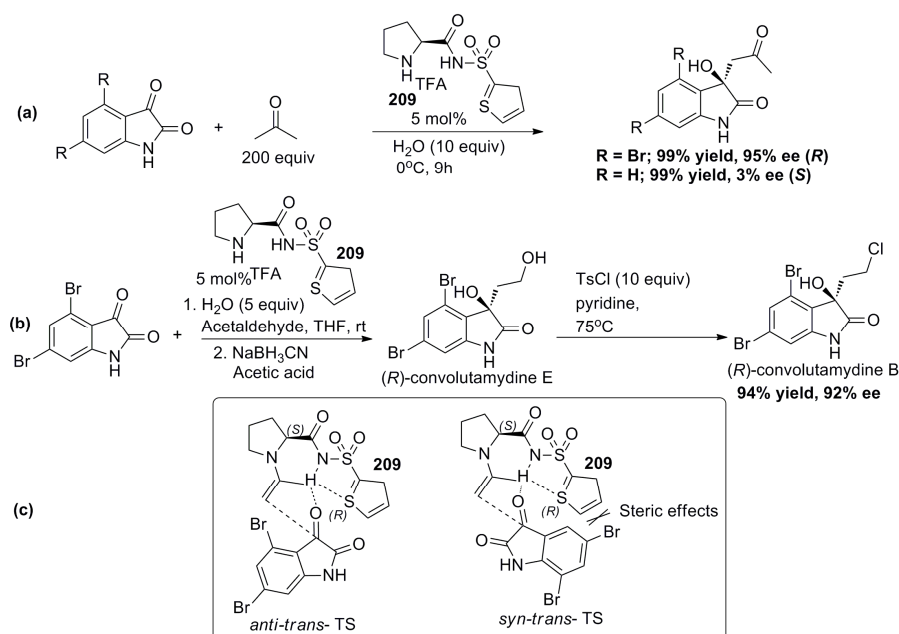
Scheme 3.25: (a) Enantioselective synthesis of (*R*)-convolutamydine B and E using *N*-(2-thenylsulfonyl)prolinamide catalyst **209** (b) Enantioselective synthesis of (*R*)-convolutamydine B & E using catalyst **209**. (c) Proposed transition states favouring the (*R*)-product.[320]

In 2008, Tomasini *et al.* conducted detailed mechanistic investigations into the (*S*)-proline catalysed reactions of isatin and 4,6-dibromoisatin with acetone using DFT calculations.[322] DFT results for the isatin reaction with acetone produced two low energy transition states *anti-S-cis* and *anti-R-trans*, consistent with the experimental formation of the (*S*)-product (Figure 3.15). However, the energy gap between these two transition states predicted a higher preference for the (*S*)-product than the experimental finding and this difference was initially

suggested to be due to solvation effects decreasing the energy difference between the states in solution. Calculations suggested that oxazolidinone intermediates, steric interactions, dipole moment and charge distribution had no effect on the enantioselectivity of the reaction. Further analysis showed that the bonds in the *anti-S-cis* and *anti-R-trans* states were equivalent but a greater degree of proton transfer from the carboxylic acid to the forming alkoxide ion in the lower energy transition state (*anti-S-cis*) was observed.

They also found that water preferentially formed H-bonds to the outside lone pair electrons of the ketone carbonyl group. This H-bonding avoids unfavourable electrostatic interactions between the electronegative amide oxygen and proline carboxylic acid oxygen and also creates a structure which only needs to rotate clockwise around the H-bond to give a conformation similar to the lowest energy *anti-S-cis* transition state (Figure 3.15). A large rotation anticlockwise and through a higher energy conformation would lead to the second lowest transition state *anti-R-trans*. These results explained the preferential formation of the (*S*)-product in the (*S*)-proline catalysed reaction of isatin with acetone with water as additive.

anti-R-trans

anti-S-cis
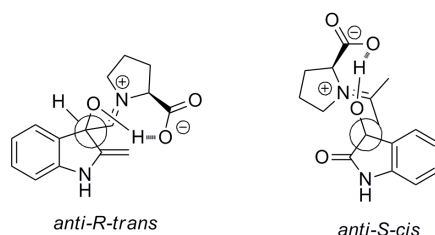
Figure 3.15: Newman projections showing the two lowest energy transition states proposed by Tomasini based on calculations on the reaction of isatin with acetone.[322]

In 2009, Tomasini *et al.* further studied the effects of water on the (*R*)-proline and prolinamide catalysed reaction of acetone with isatin.[319] Initial results showed that when too little or too much water was used as additive in the (*R*)-proline or the previously successful dipeptide **205** catalysed reaction, the ee of product decreased.[318] In the case of both reactions, the authors defined an optimum level of water and found a small increase in ee as the reaction proceeded which was attributed to the formation of diastereomeric complexes between the catalyst and the aldol adduct product, a process which was not observed in the presence of large excess of water or solvent. Overall, the effects of water were explained by including water molecules in DFT calculations of transition states. These calculations showed that a water molecule could

163

either actively or passively participate in the transition state (Figure 3.16) and calculations suggested there was a larger energy gap between the hydrated diastereomeric transition states than the unhydrated states. A number of the lowest energy transition states were also more stable in the presence of water, producing a higher ee and shorter reaction time in wet conditions.
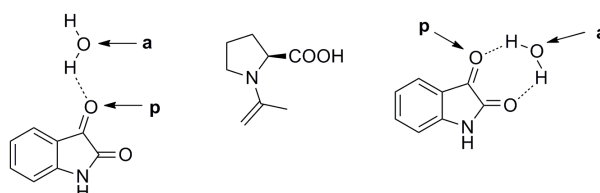
Figure 3.16: Proposed water/isatin hydrogen bonded structures where a and p represent a H-bonding site for the acid group of acetone-(S)-proline enamine where water may actively or passively participate.

In 2009 and 2010, two groups independently investigated the reaction of acetaldehyde with a range of isatin derivatives using 4-hydroxydiaryprolinol catalyst **210** to produce important intermediates for 3-hydroxyalkaloid synthesis.[323,324] Hayashi *et al.* used catalyst **210** in the reaction of isatin derivatives with acetaldehyde to yield the product in high enantioselectivities in excess of 82% (entries 1-4, Table 3.15).[323] Yuan *et al.* also used a wide range of isatins with acetaldehyde in the 210 catalysed aldol reaction and did obtained successful results without the need for an acid additive.[324] In this work, they obtained products in good yield and ee values of the order 80-99% and (R)-Convolutamydine E in 97% ee (entry 6, Table 3.15). They also reported the synthesis of (R)-Convolutamydine B in 50% yield and 97% ee.

Table 3.15: Reaction of isatin and isatin derivatives with ketones using a number of proline derived catalysts.

Entry	Isatin substrate	Conditions	Yield	ee	Config
1[323]	R = H; Y = Bn	30 mol% catalyst, 20 mol% ClCH$_2$CO$_2$H, 4°C, 48 hours. Followed by NaBH$_4$ reduction	55	85	*R*
2[323]	R = H; Y = H		<5	-	-
3[323]	R = H, Y = CH$_2$OTIPS		73	85	*R*
4[323]	R = Br, Y = CH$_2$OTIPS		86	82	*S*
5[324]	R = H Y = H	0.5 mL DME, 20 mol% catalyst, -20°C, 72 hours. Followed by NaBH$_4$ reduction	25	75	*R*
6[324]	R = Br Y = H		73	97	*R*

164

3.6 Conclusions

This Chapter has detailed a selection of proline and proline derivatised organocatalysts in the intermolecular ketone:aldehyde and ketone:ketone aldol reaction. In addition, several examples of the useful application of these reactions towards natural products have been given such as enantioselective oxindole synthesis. Chapter 4 will describe experimental work involving the application of novel pyrrolidine based organocatalysts with a focus on enantioselective synthesis of oxindoles.

4 Chapter 4

Screening of Simple *N*-aryl and *N*-heteroaryl Pyrrolidine Amide Organocatalysts for the Enantioselective Aldol Reaction of Acetone with Isatin.

4.1 Background

As discussed previously, the synthesis of enantiomerically pure compounds is a significant challenge for the organic chemist. Enantiomers differ only in spatial orientation of atoms around a chiral centre while mainly possessing identical physical and chemical properties.[221,228] One of the most efficient and widely used techniques for enantioselective synthesis is chiral catalysis.[9] The vast growth in the area of organocatalysis prompted the experimental work described in this Chapter which focuses on the development of novel chiral organocatalysts employing suitable characteristics of supramolecular binding systems for the highly useful aldol reaction towards natural products was considered.

Compounds based on the indole substructure appear in many natural products and drug molecules. For example, oxindoles, which possess a carbonyl group at the 2-position of the 5-membered ring and a quaternary carbon centre at the 3-position of this ring (Figure 4.1) are present in many biologically active alkaloids and pharmacological agents.[294-300] Structure-Activity Relationships have shown the substitution pattern and absolute configuration at the C-3 position of these compounds control their biological activities,[301] creating a need to develop methods towards their stereoselective synthesis. The work described in this Chapter focuses on the aldol addition of ketones to substituted and unsubstituted isatins towards these important biological compounds.[312-315]
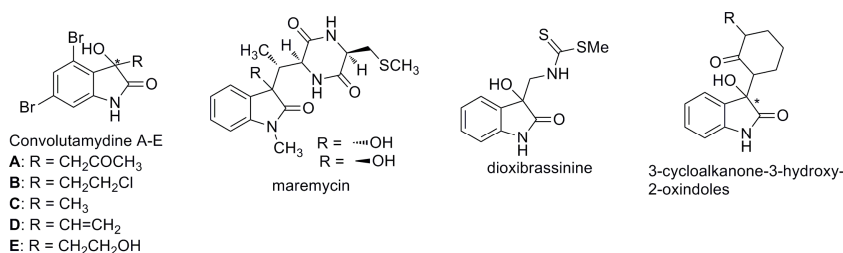
Figure 4.1:General structure of 3-substituted-3-hydroxyindoline-2-one natural products.

4.1.1 Hydroxyindole Synthesis – Proline Based Catalysts

Isatin and isatin based molecules belong to an important class of 3-substituted-3-hydroxyindolin-2-one substituted molecules which have applications as hair dyes, in the development of colour photographic materials and inhibition of corrosion in some metals.[325]

167

As described in Chapter 3, several authors have enantioselectively synthesised hydroxyindole based molecules using proline and prolinamide based catalysts and a summary of this work is given in (Scheme 4.1).[312,314,318]
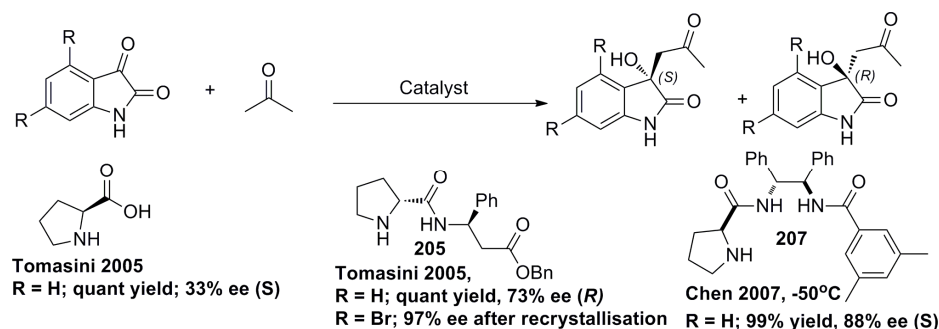
Scheme 4.1: Summary of literature examples of reaction of isatin and 4,6-dibromoisatin with acetone. [312,314,318]

4.1.2 Oxindoles from Non-proline Derived Organocatalysts

The enantioselective synthesis of oxindoles through the aldol reaction has also been achieved using non-proline derived H-bonding catalysts. In 2007, Malkov and co-workers studied the reaction of a number of substituted and unsubstituted isatins with acetone using novel amino alcohol organocatalysts derived from leucine and valine containing primary amino and terminal hydroxyl groups.[311] They produced high yields and ee values up to 95% in the reaction of *N*-methylisatin with acetone (Scheme 4.2a). The reaction was thought to proceed *via* equilibration of an oxazolidinone by-product which consumed the catalyst, avoided the build up of a stable imine and acted as a stable resting state (Scheme 4.2b).
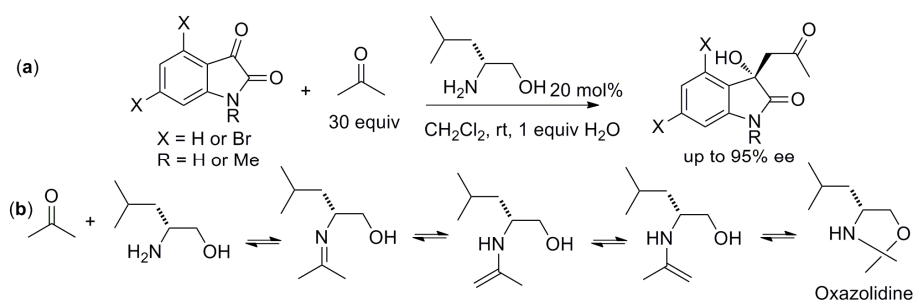
Scheme 4.2: (a) Reaction of isatin and isatin derivatives catalysed by leucinol.[311] (b) Proposed equilibrium between acetone and leucinol to form the oxazolidine stable resting state.

The enantioselective synthesis of 3-cycloalkanone-3-hydroxy-2-oxindoles has been reported including the aldol reaction of isatin with cyclohexanone to give a product with known anti-

convulsant properties.[317,326] The primary-tertiary diamine based catalyst **211** enhanced the reaction with impressive results (Scheme 4.3a). The catalytic ability was ascribed to formation of a hydrophobic cavity by the catalyst aromatic group in an aqueous medium with TFA as additive facilitating the reaction within the cleft. Yields of up to 90%, ee values up to 98% of (*S*)-product and dr up to 97:3 *syn:anti* were achieved in water, slightly inferior to DMF. Recently, Chen *et al.* reported a number of carbohydrate derived amino alcohol catalysts for the asymmetric reaction of isatin with acetone (Scheme 4.3b).[327] They observed a high dependence on solvent with optimum results in CH$_2$Cl$_2$ (91% yield; 67% ee) but racemic product in MeOH. Their catalysts were not significantly affected by a protecting group on isatin but obtained greater yields and enantioselectivites for isatin substrates with electron withdrawing substituents.
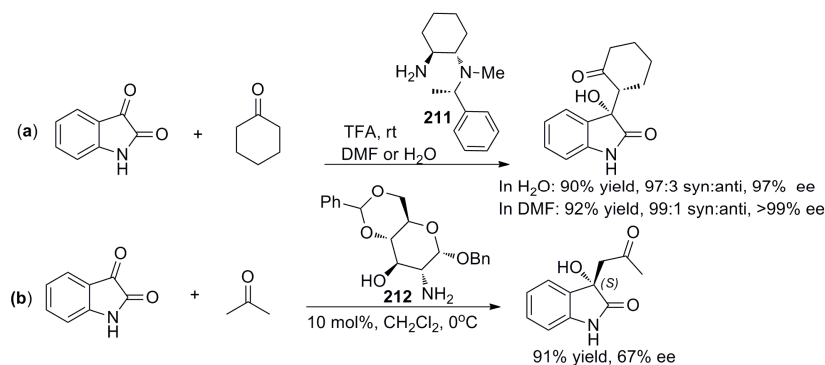
Scheme 4.3: (a) Reaction of cyclohexanone with isatin using primary-tertiary diamine catalyst **211** conducted by Raj *et al.*[317] (b) Successful carbohydrate derived amino alcohol catalyst **212** reported by Chen et al.[327]

Recently in 2011, Wang *et al.* reported the first enantioselective synthesis of biologically important 3-hydroxy-phospho substituted oxindoles through the reaction of isatin derivatives with phospho-nucleophiles.[328] The authors incorporated a tertiary amino group and hydroxyl or thiourea functionality into the scaffold of a cinchona alkaloid to activate the phosphate and isatin through H-bonding. A quinine derived catalyst **213** gave 99% yield and 67% ee under optimised conditions in the reaction of 1-methylisatin with diphenyl phosphate (Scheme 4.4). A transition state based on a ternary complex between the catalyst, 1-methylisatin and diphenyl phosphite was proposed (Scheme 4.4). The carbonyl group in 1-methylisatin was activated by H-bonding to the catalyst OH and the phosphite hydrogen was activated through a separate H-bonding effect with the tertiary amine. Synergistic cooperation allowed attack of the phosphite group on 1-methylisatin.

169
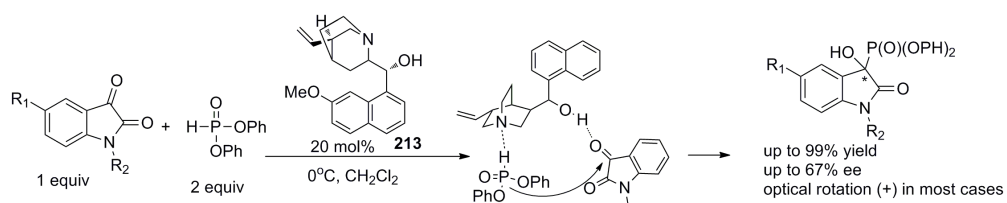
Scheme 4.4: Reaction of diphenyl phosphite with substituted isatins catalysed by quinine based catalyst **213** studied by Wang *et al.*[328] Proposed transition state model also shown.

4.1.3 Baylis-Hillman Reaction of Isatin Derivatives

The previous section described the organocatalytic enantioselective synthesis of 3-substituted-3-hydroxy-2-oxindoles through addition of carbonyl compounds to isatins. An alternative synthetic route to these compounds involves the Morita-Baylis-Hillman reaction, a reaction which was reviewed in detail in Chapter 2. The chiral variant of this reaction has been extensively examined using either chiral amine, urea or phosphine catalysts.[329] In general, aldehyde or imine electrophiles are used in this reaction; however in 2002, Garden *et al.* reported that the isatin keto-carbonyl carbon at the 3-position was sufficiently electrophilic for the Morita-Baylis-Hillman (MBH) reaction with acrylate esters or acryonitrile.[330] Following this report, Shanmugam *et al.* developed a synthetic protocol towards 2-spirocyclopropane-2-indolones, biologically active compounds and also important starting materials for alkaloid synthesis.[331]

A number of groups reported the successful application of *β*-isocupreidine **214** in the asymmetric MBH reaction using isatin derivatives.[301,332,333] In 2010, Zhou *et al.* used acrolein as the nucleophile to give the corresponding 3-hydroxy-2-oxindole in excellent enantioselectivity (Scheme 4.5).[332] Also in 2010, Shi *et al.* obtained product in good yields and ee from the using catalyst **214** in the reaction of isatin derivatives with electron deficient alkenes.[301] The most successful substrates were 1-naphthyl acrylate with unsubstituted isatins (Scheme 4.5). The proposed mechanism suggested that repulsion between the ester group and *N*-substituents of isatin disfavoured the transition state leading to the (*R*)-product, producing an excess of (*S*)-product.

170
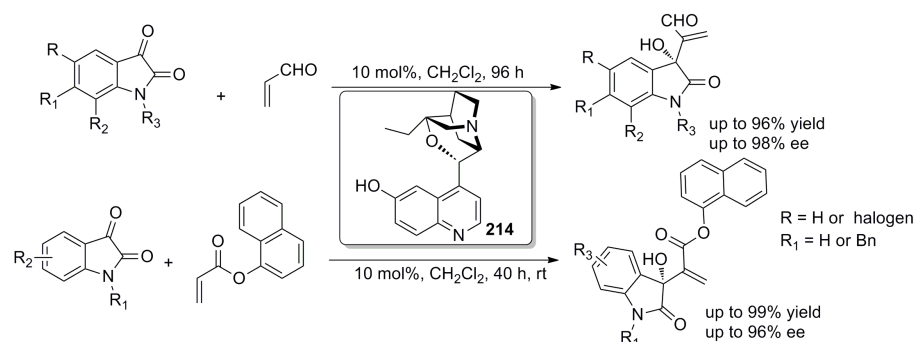
Scheme 4.5: Use of β-isocupreidine in Morita Baylis-Hillman reaction of isatin derivatives with acrolein[332] and also with 1-naphthyl acrylate by Shi *et al.*[301]

In 2011, Lu *et al.* used *β*-isocupreidine **214** in the MBH reaction of isatins with acrylates to give the products in excellent yields and enantioselectivities at ambient temperatures (83% yield, 96% ee) with protected isatins.[333] A mechanism was proposed where the enolate **A** generated by nucleophilic addition of catalyst **124** to the acrylate was stabilised by intermolecular H-bonding with the C6'-OH group. Following synthesis of Zwitterionic **B** through aldol reaction of enolate **A** with isatin, the key proton transfer step was facilitated by the C6'-OH group which acted as a proton shuttle allowing intramolecular proton transfer which selectively lead to isomer **C** (Scheme 4.6).
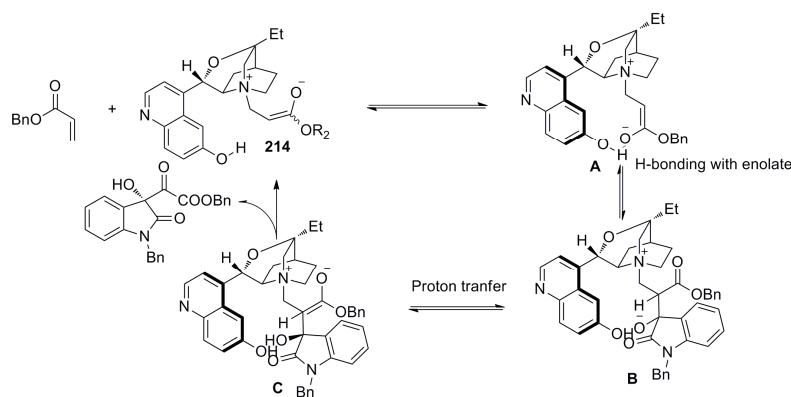
Scheme 4.6: Proposed mechanism of MBH reaction of *tert*-butyl acrylate with *N*-benzylisatin catalysed by β-isocupreidine **214** as outlined by Lu *et al.*[333]

4.2 Project Scope

The aldol addition of ketones to substituted and unsubstituted isatins has been shown to be an effective synthetic route towards important natural products such as Convolutamydines as discussed in the previous section and in Chapter 3. Significant work has been conducted by a

number of research groups towards successful organocatalytic enantioselective reactions of isatin and isatin derivatives with ketones such as acetone.[311,313,314,318,334] Overall, this has produced varied results and there still existed a need to develop new, successful enantioselective catalytic systems for this reaction. A large number of research groups have studied organocatalysts for the ketone:aldehyde aldol reaction[221] however the inherently more challenging ketone:ketone reaction has attracted significantly less attention. This reaction has the potential to create useful products and as a result, was chosen for this project with the ultimate aim of developing novel catalysts towards biologically interesting intermediates. With this goal in mind, a library of catalysts was designed and tested in the aldol reaction of isatin with acetone. This reaction was chosen as a model for other more complex syntheses due to the commercial availability of the starting materials and the challenging nature of the ketone/ketone aldol reaction.

4.2.1 Catalyst Design

In order to design potential catalysts for the aldol reaction of isatin and acetone, natural enzymatic processes were considered as optimum systems. Many enzymatic processes function through molecular recognition between enzymes and substrates and artificial systems have been developed based on the enzyme-substrate model, for example the use of organocatalysts as enzyme mimics for the aldol reactions where synthetic catalysts function in a similar way to aldolase enzymes.[118] In particular, it was highly desirable to draw key information from supramolecular systems and design catalysts capable of forming suitable non-covalent interactions with reaction intermediates. The close relationship between supramolecular interactions and catalysis has been reported[19] and this work endeavoured to provide more insight on this relationship. One notable application of supramolecular interactions in the design of chiral catalysis systems for the aldol reaction was conducted by Gong *et al.* as described in Chapter 3.[176,291] The basis of their work came from Hamilton *et al.* who found that a *bis-N*-aminopyridyl carboxamide group could successfully form H-bonds with a dicarboxylic acid as illustrated for adipic acid and a *bis*-picolinamide molecule.[53]

Hamilton's initial finding led to a significant amount of work utilising the binding properties of the *N*-aminopyridyl carboxamide functionality for a number of applications including self assembly[335] and organocatalysis.[176,291] The experimental work detailed in this Chapter was inspired by the findings of Hamilton, the constantly evolving inter-relationships between molecular recognition, active site considerations in enzyme catalysis and organocatalysis[19] and also previous results detailing the successful application of molecular receptors as catalysts (Chapter 1).[336] It aimed to apply a similar strategy to the aldol reaction of isatin with acetone by designing a number of chiral amide based catalysts incorporating *N*-pyridyl and *N*-quinolinyl groups. It was hoped to exploit cooperatively the H-bond donating and accepting properties of such catalysts. It was envisioned that the H-bond donating amide N-H group in the catalyst would bind to and activate the isatin ketone group and also possibly bind to the isatin amide carbonyl group while the H-bond accepting pyridine moiety could simultaneously form hydrogen bonds with the isatin amide N-H group (Figure 4.2). A cooperative effect was expected to enhance binding effects and hence improve reaction rate and enantioselectivity.
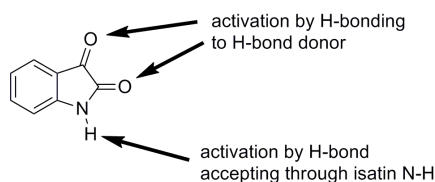
Figure 4.2: Design considerations for use of isatin as an aldol substrate (aldol acceptor).

To this end, a number of chiral amide based catalysts incorporating *N*-pyridyl and *N*-quinolinyl groups were considered. It was decided to initially generate 'reverse amide' catalysts **215-218** incorporating methyl pyrrolidine as the chiral unit in order to promote enamine formation whilst the amide H-bonding to the isatin substrate (Figure 4.3). This class of catalysts is referred to as 'reverse amides' due to the fact that they incorporate an amide group in the reverse order compared to a prolinamide (the amide N-H group resides adjacent to the pyrrolidine ring for 'reverse amide' compounds but is adjacent to the aryl ring for conventional prolinamides). 'Reverse amides' were expected to be of suitable size and have H-bond donating and accepting groups located at appropriate positions for efficient binding. This moiety also possessed an extra degree of flexibility compared to 'traditional' prolinamide catalysts due to the CH_2 group between the pyrrolidine ring and the H-bonding groups, potentially allowing the catalyst to orient itself around the substrate.
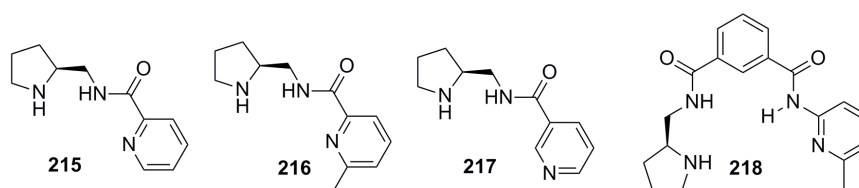
Figure 4.3: Structure of 'reverse amide' catalysts **215-218**.

Various interactions between catalyst and substrate were deemed possible (Figure 4.4). One possibility was H-bonding between the pyridine nitrogen of the catalyst and the isatin amide N-H group with concurrent H-bonding between the isatin amide carbonyl group and the catalyst amide N-H group. Alternatively, another possible but less efficient mode of binding involves one point H-bonding between the catalyst amide group and the isatin ketone functionality (Figure 4.4). In both cases, H-bonding could activate the electrophilic isatin ketone group and hold it in close proximity to the incoming enamine nucleophile. The aromatic pyridine group present could also possibly form π-π stacking interactions with the isatin substrate, leading to enhanced enantioselectivity.
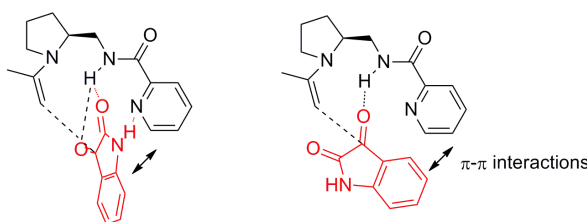
Figure 4.4: Potential H-bonding interactions between enamine modified reverse amide catalysts and isatin. Possible π-π interactions between aromatic groups also shown.

A bifunctional catalyst was also considered incorporating a 'reverse amide' group and an aminopyridine moiety separated by an achiral spacer group. Previous results obtained (see Chapters 1 & 2) showed that an isophthalamide successfully bound anions through H-bonding using complementary N-H groups in a cleft-like structure. Hamilton reported the catalysis of a phosphoryl transfer reaction[172] and also a Diels alder reaction[174] using isophthaloyl derived compounds following verification of their binding ability to reaction intermediates.

The bifunctional catalyst **218** consisted of a chiral methylpyrrolidine ring bound to one amide unit of an isophthaloyl skeleton and a substituted pyridyl group bound to the other amide unit. Isophthalamides are known to exist in their *syn-anti* lowest energy conformation but adopt the

174

syn-syn conformation in the presence of an anionic guest forming a cleft-like structure for binding and in this case could bind to one or both carbonyl groups.[56] This could activate isatin towards attack and hold it close to the enamine on the pyrrolidine ring with possible cooperative additional interactions between the pyridyl nitrogen and isatin amide N-H group (Figure 4.5).
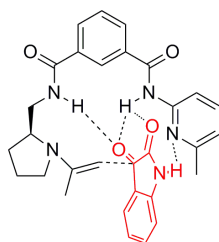
Figure 4.5: Proposed binding of bifunctional enamine modified catalyst **218** to isatin.

4.2.2 Development of Synthetic Protocol

The common intermediate for the synthesis of the 'reverse amide' catalysts was the *N*-protected methyl pyrrolidine amine **219** (Scheme 4.7) and two possible routes for this synthesis from (*S*)-proline were identified from several published routes.[337,338] One procedure conducted by Adolfsson *et al.*[337] involved a five step reaction starting from *N*-Boc-proline (Scheme 4.7). However, this method was deemed to be time-consuming, relatively inefficient and produced a low yield of amine product.[339]
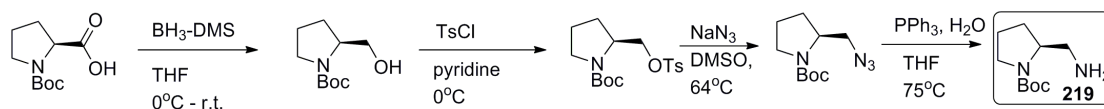
Scheme 4.7: Synthetic route towards methyl pyrrolidine amine **219** conducted by Adolfsson *et al.*[337]

An alternative more efficient methodology was also considered. Wang *et al.* synthesised the Cbz-protected methyl pyrrolidine amine starting from the commercially available (*S*)-2-carbamoyl-1-*N*-Cbz-pyrrolidine *via* a selective reduction reaction[338] based on a method previously reported by Brown and Curran.[340] The amide reduction step used borane-THF as reducing agent without loss of the carbamoyl ptotecting group (Scheme 4.8). However, Cbz removal can prove troublesome at the end of the synthetic sequence. The possibility of adapting the procedure to use the easily attachable and removable, Boc group in place of the CBz group was considered as part of an overall scheme to the amine.[341]
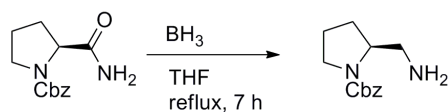
Scheme 4.8: Reaction towards methyl pyrrolidine amine by borane reduction of Cbz-protected prolinamides.[338]

Traditionally, amide reduction using Borane-THF is accompanied by a strong acid product work-up in order to cleave the intermediate Borane-amine complex but a modification of this procedure was essential to retain the acid labile Boc protecting group.[342] This involved the addition of chilled methanol to a cooled solution of reaction mixture followed by heating to reflux for 1 hour.[343] In this way, the borane amine complex was broken by complexation to methanol leading to formation of trimethylborate. Trimethylborate forms an azeotrope with methanol with evaporation of the salt at approximately 60°C *in vacuo* (Scheme 4.9).
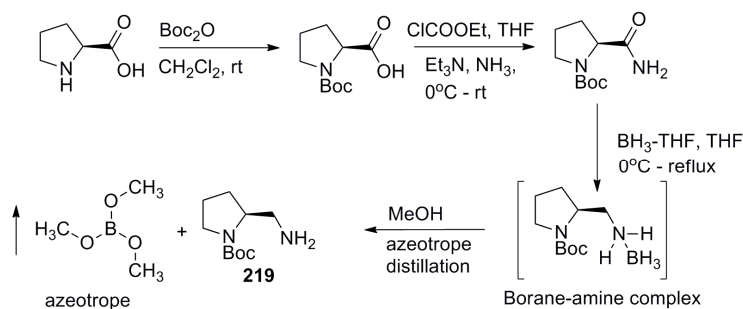
Scheme 4.9: Synthetic protocol undertaken including reduction of amide to methyl pyrrolidine amine **219** using Borane-THF followed by azeotrope distillation to cleave the borane-amine complex.

4.2.3 Methyl-Pyrrolidine Catalyst Synthesis

The complete synthetic route to *N*-Boc protected methyl-pyrrolidine amine **219** involved an initial *N*-Boc-protection of *L*-proline using Boc-anhydride (Scheme 4.10) in a procedure detailed by Chang *et al.*[341] This reaction mixture was stirred in dichloromethane for 48 hours. *N*-Boc-protected proline was obtained in 99% yield after extractive work-up and flash chromatography and its identity was confirmed by GC-MS, LC-MS and ^{1}H NMR spectroscopy. The *tert*-butyl signal integrating for 9 protons at approximately 1.45 ppm and loss of the N-H signal from the ^{1}H NMR confirmed the presence of the Boc protecting group on the secondary amine. Additionally, fragmentation of the molecular ion (m/z 215) was observed by GC-MS via loss of the *tert*-butyl group from the Boc group with protonation of

the oxygen atom to give an ion at m/z 160 in a McLafferty type rearrangement, a common fragment for Boc groups (Scheme 4.10).[344]
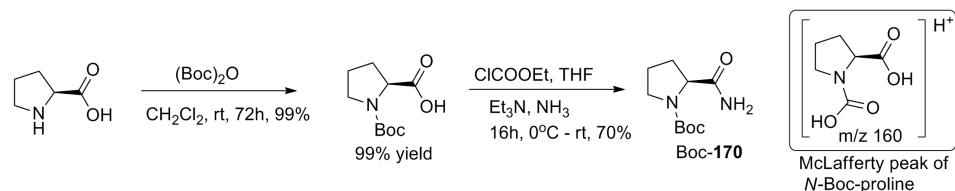
Scheme 4.10: Synthesis of Boc-proline and subsequent ethyl chloroformate coupling to form, Boc-**170**. McLafferty fragment ion of Boc-proline also shown.

Boc-proline was subsequently converted into the corresponding primary amide Boc-**170** through ethyl chloroformate coupling[176] with ammonia in THF (Scheme 4.10). Following extractive work-up and purification by flash chromatography, the white solid product amide was isolated in 70% yield. The identity of the product was confirmed by GC-MS, LC-MS and ^{1}H NMR spectroscopy with evidence of amide rotation observed by broad N-H peaks between 5.4-6.9 ppm in ^{1}H NMR spectroscopy observed due to *cis* and *trans* isomers as previously reported.[345] Additionally, *t*-Bu protons were observed at 1.46 ppm and all characterisation data corresponded to previous literature synthesis of this compound.[345] This amide displayed similar fragmentation patterns to Boc-proline by GC-MS with McLafferty rearrangement of the Boc group producing an ion at m/z 159 and the peak at m/z 115 corresponded to loss of the Boc group from the molecule.[344]

As discussed earlier, the reduction step was subsequently necessary to convert the amide group to an amine, a reaction which proved to be the most challenging step of the synthetic sequence. In particular, hydrolysis of borane amide salt initially proved difficult. The reduction was eventually achieved using 4 equivalents of 1M solution of borane in THF. Initially, the reaction was cooled to 0°C for 2 hours, stirred at room temperature for 24 hours and heated gently to approximately 50 °C for a number of hours with the progression of the reduction monitored by GC-MS and LC-MS. Reaction time was a critical factor for the success of this reaction due to the formation of a byproduct with m/z 384 with increasing reaction times and temperatures which was tentatively identified to be a dimer complex of the amine product by high resolution mass spectrometry. This was minimised using mild

conditions and use of reaction time not exceeding 6 hours at 50 °C despite the presence of a fraction of unreacted amide at this reaction time.
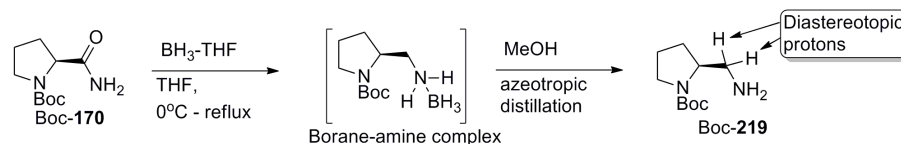
Scheme 4.11: Reduction of Boc-prolinamide to its amine counterpart Boc-**219** using BH$_3$-THF.

After the 6 hour reaction time, the mixture was quenched with methanol at 0°C and stirred for 1 hour, heated to 50°C for 1 hour after solvent removal *in vacuo*. This step was repeated in order to eliminate the borate salts by azeotropic distillation (Scheme 4.11).[343] This Boc protected amine was used without further purification due to the difficulties with chromatographic purification. The amine Boc-**219** was estimated as approximately 66% pure based on relative peak areas of the product versus the starting Boc-**170** by GC-MS. Mass spectral evidence along with NMR spectroscopic characterisation of the crude product confirmed the presence of the amine product; specifically evidence of diastereotopic methylene protons from 2.6-2.7 ppm and 3.3-3.5 ppm in the ^{1}H NMR spectrum due to the reduction of the carbonyl group verified the success of the reaction. Mass spectral data showed the molecular ion (MH$^+$) at m/z 201 and a McLafferty fragment ion at m/z 145.[345]

Catalyst	Ar	% Yield Boc protected	% Yield over 2 steps (α_D)
215	2-Py	45	43 (+27.6, CH$_2$Cl$_2$)
216	6-Me-2-Py	36	32 (+26.6, CH$_2$Cl$_2$)
217	3-Py	62	53 (+22.6, CH$_2$Cl$_2$)
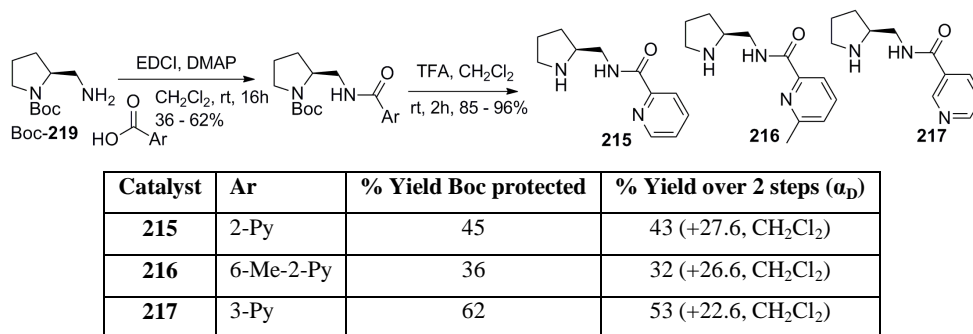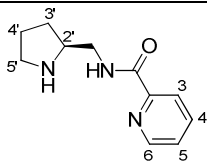
Scheme 4.12: Coupling of methyl pyrrolidine amine Boc-**219** to pyridine carboxylic acids and Boc-deprotection to give **215-217**.

This amine Boc-**219** was an important intermediate for the synthesis of each of the 'reverse amide' catalysts. In each case, the required amide catalyst was formed by EDCI coupling of the amine with the appropriate pyridine-carboxylic acid. The Boc-protected 'reverse amide' catalysts **215-217** were obtained in moderate yields (up to 65% yield) following chromatographic purification (Scheme 4.12). Structural confirmation was carried out by NMR

spectroscopy and LC-MS. LC-MS analysis produced identical results for Boc-**215** and Boc-**217** as expected with both the Na adducts at m/z 328 and the MH$^+$ ion detected at m/z 306 with McLafferty rearrangement and cleavage of the Boc-group also observed while GC-MS produced the M$^+$ ion at m/z 320 for Boc-**216**. ^{1}H NMR spectroscopic evidence for the identity of the compounds included amide N-H peaks in the range of 8.2-8.8 ppm along with the relevant pyridyl and aliphatic pyrrolidine ring peaks. Boc-**215** and Boc-**216** possessed very similar ^{1}H NMR spectra with an additional methyl group at 2.56 ppm present in the case of the latter. The aromatic NMR spectroscopic resonances of Boc-**217** were altered due to the different substitution of the pyridyl ring with the main difference being the H-2 signal at 9.08 ppm, *ortho* to the amide group and pyridine nitrogen in the ring.

Boc-deprotection was conducted by adding trifluoroacetic acid to a chilled solution of the protected catalyst in dichloromethane and stirring at room temperature for 2 hours. After removal of solvent and TFA salts *in vacuo*, the residue was dissolved in dichloromethane, neutralized with NaOH, extracted with dichloromethane and dried with MgSO$_4$ to give the 'reverse amide' catalysts in moderate yields over both steps (Scheme 4.12). The purity and structures were confirmed using ^{1}H & ^{13}C NMR spectroscopy and GC-MS or LC-MS.

Table 4.1: List of HMQC correlations and ^{1}H & ^{13}C NMR spectroscopic peak assignments of **215**.

Catalyst Structure	^{13}C NMR δ (ppm)	^{1}H NMR δ (ppm)	Assignment
	148.5	8.56 (d, J = 4.58 Hz, 1H)	C-6 & H-6
	137.4	7.81-7.87 (m, 1H)	C-4 & H-4
	126.6	7.39-7.44 (m, 1H)	C-5 & H-5
	122.5	8.18 (d, J = 8.39 Hz, 1H)	C-3 & H-3
	59.9	3.59-3.66 (m, 1H)	C-2' & H-2'
	24.3, 27.9	1.45-2.0 (m, br, 4H)	C-4' & H-4'; C-3' & H-3'
	41.0	3.31-3.49 (m, br, 2H)	CONH-C*H*$_2$

The ^{13}C and ^{1}H NMR signals of **215** and **217** were assigned through DEPT and HMQC experiments (Table 4.1 & Table 4.2) as well as COSY experiments to aid peak assignment in ^{1}H NMR spectroscopy (Table 4.3). Catalyst 216 was characterised using similar these techniques and showed an extra methyl group signal at 2.53 ppm and one less aromatic proton compared to catalyst **215**. In the cases of catalysts **215** & **217**, purification of the deprotected

catalyst was achieved by preparative TLC in 100% ethyl acetate. High resolution mass spectral analysis confirmed the approporiate MH[+] in each case.

Table 4.2: List of HMQC correlations and ^{1}H & ^{13}C NMR spectropscoic resonance assignments of **217**.
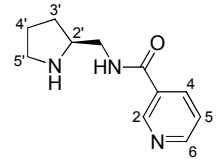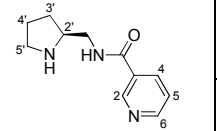
Catalyst Structure	^{13}C NMR δ (ppm)	^{1}H NMR δ (ppm)	Assignment
	151.9	8.61 (dd, J = 3.05 & 1.53 Hz, 1H)	C-6 & H-6
	148.3	8.99 (d, J = 1.53 Hz, 1H)	C-2 & H-2
	135.3	8.05-8.09 (m, 1H)	C-4 & H-4
	123.3	7.27-7.30 (m, 1H)	C-5 & H-5
	59.0	3.31-3.72 (m, 1H)	C-2' & H-2'
	42.1	3.31-3.72 (m, 2H)	CONH-CH_2
	24.7, 28.4	1.50-2.05 (m, 4H)	C-4' & H-4'; C-3' & H-3')

Table 4.3: COSY interactions of **217**.

Catalyst Structure	Proton	δ (ppm)	Correlated With δ (ppm)	Correlated With
	H-5	7.27-7.20 (m, 1H)	8.05-8.09 (m, 1H) & 8.61 (dd, J = 3.05 & 1.53 Hz, 1H)	H-4 & H-6
	CONH-CH_2	3.40 (m, 1H)	3.70 (m, 1H)	CONH-CH_2

In all cases for **215-217** in the ^{1}H NMR spectra, the presence of diastereotopic methylene protons from approximately 3.3 – 3.7 ppm for the CONHCH_2 group and 1.3 – 2.1 ppm for the ring diastereotopic protons (H-3') along with the pyrrolidine N-H, amide N-H and pyridyl signals confirmed the reverse amide structure. The ^{1}H NMR spectra of all catalysts differed from their Boc-protected forms only by the substitution of the *tert*-butyl signal for the secondary amine proton.

A number of additional steps were necessary to synthesise the pyridine-carboxylic acid portion of the bifunctional catalyst **219** (Scheme 4.13). The methyl pyrrolidine amine portion was synthesised as described previously in Scheme 4.9. The acid portion was synthesised in 2 steps using an initial EDCI coupling of 2-amino-6-picoline with mono-methyl isophthalate (Scheme 4.13). The corresponding ester product **220** was obtained in 97% yield after purification by flash chromatography. The structure and purity of this bifunctional ester/amide intermediate was confirmed by ^{1}H and ^{13}C NMR spectroscopy and LC-MS. In the case of ^{1}H NMR, two separate sets of signals corresponding to aromatic and pyridyl protons, the amide

N-H signal at 8.63 ppm and ester methoxy protons at 3.95 ppm were identified. LC-MS showed the MH$^+$ ion at m/z 271.
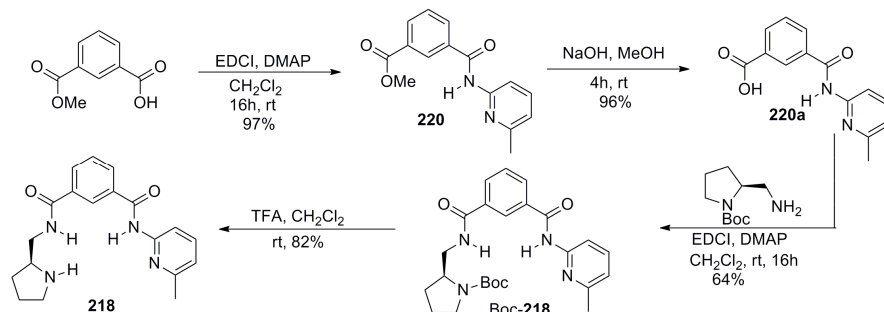
Scheme 4.13: Synthesis of 'reverse amide' bifunctional catalyst **218**

Subsequent ester hydrolysis of **220** using NaOH in methanol yielded the acid intermediate **220a** in 96% yield as a white solid. The ^{1}H NMR spectrum showed the loss of methoxy signals at 3.95 ppm compared to ester **220** and FTIR analysis showed a broad OH signal consistent with carboxylic acid formation. All ^{1}H NMR spectroscopic resonances were assigned with the aid of COSY analysis (Table 4.4). LC-MS showed a molecular ion at m/z 257 (MH$^+$)

Table 4.4: COSY data and associated ^{1}H NMR spectroscopic resonance assignments for acid **220a**

Structure	Protons	δ (ppm)	Correlated with δ (ppm)	Correlated with
	H-5	7.62 (app t)	8.11 (d, J = 7.63 Hz, 1H) & 8.26 (d, J = 7.63 Hz, 1H)	H-4, H-6
	H-4'	7.85 (app t)	8.04 (d, J = 8.39 Hz, 1H) 7.85 (app t, J = 8.39 Hz, 1H)	H-3', H-5'

This acid **220a** was coupled with the chiral methylpyrrolidine amine Boc-**219** to give the Boc-protected bifunctional catalyst Boc-**218** in 64% yield as a colourless oil following chromatographic purification. Boc-deprotection using TFA produced the catalyst in 48% overall yield over the four steps and its structure was confirmed through ^{1}H & ^{13}C NMR spectroscopy and LC-MS. The ^{1}H & ^{13}C NMR spectroscopic resonances of this catalyst were assigned based on analysis of ^{13}C, HMQC and DEPT experiments (Table 4.5). ^{1}H NMR analysis identified key diastereotopic protons CONHC$\underline{H}_2$ from 3.37 – 3.68 ppm, H-3'' from 1.35 – 1.70 ppm and 1.85 – 2.12 ppm. In addition to these, the catalyst contained two sets of

aromatic signals including one set of pyridyl ring protons, two amide N-H signals at 8.89 and 6.08 ppm and a CH$_3$ signal at 2.30 ppm which were all used to verify the success of the coupling reaction and deprotection. LC-MS analysis showed the protonated parent ion at *m/z* 339 and High Resolution Mass Spectroscopy further identified the product.

Table 4.5: List of HMQC correlations and assignment of ^{1}H & ^{13}C NMR spectroscopic resonances for **219.**

Structure	^{13}C NMR δ (ppm)	^{1}H NMR δ (ppm)	Assignment
	138.8	7.48-7.54 (m, 1H)	C-5 & H-5
	131.0 & 131.2	7.87-7.93 (m, 2H)	C-6 & H-6; C-3' & H-3'
	129.1	7.29-7.34 (m, 1H)	C-4' & H-4'
	126.0	8.34 (s, 1H)	C-2 & H-2
	119.7	6.78-6.82 (m, 1H)	C-5' & H-5'
	111.6	7.93-7.98 (m, 1H)	C-4 & H-4
	59.9	3.67-3.76 (m, 1H)	C-2'' & H-2''
	41.5	3.37-3.68, (m, 2H)	CONH-C$\underline{H}_2$
	45.2	3.03-3.23 (m, 2H)	C-5'' & H-5''
	28.1	1.85-2.12 (m, 1H), 1.35-1.70 (m, 1H)	C-3'' & H-3''
	24.1	1.70-2.02 (m, 2H)	C-4'' & H-4''
	23.9	2.30 (s, 3H)	Ar-CH$_3$

4.2.4 Catalytic Performance of Methylpyrrolidine Catalysts

As a control catalyst, (*S*)-proline was tested at 10 mol% loading at room temperature in the aldol reaction of isatin with acetone in order to develop chiral HPLC conditions and replicate published results.[318] The expected product was synthesised in quantitative yield after 16 hours with 25% ee of the (*S*)-product, consistent with previous results (Scheme 4.14).[313,314,318] The ee was determined on the crude reaction mixture using chiral HPLC with a Chiralpak AD-H column and isocratic elution consisting of 70:30 hexane: *iso*-propanol with UV detection at 254 nm. The 3-substituted-3-hydroxy-indolin-2-one reaction product **208** was isolated after removal of solvent *in vacuo* and purification by flash chromatography. The product was verified by LC-MS where its Na-adduct was found when analysed in positive mode (m/z 228) and also by NMR spectroscopy with its ^{1}H & ^{13}C NMR signals corresponding to previous reports (Table 4.6).[314,318] The presence of diastereotopic methylene ^{1}H NMR spectroscopic

resonances at 3.36 and 3.15 ppm and methyl peaks at 2.04 ppm confirmed the aldol reaction had successfully occurred.
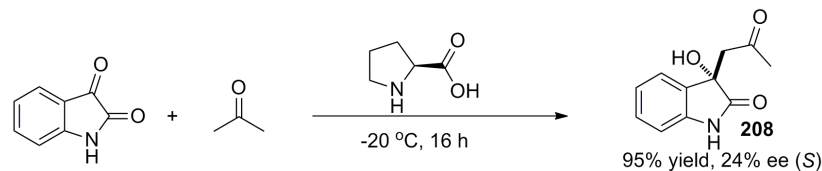
Scheme 4.14: Reaction of isatin with acetone catalysed by (S)-proline.

Table 4.6: List of HMQC correlations and assignment of ^{1}H & ^{13}C NMR spectroscopic resonances for product of reaction of isatin with acetone.

Structure	^{13}C NMR δ (ppm)	^{1}H NMR δ (ppm)	Assignment
	123.5	7.29 (d, J = 7.33 Hz, 1H)	C-4 & H-4
	129.4	7.21 (dt, J = 7.63 & 1.53 Hz, 1H)	C-6 & H-6
	122.1	6.98 (t, J = 7.63 Hz, 1H)	C-5 & H-5
	109.9	6.86 (m, 1H)	C-7 & H-7
	49.8	3.36 (d, J = 16.78 Hz, 1H,) & 3.15 (d, J = 16.78 Hz, 1H)	CH$_2$
	29.3	2.04 (s, 3H)	CH$_3$

The 'reverse amide' catalysts **215**-**218** (Figure 4.1) were tested in the aldol reaction of isatin with acetone under a variety of conditions including temperature, catalyst loading and additive. All reactions were monitored by TLC and HPLC and reactions were stopped once the reaction was deemed to be at or near completion. The ee of product was obtained on the crude reaction mixture and also on the purified product and no obvious differences were observed, contrary to some previous contradictory reports of enantiomeric enrichment[318] and partial racemisation[311] during chromatographic purification.

Catalyst **215** was tested using 10 mol% catalyst loading at room temperature and at -20 °C with the use of acetic acid (AcOH) as an aldol additive also investigated. The effect of added AcOH was investigated at room temperature and -20°C and in all cases, a high yield of product was obtained with reaction times varying from 15 to 60 hours. The use of AcOH additive resulted in a 75% reduction in reaction times, presumably due to the enhanced rate of enamine formation in the presence of AcOH. However, at room temperature the ee reduced by 4% through use of 20 mol% AcOH additive while at the lower temperature (-20 °C), a 4% improvement to 30% ee was observed (entries 3 & 5, Table 4.7) with the (R)-enantiomer

favoured in all cases. The configuration of the product was assigned through comparison of reports using the same HPLC chiral phases[314,318] and specific optical rotation data.

Table 4.7: Reaction of isatin with acetone catalysed by 'reverse amide' catalyst **215** under a number of conditions. Performance of (S)-proline also shown.
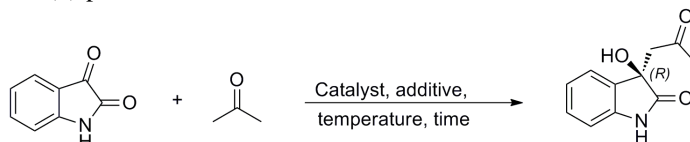
Entry	Catalyst	Catalyst Loading	Solvent	Additive	Temp (°C)	Time (h)	Yield[b] (%)	ee[c] (%)	Config
1		10	Acetone	-	Rt	16	95	24	*S*
2		10	Acetone	-	Rt	44	85	22	*R*
3		10	Acetone	AcOH	Rt	16.5	70	18	*R*
4		10	Acetone	-	-20	63	95	26	*R*
5		10	Acetone	AcOH	-20	15	98	30	*R*

[a]All reactions were conducted with 0.3 mmol of isatin and 2 mL of acetone. In cases where additive was employed, 20 mol% AcOH was used. TLC and HPLC were used to monitor the progression of reaction [b]Isolated yield. [c]Determined by chiral HPLC.

The presence of an electron donating methyl group at the 6-position of the pyridyl ring in catalyst **216** was expected to release electron density to the pyridine nitrogen and was therefore expected to enhance its H-bond accepting properties. Catalyst **216** was tested with a 10 mol% loading with and without a number of additives favouring the (R)-product in all cases. Use of 20 mol% AcOH additive gave a more successful result compared to no additive, 32% ee of (R)-product after 18 hours at -20°C compared to 19% ee when no additive was used (entry 1 vs 6, Table 4.8). A number of acids including TFA, *p*-toluenesulfonic acid and benzoic acid were subsequently tested and AcOH was found to be the most successful additive for this catalyst. In addition, the concentration of acetone was found to have a negligible affect on yield and only a slight reduction in ee in the more concentrated systems of 0.5 M and 1M was observed (entries 6-8, Table 4.8).

Table 4.8: Results of the variation of additive in the **216** catalysed aldol reaction of isatin with acetone..
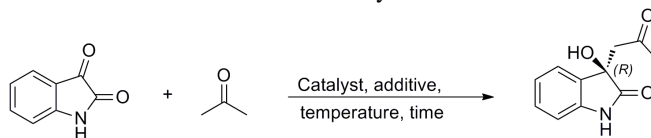
Entry	Catalyst	Catalyst Loading	Solvent	Additive	Temp (°C)	Time (h)	Yield[b] (%)	ee[c] (%)	Config
1		10	Acetone	-	Rt	15	Quant	19	R
2		10	Acetone	AcOH	Rt	15	93	20	R
3		10	Acetone	TFA	Rt	120	52	10	R
4		10	Acetone	p-TSA	Rt	120	<10	8	R
5		10	Acetone	AcOH	4	11	93	25	R
6		10	Acetone	AcOH	-20	18	95	32	R
7[d]		10	Acetone	AcOH	-20	11	93	31	R
8[e]		10	Acetone	AcOH	-20	11	97	31	R

[a]All reactions were conducted with 0.3 mmol of isatin and 2 mL of acetone. In cases where additive was employed, 20 mol% of additive was used. TLC and HPLC were used to monitor the progression of reaction [b]Isolated yield. [c]Determined by chiral HPLC. [d]0.6 mL acetone used. [e]0.3 mL acetone used.

The 'reverse amide' catalyst **217** derived from pyridine-3-carboxylic acid (nicotinic acid) coupled to the pyrrolidine ring was subsequently tested. Upon initial study, the extremely active catalyst brought the reaction to completion after approximately 6 hours at -20 °C with a disappointing ee of less than 10% ee of (R)-product. In systems using no additive at room temperature and using AcOH at -20°C, a slight excess of the (S)-product was obtained but in general, the reaction was almost racemic (entries 1-5, Table 4.9). Several experiments were undertaken in an attempt to improve the enantioselectivity of the **217** catalysed reaction of isatin with acetone including the variation of solvents, temperatures, additives, catalyst loading and concentrations. The use of water as an additive was investigated due to previous reports of its ability to enhance the ee of aldol reactions including the aldol reaction of isatin with acetone.[319] For the solvent study, a wide range of solvent polarities was studied including non-polar hexane and toluene and also polar solvents such as DMF, dioxane and brine. The (S)-enantiomer was consistently preferentially formed in toluene co-solvent regardless of additive used (entries 6-8, Table 4.9) In this solvent, the ee values varied considerably depending on the additive used; 7% ee without additive, 2.5% ee with 40 equiv H_2O additive but an encouraging 18% ee of (S)-product was obtained through the use of 20 mol% AcOH. In the case of DMF, 21% ee of the (R)-product was obtained when using either 20 mol% AcOH

or 40 equiv H_2O as additive with 20 mol% catalyst loading (entries 11 & 12, Table 4.9). All other solvents tested produced inferior ee values (entries 9, 10 & 13-15, Table 4.9), therefore toluene and DMF were considered to be the optimal solvents for catalyst **217** in this reaction.

With the optimum solvents in hand (toluene to generate an excess of (*S*)-product and DMF for excess of (*R*)-product), a number of other variables were modified in an attempt to further enhance the enantioselectivity. Initially, the concentration of acetone was reduced in order to possibly decrease the overall rate of reaction and thereby possibly impart improved enantioselectivity. The concentration of acetone was reduced from 2 mL to 5 equiv and also 2 equiv with respect to isatin for the reaction with 20 mol% AcOH additive in toluene and DMF. As expected, the reaction rates were reduced considerably; in the case of DMF, a 3% increase in ee to 24% ee of (*R*)-product was obtained when 2 equiv of acetone was used, albeit with a low yield of 31% (entry 17, Table 4.9). For toluene, use of 5 equiv acetone gave a very low yield of product after 284 hours and a disappointing ee of 7% in favour of the (*S*)-product (entry 18, Table 4.9). As a result of this unacceptably slow reaction using 5 equiv acetone, the corresponding system using 2 equiv acetone in toluene as reaction medium was not tested.

Finally, reaction temperature was further reduced in an attempt to increase enantioselectivity. Reactions comprising 1 mL acetone, 20 mol% AcOH and 20 mol% catalyst loading at -42°C for DMF and also at -80°C for toluene and DMF were tested. In the case of toluene at -80°C, a disappointing ee of 10% in favour of the (*S*)-product was obtained while in DMF, ee values of 22% and 18% of (*R*)-product at -42 °C and -80 °C were obtained respectively (entries 19-21, Table 4.9). Therefore, this catalyst was most significantly affected by solvent; use of non-polar toluene solvent and the polar aprotic DMF solvent produced the (*S*) and (*R*) isomers of product respectively, albeit in low selectivity but with high catalytic activity.

Table 4.9: Testing of catalyst **217** under a number of conditions including varying solvent, temperature, catalyst loading, and concentration of acetone used. Catalystic properties of catalyst **218** also presented
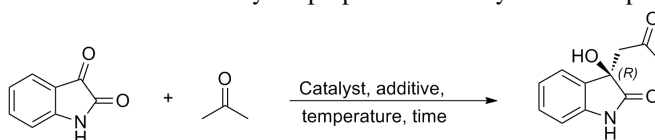
Entry	Catalyst	Catalyst Loading (mol%)	Solvent	Additive	Temp (°C)	Time (h)	Yield[b] (%)	ee[c] (%)	Config
1	**217**	10	Acetone	AcOH	Rt	14	Quant	5	*R*
2		20	Acetone	-	-20	48	Quant	7	*R*
3		20	Acetone	AcOH	-20	14	Quant	7	*S*
4		30	Acetone	H$_2$O	-20	13	Quant	8	*R*
5		10	Acetone	-	Rt	44	84	6	*S*
6		20	Toluene	-	-20	20	80	7	*S*
7		20	Toluene	H$_2$O	-20	12	72	2.5	*S*
8		20	Toluene	AcOH	-20	18	85	18	*S*
9		20	Hexane	-	-20	19	83	2	*R*
10		20	Hexane	AcOH	-20	19	86	2	*S*
11		20	DMF	AcOH	-20	16	87	21	*R*
12		20	DMF	H$_2$O	-20	22	87	21	*R*
13		20	THF	AcOH	-20	16	85	1	*S*
14		20	Dioxane	AcOH	-20	24	90	3	*S*
15		20	Brine	AcOH	-20		No Reaction		
16[d]		20	DMF	AcOH	-20	40	94	23	*R*
17[e]		20	DMF	AcOH	-20	135	31	24	*R*
18[d]		20	Toluene	AcOH	-20	284	28	7	*S*
19		20	DMF	AcOH	-42	10	72	22	*R*
20		20	DMF	AcOH	-80	165	<20	18	*R*
21		20	Toluene	AcOH	-80	165	<10	10	*S*
22	**218**	10	Acetone	-	Rt	44	84	6	*S*

[a]All reactions in neat acetone were conducted with 0.3 mmol of isatin and 2 mL of acetone unless stated otherwise. Where the reaction was conducted in an alternative solvent, 2 mL of solvent and 1 mL acetone were used. In cases where additive was employed, 20 mol% AcOH or 40 equiv H$_2$O was used. TLC and HPLC were used to monitor the progression of reaction [b]Isolated yield. [c]Determined by chiral HPLC. [d]5 equivalents (0.11 mL) acetone used. [e]2 equivalents (0.044 mL) acetone used.

The bifunctional reverse amide based catalyst **218** based on the isophthalamide substructure was finally evaluated. This catalyst produced a disappointing result of 6% ee in favour of the

(*S*)-product at room temperature after 44 hours reaction time (entry 22, Table 4.9). The poor performance of this catalyst may have been due to the chiral binding pocket of the catalyst being too small and inaccessible for efficient binding of isatin aldol intermediates. Alternatively, the isophthalamide may have existed in a conformation which where binding may have occurred at the exterior of the molecule rather than in the cleft.

4.2.5   Summary of 'Reverse Amide' Catalyst performance

Overall, disappointingly the 'reverse amide' pyrrolidine catalysts proved catalytically active but lacked a significant degree of enantioselectivity. Although catalyst flexibility was desired to bind the intermediates efficiently, the flexibility of the binding cleft due to the methyl pyrrolidine functionality may have been too great for high enantioselectivity. The enhanced flexibility of the catalyst was thought to have a negative impact on enantioselectivity with similar likelihood of *Re* and *Si* attack of the enamine on the isatin ketone (Figure 4.6). The high catalytic activity may have been due to a very small degree of steric strain for enamine attack on the isatin ketone. Also, the flexibility of the catalyst may have provided unrestricted access for the isatin substrate to efficiently bind to the catalyst via H-bonding which may have been facilitated by π-π stacking interactions between the aromatic rings of the catalyst and substrate. These factors combined were suggested to explain the high reactivity and low enantioselectivity of these catalysts.
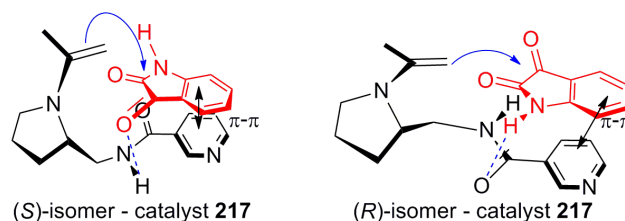
Figure 4.6: Suggested binding modes of explanation of poor enantioselectivity of reverse amide catalysts – due to enhanced flexibility and ease of attack on both the *Re* and *Si* faces of isatin ketone.

The negative effects of catalyst flexibility were previously observed in the aldol reaction of 4-nitrobenzaldehyde with acetone in water conducted by Chimni *et al.*[253] They compared the catalytic properties of a prolinamide catalyst derived from aniline with a benzyl amine derived prolinamide. The extra flexibility associated with the latter catalyst afforded significantly higher activity but lower enantioselectivity compared to the more rigid aniline analogue.

Solvation may have played a key role in the enantioselectivity of the 'reverse amide' catalysed reaction with the formation of opposite enantiomers in solvents of varying polarities. The catalyst may have existed in different conformations in non-polar versus polar solvents, although we do not have any direct evidence of this. In addition, in non-polar toluene, H-bonding effects would be enhanced due to less competitive solvent binding while polar solvents would compete with the catalyst for H-bonding to isatin, altering binding modes. Similar reversal of enantioselectivites depending on reaction solvent was recently reported by Wennemers *et al.* for their proline dipeptide catalysts in the aldol reaction of benzaldehyde and acetone. They proposed the difference in enantiomers was caused by different catalyst conformations in methanol compared to methanol/water mixtures.[346]

4.3 Prolinamide Catalysts

With the limited success of the 'reverse amide' catalysts, a series of prolinamide catalysts derived from aminopyridines and aminoquinolines were designed and synthesised. While some *N*-pyridyl prolinamides had previously been successful for ketone-aldehyde[253] and ketone-ketone aldol reactions via H-bonding,[176,291] none had been applied to the isatin/acetone aldol reaction.

In 2006, Chimni *et al.* tested *N*-pyridyl prolinamide catalysts in their protonated form for the aldol reaction of acetone with 4-nitrobenzaldehyde in water.[253] Using 20 mol% catalyst loading, the 2- and 4-aminopyridine derivatives proved unsuccessful while the 3-aminopyridyl derivative showed modest success; 52% yield after 10 days to give (*R*)-product in 31% ee (Scheme 4.15). In 2007, Luo *et al.* developed asymmetric catalysts through combination of chiral *N*-pyridyl prolinamides and surfactant Brønsted acids via non-covalent acid-base interactions in water.[265] The catalyst and reaction mixture formed colloidal dispersions in water, indicating the reaction occurred in micelles. Using *p*-dodecyl benzenesulfonic acid (DBSA) additive for the reaction of cyclohexanone with 4-nitrobenzaldehyde in water, they observed most success for the 3- and 4- aminopyridyl derivatives with varying yields and ee values depending on reaction media (Scheme 4.15). In 2006, Gong *et al.* reported the use of *N*-pyridyl prolinamide catalysts for the aldol reaction of acetone with α-keto acids and found

that a catalyst derived from proline and 2-aminopyridine to be in the optimum for transition state binding for this reaction while the 3-aminopyridine variant proved ineffective (Scheme 4.15).
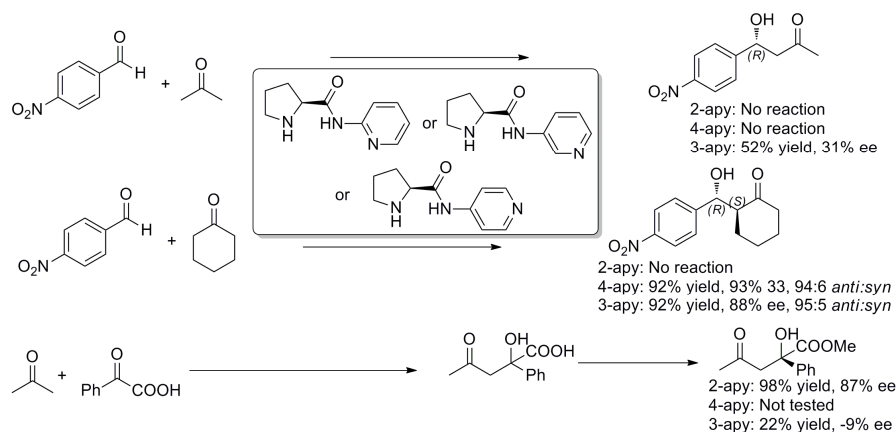
Scheme 4.15: Aldol reactions conducted by Chimni[253], Luo[265] and Gong[176] using *N*-pyridyl prolinamide catalysts.

4.3.1   Prolinamide Catalysts in Isatin/Acetone Aldol Reaction

It was postulated that *N*-pyridyl prolinamide catalysts of this type may bind to isatin in a similar way to that of the *N*-pyridyl methylpyrrolidine catalysts *via* H-bonding. The *N*-pyridyl prolinamide catalysts contain a H-bond donating amide N-H group, a H-bond accepting pyridine nitrogen atom and also a chiral secondary amine ring at which enamine formation could occur in a more rigid structure when compared to 'reverse amide' catalysts **215-218**. The increased rigidity may give rise to a larger energy gap between attack by the nucleophilic enamine on the *Re* and *Si* faces of the ketone, resulting in higher enantioselectivity. It was also postulated that *N*-quinolinyl prolinamides could rigidify the cleft further whilst providing H-bonding and π-π stacking effects.

Initially, catalysts **221** & **222** derived from 2-aminopyridine and 2-amino-6-picoline coupled to proline were considered. These catalysts were previously found to be the most successful catalysts for the aldol reaction of α-keto-acids with ketones and the mechanism of catalysis was suggested to originate from successful binding of the keto acid substrate to the aminopyridine functionality and the amide group.[176] This binding enhanced nucleophilic attack by the enamine and it was hoped that similar binding and activation would be possible

in the case of isatin through a combination of H-bonding of the catalyst amide N-H to the ketone and amide carbonyl groups of isatin and H-bonding of pyridine nitrogen to isatin amide N-H group (Figure 4.7).
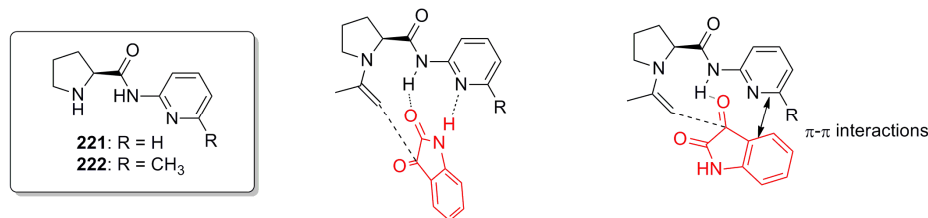
Figure 4.7: Structure of *N*-pyridyl prolinamide catalysts **221** & **222** and potential alternative binding interactions of enamine modified catalysts with isatin.

4.3.2   *N*-Pyridyl Prolinamide Catalyst Synthesis

The *N*-pyridyl prolinamide catalysts were synthesised in a two step sequence as outlined in Scheme 4.16. The first step involved Boc protection of (*S*)-proline and was achieved in high yield followed by ethyl chloroformate coupling of Boc-proline to the appropriate aminopyridine (2-aminopyridine or 6-methyl-2-aminopyridine). The conditions for successful coupling required the *N*-protected amino acid to be dissolved in anhydrous solvent and tertiary amine base and the ethyl chloroformate was added dropwise at 0°C over 15 minutes to form an unsymmetrical anhydride. Following an activation period of approximately 30 minutes, the relevant amine was added which reacted with the anhydride generated to form the Boc-amide product. This method has been extensively used in the synthesis of peptides.[347]
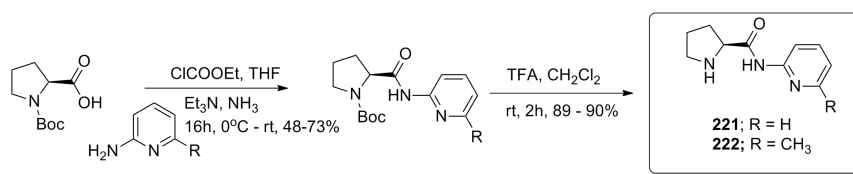
Catalyst	R	% Yield Boc protected	% Yield over 2 steps (α_D)
221	H	48	43 (-56.2, EtOAc)
222	CH$_3$	73	66 (-40.2, EtOAc)
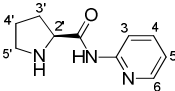
Scheme 4.16: Synthesis of *N*-pyridyl prolinamide catalysts **221** & **222**.

The reaction mixture was left to stir at 0 °C for 1 hour, at room temperature for 16 hours and heated to reflux for up to 3 hours with reaction monitoring by TLC. After dilution with ethyl acetate, the triethylamine triethylamine hydrochloride salt by-product was filtered and the

organic layer washed with saturated aqueous ammonium chloride, dried over MgSO$_4$ and solvent removed *in vacuo*. Chromatographic purification gave Boc protected **221** & **222** in 48% and 73% yields respectively. Boc-deprotection was conducted using TFA in CH$_2$Cl$_2$ to give the *N*-pyridyl prolinamide catalysts **221** & **222** in good yields (Scheme 4.16).
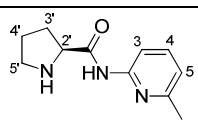
An enhanced yield from coupling of the 6-methyl substituted derivative **222** was observed possibly due to enhanced electron density on the amine group (73% yield compared to 48%). LC-MS analysis of Boc-**221** & Boc-**222** furnished MH$^+$ ions at m/z 292 and m/z 306 respectively. Typical fragmentation of these compounds was through the previously described fragmentation of the Boc group via McLafferty rearrangement (m/z 236 & 250) and also cleavage of the Boc group from MH$^+$ ion (m/z 192 & 206). Following Boc-deprotection, catalysts **221** & **222** were obtained in 43% & 66% overall yields.

Table 4.10: List of HMQC correlations and assignment of NMR spectroscopic resonances for **221.**

Structure	^{13}C NMR δ (ppm)	^{1}H NMR δ (ppm)	Assignment
	148.0	8.20-8.31 (m, 2H)	C-6 & H-6; C-3 & H-3
	138.3	7.65-7.72 (m, 1H)	C-4 & H-4
	119.7	6.99-7.04 (m, 1H)	C-5 & H-5
	61.0	3.86-3.92 (m, 1H)	C-2' & H-2'
	47.3	2.98-3.12 (m, 2H)	C-5' & H-5'
	30.9	1.98-2.25 (m, 2H)	C-3' & H-3'
	26.1	1.71-1.81 (m, 2H)	C-4' & H-4'
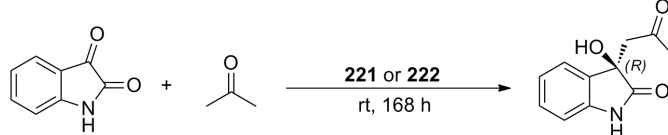
GC-MS analysis showed peaks at m/z 191 & 205 respectively corresponding to the M$^+$ ions of **221** & **222**. The structure of Boc-protected and deprotected catalysts were also confirmed by ^{1}H & ^{13}C NMR spectroscopy using DEPT, HMQC and COSY experiments. Detailed assignment of signals was conducted for the deprotected catalysts and show that **221** & **222** possessed very similar ^{1}H & ^{13}C NMR spectra. In ^{1}H NMR spectroscopy, aromatic protons from the pyridyl ring appeared in the range 6.8 – 8.2 ppm and pyrrolidine ring protons ranged from 1.7 – 3.9 ppm with diastereotopic H-3' protons from 1.95 – 2.30 ppm. In each case, amide N-H peaks appeared in the range 10.1-10.2 ppm and pyrrolidine N-H signals were present between 1.8 & 2.4 ppm (Table 4.10 & Table 4.11).
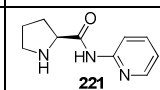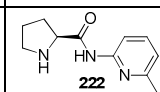
Table 4.11: COSY interactions and assignment of ^{1}H NMR spectroscopic resonances for **222**.

Structure	Protons	δ (ppm)	Correlated with δ (ppm)	Correlated with
	H-3	8.04 (d, J = 8.2 Hz, 1H)	7.56 (t, J = 8.2 Hz, 1H)	H-4
	H-4	7.56 (t, J = 8.2 Hz, 1H)	6.86-6.89 (m, 1H)	H-5
	H-5	6.86-6.89 (m, 1H)	2.46 (s, 3H)	Ar-CH$_3$
	H-2'	3.83-3.88 (m, 1H)	1.97-2.26 (m, 2H)	H-3'
	H-5'	2.99-3.10 (m, 2H)	1.67-1.81 (m, 2H)	H-4'
	H-4'	1.67-1.81 (m, 2H)	1.97-2.26 (m, 2H)	H-3'

Catalysts **221** & **222** were tested in the reaction of isatin with acetone using a 20 mol% catalyst loading at room temperature without additives as an initial trial of catalytic performance. The 2-aminopyridine derivative **221** gave 11% ee of (*R*)-product with a long reaction time and its closely related methyl substituted analogue **222** gave a marginally better result yielding 15% ee of (*R*)-product under the same conditions (entries 1 & 2, Table 4.12). These results proved disappointing as catalysts **221** & **222** had previously been successful for reaction of α-keto acids with acetone.[176] This lack of success may have been due to the relative positioning of the pyridyl and amide groups and this was subsequently investigated.

Table 4.12: Aldol reaction of isatin with acetone catalysed by 2-aminopyridyl based catalysts **221** & **222**.

Entry	Catalyst	Catalyst Loading (mol%)	Yield[b] (%)	ee[c] (%)	Config
1	**221**	20	80	11	*R*
2	**222**	20	74	15	*R*

[a]All reactions in neat acetone were conducted with 0.3 mmol of isatin and 2 mL of acetone. TLC and HPLC were used to monitor the progression of reaction [b]Isolated yield. [c]Determined by chiral HPLC.

4.3.3 Synthesis of *N*-Pyridyl Prolinamide Catalysts 223 & 224

Next, the effect of relative position of the pyridyl nitrogen atom in the aromatic ring was varied. The 3- and 4- substituted versions of *N*-pyridyl prolinamides **223** & **224** were synthesised in the same manner as for **221** & **222** using 3-aminopyridine and 4-aminopyridine

as starting materials (Scheme 4.17). The Boc-protected versions of **223** & **224** were obtained in 46% and 35% yields. LC-MS analysis for both Boc-protected catalysts produced MH[+] ions at m/z 292 and fragment ions at m/z 218 (fragmentation of the Boc group) and m/z 190 (loss of Boc group). Boc-deprotection using TFA afforded **223** & **224** in 40% and 31% overall yields over 2 steps respectively. LC-MS analysis of **223** gave the MH[+] ion at m/z 192 and GC-MS analysis of **224** gave the M[+] ion at m/z 191.
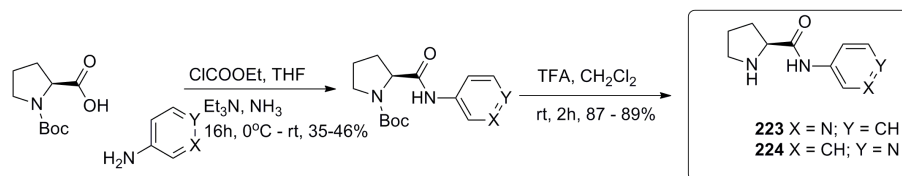
Catalyst	X	Y	% Yield Boc protected	% yield over 2 steps (α_D)
223	N	CH	46	40 (-65.8, CHCl$_3$)
224	CH	N	35	31 (-84.2 (CHCl$_3$)
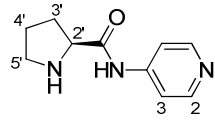
Scheme 4.17: Synthesis of 3-aminopyridine and 4-aminopyridine derived *N*-pyridyl prolinamides **223** & **224**.

The structure of Boc-protected and deprotected catalysts **223** & **224** were also confirmed by NMR spectroscopy using ^{1}H, ^{13}C, DEPT, and COSY experiments. Detailed assignment of signals conducted for the deprotected catalysts showed that both catalysts had similar spectra but differences were present reflecting the differences in the pyridyl ring substitution pattern of both catalysts. ^{1}H NMR spectra showed aromatic protons from the pyridyl ring appearing in the range 7.2 – 8.6 ppm and pyrrolidine ring protons ranging from 1.7 – 3.9 ppm with diastereotopic H-3' protons in the range of 1.9 – 2.3 ppm. In each case, amide protons appeared at approximately 9.9 ppm and pyrrolidine N-H signals appeared within the range of 1.7 -2.25 ppm (Table 4.13 & Table 4.14).

Table 4.13: COSY interactions and ^{1}H NMR spectroscopy assignments for **223**.

Structure	Protons	δ (ppm)	Correlated with δ (ppm)	Correlated with
	H-2	8.59 (d, *J* = 2.75 Hz, 1H)	8.28- 8.32 (m, 1H)	H-4
	H-6	8.21-8.25 (m, 1H)	7.20-7.26 (m, 1H)	H-5
	H-4	8.28- 8.32 (m, 1H)	7.20-7.26 (m, 1H)	H-5
	H-2'	3.83-3.89 (m, 1H)	1.97-2.25 (m, 2H)	H-3'
	H-5'	2.92-3.12 (m, 2H)	1.70-1.81 (m, 2H)	H-4'
	H-4'	1.70-1.81 (m, 2H)	1.97-2.25 (m, 2H)	H-3'

Table 4.14: COSY interactions and ^{1}H NMR spectroscopy assignments for **224**.
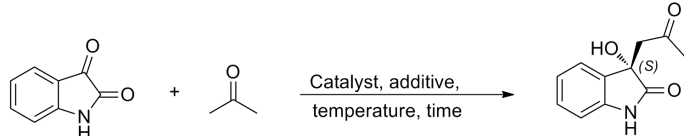
Structure	Protons	δ (ppm)	Correlated with δ (ppm)	Correlated with
	H-2	8.43-8.51 (m, 2H)	7.49-7.55 (m, 2H)	H-3
	H-2'	3.83-3.89 (m, 1H)	1.98-2.28 (m, 2H)	H-3'
	H-5'	2.92-3.13 (m, 2H)	1.68-1.88 (m, 2H)	H-4'
	H-3'	1.98-2.28 (m, 2H)	1.68-1.88 (m, 2H)	H-4'
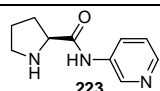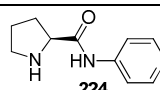
4.3.4 Catalytic Studies of 223 & 224

Catalysts **223** & **224** were tested in the reaction of isatin with acetone with varying additives, temperatures and catalyst loadings. Initially, **223** was tested using 20 mol% catalyst loading at different temperatures in the presence and absence of additives. Interestingly, an excess of the (*S*)-product was formed, opposite to that observed from the 2-aminopyridine based catalysts **221** & **222**. Gratifyingly, the ee values obtained from catalyst **223** were of the order of 55 – 69% ee. For the reaction without additives, temperature had a minor effect with a 2% improvement in ee value upon reduction of temperature to -20°C (entries 1 & 2, Table 4.15). A more significant 9% improvement in ee was obtained when 20 mol% AcOH additive was used at -20°C (entries 2 vs 4, Table 4.15). Addition of 40 mol% AcOH had no further effects on the enantioselectivity but decreased reaction rate compared to 20 mol% AcOH (entry 4 vs 5, Table 4.15).

The use of water as an aldol additive has been studied in a large number of aldehyde:ketone aldol reactions and was also studied by Tomasini *et al.* in 2009 for the aldol reaction of isatin with acetone.[319] In this work, the authors found that a required quantity of water was beneficial when compared to reaction without additive. In the work reported in this Chapter, the use of 6.6 equiv of water gave in a small increase in ee but the reaction rate appeared slower when compared to the system without additive (entry 2 vs 6, Table 4.15). The highest ee of 69% in favour of the (*S*)-isomer was found at -20°C using 40 equiv of water (entry 7, Table 4.15).

Table 4.15: Testing of catalyst **223** & **224** in aldol reaction of isatin with acetone.

Entry	Catalyst	Additive	Temp (°C)	Time (h)	Yield[b] (%)	ee[c] (%)	Config
1		-	Rt	17	98	55	S
2		-	-20	32	96	57	S
3		AcOH	Rt	15	92	60	S
4		AcOH	-20	30	95	66	S
5[d]		AcOH[d]	-20	37	84	66	S
6[e]		H$_2$O[e]	-20	37	76	58	S
7		H$_2$O	-20	37	72	69	S
8		AcOH[f]	Rt	22	95	58	S
9		AcOH	-20	22	89	65	S
10		H$_2$O	-20	24	87	54	S

[a]All reactions were conducted with 0.3 mmol of isatin and 2 mL of acetone with 20 mol% of **223** or **224**. In cases where additive was employed, 20 mol% additive or 40 equiv H$_2$O was used unless otherwise specified. TLC and HPLC were used to monitor the progression of reaction [b]Isolated yield. [c]Determined by chiral HPLC. [d]40 mol% AcOH used. [e]6.6 equiv H$_2$O used. [f]10 mol% catalyst employed.

The 4-aminopyridyl derivative **224** completed the study of the *N*-pyridyl prolinamide catalysts and produced good yields in reasonable reaction times with only slightly decreased ee values compared to **223**. Interestingly, in the case of this catalyst, 20 mol% AcOH appeared more successful than 40 equiv H$_2$O as an additive for the reaction (entries 8 – 10, Table 4.15).

To summarise the performance of the *N*-pyridyl prolinamide catalysts **221** – **224**, the 4-pyridyl derivative **224** proved slightly inferior to the 3-pyridyl derivative **223** in terms of both yield and ee in particular when H$_2$O was used as an additive. Both **223** and **224** produced an excess of (*S*)-product and were far superior to the 2-pyridyl derivatives **221** & **222** which favoured the (*R*)-product in low enantioselectivities in extended reaction times. Similar work highlighting significant differences in reactivity between the structurally similar catalysts **221**, **223** & **224** in alternative aldol reactions has been previously reported. Differences appeared to be both substrate and reaction dependant; Gong *et al.* found that the 2-pyridyl **221** was more successful than the 3- or 4-pyridyl derivatives **222** or **223** in the aldol reaction of an *α*-keto acid and a ketone.[176] In addition, Luo *et al.* compared the performance of **221, 223** & **224** in the aldol reaction of 4-nitrobenzaldehyde with cyclohexanone in water with the addition of a

surfactant.[265] They found the 2-pyridyl derivative **221** to be catalytically inactive and the 4-pyridyl **224** more successful than the 3-pyridyl **223**, explained by basicity and geometrical differences.

In the case of the aldol reaction with isatin, this work has shown the 3-pyridyl catalyst **223** to be most effective. The relative position of the pyridyl and amide groups appeared key to this success possibly due to suitable spatial fit for H-bonding interactions between isatin and **223**. In addition, the acidity of the amide N-H may have played a role in efficient catalysis. This work further extends the scope and use of catalysts **221** – **224** to the aldol reaction of isatin with acetone. The results from this study were also affected by common aldol additives such as acid additives or water with enhancement in yield and/or enantioselectivity in many cases.[221] In general, the inclusion of 20 mol% AcOH and conducting the reaction at -20°C resulted in improved yield and ee values.[267,314] The addition of an appropriate quantity of H_2O was also effective at improving ee (entries 6-7, Table 4.15), but it decreased the reaction rate as previously observed.[319,320,334]

4.4 *N*-Quinolinyl Derived Prolinamide Catalysts

Following the study of the *N*-pyridyl prolinamide catalysts, a number of *N*-quinolyl prolinamide catalysts were considered in the hope that the larger aromatic ring system might make the catalyst cleft more rigid and enantioselective. Three different *N*-quinolyl prolinamides were considered which were similar to the *N*-pyridyl prolinamides in terms of the relative position of heteroaromatic nitrogen and the amide group and were derived from 2-aminoquinoline, 3-aminoquinoline and 8-aminoquinoline (catalysts **225**-**227**; Scheme 4.18).

4.4.1 *N*-Quinolinyl Catalyst Synthesis

Synthesis of these catalysts was achieved in the same manner as for the *N*-pyridyl prolinamide catalysts through ethyl chloroformate coupling of the appropriate aminoquinoline to Boc-proline to give the Boc-protected *N*-quinolinyl prolinamides in variable yields; 56% for the 2-aminoquinoline derivative Boc-**225**, 28% for the 3-aminoquinoline derivative Boc-**226** and

93% for the 8-aminoquinoline analogue Boc-**227**. As expected, LC-MS analysis of these isomers produced ions with m/z 342 corresponding to the protonated MH$^+$ ion in each case.
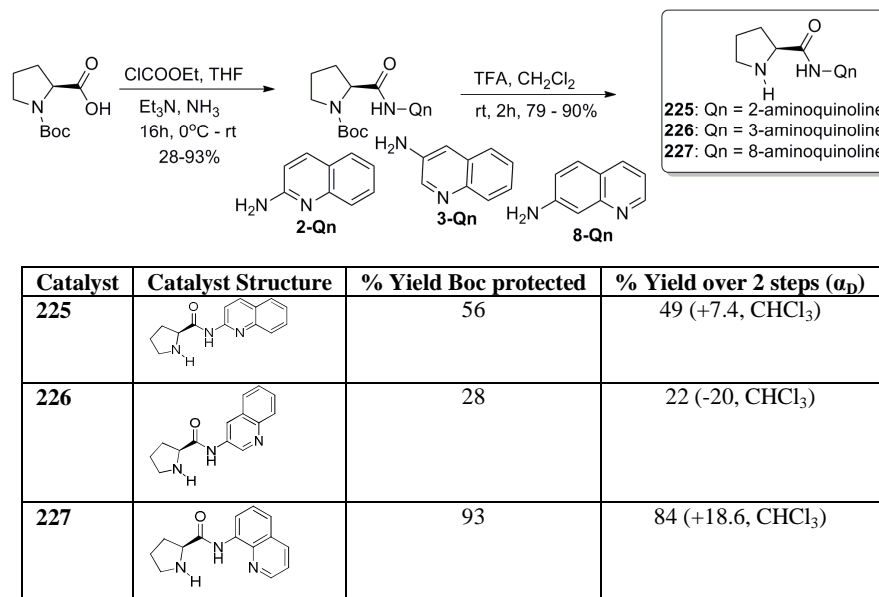
Scheme 4.18: Synthesis of *N*-quinolinyl prolinamide based catalysts.

Catalyst	Catalyst Structure	% Yield Boc protected	% Yield over 2 steps (α_D)
225		56	49 (+7.4, CHCl$_3$)
226		28	22 (-20, CHCl$_3$)
227		93	84 (+18.6, CHCl$_3$)

Boc-deprotection was conducted using TFA in dichloromethane to give **225**-**227**. Again, these isomers produced identical mass spectra with the MH$^+$ ion at m/z 242 detected as the major LC-MS peak in each case. The structure of the Boc-protected and deprotected catalysts were also confirmed by NMR spectroscopy using ^{1}H, ^{13}C, DEPT and COSY experiments. The ^{1}H & ^{13}C NMR spectra appeared similar for **225** – **227** with moderate differences due to relative arrangement of the quinolinyl aromatic peaks. Detailed assignment of signals was conducted for the deprotected catalysts using these NMR techniques (Table 4.16, Table 4.17 & Table 4.18). The key ^{1}H NMR spectroscopic resonances indentified included 6 aromatic protons in the range 7.6 – 8.9 ppm, aliphatic pyrrolidine protons including diastereotopic H-3' protons from 2.0 – 2.3 ppm, pyrrolidine amine N-H group at 2.1 – 2.2 ppm and also the prolinamide N-H proton varying from 10.1 – 11.6 ppm.

Table 4.16: ^{1}H NMR spectroscopic assignments and COSY interactions for **225**
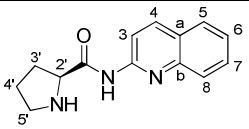
Structure	Protons	δ (ppm)	Correlated with δ (ppm)	Correlated with
	H-3	8.48 (d, J = 8.70 Hz, 1H)	8.16 (d, J = 9.16 Hz)	H-4
	H-8	7.86 (d, J = 8.70 Hz, 1H)	7.61-7.68 (m, 1H)	H-7
	H-5	7.76 (d, J = 9.16 Hz, 1H)	7.40-7.46 (m, 1H)	H-6
	H-7	7.61-7.68 (m, 1H)	7.40-7.46 (m, 1H)	H-6
	H-2'	3.88-3.95 (m, 1H)	2.01-2.30 (m, 2H)	H-3'
	H-5'	3.04-3.15 (m, 2H)	1.73-1.85 (m, 2H)	H-4'
	H-3'	2.01-2.30 (m, 2H)	1.73-1.85 (m, 2H)	H-4'

Table 4.17: ^{1}H NMR spectroscopic assignments and COSY interactions for **226**
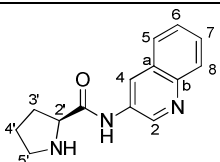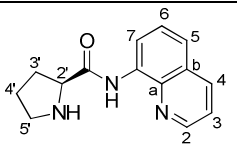
Structure	Protons	δ (ppm)	Correlated with δ (ppm)	Correlated with
	H-2	8.83-8.85 (m, 1H)	8.75-8.77 (m, 1H)	H-4
	H-5	8.0-8.04 (m, 1H)	7.57-7.62 (m, 1H)	H-6
	H-7	7.77-7.81 (m, 1H)	7.49-7.53 (m, 1H)	H-8
	H-2'	3.91-3.97 (m, 1H)	2.01-2.31 (m, 2H)	H-3'
	H-5'	3.0-3.20 (m, 2H)	1.75-1.85 (m, 2H)	H-4'
	H-3'	2.01-2.31 (m, 2H)	1.75-1.85 (m, 2H)	H-4'

Table 4.18: ^{1}H NMR spectroscopic assignments and COSY interactions for **227**

Structure	Protons	δ (ppm)	Correlated with δ (ppm)	Correlated with
	H-2 & H-7	8.81-8.89 (m, 2H)	7.48-7.56 (m, 2H)	H-5 & H-6
	H-4	8.12-8.16 (m, 1H)	7.41-7.45 (m, 1H)	H-3
	H-2'	3.98-4.05 (m, 1H)	2.08-2.33 (m, 2H)	H-3'
	H-5'	3.11-3.21 (m, 2H)	1.71-1.90 (m, 2H)	H-4'
	H-3'	2.08-2.33 (m, 2H)	1.71-1.90 (m, 2H)	H-4'

4.4.2 Catalytic Properties of *N*-Quinolinyl Catalysts

Catalysts **225** – **227** were tested in the aldol reaction of isatin with acetone and major variations in reactivity and enantioselectivity were observed between them; however interestingly their profiles followed a similar pattern to that of the *N*-pyridyl prolinamide isomers **221-224**. The 2-aminoquinoline derivative catalyst **225** effected product in 17% ee of the (*R*)-isomer in an unacceptably low yield of less than 20% using 20 mol% catalyst loading with 20 mol% AcOH at -20°C (entry 2, Table 4.19). To try optimise this further, variation in reaction temperature and use of water as an additive were investigated but resulted in lower ee. Interestingly, when **225** was used in 20 mol% loading with 40 equiv water additive, a

slight excess of 7% ee of the (*S*)-product was observed, opposite to the system when AcOH was used as additive (entry 3, Table 4.19).

Table 4.19: Testing of *N*-quinolinyl prolinamide catalysts **225-227**.
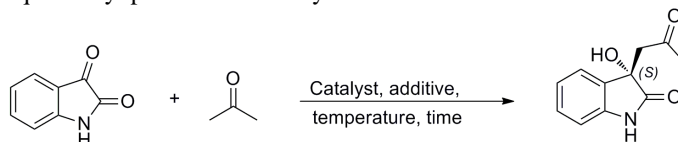
Entry	Catalyst	Catalyst Loading (mol%)	Additive	Temp (°C)	Time (h)	Yield[b] (%)	ee[c] (%)	Config
1	**225**	10	AcOH	Rt	192	<10	2	*R*
2		20	AcOH	-20	504	<20	17	*R*
3		20	H₂O	-20	312	<20	7	*S*
4	**226**	10	AcOH	Rt	24	95	59	*S*
5		20	AcOH	-20	50	71	64	*S*
6[d]		20	AcOH[d]	-20	50	69	62	*S*
7		20	H₂O	-20	44	89	66	*S*
8	**227**	10	-	Rt	23	82	17	*R*
9		10	AcOH	Rt	21	94	18	*R*
10		20	AcOH	-20	44	76	13	*R*
11[d]		20	AcOH[d]	-20	44	86	13	*R*
12		20	H₂O	-20	60	75	5	*R*

[a]All reactions were conducted with 0.3 mmol of isatin and 2 mL of acetone. In cases where additive was employed, 20 mol% additive was used. TLC and HPLC were used to monitor the progression of reaction [b]Isolated yield. [c]Determined by chiral HPLC. [d]40 mol% AcOH used.

The 3-aminoquinoline derivative **226** was tested under a number of conditions and temperatures. Due to previous results showing that the reactions were more efficient in the presence of additives such as AcOH and H₂O, these additives were used in this testing. For catalyst **226**, enantioselectivities of the order 59-66% ee in favour of the (*S*)-product were obtained with the optimum ee of 66% observed with 20 mol% catalyst loading, 40 equiv H₂O additive at -20°C to give a yield of 89% after 44 hours (entry 7, Table 4.19). In all instances, the (*S*)-product was favoured when using the 3-aminoquinoline derived catalysts as observed with the 3-aminopyridine derivative (catalyst **223**).

The 8-aminoquinoline derivative **227** was also examined under a variety of conditions varying reaction temperature, catalyst loading and additive type. In all cases, **227** preferentially formed

excess of (*R*)-product and provided good yields of product in poor enantioselectivities with reaction time up to 44 hours. Use of a 10 mol% catalyst loading with 20 mol% AcOH at room temperature gave the product in slightly better ee compared to use of a higher catalyst loading at lower temperatures (entries 8-12, Table 4.19). It is interesting to note that derivatives in which the heterocyclic nitrogen was in relatively close proximity to the amide group such as catalyst **221**, **222**, **225** & **227** tended to favour the (*R*)-product in low enantioselectivity but derivatives where the moieties are relatively separate afforded an excess of (*S*)-product.

4.5   *Bis-N*-pyridyl Prolinamide 228

A final C2 symmetric *bis-N*-pyridyl prolinamide was considered. Catalyst **228** derived from coupling of proline to 2,6-diaminopyridine represented a *bis*-prolinamide version of catalyst **221** which could enhance possible binding effects. Synthesis of **228** was achieved in poor yield through ethyl chloroformate coupling of Boc-protected proline with 2,6-diaminopyridine to give Boc-**228**. LC-MS analysis of this product produced a Na adduct MNa$^+$ at m/z 526 and MH$^+$ ion at m/z 504.
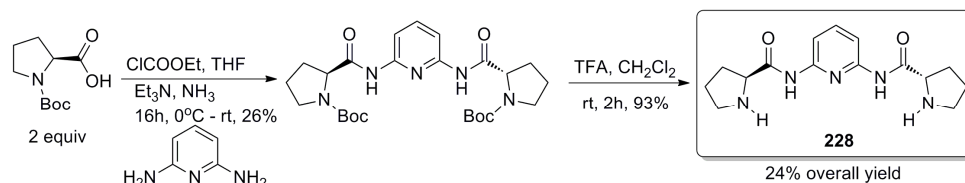
Scheme 4.19: Synthesis of C-2 symmetric *bis-N*-pyridyl prolinamide catalyst **228**

Boc-deprotection using TFA in dichloromethane completed the synthesis (Scheme 4.19). The structure and purity of the catalyst was assessed by LC-MS and ^{1}H NMR spectroscopy. LC-MS analysis gave the MNa$^+$ ion at m/z 326 and the MH$^+$ ion at m/z 304. Due to the symmetrical nature of the catalyst, the ^{1}H NMR spectrum featured a relatively small number of peaks. Key peaks identified included pyrrolidine signals, in particular diastereotopic H-3' protons in the range of 1.6 – 2.3 ppm and amide N-H signal at 9.97 ppm. The aromatic protons from the 2,6-pyridinedicarboxyl ring consisted of two signals with a doublet at 7.95 ppm representing H-3 and a triplet at 7.70 ppm corresponding to H-4.

4.5.1 Catalytic Performance of *Bis*-Prolinamide Catalyst 228

Various parameters were examined during catalyst testing including catalyst loading, level and type of acid additive and temperature. In all cases, an excess of the (*S*)-product was produced, opposite to that favoured with the 2-pyridyl mono-prolinamide (catalyst **221**).

Table 4.20: Testing of catalyst **228** under various conditions in the reaction of isatin with acetone.
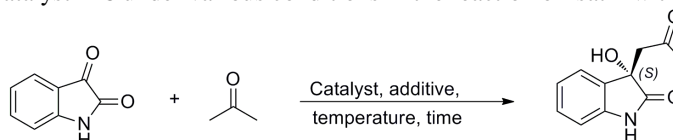
Entry	Catalyst	Catalyst Loading (mol%)	Additive	Temp (°C)	Yield[b] (%)	ee[c] (%)	Config
1		10	-	Rt	99	28	*S*
2		10	-	-20	77	45	*S*
3		10	AcOH	-20	81	47	*S*
4		20	-	-20	78	43	*S*
5		20	AcOH	-20	99	39	*S*
6		20	20 eq H$_2$O	-20	99	36	*S*
7		20	H$_2$O	-20	99	43	*S*
8		20	60 mol% AcOH	-20	95	39	*S*

[a]All reactions were conducted with 0.3 mmol of isatin and 2 mL of acetone using 88 hours reaction time. In cases where additive was employed, 20 mol% additive or 40 equiv H$_2$O was used. TLC and HPLC were used to monitor the progression of reaction [b]Isolated yield. [c]Determined by chiral HPLC.

For reactions in the absence and presence of AcOH, decreasing the catalyst loading from 20 mol% to 10 mol% and use of 20 mol% AcOH resulted in an increase in ee of up to 8% in some cases (entries 2-5, Table 4.20) The addition of 20 equiv water caused a slight reduction in ee (entry 4 vs 6, Table 4.20) while the use of 40 equiv water increased ee values equivalent to the system without additive (entry 4 vs 6 & 7, Table 4.20). The reaction using 60 mol% AcOH had no effect on enantioselectivity and only a slight yield reduction (entry 5 vs 8, Table 4.20). The optimum result was achieved through the use of 10 mol% catalyst with 20 mol% AcOH at -20 °C for 88 hours to give 47% ee of (*S*)-product (entry 3, Table 4.20), a considerable increase and in opposite configuration compared to the mono-prolinamide equivalent **221**. This increase in yield and selectivity may be due to more efficient binding of the substrate to the amide N-H groups of **228** potentially through H-bonding to both isatin

carbonyl groups. This could allow better spatial fit of the catalyst and isatin without interaction from the pyridine nitrogen.

4.5.2   Summary of Performance of Catalysts 221-228

From the results obtained from *N*-pyridyl prolinamide and also *N*-quinolinyl prolinamide catalysts, the best result was obtained using the 3-aminopyridine based catalyst **223** with a 20 mol% loading of catalyst in the presence of 40 equiv H_2O at -20°C for 37 hours, producing a yield of 72% and 69% ee of (*S*)-product (entry 7, Table 4.15). Geometrical differences and spatial effects appeared to have played a key role in binding and therefore catalytic performance. It appeared that having the amide group and pyridine nitrogen too close or too far from one another led to less efficient results with the 3-positioning of the pyridyl prolinamide having the optimal catalyst arrangement. The apparent size of the binding cleft for **223** may have been most suitable for this reaction with the smaller binding site in **221**, **222**, **225** & **228** unsuitable and this will be discussed in more detail later.

4.6   Hydroxyprolinamide & Ring Derivatised Catalysts

There have been reports of the use of hydroxyproline and other pyrrolidine ring derivatised compounds as organic catalysts and in some cases, such catalysts perform better than the non-derivatised versions.[262] With this in mind, prolinamide catalysts starting from 4-hydroxyl-*L*-proline were synthesised. These bifunctional ring-substituted prolinamide catalysts were based on the most successful catalyst to date (3-pyridyl prolinamide **223**) and examined with respect to the effect of the additional chiral centre on the pyrrolidine ring and also the effect of protecting the additional OH group with a bulky benzyloxy group (catalyst **229**) or leaving it unprotected (catalyst **230**).
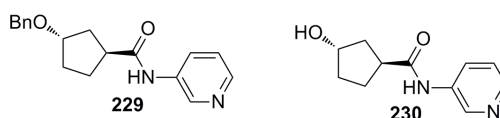
Figure 4.8: Structure of hydroxyprolinamide and ring derivatised catalysts **229** & **230**.

4.6.1 Synthesis of Benzyloxy-3-Pyridyl Prolinamide 229

Catalyst **229** was synthesised in 4 steps with moderate yield starting with *N*-Boc-trans-4-hydroxy-*L*-proline methyl ester (Scheme 4.20). To protect the commercially available ester hydroxyl group, it was stirred with benzyl bromide in anhydrous DMF with sodium hydride. After approximately 4 hours, the reaction was quenched with H_2O and following mild acidic work up and chromatographic purification, the expected product **231** was obtained in 38% yield. LC-MS analysis produced an MNa^+ adduct at m/z 358 and an MH^+ adduct at m/z 326. The structure of this compound was also confirmed by ^1H NMR spectroscopy with ^{13}C, DEPT and COSY analysis used to aid peak assignment. The key ^1H NMR spectroscopic resonances which confirmed the successful reaction and verified the protected intermediate were the benzyl methylene peaks from 4.27 – 4.52 ppm and the additional phenyl ring aromatic peaks from 7.23 – 7.36 ppm.
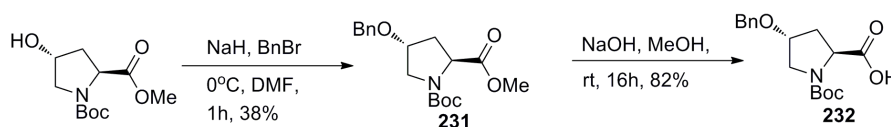
Scheme 4.20: Protection of *N*-Boc-trans-4-hydroxy-*L*-proline methyl ester with benzyl bromide forming **231** followed by hydrolysis to the corresponding carboxylic acid **232**.

Table 4.21: COSY analysis of benzyl protected intermediate **231**.

Structure	Proton	δ (ppm)	Correlated with δ (ppm)	Correlated with
	H-2'	4.27-4.52 (m, 3H)	2.0-2.42 (m, 2H)	H-3'
	H-4'	4.05-4.20 (m, 1H)	2.0-2.42 (m, 2H), 3.48-3.70 (m, 2H, H-5')	H-3' & H-5'

Ester **231** was hydrolysed to the corresponding acid using NaOH in methanol at room temperature. Upon completion, the reaction mixture was diluted with water and following a mild acid/base work-up, was extracted with ethyl acetate, dried with $MgSO_4$ and solvent removed *in vacuo* to give a yield of 81% of the acid intermediate **232**. LC-MS analysis produced the Na adduct at m/z 344. ^1H NMR spectroscopic resonances were assigned through comparison with the previously synthesised ester intermediate with an extra broad signal at 9.90 ppm ascribed to the carboxylic acid group and also the loss of the methoxy group, evident in both the ^1H and ^{13}C NMR spectroscopy.

This carboxylic acid **232** was subsequently reacted with 3-aminopyridine through ethyl chloroformate coupling in the same manner as the *N*-pyridyl and *N*-quinolinyl prolinamide catalysts (Scheme 4.21). This coupling appeared to be very sensitive to reaction concentration and also rate of addition of 3-aminopyridine, observed from the failure of the reaction at more concentrated levels than 122 mM and also with fast addition of 3-aminopyridine. A concentration of 58 mM of acid in THF was deemed to be optimal. The Boc-protected 4-benzyloxyprolinamide version of catalyst **229** was synthesised in 45% yield following chromatographic purification using a mixture of petroleum ether and ethyl acetate and LC-MS analysis produced a peak at m/z 398 corresponding to MH$^+$ and also at m/z 298 due to loss of the Boc group from the molecular ion.
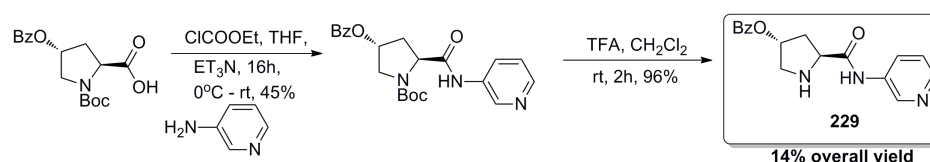
Scheme 4.21: Synthesis of catalyst **229.**

Table 4.22: List of HMQC correlations and assignment of NMR spectroscopic resonances for **229.**

Structure	^{13}C NMR δ (ppm)	^{1}H NMR δ (ppm)	Assignment
	145.1	8.28-8.31 (m, 1H)	C-4 & H-4
	141.0	8.58-8.61 (m, 1H)	C-2 & H-2
	126.6-128.7	7.20-7.38 (m, 5H)	Ar-C & Ar-H
	126.5	8.19-8.23 (m, 1H)	C-6 & H-6
	123.7	7.20-7.38 (m, 1H)	C-5 & H-5
	80.5	4.12 (s, 1H)	C-4' & H-4'
	70.8	4.41-4.52 (m, 2H)	OC$\underline{H}_2$-Ph
	60.4	4.03-4.09 (s, 1H)	C-2' & H-2'
	52.8	3.20-3.25 (m, 1H) & 2.76-2.82 (m, 1H)	C-5' & H-5'
	36.3	2.47-2.56 (m, 1H) & 1.93-2.0 (m, 1H)	C-3' & H-3'

The protected catalyst Boc-**229** was deprotected using TFA in dichloromethane at room temperature to give **229** in 96% yield from the deprotection and 14% overall from the 4-step synthetic sequence. LC-MS analysis gave an MH$^+$ peak at m/z 298 and NMR spectroscopic analysis using ^{1}H, ^{13}C, DEPT & HMQC experiments were used to verify the catalyst and to assign all NMR signals (Table 4.22). The key ^{1}H NMR spectroscopic resonances which confirmed the success of this synthesis included the amide N-H peak at 9.85 ppm, two

separate sets of aromatic protons, pyrrolidine ring protons in the range 1.9 – 4.1 ppm, the benzyl disatereotopic protons from 4.41-4.52 ppm and the pyrrolidine N-H proton at 2.55 ppm.

4.7 Synthesis of Hydroxy-Prolinamide Catalyst 230

The unprotected catalyst **230** possessing a free hydroxyl group *trans* to the amide group was synthesised as outlined in Scheme 4.22. Initial Boc protection of *trans*-4-hydroxy-*L*-proline was attained in 35% yield by reaction with di-*tert*-butyl-dicarbonate in a 1:1 mixture of water and dioxane in the presence of saturated aqueous sodium bicarbonate. After 16 hours reaction at room temperature, product extraction was conducted at pH 3 and following drying over MgSO$_4$, removal of solvent *in vacuo* and flash chromatography, the pure *N*-Boc-protected acid was obtained. ^{1}H NMR spectroscopic characterisation corresponded to previous synthetic reports of this compound with the presence of the *t*-Bu signal from 1.39 – 1.45 ppm confirming the success of the reaction.[262]
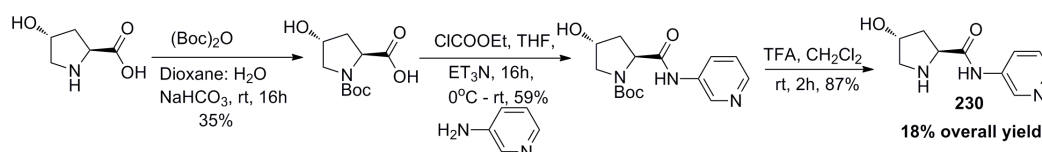
Scheme 4.22: Synthesis of Boc-protected 4-hydroxy-*L*-proline followed by coupling and deprotection towards ring substituted catalyst **230**.

Ethyl choroformate coupling of the *N*-Boc-protected hydroxyproline with 3-aminopyridine produced Boc-**230** in 59% yield. LC-MS analysis displayed a peak at m/z 308 corresponding to the MH$^+$ ion and m/z 208 due to complete loss of the Boc group. Boc deprotection using TFA in dichloromethane at room temperature gave catalyst **230** in 87% yield and 18% yield overall. LC-MS analysis of **230** produced an ion at m/z 208 corresponding to the MH$^+$ ion. NMR spectroscopic analysis was used to confirm **230** and ^{1}H, ^{13}C and HMQC experiments were used as an aid for peak assignment. Key ^{1}H NMR spectroscopic resonances included the pyrrolidine diastereotopic H-3' signals from 2.01 – 2.10 ppm and 2.36 – 2.43 ppm, H-5' protons from 3.11 – 3.28 ppm, aromatic pyridyl signals and also the amide N-H peak at 6.93 ppm.

Table 4.23: List of HMQC correlations and assignment of NMR spectroscopic resonances for **230.**

Structure	^{13}C NMR δ (ppm)	^{1}H NMR δ (ppm)	Assignment
	144.3	8.26-8.29 (m, 1H)	C-4 & H-4
	140.8	8.77-8.81 (m, 1H)	C-2 & H-2
	127.8	8.08-8.14 (m, 1H)	C-6 & H-6
	124.0	7.37-7.42 (m, 1H)	C-5 & H-5
	71.1	4.51 (s, 1H)	C-4' & H-4'
	59.8	4.31-4.37 (m, 1H)	C-2' & H-2'
	54.2	3.11-3.28 (m, 2H)	C-5' & H-5'
	39.0	2.36-2.43 (m, 1H) & 2.01-2.10 (m, 1H)	C-3' & H-3'

4.7.1 Catalytic Properties of 229 & 230

The *trans*-benzyl protected catalyst **229** was tested under a number of conditions including using AcOH and H_2O as additives for the reaction. The most successful system employed 20 mol% catalyst loading with 40 equiv H_2O at -20 °C, in an extended reaction time of 70 hours resulting in 54 % ee of (*S*)-product (entry 2, Table 4.24). The unprotected *trans*-hydroxyl derivative **230** furnished product in up to 58% ee of (*S*)-product, again using 20 mol% catalyst loading and 40 equiv of H_2O at -20 °C (entry 4, Table 4.24). These results showed that incorporation of a second bulky H-bond donating functionality and chiral centre *trans* to the amide in the pyrrolidine ring of the prolinamide catalyst resulted in a slight reduction in ee compared to the unsubstituted system.

Table 4.24: Testing of pyrrolidine ring substituted prolinamide catalysts **229** & **230.**

Entry	Catalyst	Catalyst Loading (mol%)	Additive	Temp (°C)	Time (h)	Yield[b] (%)	ee[c] (%)	Config
1	**13**	20	AcOH	-20	90	77	50	*S*
2	**13**	20	H_2O	-20	90	79	54	*S*
3	**14**	20	AcOH	-20	15	85	44	*S*
4	**14**	20	H_2O	-20	17	87	58	*S*

[a]All reactions were conducted with 0.3 mmol of isatin and 2 mL of acetone. In cases where additive was employed, 20 mol% additive or 40 equiv H_2O was used. TLC and HPLC were used to monitor the progression of reaction [b]Isolated yield. [c]Determined by chiral HPLC.

From the above series of catalysts (**221-230**); overall it was apparent that **223** possessed the most potential for the reaction. Work was subsequently conducted aiming to enhance further the yield and enantioselectivity of the reaction catalysed by **223** (Figure 4.9).
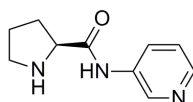
Figure 4.9: Structure of most successful catalyst **223** based on 3-aminopyridine and prolinamide coupling.

4.8   Effects of Acid Additives on Catalytic Performance

Having observed the positive influence of AcOH as an additive on yield and enantioselectivity, the effect of strength of acid additive was then considered. Xiao *et al.* previously studied the isatin/acetone aldol reaction and conducted all reactions in the presence of AcOH.[314] However, several other acid additives have also been used in aldol reactions with a number of these studies detailed in Chapter 3.[267] A range of acid additives across a pK_a range of -2 to 16 were examined for the **223** catalysed reaction of isatin and acetone and a correlation between pK_a of acid additive and enantioselectivity was observed (Table 4.25). Interestingly, a plot of pK_a versus enantioselectivity resembled a pH titration curve. The ee appeared to rise sharply and linearly between additive pK_a of 2-6. A plateau was reached at pK_a 7 after which point an essentially constant ee value was obtained regardless of the pK_a of the additive (Figure 4.10).

A relationship between pK_a of additive and reaction yield was also observed. It was noted that the reaction proceeded at a slower rate when using additives with pK_a values >6 (entry 6 vs entries 8 and 9, Table 4.25). Additionally, an increase in ee was observed to be obtained at the expense of product yield and it could therefore be stated that the optimum acid additive for yield and enantioselectivity should possess a pK_a value of approximately 4.0-6.0.

Table 4.25: Variation of acid additive & relationship between pK_a of additive and ee of (S)-product catalysed ny 223.[a]
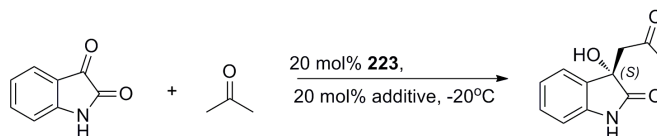
Entry	Additive	Additive pK_a	Time (h)	Yield[b] (%)	ee[c] (%)
1	p-TSA	-1.34	88	52	13
2	TFA	0.26	12	97	12
3	ClCH$_2$COOH	2.85	6	98	37
4	HCOOH	3.75	14	94	58
5	PhCOOH	4.21	14	90	63
6	AcOH	4.76	65	95	66
7	4-NO$_2$-Phenol	7.14	78	84	69
8	4-Cl-Phenol	9.38	89	85	70.5
9	Phenol	9.94	89	80	71
10	Methanol	15	89	77	69
11	Water	15.7	32	96	57

[a]All reactions were conducted with 0.3 mmol of isatin and 2 mL of acetone. In cases where additive was employed, 20 mol% additive. TLC and HPLC were used to monitor the progression of reaction [b]Isolated yield. [c]Determined by chiral HPLC. Literature pK_a data as measured in water.[348]
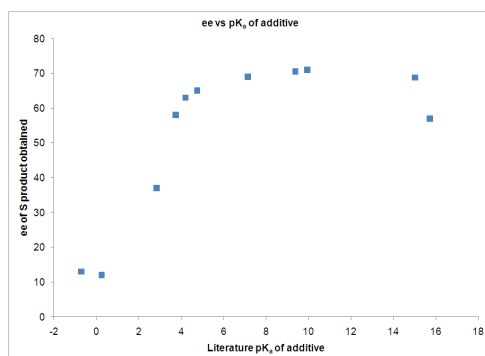
Figure 4.10: Relationship between pK_a of acid additive and ee of product using 20 mol% catalyst **232** and 20 mol% additive.

Water as an additive was found to be an exception to the aforementioned trends producing product with lower ee and higher yield than expected based on its pK_a of 15.7 when used at 20 mol% levels (entry 11, Table 4.25). It must be noted however that the quantity of water present in the medium has been demonstrated to be critical to the level of enantioselectivity.[319] A quantity of 40 equiv (4000 mol%) has been found to be optimal by Tomasini *et al.* for a

dipeptide catalyst and above this level, a decrease in ee occurred with increasing water concentrations.[319] This was also observed in this work for *N*-pyridyl prolinamide catalyst **223**.

4.9   Role of Solvent in 223 Catalysed Reaction

A detailed solvent study was undertaken investigating the effects of reaction solvent (Table 4.26). Due to the similar performance of **223** using AcOH or 40 equiv H_2O as additive, the study was undertaken for both additives independently. Solvents of varying polarities were examined and in the case of AcOH additive, toluene produced 91% yield of product in 66% ee with a reaction time of 22 hours compared to 65 hours reaction time in neat acetone. This faster reaction in non-polar toluene may have been due to potentially more efficient catalyst-substrate H-bonding in a non-polar solvent with less H-bonding competition from the solvent. A marginally higher ee value could be obtained when the reaction with AcOH additive was conducted in relatively non-polar $CHCl_3$ or CH_2Cl_2 (entries 7 & 8, Table 4.26) but this came at the expense of reaction yield.

When using H_2O as additive, the reaction in acetone was found to be marginally superior in terms of ee compared to the use of alternative reaction solvents and this reaction gave the most successful results overall. When relatively non polar co-solvents such as hexane or $CHCl_3$ were used, an increase in reaction yield was observed but longer reaction times were required (entries 9-16, Table 4.26).

Table 4.26: Variation of solvent in reaction catalysed by **223**.[a]
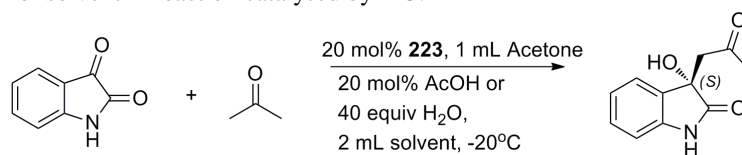
Entry	Solvent	Additive	Time (h)	Yield[b] (%)	ee[c] (%)
1	Acetone	AcOH	65	95	66
2	Toluene	AcOH	22	91	66
3	DMF	AcOH	61	78	54
4	Dioxane	AcOH	42	85	64
5	THF	AcOH	48	78	64
6	Hexane	AcOH	38	96	58
7	CH_2Cl_2	AcOH	46	82	68.5
8	$CHCl_3$	AcOH	40	80	69
9	Acetone	H_2O	37	72	69
10	Toluene	H_2O	108	72	63
11	DMF	H_2O	108	85	61
12	Dioxane	H_2O	13.5	97	50
13	THF	H_2O	41	92	63
14	Hexane	H_2O	88	98	68
15	CH_2Cl_2	H_2O	108	68	66
16	$CHCl_3$	H_2O	90	85	68
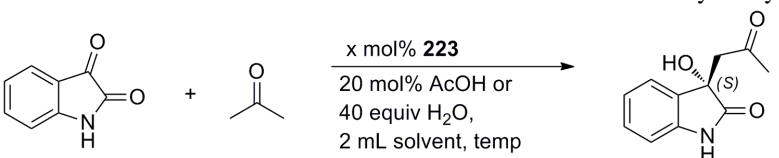
[a]All reactions were conducted with 0.3 mmol of isatin and 2 mL of co-solvent and 1 mL acetone using 20 mol% of **223** at -20°C with either 20 mol% AcOH or 40 equiv H_2O. An excess of the (S)-product was obtained in all cases. TLC and HPLC were used to monitor the progression of reaction [b]Isolated yield. [c]Determined by chiral HPLC.

4.10   Study of Conditions for Optimal Enantioselectivity using 223

The catalytic conditions were optimised further for the most successful catalyst **223**. The effects of catalyst loading, temperature additive and additive loading were examined in turn. As close values yield and ee values were obtained for chloroform, hexane and acetone as solvents with H_2O additive, these were examined at a loading of 30 mol%. The reaction in neat acetone with H_2O was the most efficient in terms of ee giving the product in 72% ee compared to 68% ee for both chloroform and hexane. Interestingly, the concentration at which the acetone reaction was conducted did not have any effect on yield or enantioselectivity with no difference in results between the reaction at 0.15 M and 0.3 M of isatin in acetone (entry 5

vs 8, Table 4.27). A further increased loading of 40 mol% produced a slightly reduced ee value of 69%, indicating that 30 mol% was the optimum catalyst loading (entry 5 vs 9, Table 4.27). The use of AcOH additive prodced slightly inferior enantioselectivities compared to water as an additive. Overall, the best result was obtained using 30 mol% loading of catalyst in the presence of 40 equiv H_2O at -20°C for 37 hours, producing a yield of 88% and 72% ee of (*S*)-product (entry 5, Table 4.27).[319]

Table 4.27: Variation of conditions and additives in reaction of isatin and acetone catalysed by **7**.[a]

Entry	Loading	Additive	Temp (°C)	Time (h)	Yield (%)	ee (%)
1	30	AcOH	Rt	15	95	60
2	30	AcOH	-20	37	95	63
3	30	AcOH[b]	-20	37	84	69
4	20	H_2O[c]	-20	37	76	58
5	**30**	**H_2O**	**-20**	**37**	**88**	**72**
6	30	H_2O/Hexane	-20	37	90	68
7	30	H_2O/CHCl$_3$	-20	37	67	68
8	30[d]	H_2O	-20	37	87[d]	72[d]
9	40	H_2O	-20	33	68	69

[a]Unless otherwise noted, all reactions for catalyst optimisation study were conducted using 30 mol% catalyst loading of **223** with either 20 mol% AcOH or 40 equiv H_2O additive to yield and excess of (*S*)-product. TLC and HPLC were used to monitor the progression of the reaction. [b]40 mol% AcOH used. [c]6.6 equiv H_2O used. [d]1 mL acetone used to give a concentration of 0.3 M isatin in acetone.

4.11 Structural Considerations

Overall, this study identified several key structural design parameters critical to yield and enantioselectivity. Firstly, the results indicate that the relative position of the pyridyl nitrogen with the amide in the prolinamide catalyst was most important to achieve high yield and enantioselectivity. The loss of yield and enantioselectivity in the 2-pyridyl catalysts **221** & **222** and 2- and 8-quinolyl catalysts **225** & **227** was possibly due to electron repulsion between the lone pair of electrons in the pyridine nitrogen and the non H-bonded carbonyl group of isatin upon H bonding of the reactive carbonyl with the amide N-H. This repulsion may not

arise when the *N* lies at position 3 or 4 in the pyridyl ring or 8-positon in the quinolyl analogue. The pK_a of acid additive was also key to yield and enantioselectivity. Loss in enantioselectivity appeared to occur when an additive with a pK_a lower than 4 was employed. Using acid with a lower pK_a could lead to possible protonation of the pyridine nitrogen with disruption of H-bonding and/or acceleration of the direct reaction of acetone with isatin which could account for loss of selectivity. Water may alternatively be used as an additive, with 40 eq at -20 °C giving the high yield and best enantioselectivity (entry 5, Table 4.27). It can be envisaged that water may bind the isatin substrate in an active/passive model similar to that proposed by Tomasini *et al.* and discussed previously.[319]
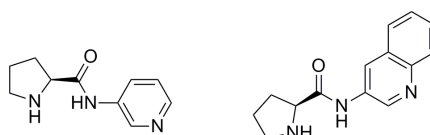
Figure 4.11: Structure of the two most successful catalysts; 3-pyridyl and 3-quinolinyl catalysts **223** & **226.**
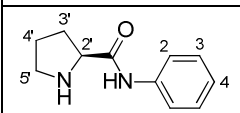
In order to further probe the impact of the pyridine *N* in the ring and hence determine the potential mode of action of **223**, catalyst **233**, in which a phenyl ring replaced the pyridine ring was prepared. The synthesis of this catalyst began with Boc-protection of *L*-proline followed by ethyl chloroformate coupling of the purified Boc-proline with aniline to give 33% yield of the white solid Boc-**233** following chromatographic purification (Scheme 4.23). LC-MS analysis of this compound showed a peak at m/z 321 corresponding to the MNa$^+$ adduct.
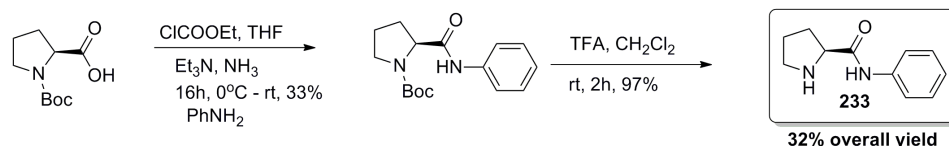
Scheme 4.23: Synthesis of catalyst **233** derived from *N*-Boc proline and aniline.

Boc deprotection was conducted using TFA in dichloromethane to give 97% yield of **233** and 32% yield over 2 steps. GC-MS analysis showed an ion at m/z 191 corresponding to the MH$^+$ ion. ^{1}H & ^{13}C NMR spectroscopic analysis were used to confirm the product and HMQC, COSY & DEPT experiments were used to aid peak assignment. Key ^{1}H NMR spectroscopic resonances verifying **233** and the success of the coupling included the amide N-H signal at 9.72 ppm, pyrrolidine N-H signal in the range of 1.97 – 2.2 ppm, diastereotopic H-3' protons from 1.97 – 2.23 ppm and aromatic protons from 7.0 – 7.6 ppm.

Table 4.28: List of HMQC correlations and assignment of ^{1}H & ^{13}C NMR spectroscopic resonances for **233.**

Structure	^{13}C NMR δ (ppm)	^{1}H NMR δ (ppm)	Assignment
	129.0	7.30 (t, $J = 7.79$ Hz, 2H)	C-3 & H-3
	124.0	7.04-7.10 (m, 1H)	C-4 & H-4
	119.3	7.59 (d, $J = 7.79$ Hz, 2H)	C-2 & H-2
	61.1	3.80-3.85 (m, 1H)	C-2' & H-2'
	47.4	2.92-3.10 (m, 2H)	C-5' & H-5'
	30.8	1.97-2.23 (m, 2H)	C-3' & H-3'
	26.4	1.69-1.80 (m, 2H)	C-4' & H-4'

Catalyst **233** was tested under a number of conditions in the reaction of isatin with acetone and surprisingly, product with high ee values was obtained when a 30 mol% loading with 40 equiv water additive at -20°C was used. The reaction appeared considerably slower with catalyst **233** compared to **223** which furnished a yield of 88% with 72% ee after 37 hours. This showed a 7% reduction in ee in the absence of the pyridyl nitrogen with an increase in reaction time of 54 hours. Therefore, it can be stated that the pyridyl nitrogen played a role in enhancing the ee of product.

Table 4.29: Reaction of isatin with acetone catalysed by aniline prolinamide catalyst **233.**
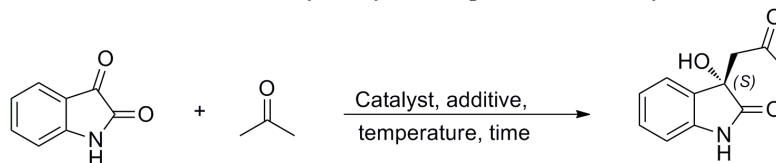
Entry	Catalyst	Cat loading (mol %)	Additive	Time (h)	Yield^b (%)	ee^c (%)
1		20	-	91	90	58
2	**233**	20	AcOH	91	92	61
3		30	H$_2$O	91	89	65

^{a}All reactions were conducted with 0.3 mmol of isatin and 2 mL of acetone. An excess of the (S)-product was obtained in each case. TLC and HPLC were used to monitor the progression of reaction ^{b}Isolated yield. ^{c}Determined by chiral HPLC.

4.12 *N*-Methylated Catalysts 234 & 235

In order to assess the role of the amide N-H proton, prolinamides **234** and **235** were synthesised from proline coupled to the appropriate methyl amine. In the case of 4-methylaminopyridine derivative **234**, Boc protected catalyst was obtained in 33% yield after

work-up and chromatographic purification. LC-MS analysis produced an ion at m/z 306 corresponding to the MH$^+$ ion. Boc-**234** derived from coupling Boc-proline with *N*-methyl aniline was obtained in 29% yield following purification by flash chromatography. GC-MS analysis gave an ion at m/z 304 corresponding to the M$^+$ ion and LC-MS analysis produced a peak at m/z 327 due to the Na adduct of the molecular ion.
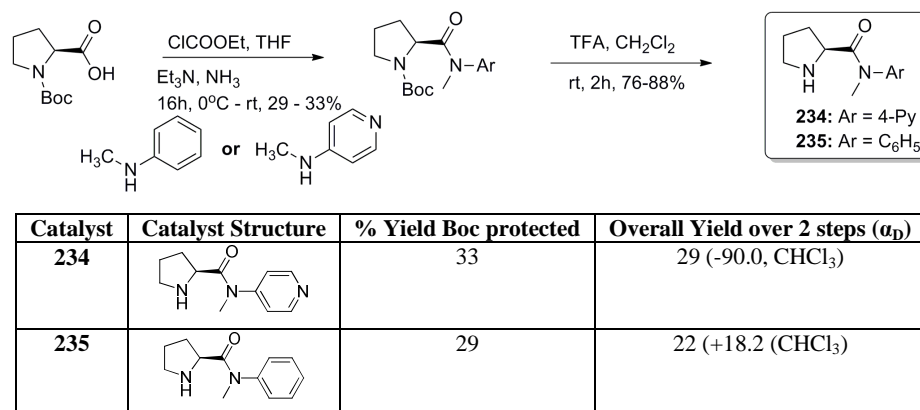
Scheme 4.24: Synthesis of *N*-methylated prolinamide catalysts **234** & **235**.

Catalyst	Catalyst Structure	% Yield Boc protected	Overall Yield over 2 steps (α_D)
234		33	29 (-90.0, CHCl$_3$)
235		29	22 (+18.2 (CHCl$_3$)

Boc-deprotection using TFA in dichloromethane of both the Boc protected versions of **234** & **235** and gave product in good yields; 88% for **234** giving a 29% yield over 2 steps and 76% yield for **235** corresponding to 22% over 2 steps. LC-MS analysis of **234** produced an ion at m/z 206 due to the MH$^+$ ion while an ion at m/z 204 by GC-MS corresponded to the M$^+$ ion for **235**. ^{1}H NMR spectroscopy and the use of ^{13}C, DEPT, COSY and HMQC experiments were used to confirm the identity of **234** & **235** and assign the relevant peaks (Table 4.30, Table 4.31 & Table 4.32). Key ^{1}H NMR spectroscopic resonances in the case of **234** included the *N*-CH$_3$ group at 2.70 ppm, pyrrolidine ring protons including the diastereotopic H-3' signals from 2.14 – 2.21 ppm and pyridyl ring protons at 6.0 ppm and 8.0 ppm with no amide N-H peak visible as expected. The pyrrolidine N-H signal was present as a broad signal at 6.75 ppm. For **17**, key peaks included the *N*-CH$_3$ signal at 3.15 ppm, pyrrolidine ring protons in particular diastereotopic protons in the range 1.50 – 1.78 ppm and aromatic peaks from 7.1 – 7.4 ppm while as expected, there was no amide N-H peak observed.

Table 4.30: List of HMQC correlations and assignment of ^{1}H & ^{13}C NMR spectroscopic resonances for **234**.
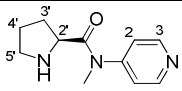
Structure	^{13}C NMR δ (ppm)	^{1}H NMR δ (ppm)	Assignment
	149.8	8.07-8.10 (m, 2H)	C-3 & H-3
	108.1	6.31-6.34 (m, 2H)	C-2 & H-2
	63.1	3.99-4.02 (m, 1H)	C-2' & H-2'
	48.6	3.50-3.56 (m, 1H) & 3.16-3.23 (m, 1H)	C-5' & H-5'
	31.3	2.14-2.21 (m, 2H)	C-3' & H-3'
	26.3	2.68-2.71 (m, 3H)	N-$\underline{CH_3}$
	23.8	1.87-2.03 (m, 2H)	C-4' & H-4'

Table 4.31: ^{1}H NMR spectroscopy peak assignment and COSY interactions of **234**.
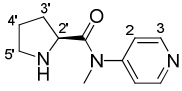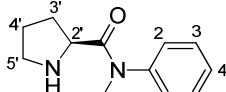
Structure	Proton	δ (ppm)	Correlated with δ (ppm)	Correlated with
	H-3	8.07-8.10	6.31-6.34	H-2
	H-2'	3.99-4.02	2.14-2.21	H-3'
	H-3'	2.14-2.21	1.87-2.03	H-4'
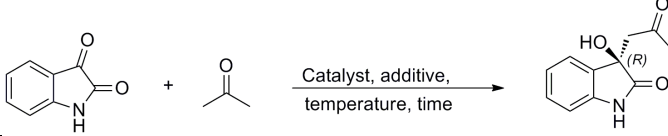
Table 4.32: List of HMQC correlations and assignment of ^{1}H & ^{13}C NMR spectroscopic peaks for **235**.

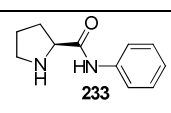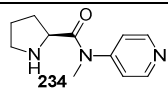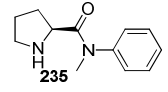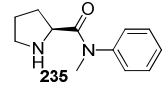| Structure	^{13}C NMR δ (ppm)	^{1}H NMR δ (ppm)	Assignment
	130.1	7.28-7.34 (m, 2H)	C-3 & H-3
	127.7	7.13-7.18 (m, 2H)	C-2 & H-2
	58.4	3.86-3.93 (m, 1H)	C-2' & H-2'
	46.7	2.90-3.29 (m, 2H)	C-5' & H-5'
	38.0	3.15 (s, 3H)	N-$\underline{CH_3}$
	30.4	1.50-1.78 (m, 2H)	C-3' & H-3'
	25.4	1.50-1.78 (m, 2H)	C-4' & H-4'

The *N*-methylated catalysts **234** & **235** were tested in the aldol reaction of acetone with isatin in order to investigate the effects of the removal of the amide N-H group. The *N*-methylated 4-methylaminopyridine derived prolinamide catalyst **234** failed to catalyse the reaction with only a trace quantity of product formed after a long reaction time (entry 1, Table 4.33). In the case of the *N*-methylaniline prolinamide derivative **235**, product was obtained in high yield using both AcOH and also H_2O additives. In this case, significantly lower enantioselectivity compared to **223** was obtained and in favour of the (*R*)-product, the opposite enantiomer to that obtained from **223** & **224** (entries 2 & 3, Table 4.33). The most successful result for **235** was 46% ee after 12 hours while **224**, the non-methylated version of **235** gave a yield of 89% in 65% ee of (*S*)-product after 22 hours. These results show that the amide N-H had a significant effect on the enantioselectivity and the substitution of the N-H group for a *N*-CH$_3$

moiety significantly affected the binding properties of the reaction resulting in preferential formation of the (*R*)-product.

Table 4.33: Aldol reaction of isatin and acetone catalysed by methylated catalysts **234 & 235**.

Entry	Catalyst	Cat loading (mol %)	Additive	Time (h)	Yield[b] (%)	ee[c] (%)
1	**234**	20	AcOH	336	Trace	-
2[d]	**235**	20	AcOH	12	99	46[d]
3[d]		30	H_2O	12	96	37[d]

[a]Unless otherwise noted all reactions were conducted with 0.3 mmol of isatin and 2 mL of acetone at -20°C to yield an excess of (*S*)-product. 20 mol% AcOH or 40 equiv H_2O additives were used. TLC and HPLC were employed to monitor the progression of the reaction. [b]Isolated yield. [c]determined by chiral HPLC. [d](*R*)-product was obtained as major enantiomer.

Therefore, it appears that in the case of *N*-pyridyl prolinamide and *N*-quinolinyl prolinamide catalysts, the pyridine nitrogen atom was important to achieve high enantioselectivity as shown by the lower enantioselectivity of product obtained for catalyst **233**. Also, the amide N-H group played a significant role. Loss of the amide N-H in catalysts **234 & 235** resulted in complete loss of enantioselectivity for **234** and reduction in ee with preferential formation of the opposite enantiomer for **234**. There was also a significant difference in reactivity and enantioselectivity for the 2-aminopyridyl catalysts **221 & 222** compared to its 3-aminopyridyl analogue **223**. Collectively, these results display the importance of the heteroaromatic nitrogen atom, the amide N-H group and in particular the relative position of the amide group and the heteroaromatic nitrogen atom in imparting good enantioselectivity to this ketone-ketone aldol reaction.

4.13 Synthesis of Catalysts with Enhanced N-H Binding Ability

Due to the relatively high ee obtained using the aniline derived catalyst **233** and the demonstration of the importance of the N-H in the binding of both **223** and **233**, compounds **236 & 237** with enhanced N-H acidities compared to **233** were considered as a final probe into

the catalyst design. Catalyst **236** was derived from proline coupled to 3,5-*bis*(trifluoromethyl) aniline and **19** derived from 3,5-*bis*(trifluoromethyl)benzenesulfonamide (**154**).[260,262,285,349] The application of acidic amides and *N*-acyl sulfonamides as successful anion receptors and organocatalysts for the Baylis-Hillman reaction was detailed in Chapter 2 and therefore it was interesting to also monitor the effects of increased N-H acidity on the ee and yield in the isatin/acetone aldol reaction.[336]

Catalyst **236** was synthesised through ethyl chloroformate coupling of Boc-proline with 3,5-*bis*(trifluoromethyl)aniline and Boc-**236** was obtained in 20% yield as a white solid following an acidic and basic work-up and chromatographic purification. LC-MS analysis in positive mode produced a peak at m/z 327 corresponding to the MH$^+$ ion following loss of the Boc-protecting group by fragmentation in the MS. LC-MS in negative mode produced an ion at m/z 425 due to the M-H ion.
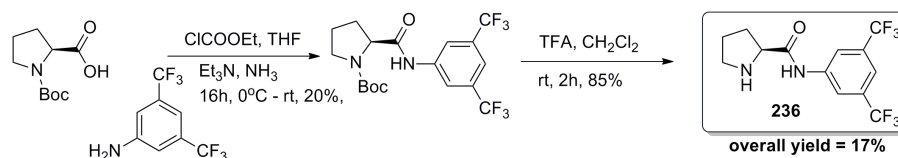
Scheme 4.25: Synthesis of acidic catalyst **236** derived from 3,5-*bis*(trifluoromethyl)aniline.

Subsequent Boc-deprotection using TFA in dichloromethane proceeded with a yield of 85% corresponding to a yield of 17% over 2 steps. LC-MS analysis produced a peak at m/z 327 due to the MH$^+$ ion. ^{1}H & ^{13}C NMR spectroscopic analysis were used to confirm the identity and purity of **236**. Key ^{1}H NMR spectroscopic resonances include the amide N-H signal at 10.10 ppm, aromatic C-H signals at 7.54 & 8.12 ppm, aliphatic diastereotopic pyrrolidine protons H-3' and pyrrolidine N-H signals in the range 1.95 – 2.27 ppm.

Table 4.34: HMQC correlations for catalyst **236**.

Structure	^{13}C NMR δ (ppm)	^{1}H NMR δ (ppm)	Assignment
	119.2	8.10 (s, 2H)	H-2 & C-2
	117.1	7.54 (s, 1H)	H-4 & C-4
	61.0	3.84-3.90 (m, 1H)	H-2' & C-2'
	47.4	2.94-3.13 (m, 2H)	H-5' & C-5'
	30.8	1.95-2.27 (m, 2H)	H-3' & C-3'
	26.4	1.71-1.79 (m, 2H)	H-4' & C-4'

Catalyst **237** incorporated the highly acidic 3,5-*bis*(trifluoromethyl)benzene sulfonamide group with a pyrrolidine ring and the synthetic route towards this catalyst was modified when compared to other prolinamide catalysts. In this case, commercially available 3,5-*bis*(trifluoromethyl)benzene sulfonyl chloride was reacted with aqueous ammonia as described in Chapter 2 to synthesise sulfonamide **154** in 98% yield as a white solid. The synthesis of **237** was subsequently achieved through EDCI coupling of Boc-proline with this sulfonamide **154**. In this reaction, Boc-proline was dissolved in a mixture of 1:1 dichloroethane: *tert*-butanol and an excess of DMAP and EDCI were added. Following this mixing, the previously synthesised sulfonamide compound was added and the reaction mixture was stirred for 16 hours. After addition of Amberlyst 15 anion exchange resin and dilution of the mixture with ethyl acetate, solvent was removed *in vacuo*, the residue was reconstituted in dichloromethane, washed with sodium bicarbonate and dried to give 38% of the white solid product. LC-MS analysis in negative mode produced a peak at m/z 489 corresponding to the (M-H)⁻ ion.
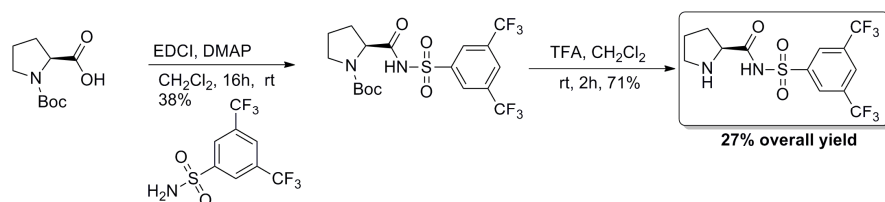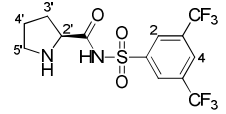
Scheme 4.26: Synthesis of catalyst **237** from Boc-protected *L*-proline.

Boc-deprotection was conducted using TFA in dichloromethane and during the neutralisation step, it was very difficult to achieve a pH where the compound existed in its neutral state and was soluble in dichloromethane. This was ascribed to deprotonation of the acidic sulfonamide N-H group in basic conditions and protonation of the pyrrolidine N-H group under acidic conditions resulting in **237** acting as a Zwitterionic molecule. The catalyst was isolated as a zwitterion in 27% overall yield over 2 steps. LC-MS analysis in negative mode showed a peak at m/z 389 corresponding to the (M-H)⁻ ion and ¹H & ¹³C NMR spectroscopic analysis was used to confirm the product with HMQC experiments confirming peak assignments. Key ¹H NMR spectroscopic resonances included the aliphatic diastereopic H-3' protons from 2.06 – 2.12 ppm and 1.62 – 1.83 ppm and 2 separate aromatic signals integrating for 1 and 2 protons at 8.24 and 8.30 ppm. The pyrrolidine N-H and sulfonamide N-H groups were not visible by

^{1}H NMR spectroscopy. ^{13}C NMR spectroscopy showed the correct number of signals for the free amine including only the amide C=O signal at 173 ppm, confirming that the TFA salt of **237** was not isolated.
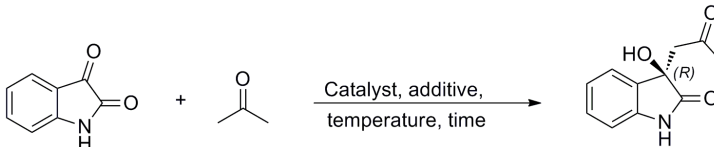
Table 4.35: HMQC correlations for catalyst **237**.
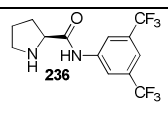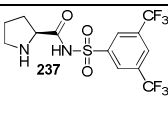
Structure	^{13}C NMR δ (ppm)	^{1}H NMR δ (ppm)	Assignment
	128.2	8.30 (s, 2H)	H-2 & C-2
	124.9	8.24 (s, 1H)	H-4 & C-4
	62.4	3.86 (t, J = 6.9 Hz, 1H)	H-2' & C-2'
	45.8	2.94-3.13 (m, 2H)	H-5' & C-5'
	29.4	2.06-2.12 (m, 1H), 1.62-1.83 (m, 1H)	H-3' & C-3'
	24.2	1.62-1.83 (m, 2H)	H-4' & C-4'

4.13.1 Catalytic Activity of Acidic Catalysts 236 & 237

The catalytic results for these acidic catalysts, in particular **237** whose acidity is expected to be similar or less than proline,[198,350] were quite surprising (Table 4.36). Catalyst **236** furnished the aldol product in high yield and up to 71% ee of the (*S*)-product (entry 2, Table 4.36). This result is very similar to the optimum catalyst **223** under the same conditions however **223** produced a higher yield and slightly enhanced ee of 72% (entry 5, Table 4.27). Catalyst **237** was observed to give the opposite enantiomer (*R*-product) in 92% yield and 68% ee using 20 mol% catalyst loading with 20 mol% AcOH (entry 3, Table 4.36). Interestingly, this catalyst was inactive using H_2O as additive or in the absence of acid additive. In a less acidic environment, the sulfonamide N-H group of **237** may be deprotonated, making it unavailable for H-bonding interactions. Further catalyst optimisation studies were beyond the scope of this work due to time constraints.

Table 4.36: Aldol reaction of isatin and acetone catalysed by **236 &237**.[a]

Entry	Catalyst	Cat loading (mol %)	Additive	Time (h)	Yield[b] (%)	ee[c] (%)
1	**236**	20	AcOH	39	85	69
2		30	H$_2$O	39	71	71
3[e]	**237**	20	AcOH	37	92	68[e]
4[d,e]		20	AcOH	37	87	68[e]
5[e]		20	H$_2$O	37	32	3[e]

[a]Unless otherwise noted all reactions were conducted with 0.3 mmol of isatin and 2 mL of acetone at -20°C to yield an excess of *S*-product. Unless otherwise stated, 20 mol% AcOH or 40 equiv H$_2$O was used. TLC and HPLC were used to monitor the progression of the reaction. [b]Isolated yield. [c]determined by chiral HPLC. [d]40 mol% AcOH used. [e](*R*)-product was obtained as major enantiomer.

4.14 Substrate and Further Mechanistic Studies

The final study undertaken was a substrate scope of the **223** catalysed isatin/acetone aldol reaction to obtain further mechanistic information regarding variation of the substrates and the effects on the reaction outcome. A number of substrates were examined using catalyst **223** and the optimum catalyst conditions as obtained from previously described studies. In terms of isatin derivatives, the use of *N*-benzylisatin and *N*-methylisatin were considered as alternative substrates to the unprotected isatin (Scheme 4.27). These substrates demonstrate possible H-bonding between the isatin N-H and pyridine nitrogen atom of catalyst 223. Substitution of the isatin N-H group with an alkyl group would interfere with this H-bonding and additionally, the steric effects of CH$_3$ compared to the benzyl group on the enantioselectivity of the aldol reaction would be determined.
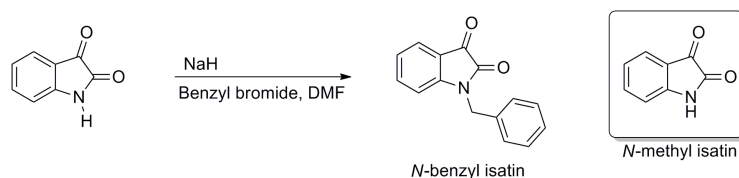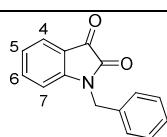
Scheme 4.27: Synthesis of *N*-benzyl isatin and structure of *N*-methyl isatin.

N-methylisatin was commercially sourced while *N*-benzylisatin was synthesised through the reaction of isatin with benzyl bromide using NaH in anhydrous DMF. Benzyl bromide was added to a cooled suspension of isatin and NaH in DMF and the reaction was stirred for 15

minutes. After the addition of water, filtration of the product and washing with hexane, a 92% yield of *N*-benzylisatin was obtained. LC-MS analysis produced ions at m/z 237.9, 259.9 & 275.9 corresponding to MH[+], MNa[+] and MK[+] adducts respectively. NMR spectroscopic analysis using COSY experiments was used to confirm the product and assign signals (Table 4.37). Key ^{1}H NMR spectroscopic peaks included the presence of benzyl CH$_2$ protons at 4.94 ppm and aromatic protons from 7.27 – 7.38 ppm along with the absence of the isatin N-H signal.

Table 4.37: COSY analysis and ^{1}H NMR assignment of *N*-benzyl isatin.

Structure	Protons	δ (ppm)	Correlated with δ (ppm)	Correlated with
	H-4	7.61 (dd, *J* = 6.0 & 1.4 Hz, 1H)	7.05-7.10 (m, 1H)	H-5
	H-6	7.48 (dt, *J* = 6.0 & 1.4 Hz, 1H)	6.74-6.77 (m, 1H)	H-7
	C*H*$_2$-Ph	4.94 (s, 2H)	6.74-6.77 (m, 1H) & 7.27-7.38 (m, 5H)	H-7 & Bz aryl protons

The reaction of *N*-benzylisatin with acetone produced a 61% ee **238** after 44 hours (entry 1, Table 4.38) with the (*S*) enantiomer assigned based on previous literature reports of this compound.[314] This result has implications for the binding to the N-H of isatin which will be discussed below and shows that substitution of the amide N-H in isatin with an *N*-benzyl group resulted in a significant decrease in ee from 72% ee for isatin to 61% for *N*-benzylisatin. The reaction of isatin with *N*-methylisatin proceeded to give 85% conversion after 99 hours but it was not possible to measure the ee of this product due to the failure of the available chiral stationary phases to successfully separate these enantiomers (Chiralpak AD-H, AS-H, IA and Chromtech AGP).

Following chromatographic purification, the presence and purity of the *N*-benzylated aldol product **238** was verified by LC-MS with MH[+] ion detected at m/z 296 and ^{1}H & ^{13}C NMR spectroscopy. Key ^{1}H NMR spectroscopic resonances included the benzyl protons from 7.37-7.41 ppm, 7.29-7.35 & 4.77 – 4.91 ppm, methylene C-H protons at 3.40 & 3.20 ppm and also the CH$_3$ group at 2.0 ppm.
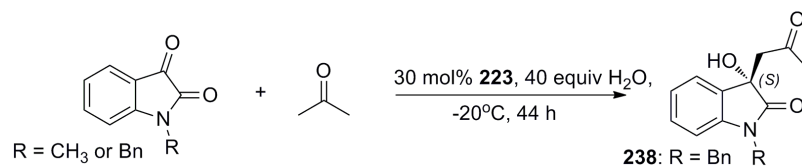
Scheme 4.28: Substrate scope varying isatin derivative for most successful catalyst **223**.

The reaction of isatin with a number of alternative ketones was also considered. Reaction of 2-butanone with isatin was studied to monitor the generality of the catalyst for linear acyclic ketones and with cyclohexanone to monitor the performance with cyclic ketones. The reaction of isatin with 2-butanone gave product **239** in 72% yield, 91% regioselectivity in favour of C-C bond formation at the less substituted methyl group and 52% ee of the major regioisomer (entry 3, Table 4.38) with the enantiomer and regioisomer identified through literature comparisons.[351]

The reaction mixture was purified by flash chromatography and LC-MS analysis showed the presence of an ion at m/z 242 corresponding to the Na adduct of the product. ^{1}H and ^{13}C NMR spectroscopy were used to confirm the product with key ^{1}H NMR spectroscopic resonances detected including CH_2 protons at 3.25 & 2.97 ppm, methylene group alpha to the methyl group from 2.24 – 2.42 ppm and also the methyl group at 0.74 ppm. ^{1}H & ^{13}C NMR spectroscopy were used to determine the major regioisomer and regioisomeric ratio, the major OH signal present at 5.96 ppm and minor at 6.1 ppm with the ratio of integration traces of 9:1 respectively, comparable to a previous synthesis of this compound.[314] Additionally, a second minor set of ^{13}C NMR spectroscopic signals compared to the main signals were identified. The reaction of isatin with cyclohexanone was unsuccessful due to the formation of many products which proved inseparable from the desired and biologically active product (entry 4, Table 4.38).[317]
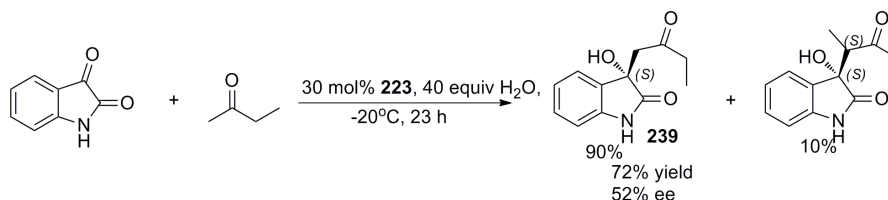
Scheme 4.29: Reaction of isatin with acetone catalysed by **223** under the optimal conditions.

Table 4.38: Substrate scope of catalyst **223** varying each component of the reaction.

Entry	Isatin	Ketone	Time (h)	Yield (%)	ee (%)
1	*N*-benzyl	Acetone	44	62	61
2	*N*-methyl	Acetone	99	85[d]	-[e]
3	Isatin	2-butanone	23	72[f]	52
4	Isatin	cyclohexanone	>100	-[g]	-[g]

[a]Unless otherwise noted, all reactions for substrate scope study were conducted using 30 mol% catalyst loading of **223** with 40 equiv H_2O additive at -20°C to give excess of (*S*)-product. [b]Isolated yield. [c]Determined by chiral HPLC [d] % Conversion. [e]Could not be determined from the available chiral HPLC columns. [f]Regioselectivity of 90:10 in favour of reaction at less substituted methyl group of 2-butanone. [g]Multiple products formed.

The reaction of isatin and *N*-benzylisatin with acetaldehyde was also studied in order to investigate the performance of catalyst **223** for the reaction of isatins with aldehyde substrates (entries 1 & 2 Table 4.39). In this case, the established optimum conditions were not used rather a previously reported method for this reaction.[323] This procedure used 30 mol% of catalyst, 0.3 mmol of isatin or *N*-benzylisatin, 5 equivalents of acetaldehyde and 0.06 mmol of chloroacetic acid at room temperature. After 48 hours reaction time, a small volume of methanol and $NaBH_4$ was added and the reaction was stirred for 1 hour at -20°C. The reaction mixture was quenched with phosphate buffer, extracted into organic solvent, dried and purified by flash chromatography. The latter reduction step was conducted as this was previously conducted in literature reports of these reactions and also to faciliatate ee measurement.

Table 4.39: Substrate scope of catalyst **223** in reactions of isatin and *N*-benzylisatin with acetaldehyde followed by $NaBH_4$ reduction
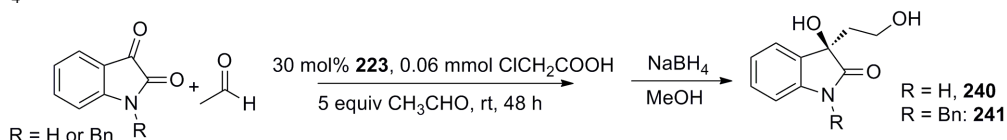
Entry	Isatin	Ketone	Time (h)	Yield (%)	ee (%)
1[a]	Isatin	Acetaldehyde[a]	48	85	39
2[a]	*N*-benzyl	Acetaldehyde[a]	48	28	32

[a]Reaction conducted using 30 mol% **223**, 0.3 mmol isatin/ *N*-benzylisatin, 5 equivalents CH_3CHO, 17 mg chloroacetic acid at r.t. and reduced ($NaBH_4$ reduction) to the alcohol product prior to analysis with excess of (*R*)-product. Absolute configurations were assigned through comparison of optical rotations and chiral chromatography with literature data.

The reaction of isatin with acetaldehyde gave 85% of reduced product in the presence of **223** with 39% ee of the (*R*)-product **240** while the reaction of *N*-benzylisatin under the same

conditions gave a yield of 28% in 32% ee of (*R*)-product **241**. It is interesting to note that the highly successful 4-hydroxydiarylprolinol catalyst was previously unsuccessful at catalysing the reaction of isatin with acetaldehyde.[323] LC-MS produced ions at m/z 216 and 306 corresponding to MNa$^+$ ions of products **240** & **241** respectively. ^{1}H NMR spectroscopic analysis of the **240** identified key peaks including CH$_2$ protons from 1.95 – 2.09 ppm, the methylene group close to the OH moiety at 3.53 – 3.59 ppm and OH signals at 2.98 & 4.30 ppm. For **241**, key ^{1}H NMR spectroscopic resonances included benzyl protons from 7.24 – 7.33 ppm and 4.77 ppm, methylene protons from 2.26 – 2.34 ppm, methylene group close to the OH group from 3.92 – 4.04 and OH signals at 4.43 and 2.99 ppm. In addition, high resolution mass spectroscopy was used to confirm the catalytic products.

4.15 Mechanistic Considerations

Results from earlier mechanistic studies and substrate scope studies suggest a combination of H-bonding and π–π stacking of the aromatic rings of catalysts with isatin may be responsible for the observed catalytic activity and enantioselectivity of **223**. Initially, the acid additive may promote the reaction of the catalyst with acetone to form a reactive enamine intermediate.
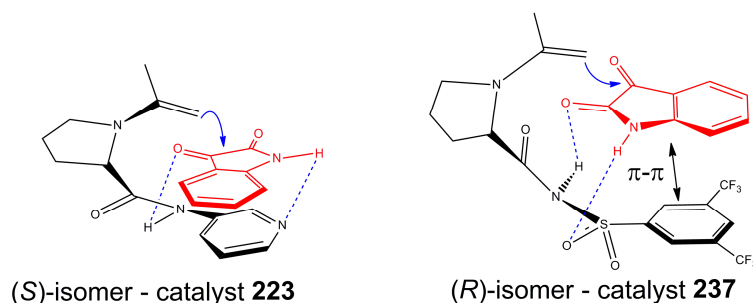
Figure 4.12: Proposed binding cleft of acetone enamine of **223** & **237** binding to isatin showing the origin of differences in configuration.

With catalyst **223**, π-stacking of isatin in the enamine modified catalyst cleft could allow H-bonding of the isatin C=O with the catalyst N-H. This would facilitate enamine attack on the *Re* face of the isatin C=O leading to the (*S*)-product and is illustrated in Figure 4.12. An additional H-bond is possible between isatin and the pyridyl *N*-atom but clearly it is not as important as shown with results using the aniline derived catalyst **233** albeit with lower enantioselectivity and longer reaction time. The relatively high ee found for *N*-benzylisatin

with **223** (entry 1, Table 4.38) also suggests that binding to the amide N-H of isatin may not play a significant role in the mechanism of addition. Similar interactions to **223** are expected to be possible with the structurally related aminoquinoline based catalyst **226**.

The proposed interactions shown in Figure 4.12 are consistent with the results for the pyrrolidine ring-substituted catalysts **229** and **230** where the added chiral centre had only minor effects as the added groups point away from the cleft. Furthermore, the importance, in the proposed model, of H-bonding to the amide group in **223,** is supported by the reduced activity and enantioselectivity of the *N*-methylated catalysts **234** and **235** and the good results found for the activated amide in catalyst **236**.

The sulfonamide catalyst **237** gave high enantioselectivity towards the (*R*)-product. With this catalyst, π-stacking of isatin in the catalyst cleft could allow formation of two H-bonds, one between the C=O on isatin and the sulfonamide N-H and the other between the N-H on isatin and the S=O of the catalyst, facilitating attack on the *Si* face leading to the (*R*)-product (Figure 4.12). In addition, when catalyst **237** was tested in the reaction of *N*-benzylisatin with acetone, the (*R*)-product was formed with a slightly lower ee compared to the reaction catalysed by **223** (78% yield and 55% ee of (*R*)-product after 39 hours). It is interesting to note the low yield and enantioselectivity when water was used as an additive instead of AcOH; this may be due to the sulfonamide group of Zwitterionic **237** in its deprotonated state in water.

With the 'reverse amide catalysts', while the catalytic activity was high, the enantioselectivity was poor and more variable between (*R*) and (*S*)-selectivity. With these catalysts the extra carbon can be expected to impart greater flexibility to the cleft site and the high observed catalytic activity may be related to the reduced steric strain involved during the enamine attack with these more flexible catalysts. Considering catalyst **217**, it is possible to envisage π-stacking of the isatin in the catalyst cleft which facilitates two H-bonds between the isatin and the amide group of the catalyst. Because of the greater flexibility of the reverse amide, similar complexes are possible by conformational change leading to either the (*R*) or (*S*)-product (Figure 4.13). The results for **217** also highlight the likely importance of solvation in all these catalytic processes.

226

(S)-isomer - catalyst **217**   (R)-isomer - catalyst **217**
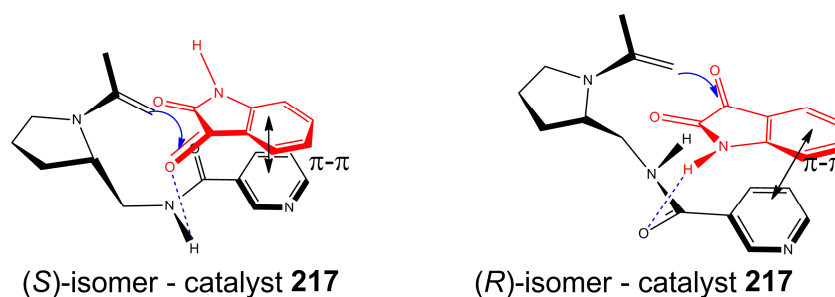
Figure 4.13: Proposed catalyst-substrate complexes for 'reverse amide' catalysts showing extra flexibility and ease of reaction at both faces, giving rise to low enantioselectivities.

4.15.1 Mechanistic Addendum

Following discussions with the external examiner at the *viva-voce*, a number of additional potential mechanistic models based on the Houk-List model were proposed to rationalise the stereochemical results obtained. In the case of the most successful catalyst **223**, the bulky amide group may favour a conformation where it is directed away from the pyridyl ring, resulting in preferential *Re*-attack of the enamine leading to an excess of the (S)-product (Figure 4.14a). H-bonding could occur between the isatin ketone group and the amide N-H, activating the electrophile. In the case of the 2-pyridyl prolinamide catalyst **221**, H-bonding between the amide N-H group of isatin and the pyridyl nitrogen atom may have resulted in preferential *Si*-attack leading to a slight excess of the (R)-product (Figure 4.14b (i)). However, in this case, electrophile activation effects may be in competition with H-bonding effects between the amide carbonyl group and the catalyst amide N-H group, explaining the significantly longer reaction time required using this catalyst.

For the *N*-acyl sulfonamide catalyst **237**, favourable H-bonding interactions between the isatin amide N-H group and the sulfonyl group may have favoured *Si*-attack giving the (R)-product while potential steric repulsion between the catalyst sulfonyl group and the isatin aromatic ring may have disfavoured *Re*-attack of the enamine (Figure 4.14c (ii)). Both of these factors combined would be expected to favour the (R)-product.
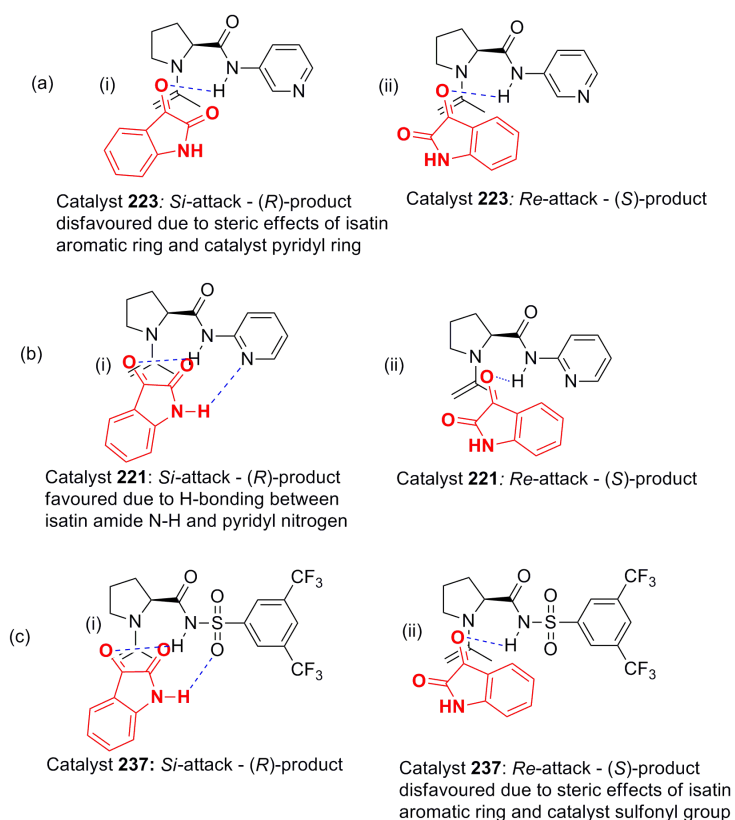
Figure 4.14: Alternative mechanistic proposals to rationalise the stereochemical results of the isatin/acetone aldol reaction.

In conclusion, a range of simple organocatalysts for the synthetically useful reaction of isatin with acetone were designed and tested. The 'reverse amide' *N*-pyridyl pyrrolidinylmethyl amide catalysts produced disappointing enantioselectivities but were highly catalytically active. More success was achieved with the *N*-pyridyl prolinamide and *N*-quinolinyl prolinamide catalysts **221-230** obtaining product up to 72% ee of (*S*)-isomer. Conditions were optimised and in particular an additive screen showed a link between the pK$_a$ of the acid additive used and yield and enantioselectivity. A small substrate screen was carried out. Investigations into the mode of action of the most successful catalyst **223** also provided interesting results and led to the discovery of two other catalysts which may be applied to the reaction; the acidic prolinamides **236** and **237**. Thus one can choose the catalyst to use based on the desired configuration of the product. Structural modifications were made to catalysts and substrate to probe the catalytic action and mechanisms are proposed for catalytic action based on π-stacking and H-bonding of the substrate in the catalyst cleft.

228

5 Chapter 5

Conclusions & Future Work

5.1   Conclusions from Chapters 1 & 2

The work described in this thesis is concerned with the use of molecular recognition phenomena in the of design successful organocatalysts. Chapters 1 & 2 considers the rational design, synthesis and analysis of minimally pre-organised, acylic amide based molecules which can act as receptors for anionic species and also organocatalysts for the Morita-Baylis-Hillman (MBH) reaction. More specifically, 6 relatively acidic amide based molecules were designed for binding anions such as halides and carboxylates. The strength of binding interactions were assessed through calculation of association constants based on ^{1}H NMR titration data, monitoring the amide N-H signals and a number of aromatic C-H signals in close proximity to the receptor binding cleft.

Significantly enhanced K_{ass} values were observed for all receptors compared to a non-acidic control molecule with up to a 70-fold enhancement in binding strength achieved. JOB plot analysis confirmed 1:1 binding stoichiometry in most cases, however where some 2:1 receptor:anion interactions were also observed including the hybrid amide/*N*-acyl sulfonamide **151**, both 1:1 and 2:1 receptor:anion K_{ass} values were calculated. Strong binding combined with proton transfer phenomena were observed for highly acidic thioamide and *N*-acyl sulfonamide derived receptors with basic carboxylate anions which prevented the calculation of K_{ass} values, however the data pointed towards significant association followed by proton transfer and possibly accompanying conformational changes.

X-ray diffraction and NOESY NMR interactions were used to probe the conformational properties of a number of receptors both in the absence and presence of anion. X-ray crystal structure of thioamide **149** showed an unexpected level of pre-organisation within the flexible thioamide motif, which existed in the *syn-syn* conformation optimal for anion binding. In solution, NOE interactions suggested that the conformations of **149** and a number of other isophthalamide based receptors were in equilibrium but preferentially adopted the *syn-syn* configuration upon addition of an anionic guest.

These successful anion receptors were subsequently applied as organocatalysts in the DABCO promoted MBH reaction of benzaldehyde with methyl acrylate with catalytic activity assessed

by product yield and kinetic measurements. These results showed considerable yield and rate constant enhancement using the H-bond donating receptors **146**-**151** compared to the uncatalysed reaction. In particular, the the hybrid amide/*N*-acyl sulfonamide catalyst **151** produced a 2.2-fold increase in product yield along with a 3.9-fold increase in rate constant. ^{1}H NMR spectroscopy catalyst-substrate and product binding studies were used in an attempt to probe the catalytic mechanism and pointed towards substrate binding and activation in the case of a number of catalysts while the acidity of **151** was also suggested to aid in its catalytic activity. This may have been achieved through promotion of the proton transfer step, thus reducing the energy barrier associated with this step. This suggestion is supported by literature mechanistic studies which state that the RDS of the uncatalysed reaction may be the proton transfer step. A substrate scope study showed that **151** produced significant product yield enhancement in all cases, in particular where deactivated aldehydes were employed, for example a 9.2-fold increase in yield for the 4-substituted methoxybenzaldehyde.

Based on the success of the newly designed diamide receptors/catalysts **146**-**151** and the known proclivity of urea and thiourea groups in organocatalysis and anion recognition, these groups were incorporated into the structure of bifunctional receptors producing hybrid urea/amide and thiourea/amide receptors **157** & **158**. Extremely strong binding to halides and carboxylates was observed with dominant binding to the (thio)urea N-H protons with K_{ass} values of the order of 10^4 M^{-1} observed in many cases. Proton transfer events prevented the calculation of K_{ass} values in the case of basic carboxylate anions, however strong binding was also evidenced in these cases. Binding studies of urea/amide hybrid **157** in DMSO-d_6 showed a particular selectivity for AcO$^-$ in this medium producing high K_{ass} values, only slightly reduced compared to binding in less competitive CD$_3$CN. Proton transfer events were also evident in DMSO-d_6 but may have been less significant than those in CD$_3$CN, possibly as a result of solvent competition for the acidic receptor binding site. X-ray crystallography of the thiourea/amide **158** displayed intermolecular interactions between the amide carbonyl and thiourea N-H groups while NMR NOESY interactions of this receptor showed it existed with the amide in the *syn*-conformation with respect to the thiourea group in the presence of anion.

Hybrid molecules **157** & **158** also proved successful organocatalysts in the MBH reaction; catalyst **157** produced a 7.2 fold increase in rate constant but a disappointing yield of 63%, ascribed to possible product inhibition. Catalyst **158** produced a 79% yield and a 5.5-fold increase in reaction rate. Based on the known anion binding proclivity of thiourea N-H groups and its previously observed participation in proton transfer events, a catalytic mechanism was proposed in an attempt to rationalise the significant catalytic ability where binding and proton shuttling effects were proposed to result in the significant catalytic activity.

Overall, this work showed that a cooperative view can be taken between the ability of a receptor to bind anions and to act as an organocatalyst while the anion binding properties of the receptors with increasing hydrogen bond donating capability provided a useful tool to probe the catalytic activity of these receptors.

5.2   Future Work Arising from Chapters 1 & 2

Possible future work arising from the results described in these Chapters would include the substitution of amide or (thio)urea groups with alternative H-bonding motifs. Quite recently, squaramide groups have emerged as molecules which possess comparable halide binding properties and increased acidities compared to equivalent ureas.[41] They can be easily synthesised starting from commercially available diethyl squarate. In addition, the synthesis of bifunctional squaramide molecules can also be conveniently achieved through reaction of 1 equivalent amine with one ester group followed by further reaction with a different amine.
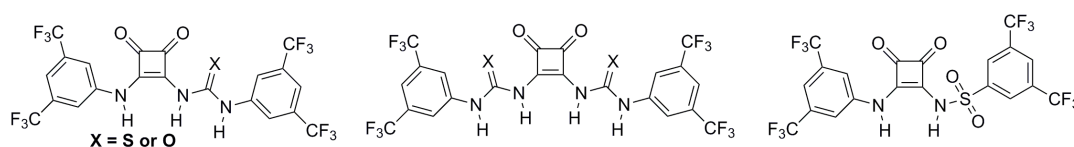
Figure 5.1: Structure of potentially successful squaramide based anion receptors/organocatalysts

Some possibly successful bifunctional squaramide based catalysts could include those shown in Figure 5.1 which include various combinations of receptor motifs. Such molecules may have the ability to cooperatively bind anions and potentially bind multiple anionic reaction transition states, therefore catalysing the MBH reaction.

232

An additional future work section would be the development of chiral organocatalysts based on the successful amide and amide/(thio)urea scaffold (Figure 5.2). A chiral *trans*-2-aminocyclohexanecarboxylic acid could be used as a substitute for the aromatic ring in hybrid (thio)urea/amide catalyst **158** to form a potentially useful chiral variant. Alternatively, the aryl side group of the (thio)urea could be replaced with a cyclohexane ring bearing either a tertiary amine or phosphine group. Chiral squaramide catalysts incorporating (thio)urea or N-acyl sulfonamide groups could also be successful catalysts in the chiral MBH reaction.
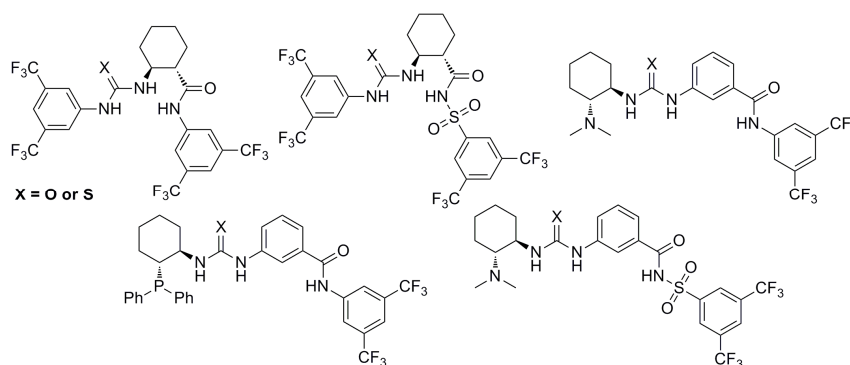
Figure 5.2: Structure of potential chiral catalysts for application in the intermolecular MBH reaction.

5.3   Conclusions from Chapters 3 & 4

Similar to Chapters 1 & 2, the work described in Chapters 3 & 4 also exploited molecular recognition phenomena which are commonly observed in natural processes such as enzyme:substrate interactions to create a series of successful organocatalysts. A number of proline-derived chiral amide catalysts incorporating *N*-pyridyl and *N*-quinolinyl groups were designed in the hope of cooperatively exploiting the H-bond donating and accepting properties of such molecules. It was envisaged that the amide N-H group would bind to and activate electrophilic species while concurrently the H-bond accepting pyridine moiety could form H-bonds to a donor molecule on the substrate. A cooperative effect of both was expected to enhance binding interactions and improve reaction rate and enantioselectivity.

Initially, a number of 'reverse amide' *N*-pyridyl pyrrolidinylmethyl amide catalysts were synthesised in four steps and tested for their catalytic activity in the model aldol reaction of acetone to isatin. Catalyst performance was assessed by isolated yield of product following

chromatographic purification and enantioselectivity was measured by chiral HPLC. The 'reverse amide' catalysts proved highly catalytically active but produced disappointing enantioselectivities. Attempts at optimisation of the most active 'reverse amide' catalyst showed a significant effect of solvent on the outcome of the reaction. When the reaction was conducted in non-polar toluene, the (*S*)-product was obtained while the (*R*)-enantiomer was preferentially formed in polar aprotic DMF with low enantioselectivities in both cases.

The *N*-pyridyl prolinamide and *N*-quinolinyl prolinamide catalysts were synthesised in 2 steps from *N*-Boc-proline. These catalysts proved more successful producting the (*S*)-isomer of product in up to 72% ee under optimised conditions using catalyst **223**. An additive screen showed a relationship between the pK_a of acid additive and yield and enantioselectivity obtained while water was identified to be the optimum additive producing the highest enantioselectivities. A small substrate screen was conducted which led to good yields and moderate enantioselectivities in many cases. Interestingly, the optimum *N*-pyridyl prolinamide was an effective catalyst for the reaction of isatin with acetaldehyde, a reaction which was previously unsuccessful using 4-hydroxydiarylprolinol as a catalyst.[323]

Investigations into the mode of action of the most successful catalyst **223** provided interesting results and led to the discovery of two successful acidic prolinamide catalysts including the proline derived *N*-acyl-sulfonamide catalyst **237** which produced an excess of the (*R*)-enantiomer. Thus one can choose the catalyst to use based on the desired configuration of the product. Structural modifications were made to the catalysts and substrates to study the catalytic action and mechanisms are proposed for the catalytic activity and enantioselectivity based on π-stacking and H-bonding of the substrate in the catalyst cleft.

5.4   Future Work Arising from Chapters 3 & 4

Possible future work based on the results obtained in Chapters 3 & 4 include further optimisation of the proline based *N*-acyl sulfonamide catalyst **237**, perhaps varying the reaction solvent and additives for the reaction of isatin with acetone in an attempt to increase the excess of (*R*)-product. Once optimum conditions for this catalyst have been identified, a

substrate scope study could be undertaken to include catalysis of the reaction of cyclohexanone with isatin, useful due to the anti-convulsant properties of the aldol product from this reaction.[317] In addition, catalyst 237 could be applied to the enantioselective synthesis of Convolutamydine A, B and E through the reactions of 4,6-dibromoisatin with acetone and also with acetaldehyde. It is reasonable to suggest that catalysts **223** & **237** could produce good yields and enantioselectivites of opposite enantiomers of Convolutamydines.

In addition, the successful catalysts **223** & **237** could be applied to alternative aldol reactions such as 4-nitrobenzaldehyde with acetone and cyclohexanone with acetone.
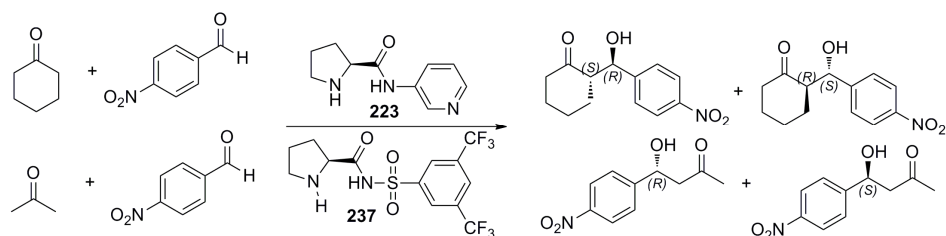
Figure 5.3: Structure of potential chiral catalysts for application in the intermolecular MBH reaction.

6 Chapter 6

Experimental

6.1   General Experimental Conditions

All commercial chemicals were obtained from Sigma and were used as received unless otherwise stated. Nuclear magnetic resonance spectroscopy (NMR) spectra were recorded on either a Joel ECX-400 spectrometer operating at 400 MHz, or a Varian NMR spectrometer operating at 500 MHz, using deuterochloroform as the solvent with tetramethylsilane as an internal reference (δ TMS = 0.0) unless otherwise stated. Coupling constants quoted are considered accurate to ±0.2 Hz. The following abbreviations (and combinations thereof) have been used to describe the signal multiplicity: b-broad, s-singlet, d-doublet, t-triplet, q-quartet, and m-multiplet.

All Infra-red spectra were recorded on a Shimadzu FTIR-8400s, melting points were determined using a Stuart Scientific melting point apparatus smp3, compounds were weighed out on an Explorer OHAUS analytical balance, GC-MS analysis was carried out on a Varian Saturn 2000 GC/MS/MS. Optical rotations were measured on an AA series polar 20 automatic polarimeter. High resolution mass spectrometry was conducted using a Waters Qevo G2 Q-TOF with leucine enkephalin used as an accurate mass reference.

Thin layer chromatography was performed using silica coated plastic plates (60 F_{254}) supplied by Merck. They were visualised using ultra-violet radiation or developed in potassium permanganate solution or iodine. Flash column chromatography was performed using flash silica 60 (230-400 mesh) 9385 supplied by Merck.

Preparative TLC was carried out on glass plates pre-coated with silica 60 Pf_{254} (1.07748) supplied by Merck, activated by heating for several hours at 50 ℃ and cooled prior to use.

The organic layers were routinely dried over anhydrous magnesium sulphate and they were concentrated by rotary evaporation. The last traces of solvent were removed on a high vacuum pump. Solvents were purchased pre-dried. Benzaldehyde was distilled prior to use; methyl acrylate was dried over 4-Å sieves prior to use.

Chiral HPLC was conducted on a HP 1050 HPLC using a chiral column (Daicel Chiralpak AD-H or IA columns).

6.2 Achiral MBH Catalyst Synthesis

N1, N3-*bis*(*n*-butyl)-1,3-dicarboxamide (145)[204]
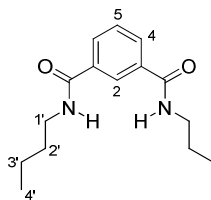
Dry DMF (30 mL) was added to *n*-butylamine (0.72 g, 9.9 mmol) and the resulting solution cooled to 0°C. To this, isophthaloyl dichloride (1.0 g, 4.9 mmol) was added in small portions over 4-5 minutes while ensuring the temperature did not increase significantly. The mixture was allowed to stir for 1 hour at room temperature with reaction monitoring by TLC, then poured into 300 mL of cold water, causing the product to precipitate out of solution as a white solid. The crude product was recrystallised from 50:50 ethanol: water to give the title product as a white solid (1.11 g, 82%), m.p. = 126-127 °C.

> ^{1}H NMR (400 MHz, CDCl$_3$) δ = 8.16 (s, 1H, H-2), 7.89 (dd, J = 7.7 & 1.6 Hz, 2H, H-4), 7.46-7.51 (t, J = 7.7 Hz, 1H, H-5), 6.35 (s, 2H, N-H), 3.46 (m, 4H, H-1'), 1.56-1.64 (m, 4H, H-2'), 1.36-1.46 (m, 4H, H-3'), 0.96 (t, J = 7.3 Hz, 6H, H-4').

> ^{13}C NMR (100 MHz, CD$_3$CN) δ = 166.2 (C=O), 135.1 (C-1), 130.7 (C-4), 128.5 (C-5), 125.5 (C-2), 39.5 (C-1'), 31.5 (C-2'), 20.3 (C-3'), 13.5 (C-4').

> IR (KBr disc) 3286, 3075, 2957, 2930, 1633, 1543, 1297 and 714 cm^{-1}.

> ESI-MS, low res, 277(M.H$^+$) HRMS (ESI); MH$^+$, found 277.1909, C$_{16}$H$_{25}$N$_2$O$_2$ requires 277.1916.

N1,N3-*bis*(4-(trifluoromethyl)phenyl)isophthalamide (146)
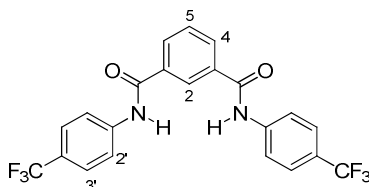
To a solution of 4-trifluoromethylaniline (1.60 g, 9.9 mmol) in DMF (30 mL) were added triethylamine (1.52 g, 15 mmol) and DMAP (1.21 g, 9.9 mmol). The reaction mixture was cooled to 0 °C in an ice bath and isophthaloyl dichloride (1.00 g, 4.9 mmol) was added slowly in small portions over 2-3 minutes with constant stirring. The solution was subsequently stirred at 90 °C for 20 hours. After this time the dark brown coloured

reaction mixture was added to water (300 mL) and extracted with ethyl acetate (3 x 50 mL). The combined organic layers were washed with 5% lithium chloride solution (2 x 80 mL) and deionised water (2 x 100 mL) to remove DMF. The product was dried with $MgSO_4$ and solvent removed *in vacuo*. The crude was purified by column chromatography, eluting with 80:20 hexane:ethyl acetate to give the title compound as a white solid (1.20 g, 54%), m.p. = 256-258 °C.

^{1}H NMR (400 MHz, CD₃CN) δ = 9.17 (s, 2H, N-H), 8.53 (t, *J* = 1.5 Hz, 1H, H-2), 8.15 (dd, *J* = 8.4 & 1.5 Hz, 2H, H-2'), 7.97 (d, *J* = 8.4 Hz, 2H, H-3'), 7.76 (d, *J* = 7.6 Hz, 2H, H-4), 7.69 (t, *J* = 7.6 Hz, 1H, H-5).

^{13}C NMR (100 MHz, CD₃CN) δ = 166.1 (C=O), 143.7 (C-1'), 135.8 (C-1), 132.7 (C-4'), 129.5 (C-4), 128.6 (C-5), 126.5 (C-3'), 126.2 (C-2), 124.2 (CF₃) *J*$_{C-F}$ = 31.63 Hz, 121.8 (C-2').

IR (KBr disc) 3296, 3144, 1651, 1605, 1537, 1321, 1258, 837 and 715 cm^{-1}.

ESI-MS, low res, 453 (M.H)$^{+}$. HRMS (ESI); MH^{+}, found 453.1026, $C_{22}H_{15}N_2O_2F_6$ requires 453.1038.

*N*1,*N*3-*bis*(3,5-*bis*(trifluoromethyl)phenyl)benzene-1,3-dicarboxamide (147)
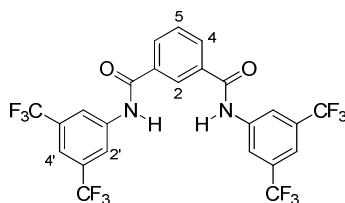
To a solution of 3,5-*bis*(trifluoromethyl)aniline (2.27 g, 9.9 mmol) in DMF (30 mL) was added triethylamine (1.52 g, 15 mmol) and 4-dimethylaminopyridine (DMAP) (1.21g, 9.9 mmol). The reaction mixture cooled to 0 °C in an ice bath and isophthaloyl dichloride (1.00 g, 4.9 mmol) was added slowly in small portions over 2-3 minutes with constant stirring. The yellow solution was stirred at 75 °C for 20 hours. After this time the dark brown coloured reaction mixture was added to water (300 mL) and back extracted with ethyl acetate (3 x 50 mL). The combined organic layers were washed with 5% lithium chloride solution (2 x 80 mL) and deionised water (2 x 100 mL) to remove DMF. The product was dried with $MgSO_4$ and solvent removed *in vacuo*. The crude was purified by column chromatography, eluting with 80/20 hexane/ethyl acetate to give the title product as a white solid (1.502 g, 52%), m.p. = 251-253 °C.

^{1}H NMR (400 MHz, CD$_3$CN) δ = 9.33 (s, 2H, N-H), 8.58 (t, J = 1.5 Hz, 1H, H-2), 8.38 (s, 4H, H-2'), 8.19 (dd, J = 7.6 & 1.5 Hz, 2H, H-4), 7.77 (s, 2H, H-4'), 7.73 (t, J = 7.6 Hz, 1H, H-5).

^{13}C NMR (CD$_3$CN, 125 MHz): δ = 165.2 (C=O), 141.3 (C-1'), 134.5 (C-1), 132.7 (C-3'), 131.7 (C-4), 131.3 (C-5), 129.5 (C-2'), 127.5 (C-2), 125.3 (CF$_3$) J_{C-F} = 35.5 Hz, 120.1 (C-4').

IR (KBr disc) 3250, 3120, 1659, 1568, 1383, 1276, 1137 and 1186 cm^{-1}.

ESI-MS, low res, 589 (M.H$^+$). HRMS (ESI); MH$^+$, found 589.0791, C$_{24}$H$_{13}$N$_2$O$_2$F$_{12}$ requires 589.0785.

*N*1,*N*3-*bis*(3,5-*bis*(trifluoromethylphenyl)benzene-1,3-dicarboxamide (148)

To a solution of 3,5-*bis*(trifluoromethyl)aniline (2.27 g, 9.9 mmol) in DMF (30 mL) was added triethylamine (1.52 g, 15 mmol) and DMAP (1.21g, 9.9 mmol). The mixture was cooled to 0 °C and pyridine-2,6-dicarboxyl chloride (0.99 g, 1 mmol) was added slowly in small portions with constant stirring over 4-5 minutes ensuring that the temperature in the flask did not increase. The reaction was held at 75-80 °C for 18 hours and subsequently poured into water (300 mL). The resulting white solid product was isolated from the solvent by filtration. The crude was purified by trituration using ethyl acetate to give the title product as a white solid (0.96 g, 34%), m.p. = 341-342 °C.

^{1}H NMR (400 MHz, CD$_3$CN) δ = 10.51 (s, 2H, N-H), 8.60 (s, 4H, H-2'), 8.50 (d, J = 8.2 Hz, 2H, H-4), 8.29 (t, J = 8.2 Hz, 1H, H-5), 7.82 (s, 2H, H-4').

^{13}C NMR (100 MHz, CD$_3$CN): δ = 164.4 (C=O), 149.6 (C-2), 141.1 (C-5), 137.2 (C-1'), 133.8 (C-3'), 132.6 (C-4'), 125.7 (C-2'), 123.0 (CF$_3$) J_{C-F} = 35.7 Hz, 121.4 (C-4).

IR (KBr disc) 3284, 3101, 1686, 1550, 1572, 1472, 1437, 1383, 1279, 1175, 1146, 1068, 1001, 936, 889, 840 and 683 cm^{-1}

ESI-MS, low res, 590 (MH$^+$). HRMS (ESI); MH$^+$, found 590.0716, C$_{23}$H$_{12}$N$_3$O$_2$F$_{12}$ requires 590.0738.

N1,N3-bis(3,5-bis(trifluoromethylphenyl)benzene-1,3-dicarbothioamide (149)
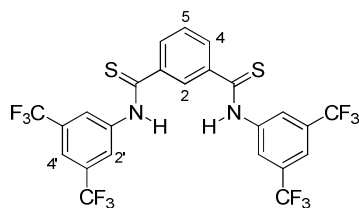
Amide **147** (0.456 g, 0.775 mmol), Lawessons reagent (0.846 g, 2.092 mmol) and 30 mL dry toluene were heated to reflux under nitrogen for 16 hours. The yellow coloured reaction mixture was allowed to cool and loaded directly onto a column of silica gel pre-packed with 50:50 dichloromethane: hexane solvent system. The column was eluted using gradient elution (100% dichloromethane followed by 5% methanol: 95% dichloromethane. Solvent was removed *in vacuo* to give the yellow solid title compound (0.46 g, 96%), m.p. = 78.5-79.4 °C, lit m.p. = 79-81 °C.[352]

^{1}H NMR (600 MHz, CD$_3$CN) δ = 10.77 (s, 2H, N-H), 8.53 (s, 4H, H-2'), 8.36 (s, 1H, H-2), 8.04 (d, *J* = 7.6 Hz, 2H, H-4), 7.91 (s, 2H, H-4'), 7.57 (t, *J* = 7.6 Hz, 1H, H-5).

^{13}C NMR (125 MHz, CD$_3$CN): δ = 200.4 (C=S), 143.5 (C-1), 142.4 (C-1'), 133.2 (C-2'), 132.8 (C-3'), 131.7 (C-2), 127.3 (C-4), 125.8 (C-5), 124.1 (CF$_3$) J_{C-F} = 36.7 Hz, 121.2 (C-4')

IR (KBr disc) 3208, 3058, 1601, 1549, 1466, 1373, 1278, 1189, 1138 and 895 cm^{-1}.

ESI-MS, low res, 621 (MH$^+$). HRMS (ESI); MH$^+$, found 621.0337, C$_{24}$H$_{13}$N$_2$S$_2$F$_{12}$ requires 621.0329.

N1,N3-bis(3,5-bis(trifluormethylphenyl)-5-nitrobenzene-1,3-dicarboxamide (150)
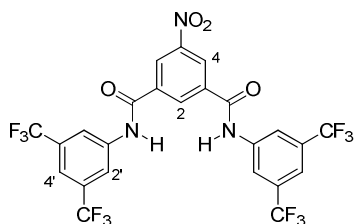
To dry dichloromethane (30 mL) was added 5-nitroisophthalic acid (1g, 4.74 mmol) and the solution was maintained under a nitrogen atmosphere. To this solution was added DMAP (1.16 g, 9.47 mmol), EDCI (1.82 g, 9.47 mmol) and 3,5-*bis* (trifluoromethyl)aniline (2.17 g, 9.47 mmol) and the off-white coloured suspension was stirred at room temperature for 16 hours. The yellow reaction mixture was washed with 1 M HCl, 10% aqueous sodium bicarbonate, saturated NaCl, and the product dried with

MgSO₄. The solvent was removed *in vacuo* and the crude was purified by flash chromatography (85% hexane: 15% ethyl acetate) to give the title compound as a white solid (1.523 g, 51%), m.p. = 310-312 °C.

^{1}H NMR (400 MHz, CD₃CN) δ = 9.53 (s, 2H, N-H), 8.99 (d, *J* = 1.5 Hz, 2H, H-4), 8.94 (t, *J* = 1.5 Hz, 1H, H-2), 8.38 (s, 4H, H-2'), 7.81 (s, 2H, H-4').

^{13}C NMR (125 MHz, CD₃CN): δ = 163.8 (C=O), 148.5 (C-5), 140.7 (C-1'), 136.3 (C-1), 132.5 (C-3'), 131.5 (C-2), 125.5 (C-2'), 124.5 (CF₃) $J_{C\text{-}F}$ = 35.5 Hz, 122.8 (C-4), 120.6 (C-4').

IR (KBr disc) 3245, 3084, 1659, 1549, 1381, 1280, 1179, 1136 and 893 cm^{-1}.

ESI-MS, low res, 634 (MH⁺). HRMS (ESI) M-H⁻, found 632.0497, C₂₄H₁₀N₃O₄F₁₂ requires 632.0480.

Methyl-*N*3-(3,5-*bis*(trifluoromethyl)phenylcarbamoyl)-1-benzoate (152)
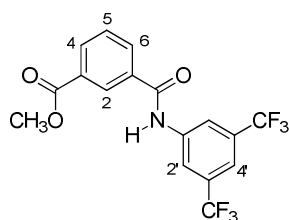
To a solution of mono-methyl isophthalate (1.0 g, 5.55 mmol) in dichloromethane (30 mL) was added DMAP (0.68 g, 5.55 mmol), EDCI (1.06 g, 5.55 mmol) and 3,5-*bis*(trifluoromethyl)aniline (1.27 g, 5.55 mmol) and the white suspension was stirred at room temperature for 16 hours. The reaction mixture was then washed with water and 1 M HCl. The white solid precipitate was collected by filtration and purified by flash chromatography (80% Hexane: 20% ethyl acetate) to give the title product as a white solid (2.0 g, 92%), m.p. = 293-295 °C.

^{1}H NMR (400 MHz, CDCl₃) δ = 8.51 (s, 1H, H-2), 8.32 (s, 1H, N-H), 8.26 (d, *J* = 7.6 Hz, 1 H, H-6), 8.23 (s, 2 H, H-2'), 8.17 (d, *J* = 7.6 Hz, 1H, H-4), 7.68 (s, 1H, H-4'), 7.64 (app t, 1H, H-5), 3.98 (s, 3H, OCH₃)

^{13}C NMR (100 MHz, DMSO-*d₆*): δ = 166.1 (*C*OOCH₃), 165.6 (H-N-*C*=O), 141.4 (C-1'), 134.8 (C-3), 133.1 (C-4), 133.0 (C-6), 130.5 (C-3), 129.7 (C-5), 128.8 (C-2), 125.1 (CF₃) $J_{C\text{-}F}$ = 35.8 Hz, 122.4 (C-1), 120.5 (C-2'), 117.0 (C-4'), 52.9 (O-*C*H₃).

IR (KBr disc) 3416, 3271, 3104, 3003, 2958, 1717, 1661, 1569, 1471, 1443, 1382, 1278, 1258, 1172, 1123, 943, 891, 720 and 686 cm^{-1}.

ESI-MS, low res, 392 (MH$^+$). GC-MS; m/z 392, 372, 360, 163, 135, 103, 76. HRMS (ESI) M-H$^-$, found 390.0562, C$_{17}$H$_{10}$NO$_3$F$_6$ requires 390.0565.

*N*3-(3,5-*bis*(trifluoromethyl)phenylcarbamoyl)-1-benzoic acid (153)
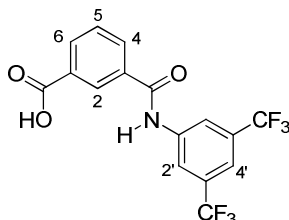
The ester **152** (1.67g, 4.26 mmol) was dissolved in hot methanol (40 mL). To this solution was added 1 M NaOH, (20 ml, 20 mmol) and the mixture heated to reflux for one hour. Distilled water (100 mL) was subsequently added and the mixture was acidified to pH 3 using concentrated HCl. The mixture was cooled and filtered to give the title product as a white solid of sufficient purity for further synthesis (1.24 g, 77%), m.p. = 194-196 °C.

^{1}H NMR (400 MHz, DMSO-d_6) δ = 13.3 (s, br, 1H, OH), 11.02 (s, 1H, N-H), 8.57 (s, 1H, H-2), 8.51 (s, 2H, H-2'), 8.21 (d, *J* = 7.6 Hz, 1H, H-6), 8.15, (d, *J* = 7.6 Hz, 1H, H-4), 7.80 (s, 1H, H-4'), 7.67 (app t, 1H, H-5).

^{13}C NMR (100 MHz, DMSO-d_6) δ = 166.7 (*C*OOH), 165.4 (*C*ONH), 141.5 (C-1'), 134.7 (C-3), 133.3 (C-4), 132.7 (C-6), 131.7 (C-3), 129.5 (C-5), 129.0 (C-2), 125.1 (CF$_3$) *J*$_{C-F}$ = 31.6 Hz, 122.5 (C-1), 120.5 (C-2'), 116.8 (C-4').

IR (KBr disc) 3292, 3092, 2662, 2551, 1690, 1651, 1562, 1470, 1441, 1381, 1305, 1279, 1175, 1146, 943, 893, 728 and 683 cm^{-1}.

ESI-MS, low res, 378 (MH$^+$). HRMS (ESI); MH$^+$, found 376.0423, C$_{16}$H$_8$NO$_3$F$_6$ (M$^-$) requires 376.0484.

3,5-*bis*(trifluoromethylaniline)-benzene-1-sulfonamide (154)
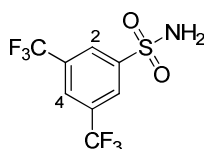
Aqueous ammonia (2 mL) and triethylamine (3.64 mmol, 0.5 mL) were added to DMF (20 mL), the reaction mixture cooled to 0 °C. To this mixture was added 3,5-*bis*(trifluoromethyl)benzene sulfonyl chloride (0.5 g, 1.6 mmol) in small portions over 5-

10 minutes and the reaction mixture was stirred at room temperature for 16 hours followed by addition of distilled water (300 mL). The basic reaction mixture was acidified to pH 2 by addition of concentrated HCl causing the product to precipitate out of solution. The off-white precipitate was collected by filtration (0.46 g, 98%), m.p. = 145.9-146.7 °C, lit m.p. = 146-147 °C.[353]

^{1}H NMR (400 MHz, DMSO-d_6) δ = 8.46 (s, 1H, H-4), 8.40 (s, 2H, H-2), 7.79 (s, 1H, NH$_2$)

^{13}C NMR (100 MHz, DMSO-d_6) δ = 147.1 (C-1), 131.1 (C-3), 127.6 (C-4), 124.6 (CF$_3$) J_{C-F} = 35.5 Hz, 121.9 (C-2).

IR (KBr disc) 3356, 3262, 3097, 3067, 1862, 1833, 1626, 1531, 1197 and 907 cm^{-1}.

ESI-MS, low res, 294 (MH$^+$). GC-MS; m/z 294, 277, 261, 229, 213, 163, 131, 99, 69. HRMS (ESI); M-H$^-$, found 291.9864, C$_8$H$_4$NO$_2$F$_6$S, requires 291.9867.

N1-(3,5-bis(trifluoromethyl)phenyl)-N3-(3,5-bis(trifluoromethyl)phenylsulfonyl)-benzene 1,3-dicarboxamide (151)
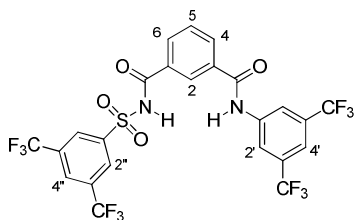
Acid **153** (0.371g, 0.983 mmol) was dissolved in a 50:50 mixture of dichloroethane:t-butanol (20 mL) and to this stirred suspension was added DMAP (0.360 g, 2.949 mmol), EDCI (0.472 g, 2.457 mmol) and sulfonamide **154** (0.200 g, 0.683 mmol). The reaction mixture was stirred for 72 hours at room temperature and after this time Amberlyst 15 anion exchange resin (2 g) was added and the mixture was diluted with ethyl acetate (10 mL). This mixture was stirred for a further 2 hours and subsequently passed through a plug of silica gel and washed with ethyl acetate. The filtrate was collected and solvent removed *in vacuo*. The mixture was purified by flash chromatography (98% dichloromethane: 2% methanol) to give the title product as an off white solid (0.187 g, 43%), m.p. = 241.5-242.3 °C.

^{1}H NMR (400 MHz, DMSO-d_6) δ = 10.92 (s, 1H, Amide N-H), 8.50 (s, 1H, H-2), 8.49 (s, 2H, H-2''), 8.39 (s, 2H, H-2'), 8.21 (s, 1H, H-4''), 8.11 (d, J = 7.6 Hz, 1H, H-4), 7.97 (d, J = 7.6 Hz, 1H, H-6), 7.77 (s, 1H, H-4'), 7.49 (app t, 1H, H-5).

^{13}C NMR (100 MHz, DMSO-d_6) δ = 169.1 (<u>C</u>ONH-SO$_2$), 166.3 (<u>C</u>ONH), 148.2 (C-1''), 141.1 (C-1'), 138.5 (C-3''), 133.6 (C-3'), 132.7 (C-1), 130.1 (C-3), 128.6 (C-6), 127.9 (C-4), 127.6 (C-2'), 124.7 (C-5), 124.4 (C-2''), 123.9 (C-2), 122.7 (CF$_3$''), 121.7 (CF$_3$') J_{C-F} = 35.5 Hz, 116.6 (C-4').

IR (KBr disc) 3450, 3318, 3093, 2927, 1667, 1608, 1553, 1380, 1179 and 888 cm^{-1}.

ESI-MS, low res, 651 (M$^-$). HRMS (ESI); M-H$^-$, found 651.0242, C$_{24}$H$_{11}$N$_2$O$_4$F$_{12}$S requires 651.0248.

*N*1,*N*3-*bis*(3,5-*bis*(trifluoromethyl)phenylsulfonyl)isophthalamide (156)
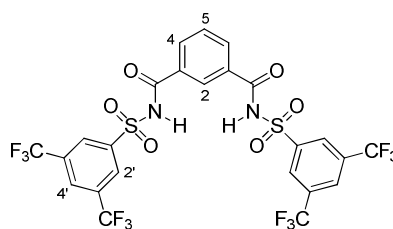
Isophthalic acid (0.113 g, 0.683 mmol) was dissolved in a 50:50 mixture of dichloroethane:*t*-butanol (20 mL) and to this stirred suspension was added DMAP (0.292 g, 2.389 mmol), EDCI (0.529 g, 3.412 mmol) and sulfonamide **154** (0.500 g, 1.706 mmol). The reaction mixture was stirred for 16 hours at room temperature and after this time Amberlyst 15 anion exchange resin (2 g) was added and the mixture was diluted with ethyl acetate (10 mL). This mixture was stirred for a further 2 hours and subsequently passed through a plug of silica gel and washed with 95:5 ethyl acetate:methanol. The filtrate was collected and solvent removed *in vacuo*. The crude product was purified by flash chromatography (85:15 ethyl acetate: petroleum ether) to give the title product as a white solid (0.300 g, 61%), m.p. >350 °C

^{1}H NMR (400 MHz, DMSO-d_6) δ = 8.49 (s, 1H, H-2), 8.38 (s, 4H, H-2'), 8.19 (s, 2H, H-4'), 7.86 (dd, J = 7.8 & 1.8 Hz, 2H, H-4), 7.24 (t, J = 7.8 Hz, 1H, H-5).

^{13}C NMR (DMSO-d_6, 100 MHz) δ = 170.7 (C=O), 149.4 (C-1), 138.3 (C-2), 130.8 (C-3'), 130.1 (C-4), 129.6 (C-4'), 128.3 (C-2'), 127.4 (C-5), 124.2 (CF$_3$) J_{C-F} = 38.3 Hz, 122.3 (C-2).

IR (KBr disc) 3543, 3093, 1603, 1555, 1362, 1280, 1139 and 897 cm^{-1}.

ESI-MS, low res, 715 (M-H); HRMS (ESI); M-H$^-$, found 714.9871, C$_{24}$H$_{11}$N$_2$O$_6$F$_{12}$S$_2$, requires 714.9867.

*N*1-(3,5-*bis*(trifluoromethyl)phenyl)-3-nitrobenzamide (159)
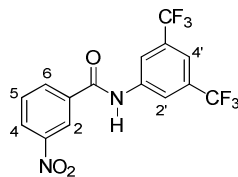
To a solution of 3-nitrobenzoic acid (1.00 g, 5.98 mmol) dissolved in dichloromethane (30 mL) was added DMAP (0.73 g, 5.98 mmol), EDCI (1.15 g, 5.98 mmol) and 3,5-*bis*(trifluoromethyl) aniline (1.37 g, 5.98 mmol). The reaction mixture was stirred for 16 hours at room temperature before being washed with 50 mL 1 M HCl causing the white solid product to crash out of solution. This solid was collected by filtration and recrystallised from dichloromethane to give the white solid title compound (1.92 g, 85%), m.p. = 233.6-234.2 °C.

> ^{1}H NMR (400 MHz, CD$_3$CN) δ = 9.38 (s, 1H, N-H), 8.73-8.75 (m, 1H, H-2), 8.37-8.41 (m, 1H, H-4), 8.31 (s, 2H, H-2'), 8.27-8.31 (m, 1H, H-6), 7.75 (s, 1H, H-4'), 7.74 (m, 1H, H-5)

> ^{13}C NMR (100 MHz, CD$_3$CN) δ = 164.2 (C=O), 148.4 (C-3), 140.3 (C-1'), 135.6 (C-1), 133.9 (C-6), 131.5 (C-3'), 130.3 (C-2'), 126.8 (C-5), 124.8 (CF$_3$) J_{C-F} = 32.6 Hz, 122.5 (C-4), 122.3 (C-2), 120.3 (C-4').

> IR (KBr disc) 3265, 1660, 1524, 1472, 1382, 1280, 1177 and 895 cm^{-1}.

> ESI-MS, low res, 379 (MH$^+$). GC-MS; m/z 378, 359, 329, 263, 228, 188, 150, 134, 120, 104, 76. HRMS (ESI); M-H$^-$, found 377.0376, C$_{15}$H$_7$N$_2$O$_3$F$_6$, requires 377.0361.

3-amino-*N*-(3,5-*bis*(trifluoromethyl)phenyl)benzamide (160)
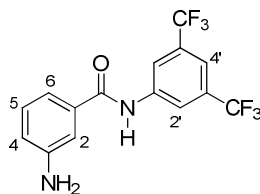
To a stirred suspension of **159** (1.0 g, 2.65 mmol) in ethanol (200 mL) was added 10% Pd/C (0.03 g, 0.03 mmol). Hydrazine monohydrate (1.5 mL) was subsequently added dropwise. The reaction mixture was heated to reflux with stirring for 16 hours. Upon completion (reaction monitored by TLC), the mixture was filtered through a silica plug and solvent removed *in vacuo.* The crude solid was dissolved in ethyl acetate, washed with water (30 mL x 2) and saturated NaCl (20 mL x 2), dried with MgSO$_4$, filtered and solvent

removed *in vacuo*. The product was purified by flash chromatography using a gradient starting with 100% dichloromethane followed by product elution with 95% dichloromethane: 5% methanol to give the title compound as a white solid, (0.63 g, 69%), m.p. = 169.5-170.8 °C.

^{1}H NMR (400 MHz, CD$_3$CN) δ = 9.03 (s, 1H, Amide N-H), 8.34 (s, 2H, H-2'), 7.73 (s, 1H, H-4'), 7.24 (app t, 1H, H-5), 7.19 (s, 1H, H-2), 7.16-7.20 (m, 1H, H-6), 6.84-6.89 (m, 1H, H-4), 4.40 (s, br, 2H, NH$_2$).

^{13}C NMR (100 MHz, DMSO-d_6) δ = 167.3 (C=O), 149.8 (C-3), 141.3 (C-1'), 134.8 (C-1), 129 (C-3'), 124.7 (CF$_3$) J_{C-F} = 33.6 Hz, 122.8 (C-2'), 122.7 (C-5), 119.7 (C-4'), 117.5 (C-4), 116.3 (C-6), 114.8 (C-2).

IR (KBr disc) 3300-3220, 1671, 1595, 1474, 1384, 1280, 1181, 1115 and 888 cm^{-1}.

ESI-MS, low res, 349 (MH$^+$). GC-MS; m/z 348, 329, 309, 279, 236, 163, 120, 92, 65. HRMS (ESI); M-H$^-$, found 347.0628, C$_{15}$H$_9$N$_2$OF$_6$ requires 347.0619.

N-(3,5-*bis*(trifluoromethyl)phenyl)-3-(3,5-*bis*(trifluoromethyl)phenyl)ureido-1-benzamide (157)
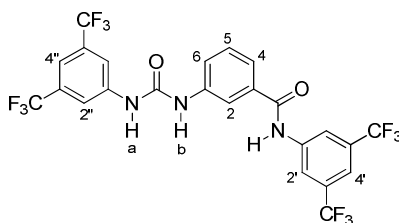
To a solution of **160** (0.40 g, 1.15 mmol) in dichloromethane (30 mL) was added 3,5-*bis*(trifluoromethyl) phenyl isocyanate (0.29 g, 1.15 mmol). The reaction mixture was stirred at room temperature for 24 hours and monitored by TLC. After this time the product was isolated by filtration to give a white solid product (0.68 g, 98%), m.p. = 208.8-209.7 °C.

^{1}H NMR (400 MHz, DMSO-d_6) δ = 10.83 (s, 1H, Amide N-H), 9.48 (s, 1H, NH-a), 9.27 (s, 1H, NH-b), 8.51 (s, 2H, H-2'), 8.15 (s, 2H, H-2''), 8.09 (s, 1H, H-2), 7.78 (s, 1H, H-4''), 7.71 (d, *J* = 7.6 Hz, 1H, H-6), 7.65 (d, *J* = 7.6 Hz, 1H, H-4), 7.62 (s, 1H, H-4'), 7.49 (app t, 1H, H-5).

^{13}C NMR (100 MHz, CD$_3$CN) δ = 166.2 (Amide C=O), 152.4 (urea C=O), 141.2 (C-1), 140.7 (C-1''), 139.3 (C-1'), 134.8 (C-3), 131.6 (C3' & C-3''), 129.2 (C-5),

125.0 (CF$_3$), 123.0 (C-6), 122.2 (CF$_3$) $J_{C\text{-}F}$ = 35.5 Hz, 121.9 (C-4), 120.2 (C-2'), 118.7 (C-2''), 117.4 (C-2 & C-4'') 115.5 (C-4').

IR (KBr disc) 3483-3250, 1707, 1585, 1474, 1381, 1279, 1138 and 89 cm^{-1}.

ESI-MS, low res, 604 (MH$^+$), 621 (M.H$_2$O$^+$), 626 (M.Na$^+$). HRMS (ESI); M-H$^-$, found 602.0734, C$_{24}$H$_{12}$N$_3$O$_2$F$_{12}$, requires 602.0738

N-(3,5-*bis*(trifluoromethyl)phenyl)-3-(3,5-*bis*(trifluoromethyl)phenyl)thioureido-1-benzamide (158)
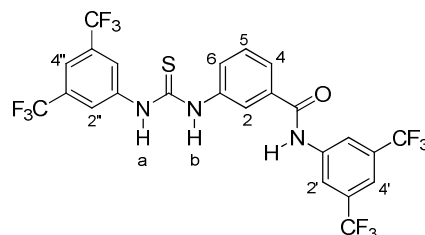
To a solution of **160** (0.30 g, 0.86 mmol) in dichloromethane (30 mL) was added 3,5-*bis*(trifluoromethyl) phenyl isothiocyanate (0.23 g, 0.86 mmol). The reaction mixture was stirred at room temperature for 72 hours and monitored by TLC. After this time the solvent was removed *in vacuo* and the mixture was purified by flash chromatography (80% hexane: 20% ethyl acetate) to give the white solid title product (0.53 g, 96%), m.p. = 168.2-169 °C

^{1}H NMR (400 MHz, CD$_3$CN) δ = 9.19 (s, 1H, Amide N-H), 8.77(s, 1H, NH-b), 8.69 (s, 1H, NH-a), 8.34 (s, 2H, H-2'), 8.14 (s, 2H, H-2''), 8.01 (s, 1H, H-2), 7.83 (d, J = 7.6 Hz, 1H, H-4), 7.79 (s, 1H, H-4''), 7.75 (s, 1H, H-4'), 7.68 (d, J = 7.6 Hz, 1H, H-6), 7.58 (app t, 1H, H-5).

^{13}C NMR (100 MHz, DMSO-d_6) δ = 180.2 (C=S), 166.7 (C=O), 142.5 (C-1), 141.6 (C-1''), 139.2 (C-1'), 131.1 (C-3), 130.8 (C-3'), 130.5 (C-3''), 130.0 (C-5), 129.5 (CF$_3$), 128.7 (C-6), 125.8 (C-4), 124.2 (CF$_3$) $J_{C\text{-}F}$ = 35.5 Hz, 122.2 (C-2'), 119.7 (C-2''), 118.4 (C-2), 117.6 (C-4''), 116.8 (C-4').

IR (KBr disc) 3419, 3252, 1669, 1548, 1472, 1381, 1280, 1170 and 894 cm^{-1}.

ESI-MS, low res, 620 (MH$^+$). HRMS (ESI); M-H$^-$, found 618.0487, C$_{24}$H$_{12}$N$_3$OF$_{12}$S calc 618.0509.

6.3 ^{1}H NMR Binding Studies

6.3.1 ^{1}H-NMR Titration Experiments[200]

A solution of the receptor at a concentration of 1 mM was prepared in an appropriate deuterated solvent. A measured amount (500µL) of this solution was immediately transferred into an NMR tube. A solution of the guest (tetrabutylammonium (TBA) anion) at a concentration of 20 mM was prepared in the same solvent. Aliquot amounts of the guest solution were added to the NMR tube *via* an autopipette. The number of additions varied between 25 and 30 with an increase in the amount of guest solution added until a total of 10 equivalents of the guest was attained. A ^{1}H NMR spectrum was recorded after each addition following an equilibration and mixing time of 2 minutes after each addition. The chemical shift of the protons associated with the recognition process was recorded after each ^{1}H NMR spectrum was run. The collected data was analyzed using WINEQNMR for calculation of association constants.[202]

6.3.2 Binding Stoichiometry – JOB Plot[200]

Solutions of the receptor (5 mM) and of the anion (5 mM) in acetonitrile-d_3 were accurately prepared. Twelve NMR tubes were filled with different proportions of these equimolar solutions present varying from 10:0 receptor: anion to 1:9 receptor:anion. The ^{1}H-NMR spectrum of each solution was subsequently recorded monitoring the amide N-H protons and also other C-H protons. A plot of mole fraction of receptor multiplied by change in chemical shift ($X_R\Delta\delta$) versus mole fraction receptor (X_R) was constructed in order to determine the binding stoichiometry.[200]

6.4 Conformational Studies & X-Ray Crystallography

In some cases, diffraction grade crystals of receptors were grown through slow evaporation. Instances where crystal growth was not successful and/or where compounds were amorphous resulted in conformational analysis being conducted using 2D NOESY and also 1D NOESY spectroscopy.

Crystal Data for Compound Receptor 149:

Crystal Data: $C_{24}H_{12}F_{12}N_2S_2$, M = 620.48, monoclinic, a = 21.592(4) Å, b = 11.3048(19) Å, c = 9.6396(16) Å, β = 90.132(4) $^{\circ}$, V = 2353.0(7) Å^3, T = 100(2) K, space group $C2/c$, Z = 4, 20279 reflections measured, 2397 unique (R_{int} = 0.0443). The final R_1 values were 0.0328 ($I > 2\sigma(I)$) and 0.0359 (all data). The final $wR(F^2)$ values were 0.0761 ($I > 2\sigma(I)$) and 0.0781 (all data).

Crystal Data for Compound Receptor 158:

Crystal Data: $C_{24}H_{13}F_{12}N_3OS$, M = 619.43, monoclinic, a = 18.444(3) Å, b = 19.411(3) Å, c = 14.5722(18) Å, β = 97.489(3) $^{\circ}$, V = 5172.59(7) Å^3, T = 296(2) K, space group $P2_1/c$, Z = 8, 53520 reflections measured, 8972 unique (R_{int} = 0.1499). The final R_1 values were 0.0862 ($I > 2\sigma(I)$) and 0.2020 (all data). The final $wR(F^2)$ values were 0.1603 ($I > 2\sigma(I)$) and 0.2183 (all data).

6.5 Morita-Baylis-Hillman Catalysis Reactions

6.5.1 General Method A for Baylis-Hillman Reaction[145]

To a clean dry 10 mL flask under a nitrogen atmosphere was added DABCO (112.2 mg, 1 mmol), aldehyde (1 mmol), methyl acrylate, *t*-butyl acrylate or cyclohexenone (3 mmol) and organocatalyst **151** (20 mol%, 130.4 mg) and the reaction was allowed to stir at room temperature for the specified time. The solution was extracted with ethyl acetate, washed with brine and dried with MgSO$_4$. Purification was achieved by flash chromatography using 80% hexane: 20% ethyl acetate to elute the product.

Methyl 2-(hydroxy(phenyl)methyl)acrylate 155
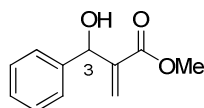
This product was synthesised according to general method **A** using benzaldehyde (106 mg, 1 mmol) and methyl acrylate (258.3 mg, 3 mmol) and was extracted and purified after 20 hours to give the title compound as a yellow oil (146 mg, 76%).

^{1}H NMR (500 MHz, CDCl$_3$) δ = 7.40-7.24 (m, 5H, Ar-H), 6.35 (s, 1H, C=C$\underline{H}_2$), 5.83 (m, 1H, C=C$\underline{H}_2$), 5.57 (d, J = 5.6 Hz, 1H, H-3), 3.72 (s, 3H, OC$\underline{H}_3$), 3.01 (s, 1H, OH).

^{13}C NMR (125 MHz; CDCl$_3$) δ = 166.3 (C=O), 141.5 (C-1), 140.7 ($\underline{C}$=CH$_2$), 127.2 (C-3), 126.8 (C-4), 125.2 (C-2), 125.4 (C=$\underline{C}$H$_2$), 72.6 ($\underline{C}$-OH), 51.8 (O$\underline{C}$H$_3$)

ESI-MS, low res, M$^+$ 192, 191, 175, 160, 132, 105, 77.

Methyl 2-(hydroxy(2-nitrophenyl)methyl)acrylate (155a)

This product was synthesised according to general method A using 2-nitrobenzaldehyde (161 mg, 1 mmol) and methyl acrylate (258.3 mg, 3 mmol) and was extracted and purified after 1 hour to give the title compound as a yellow oil (204 mg, 86%).

^{1}H NMR (400 MHz, CDCl$_3$) δ = 7.87-7.91 (m, 1H, H-6), 7.69-7.72 (m, 1H, H-3), 7.59 (t, J = 6.4 Hz, 1H, H-4), 7.41 (t, J = 6.4 Hz, 1H, H-5), 6.31 (s, 1H, C=C$\underline{H}_2$), 6.16 (s, 1H, C$\underline{H}$-OH), 5.68 (s, 1H, C=C$\underline{H}_2$), 3.67 (s, 3H, OC$\underline{H}_3$).

^{13}C NMR (100 MHz; CDCl$_3$) δ = 166.5 (C=O), 148.3 (C-1), 141.0 ($\underline{C}$=CH$_2$), 136.3 (C-2), 133.5 (C-4), 129.0 (C-3), 128.7 (C-5), 126.5 (C=$\underline{C}$H$_2$), 124.6 (C-6), 67.5 ($\underline{C}$-OH), 52.2 (O$\underline{C}$H$_3$).

ESI-MS, low res, M$^+$ 220, 206, 188, 160, 132, 117, 104, 89, 77, 65.

Methyl 2-(hydroxy(o-tolyl)methyl)acrylate (155b)

This product was synthesised according to general method A using 2-methylbenzaldehyde (120 mg, 1 mmol) and methyl acrylate (258.3 mg, 3 mmol) and was extracted and purified after 42 hours to give the title compound as a yellow oil (45 mg, 22%).

^{1}H NMR (400 MHz, CDCl$_3$) δ = 7.39-7.42 (m, 1H, H-6), 7.19-7.23 (m, 2H, H-3 & H-5), 7.13-7.18 (m, 1H, H-4), 6.30 (s, 1H, C=C$\underline{H}_2$), 5.78 (s, 1H, C$\underline{H}$-OH), 5,59 (s, 1H, C=C$\underline{H}_2$), 3.74 (s, 3H, OC$\underline{H}_3$), 2.87 (s, 1H, OH), 2.30 (s, 3H, Ar-CH$_3$).

^{13}C NMR (100 MHz; CDCl$_3$) δ = 167.1 (C=O), 141.7 (<u>C</u>=CH$_2$), 136.7 (C-2), 135.6 (C-1), 130.4 (C-6), 127.8 (C-5), 126.3 (C-3), 126.2 (C=<u>C</u>H$_2$), 126.2 (C-4), 69.2 (<u>C</u>-OH), 52.0 (O<u>C</u>H$_3$), 19.1 (<u>C</u>H$_3$).

ESI-MS, low res, M$^+$ 206, 189, 175, 159, 145, 129, 119, 91, 77.

Methyl 2-(hydroxy(2-methoxyphenyl)methyl)acrylate (155c)
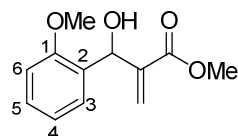
This product was synthesised according to general method A using 2-methoxybenzaldehyde (136 mg, 1 mmol) and methyl acrylate (258.3 mg, 3 mmol) and was extracted and purified after 72 hours to give the title compound as clear oil (122 mg, 55%).

^{1}H NMR (400 MHz, CDCl$_3$) δ = 7.31-7.35 (m, 1H, H-3), 7.21-7.27 (m, 1H, H-5), 6.91-6.96 (m, 1H, H-4), 6.83-6.87 (m, 1H, H-6), 6.29 (s, 1H, C=C<u>H</u>$_2$), 5.87 (m, 1H, C<u>H</u>-OH), 5.72 (m, 1H, C=C<u>H</u>$_2$), 3.80 (s, 3H, Ar-OC<u>H</u>$_3$), 3.72 (s, 3H, OC<u>H</u>$_3$), 3.47 (m, 1H, OH).

^{13}C NMR (100 MHz; CDCl$_3$) δ = 167.2 (C=O), 156.7 (C-1), 141.5 (<u>C</u>=CH$_2$), 129.3 (C-2), 129.0 (C-5), 127.7 (C-3), 125.8 (C=<u>C</u>H$_2$), 120.8 (C-4), 110.7 (C-6), 68.3 (C<u>H</u>-OH), 55.5(Ar-O<u>C</u>H$_3$), 52.0 (O<u>C</u>H$_3$).

ESI-MS, low res, M$^+$ 222, 221, 205, 191, 161, 145, 135, 107, 91, 77.

Methyl 2-((4-fluorophenyl)(hydroxy)methyl)acrylate (155d)
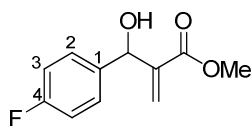
This product was synthesised according to general method A using 4-fluorobenzaldehyde (124 mg, 1 mmol) and methyl acrylate (258.3 mg, 3 mmol) and was extracted and purified after 42 hours to give the title compound as a clear oil (172 mg, 82%).

^{1}H NMR (400 MHz, CDCl$_3$) δ = 7.27-7.33 (m, 2H, H-2), 6.96-7.02 (m, 2H, H-3), 6.30 (s, 1H, C=C<u>H</u>$_2$), 5.82 (s, 1H, C=C<u>H</u>$_2$), 5.50 (m, 1H, C<u>H</u>-OH), 3.70 (s, 3H, OC<u>H</u>$_3$), 3.30 (s, 1H, OH).

^{13}C NMR (100 MHz; CDCl$_3$) δ = 166.7 (C=O), 163.6 (C-4) J_{C-F} = 246.3 Hz, 142.1 (C=CH$_2$), 137.2 (C-1), 128.4 (C-2), 126.1 (C=CH$_2$), 115.4 (C-3), 72.5 (CH-OH), 52.1 (OCH$_3$).

ESI-MS, low res, M$^+$ 210, 193, 177, 150, 133, 123, 97, 77.

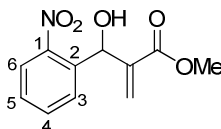## Methyl 2-(hydroxy(*p*-tolyl)methyl)acrylate (155e)
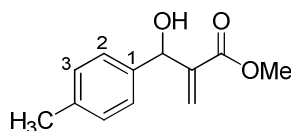
This product was synthesised according to general method A using 4-methylbenzaldehyde (120 mg, 1 mmol) and methyl acrylate (258.3 mg, 3 mmol) and was extracted and purified after 36 hours to give the title compound as a clear oil (78 mg, 38%).

^{1}H NMR (400 MHz, CDCl$_3$) δ = 7.23-7.27 (m, 2H, H-2), 7.13-7.16 (m, 2H, H-3), 6.32 (s, 1H, C=CH_2), 5.85 (s, 1H, C=CH_2), 5.51 (s, 1H, CH-OH), 3.70 (s, 3H, OCH_3), 3.03 (s, br, 1H, OH), 2.33 (s, 3H, Ar-CH_3).

^{13}C NMR (100 MHz; CDCl$_3$) δ = 166.7 (C=O), 142.0 (C=CH$_2$), 138.3 (C-1), 137.5 (C-4), 129.1 (C-3), 126.5 (C-2), 125.8 (C=CH$_2$), 73.0 (CH-OH), 51.9 (OCH$_3$), 21.1 (Ar-CH$_3$).

ESI-MS, low res, M$^+$ 206, 189, 174, 159, 146, 131, 119, 91, 77.

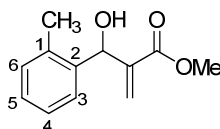## Methyl 2-(hydroxy(4-methoxyphenyl)methyl)acrylate (155f)
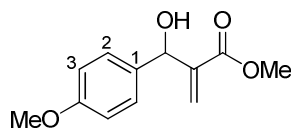
This product was synthesised according to general method A using 4-methoxybenzaldehyde (136 mg, 1 mmol) and methyl acrylate (258.3 mg, 3 mmol) and was extracted and purified after 96 hours to give the title compound as a clear oil (42 mg, 19%).

^{1}H NMR (400 MHz, CDCl$_3$) δ = 7.25-7.30 (m, 2H, H-2), 6.84-6.89 (m, 2H, H-3), 6.31 (s, 1H, C=CH_2), 5.84 (s, 1H, C=CH_2), 5.52 (s, 1H, CH-OH), 3.78 (s, 3H, Ar-OCH_3), 3.71 (s, 3H, OCH_3), 2.92 (s, br, 1H, OH).

^{13}C NMR (100 MHz; CDCl$_3$) δ = 166.9 (C=O), 159.3 (C-4), 142.3 (C=CH$_2$), 133.5 (C-1), 128.0 (C-2), 125.7 (C=CH$_2$), 113.9 (C-3), 72.9 (CH-OH), 55.3 (Ar-OCH$_3$), 52.0 (COOCH$_3$).

253

ESI-MS, low res, M$^+$ 222, 205, 190, 162, 135, 108.

2-(hydroxy(4-methoxyphenyl)methyl)-4,4-dimethylpent-1-en-3-one (155g)
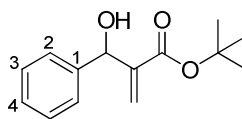
This product was synthesised according to general method A using benzaldehyde (106 mg, 1 mmol) and *tert*-butyl acrylate (384 mg, 3 mmol) and was extracted and purified after 20 hours to give the title compound as an off-yellow coloured oil (66 mg, 28%).

^{1}H NMR (400 MHz, CDCl$_3$) δ = 7.24-7.37 (m, 5H, Ar-H), 6.24 (s, 1H, C=C*H*$_2$), 5.72 (s, 1H, C=C*H*$_2$), 5.47-5.50 (m, 1H, C*H*-OH), 3.15-3.19 (m, 1H, OH), 1.39 (s, 9H, O-*t*Bu).

^{13}C NMR (100 MHz; CDCl$_3$) δ = 165.6 (C=O), 143.4 (C-1), 141.6 (*C*=CH$_2$), 128.3 (C-3), 127.6 (C-4), 126.5 (C-2), 125.2 (C=*C*H$_2$), 81.6 (*C*-(CH$_3$)$_3$), 73.5 (*C*H-OH), 27.9 (C-(*C*H$_3$)$_3$).

ESI-MS, low res, M$^+$ 217, 177, 161, 132, 105, 77, 51.

2-(hydroxy(4-methoxyphenyl)methyl)cyclohex-2-enone (155h)
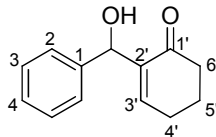
This product was synthesised according to general method A using benzaldehyde (106 mg, 1 mmol) and cyclohexenone (288 mg, 3 mmol) and was extracted and purified after 20 hours to give the title compound as an off-yellow coloured oil (119 mg, 59%).

^{1}H NMR (400 MHz, CDCl$_3$) δ = 7.2-7.35 (m, 5H, Ar-H), 6.74 (t, *J* = 4.1 Hz, 1H, H-3'), 5.53 (s, 1H, C*H*-OH), 3.66 (s, 1H, OH), 2.3-2.41 (m, 4H, H-4' & H-6'), 1.95 (m, 2H, H-5').

^{13}C NMR (100 MHz, CDCl$_3$) δ = 200.4 (C=O), 147.5 (C-3'), 141.9 (C-1), 141.2 (C-2'), 128.4 (C-3), 127.5 (C-4), 126.6 (C-2), 72.2 (*C*H-OH), 38.6 (C-6'), 25.8 (C-4'), 22.6 (C-5').

ESI-MS, low res, M$^+$ 202, 201, 185, 157, 128, 115, 105, 77, 65.

6.6 Kinetics

6.6.1 Kinetics – General Procedure[145]

Into a 10 mL round bottomed flask was placed a magnetic stirring bar, organocatalyst (20 mol%, 0.2 mmol), DABCO (113.7 mg, 1 mmol), (*E*)-stilbene (22.8 mg, 0.126 mmol) and benzaldehyde (106 mg, 1 mmol). The flask was then fitted with a septum and flushed with N_2. Methyl acrylate (0.92 ml, 10.14 mmol) was subsequently added by syringe and the reaction mixture was stirred at room temperature. Upon addition of the methyl acrylate, a sample (50 µL) was taken from the flask, diluted to 500 µL with $CDCl_3$ and analysed by ^{1}H NMR as t_0. Further samples of 50 µL were taken every 2 hours for 8 hours, diluted to 500 µL total volume and the NMR spectrum obtained. The change in integration ratio of benzaldehyde: (*E*)-stilbene peak in the ^{1}H NMR spectrum of the reaction mixture was monitored as a function of time. A rate plot of this pseudo-first order kinetics system was constructed (plot of –Log_e[benzaldehyde] versus time) and the rate constant of the reaction was assessed from the slope of this plot.

6.7 Synthesis of Chiral Catalysts for the Aldol Reaction

N-**Boc-(*S*)-proline**[341]
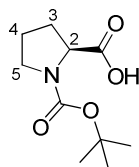
To (*S*)-Proline (3.54 g, 30 mmol) in dichloromethane (20 mL) was added a solution of di-*tert*-butyl-dicarbonate (Boc$_2$O) (7.86 g, 36 mmol) in dichloromethane (30 mL). The mixture was stirred for 72 hours at room temperature, extracted with dichloromethane (2 x 30 mL) and washed with brine. The crude reaction mixture was purified by flash chromatography (50:50 ethyl acetate: hexane) to give the title product as a white solid (3.20 g, 99%), m.p. = 134-136 °C; $[\alpha]_D^{21}$ = -65.2 (c = 0.1, CHCl$_3$). Lit m.p. = 132-134 °C, Lit $[\alpha]_D^{21}$ = +57.0 (c = 1.0, CHCl$_3$).[354]

> ^{1}H NMR (400 MHz, CDCl$_3$) δ = 4.20-4.37 (m, 1H, H-2), 3.30-3.60 (m, 2H, H-5), 2.0-2.40(m, 2H, H-3), 1.83-1.98 (m, 2H, H-4), 1.39-1.51 (m, 9H, Boc-H), OH proton not visible.

ESI-MS, low res, 238 (M.Na$^+$), 216 (MH$^+$), 160, 116. GC-MS; *m/z* 215, 214, 160, 116, 114, 98, 83.

N-Boc-(*S*)-prolinamide (170)[176]
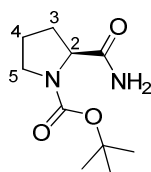
N-Boc-proline (2.15 g, 10 mmol) was dissolved in dry THF (30 mL) and treated with triethylamine (10 mmol, 1.01 g, 1.38 mL). The stirred reaction mixture was cooled to 0 °C and ethyl chloroformate (1.09 g, 10 mmol) was added dropwise over 15 minutes. After the mixture had been stirred for a further 30 minutes aqueous ammonia (11 mL, 12.5 mmol) was added slowly by syringe over 15 minutes. This reaction mixture was stirred for 1 hour at 0 °C, 16 hours at room temperature and heated to reflux for 3 hours. The reaction was diluted with ethyl acetate and solvent removed *in vacuo*. The resulting residue was dissolved in ethyl acetate, washed with saturated aqueous ammonium chloride, dried with MgSO$_4$, filtered and solvent removed *in vacuo*. The crude product was purified by flash chromatography (50:50 ethyl acetate: petroleum ether) to give a white solid product (1.50 g, 70%), m.p. = 105-108 °C; $[\alpha]_D^{19}$ = - 34.2 (c = 0.1, EtOH). Lit m.p. = 104-106 °C, Lit $[\alpha]_D^{26}$ = - 43.4 (c = 1.0, EtOH).[345]

> ^{1}H NMR (400 MHz, CDCl$_3$) δ = 6.84 (s, 1H, N-H), 6.01 (s, 1H, N-H'), 5.35-5.58 (m, 1H, H-2), 4.11-4.38 (m, 2H, H-5), 3.25-3.57 (m, 2H, H-3), 2.04-2.42 (m, 2H, H-4), 1.46 (s, 9H, Boc-H).

> ESI-MS, low res, 237 (M.Na$^+$), 215 (MH$^+$), 195, 181, 159, 137, 115. GC-MS; m/z 214, 199, 159, 141, 115, 70.

N-Boc-(*S*)-prolinamine (219)[340]
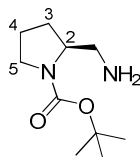
To a solution of prolinamide **170** (1 g, 4.67 mmol) in dry THF (30 mL) at 0 °C under an inert atmosphere in oven dried glassware was added Borane-THF 1 M solution (20 ml, 20 mmol) dropwise. The reaction mixture was held at 0 °C for 1 hour, warmed to room temperature slowly and stirred for 16 hours and heated to reflux for 6 hours. The reaction

mixture was then cooled to 0 °C and quenched by slow addition of methanol (20 mL), taking extreme care with the evolution of H_2 gas. This mixture was evaporated to remove solvent and boric acid salts [340,343]. The colourless oil was used without further purification due to difficulty with retention of the amine product on a silica flash chromatography column. Ratio of title product: unreacted amide = 2.4:1. Approx 60% pure by ^{1}HNMR, (0.81 g, 86% crude), $[\alpha]_D^{19}$ = -28.6 (c = 0.1, CHCl$_3$). Lit $[\alpha]_D^{19}$ = -56.2 (c = 1.1, CHCl$_3$).[355]

^{1}H NMR (400 MHz, CDCl$_3$) δ = 3.78-4.05 (m, br, 1H, H-2), 3.63-3.69 (m, 2H, NH$_2$), 3.35-3.46 (m, 1H, C$\underline{H}_2$-NH$_2$ diastereotopic), 3.03-3.33 (m, 2H, H-5), 2.63-2.74 (m, 1H, C$\underline{H}_2$-NH$_2$ diastereotopic), 1.73-1.99 (m, 4H, H-3 & H-4), 1.46 (s, 9H, Boc-H).

IR (Thin Film) 3467, 2977, 2887, 2076, 1671, 1478, 1456, 1410, 1368, 1253, 1169, 1122, 1050 and 936 cm^{-1}.

ESI-MS, low res, 201 (MH$^+$), 145, 101; GC-MS; m/z 201 (M.H$^+$), 200, 185, 170, 145, 127, 114, 101, 84, 70, 57.

Methyl-3-(6-methylpyridin-2-ylcarbamoyl)benzoate (220)
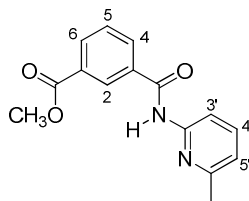
To a stirred solution of mono-methyl isophthalate (750 mg, 4.162 mmol) in dichloromethane (30 mL) was added DMAP (509 mg, 4.162 mmol) and EDCI (800 mg, 4.162 mmol). To this was added 2-amino-6-picoline (450 mg, 4.162 mmol) slowly and the reaction was stirred for 16 hours at room temperature. After this time solvent was removed from the reaction *in vacuo* and the crude yellow oil was purified by flash chromatography (90:10 hexane:ethyl acetate with polarity subsequently increased to 80:20 hexane:ethyl acetate) to give the title product as a white solid (1.09 g, 97%), m.p. = 100.1 – 102.5 °C.

^{1}H NMR (400 MHz, CDCl$_3$) δ = 8.63 (s, 1H, N-H), 8.56 (s, 1H, H-2), 8.22 (d, J = 8.4 Hz, 1H, H-6), 8.18 (d, J = 8.4 Hz, 1H, H-4), 8.16 (d, J = 7.6 Hz, 1H, H-5'), 7.66 (t, J = 8.4 Hz, 1H, H-5), 7.59 (app t, 1H, H-4'), 6.95 (d, J = 7.6 Hz, 1H, H-3'), 3.95 (s, 3H, OCH$_3$), 2.47 (s, 3H, Ar-CH$_3$).

^{13}C NMR (100 MHz, CDCl$_3$) δ = 166.0 (CH$_3$-O-$\underline{C}$=O), 164.7 (HN$\underline{C}$=O) 157.2 (C-2'), 150.5 (C-6'), 138.7 (C-4'), 134.7 (C-3), 133.2 (C-6) 130.7 (C-5), 129.4 (C-2), 127.9 (C-4), 119.7 (C-1), 111.2 (C-5'), 100.4 (C-3'), 52.5 (O$\underline{C}$H$_3$), 24.2 (Ar-$\underline{C}$H$_3$).

IR (KBr disc) 3300-2900 (br), 1691, 1615, 1582, 1456, 1316, 1277, 1164, & 717 cm^{-1}.

ESI-MS, low res, 271 (M.H$^+$), 241, 209, 163, 135, 119, 103, HRMS (ESI); MH$^+$, found 271.1084, C$_{15}$H$_{15}$N$_2$O$_3$ requires 271.1083.

3-(6-methylpyridin-2-ylcarbamoyl)benzoic acid (220a)
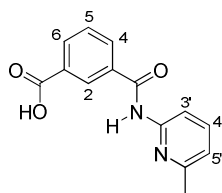
To a solution of **220** (1.09 g, 4 mmol) in hot methanol (40 mL) was added 1 M NaOH (8 ml, 8 mmol) and the mixture was stirred at room temperature for 4 hours. After this time deionised water (100 mL) was added and the reaction mixture was acidified to pH 3.0 using concentrated HCl. The precipitated product was collected by filtration to give the title product as a white solid (1.05 g, 96%), m. p. = 290.5 – 292 °C.

^{1}H NMR (400 MHz, DMSO-d_6) δ = 11.2 (s, 1H, N-H), 8.53 (s, 1H, H-2), 8.26 (d, J = 7.6 Hz, 1H, H-6), 8.11 (d, J = 7.6 Hz, 1H, H-4), 8.04 (d, J = 8.4 Hz, 1H, H-3'), 7.85 (app t, 1H, H-4'), 7.62 (t, J = 7.6 Hz, 1H, H-5), 7.12 (d, J = 8.4 Hz, 1H, H-5'), 2.42 (s, 3H, Ar-CH$_3$).

^{13}C NMR (100 MHz, DMSO-d_6) δ = 166.3 ($\underline{C}$OOH), 165.5 ($\underline{C}$ONH), 155.7 (C-2'), 150.8 (C-6'), 140.6 (C-4'), 134.2 (C-3), 132.7 (C-6), 132.2 (C-4), 131.0 (C-5), 129.1 (C-1), 128.8 (C-2), 119.7 (C-5'), 112.5 (C-3'), 23.8 (Ar-$\underline{C}$H$_3$).

IR (KBr disc) 2947, 1730, 1672, 1575, 1457, 1315, 1296, 1236, 1136, 788 & 726 cm^{-1}.

ESI-MS low res, 257 (M.H$^+$), 239, 221, 130, 110, 92 HRMS (ESI); MH$^+$, found 257.0930, C$_{14}$H$_{13}$N$_2$O$_3$ requires 257.0926.

6.8 General Method B for *N*-Boc deprotection

A solution of Boc-protected catalyst (5 mmol) in dichloromethane (5 mL) was cooled to 0 °C. To this chilled solution was added dropwise trifluoroacetic acid (5 mL) and the reaction mixture stirred at 0 °C for 2 hours. After this time, the solvent and excess TFA were removed in *vacuo*. The residue was redissolved in dichloromethane (10 mL), neutralised with 5% NaOH and the aqueous layer extracted with dichloromethane (5 x 15 mL). The combined extracts were washed with saturated NaCl, dried with MgSO₄, filtered and solvent removed in *vacuo* to give the catalyst with sufficient purity in most cases. Where necessary, the deprotected catalyst was purified by preparative TLC.

(S)-tert-butyl-2-(picolinamidomethyl)pyrrollidine-1-carboxylate (Boc-215)
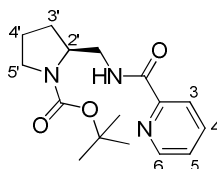
To a suspension of pyridine-2-carboxylic acid (0.616 g, 5 mmol) in dichloromethane (30 mL) was added EDCI (0.959 g, 5 mmol) and DMAP (0.611g, 5 mmol) and this suspension was stirred for 10 minutes. Boc-prolinamine **219** (1g, 5 mmol) was added slowly as a solution in dichloromethane (20 mL) and the reaction mixture was stirred at room temperature for 16 hours. After this time, solvent was removed from the dark brown reaction mixture in *vacuo* and the product was purified by flash chromatography (90:10 hexane: ethyl acetate with polarity subsequently increased to 70:30 hexane: ethyl acetate) eluting the title product as a colourless oil (272 mg, 45%), $[\alpha]_D^{18}$ = -14.0 (c = 0.35, CH₂Cl₂).

> ¹H NMR (400 MHz, CDCl₃) δ = 8.7, 8.25 (s, 1H N-H (rotation present)), 8.55 (d, *J* = 4.6 Hz, 1H, H-6), 8.14-8.30 (m, 1H, H-3), 7.76-7.87 (m, 1H, H-4), 7.45-7.5 (m, 1H, H-5), 4.0-4.1 (m, br, 1H, H-2'), 3.42-3.68 (m, br, 2H, H-5'), 3.31-3.41 (m, br, 2H, CONH-C*H₂*), 1.75-2.05 (m, br, 4H, H-3' & H-4'), 1.45 (s, 9H, Boc-H).

> ¹³C NMR (100 MHz, CDCl₃,) δ = 164.7 (Amide C=O), 155.3 (Boc C=O), 149.7 (C-2), 148.0 (C-6), 137.0 (C-4), 125.9 (C-5), 122.0 (C-3), 79.8 (*C*-(CH₃)₃), 56.4 (C-2'), 46.4 (C-5'), 42.8 (*C*H₂-NH), 28.8 (C-3'), 28.2 (C-(*C*H₃)₃), 23.8 (C-4')

> IR (KBr disc) 3340, 3259, 2976, 1694, 1585, 1507, 1410, 1300, 1160 and 815cm⁻¹

ESI-MS: LC-MS; (ESI) 328 (M.Na$^+$), 306 (MH+), 250, 206, 188, 124, 84. HRMS (ESI); MH$^+$, found 306.1832, C$_{16}$H$_{24}$N$_3$O requires 306.1818.

(*S*)-*N*-(pyrrolidin-2-ylmethyl)picolinamide (215)
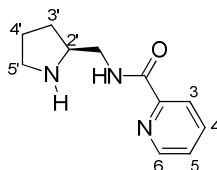
Following general method **B** for *N*-Boc-deprotection, the title compound was obtained as a brown oil (258mg, 43%), $[\alpha]_D^{21} = +27.6$ (c = 0.515, CH$_2$Cl$_2$).

^{1}H NMR (400 MHz, CDCl$_3$) δ = 8.54-8.57 (m, 1H, H-6), 8.44 (s, br, 1H, Amide N-H), 8.18 (d, *J* = 8.4 Hz, 1H, H-3), 7.81-7.87 (m, 1H, H-4), 7.39-7.44 (m, 1H, H-5), 3.59-3.66 (m, 1H, H-2'), 3.31-3.49 (m, br, CONH-CH$_2$), 2.96-3.03 (m, 2H, H-5'), 2.66 (s, br, 1H N-H), 1.45-2.0 (m, br, 4H, H-3' & H-4').

^{13}C NMR (100 MHz, CDCl$_3$) δ = 166.3 (Amide C=O), 149.1 (C-2), 148.5 (C-6), 137.4 (C-4), 126.6 (C-5), 122.4 (C-3), 59.9 (C-2'), 45.2 (C-5'), 41.0 (*C*H$_2$-NH), 27.9 (C-3'), 24.3 (C-4').

IR (KBr disc) 3379, 2963, 1664, 1529, 1269, 997, 750 and 694 cm^{-1}

ESI-MS, low res, 205 (M$^+$). HRMS (ESI); MH$^+$, found 206.1298, C$_{11}$H$_{16}$N$_3$O requires 206.1293

(*S*)-*tert*-butyl-2-((6-methylpicolinamido)methyl)pyrrolidine-1-carboxylate (Boc-216)
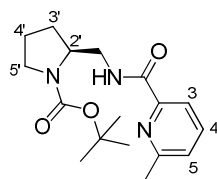
To a suspension of 6-methylpicolinic acid (0.4416 g, 3.22 mmol) in dichloromethane (20 mL) was added EDCI (0.767 g, 4 mmol) and DMAP (0.489 g, 4 mmol) and this suspension was stired for 10 minutes. Boc-prolinamine **219** (1.044 g, 5.19 mmol) was added slowly as a solution in 20 mL dichloromethane and the dark brown coloured reaction mixture was stirred at room temperature for 16 hours. After this time, solvent was removed from the dark brown reaction mixture *in vacuo* and the product was purified by flash chromatography (80:20 petroleum ether: ethyl acetate with polarity subsequently

increased to 70:30 petroleum ether: ethyl acetate) eluting the title product as a colourless oil (0.367 g, 36%), $[\alpha]_D^{19}$ = -9.15 (c = 0.184, EtOAc),

^{1}H NMR (400 MHz, CDCl$_3$) δ = 8.82, 8.18 (s, 1H, N-H rotation present), 7.87-8.03 (m, 1H, H-3), 7.62-7.74 (m, 1H, H-4), 7.18-7.28 (m, 1H, H-5), 3.95-4.13 (m, br, 1H, H-2'), 3.28-3.71 (m, br, 4H, H-5' & CONH-C$\underline{H}_2$), 2.56 (s, 3H, Ar-CH$_3$), 1.74-2.04 (m, br, 4H, H-3' & H-4'), 1.46 (s, 9H, Boc-H).

^{13}C NMR (100 MHz, CDCl$_3$) δ = 178.8 (Amide C=O), 165.6 (C-6), 157.2 (Boc C=O), 149.0 (C-2), 137.4 (C-4), 126.0 (C-5), 119.3 (C-3), 77.4 ($\underline{C}$-(CH$_3$)$_3$), 58.7 (C-2'), 45.4 (C-5'), 41.6 ($\underline{C}$H$_2$-NH), 28.6 (C-3' & C-($\underline{C}$H$_3$)$_3$), 24.9 (C-4'), 24.3 (Ar-$\underline{C}$H$_3$)

IR (KBr disc) 3325, 3250, 2968, 1690, 1670, 1410, 1350, 1160 and 815cm^{-1}

ESI-MS, low res, 320 (M$^+$), 246, HRMS (ESI); MH$^+$, found 320.1977, C$_{17}$H$_{26}$N$_3$O$_3$ requires 320.1974

(*S*)-6-methyl-*N*-(pyrrolidin-2-ylmethyl)picolinamide (216)
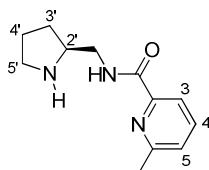
Following general method **B** for *N*-Boc-deprotection, the title compound was obtained as a thick yellow oil; (330mg, 32%), $[\alpha]_D^{19}$ = + 26.63 (c = 0.184, CH$_2$Cl$_2$)

^{1}H NMR (400 MHz, CDCl$_3$) δ = 8.42 (s, br, 1H Amide N-H), 7.95 (d, 1H, *J* = 7.6 Hz, H-3), 7.67 (app t, 1H, H-4), 7.23 (d, 1H, *J* = 7.6 Hz, H-5), 3.52-3.54(m, 1H, H-2'), 3.25-3.42(m, 2H, CONH-C$\underline{H}_2$'), 2.88-2.99 (m, 2H, H-5'), 2.53 (s, 3H, Ar-CH$_3$), 2.47 (s, 1H, N-H), 1.38-1.95 (m, 4H, H-3' & H-4').

^{13}C NMR (100 MHz, CDCl$_3$) δ = 164.8 (Amide C=O), 157.2 (C-6), 149.3 (C-2), 137.4 (C-4), 125.8 (C-5), 119.2 (C-3), 58.1 (C-2'), 46.6 (C-5'), 44.2 ($\underline{C}$H$_2$-NH), 29.4 (C-3'), 25.8 (C-4'), 24.3 (Ar-$\underline{C}$H$_3$).

IR (KBr disc) 3379, 3290, 2959, 1662, 1593, 1406, 994 and 761 cm^{-1}

ESI-MS, low res 220 (MH$^+$). HRMS (ESI); MH$^+$, found 220.1455, C$_{12}$H$_{18}$N$_3$O requires 220.1450

(*S*)-*tert*-butyl-2-(nicotinamidomethyl)pyrrolidine-1-carboxylate (Boc-217)
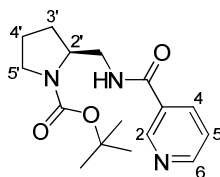
To a suspension of pyridine-3-carboxylic acid (0.616 g, 5 mmol) in dichloromethane (20 mL) was added EDCI (0.958 g, 5 mmol) and DMAP (0.610 g, 5 mmol) and this solution was stired for 10 minutes. Boc-prolinamine **219** (0.647 g, 3.22 mmol) was added slowly as a solution in 20 mL dichloromethane and the reaction mixture was stirred at room temperature for 16 hours. After this time, solvent was removed *in vacuo* and the product was purified by flash chromatography (80:20 hexane: ethyl acetate) to yield the title compound as a thick colourless oil (0.9416 g, 62%) $[\alpha]_D^{22} = +3$ (c = 0.1, CHCl$_3$);

^{1}H NMR (400 MHz, CDCl$_3$) δ = 9.08 (s, 1H, H-2), 8.71-8.81 (m, br, 1H, N-H), 8.65-8.70 (m, 1H, H-6), 8.16 (d, *J* = 7.6 Hz, 1H, H-4), 7.30-7.39 (m, 1H, H-5), 4.12-4.24 (m, 1H, H-2'), 3.29-3.60 (m, 4H, H-5' & CONH-C$\underline{H}_2$), 1.68-2.15 (m, br, 4H, H-3' & H-4'), 1.44 (s, 9H, Boc-H).

^{13}C NMR (100 MHz, CDCl$_3$) δ = 166.1 (Amide C=O), 152.3 (C-6), 149.0 (C-2), 136.4 (C-4), 130.2 (C-1), 125.3 (C-3), 80.2 ($\underline{C}$-(CH$_3$)$_3$), 58.1 (C-2'), 44.0 (C-5'), 42.1 ($\underline{C}$H$_2$-NH), 28.4 (C-3'), 27.5 (C-($\underline{C}$H$_3$)$_3$), 24.7 (C-4').

IR (KBr disc) 3352, 3260, 2870, 1680, 1610, 1507, 1410, 1300, 1160, and 815cm^{-1}

ESI-MS: 328 (MNa$^+$), 306 (MH+). HRMS (ESI); MH$^+$, found 306.1835, C$_{16}$H$_{24}$N$_3$O requires 306.1818.

(*S*)-*N*-(pyrrolidin-2-ylmethyl)nicotinamide (217)
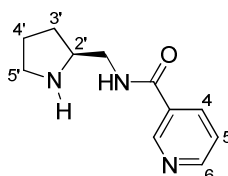
Following general method **B** for *N*-Boc-deprotection, the title compound was obtained as a brown coloured oil (450mg, 53%), $[\alpha]_D^{21} = +22.6$ (c = 0.1, CHCl$_3$).

^{1}H NMR (400 MHz, CDCl$_3$) δ = 8.99 (d, *J* = 1.5 Hz, 1H, H-2), 8.61 (dd, *J* = 3.1 & 1.5 Hz, 1H, H-6), 8.05-8.09 (m, 1H, H-4), 7.89 (s, br, 1H, Amide N-H), 7.27-7.30

(m, 1H, H-5), 4.19 (s, br, 1H, Aliphatic N-*H*), 3.31-3.72 (m, 3H, H-2'&CONH-C*H*₂), 3.03-3.10 (m, 2H, H-5'), 1.50-2.05 (m, 4H, H-3' & H-4')

^{13}C NMR (100 MHz, CDCl₃) δ = 166.1 (Amide C=O), 151.9 (C-6), 148.3 (C-2), 135.3 (C-4), 129.6 (C-1), 123.3 (C-3), 59.0 (C-2'), 45.3 (C-5'), 42.1 (*C*H₂-NH), 28.4 (C-3'), 24.7 (C-4')

IR (KBr disc) 3407, 3066, 2968, 1655, 1545, 1420, 1133 and 708 cm^{-1}

ESI-MS, low res, 206 (MH$^+$), 136, 106, 70 HRMS (ESI); MH$^+$, found 206.1299, C₁₁H₁₆N₃O requires 206.1293

(S)-*tert*-butyl-2-((3-(6-methylpyridin-2-ylcarbamoyl)benzamido)methyl)pyrrolidine-1-carboxylate (Boc-218)
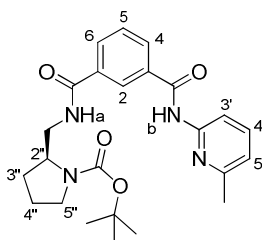
To a suspension of **220a** (1.0 g, 3.9 mmol) in dichloromethane 50 mL was added EDCI (958.5 mg, 5 mmol) and DMAP (611 mg, 5 mmol). This suspension was left to stir for 10 minutes. Boc-prolinamine (1g, 5 mmol) was added slowly as a solution in 20 mL dichloromethane and the reaction mixture was stirred at room temperature for 16 hours. After this time, solvent was removed from the clear solution reaction mixture *in vacuo* and the product was purified by flash chromatography (100% hexane with polarity subsequently increased to 80:20 hexane: ethyl acetate) to give the title product as a colourless oil (1.1 g, 64%), $[\alpha]_D^{19}$ = +5.0 (c = 0.1, CHCl₃).

^{1}H NMR (400 MHz, CDCl₃) δ = 9.24 (s, 1H, Amide N-H$_b$), 8.57 (s, 1H, Amide N-H$_a$), 8.37 (s, 1H, H-2), 8.05 (d, *J* = 8.4 Hz, 1H, H-4), 7.99 (d, *J* = 7.6 Hz, 1H, H-6), 7.95 (d, *J* = 7.6 Hz, 1H, H-3'), 7.51 (app t, 1H, H-5), 7.41 (app t, 1H, H-4'), 6.79 (d, *J* = 7.6 Hz, 1H, H-5'), 4.04-4.22 (m, 1H, H-2''), 3.17-3.57 (m, br, 4H, H-5'' & CONH-C*H*₂), 2.30 (s, 3H, Ar-C*H*₃), 1.59-2.05 (m, br, 4H, H-3'' and H-4''), 1.31 (s, 9H, Boc-H)

^{13}C NMR (100 MHz, CDCl₃) δ = 166.3 (CONHCH₂), 165.6 (CONH-Py), 156.2 (Boc C=O), 150.7 (C-2' & C-6'), 138.6 (C-5), 134.4 (C-3), 130.0 (C-3' & C-6), 128.7 (C-4'), 125.6 (C-2), 119.6 (C-5'), 111.5 (C-4), 80.9 (*C*-(CH₃)₃), 60.5 (C-2''),

47.9 (C-5''), 46.7 (CH$_2$), 29.9 (C-3''), 28.1 (C-($\underline{C}$H$_3$)$_3$), 23.4 (C-4''), 20.5 (Ar-CH$_3$).

IR (KBr disc) 3328, 3067, 2975, 1676, 1608, 1537, 1397, 1165 and 754 cm^{-1}

ESI-MS, low res, 439 (M.H$^+$), 461 (M.Na$^+$), 339 HRMS (ESI); MH$^+$, found 439.2348, C$_{24}$H$_{31}$N$_4$O$_4$, requires 439.2345

(S)-*N*1-(6-methylpyridin-2-yl)-*N*3-(pyrrolidin-2-ylmethyl)isophthalamide (218)
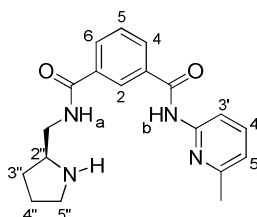
Following general method **B** for *N*-Boc-deprotection, the title compound was obtained as a colourless oil (500mg, 38%) $[\alpha]_D^{14} = +19.0$ (c = 0.1, EtOAc).

^{1}H NMR (400 MHz, CDCl$_3$) δ = 8.89 (s, 1H, N-H$_b$); 8.34 (s, 1H, H-2), 7.93-7.98 (m, 1H, H-4), 7.87-7.93 (m, 2H, H-6 & H-3'), 7.48-7.54 (m, 1H, H-5), 7.29-7.34 (m, 1H, H-4'), 6.78-6.82 (m, 1H, H-5'), 6.08 (s, br, 1H, N-Ha), 3.67-3.76 (m, 1H, H-2''), 3.37-3.68, (m, 2H, CONH-C$\underline{H}_2$), 3.03-3.23 (m, 2H, H-5''), 2.30 (s, 3H, Ar-CH$_3$), 1.85-2.12 (m, 1H, H-3''), 1.35-1.70 (m, 1H, H-3''), 1.70-2.02 (m, 2H, H-4'')

^{13}C NMR (100 MHz, CDCl$_3$) 167.8 (CONHCH$_2$), 165.3 (CONH-Py), 156.9 (C-2'), 150.8 (C-6'), 138.8 (C-5), 134.3 (C-3), 133.8 (C-1), 131.2 (C-3'), 131.0 (C-6), 129.1 (C-4'), 126.0 (C-2), 119.7 (C-5'), 111.6 (C-4), 59.9 (C-2''), 45.2 (C-5''), 41.5 (CH$_2$), 28.1 (C-3''), 24.1 (C-4''), 23.9 (Ar-CH$_3$).

IR (KBr disc) 3400, 3332, 2932, 1675, 1603, 1538, 1398 and 1113 cm^{-1}

ESI-MS, low res 339 (MH$^+$). HRMS (ESI): MH$^+$, found 339.1823, C$_{19}$H$_{23}$N$_4$O$_2$ requires 339.1821.

(S)-*tert*-butyl 2-(pyridin-2-ylcarbamoyl)pyrrolidine-1-carboxylate (Boc-221)
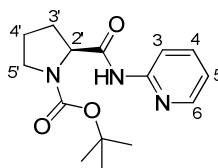
N-Boc-proline (2.153 g, 10 mmol) was dissolved in dry THF (30 mL) and treated with triethylamine (10 mmol, 1.011 g, 1.377 mL). The stirred reaction mixture was cooled to 0

°C and ethyl chloroformate (1.085 g, 10 mmol) was added dropwise over 15 minutes. After the mixture had been stirred for a further 30 minutes, 2-aminopyridine (0.941g, 10 mmol) was added slowly over 15 minutes. This reaction mixture was stirred for 1 hour at 0 °C, 16 hours at room temperature and heated to reflux for 3 hours. The mixture was subsequently diluted with ethyl acetate, filtered and solvent removed *in vacuo.* The resulting crude product was dissolved in ethyl acetate, washed with saturated aqueous ammonium chloride, dried with MgSO₄, filtered and evaporated. Purification was conducted by flash chromatography using (50:50 ethyl acetate: petroleum ether) to give the title compound as a colourless solid (1.42 g, 48%), m.p. = 135.9-136.8 °C; $[\alpha]_D^{19.5}$ = -80.4 (c = 0.1, CH₂Cl₂). Lit $[\alpha]_D$ = -71.0 (c = 0.25, CH₃OH).[356]

^{1}H NMR (400 MHz, CDCl₃) δ = 9.60, 8.87 (s, br, 1H, N-H (rotation present)), 8.22-8.27 (m, 2H, H-6 & H-3), 7.69 (m, 1H, H-4), 6.98 (m, 1H, H-5), 4.23-4.52 (m, 1H, H-2'), 3.31-3.59 (m, 2H, H-5'), 2.01-2.4 (m, br, 2H, H-3'), 1.86-1.99 (m, 2H, H-4'), 1.45 (s, 9H, Boc-H).

^{13}C NMR (100 MHz, CDCl₃) δ = 171.7 (Amide C=O), 155.0 (Boc C=O), 151.8 (C-2), 146.8 (C-6), 138.8 (C-4), 119.8 (C-5), 114.2 (C-3), 80.8 (*C*-(CH₃)₃), 61.5 (C-2'), 47.3 (C-4'), 31.0 (C-2'), 28.3 (C-(*C*H₃)₃), 23.9 (C-3').

IR (KBr disc) 3220, 2980, 1708, 1688, 1582, 1436, 1391, 1154 and 800 cm^{-1}

ESI-MS, low res, 292 (MH$^+$), 236, 192 HRMS (ESI); MH$^+$, found 504.2824, C₁₅H₂₂N₃O₃ requires 504.2822.

(*S*)-*N*-(pyridin-2-yl)pyrrolidine-2-carboxamide (221)
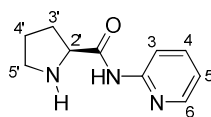
Following general method **B** for *N*-Boc-deprotection, the title compound was obtained as a viscous brown oil (900 mg, 43%) m.p. = 48-51 °C; $[\alpha]_D^{22}$ = -56.2 (c = 0.4, EtOAc). Lit m.p. = 45-50 °C, Lit $[\alpha]_D^{26}$ = -62.5 (c = 0.44, EtOAc).[176]

^{1}H NMR (400 MHz, CDCl₃) δ = 10.20 (s, 1H, Amide N-H), 8.20-8.31 (m, 2H, H-6 & H-3), 7.65-7.72 (m, 1H, H-4), 6.99-7.04 (m, 1H, H-5), 3.86-3.92 (m, 1H, H-2'), 2.98-3.12 (m, 2H, H-5'), 2.39 (s, br, 1H, Aliphatic N-H), 1.98-2.25 (m, 2H, H-3'), 1.71-1.81 (m, 2H, H-4').

^{13}C NMR (100 MHz, CDCl$_3$) δ = 174.0 (Amide C=O), 151.2 (C-2), 148.0 (C-6), 138.3 (C-4), 119.7 (C-5), 113.7 (C-3), 61.0 (C-2'), 47.3 (C-5'), 30.9 (C-3'), 26.1 (C-4').

ESI-MS, low res, 191 (M$^+$).

(*S*)-*tert*-butyl-2-(6-methylpyridin-2-ylcarbamoyl)pyrrolidine-1-carboxylate (Boc-222)
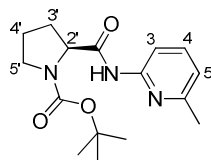
This compound was synthesised as per the procedure given for Boc-**221** using 2-amino-6-picoline (1.081g, 10 mmol) and purified by flash chromatography (50:50 ethyl acetate: petroleum ether) to give the title compound as a yellow solid (2.23 g, 73%), m.p. = 145.8-146.5 °C; [α]$_D^{20}$ = -89.4 (c = 0.1, CH$_2$Cl$_2$).

^{1}H NMR (400 MHz, CDCl$_3$) δ = 8.89, 8.29 (s, br, 1H, N-H (Rotation visible)), 7.95-8.01 (m, 1H, H-4), 7.49-7.60 (m, 1H, H-3), 6.80-6.91 (m, 1H, H-5), 4.20-4.48 (m, 1H, H-2'), 3.31-3.59 (m, br, 2H, H-5'), 2.41 (s, 3H, Ar-C*H*$_3$), 1.95-2.35 (m, 2H, H-3'), 1.83-1.96 (m, br, 2H, H-4'), 1.45 (s, 9H, Boc-H).

^{13}C NMR (100 MHz, CDCl$_3$) δ = 171.0 (Amide C=O), 157.0 (Boc C=O), 154.6 (C-6), 150.5 (C-2), 138.6 (C-4), 119.4 (C-5), 110.5 (C-3), 81.0 (*C*-(CH$_3$)$_3$), 62.2 (C-2'), 47.2 (C-5'), 31.1 (C-3'), 28.4 (C-(*C*H$_3$)$_3$), 24.1 (C-4').

IR (KBr disc) 3228, 2971, 2876, 1714, 1657, 1450, 1301, 1154 and 799 cm^{-1}

ESI-MS, low res, 306 (MH$^+$), 250, 206, 188 HRMS (ESI); MH$^+$, found 306.1819, C$_{16}$H$_{24}$N$_3$O$_3$ requires 306.1818.

(*S*)-*N*-(6-methylpyridin-2-yl)pyrrolidine-2-carboxamide (222)
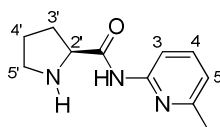
Following general method **B** for *N*-Boc-deprotection, the title compound was obtained as an off-white coloured solid (1.50g, 66%), m.p. = 59-62 °C; [α]$_D^{22}$ = -40.2 (c = 0.4, EtOAc). Lit m.p. = 60-63°C, Lit [α]$_D^{26}$ = -39.2 (c = 0.45, EtOAc).[176]

^{1}H NMR (400 MHz, CDCl$_3$) δ = 10.1 (s, br, 1H, N-H), 8.04 (d, J = 8.2 Hz, 1H, H-3), 7.56 (t, J = 8.2 Hz, 1H, H-4), 6.86-6.89 (m , 1H, H-5), 3.83-3.88 (m, 1H, H-2'), 2.99-3.10 (m, 2H, H-5'), 2.46 (s, 3H, Ar-CH$_3$), 1.97-2.26 (m, 2H, H-3'), 1.8 (s, br, 1H, Aliphatic N-H) 1.67-1.81 (m, 2H, H-4').

^{13}C NMR (100 MHz, CDCl$_3$) δ = 174.4 (Amide C=O), 156.9 (C-6), 150.5 (C-2), 138.5 (C-4), 119.1 (C-5), 110.4 (C-3), 61.0 (C-2'), 47.3 (C-5'), 30.9 (C-3'), 26.2 (C-4'), 24.2 (Ar-CH$_3$).

ESI-MS, low res, 205(M$^+$)

(*S*)-*tert*-butyl 2-(pyridin-3-ylcarbamoyl)pyrrolidine-1-carboxylate (Boc-223)
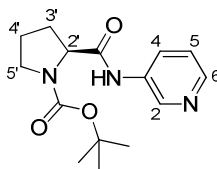
This compound was synthesised as per the procedure given for Boc-**221** using 2-amino-6-picoline (0.941 g, 10 mmol) and purified by flash chromatography in 70:30 ethyl acetate: petroleum ether to yield the title compound as an off-white solid (1.53 g, 46%), m.p. = 163.8-164.5 °C; [α]$_D^{19}$ = -90.6 (c = 0.1, CHCl$_3$).

^{1}H NMR (400 MHz, CDCl$_3$) δ = 9.80 (s, br, 1H, N-H), 8.57-8.59 (m, 1H, H-2), 8.27-8.33 (m, 1H, H-4), 8.04-8.12 (m, 1H, H-6). 7.18-7.27 (m, 1H, H-5), 4.46-4.55 (m, 1H, H-2'), 3.33-3.51 (m, 2H, H-5'), 2.47-2.58 (m, 1H, H-3'), 1.84-2.03 (m, 3H, H-3' & H-4'), 1.50 (s, 9H, Boc-H).

^{13}C NMR (100 MHz, CDCl$_3$) δ = 170.5 (Amide C=O), 156.8 (Boc C=O), 144.9 (C-4), 141.2 (C-6), 135.3 (C-2), 126.6 (C-5), 123.6 (C-3), 81.3 (C-(CH$_3$)$_3$), 60.4 (C-2'), 47.3 (C-5'), 28.4 (C-(CH$_3$)$_3$), 27.0 (C-3'), 24.6 (C-4').

IR (KBr disc) 3267, 3186, 3123, 2877, 1703, 1664, 1604, 1547, 1159 and 808 cm^{-1}

ESI-MS, low res, 292(MH$^+$) HRMS (ESI); MH$^+$, found 292.1661, C$_{15}$H$_{22}$N$_3$O$_3$ requires 292.1661

(*S*)-*N*-(pyridin-3-yl)pyrrolidine-2-carboxamide (223)
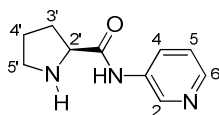
Following general method **B** for *N*-Boc-deprotection, the title compound was obtained as a colourless sticky oil (1.15g, 40%), $[\alpha]_D^{18}$ = -65.8 (c = 0.1, CHCl$_3$). Lit $[\alpha]_D^{25}$ = -54.1 (c = 1.0, CHCl$_3$).[357]

> ^{1}H NMR (400 MHz, CDCl$_3$) δ = 9.87 (s, br, 1H, Amide N-H), 8.59 (d, *J* = 2.8 Hz, 1H, H-2), 8.28- 8.32 (m, 1H, H-4), 8.21-8.25 (m, 1H, H-6), 7.20-7.26 (m, 1H, H-5), 3.83-3.89 (m, 1H, H-2'), 2.92-3.12 (m, 2H, H-5'), 2.25 (s, br, 1H, aliphatic N-H), 1.97-2.25 (m, 2H, H-3'), 1.70-1.81 (m, 2H, H-4')

> ^{13}C NMR (100 MHz, CDCl$_3$) δ = 174.3 (Amide C=O), 145.1 (C-4), 141.0 (C-6), 134.7 (C-2), 126.4 (C-5), 123.7 (C-3), 61.1 (C-2'), 47.5 (C-5'), 30.8 (C-3'), 26.4 (C-4').

> ESI-MS, low res, 192 (MH$^+$)

(*S*)-*tert*-butyl 2-(pyridin-4-ylcarbamoyl)pyrrolidine-1-carboxylate (Boc-224)
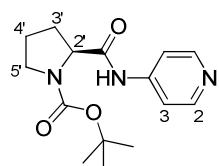
This compound was synthesised as per the procedure given for Boc-**221** using 4-aminopyridine (0.941g, 10 mmol) and purified by flash chromatography in 80:20 hexane: ethyl acetate to yield the title compound as an off- white solid (0.751 g, 35%), m. p. = 204.5-205.4 °C; $[\alpha]_D^{18}$ = -93.4 (c = 0.1, CHCl$_3$).

> ^{1}H NMR (400 MHz, CDCl$_3$) δ = 9.95 (s, br, 1H, Amide N-H), 8.41-8.49 (m, 2H, H-2), 7.41-7.46 (m, 2H, H-3), 4.40-4.51 (s, 1H, H-2'), 3.30-3.51 (m, 2H, H-5'), 2.50-2.59 (m, 1H, H-3'), 1.85-2.03 (m, 3H, H-3' & H-4'), 1.50 (s, 9H, Boc-H).

> ^{13}C NMR (100 MHz, CDCl$_3$) δ = 171.2 (Amide C=O), 156.6 (Boc C=O), 150.6 (C-2), 145.4 (C-4), 113.7 (C-3), 81.3 (<u>C</u>-(CH$_3$)$_3$), 60.7 (C-2'), 47.4 (C-5'), 28.5 ((C-(<u>C</u>H$_3$)$_3$), 27.7 (C-3'), 24.7 (C-4')

> IR (KBr disc) 3246, 3162, 2972, 2878, 1713, 1597, 1635, 1391, 1183 and 835; cm^{-1}

ESI-MS, low res, 292 (M.H$^+$), 218, 190, 114, 70; HRMS (ESI); MH$^+$, found 292.1671, $C_{15}H_{22}N_3O_3$ requires 292.1661

(*S*)-*N*-(pyridin-4-yl)pyrrolidine-2-carboxamide (224)
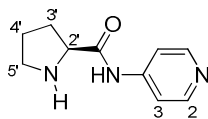
Following general method **B** for *N*-Boc-deprotection, the title compound was obtained as a white solid (500mg, 31%), m. p. = 171-173 °C; $[\alpha]_D^{18}$ = -84.2 (c = 0.2, CHCl$_3$). Lit m.p. = 172-174 °C, Lit $[\alpha]_D^{25}$ = -70.1 (c = 0.55, CH$_3$OH).[357]

^{1}H NMR (400 MHz, CDCl$_3$) δ = 9.93 (s, br, 1H, Amide N-H), 8.43-8.51 (m, 2H, H-2), 7.49-7.55 (m, 2H, H-3), 3.83-3.89 (m, 1H, H-2'), 2.92–3.13 (m, 2H, H-5'), 1.98–2.28 (m, 2H, H-3'), 1.77 (s, br, 1H, Aliphatic N-H), 1.68-1.88 (m, 2H, H-4').

^{13}C NMR (100 MHz, CDCl$_3$) δ = 174.6 (Amide C=O), 150.8 (C-4), 144.6 (C-2), 113.4 (C-3), 61.2 (C-2'), 47.5 (C-5'), 30.8 (C-3'), 26.4 (C-4').

ESI-MS, low res, 191(M$^+$)

(*S*)-*tert*-butyl 2-(quinolin-2-ylcarbamoyl)pyrrolidine-1-carboxylate (Boc-225)
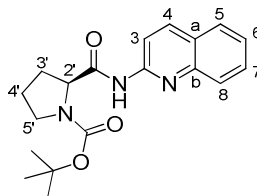
This compound was synthesised as per the procedure given for Boc-**221** using 2-aminoquiniline (1.1015 g, 7.64 mmol) and purified by flash chromatography in 80: 20 petroleum ether: ethyl acetate to yield the title compound as an off-white solid (1.9 g, 56%), m. p. = 192.2-193.5 °C; $[\alpha]_D^{14}$ = -81.8 (c = 0.1, CHCl$_3$).

^{1}H NMR (400 MHz, CDCl$_3$) δ = 9.42, 8.82 (s, 1H, Amide N-H (rotation present), 8.38-8.48 (m, 1H, H-3), 8.12-8.21 (m, 1H, H-4), 7.82-7.86 (m, 1H, H-5), 7.73-7.83 (m, 1H, H-8), 7.62-7.68 (m, 1H, H-7), 7.40-7.48 (m, 1H, H-6), 4.25-4.55 (m, 1H, H-2'), 3.35-3.68 (m, 2H, H-5'), 1.88-2.48 (m, 4H, H-3' & H-4'), 1.47 (s, 9H, Boc-H).

^{13}C NMR (100 MHz, CDCl$_3$) δ = 171.9 (Amide C=O), 155.0 (Boc C=O), 150.6 (C-2), 146.5 (C-b), 138.6 (C-4), 129.9 (C-7), 127.4 (C-5), 127.3 (C-8), 126.3 (C-a),

125.1 (C-6), 114.0 (C-3), 80.9 ($\underline{C}$-(CH$_3$)$_3$), 61.3 (C-2'), 47.2 (C-5'), 31.0 (C-3'), 28.3 (C-($\underline{C}$H$_3$)$_3$), 24.0 (C-4').

IR (KBr disc) 3220, 2976, 2876, 1716, 1657, 1597, 1425, 1318, 1178 and 838 cm^{-1}

ESI-MS, low res, 342 (M.H$^+$) HRMS (ESI); MH$^+$, found 342.1819, C$_{19}$H$_{24}$N$_3$O$_3$ requires 342.1818

(S)-N-(quinolin-2-yl)pyrrolidine-2-carboxamide (225)
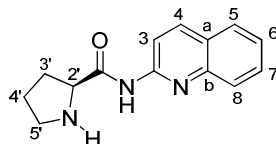
Following general method **B** for *N*-Boc-deprotection, the title compound was obtained as an off-white solid (1.4g, 49%,) m. p. = 108.3-109.1 °C; $[\alpha]_D^{14}$ = +7.4 (c = 0.1, CHCl$_3$).

^{1}H NMR (400 MHz, CDCl$_3$) δ = 10.43 (s, br, 1H, Amide N-H), 8.48 (d, *J* = 8.7 Hz, 1H, H-3), 8.16 (d, *J* = 9.2 Hz, 1H, H-4), 7.86 (d, *J* = 8.7 Hz, 1H, H-8), 7.76 (d, *J* = 9.2 Hz, 1H, H-5), 7.61-7.68 (m, 1H, H-7), 7.40-7.46 (m, 1H, H-6), 3.88-3.95 (m, 1H, H-2'), 3.04-3.15 (m, 2H, H-5'), 2.01-2.30 (m, 2H, H-3'), 2.15(s, br, 1H, aliphativ N-H) 1.73-1.85 (m, 2H, H-4')

^{13}C NMR (100 MHz, CDCl$_3$) δ = 174.9 (Amide C=O), 150.7 (C-2), 146.8 (C-b), 138.4 (C-4), 129.8 (C-7), 127.5 (C-5), 127.4 (C-8), 126.3 (C-a), 124.9 (C-6), 113.9 (C-3), 61.1 (C-2'), 47.4 (C-5'), 30.9 (C-3'), 26.2 (C-2').

IR (KBr disc) 3347, 3213, 2967, 1678, 1499, 1233, 1105 and 828 cm^{-1}

ESI-MS, low res, 242(M.H$^+$) HRMS (ESI); MH$^+$, found 242.1297, C$_{14}$H$_{16}$N$_3$O requires 242.1293

(S)-tert-butyl 2-(quinolin-3-ylcarbamoyl)pyrrolidine-1-carboxylate (Boc-226)
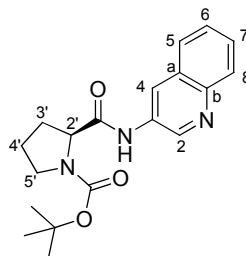
This compound was synthesised as per the procedure given for Boc-**221** using 3-aminoquiniline (1.102 g, 7.64 mmol) and purified by flash chromatography in 80:20

petroleum ether: ethyl acetate to yield the title compound as a brown solid (0.725 g, 28%), m. p. = 185-186.5 °C; $[\alpha]_D^{20}$ = -50 (c = 0.1, CHCl$_3$).

^{1}H NMR (400 MHz, CDCl$_3$) δ = 10.1 (s, br, 1H, N-H), 8.69 (s, 2H, H-2 & H-8), 7.88-7.96 (m, 1H, H-5), 7.60-7.69 (m, 1H, H-7), 7.47-7.55 (m, 1H, H-6), 7.37-7.45 (m, 1H, H-4), 4.51-4.62 (m, 1H, H-2'), 3.32-3.55 (m, 2H, H-5'), 2.22-2.57 (m, 1H, H-3'), 1.87-2.09 (m, 3H, H-3' & H-4'), 1.40-1.58 (m, 9H, Boc-H).

^{13}C NMR (100 MHz, CDCl$_3$) δ = 170.7 (Amide C=O), 156.8 (Boc C=O), 144.9 (C-b), 144.1 (C-2), 132.0 (C-3), 128.9 (C-4), 128.2 (C-a), 127.9 (C-6), 127.6 (C-7), 127.0 (C-8), 123.2 (C-5), 81.3 ($\underline{C}$-(CH$_3$)$_3$), 60.4 (C-2'), 47.3 (C-5'), 28.4 ((C-(C$\underline{H}_3$)$_3$), 27.1 (C-3'), 24.6 (C-4').

IR (KBr disc) 3298, 2976, 2873, 1702, 1666, 1555, 1417, 1160 and 756 cm^{-1}

ESI-MS, low res, 342 (M.H$^+$) HRMS (ESI); MH$^+$, found 342.1823, C$_{19}$H$_{24}$N$_3$O$_3$ requires 342.1818

(*S*)-*N*-(quinolin-3-yl)pyrrolidine-2-carboxamide (226)
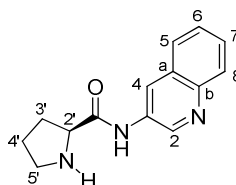
Following general method **B** for *N*-Boc-deprotection, the title compound was obtained as a thick brown pasty solid (400mg, 22%), $[\alpha]_D^{17}$ = -20 (c = 0.05, CHCl$_3$).

^{1}H NMR (400 MHz, CDCl$_3$) δ = 10.11 (s, br, 1H, Amide N-H), 8.83-8.85 (m, 1H, H-2), 8.75-8.77 (m, 1H, H-4), 8.0-8.04 (m, 1H, H-5), 7.77-7.81 (m, 1H, H-7), 7.57-7.62 (m, 1H, H-6), 7.49-7.53 (m, 1H, H-8), 3.91-3.97 (m, 1H, H-2'), 3.0-3.20 (m, 2H, H-5'), 2.01-2.31 (m, 2H, H-3'), 2.09 (s, 1H, Aliphatic N-H), 1.75-1.85 (m, 2H, H-4').

^{13}C NMR (100 MHz, CDCl$_3$) δ = 174.4 (Amide C=O), 145.2 (C-b), 144.0 (C-2), 131.4 (C-3), 128.8 (C-4), 128.2 (C-a), 128.1 (C-6), 127.7 (C-7), 127.1 (C-8), 123.0 (C-5), 61.1 (C-2'), 47.5 (C-5'), 30.9 (C-3'), 26.5 (C-4').

IR (KBr disc) 3354, 2969, 1686, 1523, 1490, 1369, 902 and 751 cm^{-1}

ESI-MS, low res, 242 (M.H$^+$) HRMS (ESI); MH$^+$, found 242.1297, $C_{14}H_{16}N_3O$ requires 242.1293.

(*S*)-*tert*-butyl 2-(quinolin-8-ylcarbamoyl)pyrrolidine-1-carboxylate (Boc-227)
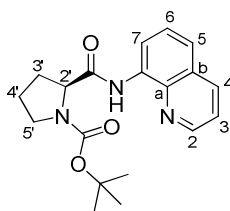
This compound was synthesised as per the procedure given for Boc-**221** using 8-aminoquiniline (1.1015 g, 7.64 mmol) and purified by flash chromatography in 90:10 hexane: ethyl acetate to yield the title compound as an off- white solid (2.43 g, 93%), m.p. = 154.8-156.2 °C; $[\alpha]_D^{16}$ = -127.4 (c = 0.1, CHCl$_3$). Lit $[\alpha]_D^{26}$ = -304.6 (c = 1.0, CHCl$_3$).[358]

^{1}H NMR (400 MHz, CDCl$_3$) δ = 10.28-10.64 (m, 1H, N-H), 8.72-8.79 (m, 2H, H-2 & H-7), 8.07-8.15 (m, 1H, H-4), 7.45-7.55 (m, 2H, H-3 & H-5), 7.39-7.47 (m, 1H, H-6), 4.55 (m, 1H, H-2'), 3.60 (m, 2H, H-5'), 2.30 (m, 2H, H-3'), 1.96 (m, 2H, H-4'), 1.45 (m, 9H, Boc-H).

^{13}C NMR (CDCl$_3$, 100 MHz) δ = 171.0 (Amide C=O), 154.8 (Boc C=O), 148.3 (C-2), 138.6 (C-a), 136.1 (C-4), 134.1(C-8), 127.9 (C-b), 127.2 (C-6 & C-5), 121.6 (C-3), 116.4 (C-7), 80.3 ($\underline{C}$-(CH$_3$)$_3$), 61.9 (C-2'), 47.0 (C-5'), 31.3 (C-3'), 28.4 ((C-($\underline{C}$H$_3$)$_3$), 24.1 (C-4')

IR (KBr disc) 3288, 2974, 2869, 1696, 1675, 1527, 1485, 1365, 1124 and 829 cm^{-1}

ESI-MS, low res, 342 (M.H$^+$) HRMS (ESI); MH$^+$, found 342.1819, $C_{19}H_{24}N_3O_3$ requires 342.1818.

(*S*)-*N*-(quinolin-8-yl)pyrrolidine-2-carboxamide (227)
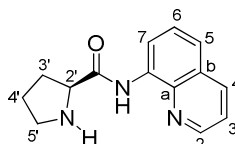
Following general method **B** for *N*-Boc-deprotection, the title compound was obtained as a dark brown viscous oil (1.8g, 84%), $[\alpha]_D^{24}$ = +18.6 (c = 0.1, CHCl$_3$). Lit $[\alpha]_D$ = +19.1 (c = 1.0, CHCl$_3$).[358]

^{1}H NMR (400 MHz, CDCl$_3$) δ = 11.61 (s, br, 1H, Amide N-H), 8.81-8.89 (m, 2H, H-2 & H-7), 8.12-8.16 (m, 1H, H-4), 7.48-7.56 (m, 2H, H-5 & H-6), 7.41-7.45 (m, 1H, H-3), 3.98-4.05 (m, 1H, H-2'), 3.11-3.21 (m, 2H, H-5'), 2.08–2.33 (m, 2H, H-3'), 2.18 (s, br, 1H, aliphatic N-H), 1.71-1.90 (m, 2H, H-4').

^{13}C NMR (100 MHz, CDCl$_3$) δ = 174.3 (Amide C=O), 148.6 (C-2), 139.2 (C-a), 136.1 (C-4), 134.5 (C-8), 128.1 (C-b), 127.2 (C-6), 121.6 (C-5), 121.4 (C-3), 116.4 (C-7), 61.8 (C-2'), 47.5 (C-5'), 31.0 (C-3'), 26.3 (C-4').

IR (KBr disc) 3257, 2965, 1670, 1516, 1382, 1102, 824 and 791 cm^{-1}

ESI-MS, low res, 242 (M.H$^+$) HRMS (ESI); MH$^+$, found 242.1296, C$_{14}$H$_{16}$N$_3$O requires 242.1293

(2*S*,2'*S*)-*tert*-butyl-2,2'-(pyridine-2,6-diyl*bis*(azanediyl))*bis*(oxomethylene) dipyrrolidine-1-carboxylate (Boc-228)
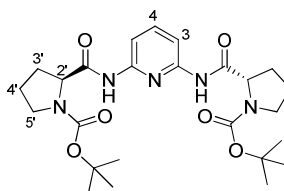
This compound was synthesised as per the procedure given for Boc-**221** using 2,6-diaminopyridine (1.069 g, 9.805 mmol) and purified by flash chromatography in 70:30 petroleum ether: ethyl acetate to yield the title compound as a white solid (1.29 g, 26%), m. p. = 218.5-220 °C; [α]$_D^{20}$ = -86.4 (c = 0.1, CHCl$_3$).

^{1}H NMR (400 MHz, CDCl$_3$) δ = 9.20, 8.12 (s, br, 2H, N-H (rotation present)), 7.90 (d, *J* = 7.6 Hz, 2H, H-3), 7.87 (s, 1H, H-4), 4.1-4.52 (m, 2H, H-2'), 3.15-3.65 (m, 4H, H-5'), 1.78-2.48 (m, 8H, H-3' & H-4'), 1.45 (s, 18H, Boc-H).

^{13}C NMR (100 MHz, CDCl$_3$) δ = 171.0 (Amide C=O), 155.2 (Boc C=O), 149.4 (C-2), 140.7 (C-5), 109.9 (C-3), 81.1 (*C*-(CH$_3$)$_3$), 62.2 (C-2'), 47.3 (C-5'), 31.2 (C-3'), 28.5 (C-(*C*H$_3$)$_3$), 24.4 (C-4').

IR (KBr disc) 3345, 3261, 2976, 1692, 1585, 1509, 1405, 1300, 1156, and 804cm^{-1}

ESI-MS, low res 526 (MNa$^+$), 504 (MH$^+$) HRMS (ESI); MH$^+$, found 504.2834, C$_{25}$H$_{38}$N$_5$O$_6$Na requires 504.2822.

## (2S,2'S)-N,N'-(pyridine-2,6-diyl)dipyrrolidine-2-carboxamide (228)
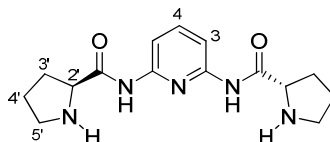
Following general method **B** for *N*-Boc-deprotection, the title compound was obtained as an off-white solid (800mg, 21%) m.p. = 177.5-179 °C; $[\alpha]_D^{20}$ = +10 (c = 0.1, CHCl$_3$). Lit $[\alpha]_D$ = +12.0 (c = 0.1, CHCl$_3$).[359]

> ^{1}H NMR (400 MHz, CDCl$_3$) δ = 9.97 (s, br, 2H, Amide N-H), 7.95 (d, *J* = 7.6 Hz, 2H, H-3), 7.70 (t, *J* = 7.6 Hz, 1H, H-4), 3.78-3.87 (m, 2H, H-2'), 2.9-3.13 (m, 4H, H-5'), 1.62-2.25 (m, 10H, H-3', H-4' & aliphatic N-H).

> ^{13}C NMR (100 MHz, CDCl$_3$) δ = 174.2 (Amide C=O), 149.4 (C-2), 140.2 (C-4), 108.9 (C-3), 61.0 (C-2'), 47.3 (C-5'), 30.8 (C-3'), 26.2 (C-4').

> ESI-MS, low res 326 (MNa$^+$), 304 (MH$^+$)

(2S,4R)-1-(*tert*-butoxycarbonyl)-4-hydroxypyrrolidine-2-carboxylic acid
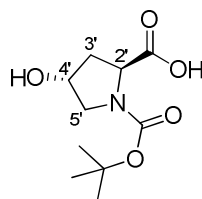
To a solution of trans-4-hydroxy-*L*-Proline (1.967 g, 15 mmol) in 20 ml of 1:1 dioxane:H$_2$O saturated aqueous sodium bicarbonate was added and the reaction mixture cooled to 0°C.A solution of (Boc)$_2$O (6.548 g, 30 mmol) in dioxane (10 mL) was added slowly and this mixture was stirred at room temperature for 16 hours. After this time, the mixture was concentrated to approximately 30 ml by removal of solvent *in vacuo*, 50 mL of ethyl acetate was added and the reaction mixture acidified to pH 3 with 1M HCl and the organic and aqueous layers were separated. The aqueous layer was extracted with a further 2 x 40 mL ethyl acetate and the combined organic layers were washed with saturated NaCl, dried with MgSO$_4$, filtered and solvent removed *in vacuo*. Flash chromatography using a gradient from 90:10 chloroform:methanol to 50:50 chloroform:methanol gave the title compound as a thick, colourless waxy solid (1.2 g, 35%), $[\alpha]_D^{17}$ = -55.6 (c = 0.1, CHCl$_3$).

^{1}H NMR (400 MHz, CDCl$_3$) δ = 5.50 (s, br, 1H, CHO*H*), 4.33-4.49 (m, 2H, H-2 & H-4), 3.43-3.63 (m, 2H, H-5), 2.05-2.38 (m, br, 2H, H-3), 1.45-1.39 (m, 9H, Boc-H).

^{13}C NMR (100 MHz, CDCl$_3$) δ (cis & trans conformers) = 177.6 & 174.6 (Amide C=O), 156.4 & 154.2 (Boc C=O), 81.8 & 81.0 (*C*-(CH$_3$)$_3$), 69.6 & 69.3 (C-4), 57.8 (C-2), 54.6 & 54.5 (C-5), 38.9 & 37.4 (C-3), 28.3 & 28.2 ((C-(*C*H$_3$)$_3$).

(2*S*,4*R*)-1-*tert*-butyl 2-methyl 4-(benzyloxy)pyrrolidine-1,2-dicarboxylate (231)
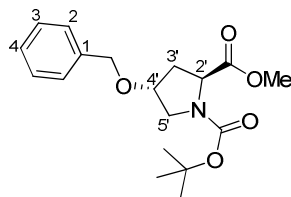
A solution of *N*-Boc-trans-4-hydroxy-*L*-proline methyl ester (0.8g, 3.262 mmol) in dry DMF (12 mL) was chilled to 0°C while sodium hydride (60% dispersion in mineral oil) (0.130 g, 3.262 mmol) was carefully added. After approximately 10 minutes, benzyl bromide (0.58 g, 0.404 mL, 3.4 mmol) was added slowly and the mixture was allowed to gradually heat up to room temperature with stirring over 4 hours. Water (15 mL) was then added to the reaction mixture and was followed by pH adjustment to pH 2 using 6 M HCl. This reaction mixture was then extracted with ethyl acetate (3 x 30 mL), washed with 10% LiCl solution (2 x 25 mL) and dried using MgSO$_4$. Flash chromatography using 90:10 petroleum ether: ethyl acetate yielded the title compound as a colourless oil, (0.415g, 38%), $[\alpha]_D^{20}$ = -5 (c = 0.1, EtOAc).

^{1}H NMR (400 MHz, CDCl$_3$) δ = 7.23-7.36 (m, 5H, aromatic protons), 4.27-4.52 (m, 3H, H-2' & O-C*H*$_2$Ar), 4.05-4.20 (m, 1H, H-4'), 3.70 (s, 3H, OC*H*$_3$), 3.48-3.70 (m, 2H, H-5'), 2.0-2.42 (m, 2H, H-3'), 1.38-1.46 (m, 9H, Boc-H).

^{13}C NMR (100 MHz, CDCl$_3$) δ = 171.2 (Amide C=O), 153.8 (Boc C=O), 137.8 (C-1), 128.6 (C-3), 127.9 (C-4), 127.7 (C-2), 80.2 (C-4'), 76.1 (*C*-(CH$_3$)$_3$), 71.1 (O-*C*H$_2$-Ph), 60.4 (C-2'), 58.1 (C-5'), 51.4 (O-*C*H$_3$), 36.2 (C-3'), 28.4 (C-(*C*H$_3$)$_3$).

ESI-MS, low res, 336 (MH$^+$), 358 (MNa$^+$), HRMS (ESI): MNa$^+$, found 358.1632, C$_{18}$H$_{25}$NO$_5$Na requires 358.1630.

(2S,4R)-4-(benzyloxy)-1-(*tert*-butoxycarbonyl)pyrrolidine-2-carboxylic acid (232)
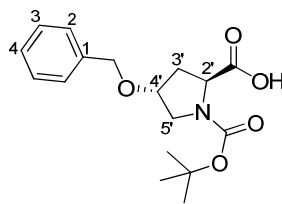
The above ester **231** (0.4 g, 1.194 mmol) was dissolved in methanol (9 mL) and to the reaction mixture was added 1M NaoH (10 ml) and the reaction mixture was stirred for 16 hours at room temperature. After addition of deionised water (10 mL), the pH of the mixture was adjusted to 10 by careful addition of 6 M NaOH. The reaction mixture was extracted with diethyl ether (2 x 10 mL). The aqueous layer was then acidified further to pH 4 and the solution was extracted with ethyl acetate (3 x 40 mL), the combined ethyl acetate organics were washed with saturated sodium chloride, dried with MgSO$_4$, filtered and solvent removed *in vacuo*. This compound was obtained as a colourless waxy solid (0.315 g, 82%), $[\alpha]_D^{21}$ = -11.2 (c = 0.1, CHCl$_3$);

> ^{1}H NMR (400 MHz, CDCl$_3$) δ = 9.90 (s, br, 1H, COOH), 7.21-7.33 (m, 5H, aromatic protons), 4.29-4.52 (m, 3H, H-2' & O-C$\underline{H}_2$-Ph), 4.02-4.17 (m, 1H, H-4'), 3.47-3.72 (m, 2H, H-5'), 2.05-2.50 (m, 2H, H-3'), 1.35-1.44 (m, 9H, Boc-H).

> ESI-MS, low res, 344 (MNa$^+$ adduct), HRMS (ESI): MNa$^+$, found 344.1483, C$_{17}$H$_{23}$NO$_5$Na requires 344.1474.

(2S,4R)-*tert*-butyl-4-(benzyloxy)-2-(pyridin-3-ylcarbamoyl)pyrrolidine-1-carboxylate (Boc-229)
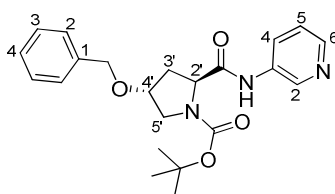
Acid **232** (0.275g, 0.857 mmol) was dissolved in dry THF (25 ml) under an inert atmosphere and to this was added triethylamine (0.14 mL, 0.087g). The stirred reaction mixture was cooled to 0 °C and ethyl chloroformate (0.238 g, 0.100 mL, 0.857 mmol) was added dropwise over 15 minutes. After the mixture had been stirred for a further 30 minutes, 3-aminopyridine (0.081 g, 0.857 mmol) was added slowly over 15 minutes. This reaction mixture was stirred for 1 hour at 0 °C, 16 hours at room temperature and heated to reflux for 3 hours. The mixture was subsequently diluted with ethyl acetate and the TEA.HCl removed by filtration and solvent removed from the filtrate *in vacuo*. Flash

chromatography in 80: 20 petroleum ether: ethyl acetate yielded the title compound as an off-white waxy solid (0.153 g, 45%), $[\alpha]_D^{21}$ = -46.8 (c = 0.1, CHCl$_3$).

^{1}H NMR (400 MHz, CDCl$_3$) δ = 9.81 (s, 1H, Amide N-H), 8.58 (s, 1H, H-2), 8.17 (s, 1H, H-4), 7.91 (s, 1H, H-6), 7.27 (m, 5H, aromatic benzyl protons), 7.06 (s, 1H, H-5), 4.56-4.68 (m, 1H, H-2') 4.45-4.53 (m. 2H, O-C$\underline{H}_2$Ar) 4.23-4.30 (m, 1H, 4H'), 3.56 (s, 2H, H5'), 2.1-2.6 (m, 2H, H-3'), 1.39-1.50 (m, 9H, Boc-H).

^{13}C NMR (100 MHz, CDCl$_3$) δ = 170.0 (Amide C=O), 157.0 (Boc C=O), 145.0 (C-4), 141.3 (C-6), 137.8 (C-1''), 135.2 (C-3), 128.6 (C-3'), 128.0 (C-4''), 127.8 (C-2''), 126.9 (C-2), 123.7 (C-5), 81.7 (C-($\underline{C}$H$_3$)$_3$), 77.0 (C-4'), 71.6 (O-$\underline{C}$H$_2$-Ph), 59.3 (C-2'), 51.9 (C-5'), 32.8 (C-3'), 28.4 (C-($\underline{C}$H$_3$)$_3$)

IR (KBr disc) 3421, 3197, 2967, 1682, 1655, 1368, 1156 and 742 cm^{-1}

ESI-MS, low res, 398 (MH$^+$) HRMS (ESI); MH$^+$, found 398.2082, C$_{22}$H$_{28}$N$_3$O$_4$ requires 398.2080

(2S,4R)-4-(benzyloxy)-N-(pyridin-3-yl)pyrrolidine-2-carboxamide (229)
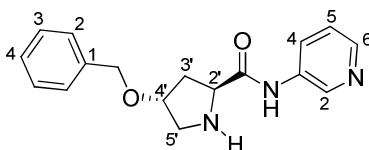
Following general method **B** for N-Boc-deprotection, the title compound was obtained as a brown oil (95mg, 29%), $[\alpha]_D^{14}$ = -22.5 (c = 0.05, CHCl$_3$)

^{1}H NMR (400 MHz, CDCl$_3$) δ = 9.85 (s, 1H, Amide N-H), 8.58-8.61 (m, 1H, H-2), 8.28-8.31 (m, 1H, H-4), 8.19-8.23 (m, 1H, H-6), 7.20-7.38 (m, 6H, H-5 & aromatic benzyl protons), 4.41-4.52 (m, 2H, OC$\underline{H}_2$Ph), 4.12 (s, 1H, H-4'), 4.03-4.09 (m, 1H, H-2'), 3.20-3.25(m, 1H, H-5'), 2.76-2.82 (m, 1H, H-5'), 2.55 (s, br, 1H, N-H), 2.47-2.56 (m, 1H, H-3'), 1.93-2.0 (m, 1H, H-3').

^{13}C NMR (100 MHz, CDCl$_3$) δ = 173.7 (Amide C=O), 145.1 (C-4), 141.0 (C-6), 138.0 (C-1''), 134.6 (C-3), 128.6 (C-3''), 127.9 (C-4''), 127.7 (C-2''), 126.5 (C-6), 123.7 (C-5), 80.5 (C-4'), 70.8 (O-$\underline{C}$H$_2$-Ph), 60.4 (C-2'), 52.8 (C-5'), 36.3 (C-3').

IR (KBr disc) 3377, 2921, 1670, 1583, 1425, 1259, 806 and 741 cm^{-1}

ESI-MS, low res, 298 (MH$^+$) HRMS (ESI); MH$^+$, found 298.1559, C$_{17}$H$_{20}$N$_3$O$_2$ requires 298.1556

(2S,4R)-tert-butyl-4-hydroxy-2-(pyridin-3-ylcarbamoyl)pyrrolidine-1-carboxylate (Boc-230)
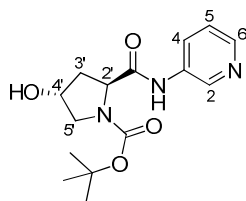
N-Boc-4-hydroxy-*L*-proline (0.403 g, 1.745 mmol) was dissolved in dry THF (30 mL) and treated with triethylamine (0.202 g, 0.280 mL, 2 mmol). The stirred reaction mixture was cooled to 0 °C and ethyl chloroformate (0.395 g, 0.166 mL, 1.754 mmol) was added dropwise over 15 minutes. After the mixture had been stirred for a further 30 minutes, 3-aminopyridine (0.164 g, 1.745 mmol) was added slowly over 15 minutes. This reaction mixture was stirred for 1 hour at 0 °C, 16 hours at room temperature and heated to reflux for 3 hours. The mixture was subsequently diluted with ethyl acetate and the TEA.HCl removed by filtration and solvent removed from the filtrate *in vacuo*. Flash chromatography in 80:20 ethyl acetate: petroleum ether yielded the title compound as an off-white solid (0.315 g, 59%), m.p. = 220 – 221.5 °C; $[\alpha]_D^{21}$ = -92 (c = 0.05, CH$_3$OH);

^{1}H NMR (400 MHz, CD$_3$OD) 8.72-8.78 (m, 1H, H-2), 8.22-8.30 (m, 1H, H-4), 8.08-8.19 (m, 1H, H-6), 7.34-7.44 (m, 1H, H-5), 4.39-4.52 (m, 2H, H-2' & H-4'), 3.44-3.66 (m, 2H, H-5'), 2.02-2.35 (m, 2H, H-3'), 1.30-1.49 (m, 9H, Boc-H);

^{13}C NMR (100 MHz, CD$_3$OD) δ = 172.8 (Amide C=O), 155.2 (Boc C=O), 144.1 (C-6), 140.5 (C-4), 136.0 (C-2), 127.9 (C-5), 124.0 (C-1), 80.4 (*C*-(CH$_3$)$_3$), 68.9 (C-4), 59.9 (C-2'), 55.1 (C-5'), 39.3 (C-3'), 27.4 ((C-(*C*H$_3$)$_3$).

IR (KBr disc) 3421, 3197, 2976, 1682, 1655, 1531, 1416, 1368, 1128 and 742 cm^{-1};

ESI-MS, low res, 308 (MH$^+$), 251.9, 207.9, 94.9. HRMS (ESI); MH$^+$, found 308.1612, C$_{15}$H$_{22}$N$_3$O$_4$ requires 308.1610

(2S,4R)-4-hydroxy-*N*-(pyridin-3-yl)pyrrolidine-2-carboxamide (230)
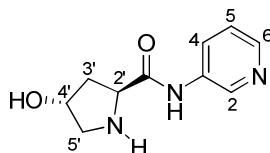
Following general method **B** for *N*-Boc-deprotection, the title compound was obtained as an orange coloured solid (200 mg, 42%), m.p. = 142.5 – 143.2 °C; $[\alpha]_D^{18}$ = -1.0 (c = 0.1, CHCl$_3$).

^{1}H NMR (400 MHz, CD$_3$OD) δ = 8.77-8.81 (m, 1H, H-2), 8.26-8.29 (m, 1H, H-4), 8.08-8.14 (m, 1H, H-6), 7.37-7.42 (m, 1H, H-5), 6.93 (s, 1H, Amide N-H), 4.51 (s, 1H, H-4'), 4.31-4.37 (m, 1H, H-2'), 3.11-3.28 (m, 2H, H-5'), 2.36-2.43 (m, 1H, H-3'), 2.01-2.10 (m, 1H, H-3'),

^{13}C NMR (100 MHz, CD$_3$OD) δ = 161.8 (Amide C=O), 144.3 (C-4), 140.8 (C-2), 127.8 (C-6), 124.0 (C-5), 118.2 (C-3), 71.1 (C-4'), 59.8 (C-2'), 54.2 (C-5'), 39.0 (C-3').

IR (KBr disc) 3406, 1682, 1501, 1206, 1139 and 802 cm^{-1};

ESI-MS, low res, 208 (M.H$^+$), HRMS (ESI): MH$^+$, found 208.1089, C$_{10}$H$_{14}$N$_3$O$_2$ requires 208.1086.

(*S*)-*tert*-butyl 2-(phenylcarbamoyl)pyrrolidine-1-carboxylate (Boc 233)
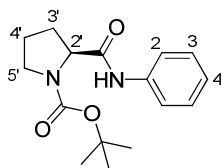
N-Boc-proline (1.075 g, 5 mmol) was dissolved in dry THF (25 mL) and treated with triethylamine (0.506 g, 0.69 mL, 5 mmol). The stirred reaction mixture was cooled to 0 °C and ethyl chloroformate (0.54 g, 5 mmol) was added dropwise over 15 minutes. After the mixture had been stirred for a further 30 minutes at 0 °C, aniline (0.465 g, 5 mmol) was added slowly over 15 minutes. This reaction mixture was stirred for 1 hour at 0 °C and 16 hours at room temperature. The mixture was worked up in the standard manner and subsequently dissolved in approx 40 ml dichloromethane, washed with 0.001 M HCl, dried with saturated NaCl and MgSO$_4$, filtered and solvent removed *in vacuo*. Flash chromatography in 90:10 petroleum ether: ethyl acetate yielded the title compound as a colourless solid (0.471 g, 33%), m. p. = 189.8-190.5 °C; $[\alpha]_D^{21}$ = -127.8 (c = 0.1, CHCl$_3$). Lit m.p. = 185-188 °C, Lit $[\alpha]_D$ = -138.3 (c = 0.24, CHCl$_3$).[360]

^{1}H NMR (400 MHz, CDCl$_3$) δ = 9.45, 7.74 (s, br, 1H, Amide N-H (rotation present)), 7.47-7.52 (m, 2H, H-2), 7.25-7.32 (m, 2H, H-3), 7.02-7.11 (m, 1H, H-4),

4.23-4.51 (m, 1H, H-2'), 3.25-3.6 (m, 2H, H-5'), 1.75-2.60 (m, br, 4H, H-3' & H-4'), 1.47 (s, 9H, Boc-H).

^{13}C NMR (100 MHz, CDCl$_3$) δ = 170.0 (Amide C=O), 156.7 (Boc C=O), 138.5 (C-1), 129.0 (C-3) 123.9 (C-4), 119.7 (C-2), 81.0 ($\underline{C}$-(CH$_3$)$_3$), 60.6 (C-2'), 47.3 (C-5'), 28.5 (C-($\underline{C}$H$_3$)$_3$), 27.3 (C-3'), 24.7 (C-4').

ESI-MS, low res, 313 (M.Na$^+$)

(*S*)-*N*-phenylpyrrolidine-2-carboxamide (233)
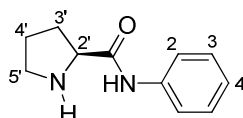
Following general method **B** for *N*-Boc-deprotection, the title compound was obtained as an off-white solid (250 mg, 29%), m. p. = 167.6-169.0 °C; [α]$_D^{19}$ = -62 (c = 0.1, CHCl$_3$). Lit m.p. = 170-172 °C, Lit [α]$_D$ = -44.2 (c = 0.5, EtOH).[253]

^{1}H NMR (400 MHz, CDCl$_3$) δ = 9.72 (s, br, 1H, N-H), 7.59 (d, *J* = 7.8 Hz, 2H, H-2), 7.30 (t, *J* = 7.8 Hz, 2H, H-3), 7.04-7.10 (m, 1H, H-4), 3.80-3.85 (m, 1H, H-2'), 2.92-3.10 (m, 2H, H-5'), 1.97-2.23 (m, 3H, H-3' & Aliphatic N-H), 1.69-1.80 (m, 2H, H-4').

^{13}C NMR (100 MHz, CDCl$_3$) δ = 173.6 (Amide C=O), 138.0 (C-1), 129.0 (C-3), 124.0 (C-4), 119.3 (C-2), 61.1 (C-2'), 47.4 (C-5'), 30.8 (C-3'), 26.4 (C-4').

ESI-MS, low res, 191 (MH$^+$)

(*S*)-*tert*-butyl-2-(methyl(pyridin-4-yl)carbamoyl)pyrrolidine-1-carboxylate (Boc-234)
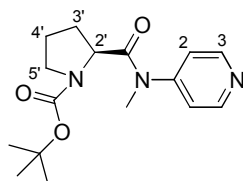
N-Boc-proline (0.425 g, 1.98 mmol) was dissolved in dry THF (25 mL) and treated with triethylamine (0.202 g, 0.275 mL, 2 mmol). The stirred reaction mixture was cooled to 0 °C and ethyl chloroformate (0.217 g, 2 mmol) was added dropwise over 15 minutes. After the mixture had been stirred for a further 30 minutes at 0 °C, 4-methylaminopyridine (0.214 g, 1.98 mmol) was added slowly over 15 minutes. This reaction mixture was stirred for 1 hour at 0 °C and 16 hours at room temperature. The mixture was worked up in the

standard manner and purified by flash chromatography using a gradient from 50:50 petroleum ether: ethyl acetate changing to 80:20 ethyl acetate: petroleum ether to yield the title compound as a colourless oil (0.202 g, 33%), $[\alpha]_D^{16} = +101.8$ (c = 0.1, CHCl$_3$)

^{1}H NMR (400 MHz, CDCl$_3$) δ = 8.55-8.62 (m, 2H, H-3), 7.28-7.32 (m, 1H, H-2), 7.12-7.16 (m, 1H, H-2), 4.16-4.42 (m, 1H, H-2'), 3.27-3.57 (m, 2H, H-5'), 3.22-3.27 (m, 3H, N-CH$_3$), 1.63-1.99 (m, 4H, H-3' & H-4'), 1.37 (s, 9H, Boc-H).

^{13}C NMR (100 MHz, CDCl$_3$) (Rotation present) δ = 172.5 & 172.3 (Amide C=O), 154.4 & 153.6 (Boc C=O), 151.4 (C-3), 150.9 & 151.1 (C-1), 121.9 & 121.5 (C-2), 79.9 & 79.5 (C-(CH$_3$)$_3$), 57.1 & 56.9 (C-2'), 47.1 & 47.0 (C-5'), 37.2 & 37.1 (N-CH$_3$), 30.3 (C-3'), 28.5 (C-(CH$_3$)$_3$), 24.3 & 23.5 (C-4')

ESI-MS, low res, 306 (MH)$^+$

(S)-N-methyl-N-(pyridin-4-yl)pyrrolidine-2-carboxamide (234)
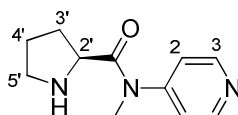
Following general method **B** for *N*-Boc-deprotection, the title compound was obtained as a colourless oil (120mg, 29%), $[\alpha]_D^{14} = -90$ (c = 0.05, CHCl$_3$). Lit $[\alpha]_D^{20} = -81.6$ (c = 0.5, CHCl$_3$).[265]

^{1}H NMR (400 MHz, CDCl$_3$) δ = 8.07-8.10 (m, 2H, H-3), 6.75 (s, br, 1H, aliphatic N-H) 6.31-6.34 (m, 2H, H-2), 3.99-4.02 (m, 1H, H-2'), 3.50-3.56 (m, 1H, H-5'), 3.16-3.23 (m, 1H, H-5'), 2.68-2.71 (m, 3H, N-CH$_3$), 2.14-2.21 (m, 2H, H-3'), 1.87-2.03 (m, 2H, H-4').

^{13}C NMR (100 MHz, CDCl$_3$) δ = 172.9 (C=O), 152.0 (C-1), 149.8 (C-3), 108.1 (C-2), 63.1 (C-2'), 48.6 (C-5'), 31.3 (C-3'), 26.3 (*N*-CH$_3$), 23.8 (C-4')

ESI-MS, low res, 206 (MH)$^+$

(S)-tert-butyl-2-(methyl(phenyl)carbamoyl)pyrrolidine-1-carboxylate (Boc-235)
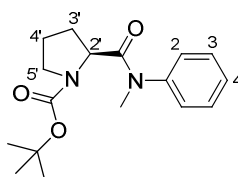
This compound was synthesised as per the procedure given for Boc-**221** using *N*-methylaniline (1.072 g, 10 mmol), the crude mixture was washed with with 0.5 M NaOH, dried with saturated NaCl and MgSO$_4$, filtered and solvent removed *in vacuo*. Flash chromatography in 90:10 petroleum ether: ethyl acetate yielded the title compound as a colourless oil (0.887 g, 29%), $[\alpha]_D^{11}$ = +66.8 (c = 0.1, CHCl$_3$).

^{1}H NMR (400 MHz, CDCl$_3$) δ = 7.38-7.45 (m, 2H, H-3), 7.28-7.37 (m, 2H, H-2), 7.20-7.24 (m, 1H, H-4), 4.1-4.3 (m, 1H, H-2'), 3.30-3.59 (m, 2H, H-5), 3.24-3.27 (m, 3H, N-C*H*$_3$), 1.60-2.01 (m, 4H, H-3' & H-4'), 1.42-1.48 (m, 9H, Boc-H).

^{13}C NMR (100 MHz, CDCl$_3$) (rotation present) δ = 172.7 & 172.6 (Amide C=O), 154.4 & 153.9 (Boc C=O), 143.6 & 143.4 (C-1), 129.9 (C-3), 128.1 & 128.0 (C-3), 127.9 & 127.8 (C-4), 79.7 & 79.3 (*C*-(CH$_3$)$_3$), 57.2 & 56.9 (C-2'), 47.3 & 47.1 (C-5'), 37.9 & 37.8 (N-*C*H$_3$), 31.7 & 30.4 (C-3'), 28.7 & 28.6 (C-(*C*H$_3$)$_3$), 24.3 & 23.6 (C-4').

IR (KBr disc) 2971, 2359, 1689, 1661, 1493, 1408, 1364, 1162 and 770 cm^{-1}

ESI-MS, low res, 304 (M)$^+$ HRMS (ESI); MNa$^+$, found 327.1695, C$_{17}$H$_{24}$N$_2$O$_3$ Na requires 327.1685

(*S*)-*N*-methyl-*N*-phenylpyrrolidine-2-carboxamide (235)
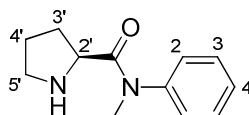
Following general method **B** for *N*-Boc-deprotection, the title compound was obtained as a colourless oil (500mg, 22%), $[\alpha]_D^{14}$ = +18.2 (c = 0.1, CHCl$_3$).

^{1}H NMR (400 MHz, CDCl$_3$) δ = 7.62 (s, br, 1H, aliphatic N-H), 7.28-7.34 (m, 2H, H-3), 7.21-7.27 (m, 1H, H-4), 7.13-7.18 (m, 2H, H-2), 3.86-3.93 (m, 1H, H-2'), 2.90-3.29 (m, 2H, H-5'), 3.15 (s, 3H, N-C*H*$_3$), 1.50-1.78 (m, 4H, H-3' & H-4').

^{13}C NMR (100 MHz, CDCl$_3$) δ = 170.8 (C=O), 141.9 (C-1), 130.1 (C-3), 128.7 (C-4), 127.7 (C-2), 58.4 (C-2'), 46.7 (C-5'), 38.0 (N-*C*H$_3$), 30.4 (C-3'), 25.4 (C-4')

ESI-MS, low res, 204 (M)$^+$

(*S*)-*tert*-butyl-2-(3,5-*bis*(trifluoromethyl)phenylcarbamoyl)pyrrolidine-1-carboxylate (Boc-236)
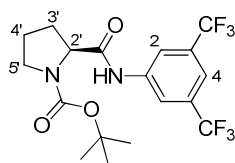
N-Boc-proline (1.254 g, 5.83 mmol) was dissolved in dry THF (25 mL) and treated with triethylamine (0.590 g, 0.813 mL, 5.83 mmol). The stirred reaction mixture was cooled to 0 °C and ethyl chloroformate (0.630 g, 0.555 ml 5.83 mmol) was added dropwise over 15 minutes. After the mixture had been stirred for a further 30 minutes at 0°C, 3,5-*bis*(trifluoromethyl)aniline (1.336 g, 5.83 mmol) was added slowly as a solution in 2 ml dry THF over 15 minutes. This reaction mixture was stirred for 1 hour at 0 °C, 16 hours at room temperature and heated to reflux for 4 hours. The mixture was subsequently dissolved in ethyl acetate (40 mL), washed with 0.2 M HCl, (30 ml) saturated aqueous sodium bicarbonate (30 ml), dried with saturated NaCl and MgSO$_4$, filtered and solvent removed *in vacuo*. Flash chromatography in 95:5 petroleum ether: ethyl acetate yielded the title compound as a colourless solid (0.489 g, 20%), m. p. = 193.5-119.4 °C; $[\alpha]_D^{18}$ = -89.8 (c = 0.1, CHCl$_3$)

> ^{1}H NMR (400 MHz, CDCl$_3$) δ = 10.22 (s, br, 1H, Amide N-H), 7.89 (s, 2H, H-2), 7.36 (s, 1H, H-4), 4.47-4.56 (s, 1H, H-2'), 3.37-3.62 (m, 2H, H-5'), 1.87-2.31 (m, 4H, H-3' & H-4'), 1.51 (s, 9H, Boc-H).

> ^{13}C NMR (100 MHz, CDCl$_3$) δ = 171.2 (Amide C=O), 156.2 (Boc C=O), 140.1 (C-1), 131.8 (C-3), 124.5 (CF$_3$) J_{C-F} = 34.5 Hz, 118.8 (C-2), 116.7 (C-4), 81.3 (*C*-(CH$_3$)$_3$), 60.7 (C-2'), 47.4 (C-5'), 29.0 (C-3') 28.8 (C-(*CH$_3$*)$_3$), 24.6 (C-4')

> IR (KBr disc) 3304, 3269, 3120, 1714, 1661, 1578, 1431, 1384, 1169 and 881 cm^{-1}

> ESI-MS, low res, 327 (MH$^+$- Boc group) HRMS (ESI); M$^-$, found 425.1341, C$_{18}$H$_{19}$F$_6$N$_2$O$_3$ requires 425.1300

(*S*)-*N*-(3,5-*bis*(trifluoromethyl)phenyl)pyrrolidine-2-carboxamide (236)
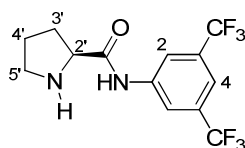
Following general method **B** for *N*-Boc-deprotection, the title compound was obtained as a pale yellow oil (230 mg, 17%); $[\alpha]_D^{18}$ = -37 (c = 0.05, CHCl$_3$). Lit $[\alpha]_D^{25}$ = -37.5 (c = 1.33, CHCl$_3$).[361]

> ^{1}H NMR (400 MHz, CDCl$_3$) δ = 10.10 (s, br, 1H, Amide N-H), 8.10 (s, 2H, H-2), 7.54 (s, 1H, H-4), 3.84-3.90 (m, 1H, H-2'), 2.94-3.13 (m, 2H, H-5'), 1.95-2.27 (m, 3H, H-3' & aliphatic N-H), 1.71-1.79 (m, 2H, H-4').

> ^{13}C NMR (100 MHz, CDCl$_3$) δ = 174.3 (Amide C=O), 139.3 (C-1), 132.4 (C-3), 124.6 (CF$_3$) $J_{C\text{-}F}$ = 32.6 Hz, 119.2 (C-2), 117.1 (C-4), 61.0 (C-2'), 47.4 (C-5'), 30.8 (C-3'), 26.4 (C-4').

> ESI-MS, low res, 327 (MH$^+$)

(*S*)-*tert*-butyl-2-(3,5-*bis*(trifluoromethyl)phenylsulfonylcarbamoyl)pyrrolidine-1-carboxylate (Boc-237)
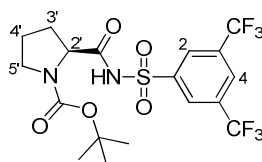
N-Boc-proline (824 mg, 3.83 mmol) was dissolved in a 50:50 mixture of dichloroethane:*t*-butanol (20 mL) and to this stirred suspension was added DMAP (1.404 g, 11.49 mmol), EDCI (1.839 g, 9.576 mmol) and 3,5-*bis*(trifluoromethyl)-benzene sulphonamide (2.66 mmol, 780 mg). The reaction mixture was stirred for 16 hours at room temperature and after this time Amberlyst 15 anion exchange resin (2 g) was added and the mixture was diluted with ethyl acetate (10 mL). This mixture was stirred for a further 2 hours and subsequently passed through a plug of silica gel and washed with ethyl acetate. The filtrate was collected and solvent removed *in vacuo*. The mixture was redissolved in dichloromethane (20 mL), washed with distilled water (20 ml), the aqueous layer was extracted with a further 2 x 10 ml portions of dichloromethane, the combined organics were washed with 0.2 M HCl, saturated NaCl, dried with MgSO$_4$, filtered and solvent removed *in vacuo*. The mixture was purified by flash chromatography (50:50 ethyl acetate: petroleum ether) to give the title product as a white solid (496 mg, 38%), m. p. = 122.8-124.2 °C; $[\alpha]_D^{21}$ = -81.2 (c = 0.05, CHCl$_3$).

¹H NMR (400 MHz, CDCl₃) δ = 8.34 (s, 2H, H-2), 7.73 (s, 1H, H-4). 4.1-4.25 (m, 1H, H-2'), 3.25-3.46 (m, 2H, H-5'), 1.68-2.18 (m, 4H, H-3' & H-4'), 1.29-1.40 (m, 9H, Boc-H).

^{13}C NMR (100 MHz, CDCl₃) δ = 181.4 (Amide C=O), 155.9 (Boc C=O), 145.5 (C-1), 132.2 (C-3), 126.9 (C-2), 125.0 (C-4), 124.1 (CF₃) J_{C-F} = 37.4 Hz, 81.5 (*C*-(CH₃)₃), 63.5 (C-2'), 47.3 (C-5'), 28.2 (C-(*C*H₃)₃), 29.9 (C-3'), 24.4 (C-4').

IR (KBr disc) 3472, 3089, 2982, 1670, 1582, 1425, 1362, 1138 and 904 cm⁻¹

ESI-MS, low res, 489 (M – H)⁻ HRMS (ESI); MNa⁺, found 513.0899, C₁₈H₂₀F₆N₂O₅SNa requires 513.0895

(*S*)-*N*-(3,5-*bis*(trifluoromethyl)phenylsulfonyl)pyrrolidine-2-carboxamide (237)
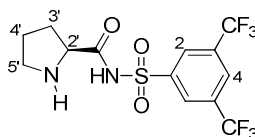
Following general method **B** for *N*-Boc-deprotection, the title compound was obtained as a White solid (200mg, 27%), m.p. = 222.3-223.1 °C;

¹H NMR (400 MHz, DMSO-*d₆*) δ = 8.30 (s, 2H, H-2), 8.24 (s, 1H, H-4), 3.86 (t, *J* = 6.9 Hz, 1H, H-2'), 2.94-3.14 (m, 2H, H-5'), 2.06-2.12 (m, 1H, H-3'), 1.62-1.83 (m, 2H, H-4'), 1.62-1.83 (m, 1H, H-3').

^{13}C NMR (100 MHz, DMSO-*d₆*) δ = 173.0 (Amide C=O), 148.3 (C-1), 130.7 (C-3), 128.2 (C-2), 124.9 (C-4), 122.1 (CF₃) J_{C-F} = 33.6 Hz, 62.4 (C-2'), 45.8 (C-5'), 29.4 (C-3'), 23.7 (C-4').

IR (KBr disc) 3447, 3187, 1622, 1361, 1310, 1279, 1128 and 852 cm⁻¹

ESI-MS, low res, 389 (M – H)⁻ HRMS (ESI); MH⁺, found 391.0551, C₁₃H₁₃N₂O₃F₆S requires 391.0551

1-benzylindoline-2,3-dione (*N*-benzyl isatin)
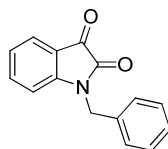
A solution of isatin (5.0 g, 34 mmol) in dry DMF (62 mL) was cooled to 0°C. NaH (60% dispersion in mineral oil, 1.4 g, 36 mmol) was carefully added in small portions. The

colour of the solution was observed to change from orange to a strong purple colour. When the H$_2$ evolution had stopped, benzyl bromide (6.7 g, 39 mmol) was slowly added and the mixture was observed to change to a brown colour. After the mixture had been stirred for a further 15 minutes at room temperature, H$_2$O (300 mL) was added, the resulting suspension was filtered by Buchner filtration and the product collected. The residue was washed with hexane and dried under vacuum to give the title compound as orange needles (7.0 g, 92%).

^{1}H NMR (400 MHz, CDCl$_3$) δ = 7.58-7.62 (m, 1H, H-4), 7.44-7.50 (m, 1H, H-6), 7.27-7.38 (m, 5H, Ar-H), 7.05-7.10 (m, 1H, H-5), 6.74-6.77 (m, 1H, H-7), 4.94 (s, 2H, Ph-C*H*$_2$);

^{13}C NMR (100 MHz; CDCl$_3$) δ = 183.2, 158.2, 150.6, 138.3, 134.4, 129.0 (2C), 128.1, 127.3 (2C), 125.3, 123.8, 117.6, 110.9, 43.9.

ESI-MS, low res, 237.9 (M.H$^+$), 259.9 (M.Na$^+$), 275.9 (M.K$^+$)

6.9   General Method of Reaction of Isatin with Acetone

The catalyst (0.03 mmol, 10 mol%) was stirred in a mixture of anhydrous acetone (2 mL) and additive (if applicable) at the temperature stated for 10 minutes. After this time, solid isatin (0.3 mmol, 44 mg) was added and the reaction mixture was stirred for the stated time. After this time, acetone was removed *in vacuo* and the mixture was purified by flash chromatography using a gradient initially eluting with 80:20 petroleum ether: ethyl acetate, gradually increasing polarity to 50:50 petroleum ether: ethyl acetate. The enantiomeric excess was determined by chiral stationary phase HPLC (Daicel-Chiralpak ASH) with the absolute configuration assigned based on literature values.[318] For the solvent screen, 2 mL of solvent and 1 mL of acetone was used for the test reactions.

(*S*)-3-hydroxy-3-(2-oxopropyl)indolin-2-one (208)
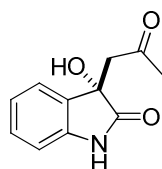
The title compound was obtained using the general procedure to give the title compound as a white solid, yield: see tables in Chapter 4, $[\alpha]_D^{18}$ = -20.0 (c = 0.03, CH$_3$OH). The ee was determined on the crude reaction mixture by chiral HPLC (Chiralpak ADH column, 70:30

^{1}H NMR (400 MHz, CD$_3$OD) δ = 7.29 (d, *J* = 7.3 Hz, 1H, Ar-H), 7.21 (dt, J = 7.6 and 1.5 Hz, 1H, Ar-H), 6.98 (t, *J* = 7.6 Hz, 1H, Ar-H), 6.86 (m, 1H, Ar-H), 3.36 (d, *J* = 16.8 Hz, 1H, CH$_2$) 3.15 (d, *J* = 16.8 Hz, 1H, CH$_2$), 2.04 (s, 3H, CH$_3$)

^{13}C NMR (100 MHz; CD$_3$OD) δ = 206.1 (CH$_3$-CO-CH$_2$), 179.8 (amide C=O), 142.3 (C-7a), 130.9 (C-3a), 129.4 (C-6), 123.5 (C-4), 122.1 (C-5), 109.9 (C-7), 73.4 (C-3), 49.8 (CH$_2$), 29.3 (CH$_3$);

IR (KBr disc) 3359, 3258, 2359, 1718, 1620, 1470, 1362 and 1057 cm^{-1}

ESI-MS, low res, 228 (MNa$^+$) HRMS (ESI); MNa$^+$, found 228.0637, C$_{11}$H$_{11}$NO$_3$Na requires 228.0637.

(*S*)-1-benzyl-3-hydroxy-3-(2-oxopropyl)indolin-2-one (238)
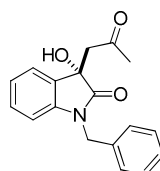
The title compound was obtained using the general procedure to give the title compound as a white solid, yield: see tables in Chapter 4, $[\alpha]_D^{19}$ = -4.0 (c = 0.05, CH$_3$OH). The ee was determined on the crude reaction mixture by chiral HPLC (Chiralpak ADH column, 90:10 hexane: *i*-PrOH, flow rate 0.7 mL/min; t_R = 39.5 min (minor enantiomer); t_R = 42.3 min (major enantiomer), λ = 254 nm).

^{1}H NMR (400 MHz, CD$_3$CN) δ = 7.37-7.41 (m, 2H, Bz protons), 7.29-7.35 (m, 3H, Bz protons), 7.25-7.28 (m, 1H, Ar-H), 7.14-7.19 (m, 1H, Ar-H), 6.96-7.01 (m, 1H, Ar-H), 6.70 (d, *J* = 7.8 Hz, 1H, Ar-H), 4.77-4.91 (m, 2H, Bz-CH$_2$), 4.25 (s, br, 1H, OH), 3.40 (d, *J* = 17.0 Hz, 1H, CH$_2$), 3.20 (d, *J* = 17.0 Hz, 1H, CH$_2$), 2.0 (s, 3H, CH$_3$)

^{13}C NMR (100 MHz, CD$_3$CN) δ = 206.9 (CH$_3$-CO-CH$_2$), 177.4 (amide C=O), 144.3 (C-7a), 137.4 (C-1'), 130.4 (C-3'), 129.6 (C-3a), 128.4 (C-6), 128.2 (C-2'), 124.4 (C-4'), 123.4 (C-5 and C-6), 110.1 (C-7), 74.0 (C-3), 50.5 (N-CH$_2$-Ph), 44.1 (CH$_2$C=O), 30.9 (CH$_3$)

IR (KBr disc) 3315, 3060, 2359, 1698, 1616, 1467, 1360 and 1079 cm^{-1}

ESI-MS, low res, 296 (MH$^+$), 318 (MNa$^+$). HRMS (ESI); MH$^+$, found 296.1294, C$_{18}$H$_{18}$NO$_3$ requires 296.1287

(S)-3-hydroxy-3-(2-oxobutyl)indolin-2-one (239)
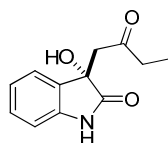
The title compound was obtained using the general procedure to give the title compound as a white solid, yield: see tables in Chapter 4, $[\alpha]_D^{14}$ = -40.0 (c = 0.01, CH$_3$OH). The ee was determined on the crude and also purified reaction mixtures using chiral HPLC (Chiralpak ADH column, 70/30 hexane/*i*-PrOH, flow rate 0.7 mL/min; t$_R$ = 9.9 min (*S* isomer); t$_R$ = 11.0 min (*R* isomer), λ = 254 nm) 91% regioselectivity of reaction, C-C bond formation at the less substituted methyl group of the ketone (determined by ^{1}H NMR).

^{1}H NMR (400 MHz, DMSO-*d*$_6$) δ = 10.20 (s, br, 1H, N-H), 7.22 (d, *J* = 7.2 Hz, 1H, H-3), 7.15 (t, *J* = 8.0 Hz, 1H, H-4), 6.88 (t, *J* = 7.6 Hz, 1H, H-5), 6.76 (d, *J* = 7.6 Hz, 1H, H-6), 5.96 (s, 1H, OH), 3.25 (d, *J* = 16.4 Hz, 1H, CH$_2$-a), 2.97 (d, *J* = 16.4 Hz, 1H, CH$_2$-a), 2.24-2.42 (m, 2H, CH$_2$-b), 0.74 (t, *J* = 7.2 Hz, 3H, CH$_3$).

^{13}C NMR (100 MHz; DMSO-*d*$_6$) δ = 207.4 (CH$_2$-CO-CH$_2$), 178.2 (amide C=O), 142.5 (C-7a), 131.5 (C-3a), 128.9 (C-6), 123.7 (C-4), 121.2 (C-5), 109.4 (C-7), 72.7 (C-3), 49.1 (C-CH$_2$CO), 35.6 (CH$_3$-CH$_2$-CO), 7.3 (CH$_3$).

IR (KBr disc) 3356, 2972, 2360, 1723, 1621, 1473, 1180 and 777 cm^{-1}

ESI-MS, low res, 228 (MNa$^+$) HRMS (ESI); MNa$^+$, found 242.0797, C$_{12}$H$_{13}$NO$_3$Na requires 242.0793

6.10 General Method for Reaction of Isatins with Acetaldehyde

These reactions were conducted using conditions which were almost identical to those previously used in the 4-hydroxydiarylprolinol catalysed reaction of benzyl Isatin with acetaldehyde.[323] To a solution of optimum catalyst **223** (30 mol%, 0.09 mmol, 17.2 mg), chloroacetic acid (60 mol%, 17 mg, 0.06 mmol) and isatin (0.3 mmol) in DMF (0.3 mL) was added acetaldehyde (84 μL, 1.50 mmol). This reaction mixture was stirred at room temperature under N$_2$ for 48 hours, subsequently, methanol (0.5 mL) and NaBH$_4$ (56 mg, 1.5 mmol) were added and the mixture was stirred for 1 hour at -20 °C. The resulting

mixture was quenched with pH 7.0 phosphate buffer solution and this mixture was extracted with ethyl acetate (3 x 25 mL) and the combined extracts were dried over anhydrous Na_2SO_4, filtered and solvent removed in *vacuo*. The product was isolated by flash chromatography (80:20 ethyl acetate: petroleum ether for the Isatin derivative **240** and 50:50 ethyl acetate: petroleum ether for the benzyl Isatin product **241**).

(*R*)-3-hydroxy-3-(2-hydroxyethyl)indolin-2-one (240)
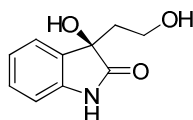
The title compound was obtained using the general procedure to give the title compound as a white solid (85%). The ee was determined on the purified reaction mixture (flash chromatography) using chiral HPLC (Chiralpak IA column, 10:1 hexane: *i*-PrOH, flow rate 0.7 mL/min; t_R = 30.9 min (minor enantiomer); t_R = 44.1 min (major enantiomer), λ = 254 nm); White solid; Yield: See Tables in Chapter 4; $[\alpha]_D^{14}$ = +19.1 (c = 0.01, $CHCl_3$);

^{1}H NMR (400 MHz, $CDCl_3$) δ = .35 (s, br, 1H, N-H), 7.30 (d, *J* = 6.9 Hz, 1H, Ar-H), 7.22 (t, *J* = 6.9 Hz, 1H, Ar-H), 7.0 (t, *J* = 7.6 Hz, 1H, Ar-H), 6.85 (d, *J* = 7.6 Hz, 1H, Ar-H), 4.30 (s, br, 1H, OH), 3.53-3.59 (m, 2H, C*H*$_2$OH), 2.98 (s, br, 1H, OH), 1.95-2.09 (m, 2H, C*H*$_2$CH$_2$OH)

^{13}C NMR (100 MHz, CD_3CN) δ = 180.0 (amide C=O), 142.0 (C-7a), 132.4 (C-3a), 130.3 (C-6), 125.1 (C-4), 123.2 (C-5), 110.8 (C-7), 76.2 (C-3), 58.3 (CH_2OH), 40.5 (C-CH_2)

IR (KBr disc) 3379, 2963, 1664, 1529, 1269, 997, 750 and 694 cm^{-1}

ESI-MS, low res, 216 (MNa$^+$) HRMS (ESI); MNa$^+$, found 216.0638, $C_{10}H_{11}NO_3Na$ requires 216.0637

(*R*)-1-benzyl-3-hydroxy-3-(2-hydroxyethyl)indolin-2-one (241)
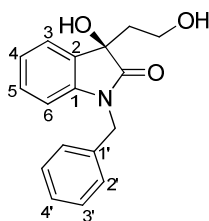
The title compound was obtained using the general procedure to give the title compound as a white solid, (28%). The ee was determined on the purified reaction mixture (after flash

chromatography) using chiral HPLC (Chiralpak IA column, 10:1 hexane: *i*-PrOH, flow rate 0.7 mL/min; t_R = 36.2 min (minor enantiomer); t_R = 40.2 min (major enantiomer), λ = 254 nm). Colourless oil; yield: see relevant table in Chapter 4, $[\alpha]_D^{14}$ = +14.0 (c = 0.01, CHCl$_3$)

^{1}H NMR (400 MHz, CDCl$_3$) δ = 7.38-7.42 (m, 1H, H-5), 7.24-7.33 (m, 5H, Bz protons), 7.17-7.22 (m, 1H, H-4), 7.03-7.09 (m, 1H, H-3), 6.68-6.72 (m, 1H, H-6), 4.96 (d, *J* = 16.0 Hz, 1H, C*H*$_2$-Ph), 4.77 (d, *J* = 16.0 Hz, 1H, C*H*$_2$-Ph), 4.43 (s, br, 1H, OH), 3.92-4.04 (m, 2H, C*H*$_2$-OH), 2.99 (s, br, 1H, OH), 2.26-2.34 (m, 1H, C*H*$_2$-C(OH)), 2.03-2.12 (m, 1H, C*H*$_2$-C(OH)).

^{13}C NMR (100 MHz; CDCl$_3$) δ = 178.4 (C=O), 141.9 (C-1), 135.3 (C-1'), 130.6 (C-2), 129.6 (C-4), 128.8 (C-3'), 127.7 (C-4'), 127.2 (C-2'), 123.9 (C-5), 123.3 (C-3), 109.6 (C-6), 58.6 (*C*H$_2$-OH), 43.8 (*C*H$_2$-Ph), 39.3 (*C*H$_2$-C(OH)).

IR (KBr disc) 3395, 2924, 1705, 1613, 1269, 1468, 1174 and 753 cm^{-1}

ESI-MS, low res, 306 (MNa$^+$) HRMS (ESI); MNa$^+$, found 306.1107, C$_{17}$H$_{17}$NO$_3$Na requires 306.1106
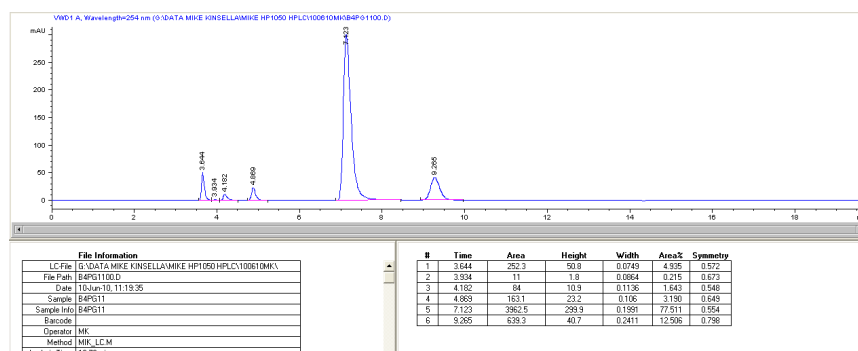
Figure 6.1: Product **223** catalysed reaction of isatin with acetone to give 72% ee of (S)-product **208**.
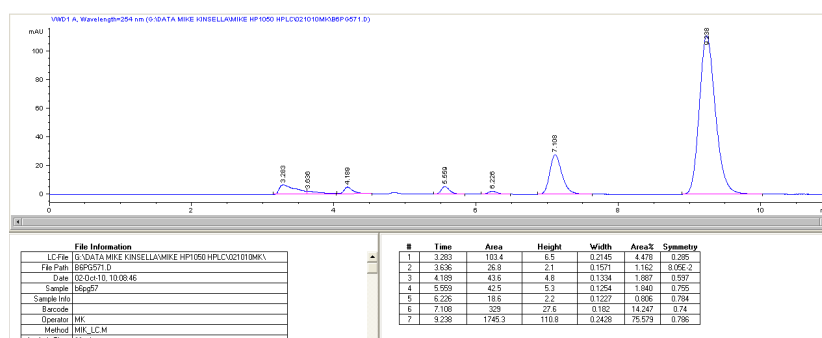
Figure 6.2: Product of **237** catalysed reaction of isatin with acetone to give 68% ee of *(R)*-product **208**.

References

1. Bates, G. W.; Gale, P. A. In *Recognition of Anions*, 2008; pp. 1-44.
2. Caltagirone, C.; Gale, P. A. *Chemical Society Reviews* **2009,** *38*, 520-563.
3. For an example of an indole based receptor see:Pfeffer, F. M.; Lim, K. F.; Sedgwick, K. J. *Organic & Biomolecular Chemistry* **2007,** *5*, 1795-1799.
4. For an example of a pyrrole based receptor see:Zielinski, T.; Jurczak, J. *Tetrahedron* **2005,** *61*, 4081-4089.
5. For an example of a sulfonamide based receptor see:Huggins, M. T.; Butler, T.; Barber, P.; Hunt, J. *Chemical Communications* **2009**, 5254-5256.
6. For an example of a urea based receptor see:Lin, C.; Simov, V.; Drueckhammer, D. G. *Journal Of Organic Chemistry* **2007,** *72*, 1742-1746.
7. Hughes, M. P.; Smith, B. D. *Journal Of Organic Chemistry* **1997,** *62*, 4492-4499.
8. Santacroce, P. V.; Davis, J. T.; Light, M. E.; Gale, P. A.; Iglesias-Sanchez, J. C.; Prados, P.; Quesada, R. *Journal Of The American Chemical Society* **2007,** *129*, 1886-1887.
9. Bhadury, P. S.; Song, B. A.; Yang, S.; Hu, D. Y.; Xue, W. *Current Organic Synthesis* **2009,** *6*, 380-399.
10. Sohtome, Y., Takemura, N., Takagi, R., Hashimoto, Y., Nagasawa, K. *Tetrahedron* **2008,** *64*, 9423-9429.
11. Connon, S. J. *Chemistry-A European Journal* **2006,** *12*, 5418-5427.
12. Jones, C. E. S., Turega, S. M., Clarke, M. L., Philp, D. *Tetrahedron Letters* **2008,** *49*, 4666-4669.
13. Kotke, M.; Schreiner, P. R. *Tetrahedron* **2006,** *62*, 434-439.
14. Fan, E. K.; Vicent, C.; Hamilton, A. D. *New Journal Of Chemistry* **1997,** *21*, 81-85.
15. Reisman, S. E.; Doyle, A. G.; Jacobsen, E. N. *Journal of the American Chemical Society* **2008,** *130*, 7198-7199.
16. Raheem, I. T.; Thiara, P. S.; Peterson, E. A.; Jacobsen, E. N. *Journal of the American Chemical Society* **2007,** *129*, 13404-+.
17. Crabtree, R. H., Kavallieratos, K. *Chemical Communications* **1999**, 2109-2110.
18. Zuend, S. J.; Jacobsen, E. N. *Journal Of The American Chemical Society* **2009,** *131*, 15358-15374.
19. Zhang, Z. G.; Schreiner, P. R. *Chemical Society Reviews* **2009,** *38*, 1187-1198.
20. Beer, P. D.; Gale, P. A. *Angewandte Chemie-International Edition* **2001,** *40*, 486-516.
21. Park, C. H.; Simmons, H. E. *Journal of the American Chemical Society* **1968,** *90*, 2431-&.
22. Bowman-James, K., E Garcia-Espana *Supramolecular Chemistry of Anions*, ed.; Wiley-VCH: New York, 1997.
23. Sessler, J. L.; Gale, P. A.; Cho, W. S. *Anion receptor chemistry*; Royal Society of Chemistry, 2006.
24. Kavallieratos, K.; deGala, S. R.; Austin, D. J.; Crabtree, R. H. *Journal Of The American Chemical Society* **1997,** *119*, 2325-2326.
25. Kubik, S. *Chemical Society Reviews* **2010,** *39*, 3648-3663.
26. Ojida, A.; Takashima, I.; Kohira, T.; Nonaka, H.; Hamachi, I. *Journal of the American Chemical Society* **2008,** *130*, 12095-12101.
27. Kim, Y.; Gabbai, F. P. *Journal of the American Chemical Society* **2009,** *131*, 3363-3369.
28. Davis, A. P.; Sheppard, D. N.; Smith, B. D. *Chemical Society Reviews* **2007,** *36*, 348-357.
29. Fowler, C. J.; Haverlock, T. J.; Moyer, B. A.; Shriver, J. A.; Gross, D. E.; Marquez, M.; Sessler, J. L.; Hossain, M. A.; Bowman-James, K. *Journal of the American Chemical Society* **2008,** *130*, 14386-+.
30. Bazzicalupi, C.; Bencini, A.; Lippolis, V. *Chemical Society Reviews* **2010,** *39*, 3709-3728.
31. Steed, J. W. *Chemical Society Reviews* **2009,** *38*, 506-519.
32. Mercer, D. J.; Loeb, S. J. *Chemical Society Reviews* **2010,** *39*, 3612-3620.
33. Galbraith, E.; James, T. D. *Chemical Society Reviews* **2010,** *39*, 3831-3842.
34. Schottel, B. L.; Chifotides, H. T.; Dunbar, K. R. *Chemical Society Reviews* **2008,** *37*, 68-83.

35. Kang, S. O.; Begum, R. A.; Bowman-James, K. *Angewandte Chemie-International Edition* **2006,** *45*, 7882-7894.
36. Gale, P. A. *Accounts Of Chemical Research* **2006,** *39*, 465-475.
37. Li, A. F.; Wang, J. H.; Wang, F.; Jiang, Y. B. *Chemical Society Reviews* **2010,** *39*, 3729-3745.
38. Gale, P. A. *Chemical Society Reviews* **2010,** *39*, 3746-3771.
39. Kang, S. O.; Hossain, M. A.; Bowman-James, K. *Coordination Chemistry Reviews* **2006,** *250*, 3038-3052.
40. Rostami, A.; Colin, A.; Li, X. Y.; Chudzinski, M. G.; Lough, A. J.; Taylor, M. S. *Journal of Organic Chemistry* **2010,** *75*, 3983-3992.
41. Amendola, V.; Bergamaschi, G.; Boiocchi, M.; Fabbrizzi, L.; Milani, M. *Chemistry-a European Journal* **2010,** *16*, 4368-4380.
42. Boyle, E. M.; McCabe, T.; Gunnlaugsson, T. *Supramolecular Chemistry* **2010,** *22*, 586-597.
43. Caltagirone, C.; Gale, P. A.; Hiscock, J. R.; Brooks, S. J.; Hursthouse, M. B.; Light, M. E. *Chemical Communications* **2008**, 3007-3009.
44. Brooks, S. J., Light, M. E., Gale, P. A. *Chemical Communications* **2006**, 4344-4346.
45. Gomez, D. E.; Fabbrizzi, L.; Licchelli, M.; Monzani, E. *Organic & Biomolecular Chemistry* **2005,** *3*, 1495-1500.
46. Dahan, A.; Ashkenazi, T.; Kuznetsov, V.; Makievski, S.; Drug, E.; Fadeev, L.; Bramson, M.; Schokoroy, S.; Rozenshine-Kemelmakher, E.; Gozin, M. *Journal of Organic Chemistry* **2007,** *72*, 2289-2296.
47. Dydio, P.; Lichosyt, D.; Jurczak, J. *Chemical Society Reviews* **2011,** *40*, 2971-2985.
48. Bates, G. W.; Gale, P. A.; Light, M. E.; Ogden, M. I.; Warriner, C. N. *Dalton Transactions* **2008**, 4106-4112.
49. Caltagirone, C.; Hiscock, J. R.; Hursthouse, M. B.; Light, M. E.; Gale, P. A. *Chemistry-A European Journal* **2008,** *14*, 10236-10243.
50. Chmielewski, M. J.; Jurczak, J. *Tetrahedron Letters* **2005,** *46*, 3085-3088.
51. Kavallieratos, K.; Bertao, C. M.; Crabtree, R. H. *Journal Of Organic Chemistry* **1999,** *64*, 1675-1683.
52. Chang, S. K.; Vanengen, D.; Fan, E.; Hamilton, A. D. *Journal Of The American Chemical Society* **1991,** *113*, 7640-7645.
53. Tellado, F. G., Goswami, S., Chang, S.K., Geib, S.J., Hamilton, A.D. *Journal Of The American Chemical Society* **1990,** *112*, 7393-7394.
54. Pinter, T.; Jana, S.; Courtemanche, R. J. M.; Hof, F. *Journal of Organic Chemistry* **2011,** *76*, 3733-3741.
55. Hamilton, A. D.; Van Engen, D. *Journal of the American Chemical Society* **1987,** *109*, 5035-5036.
56. Hunter, C. A., Purvis, D. H. *Angewandte Chemie-International Edition* **1992,** *31*, 792-795.
57. Coles, S. J.; Frey, J. G.; Gale, P. A.; Hursthouse, M. B.; Light, M. E.; Navakhun, K.; Thomas, G. L. *Chemical Communications* **2003**, 568-569.
58. Brooks, S. J., Evans, L. S., Gale, P. A., Hursthouse, M. B., Light, M. E. *Chemical Communications* **2005**, 734 - 736.
59. Bates, G. W.; Gale, P. A.; Light, M. E. *Chemical Communications* **2007**, 2121-2123.
60. Gale, P. A.; Garric, J.; Light, M. E.; McNally, B. A.; Smith, B. D. *Chemical Communications* **2007**, 1736-1738.
61. Duke, R. M.; O'Brien, J. E.; McCabe, T.; Gunnlaugsson, T. *Organic & Biomolecular Chemistry* **2008,** *6*, 4089-4092.
62. Duke, R. M.; Gunnlaugsson, T. *Tetrahedron Letters* **2010,** *51*, 5402-5405.
63. Gale, P. A.; Camiolo, S.; Chapman, C. P.; Light, M. E.; Hursthouse, M. B. *Tetrahedron Letters* **2001,** *42*, 5095-5097.
64. Camiolo, S.; Gale, P. A.; Hursthouse, M. B.; Light, M. E. *Tetrahedron Letters* **2002,** *43*, 6995-6996.
65. Camiolo, S.; Gale, P. A.; Hursthouse, M. B.; Light, M. E.; Shi, A. J. *Chemical Communications* **2002**, 758-759.

66.	Camiolo, S.; Gale, P. A.; Hursthouse, M. B.; Light, M. E. *Organic & Biomolecular Chemistry* **2003,** *1*, 741-744.

67.	Evans, L. S.; Gale, P. A.; Light, M. E.; Quesada, R. *New Journal Of Chemistry* **2006,** *30*, 1019-1025.

68.	Vega, I. E. D., Camiolo, S., Gale, P. A., Hursthouse, M. B., Light, M.E. *Chemical Communications* **2003**, 1686-1687.

69.	Vega, I. E.; Gale, P. A.; Hursthouse, M. B.; Light, M. E. *Organic & Biomolecular Chemistry* **2004,** *2*, 2935-2941.

70.	Zhang, Y. H.; Yin, Z. M.; Li, Z. C.; He, J. Q.; Cheng, J. P. *Tetrahedron* **2007,** *63*, 7560-7564.

71.	Bates, G. W.; Triyanti; Light, M. E.; Albrecht, M.; Gale, P. A. *Journal of Organic Chemistry* **2007,** *72*, 8921-8927.

72.	Makuc, D.; Lenarcic, M.; Bates, G. W.; Gale, P. A.; Plavec, J. *Organic & Biomolecular Chemistry* **2009,** *7*, 3505-3511.

73.	Caltagirone, C.; Gale, P. A.; Hiscock, J. R.; Hursthouse, M. B.; Light, M. E.; Tizzard, G. J. *Supramolecular Chemistry* **2009,** *21*, 125-130.

74.	Dydio, P.; Zielinski, T.; Jurczak, J. *Organic Letters* **2010,** *12*, 1076-1078.

75.	Amendola, V.; Fabbrizzi, L.; Mosca, L. *Chemical Society Reviews* **2010,** *39*, 3889-3915.

76.	Smith, P. J.; Reddington, M. V.; Wilcox, C. S. *Tetrahedron Letters* **1992,** *33*, 6085-6088.

77.	Kelly, T. R.; Kim, M. H. *Journal Of The American Chemical Society* **1994,** *116*, 7072-7080.

78.	Buhlmann, P.; Nishizawa, S.; Xiao, K. P.; Umezawa, Y. *Tetrahedron* **1997,** *53*, 1647-1654.

79.	Snellink-Ruel, B. H. M., Antonisse, M. M. G., Engbersen, J. F. J., Timmerman, P., Reinhoudt, D. N. *European Journal Of Organic Chemistry* **2000,** *2000*, 165.

80.	Kato, R.; Nishizawa, S.; Hayashita, T.; Teramae, N. *Tetrahedron Letters* **2001,** *42*, 5053-5056.

81.	Boiocchi, M.; Del Boca, L.; Gomez, D. E.; Fabbrizzi, L.; Licchelli, M.; Monzani, E. *Journal of the American Chemical Society* **2004,** *126*, 16507-16514.

82.	Amendola, V.; Esteban-Gomez, D.; Fabbrizzi, L.; Licchelli, M. *Accounts Of Chemical Research* **2006,** *39*, 343-353.

83.	Gunnlaugsson, T.; Kruger, P. E.; Jensen, P.; Tierney, J.; Ali, H. D. P.; Hussey, G. M. *Journal of Organic Chemistry* **2005,** *70*, 10875-10878.

84.	Brooks, S. J.; Gale, P. A.; Light, M. E. *Chemical Communications* **2005**, 4696-4698.

85.	Brooks, S. J.; Edwards, P. R.; Gale, P. A.; Light, M. E. *New Journal Of Chemistry* **2006,** *30*, 65-70.

86.	dos Santos, C. M. G.; McCabe, T.; Watson, G. W.; Kruger, P. E.; Gunnlaugsson, T. *Journal of Organic Chemistry* **2008,** *73*, 9235-9244.

87.	Hay, B. P.; Firman, T. K.; Moyer, B. A. *Journal of the American Chemical Society* **2005,** *127*, 1810-1819.

88.	Clare, J. P.; Statnikov, A.; Lynch, V.; Sargent, A. L.; Sibert, J. W. *Journal of Organic Chemistry* **2009,** *74*, 6637-6646.

89.	Caltagirone, C., Bates, G. W., Gale, P. A., Light, M. E. *Chemical Communications* **2008**, 61-63.

90.	Mammoliti, O., Allasia, S., Dixon, S., Kilburn, J. D. *Tetrahedron* **2009,** *65*, 2184-2195.

91.	Prohens, R.; Rotger, M. C.; Pina, M. N.; Deya, P. M.; Morey, J.; Ballester, P.; Costa, A. *Tetrahedron Letters* **2001,** *42*, 4933-4936.

92.	Pina, M. N.; Rotger, M. C.; Costa, A.; Ballester, P.; Deya, P. M. *Tetrahedron Letters* **2004,** *45*, 3749-3752.

93.	Ramalingam, V.; Domaradzki, M. E.; Jang, S.; Muthyala, R. S. *Organic Letters* **2008,** *10*, 3315-3318.

94.	Al-Sayah, M. H.; Branda, N. R. *Thermochimica Acta* **2010,** *503*, 28-32.

95.	Amendola, V.; Fabbrizzi, L.; Mosca, L.; Schmidtchen, F. P. *Chemistry-a European Journal* **2011,** *17*, 5972-5981.

96.	Corey, E. J., Cheng, X.-M. *The logic of chemical synthesis*; John Wiley & Sons: New York, 1989.

293

97. Jacobsen, E. N.; MacMillan, D. W. C. *Proceedings of the National Academy of Sciences of the United States of America* **2010,** *107*, 20618-20619.
98. Knowles, W. S.; Sabacky, M. J. *Chemical Communications* **1968**, 1445-&.
99. Knowles, W. S.; Vineyard, B. D.; Sabacky, M. J. *Journal of the Chemical Society-Chemical Communications* **1972**, 10-&.
100. Kagan, H. B.; Dang, T. P. *Journal of the American Chemical Society* **1972,** *94*, 6429-&.
101. Knowles, W. S. *Accounts of Chemical Research* **1983,** *16*, 106-112.
102. Erre, G.; Enthaler, S.; Junge, K.; Gladiali, S.; Beller, M. *Coordination Chemistry Reviews* **2008,** *252*, 471-491.
103. Clayden, J. *Organic chemistry*; Oxford Univ. Press, 2009.
104. Weber, D. J., Meeker, A.K., Mildvan, A.S., . *Biochemistry* **1989,** *30*, 6103.
105. Jubian, V.; Dixon, R. P.; Hamilton, A. D. *Journal Of The American Chemical Society* **1992,** *114*, 1120-1121.
106. Eder, U., Wiechert, R., Sauer, G. *Chemical Abstracts* **1972,** *76*, 14180.
107. Hajos, Z. G., Parrish, D. R., . *Chemical Abstracts* **1972,** *76*, 59072.
108. Hine, J.; Linden, S. M.; Kanagasabapathy, V. M. *Journal of the American Chemical Society* **1985,** *107*, 1082-1083.
109. Kelly, T. R., Meghani, P., Ekkundi, V.S. *Tetrahedron Letters* **1990,** *31*, 3381-3384.
110. Pellissier, H. *Tetrahedron* **2007,** *63*, 9267-9331.
111. Fonseca, M. H.; List, B. *Current Opinion In Chemical Biology* **2004,** *8*, 319-326.
112. Dalko, P. I.; Moisan, L. *Angewandte Chemie-International Edition* **2004,** *43*, 5138-5175.
113. Seayad, J.; List, B. *Organic & Biomolecular Chemistry* **2005,** *3*, 719-724.
114. Marcelli, T.; Hiemstra, H. *Synthesis-Stuttgart* **2010**, 1229-1279.
115. Gaunt, M. J.; Johansson, C. C. C.; McNally, A.; Vo, N. T. *Drug Discovery Today* **2007,** *12*, 8-27.
116. Takemoto, Y. *Organic & Biomolecular Chemistry* **2005,** *3*, 4299-4306.
117. McCooey, S. H.; Connon, S. J. *Organic Letters* **2007,** *9*, 599-602.
118. List, B.; Lerner, R. A.; Barbas, C. F. *Journal of the American Chemical Society* **2000,** *122*, 2395-2396.
119. Ahrendt, K. A.; Borths, C. J.; MacMillan, D. W. C. *Journal of the American Chemical Society* **2000,** *122*, 4243-4244.
120. Hashimoto, T.; Maruoka, K. *Chemical Reviews* **2007,** *107*, 5656-5682.
121. Maruoka, K.; Ooi, T. *Chemical Reviews* **2003,** *103*, 3013-3028.
122. Lygo, B.; Wainwright, P. G. *Tetrahedron Letters* **1997,** *38*, 8595-8598.
123. Corey, E. J.; Xu, F.; Noe, M. C. *Journal of the American Chemical Society* **1997,** *119*, 12414-12415.
124. O'Donnell, M. J.; Delgado, F.; Hostettler, C.; Schwesinger, R. *Tetrahedron Letters* **1998,** *39*, 8775-8778.
125. Ooi, T.; Kameda, M.; Maruoka, K. *Journal of the American Chemical Society* **2003,** *125*, 5139-5151.
126. Li, H. M.; Wang, Y.; Tang, L.; Deng, L. *Journal of the American Chemical Society* **2004,** *126*, 9906-9907.
127. Schreiner, P. R. *Chemical Society Reviews* **2003,** *32*, 289-296.
128. Akiyama, T.; Itoh, J.; Fuchibe, K. *Advanced Synthesis & Catalysis* **2006,** *348*, 999-1010.
129. Taylor, M. S.; Jacobsen, E. N. *Angewandte Chemie-International Edition* **2006,** *45*, 1520-1543.
130. Hiemstra, H.; Wynberg, H. *Journal of the American Chemical Society* **1981,** *103*, 417-430.
131. Lou, S.; Taoka, B. M.; Ting, A.; Schaus, S. E. *Journal of the American Chemical Society* **2005,** *127*, 11256-11257.
132. McDougal, N. T.; Schaus, S. E. *Journal Of The American Chemical Society* **2003,** *125*, 12094-12095.
133. Huang, Y.; Unni, A. K.; Thadani, A. N.; Rawal, V. H. *Nature* **2003,** *424*, 146-146.
134. Akiyama, T.; Itoh, J.; Yokota, K.; Fuchibe, K. *Angewandte Chemie-International Edition* **2004,** *43*, 1566-1568.
135. Akiyama, T.; Saitoh, Y.; Morita, H.; Fuchibe, K. *Advanced Synthesis & Catalysis* **2005,** *347*, 1523-1526.

136. Hine, J., Ahn, K., Gallucci, J.C., Linden, S.M. *Journal Of The American Chemical Society* **1984,** *106*, 7980-7981.
137. Hine, J.; Ahn, K. *Journal of Organic Chemistry* **1987,** *52*, 2089-2091.
138. Etter, M. C. *Accounts Of Chemical Research* **1990,** *23*, 120-126.
139. Etter, M. C.; Panunto, T. W. *Journal Of The American Chemical Society* **1988,** *110*, 5896-5897.
140. Blake, J. F.; Jorgensen, W. L. *Journal Of The American Chemical Society* **1991,** *113*, 7430-7432.
141. Etter, M. C.; Urbanczyk-Lipkowska, Z.; Zia-Ebrahimi, M.; Panunto, T. W. *Journal of the American Chemical Society* **1990,** *112*, 8415-8426.
142. Curran, D. P.; Kuo, L. H. *The Journal of Organic Chemistry* **1994,** *59*, 3259-3261.
143. Curran, D. P.; Lung, H. K. *Tetrahedron Letters* **1995,** *36*, 6647.
144. Schreiner, P. R.; Wittkopp, A. *Organic Letters* **2002,** *4*, 217-220.
145. Maher, D. J.; Connon, S. J. *Tetrahedron Letters* **2004,** *45*, 1301-1305.
146. Okino, T.; Hoashi, Y.; Takemoto, Y. *Tetrahedron Letters* **2003,** *44*, 2817.
147. Sohtome, Y., , Tanatani, A., Hashimoto, Y., Nagasawa, K. *Tetrahedron Letters* **2004,** *45*, 5589-5592.
148. Schreiner, P. R., Wittkopp, Alexander. *Chemistry-A European Journal* **2003,** *9*, 407-414.
149. Sohtome, Y., , Tanatani, A., Hashimoto, Y., Nagasawa, K. *Chemical and Pharmaceutical Bulletin* **2004,** *52*, 477-480.
150. Kleiner, C. M.; Schreiner, P. R. *Chemical Communications* **2006**, 4315-4317.
151. Weil, T.; Kotke, M.; Kleiner, C. M.; Schreiner, P. R. *Organic Letters* **2008,** *10*, 1513-1516.
152. Kotke, M.; Schreiner, P. R. *Synthesis-Stuttgart* **2007**, 779-790.
153. Fleming, E. M.; Quigley, C.; Rozas, I.; Connon, S. J. *The Journal of Organic Chemistry* **2008,** *73*, 948-956.
154. Russo, A.; Lattanzi, A. *Advanced Synthesis & Catalysis* **2009,** *351*, 521-524.
155. Jacobsen, E. N., Gigman, M. S. *Journal Of The American Chemical Society* **1998,** *120*, 4901-4902.
156. Okino, T.; Hoashi, Y.; Takemoto, Y. *Journal Of The American Chemical Society* **2003,** *125*, 12672-12673.
157. Hamza, A.; Schubert, G.; Soos, T.; Papai, I. *Journal Of The American Chemical Society* **2006,** *128*, 13151-13160.
158. Hoashi, Y.; Okino, T.; Takemoto, Y. *Angewandte Chemie-International Edition* **2005,** *44*, 4032-4035.
159. Okino, T.; Nakamura, S.; Furukawa, T.; Takemoto, Y. *Organic Letters* **2004,** *6*, 625-627.
160. Wang, J.; Li, H.; Yu, X. H.; Zu, L. S.; Wang, W. *Organic Letters* **2005,** *7*, 4293-4296.
161. Wang, J.; Li, H.; Duan, W. H.; Zu, L. S.; Wang, W. *Organic Letters* **2005,** *7*, 4713-4716.
162. Tsogoeva, S. B.; Yalalov, D. A.; Hateley, M. J.; Weckbecker, C.; Huthmacher, K. *European Journal of Organic Chemistry* **2005,** *2005*, 4995-5000.
163. Yalalov, D. A.; Tsogoeva, S. B.; Schmatz, S. *Advanced Synthesis & Catalysis* **2006,** *348*, 826-832.
164. Robiette, R.; Aggarwal, V. K.; Harvey, J. N. *Journal of the American Chemical Society* **2007,** *129*, 15513-15525.
165. Berkessel, A.; Roland, K.; Neudorfl, J. M. *Organic Letters* **2006,** *8*, 4195-4198.
166. Yuan, K.; Zhang, L.; Song, H.-L.; Hu, Y.; Wu, X.-Y. *Tetrahedron Letters* **2008,** *49*, 6262.
167. Dong, X. Q.; Teng, H. L.; Wang, C. J. *Organic Letters* **2009,** *11*, 1265-1268.
168. Rho, H. S.; Oh, S. H.; Lee, J. W.; Lee, J. Y.; Chin, J.; Song, C. E. *Chemical Communications* **2008**, 1208-1210.
169. Peschiulli, A.; Gun'ko, Y.; Connon, S. J. *Journal of Organic Chemistry* **2008,** *73*, 2454-2457.
170. Oh, S. H.; Rho, H. S.; Lee, J. W.; Lee, J. E.; Youk, S. H.; Chin, J.; Song, C. E. *Angewandte Chemie-International Edition* **2008,** *47*, 7872-7875.
171. Palacio, C.; Connon, S. J. *Organic Letters* **2011,** *13*, 1298-1301.
172. Tecilla, P.; Chang, S. K.; Hamilton, A. D. *Journal Of The American Chemical Society* **1990,** *112*, 9586-9590.

173. Chang, S. K.; Hamilton, A. D. *Journal of the American Chemical Society* **1988,** *110*, 1318-1319.
174. Hirst, S. C.; Hamilton, A. D. *Journal Of The American Chemical Society* **1991,** *113*, 382-383.
175. McGarraugh, P. G.; Brenner, S. E. *Tetrahedron* **2009,** *65*, 449-455.
176. Tang, Z.; Cun, L.-F.; Cui, X.; Mi, A.-Q.; Jiang, Y.-Z.; Gong, L.-Z. *Organic Letters* **2006,** *8*, 1263-1266.
177. Muñiz, F. M.; Montero, V. A.; Fuentes de Arriba, Á. L.; Simón, L.; Raposo, C.; Morán, J. R. *Tetrahedron Letters* **2008,** *49*, 5050.
178. Malerich, J. P.; Hagihara, K.; Rawal, V. H. *Journal of the American Chemical Society* **2008,** *130*, 14416-+.
179. Zhu, Y.; Malerich, J. P.; Rawal, V. H. *Angewandte Chemie-International Edition* **2010,** *49*, 153-156.
180. Qian, Y.; Ma, G.; Lv, A.; Zhu, H.-L.; Zhao, J.; Rawal, V. H. *Chemical Communications* **2010,** *46*, 3004-3006.
181. Song, H.-L.; Yuan, K.; Wu, X.-Y. *Chemical Communications* **2011,** *47*, 1012-1014.
182. Bondy, C., R., Loeb, Stephen J. *Coordination Chemistry Reviews* **2003,** *240*, 77-99.
183. Morita, K.; Suzuki, Z.; Hirose, H. *Bulletin of the Chemical Society of Japan* **1968,** *41*, 2815-&.
184. Baylis, A. B., Hillman, M.E.D. *Offenlegungsschrift, 2155113* **1972**, US Patent 3,743,669: Chem Abstr, 777, 34197q.
185. Basavaiah, D.; Rao, A. J.; Satyanarayana, T. *Chemical Reviews* **2003,** *103*, 811-892.
186. Hill, J. S., Isaacs, N. S. *Journal of Physical Organic Chemistry* **1990,** *3*, 285 - 288.
187. Leonardo Silva Santos, C. H. P., Wanda P. Almeida, Fernando Coelho, Marcos N. Eberlin. *Angewandte Chemie International Edition* **2004,** *43*, 4330-4333.
188. Ameer, F.; Drewes, S. E.; Freese, S.; Kaye, P. T. *Synthetic Communications* **1988,** *18*, 495-500.
189. Aggarwal, V. K.; Fulford, S. Y.; Lloyd-Jones, G. C. *Angewandte Chemie-International Edition* **2005,** *44*, 1706-1708.
190. Price, K. E.; Broadwater, S. J.; Jung, H. M.; McQuade, D. T. *Organic Letters* **2005,** *7*, 147-150.
191. Roy, D.; Sunoj, R. B. *Organic Letters* **2007,** *9*, 4873-4876.
192. Roy, D.; Sunoj, R. B. *Chemistry-a European Journal* **2008,** *14*, 10530-10534.
193. Roy, D.; Patel, C.; Sunoj, R. B. *Journal of Organic Chemistry* **2009,** *74*, 6936-6943.
194. Price, K. E.; Broadwater, S. J.; Walker, B. J.; McQuade, D. T. *Journal of Organic Chemistry* **2005,** *70*, 3980-3987.
195. Cantillo, D.; Kappe, C. O. *Journal of Organic Chemistry* **2010,** *75*, 8615-8626.
196. Kinsella, M., Lennon, C. *Unpublished Results* **2007**.
197. Lee, H.-J.; Choi, Y.-S.; Lee, K.-B.; Park, J.; Yoon, C.-J. *The Journal of Physical Chemistry A* **2002,** *106*, 7010-7017.
198. Berkessel, A.; Koch, B.; Lex, J. *Advanced Synthesis & Catalysis* **2004,** *346*, 1141-1146.
199. Cobb, A. J. A.; Shaw, D. M.; Longbottom, D. A.; Gold, J. B.; Ley, S. V. *Organic & Biomolecular Chemistry* **2005,** *3*, 84-96.
200. Connors, K. A. *Binding Constants*; John Wiley & Sons: New York, 1987.
201. Fielding, L. *Tetrahedron* **2000,** *56*, 6151-6170.
202. Hynes, M. J. *Journal Of The Chemical Society-Dalton Transactions* **1993,** *2*, 311.
203. Huang, C. Y. *Methods in Enzymology* **1982,** *87*, 509-525.
204. Larocca, J. P., Sharkawi, M. A. Y. *Journal of Pharmaceutical Sciences* **1967,** *56*, 916-918.
205. Ozturk, T., Ertas, E., Mert, O. *Chemical Reviews* **2007,** *107*, 5210-5278.
206. Cava, M. P., Levinson, M. I. *Tetrahedron* **1985,** *41*, 5061-5087.
207. Wipt, P. *Handbook of Reagents for Organic Synthesis: reagents for high-throughput solid-phase and solution-phase organic synthesis*: Chicester, 2005.
208. Albrecht Berkessel, B. K. J. L.*: Advanced Synthesis & Catalysis*.
209. Abraham, M. H. *Chemical Society Reviews* **1993,** *22*, 73-83.
210. Sambrook, M. R.; Beer, P. D.; Wisner, J. A.; Paul, R. L.; Cowley, A. R.; Szemes, F.; Drew, M. G. B. *Journal of the American Chemical Society* **2005,** *127*, 2292-2302.

211. Cook, J. L.; Hunter, C. A.; Low, C. M. R.; Perez-Velasco, A.; Vinter, J. G. *Angewandte Chemie-International Edition* **2007,** *46*, 3706-3709.
212. Huheey, J. E., Keiter, E.A., Keiter, R.L. *Inorganic Chemistry*; Harper-Collins: New York, 1993.
213. Pfeffer, F. M.; Kruger, P. E.; Gunnlaugsson, T. *Organic & Biomolecular Chemistry* **2007,** *5*, 1894-1902.
214. X-ray structure determination was conducted by Dr S.E. Lawrence, Department of Chemistry, U.C.C.
215. Lowe, A. J.; Pfeffer, F. M. *Organic & Biomolecular Chemistry* **2009,** *7*, 4233-4240.
216. X-ray structure determination was conducted by Dr S.E. Lawrence, Department of Chemistry, U.C.C.
217. Kane, R. *Ann. Phys. Chem., Ser 2* **1838,** *44*, 475.
218. Wurtz, A. *Bulletin de la Societe Chimique de France* **1872,** *17*, 436-442.
219. Sukumaran, J.; Hanefeld, U. *Chemical Society Reviews* **2005,** *34*, 530-542.
220. Zhu, X. Y.; Tanaka, F.; Hu, Y. F.; Heine, A.; Fuller, R.; Zhong, G. F.; Olson, A. J.; Lerner, R. A.; Barbas, C. F.; Wilson, I. A. *Journal of Molecular Biology* **2004,** *343*, 1269-1280.
221. Trost, B. M.; Brindle, C. S. *Chemical Society Reviews* **2010,** *39*, 1600-1632.
222. Machajewski, T. D.; Wong, C. H. *Angewandte Chemie-International Edition* **2000,** *39*, 1352-1374.
223. Smith, A. B.; Kingerywood, J.; Leenay, T. L.; Nolen, E. G.; Sunazuka, T. *Journal of the American Chemical Society* **1992,** *114*, 1438-1449.
224. Danishefsky, S.; Cain, P. *Journal of the American Chemical Society* **1976,** *98*, 4975-4983.
225. Pidathala, C.; Hoang, L.; Vignola, N.; List, B. *Angewandte Chemie International Edition* **2003,** *42*, 2785-2788.
226. Chandler, C. L.; List, B. *Journal of the American Chemical Society* **2008,** *130*, 6737-6739.
227. List, B. *Tetrahedron* **2002,** *58*, 5573-5590.
228. Guillena, G.; Najera, C.; Ramon, D. J. *Tetrahedron-Asymmetry* **2007,** *18*, 2249-2293.
229. List, B.; Pojarliev, P.; Castello, C. *Organic Letters* **2001,** *3*, 573-575.
230. Notz, W.; List, B. *Journal of the American Chemical Society* **2000,** *122*, 7386-7387.
231. Peng, L.; Liu, H.; Zhang, T.; Zhang, F.; Mei, T.; Li, Y.; Li, Y. *Tetrahedron Letters* **2003,** *44*, 5107-5108.
232. Sakthivel, K.; Notz, W.; Bui, T.; Barbas, C. F. *Journal of the American Chemical Society* **2001,** *123*, 5260-5267.
233. Casas, J.; Sundén, H.; Córdova, A. *Tetrahedron Letters* **2004,** *45*, 6117.
234. Pihko, P. M.; Laurikainen, K. M.; Usano, A.; Nyberg, A. I.; Kaavi, J. A. *Tetrahedron* **2006,** *62*, 317-328.
235. Sun, B.; Peng, L.; Chen, X.; Li, Y.; Li, Y.; Yamasaki, K. *Tetrahedron: Asymmetry* **2005,** *16*, 1305-1307.
236. Zotova, N.; Broadbelt, L. J.; Armstrong, A.; Blackmond, D. G. *Bioorganic & Medicinal Chemistry Letters* **2009,** *19*, 3934-3937.
237. Bock, D. A.; Lehmann, C. W.; List, B. *Proceedings of the National Academy of Sciences of the United States of America* **2010,** *107*, 20636-20641.
238. Seebach, D.; Beck, A. K.; Badine, D. M.; Limbach, M.; Eschenmoser, A.; Treasurywala, A. M.; Hobi, R.; Prikoszovich, W.; Linder, B. *Helvetica Chimica Acta* **2007,** *90*, 425-471.
239. Zotova, N.; Franzke, A.; Armstrong, A.; Blackmond, D. G. *Journal of the American Chemical Society* **2007,** *129*, 15100-+.
240. Penhoat, M.; Barbry, D.; Rolando, C. *Tetrahedron Letters* **2011,** *52*, 159-162.
241. List, B., Lerner, R. A., Barbas, C. F. *Journal Of The American Chemical Society* **2000,** *122*, 2395-2396.
242. Fache, F.; Piva, O. *Tetrahedron-Asymmetry* **2003,** *14*, 139-143.
243. Shen, Z. X.; Chen, W. H.; Jiang, H.; Ding, Y.; Luo, X. Q.; Zhang, Y. W. *Chirality* **2005,** *17*, 119-120.
244. Bellis, E.; Kokotos, G. *Tetrahedron* **2005,** *61*, 8669-8676.
245. Hayashi, Y.; Sumiya, T.; Takahashi, J.; Gotoh, H.; Urushima, T.; Shoji, M. *Angewandte Chemie-International Edition* **2006,** *45*, 958-961.
246. Raj, M.; Vishnumaya; Ginotra, S. K.; Singh, V. K. *Organic Letters* **2006,** *8*, 4097-4099.

247. Zhang, F. L.; Peng, Y. Y.; Liao, S. H.; Gong, Y. F. *Tetrahedron* **2007,** *63*, 4636-4641.
248. Dodda, R.; Zhao, C. G. *Organic Letters* **2006,** *8*, 4911-4914.
249. Tang, Z.; Jiang, F.; Yu, L.-T.; Cui, X.; Gong, L.-Z.; Mi, A.-Q.; Jiang, Y.-Z.; Wu, Y.-D. *Journal of the American Chemical Society* **2003,** *125*, 5262-5263.
250. Tang, Z.; Jiang, F.; Cui, X.; Gong, L. Z.; Mi, A. Q.; Jiang, Y. Z.; Wu, Y. D. *Proceedings Of The National Academy Of Sciences Of The United States Of America* **2004,** *101*, 5755-5760.
251. Chimni, S. S.; Mahajan, D.; Babu, V. V. S. *Tetrahedron Letters* **2005,** *46*, 5617-5619.
252. Tang, Z.; Yang, Z. H.; Chen, X. H.; Cun, L. F.; Mi, A. Q.; Jiang, Y. Z.; Gong, L. Z. *Journal of the American Chemical Society* **2005,** *127*, 9285-9289.
253. Chimni, S. S.; Mahajan, D. *Tetrahedron-Asymmetry* **2006,** *17*, 2108-2119.
254. Jiang, M.; Zhu, S. F.; Yang, Y.; Gong, L. Z.; Zhou, X. G.; Zhou, Q. L. *Tetrahedron-Asymmetry* **2006,** *17*, 384-387.
255. Russo, A.; Botta, G.; Lattanzi, A. *Synlett* **2007**, 795-799.
256. Russo, A.; Botta, G.; Lattanzi, A. *Tetrahedron* **2007,** *63*, 11886-11892.
257. Chen, J. R.; An, X. L.; Zhu, X. Y.; Wang, X. F.; Xiao, W. J. *Journal of Organic Chemistry* **2008,** *73*, 6006-6009.
258. Schwab, R. S.; Galetto, F. Z.; Azeredo, J. B.; Braga, A. L.; Ludtke, D. S.; Paixao, M. W. *Tetrahedron Letters* **2008,** *49*, 5094-5097.
259. Sato, K.; Kuriyama, M.; Shimazawa, R.; Morimoto, T.; Kakiuchi, K.; Shirai, R. *Tetrahedron Letters* **2008,** *49*, 2402-2406.
260. Moorthy, J. N.; Saha, S. *European Journal of Organic Chemistry* **2009**, 739-748.
261. Zhao, J.-F.; He, L.; Jiang, J.; Tang, Z.; Cun, L.-F.; Gong, L.-Z. *Tetrahedron Letters* **2008,** *49*, 3372-3375.
262. Fu, S. D.; Fu, X. K.; Zhang, S. P.; Zou, X. C.; Wu, X. J. *Tetrahedron-Asymmetry* **2009,** *20*, 2390-2396.
263. Zhang, S.-p.; Fu, X.-k.; Fu, S.-d. *Tetrahedron Letters* **2009,** *50*, 1173-1176.
264. Okuyama, Y.; Nakano, H.; Watanabe, Y.; Makabe, M.; Takeshita, M.; Uwai, K.; Kabuto, C.; Kwon, E. *Tetrahedron Letters* **2009,** *50*, 193-197.
265. Luo, S.; Xu, H.; Li, J.; Zhang, L.; Mi, X.; Zheng, X.; Cheng, J. P. *Tetrahedron* **2007,** *63*, 11307-11314.
266. Gryko, D.; Lipinski, R. *European Journal Of Organic Chemistry* **2006**, 3864-3876.
267. Gryko, D.; Zimnicka, M.; Lipinski, R. *Journal Of Organic Chemistry* **2007,** *72*, 964-970.
268. Wang, B.; Liu, X. W.; Liu, L. Y.; Chang, W. X.; Li, J. *European Journal of Organic Chemistry* **2010**, 5951-5954.
269. Gryko, D.; Saletra, W. J. *Organic & Biomolecular Chemistry* **2007,** *5*, 2148-2153.
270. Wang, B.; Chen, G. H.; Liu, L. Y.; Chang, W. X.; Li, J. *Advanced Synthesis & Catalysis* **2009,** *351*, 2441-2448.
271. Samanta, S.; Liu, J. Y.; Dodda, R.; Zhao, C. G. *Organic Letters* **2005,** *7*, 5321-5323.
272. Guillena, G.; del Carmen Hita, M.; Nájera, C. *Tetrahedron: Asymmetry* **2006,** *17*, 729.
273. Guillena, G.; del Carmen Hita, M.; Najera, C. *Tetrahedron-Asymmetry* **2006,** *17*, 1493-1497.
274. Guillena, G.; Hita, M. D.; Najera, C.; Viozquez, S. F. *Journal of Organic Chemistry* **2008,** *73*, 5933-5943.
275. Guizzetti, S.; Benaglia, M.; Raimondi, L.; Celentano, G. *Organic Letters* **2007,** *9*, 1247-1250.
276. Ma, G.-N. Z., Yun-Peng; Shi, Min. *Synthesis* **2007,** *2*.
277. Chen, J.-R., Lu, H.-H., Li, X.-Y., Cheng, L., Wan, J., Xiao, W.-J. *Organic Letters* **2005,** *7*, 4543-4545.
278. Chen, J.-R.; Li, X.-Y.; Xing, X.-N.; Xiao, W.-J. *The Journal of Organic Chemistry* **2006,** *71*, 8198-8202.
279. Guizzetti, S.; Benaglia, M.; Pignataro, L.; Puglisi, A. *Tetrahedron-Asymmetry* **2006,** *17*, 2754-2760.
280. Guillena, G.; Najera, C.; Viozquez, S. F. *Synlett* **2008**, 3031-3035.
281. Aratake, S.; Itoh, T.; Okano, T.; Nagae, N.; Sumiya, T.; Shoji, M.; Hayashi, Y. *Chemistry-a European Journal* **2007,** *13*, 10246-10256.

282. Jia, Y. N.; Wu, F. C.; Ma, X.; Zhu, G. J.; Da, C. S. *Tetrahedron Letters* **2009,** *50*, 3059-3062.

283. Fotaras, S.; Kokotos, C. G.; Tsandi, E.; Kokotos, G. *European Journal of Organic Chemistry* **2011**, 1310-1317.

284. Tzeng, Z. H.; Chen, H. Y.; Huang, C. T.; Chen, K. M. *Tetrahedron Letters* **2008,** *49*, 4134-4137.

285. Kokotos, G., Bellis, Evagelos, Vasilatou, Konstantina, . *Synthesis* **2005,** *14*, 2407-2413.

286. Wu, Y. Y.; Zhang, Y. Z.; Yu, M. L.; Zhao, G.; Wang, S. W. *Organic Letters* **2006,** *8*, 4417-4420.

287. Yang, H.; Carter, R. G. *Organic Letters* **2008,** *10*, 4649-4652.

288. Yang, H.; Mahapatra, S.; Cheong, P. H. Y.; Carter, R. G. *Journal of Organic Chemistry* **2010,** *75*, 7279-7290.

289. Geary, L. M.; Hultin, P. G. *Tetrahedron: Asymmetry* **2009,** *20*, 131-173.

290. Li-Hua, Q.; Zong-Xuan, S.; Chang-Qing, S.; Yan-Hua, L.; Ya-Wen, Z. *Chinese Journal of Chemistry* **2005,** *23*, 584-588.

291. Xu, X. Y.; Tang, Z.; Wang, Y. Z.; Luo, S. W.; Cun, L. F.; Gong, L. Z. *Journal of Organic Chemistry* **2007,** *72*, 9905-9913.

292. Wang, F.; Xiong, Y.; Liu, X.; Feng, X. *Advanced Synthesis & Catalysis* **2007,** *349*, 2665-2668.

293. Hara, N.; Tamura, R.; Funahashi, Y.; Nakamura, S. *Organic Letters* **2011,** *13*, 1662-1665.

294. Suzuki, H.; Morita, H.; Shiro, M.; Kobayashi, J. *Tetrahedron* **2004,** *60*, 2489-2495.

295. Kitajima, M.; Mori, I.; Arai, K.; Kogure, N.; Takayama, H. *Tetrahedron Letters* **2006,** *47*, 3199-3202.

296. Suarez-Castillo, O. R.; Sanchez-Zavala, M.; Melendez-Rodriguez, M.; Castelan-Duarte, L. E.; Morales-Rios, M. S.; Joseph-Nathan, P. *Tetrahedron* **2006,** *62*, 3040-3051.

297. Goehring, R. R.; Sachdeva, Y. P.; Pisipati, J. S.; Sleevi, M. C.; Wolfe, J. F. *Journal of the American Chemical Society* **1985,** *107*, 435-443.

298. Labroo, R. B.; Cohen, L. A. *Journal of Organic Chemistry* **1990,** *55*, 4901-4904.

299. Rasmussen, H. B.; MacLeod, J. K. *Journal of Natural Products* **1997,** *60*, 1152-1154.

300. Albrecht, B. K.; Williams, R. M. *Organic Letters* **2003,** *5*, 197-200.

301. Guan, X. Y.; Wei, Y.; Shi, M. *Chemistry-a European Journal* **2010,** *16*, 13617-13621.

302. Kawasaki, T.; Nagaoka, M.; Satoh, T.; Okamoto, A.; Ukon, R.; Ogawa, A. *Tetrahedron* **2004,** *60*, 3493-3503.

303. Kohno, J.; Koguchi, Y.; Niskio, M.; Nakao, K.; Kuroda, M.; Shimizu, R.; Ohnuki, T.; Komatsubara, S. *Journal of Organic Chemistry* **2000,** *65*, 990-995.

304. Tang, Y. Q.; Sattler, I.; Thiericke, R.; Grabley, S.; Feng, X. Z. *European Journal of Organic Chemistry* **2001**, 261-267.

305. Tokunaga, T.; Hume, W. E.; Umezome, T.; Okazaki, K.; Ueki, Y.; Kumagai, K.; Hourai, S.; Nagamine, J.; Seki, H.; Taiji, M.; Noguchi, H.; Nagata, R. *Journal of Medicinal Chemistry* **2001,** *44*, 4641-4649.

306. Li, Y. M.; Zhang, Z. K.; Jia, Y. T.; Shen, Y. M.; He, H. M.; Fang, R. X.; Chen, X. Y.; Hao, X. J. *Plant Biotechnology Journal* **2008,** *6*, 301-308.

307. Lee, S.; Hartwig, J. F. *Journal of Organic Chemistry* **2001,** *66*, 3402-3415.

308. Shibata, N.; Tarui, T.; Doi, Y.; Kirk, K. L. *Angewandte Chemie-International Edition* **2001,** *40*, 4461-+.

309. Nakamura, T.; Shirokawa, S.; Hosokawa, S.; Nakazaki, A.; Kobayashi, S. *Organic Letters* **2006,** *8*, 677-679.

310. Guo, X.; Huang, H. X.; Yang, L. P.; Hu, W. H. *Organic Letters* **2007,** *9*, 4721-4723.

311. Malkov, A. V.; Kabeshov, M. A.; Bella, M.; Kysilka, O.; Malyshev, D. A.; Pluhackova, K.; Kocovsky, P. *Organic Letters* **2007,** *9*, 5473-5476.

312. Luppi, G.; Monari, M.; Correa, R. J.; Violante, F. D.; Pinto, A. C.; Kaptein, B.; Broxterman, Q. B.; Garden, S. J.; Tomasini, C. *Tetrahedron* **2006,** *62*, 12017-12024.

313. Chen, G.; Wang, Y.; He, H. P.; Gao, S.; Yang, X. S.; Hao, X. J. *Heterocycles* **2006,** *68*, 2327-2333.

314. Chen, J. R.; Liu, X. P.; Zhu, X. Y.; Li, L.; Qiao, Y. F.; Zhang, J. M.; Xiao, W. J. *Tetrahedron* **2007,** *63*, 10437-10444.

315. Nakamura, S.; Hara, N.; Nakashima, H.; Kubo, K.; Shibata, N.; Toru, T. *Chemistry - A European Journal* **2008,** *14*, 8079-8081.

316. Adachi, S.; Harada, T. *European Journal of Organic Chemistry* **2009,** *2009*, 3661-3671.

317. Raj, M.; Veerasamy, N.; Singh, V. K. *Tetrahedron Letters* **2010,** *51*, 2157-2159.

318. Luppi, G.; Cozzi, P. G.; Monari, M.; Kaptein, B.; Broxterman, Q. B.; Tomasini, C. *Journal Of Organic Chemistry* **2005,** *70*, 7418-7421.

319. Angelici, G.; Corrêa, R. J.; Garden, S. J.; Tomasini, C. *Tetrahedron Letters* **2009,** *50*, 814.

320. Nakamura, S.; Hara, N.; Nakashima, H.; Kubo, K.; Shibata, N.; Toru, T. *Chemistry-A European Journal* **2008,** *14*, 8079-8081.

321. Hara, N.; Nakamura, S.; Shibata, N.; Toru, T. *Chemistry-a European Journal* **2009,** *15*, 6790-6793.

322. Correa, R. J.; Garden, S. J.; Angelici, G.; Tomasini, C. *European Journal of Organic Chemistry* **2008**, 736-744.

323. Itoh, T.; Ishikawa, H.; Hayashi, Y. *Organic Letters* **2009,** *11*, 3854-3857.

324. Chen, W. B.; Du, X. L.; Cun, L. F.; Zhang, X. M.; Yuan, W. C. *Tetrahedron* **2010,** *66*, 1441-1446.

325. da Silva, J. F. M.; Garden, S. J.; Pinto, A. C. *Journal Of The Brazilian Chemical Society* **2001,** *12*, 273-U286.

326. Popp, F. D.; Donigan, B. E. *Journal of Pharmaceutical Sciences* **1979,** *68*, 519-520.

327. Shen, C.; Shen, F. Y.; Xia, H. J.; Zhang, P. F.; Chen, X. Z. *Tetrahedron-Asymmetry* **2011,** *22*, 708-712.

328. Peng, L.; Wang, L. L.; Bai, J. F.; Jia, L. N.; Yang, Q. C.; Huang, Q. C.; Xu, X. Y.; Wang, L. X. *Tetrahedron Letters* **2011,** *52*, 1157-1160.

329. Basavaiah, D.; Rao, K. V.; Reddy, R. J. *Chemical Society Reviews* **2007,** *36*, 1581-1588.

330. Garden, S. J.; Skakle, J. M. S. *Tetrahedron Letters* **2002,** *43*, 1969-1972.

331. Shanmugam, P.; Vaithiyanathan, V.; Viswambharan, B. *Tetrahedron* **2006,** *62*, 4342-4348.

332. Liu, Y. L.; Wang, B. L.; Cao, J. J.; Chen, L.; Zhang, Y. X.; Wang, C.; Zhou, J. A. *Journal of the American Chemical Society* **2010,** *132*, 15176-15178.

333. Zhong, F. R.; Chen, G. Y.; Lu, Y. X. *Organic Letters* **2011,** *13*, 82-85.

334. Rodrigo J. Corrêa, S. J. G. G. A. C. T. *European Journal of Organic Chemistry* **2008,** *2008*, 736-744.

335. Geib, S. J.; Vicent, C.; Fan, E.; Hamilton, A. D. *Angewandte Chemie-International Edition in English* **1993,** *32*, 119-121.

336. Kinsella, M.; Duggan, P. G.; Muldoon, J.; Eccles, K. S.; Lawrence, S. E.; Lennon, C. M. *European Journal of Organic Chemistry* **2011,** *2011*, 1125-1132.

337. Dahlin, N.; Bøgevig, A.; Adolfsson, H. *Advanced Synthesis & Catalysis* **2004,** *346*, 1101-1105.

338. Wang, J., Li, H., Lou, B., Zu, L., Guo, H., Wang, W. *Chemistry-A European Journal* **2006,** *12*, 4321-4332.

339. Burch, R. M., Patch, R. J., Shearer, B. G., Perumattam, J.J., Natalie, K.J. *Jr (Nova Pharmaceutical Corp, USA)* **1992,** *WO 9203415*.

340. Brown, H. C., Heim, P. *journal Of The American Chemical Society* **1964,** *86*, 3566-3567.

341. Park, S. H.; Kang, H. J.; Ko, S.; Park, S.; Chang, S. *Tetrahedron: Asymmetry* **2001,** *12*, 2621.

342. Amedio, J. C.; Bernard, P. J.; Fountain, M.; Van Wagenen, G. *Synthetic Communications* **1999,** *29*, 2377-2391.

343. Couturier, M.; Andresen, B. M.; Jorgensen, J. B.; Tucker, J. L.; Busch, F. R.; Brenek, S. J.; Dube, P.; am Ende, D. J.; Negri, J. T. *Organic Process Research & Development* **2002,** *6*, 42-48.

344. Wolf, C.; Villalobos, C. N.; Cummings, P. G.; Kennedy-Gabb, S.; Olsen, M. A.; Trescher, G. *Journal of the American Society for Mass Spectrometry* **2005,** *16*, 553-564.

345. Wagger, J.; Groselj, U.; Meden, A.; Svete, J.; Stanovnik, B. *Tetrahedron* **2008,** *64*, 2801-2815.

346. Messerer, M.; Wennemers, H. *Synlett* **2011**, 499-502.

347. Sewald, N.; Jakubke, H. D. *Peptides: chemistry and biology*; Wiley-VCH, 2009.

348. pKa data compiled by Williams: http://research.chem.psu.edu.bprgroup/pKa_compilation.pdf

349. He, L.; Tang, Z.; Cun, L. F.; Mi, A. Q.; Jiang, Y. Z.; Gong, L. Z. *Tetrahedron* **2006,** *62*, 346-351.

350. Yang, H.; Carter, R. G. *Synlett* **2010**, 2827-2838.

351. Determined by 1H NMR

352. Guizzetti, S.; Benaglia, M.; Puglisi, A.; Raimondi, L. *Synthetic Communications* **2009,** *39*, 3731-3742.

353. Yuriev, E.; Kong, D. C. M.; Iskander, M. N. *European Journal of Medicinal Chemistry* **2004,** *39*, 835-847.

354. Maleev, V. I.; Gugkaeva, Z. T.; Moskalenko, M. A.; Tsaloev, A. T.; Lyssenko, K. A. *Russian Chemical Bulletin* **2009,** *58*, 1903-1907.

355. Morris, D. J.; Partridge, A. S.; Manville, C. V.; Racys, D. T.; Woodward, G.; Docherty, G.; Wills, M. *Tetrahedron Letters* **2010,** *51*, 209-212.

356. Fanfoni, L.; Meduri, A.; Zangrando, E.; Castillon, S.; Felluga, F.; Milani, B. *Molecules* **2011,** *16*, 1804-1824.

357. Banerjee, M.; Das, S.; Yoon, M.; Choi, H. J.; Hyun, M. H.; Park, S. M.; Seo, G.; Kim, K. *Journal of the American Chemical Society* **2009,** *131*, 7524-+.

358. Reddy, B. V. S.; Bhavani, K.; Raju, A.; Yadav, J. S. *Tetrahedron-Asymmetry* **2011,** *22*, 881-886.

359. Xu, Z. H.; Daka, P.; Budik, I.; Wang, H.; Bai, F. Q.; Zhang, H. X. *European Journal of Organic Chemistry* **2009**, 4581-4585.

360. Doherty, S.; Knight, J. G.; McRae, A.; Harrington, R. W.; Clegg, W. *European Journal of Organic Chemistry* **2008**, 1759-1766.

361. de Arriba, A. L. F.; Simon, L.; Raposo, C.; Alcazar, V.; Moran, J. R. *Tetrahedron* **2009,** *65*, 4841-4845.

Appendix I

Publications

Synthesis and NMR Binding Studies towards Rational Design of a Series of Electron-Withdrawing Diamide Receptors/Organocatalysts

Michael Kinsella,[a] Patrick G. Duggan,[a] Jimmy Muldoon,[b] Kevin S. Eccles,[c] Simon E. Lawrence,[c] and Claire M. Lennon*[a]

A related series of bisamides have been evaluated for rational correlation between anion complexation and organocatalysis: remarkable enhancement of hydrogen bonding to anions was observed along with significant increases in catalytic activity in the Baylis–Hillman reaction. In addition, X-ray crystallography showed a large degree of pre-organisation was observed in one receptor by incorporation of bis-(trifluoromethyl)aniline groups along with a thioamide functionality. A novel bifunctional amide/N-acylsulfonamide within the series gave the best catalytic profile.

Introduction

The recognition of anions is an ever-expanding field.[1] Many hosts incorporating functional groups such as indoles, pyrroles, sulfonamides, ureas and amides have been successful in selectively complexing a range of anionic guests via hydrogen bonding.[2] Often, these receptor molecules are designed with some degree of pre-organisation in mind, for example creating a cleft-like structure.[3,4] The use of metal-free organic molecules to catalyse reactions has also received intense interest.[5] The catalytic activity of several such organocatalysts involves coordination of groups such as those listed above via hydrogen bonding to highly negative or anionic intermediates.[6] Considering a major objective of both receptor and organocatalyst design is the molecular recognition of anions, much can be gained from taking a cooperative view between both areas, giving rise to the potential of dual application of molecular receptors for anion recognition and organocatalysis.[7]

Our interest lies in the rational design of receptors for selective anion binding and catalysis, specifically reactions where hydrogen bonding and electrophile activation play key mechanistic roles. Instead of the lengthy and potentially troublesome synthesis of transition state analogues for binding studies, we look to the binding characteristics of our target receptors with anions as a guide to catalytic mechanisms and in some cases, use anion binding properties as a mechanistic probe into organic reactions.

Results and Discussion

We assessed compounds **1**–**7** (Figure 1), based on the simple, flexible, minimally pre-organised motif first evaluated by Crabtree for anion binding, using binding characteristics to predict their applicability as efficient organic catalysts.[8] The well known receptor building blocks of iso-
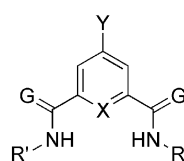
1: X = CH; G = O; Y = H;   R = *n*Bu
2: X = CH; G = O; Y = H;   R = 4-(CF$_3$)C$_6$H$_4$
3: X = CH; G = O; Y = H;   R = 3,5-(CF$_3$)$_2$C$_6$H$_3$
4: X = N; G = O; Y = H;   R = 3,5-(CF$_3$)$_2$C$_6$H$_3$
5: X = CH; G = S; Y = H;   R = 3,5-(CF$_3$)$_2$C$_6$H$_3$
6: X = CH; G = O; Y = NO$_2$; R = 3,5-(CF$_3$)$_2$C$_6$H$_3$
7: X = CH; G = O; Y = H; R = 3,5-(CF$_3$)$_2$C$_6$H$_3$; R' = SO$_2$3,5-(CF$_3$)$_2$C$_6$H$_3$

Figure 1. Structure of receptors **1**–**7** and their possible conformations.[11]

[a] Pharmaceutical and Molecular Biotechnology Research Centre, Department of Chemical and Life Sciences, Waterford Institute of Technology, Waterford, Ireland
Fax: +353-51-302679
E-mail: clennon@wit.ie
[b] Centre for Synthesis and Chemical Biology, School of Chemistry and Chemical Biology, University College Dublin, Belfield, Dublin 4, Ireland
[c] Department of Chemistry, Analytical and Biological Chemistry Research Facility, University College Cork, College Road, Cork, Ireland
Supporting information for this article is available on the WWW under http://dx.doi.org/10.1002/ejoc.201001439.

phthalic acid and 2,6-pyridinedicarboxylic acid[8] were used to generate a series of open-cleft bisamides **2–7** while **1** was used as a reference starting point.[9,10]

Each receptor differed by the nature of the groups attached to the amide skeleton, altering amide acidity and structural rigidity. To increase the acidity of the amide N–H groups and therefore increase hydrogen bonding,[12,13] the highly electron-withdrawing 4-trifluoromethylphenyl group (see **2**), 3,5-bis(trifluoromethyl)phenyl group (see **3–7**)[12] and also an additional *p*-nitro group (see **6**) were incorporated into the diamide structure. In addition, receptor **4** was designed to hold a degree of cleft pre-organisation and was expected to preferentially exist in the *syn-syn* conformation (Figure 1) most suitable for binding.[11,14] To circumvent the H-bond accepting properties of amides,[15] thioamide **5**, which is less likely to self associate[16] was also evaluated. This receptor might exist in the *syn–syn* conformation due to intramolecular interactions between acidic aromatic C–H groups and the sulfur atom as observed for some thiourea molecules.[13] Finally, a bifunctional hybrid amide/*N*-acyl-sulfonamide **7** was prepared incorporating both increased hydrogen bond donating properties and also the possibility to deprotonate the sulfonyl N–H; a potentially useful feature where proton transfer may occur and/or where activation of an electrophile plays a key role in the catalytic cycle.[17,18] In this paper, we report the synthesis, comparative anion binding properties, X-ray structure of **5** and preliminary catalytic and kinetic results in the Baylis–Hillman reaction.[19]

Receptor **1** was prepared according to literature procedures[20] while **2–6** were synthesised in a single step in good yields from commercially available starting materials. A four step synthetic sequence was employed for **7** (Scheme 1).

Initial binding studies conducted in CDCl$_3$ indicated strong association but were hindered by low solubility in some cases; therefore CD$_3$CN was used for further studies. The anion complexation properties were evaluated with tetra-*n*-butylammonium salts of bromide, chloride, acetate and benzoate. These anions represent different topologies (spherical vs. coplanar) and sizes and were chosen to give good indications of receptor selectivity and catalytic potential.

Standard ^{1}H NMR titration in CD$_3$CN at 298 K was employed with titration continued up to the addition of 10 equiv. of anion relative to receptor. Stability constants were obtained using the WINEQNMR2 program[21] (Table 1). JOB plot analysis was carried out for all receptors revealing 1:1 binding in most cases. The JOB plot for compound **6** with acetate and chloride possessed a minor contribution from 2:1 receptor: anion stoichiometry as observed by a small shoulder on the plot at 0.65 mol fraction receptor; however 1:1 stoichiometry was deemed to dominate. Interestingly, JOB plot analysis of **7** with chloride and bromide pointed solely to 2:1 receptor: anion stoichiometry. In the cases of **5** and **7** with acetate and benzoate, binding could not be accurately fitted to a 1:1 isotherm. This will be discussed later.

Table 1. Binding constants K_a (M^{-1}) for receptors **1–7** with bromide, chloride, acetate and benzoate as tetrabutylammonium salts at 298 K in CD$_3$CN. K_a values calculated based on N–H proton.

Receptor	Bromide	Chloride	Acetate	Benzoate
1	80	260	920	650
2	700	8,900	4,900	12,100
3	4,700	10,800	14,300	19,200
4	290	3,800	8,700	3,800
5	5,900	17,500	_[a,b]	_[a,b]
6	6,100	11,100	16,600	21,000
7	K_a 1:1 900	K_a 1:1 4,000	_[a,b]	_[a,b]
	K_a 2:1 6,100	K_a 2:1 3,700		

[a] Deprotonation prevented the calculation of an accurate association constant. [b] Did not reliably fit to a 1:1 model.

Receptor **1** was observed to bind all anions with association constants in the range 80–950 M^{-1}. Significantly enhanced anion complexation was found for receptors **2–6**, for example a 73-fold increase in binding strength in the case of **6** with bromide. A second notable example was thioamide **5** with chloride where, a 66-fold increase in K_a
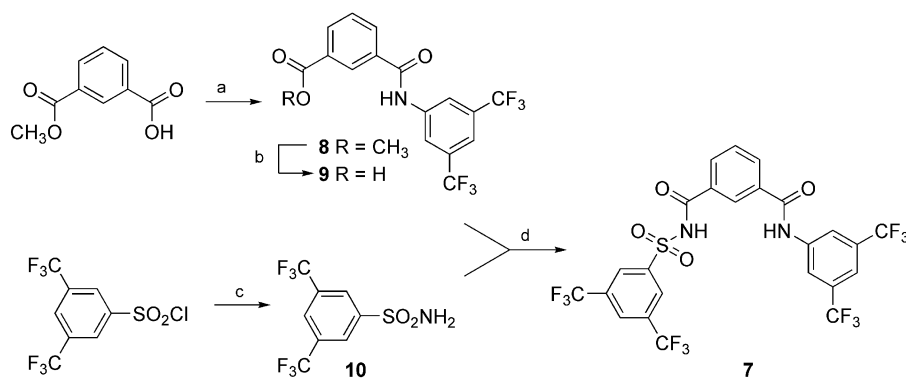
Scheme 1. Synthesis of bifunctional receptor **7**. (a) 3,5-bis(trifluoromethyl)aniline, EDCI, DMAP, dichloromethane, room temp., 16 h, 92% (b) NaOH, methanol, reflux, 1 h, 77% (c) NH$_3$, Et$_3$N, DMF, room temp., 16 h, 98% (d) EDCI, DMAP, 50:50 dichloroethane:*tert*-butyl alcohol, room temp., 16 h, 43%.

was achieved; 17,500 M^{-1} for **5** compared to 260 M^{-1} for **1**. Receptor **6** gave the best 1:1 binding characteristics with strong binding to all anions studied.[22]

In all cases, the receptors were more efficient for chloride than bromide and this was ascribed to differing hydrogen bond capabilities[23] and also the size constraint of bromide as previously observed by Crabtree et al.[8] Receptors **3**, **4** and **6** gave highly efficient binding for the coplanar acetate and benzoate ions, particularly for benzoate with receptors **3** and **6** exhibiting 30- and 33-fold increases respectively in benzoate binding over the control **1**.

When comparing binding affinity for each of the anions with structural variation and amide acidity, **3** yielded significantly enhanced binding constants compared to the mono-trifluoromethyl variant **2**. The more acidic thioamide **5** and also *p*-nitro derivative **6** gave even superior anion binding. However, the less flexible, more pre-organised **4** gave considerably lower K_a values, possibly due to electrostatic repulsion.[8]

Receptor **7** with bromide and chloride produced an excellent fit to a 1:1 and 2:1 receptor: anion species (Table 1).[24] We postulate these high 2:1 receptor: anion K_a values were due to the formation of a stable complex in which one anion is complexed between two receptors, with the higher 2:1 K_a for **7** with bromide ascribed to the large size of the bromide anion better able to accommodate this stoichiometry. Similar binding stoichiometries were previously reported by others.[25]

Receptors **5** and **7** produced interesting titration curves with acetate and benzoate as illustrated in Figure 2. For example in the case of **5** with acetate, the N–H signal disappeared and the titration was tracked using the isophthaloyl H2 proton between the thioamide groups. Initially, a minor upfield shift was observed followed by a significant downfield shift, with a second minor upfield shift upon addition

of 1 equiv. acetate followed by significant downfield migration once again. We suggest this is due to initial desolvation of the receptor,[26] followed by strong hydrogen bonding to the anion, indicated by the subsequent downfield shift. The minor upfield shift at 1 equiv. anion poses two possibilities. With the increased acidity of the thioamide N–H, proton transfer to the carboxylate from the receptor could account for the chemical shift perturbation. Alternatively, the observed behavior may purely be a consequence of changing complex stoichiometries as the titration proceeds which may be facilitated by the more acidic receptor **5**. In either case a subsequent conformational change could allow for further binding events resulting in migration downfield of the H2 signal. Similar behavior was observed in the case of **5** with benzoate.

A similar but more pronounced effect was observed in the case of the more acidic **7** with both acetate and benzoate. As the sulfonyl N–H was not visible in the NMR spectrum, the titration was monitored using the amide N–H proton. Addition of up to 0.5 equiv. anion caused a downfield shift of the N–H resonance. Upon addition of a further 0.5 equiv. anion an upfield shift occurred, with an almost linear downfield migration upon further additions. Furthermore, the isophthaloyl H2 and the H4 protons of the bis(trifluoromethyl)phenyl rings broadened significantly up to addition of 1 equiv. anion but subsequently sharpened. We suggest this was due to an overall equilibrium process involving binding of the first 0.5 equiv. of anion generating a 2:1 receptor:anion complex followed by deprotonation of the highly acidic sulfonyl N–H which is known to have a similar pK_a to carboxylic acids.[17] This equilibrium process may account for the broadened signals up to 1 equiv. anion with the equilibrium driven to a single complexed species by addition of further anion. A conformational change may have occurred following the addition of
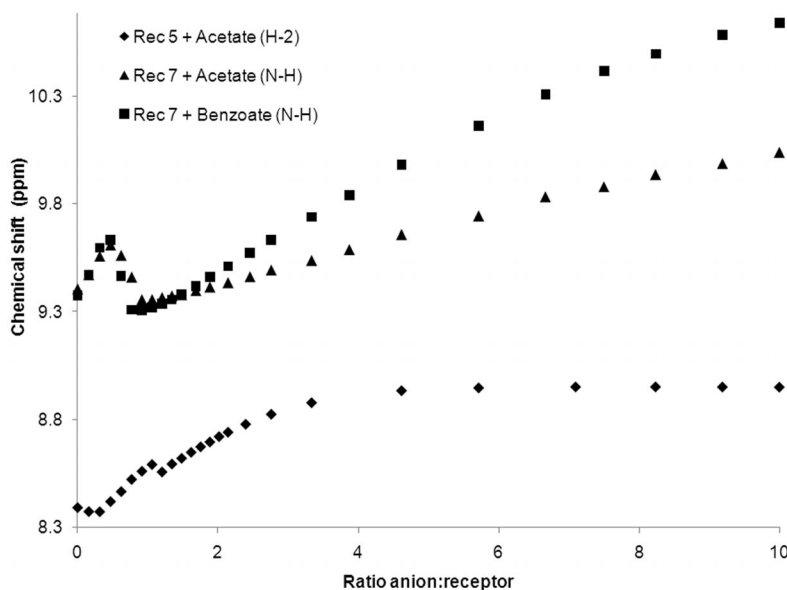
Figure 2. Binding curves of **5** with acetate and **7** with acetate and benzoate.

1 equiv. of anion allowing the amide N–H and isophthaloyl H4 to further bind anionic species. A similar trend involving deprotonation was observed for sulfonamide functionalised urea compounds[27] with evidence of conformational change allowing further binding events reported by Crabtree et al.[8] and Kilburn et al.[28]

In a number of cases, K_a values in excess of 10^4 M^{-1} were obtained for the most efficient receptors **2**, **3**, **5** and **6** with several anions. These titrations were repeated in the more competitive [D$_6$]DMSO and K_a values calculated (Table 2).[21]

Table 2. Binding constants K_a (M^{-1}) for strong binding systems in [D$_6$]DMSO at 298 K. 1:1 stoichiometry was observed in all cases.

Receptor	Chloride	Acetate	Benzoate
2	100	480	160
3	120	1,370	720
5	80	2,700[a]	2,540[a]
6	100	5,200	800

[a] Calculated based on isophthaloyl H2 signal.

For titrations conducted in [D$_6$]DMSO, the receptors appeared to possess a degree of selectivity for acetate, in particular receptor **6**. We suggest the increase in K_a values for **2**–**6** with acetate is linked to the increased acidity of the N–H bond as discussed earlier. Interestingly, **5** appeared to bind strongly to benzoate compared to **2**, **3** and **6**. This may be due to proton transfer as indicated by the broadening and subsequent loss of amide N–H signal after the addition of 1 equiv. of anion. In addition, conformational change is likely to play a role in accommodating the benzoate anion. Overall our results highlight the key role of solvent in binding and selectivity.

Gratifyingly, diffraction grade crystals of **5** (Figure 3) through slow evaporation of a chloroform/methanol mixture revealed its structure, with a crystallographic twofold axis through the middle of the molecule. The two nitrogen atoms are twisted in opposite directions out of the plane to minimise steric conflict and enable hydrogen bonding to a neighboring sulfur atom (Figure 3, b). In addition, **5** was found to exist in the solid state in its *syn-syn* conformation, possibly due to internal interactions with the polarized C–H bonds (H-7) ortho to the CF$_3$ group and the Lewis basic sulfur atom.[13] Further evidence supporting this conformation came from ^{1}H NMR spectroscopy. The chemical shift of this proton (H-7) lay further downfield in the case of thioamide **5** (δ = 8.53 ppm for **5**; 8.38 ppm for **3**), suggesting possible H-bonding interactions. Moreover, the proton *ortho* to both amide moieties (H2) was further upfield for **5** compared to the corresponding proton on **3**. This is in agreement with previously reported similar systems in which isophthaloyl H2 existed most upfield for an isophthalamide in the *syn-syn* conformation.[4] Therefore, it appears that a remarkable level of pre-organisation was achieved in this receptor, comparable to similar preorganisation effects which make some thiourea molecules effective for binding and catalysis.[13]
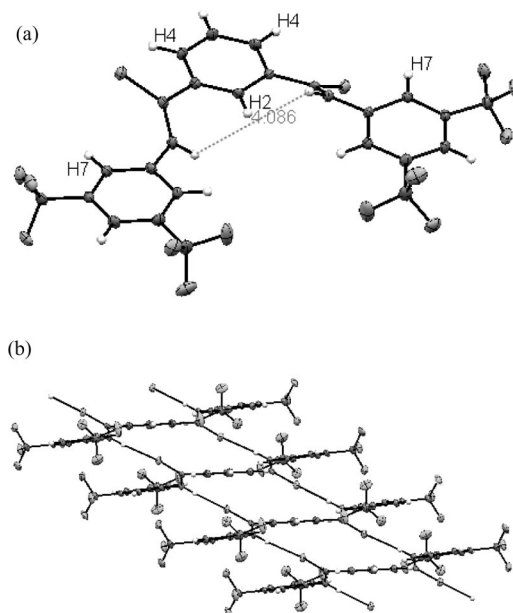
Figure 3. (a) X-ray crystal structure of **5** showing measurements between protons in the proposed anion binding cleft. (b) Crystal packing of **5**.

With the strong affinity of **2**–**7** for the acetate and benzoate anions in particular, they were applied as organocatalysts in the DABCO catalysed Baylis–Hillman reaction of benzaldehyde with methyl acrylate (Scheme 2).[19] It was envisaged that the oxyanion binding ability of these receptors would facilitate the catalysis of this highly useful reaction through stabilisation of the negative oxyanion intermediates of the reaction. In addition possible proton transfer steps could be accelerated by deprotonation of the catalyst as in the case of **5** and **7**.
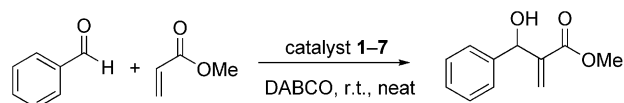
Scheme 2. Baylis–Hillman reaction of methyl acrylate and benzaldehyde.

Initial reactions conducted in acetonitrile gave inferior yields to those under neat reaction conditions (Table 3). Under neat conditions in all cases, yield and rate enhancements were observed. Reaction yield after 20 h was determined after product isolation by column chromatography. A kinetic study by ^{1}H NMR spectroscopy using (*E*)-stilbene as an internal standard was undertaken in order to calculate the rate constant (k_{obs}) during the initial stages of the reaction (< 20% conversion). Receptor **7** gave the largest yield and rate constant, producing a 76% yield, a 2.2-fold increase in product formation, a factor of 3.9 times greater rate constant than the uncatalysed process (Figure 4). In addition, in the case of **7** it was possible to recycle the catalyst 3 times with less than a 5% reduction in catalytic activity.
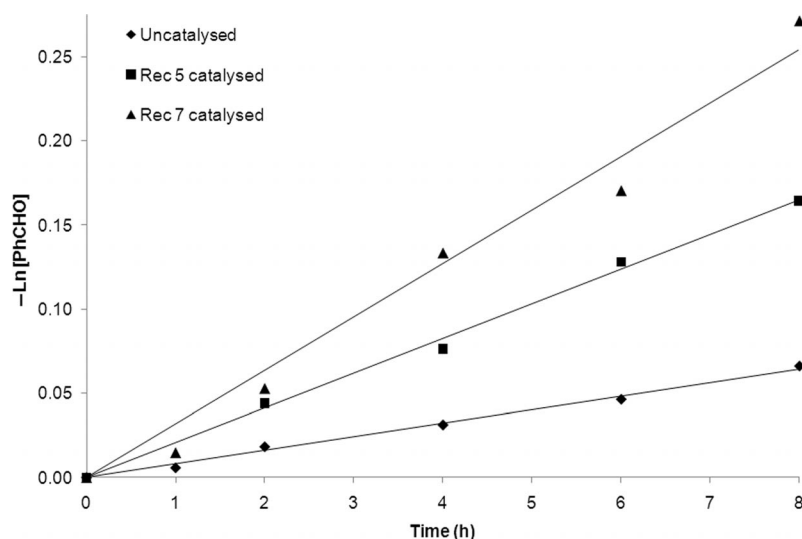
Figure 4. Kinetic plots and least square fits of –Ln[PhCHO] vs. time for receptor **5** and **7** catalysed Baylis–Hillman reaction. The uncatalysed reaction is also shown.

Table 3. Catalysis of Baylis–Hillman reaction of benzaldehyde and methyl acrylate using **1**–**7** as H-bond donating organocatalysts.

Receptor	Yield [%][a]	$k_{obsd} \times 10^{-2}$ [h^{-1}][b]	k_{rel}
Uncatalysed	34	0.82	1
1[c]	44	0.77	0.94
2[c]	50	0.55	0.67
3	68	2.38	2.9
4	_[d]	_[d]	_[d]
5	71	2.5	3.1
6	51	2.68	3.3
7	76	3.19	3.9

[a] Reagents and conditions: benzaldehyde (1 equiv.). DABCO (1 equiv.), methyl acrylate (3 equiv.), catalyst **1**–**7** (20 mol-%), room temp., 20 h. [b] Initial rates (< 20% conversion), 10 equiv. of methyl acrylate used; (E)-stilbene was used as an internal standard for ^{1}H NMR.[30] [c] Poor solubility in kinetic experiment. [d] Not determined due to complete insolubility of **4** in reactants.

We propose that binding of our anion receptors to the negative intermediates in the reaction medium through the N–H group accelerates the reaction. In general, the increase in amide N–H polarisation of the receptor led to enhanced catalytic activity which was consistent with the findings of the binding studies; in the case of **1**, **2** and **3** there was excellent correlation between acetate K_a and catalytic performance. In addition, pre-organisation of the catalytic site of **5** may have contributed to its catalytic success. In the case of **5** and **7** proton transfer as observed in the binding studies along with increased acidity may account for the further increase in yield and reaction rate, particularly in light of reported mechanistic studies.[29]

Receptor **6** produced a disappointing yield of 51%. However, it produced an initial rate constant of 2.68 h^{-1}, slightly higher than that of the more successful catalysts **3**, **5** and **7**. We propose this is linked to strong binding of one of the several anionic species involved in the reaction cycle causing inhibition. This is supported by the earlier binding studies (Table 1).

In addition, kinetic experiments conducted for **3** and **7** in the presence of 1 equiv. of tetra-*n*-butylammonium benzoate resulted in substantially diminished rate constants; 86% and 50% respectively. This was deemed to be due to competition between the anionic intermediates and benzoate for the H-bonding sites of these catalysts.

Table 4. Baylis–Hillman reaction using a variety of substrates and bases catalysed by **7**.

Ar	G	Base	mol-% 7	Time (h)	Yield %[a]
C$_6$H$_5$	OMe	DABCO	–	20	34
C$_6$H$_5$	OMe	DABCO	20	20	76
C$_6$H$_5$	OMe	DMAP	–	20	8
C$_6$H$_5$	OMe	DMAP	20	20	41
C$_6$H$_5$	OMe	DBU	–	20	33
C$_6$H$_5$	OMe	DBU	20	20	34
C$_6$H$_5$	OMe	PPh$_3$	–	20	trace
C$_6$H$_5$	OMe	PPh$_3$	20	20	trace
o-O$_2$NC$_6$H$_4$	OMe	DABCO	–	1	79
o-O$_2$NC$_6$H$_4$	OMe	DABCO	20	1	86
o-MeC$_6$H$_4$	OMe	DABCO	–	42	6
o-MeC$_6$H$_4$	OMe	DABCO	20	42	22
o-MeOC$_6$H$_4$	OMe	DABCO	–	72	6
o-MeOC$_6$H$_4$	OMe	DABCO	20	72	55
p-FC$_6$H$_4$	OMe	DABCO	–	42	69
p-FC$_6$H$_4$	OMe	DABCO	20	42	82
p-MeC$_6$H$_4$	OMe	DABCO	–	36	19
p-MeC$_6$H$_4$	OMe	DABCO	20	36	38
p-MeOC$_6$H$_4$	OMe	DABCO	–	96	4
p-MeOC$_6$H$_4$	OMe	DABCO	20	96	19
C$_6$H$_5$	O-*t*Bu	DABCO	–	20	4
C$_6$H$_5$	O-*t*Bu	DABCO	20	20	28
C$_6$H$_5$	(cyclohexenone)	DABCO	–	38	4
C$_6$H$_5$	(cyclohexenone)	DABCO	20	38	59

[a] Isolated yield after flash chromatography.

Following on from this work, we examined the generality and scope of our most successful catalyst **7**. Initially variation of the base in the reaction of benzaldehyde with methyl acrylate was examined. Triphenylphosphane, DBU and DMAP were evaluated and in all cases inferior yields compared to DABCO were obtained. Subsequently, with the optimum catalyst and base in hand, we examined the substrate scope of the reaction of methyl acrylate with activated and de-activated aldehydes. Finally, reaction of a number of different Michael acceptors with benzaldehyde were investigated. In all cases, **7** afforded significant yield enhancement compared to the uncatalysed reactions (Table 4) with catalytic effect observed for all substrates and Michael acceptors studied.

Considerable yield enhancement was observed in many cases, particularly in systems where deactivated aldehyde derivatives were employed, e.g. a 4.8- and 9.2-fold increase in product formation for deactivated 2- and 4-substituted methoxybenzaldeyde. Another notable example is reaction of benzaldehyde with 2-cyclohexen-1-one, where a 15-fold increase in product formation was observed. It is also worth noting the ease of recoverability of the catalyst in each reaction. The catalyst could be obtained with high purity during the catalytic product isolation step of flash chromatography.

Further catalytic studies are currently underway in our laboratory including application of the receptors in alternative reactions.

Conclusions

To summarise, we synthesised a series of rationally designed diamides and evaluated their properties as anion receptors and organocatalysts in the Baylis–Hillman reaction. Equilibrium binding was determined by NMR titration and catalytic activity was assessed by product yield and kinetic measurements. X-ray crystal structure of receptor **5** also showed an unexpected level of preorganisation within the flexible thioamide motif. The anion binding constants of the receptor series with increasing hydrogen bond donating capability provided a useful tool to probe the catalytic activity of these receptors. Ongoing work in this area involves further structural modification of the motif along with their application to other reactions.

Experimental Section

Synthesis of New Receptors

Receptor 2: To a solution of 4-trifluoromethylaniline (1.60 g, 9.9 mmol) in DMF (30 mL) was added triethylamine (1.52 g, 15 mmol) and DMAP (1.21 g, 9.9 mmol). The reaction mixture was cooled to 0 °C and isophthaloyl dichloride (1 g, 4.9 mmol) was added in small portions over 2–3 min. The solution was stirred at 90 °C for 20 h. After this time the dark brown mixture was added to water (300 mL) and extracted with ethyl acetate (3×50 mL). The combined organic layers were washed with 5% lithium chloride solution (2×80 mL) and deionised water (2×100 mL) to remove DMF. The product was dried with $MgSO_4$ and solvent removed in vacuo. The crude was purified by column chromatog-

raphy, eluting with 80:20 hexane/ethyl acetate. The solvent was removed in vacuo to give **2** (1.20 g, 54%) as a white solid; m.p. 256–258 °C. IR (KBr): $\tilde{v}_{max}$ = 3296, 3144, 1651, 1605, 1537, 1321, 1258, 837 and 715. ^{1}H NMR (400 MHz, CD_3CN, 22 °C): δ = 9.17 (s, 2 H, N–H), 8.53 (t, $J_{H,H}$ = 1.53 Hz, 1 H, 2-H), 8.15 (dd, $J_{H,H}$ = 8.4 and 1.53 Hz, 2 H, 2'-H), 7.97 (d, $J_{H,H}$ = 8.4 Hz, 2 H, 3'-H), 7.76 (d, $J_{H,H}$ = 7.6 Hz, 2 H, 4-H), 7.69 (t, $J_{H,H}$ = 7.6 Hz, 1 H, 5-H) ppm. ^{13}C NMR (100 MHz, CD_3CN, 22 °C): δ = 166, 143, 135, 132, 129, 128 126.5, 126.2, 124.2, 121 ppm. LRMS (ES$^+$): m/z = 453 [M + H]$^+$. HRMS: m/z for $C_{22}H_{15}N_2O_2F_6$ (M$^+$) calcd. 453.1038; found 453.1026.

Receptor 4: To a solution of 3,5-bis(trifluoromethyl)aniline (2.27 g, 9.9 mmol) in DMF (30 mL) was added triethylamine (1.52 g, 15 mmol) and DMAP (1.21 g, 9.9 mmol). The mixture was cooled to 0 °C and pyridine-2,6-dicarboxyl chloride (0.99 g, 1 mmol) was in small portions over 4–5 min. The reaction was held at 75–80 °C for 18 h and subsequently poured into a large volume of water (300 mL). The resulting white solid product was isolated from the solvent by filtration. The crude was purified by trituration using ethyl acetate to give the title product **4** (0.96 g, 34%) as a white solid; m.p. 341–342 °C. IR (KBr): $\tilde{v}_{max}$ = 3284, 3101, 1686, 1550, 1572, 1472, 1437, 1383, 1279, 1175, 1146, 1068, 1001, 936, 889, 840 and 683. ^{1}H NMR (400 MHz, CD_3CN, 22 °C): δ = 10.51 (s, 2 H, N–H), 8.60 (s, 4 H, 2'-H), 8.50 (d, $J_{H,H}$ = 8.2 Hz, 2 H, 4-H), 8.29 (t, $J_{H,H}$ = 8.2 Hz, 1 H, 5-H), 7.82 (s, 2 H, 4'-H) ppm. LRMS (ES$^+$): m/z = 590 [M + H]$^+$. HRMS: m/z for $C_{23}H_{12}N_3O_2F_{12}$ (M$^+$) calcd. 590.0738; found 590.0716.

Receptor 6: To 5-nitroisophthalic acid (1 g, 4.74 mmol) was added dry dichloromethane (30 mL) under N_2 atmosphere. To this was added DMAP (1.16 g, 9.47 mmol), EDCI (1.82 g, 9.47 mmol) and 3,5-bis(trifluoromethyl)aniline (2.17 g, 9.47 mmol) and the off-white coloured suspension was stirred at room temperature for 16 h. The resulting reaction mixture was washed with 1 M HCl, 10% aqueous sodium hydrogen carbonate, saturated NaCl, and the product dried with $MgSO_4$. The solvent was removed in vacuo to leave a yellow crude oil, 1.48 g. which was purified by flash chromatography (85% hexane:15% ethyl acetate) to give the title compound **6** (1.52 g, 51%) as a white solid; m.p. 310–312 °C. IR (KBr): $\tilde{v}_{max}$ = 3245, 3084, 1659, 1549, 1381, 1280, 1179, 1136 and 893. ^{1}H NMR (400 MHz, CD_3CN, 22 °C): δ = 9.53 (s, 2 H, N–H), 8.99 (d, $J_{H,H}$ = 1.5 Hz, 2 H, 4-H), 8.94 (t, $J_{H,H}$ = 1.5 Hz, 1 H, 2-H), 8.38 (s, 4 H, 2'-H), 7.81 (s, 2 H, 4'-H) ppm. ^{13}C NMR (125 MHz, CD_3CN, 22 °C): δ = 163, 148.5, 140, 136, 132.5, 131.5, 125.5, 124.5, 122, 120 ppm. LRMS (ES$^+$): m/z = 634 [M + H]$^+$. HRMS: m/z for $C_{24}H_{10}N_3O_4F_{12}$ (M$^-$) calcd. 632.0480; found 632.0497.

Receptor 7: To mono-methyl isophthalate (1.0 g, 5.55 mmol) in dichloromethane (30 mL) was added DMAP (0.68 g, 5.55 mmol), EDCI (1.06 g, 5.55 mmol) and 3,5-bis(trifluoromethyl)aniline (1.27 g, 5.55 mmol) and the mixture was stirred at room temperature for 16 h. The reaction mixture was then washed with water and 1 M HCl. The white solid precipitate was collected by filtration and purified by flash chromatography (80% hexane:20% ethyl acetate) to give **8** as a white solid, (2.0 g, 92%); m.p. 293–295 °C. IR (KBr): $\tilde{v}_{max}$ = 3416, 3271, 3104, 3003, 2958, 1717, 1661, 1569, 1471, 1443, 1382, 1278, 1258, 1172, 1123, 943, 891, 720 and 686. ^{1}H NMR (400 MHz, $CDCl_3$, 22 °C): δ = 8.51 (s, 1 H, 2-H), 8.32 (s, 1 H, N–H), 8.26 (d, $J_{H,H}$ = 7.6 Hz, 1 H, 6-H), 8.23 (s, 2 H, 2'-H), 8.17 [d, $J_{H,H}$ = 7.6 Hz, 1 H, 4-H], 7.68 (s, 1 H, 4'-H), 7.64 (t, $J_{H,H}$ = 7.6 Hz, 1 H, 5-H), 3.98 (s, 3 H, OCH$_3$) ppm. ^{13}C NMR (100 MHz, CD_3CN, 22 °C): δ = 166.5, 164.5, 139.2, 134.1, 133.5, 132.3, 130.9, 129.6, 127.6, 124.5, 122, 120, 118, 52.7 ppm. LRMS (ES$^+$): m/z =

392 [M + H]⁺. HRMS: m/z for $C_{17}H_{10}NO_3F_6$ (M⁻) calcd. 390.0565; found 390.0562.

To ester **8** (1.67 g, 4.26 mmol) dissolved in hot methanol (40 mL) was added 1 M NaOH, (20 mL, 20 mmol) and the mixture was refluxed with stirring for one hour. Distilled water (100 mL) was added to the mixture which was then acidified to pH 3 with concentrated aqueous HCl. The mixture was cooled and filtered to give **9** (1.24 g, 77%) as a white solid; m.p. 194–196 °C. IR (KBr): $\tilde{\nu}_{max}$ = 3292, 3092, 2662, 2551, 1690, 1651, 1562, 1470, 1441, 1381, 1305, 1279, 1175, 1146, 943, 893, 728 and 683. ¹H NMR (400 MHz; [D₆]-DMSO, 22 °C): δ = 13.3 (br. s, 1 H, OH), 11.02 (s, 1 H, N–H), 8.57 (s, 1 H, 2-H), 8.51 (s, 2 H, 2′-H), 8.21 (d, $J_{H,H}$ = 7.6 Hz, 1 H, 6-H), 8.15, (d, $J_{H,H}$ = 7.6 Hz, 1 H, 4-H), 7.80 (s, 1 H, 4′-H), 7.67 (t, $J_{H,H}$ = 7.6 Hz, 1 H, 5-H) ppm. ¹³C NMR (100 MHz; [D₆]DMSO, 22 °C): δ = 166.7, 165.4, 134.2, 132.8, 132.2, 130.8, 129.1, 128.5, 124.6, 121.9, 120, 116.6 ppm. LRMS (ES⁺): m/z = 378 [M + H]⁺. HRMS: m/z for $C_{16}H_8NO_3F_6$ (M⁻) calcd. 376.0484; found 376.0423.

Aqueous ammonia (2 mL), triethylamine (3.64 mmol, 0.5 mL) were added to DMF (20 mL), the reaction mixture cooled to 0 °C and to this was added dropwise 3,5-bis(trifluoromethyl)benzenesulfonyl chloride (0.5 g, 1.6 mmol). The reaction mixture was stirred at room temperature for 16 h and to this was added 300 mL distilled water. The basic reaction mixture was acidified to pH 2 by addition of concentrated HCl causing the product to precipitate out of solution. The off-white precipitate **10** (0.46 g, 98%) was collected by filtration; m.p. 184.5–185 °C. IR (KBr): $\tilde{\nu}_{max}$ = 3356, 3262, 3097, 3067, 1862, 1833, 1626, 1531, 1457, 1324, 1197 and 907. ¹H NMR (400 MHz; [D₆]DMSO, 22 °C): δ = 8.46 (s, 1 H, 4-H), 8.40 (s, 2 H, 2-H), 7.79 (s, 1 H, NH₂) ppm. ¹³C NMR (100 MHz; [D₆]DMSO, 22 °C): δ = 147, 131, 127, 124.6, 121.9 ppm. LRMS (ES⁺): m/z = 294 [M + H]⁺. HRMS: m/z for $C_8H_4NO_2F_6S$ (M⁻) calcd. 291.9867; found 291.9864.

Acid **9** (370.5 mg, 0.98 mmol) was dissolved in a 50:50 mixture of dichloroethane:*tert*-butyl alcohol (20 mL) and to this stirred suspension was added DMAP (360 mg, 2.95 mmol), EDCI (472 mg, 2.46 mmol) and 3,5-bis(trifluoromethyl)benzenesulfonamide (**10**) (200 mg, 0.68 mmol). The reaction mixture was stirred for 72 h at room temperature and after this time Amberlyst 15 anion exchange resin (2 g) was added and the mixture was diluted with ethyl acetate (10 mL). This mixture was stirred for a further 2 h and subsequently passed through a plug of silica gel and washed with ethyl acetate. The filtrate was collected and solvent removed in vacuo. The crude product was purified by flash chromatography (98% dichloromethane/2% methanol) to give product **7** (187 mg, 43%) as an off white solid, m.p. 241.5–242.3 °C. IR (KBr): $\tilde{\nu}_{max}$ = 3450, 3318, 3093, 2927, 1667, 1608, 1553, 1471, 1380, 1353, 1179, 888, 844 and 682. ¹H NMR (400 MHz, CD₃CN, 22 °C): δ = 9.37 (s, 1 H, Amide N–H), 8.61 (s, 1 H, 2-H), 8.52 (s, 2 H, 2′′-H), 8.33 (s, 2 H, 2′-H), 8.13 (d, $J_{H,H}$ = 7.6 Hz, 1 H, 6-H), 8.09 (s, 1 H, 4′′-H), 7.96 (d, $J_{H,H}$ = 7.6 Hz, 1 H, 4-H), 7.69 (s, 1 H, 4′-H), 7.39 (t, $J_{H,H}$ = 7.6 Hz, 1 H, 5-H) ppm. ¹³C NMR (100 MHz; [D₆]DMSO, 22 °C): δ = 169, 166, 148, 141, 138, 133, 132, 130, 128, 127.9, 127.6, 124.7, 124.4, 123.9, 122, 121.7, 120, 116 ppm. LRMS (ES⁻): m/z = 651 [M – H]⁻. HRMS: m/z for $C_{24}H_{11}N_2O_4F_{12}S$ (M⁻) calcd. 651.0248; found 651.0242.

CCDC-796511 contains the supplementary crystallographic data for **5**. These data can be obtained free of charge from The Cambridge Crystallographic Data Centre via www.ccdc.cam.ac.uk/data_request/cif.

Supporting Information (see footnote on the first page of this article): Full experimental procedures, characterisation data, NMR stack plots and rate plots.

[1] G. W. Bates, P. A. Gale, in: *Recognition of Anions*, vol. 129, **2008**, pp. 1–44; C. Caltagirone, P. A. Gale, *Chem. Soc. Rev.* **2009**, *38*, 520–563.

[2] For an example of an indole-based receptor, see: F. M. Pfeffer, K. F. Lim, K. J. Sedgwick, *Org. Biomol. Chem.* **2007**, *5*, 1795–1799; for an example of a pyrrole based receptor, see: T. Zielinski, J. Jurczak, *Tetrahedron* **2005**, *61*, 4081–4089; for an example of a sulfonamide-based receptor, see: M. T. Huggins, T. Butler, P. Barber, J. Hunt, *Chem. Commun.* **2009**, 5254–5256; for an example of a urea-based receptor, see: C. Lin, V. Simov, D. G. Drueckhammer, *J. Org. Chem.* **2007**, *72*, 1742–1746.

[3] M. P. Hughes, B. D. Smith, *J. Org. Chem.* **1997**, *62*, 4492–4499.

[4] P. V. Santacroce, J. T. Davis, M. E. Light, P. A. Gale, J. C. Iglesias-Sanchez, P. Prados, R. Quesada, *J. Am. Chem. Soc.* **2007**, *129*, 1886–1887.

[5] P. S. Bhadury, B. A. Song, S. Yang, D. Y. Hu, W. Xue, *Curr. Org. Synth.* **2009**, *6*, 380–399.

[6] Y. Sohtome, N. Takemura, R. Takagi, Y. Hashimoto, K. Nagasawa, *Tetrahedron* **2008**, *64*, 9423–9429; S. J. Connon, *Chem. Eur. J.* **2006**, *12*, 5418–5427; C. E. S. Jones, S. M. Turega, M. L. Clarke, D. Philp, *Tetrahedron Lett.* **2008**, *49*, 4666–4669; M. Kotke, P. R. Schreiner, *Tetrahedron* **2006**, *62*, 434–439; E. K. Fan, C. Vicent, A. D. Hamilton, *New J. Chem.* **1997**, *21*, 81–85; S. E. Reisman, A. G. Doyle, E. N. Jacobsen, *J. Am. Chem. Soc.* **2008**, *130*, 7198–7199; I. T. Raheem, P. S. Thiara, E. A. Peterson, E. N. Jacobsen, *J. Am. Chem. Soc.* **2007**, *129*, 13404; R. H. Crabtree, K. Kavallieratos, *Chem. Commun.* **1999**, 2109–2110.

[7] S. J. Zuend, E. N. Jacobsen, *J. Am. Chem. Soc.* **2009**, *131*, 15358–15374; Z. G. Zhang, P. R. Schreiner, *Chem. Soc. Rev.* **2009**, *38*, 1187–1198.

[8] K. Kavallieratos, S. R. de Gala, D. J. Austin, R. H. Crabtree, *J. Am. Chem. Soc.* **1997**, *119*, 2325–2326; K. Kavallieratos, C. M. Bertao, R. H. Crabtree, *J. Org. Chem.* **1999**, *64*, 1675–1683.

[9] Over the course of this work, the synthesis of **3** and **5** were reported along with application of **5** in a Diels–Alder reaction. To the best of our knowledge, a comprehensive anion binding study and application of these compounds in other reactions has not been conducted.[10]

[10] F. M. Muñiz, V. A. Montero, Á. L. Fuentes de Arriba, L. Simón, C. Raposo, J. R. Morán, *Tetrahedron Lett.* **2008**, *49*, 5050; S. Guizzetti, M. Benaglia, A. Puglisi, L. Raimondi, *Synth. Commun.* **2009**, *39*, 3731–3742.

[11] C. A. Hunter, D. H. Purvis, *Angew. Chem.* **1992**, *104*, 779; *Angew. Chem. Int. Ed. Engl.* **1992**, *31*, 792–795; J. F. Malone, C. M. Murray, G. M. Dolan, R. Docherty, A. J. Lavery, *Chem. Mater.* **1997**, *9*, 2983–2989.

[12] P. R. Schreiner, A. Wittkopp, *Org. Lett.* **2002**, *4*, 217–220.

[13] P. R. Schreiner, A. Wittkopp, *Chem. Eur. J.* **2003**, *9*, 407–414.

[14] Y. Hamuro, S. J. Geib, A. D. Hamilton, *J. Am. Chem. Soc.* **1996**, *118*, 7529–7541; M. J. Chmielewski, J. Jurczak, *Chem. Eur. J.* **2006**, *12*, 7652–7667.

[15] M. H. Abraham, *Chem. Soc. Rev.* **1993**, *22*, 73–83.

[16] H.-J. Lee, Y.-S. Choi, K.-B. Lee, J. Park, C.-J. Yoon, *J. Phys. Chem. A* **2002**, *106*, 7010–7017.

[17] A. Berkessel, B. Koch, J. Lex, *Adv. Synth. Catal.* **2004**, *346*, 1141–1146.

[18] S. A. Kavanagh, A. Piccinini, E. M. Fleming, S. J. Connon, *Org. Biomol. Chem.* **2008**, *6*, 1339–1343.

[19] A. B. Baylis, M. E. D. Hillman, *Offenlegungsschrift* 2155113, **1972**; US Patent 3,743,669; *Chem. Abstr.* **1972**, *77*, 34174q.

[20] J. P. Larocca, M. A. Y. Sharkawi, *J. Pharm. Sci.* **1967**, *56*, 916–918.

[21] M. J. Hynes, *J. Chem. Soc., Dalton Trans.* **1993**, *2*, 311.

[22] Direct comparison with **7** was not possible due to different complex stoichiometries.

[23] M. R. Sambrook, P. D. Beer, J. A. Wisner, R. L. Paul, A. R. Cowley, F. Szemes, M. G. B. Drew, *J. Am. Chem. Soc.* **2005**, *127*, 2292–2302.

[24] We would like to gratefully acknowledge the work of Professor Michael Hynes who carried out the WINEQNMR fitting of these interesting systems.

[25] S. J. Coles, J. G. Frey, P. A. Gale, M. B. Hursthouse, M. E. Light, K. Navakhun, G. L. Thomas, *Chem. Commun.* **2003**, 568–569; P. Dydio, T. Zielinski, J. Jurczak, *Org. Lett.* **2010**, *12*, 1076–1078; F. M. Pfeffer, P. E. Kruger, T. Gunnlaugsson, *Org. Biomol. Chem.* **2007**, *5*, 1894–1902.

[26] S. J. Brooks, M. E. Light, P. A. Gale, *Chem. Commun.* **2006**, 4344–4346.

[27] C. Caltagirone, G. W. Bates, P. A. Gale, M. E. Light, *Chem. Commun.* **2008**, 61–63.

[28] O. Mammoliti, S. Allasia, S. Dixon, J. D. Kilburn, *Tetrahedron* **2009**, *65*, 2184–2195.

[29] R. Robiette, V. K. Aggarwal, J. N. Harvey, *J. Am. Chem. Soc.* **2007**, *129*, 15513–15525.

[30] D. J. Maher, S. J. Connon, *Tetrahedron Lett.* **2004**, *45*, 1301–1305.

Screening of simple *N*-aryl and *N*-heteroaryl pyrrolidine amide organocatalysts for the enantioselective aldol reaction of acetone with isatin

Michael Kinsella, Patrick G. Duggan, Claire M. Lennon *

Pharmaceutical and Molecular Biotechnology Research Centre, Department of Chemical and Life Sciences, Waterford Institute of Technology, Waterford, Ireland

ABSTRACT

We have screened a range of simple *N*-aryl and *N*-heteroaryl pyrrolidine amide organocatalysts incorporating *N*-pyridyl and *N*-quinolinyl groups in the synthetically useful aldol reaction of isatin with acetone. The 'reverse amide' *N*-pyridyl pyrrolidinylmethyl amide catalysts proved highly catalytically active but gave disappointing enantioselectivities. However, an *N*-3-pyridyl prolinamide catalyst gave the aldol adduct in high yields and high enantioselectivity with up to 72% ee of the (*S*)-isomer. Conditions were optimised for this catalyst and in particular an additive screen identified a link between the pK_a of the acid additive and the yield and enantioselectivity. An *N*-arylsulfonamide prolinamide was also identified as a catalyst for this reaction giving the (*R*)-enantiomer in 68% ee.

© 2011 Elsevier Ltd. All rights reserved.

1. Introduction

The synthesis of natural products remains a significant challenge for synthetic organic chemists and is an area which requires continuing attention. In particular, compounds based on the indole substructure appear in many natural products and drug molecules. More specifically, oxindoles, which possess a carbonyl group at the 2-position of the 5 membered ring and a stereogenic quaternary carbon centre at the 3-position of this ring, are present in a number of natural products including biologically active alkaloids and pharmacological agents.[1–11] As a result, many techniques have been used to synthesise compounds bearing the aforementioned functionality with particular interest in the enantioselective addition to the 3-position.[12–17]

The aldol addition of ketones to substituted and unsubstituted isatins would appear to be a simple and suitable route towards these important biological compounds (Scheme 1).[18–21] In addition, the biological activity of oxindoles may be linked to the configuration at the stereogenic centre, creating a need to develop enantioselective methods for their synthesis.[19]
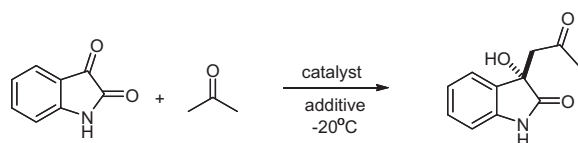
Scheme 1. Aldol reaction of acetone with isatin.

There has been renewed interest in the organocatalyst promoted aldol reaction,[22–27] in particular due to the discovery that proline is a successful catalyst for this reaction.[28–30] This discovery has pushed the resurgence of organocatalysis and has allowed previously difficult reactions to be successfully accomplished in a stereoselective manner.[31–35]

Some examples of biologically active products generated from the aldol reaction of ketones to isatins include convolutamydines **A–E** and 3-cycloalkanone-3-hydroxy-2-oxindoles[36–38] (Fig. 1). An organocatalyst promoted stereoselective aldol reaction for the synthesis of these compounds is highly attractive and prompted us to investigate this further.[20,38]

convolutamydines **A-E** 3-hydroxyindoline-2-ones 3-cycloalkanone-3-hydroxy-2-oxindoles
A: R = CH$_2$COCH$_3$
B: R = CH$_2$CH$_2$Cl
C: R = CH$_3$
D: R = CH=CH$_2$
E: R = CH$_2$CH$_2$OH
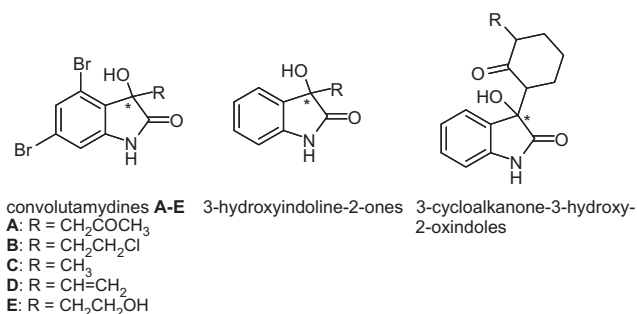
Figure 1. Examples of biologically active 3-hydroxy-indolin-2-ones.

Since 2005 work has been conducted by a number of research groups with the common aim of designing the successful organocatalytic enantioselective reactions of isatin and isatin derivatives with ketones.[16,20,21,39,40] Overall, this work has produced varied

* Corresponding author. Tel.: +353 51 304048; fax: +353 51 302679.
E-mail address: clennon@wit.ie (C.M. Lennon).

results and there still exists a strong need to develop new, successful, catalytic systems for this reaction.

In response to this challenge, we designed a library of catalysts and tested them in the aldol reaction of isatin with acetone. We chose this reaction as a model for other more complex syntheses towards larger natural products due to the commercial availability of the starting materials and also the challenging nature of this reaction which would give us a good indication of our catalysts performance; herein we report our results.

2. Results and discussion

In order to design potential catalysts for the aldol reaction of isatin and acetone, we considered natural enzymatic processes. Many of these processes function through molecular recognition between enzymes and substrates and many artificial systems have been developed based on the enzyme–substrate model.[41] In 2006, Gong and co-workers studied an organocatalytic system based on an artificial molecular recognition system.[42] They applied the discovery by Hamilton and co-workers that an *N*-pyridyl amide was a suitable group to bind a carboxyl molecule[43] and in doing so developed a successful series of hydrogen bond donating organocatalysts for the aldol reaction of α-keto acids with acetone. Our interest also lies in the application of key artificial receptor motifs as organocatalysis.

Therefore, we wanted to apply a similar strategy to the aldol reaction of isatin with acetone by designing a number of chiral amide based catalysts incorporating *N*-pyridyl and *N*-quinolinyl groups. We hoped to exploit cooperatively the hydrogen bond donating and accepting properties of such catalysts. We envisioned that the hydrogen bond donating amide N–H group would bind to and activate the isatin ketone group while concurrently the hydrogen bond accepting pyridine moiety could form hydrogen bonds with the isatin amide N–H group. A cooperative effect of both

could serve to enhance binding effects and improve reaction rate and enantioselectivity.

2.1. Pyrrolidinylmethyl amide 'reverse amide' based catalysts

We initially designed and created a series of pyrrolidinyl methyl amide based catalysts **1–4** (Fig. 2). Each of these catalysts contained the 'reverse amide' group when compared to typical prolinamide catalysts. The combination of this functionality with the hydrogen bond accepting pyridine group in a single molecule was expected to be of a suitable size and shape to bind the reaction intermediates by hydrogen bonding and thereby impart stereoselectivity to the product.[44] We postulated that the larger distance between the amide N–H and the enamine formed at the amine N–H as well as the inherent increased flexibility of these groups compared to the pyridine carboxyl group may result in a good hydrogen bonding fit for isatin.

The 'reverse amide' catalysts were synthesised in four steps with moderate yields starting from commercially available L-proline. We used a borane reduction step originally devised by Brown and Heim[45] and recently used by Wang et al. in the case of the Cbz protected analogue, to convert the Boc-amide to the Boc-amine.[46] A modified work-up procedure, which included the azeodistillation of the borane salts was employed for the acid-sensitive Boc-amine product.[47] This amine was used without further purification for ethyl chloroformate coupling with the appropriate pyridine carboxylic acid and subsequent purification followed by Boc-deprotection to yield the pyrrolidine catalysts **1–4**.

The results for catalysts **1–4** are presented in Table 1. In all cases, the absolute configuration of the aldol product was assigned through comparison of the specific rotations with the reported value[16] and of our HPLC chromatograms, based on triplicate analysis, with those in the literature.[19–21,39] In general, these catalysts were highly catalytically active at the expense of enantioselectivity; a

Figure 2. Catalysts examined herein; 'reverse amide'; *N*-pyridyl pyrrolidine amide catalysts **1–4**, *N*-pyridyl prolinamide catalysts **5–8** and **12**, *N*-quinolinyl prolinamide catalysts **9–11**, *N*-pyridyl hydroxy and benzyloxy prolinamide catalysts (**13** and **14**).

Table 1
Aldol reaction of isatin with acetone catalysed by pyrrolidine catalysts **1–4**[a]

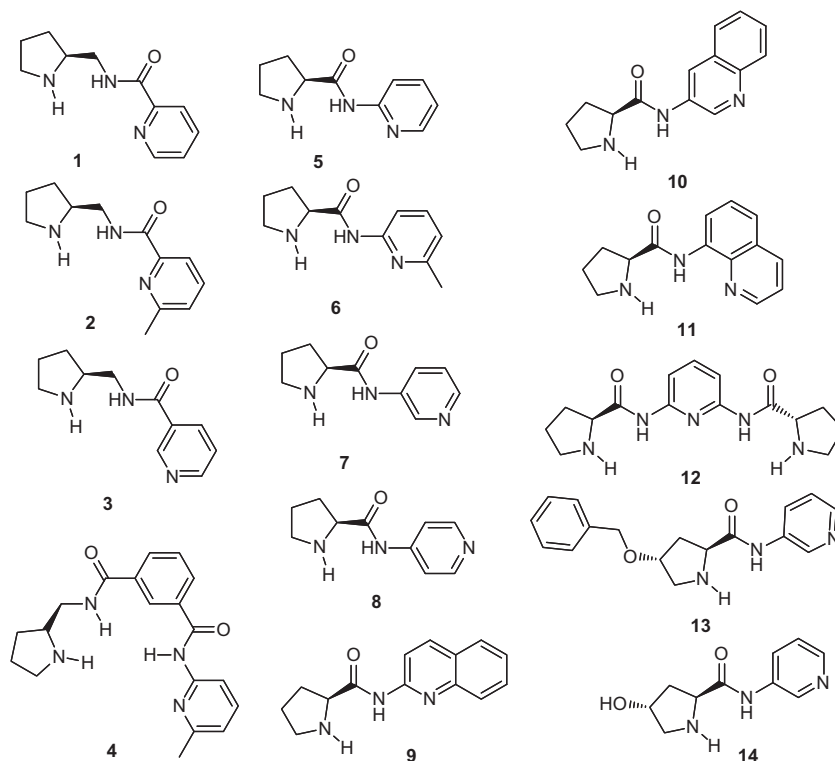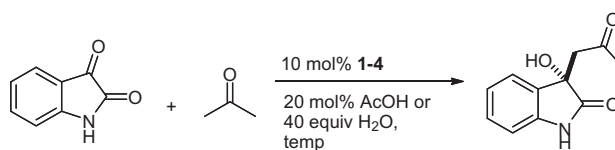| Entry	Catalyst	Additive	Temp (°C)	Time (h)	Yield[b] (%)	ee[c] (%)	Config
1	**1**	–	rt	44	85	22	(R)
2	**1**	–	−20	63	95	26	(R)
3	**1**	AcOH	rt	16.5	70	18	(R)
4	**1**	AcOH	−20	15	98	30	(R)
5	**2**	AcOH	−20	18	95	32	(R)
6	**2**[d]	AcOH	−20	11	97	31	(R)
7	**2**	TFA	rt	120	52	10	(R)
8	**2**	p-TSA	rt	120	<10	8	(R)
9	**3** (20)	AcOH	−20	14	Quant	7	(S)
10	**3** (30)	H₂O	−20	6	92	8	(R)
11	**3**[e] (20)	AcOH	−20	18	85	18	(S)
12	**3**[f] (20)	AcOH	−20	16	87	21	(R)
14	**3**[f,g] (20)	AcOH	−20	135	31	24	(R)
15	**4**	–	rt	44	84	6	(S)

[a] All reactions were conducted with 0.3 mmol of isatin and 2 mL of acetone at the temperature specified with 10 mol % catalyst loading unless catalyst loading is specified in parentheses in the Table. In cases where the additive was employed, 20 mol % acid or 40 equiv H_2O were used. TLC and HPLC were used to monitor the progression of the reaction.
[b] Isolated yield.
[c] Determined by chiral HPLC.
[d] 0.3 mL Acetone used.
[e] Toluene solvent (2 mL) used with 1 mL acetone.
[f] DMF solvent (2 mL) used with 1 mL acetone.
[g] Two equivalents (0.044 mL) acetone used.

maximum ee of 32% was obtained for catalyst **2**. After testing a number of acidic additives and also water, we concluded that AcOH was the most successful additive enhancing both the reaction rate and enantioselectivity. Attempts to improve the enantioselectivity of the most reactive catalyst **3** by varying the temperature, additive, catalyst loading and stoichiometry proved unsuccessful. However, the solvent was found to have the most significant effect on the configuration of the product and its enantioselectivity. When the reaction was conducted in non-polar toluene as a solvent, the (S)-enantiomer was formed preferentially; however, the (R)-product was obtained when using the polar aprotic DMF solvent (Table 1, entries 11–14).

2.2. Prolinamide based catalysts

With the limited success of our 'reverse amide' pyrrolidine catalysts, we subsequently synthesised and screened a series of prolinamide catalysts derived from aminopyridines and aminoquinolines.[27,42,43,48] The synthesis was achieved through the coupling of Boc-proline to an aminopyridine or aminoquinoline; subsequent Boc-deprotection yielded prolinamide catalysts **5–12** in good yields.[49]

These catalysts were tested in the reaction of isatin with acetone under similar conditions as used for the pyrrolidine catalysts; however, a 20 mol % catalyst loading was used in this screen due to a general improvement in results when using this loading for the previous screen. The 2-aminopyridine derivative **5** and its picoline derivative **6** yielded disappointing results; 11% and 15% ee of the (R)-product, respectively, with long reaction times (Table 2, entries 1 and 2). The C₂-symmetric bis-prolinamide catalyst **12** gave improved results, however, the ee was still at a moderate level of 47% in favour of the (S)-product. The position of the nitrogen in the ring proved to have the most pronounced effect on both the

yield and enantioselectivity. Overall, the 3- and 4-aminopyridinyl catalysts **7** and **8** and the 3-aminoquinolinyl catalyst **10** provided the best results (Table 2, entries 3–9, 14 and 15). As with the previous series, the use of common aldol additives enhanced yield and enantioselectivity.[22,50] In general, the inclusion of 20 mol % AcOH and a reduction in temperature to −20 °C resulted in improved yield and ee values.[21,51] The addition of an appropriate quantity of H_2O was also effective at improving the ee (Table 2, entries 8 and 9), but it decreased the reaction rate. This has previously been observed for proline-based catalysts.[18,40,52] The 4-aminopyridine derivative **8** proved slightly inferior to **7** in terms of both yield and ee, in particular when H_2O was used as an additive. Both **7** and **8** were far superior to the 2-aminopyridine derivatives **5** and **6** and the 2- and 8-aminoquinoline derivatives **9** and **11**.

In the reaction of isatin with acetone catalysed by **7** with H_2O and AcOH, the enantioselectivity of the product increased slightly as the reaction progressed. This phenomenon has been previously observed and reported for this aldol reaction using a dipeptide based catalyst and was ascribed to the formation of diastereomeric complexes between the catalyst and product.[52]

2.3. Hydroxyprolinamide based catalysts

Previous success with hydroxyproline catalysts in aldol reactions motivated us to investigate this functionality.[53] We based our bifunctional hydroxyprolinamide catalysts on our most successful catalysts to date (catalyst **7**) and examined the effect of the additional stereogenic centre, a benzyloxy group (catalyst **13**) and the unprotected hydroxyl group (catalyst **14**). Catalyst **13** was synthesised in 4 steps with moderate yield starting with N-Boc-trans-4-hydroxy-ʟ-proline methyl ester and **14** was prepared in 3 steps in an analogous way to the synthesis of **5–12**. The benzyl protected catalyst **13** produced the (S)-product in 54% ee using

Table 2
Aldol reaction of isatin with acetone catalysed by prolinamide catalysts **5–14**[a]
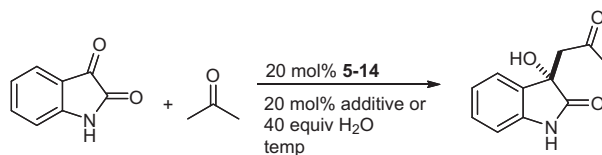
Entry	Catalyst	Additive	Temp (°C)	Time (h)	Yield[b] (%)	ee[c] (%)	Config
1	**5**	–	rt	168	80	11	(R)
2	**6**	–	rt	168	74	15	(R)
3	**7**	–	rt	17	98	55	(S)
4	**7**	–	−20	32	96	57	(S)
5	**7**	AcOH	rt	15	92	60	(S)
6	**7**	AcOH	−20	30	95	66	(S)
7	**7**	AcOH[d]	−20	37	84	66	(S)
8	**7**	H₂O[e]	−20	37	76	58	(S)
9	**7**	H₂O	−20	37	72	69	(S)
10	**8**	AcOH	−20	22	89	65	(S)
11	**8**	H₂O	−20	24	87	54	(S)
12	**9**	AcOH	−20	504	<20	17	(R)
13	**9**	H₂O	−20	312	<20	7	(S)
14	**10**	AcOH	−20	50	71	64	(S)
15	**10**	H₂O	−20	44	89	66	(S)
16	**11**	AcOH	−20	44	76	13	(R)
17	**11**	H₂O	−20	60	75	5	(R)
18	**12(10)**	AcOH	−20	88	81	47	(S)
19	**12**	AcOH	−20	88	99	39	(S)
20	**12**	H₂O	−20	88	99	43	(S)
21	**13**	AcOH	−20	90	77	50	(S)
22	**13**	H₂O	−20	90	79	54	(S)
23	**14**	AcOH	−20	15	85	44	(S)
24	**14**	H₂O	−20	17	87	58	(S)

[a] All reactions were conducted with 0.3 mmol of isatin and 2 mL of acetone at the temperature specified with 20 mol % catalyst loading unless the catalyst loading is specified in parentheses in the Table. In cases where the additive was employed, 20 mol % AcOH or 40 equiv H₂O was used unless otherwise specified. TLC and HPLC were used to monitor the progression of the reaction.
[b] Isolated yield.
[c] Determined by chiral HPLC.
[d] 40 mol % AcOH used.
[e] 6.6 equiv H₂O used.

20 mol % catalyst loading and 40 equiv H₂O at −20 °C (Table 2, entry 22). The unprotected hydroxy proline derivative **14** furnished product the (S)-product in up to 58% ee, using the same conditions (Table 2, entry 24). Therefore, the incorporation of a second functional group and stereogenic centre into the prolinamide catalyst resulted in a slight reduction in ee.

With the screening results in hand, we identified catalyst **7** as the catalyst with the most potential for the reaction. We subsequently undertook a study to optimise the reaction conditions and hence improve the yield and enantioselectivity further.

2.4. Variation of acid additive

Having observed the positive effect of AcOH as an additive on the yield and enantioselectivity in our preliminary studies we considered the effect of the strength of the acid additive. We tested a range of additives across a pK_a range of −2 to 16 (literature values) and found a correlation between the pK_a of the acid additive and the enantioselectivity (Table 3 and Fig. 3).[54,55] Interestingly, a plot of pK_a versus enantioselectivity gave a curve resembling a pH titration curve. The ee appeared to rise sharply and linearly between additive pK_a 2–6. A plateau was reached at pK_a 7 after which an essentially constant ee value was obtained regardless of the pK_a of the additive; (Fig. 3). A correlation between the pK_a of the addi-

Table 3
Variation of the acid additive and relationship between pK_a of additive and ee of (S)-product for **7** catalysed reaction[a]
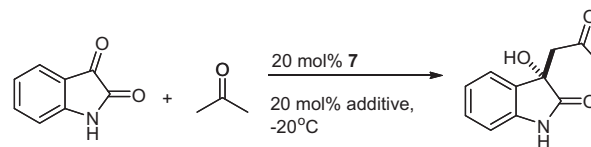
Entry	Additive	Additive pK_a	Time (h)	Yield (%)	ee (%)
1	p-TSA	−1.34	88	52	13
2	TFA	0.26	12	97	12
3	ClCH₂COOH	2.85	6	98	37
4	HCOOH	3.75	14	94	58
5	PhCOOH	4.21	14	90	63
6	AcOH	4.76	65	95	66
7	4-NO₂-phenol	7.14	78	84	69
8	4-Cl-phenol	9.38	89	85	70.5
9	Phenol	9.94	89	80	71
10	Methanol	15	89	77	69
11	Water	15.7	32	96	57

[a] Unless otherwise noted, all reactions for the acid additive study were conducted using 20 mol % catalyst loading of **7** at −20 °C with 20 mol % of additive. TLC and HPLC were used to monitor the progress of the reaction. Literature pK_a data, as measured in water.[56]
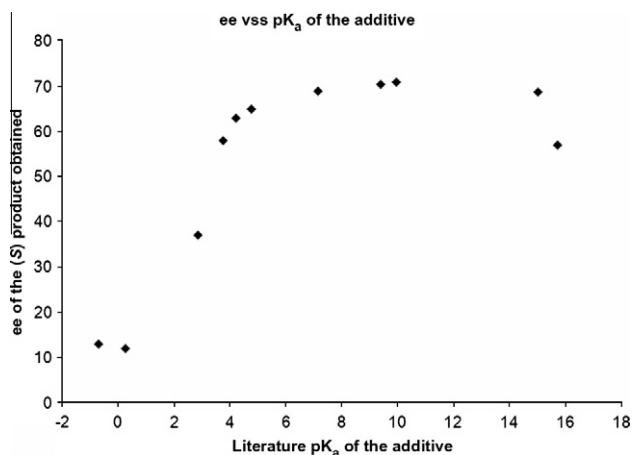
Figure 3. Relationship between the pK_a of the additive and ee of the product using 20 mol % catalyst **7** and 20 mol % additive.

Table 4
Variation of solvents in reaction catalysed by **7**[a]
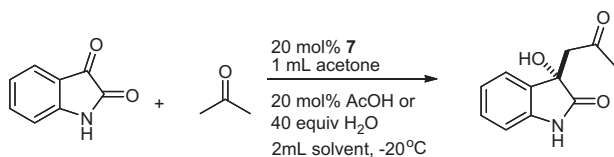
Entry	Solvent	Additive	Time (h)	Yield (%)	ee (%)
1	Acetone	AcOH	65	95	66
2	Toluene	AcOH	22	91	66
3	DMF	AcOH	61	78	54
4	Dioxane	AcOH	42	85	64
5	THF	AcOH	48	78	64
6	Hexane	AcOH	38	96	58
7	CH_2Cl_2	AcOH	46	82	68.5
8	$CHCl_3$	AcOH	40	80	69
9	Acetone	H_2O	37	72	69
10	Toluene	H_2O	108	72	63
11	DMF	H_2O	108	85	61
12	Dioxane	H_2O	13.5	97	50
13	THF	H_2O	41	92	63
14	Hexane	H_2O	88	98	68
15	CH_2Cl_2	H_2O	108	68	66
16	$CHCl_3$	H_2O	90	85	68

[a] Unless otherwise noted, all of the reactions for the solvent study were conducted using 20 mol % catalyst loading of **7** at −20 °C with either 20 mol % AcOH or 40 equiv H_2O additive to give excess of the (S)-product. TLC and HPLC were used to monitor the progress of the reaction.

tive and the reaction rate and yield was also observed. It was noted that the reaction proceeded at a slower rate when using additives with pK_a values >6 (Table 3, entry 6 vs entries 8 and 9). Additionally, an increase in ee was observed at the expense of product yield. It could, therefore, be said that the optimum acid additive for yield and enantioselectivity should have a pK_a value of approximately 4.0–6.0. Water as an additive at 20 mol % was found to be an exception to the aforementioned trends resulting in lower ee and higher yield than expected based on its pK_a of 15.7 (Table 3, entry 11). It should be noted, however, that the quantity of water present in the media has been demonstrated to be critical to the level of enantioselectivity.[52] A quantity of 40 equiv (4000 mol %) has been found to be optimum by us and also reported in the literature.[52] Additionally, above the optimum level, water was shown to have a negative effect on the enantioselectivity of the reaction.[52]

Table 5
Variation of the conditions and additives in the reaction of isatin and acetone catalysed by **7**[a]

Entry	Loading	Additive	Temp (°C)	Time (h)	Yield (%)	ee (%)
1	30	AcOH	rt	15	95	60
2	30	AcOH	−20	37	95	63
3	30	AcOH[b]	−20	37	84	69
4	20	H_2O[c]	−20	37	76	58
5	30	H_2O	−20	37	88	72
6	30	H_2O[d]	−20	37	87	72
7	40	H_2O	−20	33	68	69

[a] Unless otherwise noted, all of the reactions for the catalyst optimisation study were conducted using 30 mol % catalyst loading of **7** with either 20 mol % AcOH or 40 equiv H_2O additive to yield an excess of (S)-product. TLC and HPLC were used to monitor the progress of the reaction.
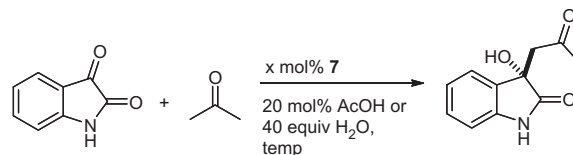[b] 40 mol % AcOH used.
[c] 6.6 equiv H_2O used.
[d] One millilitre acetone used.

2.5. Variation of solvent

We conducted a detailed study to investigate the effects of varying the reaction solvent (Table 4). Due to the similar performance of **7** using AcOH or 40 equiv H_2O as additive, we conducted the solvent study for both additives independently. We tested a range of solvents of varying polarities and in the case of the AcOH additive, found that a marginally higher ee value could be obtained when the reaction was conducted in non-polar $CHCl_3$ or CH_2Cl_2 (Table 4, entries 7 and 8) but this came at the expense of the reaction yield. However, using H_2O as an additive, the reaction in acetone was found to be marginally superior in terms of ee when compared to the use of alternative reaction solvents. When relatively non-polar solvents were used, an increase in reaction yield was observed in hexane and $CHCl_3$, however, significantly longer reaction times were required (Table 4, entries 9–16).

2.6. Optimisation of the reaction conditions

We finally attempted to further optimise conditions for **7**. We studied the effects of catalyst loading, temperature and additive loading. Overall, our best results in terms of enantioselectivity were obtained using 30 mol % loading of catalyst in the presence of 40 equiv H_2O at −20 °C for 37 h, producing the (S)-product in a yield of 88% and 72% ee (Table 5, entry 5).[52] It was noted that the reaction with the AcOH additive proceeded with marginally less enantioselectivity and improved yield; however, reactions using water were slower but provided higher enantioselectivities. To compare our catalysts with related organocatalysts, (S)-proline gave 33% ee while Tomasini et al. obtained 73% ee for their proline dipeptide catalyst[39] and up to 86% ee in the presence of H_2O.[52] Xiao et al. obtained up to 88% ee at −50 °C,[21] while Nakamura et al. produced 3% ee from their N-heteroarylsulfonamide catalyst but 95% ee for the reaction of acetone with 4,6-dibromoisatin.[18] In general, organocatalysts have been found to give better enantioselectivities with 4,6-dibromoisatin compared to isatin itself.[18,19,40] A highly efficient enantioselective example of this reaction was reported by Malkov et al. with up to 94% ee being obtained for an amino alcohol catalyst.[16] Chen et al. obtained a product in up to 67% ee using a carbohydrate derived alcohol catalyst.[57] It is worth noting that the work reported herein represents an extension of the scope

of catalyst **7** from the enantioselective aldehyde:ketone to ketone:-ketone aldol reactions.

2.7. Structural considerations

Our studies identified several key structural design parameters that were critical with regard to the yield and enantioselectivity. The results indicate that the position of the pyridyl nitrogen was important for achieving high yield and enantioselectivity. The loss of enantioselectivity in the 2-pyridyl catalyst is possibly due to electron repulsion between the lone pair of electrons in the pyridine nitrogen and the non-hydrogen bonded carbonyl group of isatin upon hydrogen bonding of the reactive carbonyl with the amide N–H. This repulsion may not arise when the N lies at the 3- or 4-position in the pyridyl ring. The pK_a of the acid additive was also key with regard to the yield and enantioselectivity. A loss in enantioselectivity seems to occur when an additive with a pK_a lower than 4 is employed. Using an acid with a lower pK_a could lead to possible protonation of the pyridine nitrogen and/or acceleration of the direct reaction of acetone with isatin, which could account for the loss of selectivity. Water may alternatively be used as an additive for **7**, with 40 equiv at −20 °C giving the highest enantioselectivity.

In order to study the effect of the pyridine *N* in the ring and hence determine the potential mode of action of **7**, catalyst **15** (Fig. 4), in which a phenyl ring was used in place of a pyridine ring, was prepared. We obtained a relatively high ee of 65% using 30 mol % loading and 40 equiv water additive at −20 °C; however, the reaction was considerably slower with catalyst **15** compared to **7** (Table 6, entry 3).

In order to assess the role of the amide N–H proton, prolinamides **16** and **17** (Fig. 4) were synthesised from proline coupled to the appropriate methylamine. As expected, the 4-methylaminopyridine prolinamide catalyst **16** failed to catalyse the reaction (Table 6, entry 4). In the case of the methylaniline prolinamide derivative **17**, the product was obtained in good yield while the enantioselectivity was significantly lower and the opposite enantiomer was obtained (Table 6, entry 5), indicating a loss of special fit.
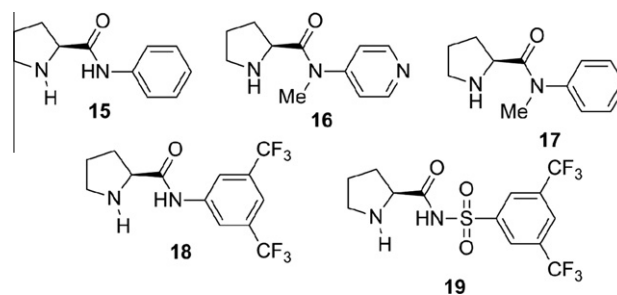
Figure 4. Catalysts synthesised and tested for mechanistic investigations.

Therefore, we suggest that in the case of aminopyridine and aminoquinoline based catalysts, the relative position of the amino group and the pyridine nitrogen atom has a major impact on the enantioselectivity of the reaction. The presence of *N* in the ring is not crucial, however, as the aniline derived prolinamide **15** also catalysed the reaction, albeit with lower enantioselectivity. In both cases the amide N–H was necessary to obtain high yields and enantioselectivity.

With a relatively high ee obtained using the aniline derived catalysts, we also considered catalysts **18** and **19** (Fig. 4) with enhanced N–H acidities compared to **15**. Catalyst **18** was derived from proline coupled to 3,5-bis(trifluoromethyl)aniline and **19** derived from 3,5-bis(trifluoromethyl)benzenesulfonamide.[53,58–60] Previously, our group reported acidic amides and *N*-acyl sulfonamides as successful acidic anion receptors and organocatalysts for the Baylis–Hillman reaction; therefore, we were interested in studying the effects of increased N–H acidity on this reaction.[61] The results for these acidic catalysts, in particular **19**, (the acidity of such a compound would be expected to be similar to carboxylic acids)[62,63] were surprising. Catalyst **18** furnished the aldol product in high yield and with up to 71% ee of the (*S*)-product using the previously determined optimum conditions (Table 6, entry 8). This result is very similar to the optimum catalyst **7** under the same conditions, however, the latter catalyst produced a higher yield

Table 6
Aldol reaction of isatin with acetone catalysed by catalysts **15–19**[a]
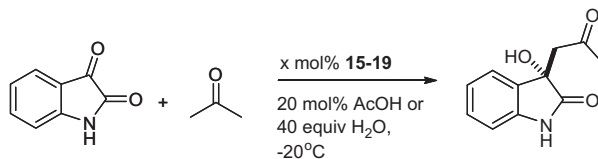
Entry	Catalyst	Cat loading (mol %)	Additive	Time (h)	Yield[b] (%)	ee[c] (%)
1	**15**	20	—	91	90	58
2	**15**	20	AcOH	91	92	61
3	**15**	30	H$_2$O	91	89	65
4	**16**	20	AcOH	336	Trace	–
5[e]	**17**	20	AcOH	12	99	46[e]
6[e]	**17**	30	H$_2$O	12	96	37[e]
7	**18**	20	AcOH	39	85	69
8	**18**	30	H$_2$O	39	71	71
9[e]	**19**	20	AcOH	37	92	68[e]
10[d,e]	**19**	20	AcOH	37	87	68[e]
11[e]	**19**	20	H$_2$O	37	32	3[e]

[a] Unless otherwise noted, all reactions were conducted with 0.3 mmol of isatin and 2 mL of acetone at −20 °C to yield an excess of (*S*)-product. Unless otherwise noted, 20 mol % AcOH was used and 40 equiv H$_2$O; TLC and HPLC were used to monitor the progress of the reaction.
[b] Isolated yield.
[c] Determined by chiral HPLC.
[d] 40 mol % AcOH used.
[e] The (*R*)-product was obtained as the major enantiomer.

Table 7
Substrate scope of catalyst **7** varying each component of the reaction[a]

Entry	Isatin	Ketone	Time (h)	Yield[b](%)	ee[c](%)
1	*N*-benzyl	Acetone	44	62	61
2	Isatin	2-Butanone	23	72	52
3	Isatin	Cyclohexanone	>100	—[d]	—[d]
4	Isatin	Acetaldehyde[e]	48	85	39
5	*N*-benzyl	Acetaldehyde[e]	48	28	32

[a] Unless otherwise noted, all reactions for the substrate scope study were conducted using 30 mol % catalyst loading of **7** with 40 equiv H_2O additive at −20 °C to give excess of the (*S*)-product.
[b] Isolated yield.
[c] Determined by chiral HPLC.
[d] Multiple products formed with product separation impossible.
[e] Reaction conducted using 30 mol % **7**, 0.3 mmol isatin/*N*-benzylisatin, 5 equiv CH_3CHO, 17 mg chloroacetic acid at rt and reduced ($NaBH_4$ reduction) to the alcohol product prior to analysis with excess of the (*R*)-product. Absolute configurations were assigned through comparison of the specific rotations and chiral chromatography with literature data.

(Table 5, entry 5 vs Table 6, entry 8). Catalyst **17** was observed to give the opposite enantiomer [the (*R*)-product] in 68% ee using 20 mol % catalyst loading with 20 mol % AcOH (Table 6, entry 9).

2.8. Substrate scope

The final study undertaken was a substrate scope of our most successful catalyst **7**. We examined a number of substrates using catalyst **7** and the optimum catalyst conditions as obtained from our previous studies. The reaction of *N*-benzylisatin with acetone produced the (*S*)-product in 61% ee after 44 h (Table 7, entry 1). This result has implications for the binding to the N–H of isatin which will be discussed below. We tested the reaction of isatin with 2-butanone and obtained the product in good ee and regioselectivity with 52% ee of the major product, 9:1 regioselectivity in favour of C–C bond formation at the less substituted methyl group (Table 7, entry 2).[64] We also attempted the reaction of isatin with cyclohexanone, but were unsuccessful in assessing the performance of this difficult substrate due to the formation of many products, which proved to be inseparable from the desired and biologically active product.[38] We also studied the reaction of isatin and *N*-benzylisatin with acetaldehyde (Table 7, entries 4 and 5). We deviated from our prescribed conditions in these cases and followed a previously reported method.[65] We observed the formation of the product from both reactions. It has been previously reported that isatin was inactive with acetaldehyde when the highly successful 4-hydroxydiarylprolinol was used as a catalyst.[65] We obtained the product (*R*)-product in 39% ee for the isatin reaction and in 33% ee for the reaction of the acetaldehyde with *N*-benzylisatin.

2.9. Mechanistic considerations

We postulate that a combination of hydrogen bonding and π–π stacking of the aromatic rings of our catalysts with isatin is responsible for the observed catalytic activity and enantioselectivity. Initially, we suggest that the acid additive promotes the reaction of the catalyst with acetone to form a reactive enamine intermediate. In the case of aminopyridine and aminoquinoline based catalysts, the relative position of the amino group and the pyridine nitrogen atom had a major impact on the enantioselectivity of the reaction.

With catalyst **7**, it is possible to envisage π-stacking of isatin in the enamine modified catalyst cleft. The hydrogen bonding of isatin C=O with the catalyst N–H could facilitate enamine attack on the *Re* face of the isatin C=O leading to the (*S*)-product. An additional hydrogen bond is possible between isatin and the pyridyl

N-atom, but clearly it is not as important as was shown with results using the aniline derived catalyst **15**, albeit with lower enantioselectivity and longer reaction time. The relatively high ee found for *N*-benzylisatin with **7** also suggests that binding to the amide N–H of isatin may not play a significant role in the mechanism. Similar interactions to **7** are possible with the structurally related aminoquinoline based catalyst **10**.

The suggested interactions above are consistent with the results for the hydroxyproline derived catalysts **13** and **14** where the added stereogenic centre had only minor effects as the added groups point away from the cleft. Furthermore, the importance of hydrogen bonding to the amide group in **7** is supported by the reduced activity and enantioselectivity of the *N*-methylated catalysts **16** and **17** and the good results found for the activated amide in catalyst **18**.

The sulfonamide catalyst **19** gave high enantioselectivity towards the (*R*)-product. With this catalyst, π-stacking of isatin in the catalyst cleft could allow the formation of two hydrogen bonds, one between the C=O on isatin and the sulfonamide N–H and the other binding between the N–H on isatin and the S=O of the catalyst, facilitating an attack on the *Si* face leading to the (*R*)-product. In addition, when catalyst **19** was tested in the reaction of *N*-benzylisatin with acetone, the (*R*)-product was formed with a slightly lower ee compared to the reaction catalysed by **7**. It is interesting to note the low yield and enantioselectivity obtained when water was used as an additive instead of AcOH; this may be due to the deprotonation of the highly acidic sulfonamide N–H in this reaction media forming a zwitterionic state which could inhibit enamine formation.

With the 'reverse amide' catalysts, while the catalytic activity was high, the enantioselectivity was poor and more variable between (*R*) and (*S*)-selectivity. With these catalysts, the extra carbon can be expected to impart greater flexibility to the cleft site and the high catalytic activity observed may be related to the reduced steric strain involved during the enamine attack with these more flexible catalysts. Considering catalyst **3**, it is possible to envisage π-stacking of isatin in the catalyst cleft, which facilitates two hydrogen bonds between isatin and the amide group of the catalyst. Due to the greater flexibility of the 'reverse amide', similar complexes are possible by a conformational change leading to either the (*R*)- or (*S*)-product. The results for **3** also highlight the likely importance of the solvation in all these catalytic processes.

3. Conclusions

In conclusion, we have designed and tested a range of simple organocatalysts for the synthetically useful reaction of isatin to acetone. Our 'reverse amide' *N*-pyridyl pyrrolidinylmethyl amide catalysts produced disappointing enantioselectivities but were highly catalytically active. We achieved more success with our *N*-pyridyl prolinamide and *N*-quinolinyl prolinamide catalysts obtaining the (*S*)-isomer product in up to 72% ee. Conditions were optimised and in particular an additive screen showed a link between the pK_a of the acid additive used and the yield and enantioselectivity. A small substrate screen was carried out. Investigations into the mode of action of the most successful catalyst **7** also provided interesting results and led to the discovery of two other catalysts, which may be applied to the reaction; the acidic prolinamides **16** and **17**. Thus one can choose the catalyst to use based on the desired configuration of the product. Structural modifications were made to the catalysts and substrates to study the catalytic action, and mechanisms are proposed for the catalytic action based on π-stacking and hydrogen bonding of the substrate in the catalyst cleft. Work is currently underway to apply these catalysts to the enantioselective synthesis of biologically active compounds.

4. Experimental section

4.1. General information

All commercial chemicals were obtained from Sigma and were used as received unless otherwise stated. Flash chromatography was conducted using 200–300 mesh silica gel. Nuclear Magnetic Resonance (NMR) spectra were measured using a Joel ECX-400 spectrometer operating at 400 MHz for ^{1}H NMR and at 100 MHz for ^{13}C NMR. Chemical shift values (δ) are reported in ppm relative to either TMS at 0.0 ppm or the NMR solvent peak. NMR data are reported as follows: chemical shift, multiplicity (s = singlet, d = doublet, t = triplet, q = quartet, m = multiplet, br = broad), coupling constant expressed in Hertz, integration, assignment of peak. Chiral HPLC was conducted on HP 1050 HPLC using a chiral column (Chiralpak AD-H or IA columns). Low resolution mass spectra were performed using an Agilent 1200 series LC-MSD Trap XCT Ultra LC–MS instrument and Varian Saturn 2000 GC/MS/MS with high resolution mass spectrometry conducted using a Waters Xevo G2 Q-TOF mass spectrometer. An external reference standard of Leucine enkephalin was infused in order to confirm mass accuracy of the HRMS data acquired. Melting points were measured on a Stuart Scientific Melting point apparatus SMP3 and are uncorrected. Optical rotations were measured on an AA series polAAr 20 automatic polarimeter. FTIR spectra were recorded on a Varian 660-IR FTIR spectrometer and KBr discs were produced using a KBr press; Spe-cac ATLAS T25.

4.2. General method for the synthesis of catalysts 1–4

To a suspension of the appropriate pyridine-carboxylic acid (5 mmol) in dichloromethane (30 mL) was added EDCI (0.959 g, 5 mmol) and DMAP (0.611 g, 5 mmol) and this suspension was stirred for 10 min. Next, Boc-pyrrolidinylmethyl amine (1 g, 5 mmol) was added slowly as a solution in dichloromethane (20 mL) and the reaction mixture was stirred at room temperature for 16 h. After this time, the solvent was removed in vacuo and the product was purified by flash chromatography (hexane:ethyl acetate gradient) eluting the Boc-protected catalysts as oily residues in moderate yields. The Boc-deprotection was conducted as per the general method.

4.3. General method for synthesis of catalysts 5–19

At first, Boc-L-proline (10 mmol, 2.15 g) was dissolved in dry THF (30 mL) and treated with triethylamine (10 mmol, 1.01 g, 1.38 mL). The stirred reaction mixture was cooled to 0 °C and ethyl chloroformate (1.09 g, 10 mmol) was added dropwise over 15 min. After the mixture had been stirred for a further 30 min at 0 °C, amine (10 mmol) was added slowly over 15 min. This reaction mixture was stirred for 1 h at 0 °C, 16 h at room temperature and heated at reflux for 3 h with the reaction monitored by TLC. The mixture was subsequently diluted with ethyl acetate and the TEA. HCl removed by filtration and the solvent removed from the filtrate in vacuo. The resulting residue was dissolved in ethyl acetate, washed with saturated aqueous ammonium chloride, dried over MgSO$_4$, filtered and evaporated. The crude product was purified by flash chromatography using ethyl acetate and petroleum ether mixtures. The Boc-deprotection was conducted as per the general method.

4.4. General method for the Boc-deprotection of 1–19

A solution of Boc-protected catalyst (5 mmol) in dichloromethane (5 mL) was cooled to 0 °C. To this chilled solution was added dropwise trifluoroacetic acid (5 mL) and the reaction mixture stirred at room temperature for 2 h. After this time, the solvent and excess TFA were removed in vacuo. The residue was redissolved in dichloromethane (10 mL), neutralised with 5% NaOH and the aqueous layer extracted with dichloromethane (5 × 15 mL). The combined extracts were washed with saturated NaCl, dried over MgSO$_4$, filtered and the solvent removed in vacuo to yield catalysts 1–19.

4.5. Catalysts 1–19

4.5.1. (S)-N-(Pyrrolidin-2-ylmethyl)picolinamide 1

Brown oil; yield: 258 mg, 43%; $[\alpha]_D^{21} = +27.6$ (c 0.5, CH$_2$Cl$_2$); v_{max} (KBr disc) 3379, 2963, 1664, 1529, 1269, 997, 750, 694 cm^{-1}; δ_H (400 MHz, CDCl$_3$) 8.54–8.57 (m, 1H, H-6), 8.44 (s, br, 1H, amide N–H), 8.18 (d, J = 8.39 Hz, 1H, H-3), 7.81–7.87 (m, 1H, H-4), 7.39–7.44 (m, 1H, H-5), 3.59–3.66 (m, 1H, H-2′), 3.31–3.49 (m, br, 2H, CONH–CH$_2$), 2.96–3.03 (m, 2H, H-5′), 2.66 (s, br, 1H N–H), 1.45–2.0 (m, br, 4H, H-3′ and H-4′); δ_C (100 MHz, CDCl$_3$) 166.3 (amide C=O), 149.1 (C-2), 148.5 (C-6), 137.4 (C-4), 126.6 (C-5), 122.4 (C-3), 59.9 (C-2′), 45.2 (C-5′), 41.0 (CH$_2$NH), 27.9 (C-3′), 24.3 (C-4′). m/z 205 (M$^+$); HRMS (ESI): MH$^+$, found 206.1298, C$_{11}$H$_{16}$N$_3$O requires 206.1293.

4.5.2. (S)-6-Methyl-N-(pyrrolidin-2-ylmethyl)picolinamide 2

Viscous yellow oil; yield: 330 mg, 32%; $[\alpha]_D^{19} = +26.6$ (c 0.2, CH$_2$Cl$_2$); v_{max} (KBr disc) 3379, 3290, 2959, 1662, 1593, 1406, 994, 761 cm^{-1}; δ_H (400 MHz, CDCl$_3$) 8.42 (s, br, 1H amide N–H), 7.95 (d, 1H, J = 7.63 Hz, H-3), 7.67 (t, 1H, J = 7.63 Hz, H-4), 7.23 (d, 1H, J = 7.63 Hz, H-5), 3.52–3.54 (m, 1H, H-2′), 3.25–3.42 (m, 2H, CONH–CH$_2$), 2.88–2.99 (m, 2H, H-5′), 2.53 (s, 3H, Ar-CH$_3$), 2.47 (s, 1H, N–H), 1.38–1.95 (m, 4H, H-3′ and H-4′); δ_C (100 MHz, CDCl$_3$) 164.8 (amide C=O), 157.2 (C-6), 149.3 (C-2), 137.4 (C-4), 125.8 (C-5), 119.2 (C-3), 58.1 (C-2′), 46.6 (C-5′), 44.2 (CH$_2$NH), 29.4 (C-3′), 25.8 (C-4′), 24.3 (Ar-CH$_3$); m/z 220 (M$^+$); HRMS (ESI): MH$^+$, found 220.1455, C$_{12}$H$_{18}$N$_3$O requires 220.1450.

4.5.3. (S)-N-(Pyrrolidin-2-ylmethyl)nicotinamide 3

Brown oil; yield: 450 mg, 53%; $[\alpha]_D^{21} = +22.6$ (c 0.1, CHCl$_3$); v_{max} (KBr disc) 3407, 3066, 2968, 1655, 1545, 1420, 1133, 708 cm^{-1}; δ_H (400 MHz, CDCl$_3$); 8.99 (d, J = 1.53 Hz, 1H, H-2), 8.61 (dd, J = 3.05 and 1.53 Hz, 1H, H-6), 8.05–8.09 (m, 1H, H-4), 7.89 (s, br, 1H, amide N–H), 7.27–7.30 (m, 1H, H-5), 4.19 (s, br, 1H, aliphatic N–H), 3.31–3.72 (m, 3H, H-2′ and CONH–CH$_2$), 3.03–3.10 (m, 2H, H-5′), 1.50–2.05 (m, 4H, H-3′ and H-4′). δ_C (100 MHz, CDCl$_3$) 166.1 (amide C=O), 151.9 (C-6), 148.3 (C-2), 135.3 (C-4), 129.6 (C-1), 123.3 (C-3), 59.0 (C-2′), 45.3 (C-5′), 42.1 (CH$_2$NH), 28.4 (C-3′), 24.7 (C-4′); m/z 206 (MH$^+$), 136, 106, 70; HRMS (ESI): MH$^+$, found 206.1299, C$_{11}$H$_{16}$N$_3$O requires 206.1293.

4.5.4. (R)-N^1-(6-Methylpyridin-2-yl)-N^3-(pyrrolidin-2-ylmethyl)isophthalamide 4

This catalyst was synthesised by first reacting mono-methyl isophthalate with 2-amino-6-picoline and hydrolysis to produce the appropriate carboxylic acid. This acid was coupled to previously synthesized Boc-pyrrolidine amine and Boc-deprotection released catalyst 4; colourless oil; yield: 500 mg, 38%; $[\alpha]_D^{14} = +19.0$ (c 0.1, EtOAc); v_{max} (KBr disc) 3400, 3332, 2932, 1675, 1603, 1538, 1398, 1113 cm^{-1}; δ_H (400 MHz, CDCl$_3$) 8.89 (s, 1H, N–Hb); 8.34 (s, 1H, H-2), 7.93–7.98 (m, 1H, H-4), 7.87–7.93 (m, 2H, H-6 and H-3′), 7.48–7.54 (m, 1H, H-5), 7.29–7.34 (m, 1H, H-4′), 6.78–6.82 (m, 1H, H-5′), 6.08 (s, br, 1H, N–Ha), 3.67–3.76 (m, 1H, H-2″), 3.37–3.68, (m, 2H, CONH–CH$_2$), 3.03–3.23 (m, 2H, H-5″), 2.30 (s, 3H, Ar-CH$_3$), 1.85–2.12 (m, 1H, H-3′), 1.35–1.70 (m, 1H, H-3″), 1.70–2.02 (m, 2H, H-4″); δ_C (100 MHz, CDCl$_3$) 167.8 (CONHCH$_2$), 165.3 (CONH–Py), 156.9 (C-2′), 150.8 (C-6′), 138.8 (C-4′), 134.3

(C-3), 133.8 (C-1), 131.2 (C-6), 131.0 (C-4), 129.1 (C-5), 126.0 (C-2), 119.7 (C-5′), 111.6 (C-3′), 59.9 (C-1″), 45.2 (CH$_2$), 41.5 (C-5″), 28.1 (C-3″), 24.1 (C-4″), 23.9 (Ar-CH$_3$). m/z 339 (MH$^+$). HRMS (ESI): MH$^+$, found 339.1823, C$_{19}$H$_{23}$N$_4$O$_2$ requires 339.1821.

4.5.5. (S)-N-(Pyridin-2-yl)pyrrolidine-2-carboxamide 5[42,66]

Viscous brown oil; yield: 900 mg, 43%; mp = 48–51 °C; $[\alpha]_D^{22} = -56.2$ (c 0.4, EtOAc); δ_H (400 MHz, CDCl$_3$) 10.20 (s, 1H, amide N–H), 8.20–8.31 (m, 2H, H-6 and H-3), 7.65–7.72 (m, 1H, H-4), 6.99–7.04 (m, 1H, H-5), 3.86–3.92 (m, 1H, H-2′), 2.98–3.12 (m, 2H, H-5′), 2.39 (s, br, 1H, aliphatic N–H), 1.98–2.25 (m, 2H, H-3′), 1.71–1.81 (m, 2H, H-4′). δ_C (100 MHz, CDCl$_3$) 174.0 (amide C=O), 151.2 (C-2), 148.0 (C-6), 138.3 (C-4), 119.7 (C-5), 113.7 (C-3), 61.0 (C-2′), 47.3 (C-5′), 30.9 (C-3′), 26.1 (C-4′); m/z 191 (M$^+$).

4.5.6. (S)-N-(6-Methylpyridin-2-yl)pyrrolidine-2-carboxamide 6[42]

Off-white solid; yield: 1.50 g, 66%; mp = 59–62 °C; $[\alpha]_D^{22} = -40.2$ (c 0.4, EtOAc); δ_H (400 MHz, CDCl$_3$) 10.1 (s, br, 1H, N–H), 8.04 (d, J = 8.2 Hz, 1H, H-3), 7.56 (t, J = 8.2 Hz, 1H, H-4), 6.86–6.89 (m, 1H, H-5), 3.83–3.88 (m, 1H, H-2′), 2.99–3.10 (m, 2H, H-5′), 2.46 (s, 3H, Ar-CH$_3$), 1.97–2.26 (m, 2H, H-3′), 1.8 (s, br, 1H, aliphatic N–H) 1.67–1.81 (m, 2H, H-4′); δ_C (100 MHz, CDCl$_3$) 174.4 (amide C=O), 156.9 (C-6), 150.5 (C-2), 138.5 (C-4), 119.1 (C-5), 110.4 (C-3), 61.0 (C-2′), 47.3 (C-5′), 30.9 (C-3′), 26.2 (C-4′), 24.2 (Ar-CH$_3$); m/z 205 (M$^+$).

4.5.7. (S)-N-(Pyridin-3-yl)pyrrolidine-2-carboxamide 7[42,66]

Colourless oil; yield: 1.15 g, 40%; $[\alpha]_D^{18} = -65.8$ (c = 0.1, CHCl$_3$); δ_H (400 MHz, CDCl$_3$) 9.87 (s, br, 1H, amide N–H), 8.59 (d, J = 2.75 Hz, 1H, H-2), 8.28- 8.32 (m, 1H, H-4), 8.21–8.25 (m, 1H, H-6), 7.20–7.26 (m, 1H, H-5), 3.83–3.89 (m, 1H, H-2′), 2.92–3.12 (m, 2H, H-5′), 2.25 (s, br, 1H, aliphatic N–H), 1.97–2.25 (m, 2H, H-3′), 1.70–1.81 (m, 2H, H-4′); δ_C (100 MHz, CDCl$_3$) 174.3 (amide C=O), 145.1 (C-4), 141.0 (C-6), 134.7 (C-2), 126.4 (C-5), 123.7 (C-3), 61.1 (C-2′), 47.5 (C-5′), 30.8 (C-3′), 26.4 (C-4′); m/z 192 (MH$^+$).

4.5.8. (S)-N-(Pyridin-4-yl)pyrrolidine-2-carboxamide 8[66]

White solid; yield: 500 mg, 31%; mp = 171–173 °C; $[\alpha]_D^{18} = -84.2$ (c 0.2, CHCl$_3$); δ_H (400 MHz, CDCl$_3$) 9.93 (s, br, 1H, amide N–H), 8.43–8.51 (m, 2H, H-2), 7.49–7.55 (m, 2H, H-3), 3.83–3.89 (m, 1H, H-2′), 2.92–3.13 (m, 2H, H-5′), 1.98–2.28 (m, 2H, H-3′), 1.77 (s, br, 1H, aliphatic N–H), 1.68–1.88 (m, 2H, H-4′); δ_C (100 MHz, CDCl$_3$) 174.6 (amide C=O), 150.8 (C-4), 144.6 (C-2), 113.4 (C-3), 61.2 (C-2′), 47.5 (C-5′), 30.8 (C-3′), 26.4 (C-4′); m/z 191 (M$^+$).

4.5.9. (S)-N-(Quinolin-2-yl)pyrrolidine-2-carboxamide 9

Off-white solid; yield: 1.4 g, 49%; mp = 108.3–109.1 °C; $[\alpha]_D^{14} = +7.4$ (c 0.1, CHCl$_3$); ν_{max} (KBr disc) 3347, 3213, 2967, 1678, 1499, 1233, 1105, 828 cm^{-1}; δ_H (400 MHz, CDCl$_3$) 10.43 (s, br, 1H, amide N–H), 8.48 (d, J = 8.70 Hz, 1H, H-3), 8.16 (d, J = 9.16 Hz, 1H, H-4), 7.86 (d, J = 8.70 Hz, 1H, H-8), 7.76 (d, J = 9.16 Hz, 1H, H-5), 7.61–7.68 (m, 1H, H-7), 7.40–7.46 (m, 1H, H-6), 3.88–3.95 (m, 1H, H-2′), 3.04–3.15 (m, 2H, H-5′), 2.01–2.30 (m, 2H, H-3′), 2.15 (s, br, 1H, aliphatic N–H), 1.73–1.85 (m, 2H, H-4′); δ_C (100 MHz, CDCl$_3$) 174.9 (amide C=O), 150.7 (C-2), 146.8 (C-b), 138.4 (C-4), 129.8 (C-7), 127.5 (C-5), 127.4 (C-8), 126.3 (C-a), 124.9 (C-6), 113.9 (C-3), 61.1 (C-2′), 47.4 (C-5′), 30.9 (C-3′), 26.2 (C-2′); m/z 242 (MH$^+$). HRMS (ESI): MH$^+$, found 242.1297, C$_{14}$H$_{16}$N$_3$O requires 242.1293.

4.5.10. (S)-N-(Quinolin-3-yl)pyrrolidine-2-carboxamide 10

Brown paste; yield: 400 mg, 22%; $[\alpha]_D^{17} = -20.0$- (c 0.05, CHCl$_3$); ν_{max} (KBr disc) 3354, 2969, 1686, 1523, 1490, 1369, 902, 751 cm^{-1}; δ_H (400 MHz, CDCl$_3$) 10.11 (s, br, 1H, amide N–H), 8.83–8.85 (m,

1H, H-2), 8.75–8.77 (m, 1H, H-4), 8.0–8.04 (m, 1H, H-5), 7.77–7.81 (m, 1H, H-7), 7.57–7.62 (m, 1H, H-6), 7.49–7.53 (m, 1H, H-8), 3.91–3.97 (m, 1H, H-2′), 3.0–3.20 (m, 2H, H-5′), 2.01–2.31 (m, 2H, H-3′), 2.09 (s, 1H, aliphatic N–H), 1.75–1.85 (m, 2H, H-4′); δ_C (100 MHz, CDCl$_3$) 174.4 (amide C=O), 145.2 (C-b), 144.0 (C-2), 131.4 (C-3), 128.8 (C-4), 128.2 (C-a), 128.1 (C-6), 127.7 (C-7), 127.1 (C-8), 123.0 (C-5), 61.1 (C-2′), 47.5 (C-5′), 30.9 (C-3′), 26.5 (C-4′); m/z 242 (MH$^+$); HRMS (ESI): MH$^+$, found 242.1297, C$_{14}$H$_{16}$N$_3$O requires 242.1293.

4.5.11. (S)-N-(Quinolin-8-yl)pyrrolidine-2-carboxamide 11

Brown viscous oil; yield: 1.8 g, 84%; $[\alpha]_D^{24} = +18.6$ (c 0.1, CHCl$_3$); ν_{max} (KBr disc) 3257, 2965, 1670, 1516, 1382, 1102, 824, 791 cm^{-1}; δ_H (400 MHz, CDCl$_3$) 11.61 (s, br, 1H, amide N–H), 8.81–8.89 (m, 2H, H-2 and H-7), 8.12–8.16 (m, 1H, H-4), 7.48–7.56 (m, 2H, H-5 and H-6), 7.41–7.45 (m, 1H, H-3), 3.98–4.05 (m, 1H, H-2′), 3.11–3.21 (m, 2H, H-5′), 2.08–2.33 (m, 2H, H-3′), 2.18 (s, br, 1H, aliphatic N–H), 1.71–1.90 (m, 2H, H-4′); δ_C (100 MHz, CDCl$_3$) 174.3 (amide C=O), 148.6 (C-2), 139.2 (C-a), 136.1 (C-4), 134.5 (C-8), 128.1 (C-b), 127.2 (C-6), 121.6 (C-5), 121.4 (C-3), 116.4 (C-7), 61.8 (C-2′), 47.5 (C-5′), 31.0 (C-3′), 26.3 (C-4′); m/z 242 (MH$^+$); HRMS (ESI): MH$^+$, found 242.1296, C$_{14}$H$_{16}$N$_3$O requires 242.1293.

4.5.12. (2S,2′S)-N,N′-(Pyridine-2,6-diyl)dipyrrolidine-2-carboxamide 12[67]

Off-white solid; yield: 800 mg, 21%; mp = 177.5–177.9 °C; $[\alpha]_D^{20} = +10.0$ (c 0.1, CHCl$_3$); δ_H (400 MHz, CDCl$_3$) 9.97 (s, br, 2H, amide N–H), 7.95 (d, J = 7.63 Hz, 2H, H-3), 7.70 (t, J = 7.63 Hz, 1H, H-4), 3.78–3.87 (m, 2H, H-2′), 2.9–3.13 (m, 4H, H-5′), 1.62–2.25 (m, 10H, H-3′, H-4′ and aliphatic N–H); δ_C (100 MHz, CDCl$_3$) 174.2 (amide C=O), 149.4 (C-2), 140.2 (C-4), 108.9 (C-3), 61.0 (C-2′), 47.3 (C-5′), 30.8 (C-3′), 26.2 (C-4′); m/z 326 (MNa$^+$), 304 (MH$^+$).

4.5.13. (2S,4R)-4-(Benzyloxy)-N-(pyridin-3-yl)pyrrolidine-2-carboxamide 13

Brown oil; yield: 95 mg, 29%; $[\alpha]_D^{14} = -22.5$ (c 0.05, CHCl$_3$); ν_{max} (KBr disc) 3377, 2921, 1670, 1583, 1425, 1259, 806, 741 cm^{-1}; δ_H (400 MHz, CDCl$_3$) 9.85 (s, 1H, amide N–H), 8.58–8.61 (m, 1H, H-2), 8.28–8.31 (m, 1H, H-4), 8.19–8.23 (m, 1H, H-6), 7.20–7.38 (m, 6H, H-5 and aromatic benzyl protons), 4.41–4.52 (m, 2H, OCH$_2$Ph), 4.12 (s, 1H, H-4′), 4.03–4.09 (m, 1H, H-2′), 3.20–3.25 (m, 1H, H-5′), 2.76–2.82 (m, 1H, H-5′), 2.55 (s, br, 1H, N–H), 2.47–2.56 (m, 1H, H-3′), 1.93–2.0 (m, 1H, H-3′); δ_C (100 MHz, CDCl$_3$) 173.7 (amide C=O), 145.1 (C-4), 141.0 (C-6), 138.0 (C-1″), 134.6 (C-3), 128.6 (C-3″), 127.9 (C-4″), 127.7 (C-2″), 126.5 (C-2), 123.7 (C-5), 80.5 (C-4′), 70.8 (O–CH$_2$–Ph), 60.4 (C-2′), 52.8 (C-5′), 36.3 (C-3′); m/z 298 (MH$^+$); HRMS (ESI): MH$^+$, found 298.1559, C$_{17}$H$_{20}$N$_3$O$_2$ requires 298.1556.

4.5.14. (2S,4R)-4-Hydroxy-N-(pyridin-3-yl)pyrrolidine-2-carboxamide 14

Orange solid; yield: 200 mg, 42%; mp = 142.5–143.2 °C; $[\alpha]_D^{18} = -1.0$ (c 0.1, CHCl$_3$); δ_H (400 MHz, CD$_3$OD) 8.77–8.81 (m, 1H, H-2), 8.26–8.29 (m, 1H, H-4), 8.08–8.14 (m, 1H, H-6), 7.37–7.42 (m, 1H, H-5), 6.93 (s, 1H, amide N–H), 4.51 (s, 1H, H-4′), 4.31–4.37 (m, 1H, H-2′), 3.11–3.28 (m, 2H, H-5′), 2.36–2.43 (m, 1H, H-3′), 2.01–2.10 (m, 1H, H-3′); δ_C (100 MHz, CD$_3$OD) 161.8 (amide C=O), 144.3 (C-4), 140.8 (C-2), 127.8 (C-6), 124.0 (C-5), 118.2 (C-3), 71.1 (C-4′), 59.8 (C-2′, 54.2 (C-5′), 39.0 (C-3′); HRMS (ESI): MH$^+$, found 208.1089, C$_{10}$H$_{14}$N$_3$O$_2$ requires 208.1086.

4.5.15. (S)-N-Phenylpyrrolidine-2-carboxamide 15[59]

Off-white solid; yield: 250 mg, 29%; mp = 115.5–116.2 °C; $[\alpha]_D^{19} = -62.0$ (c 0.1, CHCl$_3$); δ_H (400 MHz, CDCl$_3$) 9.72 (s, br, 1H, N–H), 7.59 (d, J = 7.79 Hz, 2H, H-2), 7.30 (t, J = 7.79 Hz, 2H, H-3), 7.04–7.10 (m, 1H, H-4), 3.80–3.85 (m, 1H, H-2′), 2.92–3.10 (m,

2H, H-5′), 1.97–2.23 (m, 3H, H-3′ and aliphatic N–H), 1.69–1.80 (m, 2H, H-4′); δ_C (100 MHz, CDCl$_3$) 173.6 (amide C=O), 138.0 (C-1), 129.0 (C-3), 124.0 (C-4), 119.3 (C-2), 61.1 (C-2′), 47.4 (C-5′), 30.8 (C-3′), 26.4 (C-4′); m/z 191 (MH$^+$).

4.5.16. (S)-N-Methyl-N-(pyridin-4-yl)pyrrolidine-2-carboxamide 16[66]

Colourless oil; yield: 120 mg, 29%; $[\alpha]_D^{14} = -90.0$ (c 0.05, CHCl$_3$); δ_H (400 MHz, CDCl$_3$) 8.07–8.10 (m, 2H, H-3), 6.75 (s, br, 1H, aliphatic N–H), 6.31–6.34 (m, 2H, H-2), 3.99–4.02 (m, 1H, H-2′), 3.50–3.56 (m, 1H, H-5′), 3.16–3.23 (m, 1H, H-5′), 2.68–2.71 (m, 3H, N–CH$_3$), 2.14–2.21 (m, 2H, H-3′), 1.87–2.03 (m, 2H, H-4′); δ_C (100 MHz, CDCl$_3$) 172.9 (C=O), 152.0 (C-1), 149.8 (C-3), 108.1 (C-2), 63.1 (C-2′), 48.6 (C-5′), 31.3 (C-3′), 26.3 (N–CH$_3$), 23.8 (C-4′); m/z 206 (MH$^+$).

4.5.17. (S)-N-methyl-N-phenylpyrrolidine-2-carboxamide 17[68]

Colourless oil; yield: 500 mg, 22%; $[\alpha]_D^{14} = +18.2$ (c 0.1, CHCl$_3$); δ_H (400 MHz, CDCl$_3$) 7.62 (s, br, 1H, aliphatic N–H), 7.28–7.34 (m, 2H, H-3), 7.21–7.27 (m, 1H, H-4), 7.13–7.18 (m, 2H, H-2), 3.86–3.93 (m, 1H, H-2′), 2.90–3.29 (m, 2H, H-5′), 3.15 (s, 3H, N–CH$_3$), 1.50–1.78 (m, 4H, H-3′ and H-4′); δ_C (100 MHz, CDCl$_3$) 170.8 (C=O), 141.9 (C-1), 130.1 (C-3), 128.7 (C-4), 127.7 (C-2), 58.4 (C-2′), 46.7 (C-5′), 38.0 (N–CH$_3$), 30.4 (C-3′), 25.4 (C-4′); m/z 204 (M$^+$).

4.5.18. (S)-N-(3,5-Bis(trifluoromethyl)phenyl)pyrrolidine-2-carboxamide 18[59]

Pale yellow oil; yield: 230 mg, 17%; $[\alpha]_D^{18} = -37.0$ (c 0.05, CHCl$_3$); δ_H (400 MHz, CDCl$_3$) 10.10 (s, br, 1H, amide N–H), 8.10 (s, 2H, H-2), 7.54 (s, 1H, H-4), 3.84–3.90 (m, 1H, H-2′), 2.94–3.13 (m, 2H, H-5′), 1.95–2.27 (m, 3H, H-3′ and aliphatic N–H), 1.71–1.79 (m, 2H, H-4′); δ_C (100 MHz, CDCl$_3$) 174.3 (amide C=O), 139.3 (C-1), 132.4 (C-3), 127.3, 124.6 (CF$_3$), 121.9, 119.2 (C-2), 117.1 (C-4), 61.0 (C-2′), 47.4 (C-5′), 30.8 (C-3′), 26.4 (C-4′); m/z 327 (MH$^+$).

4.5.19. (S)-N-(3,5-Bis(trifluoromethyl)phenylsulfonyl)-pyrrolidine-2-carboxamide 19

A deviation from the general procedure was used to synthesise this catalyst. The synthesis was achieved through EDCI coupling of Boc-L-proline with the previously synthesized 3,5-bis(trifluoromethyl)benzylsulfonamide[61] to give Boc-19; subsequent Boc-deprotection produced 19; white solid; yield: 200 mg, 27%; mp = 222.3–223.1 °C; ν_{max} (KBr disc) 3447, 3187, 1622, 1361, 1310, 1279, 1128, 852 cm^{-1}; δ_H (400 MHz, DMSO-d_6) 8.30 (s, 2H, H-2), 8.24 (s, 1H, H-4), 3.86 (t, J = 6.9 Hz, 1H, H-2′), 2.94–3.14 (m, 2H, H-5′), 2.06–2.12 (m, 1H, H-3′), 1.62–1.83 (m, 2H, H-4′), 1.62–1.83 (m, 1H, H-3′); δ_C (100 MHz, DMSO-d_6) ^{13}C NMR (100 MHz, DMSO-d_6) δ = 173.0 (amide C=O), 148.3 (C-1), 130.7 (C-3), 128.2 (C-2), 124.9 (C-4), 122.1 (CF$_3$), 62.4 (C-2′), 45.8 (C-5′), 29.4 (C-3′), 23.7 (C-4′); m/z 389 (M–H); HRMS (ESI): MH$^+$, found 391.0551, C$_{13}$H$_{13}$N$_2$O$_3$F$_6$S requires 391.0551.

4.5.20. General procedure for the aldol reaction of isatin with acetone[21]

The organocatalyst 20 mol % (0.06 mmol) and additive (either 40 equiv H$_2$O or 20 mol % acid additive) were stirred in 2 mL anhydrous acetone for 10 min at the specified temperature. Isatin (0.3 mmol, 44 mg) was subsequently added and the mixture was stirred at the desired temperature for the specified time. The progression of the reaction was monitored by TLC and HPLC. Acetone was subsequently removed in vacuo and the mixture was purified by flash chromatography (petroleum ether:ethyl acetate 2:1). The ee of the product was determined by chiral HPLC on the crude reaction mixture.

4.5.21. (S)-3-Hydroxy-3-(2-oxopropyl)indolin-2-one 20[21]

The ee was determined on the crude reaction mixture using chiral HPLC–Chiralpak ADH column, hexane/i-PrOH 70/30, flow rate 1 mL/min; t_R = 7.0 min [(S)-isomer]; t_R = 9.0 min [(R)-isomer], λ = 254 nm. Off-white solid; yield: see Tables; $[\alpha]_D^{18} = -20.0$ (c 0.03, CH$_3$OH); ν_{max} (KBr disc) 3359, 3258, 2359, 1718, 1620, 1470, 1362, 1057 cm^{-1}; δ_H (400 MHz, CD$_3$OD) 7.29 (d, J = 7.33 Hz, 1H, Ar-H), 7.21 (dt, J = 7.63 and 1.53 Hz, 1H, Ar-H), 6.98 (t, J = 7.63 Hz, 1H, Ar-H), 6.86 (m, 1H, Ar-H), 3.36 (d, J = 16.78 Hz, 1H, CH$_2$), 3.15 (d, J = 16.78 Hz, 1H, CH$_2$), 2.04 (s, 3H, CH$_3$); δ_C (100 MHz, CD$_3$OD) 206.1 (CH$_3$–CO–CH$_2$), 179.8 (amide C=O), 142.3 (C-7a), 130.9 (C-3a), 129.4 (C-6), 123.5 (C-4), 122.1 (C-5), 109.9 (C-7), 73.4 (C-3), 49.8 (CH$_2$), 29.3 (CH$_3$); m/z 228 (MNa$^+$); HRMS (ESI): MNa$^+$, found 228.0637, C$_{11}$H$_{11}$NO$_3$Na requires 228.0637.

4.5.22. (S)-1-Benzyl-3-hydroxy-3-(2-oxopropyl)indolin-2-one 21[21]

The ee was determined on the crude reaction mixture using chiral HPLC–Chiralpak ADH column, hexane/i-PrOH 90/10, flow rate 0.7 mL/min; t_R = 39.5 min (minor isomer); t_R = 42.3 min (major isomer), λ = 254 nm; Off-white solid; yield: see Tables; $[\alpha]_D^{19} = -4.0$ (c 0.05, CH$_3$OH); ν_{max} (KBr disc) 3315, 3060, 2359, 1698, 1616, 1467, 1360, 1079 cm^{-1}; δ_H (400 MHz, CD$_3$CN) 7.37–7.41 (m, 2H, Bz protons), 7.29–7.35 (m, 3H, Bz protons), 7.25–7.28 (m, 1H, Ar-H), 7.14–7.19 (m, 1H, Ar-H), 6.96–7.01 (m, 1H, Ar-H), 6.70 (d, J = 7.79 Hz, 1H, Ar-H), 4.77–4.91 (m, 2H, Bz-CH$_2$), 4.25 (s, br, 1H, OH), 3.40 (d, J = 17.0 Hz, 1H, CH$_2$), 3.20 (d, J = 17.0 Hz, 1H, CH$_2$), 2.0 (s, 3H, CH$_3$); δ_C (100 MHz, CD$_3$CN) 206.9 (CH$_3$–CO–CH$_2$), 177.4 (amide C=O), 144.3 (C-7a), 137.4 (C-1′), 130.4 (C-3′), 129.6 (C-3a), 128.4 (C-6), 128.2 (C-2′), 124.4 (C-4′), 123.4 (C-5 and C-6), 110.1 (C-7), 74.0 (C-3), 50.5 (N-CH$_2$-Ph), 44.1 (CH$_2$C=O), 30.9 (CH$_3$); m/z 296 (MH$^+$); HRMS (ESI): MH$^+$, found 296.1294, C$_{18}$H$_{18}$NO$_3$ requires 296.1287.

4.5.23. (S)-3-Hydroxy-3-(2-oxobutyl)indolin-2-one 22[21]

The ee was determined on the crude reaction mixture using chiral HPLC–Chiralpak ADH column, hexane/i-PrOH 70/30, flow rate 0.7 mL/min; t_R = 10.0 min (major isomer); t_R = 11.0 min (minor isomer), λ = 254 nm. 91% regioselectivity of reaction, C–C bond formation at the less substituted methyl group of the ketone (as determined by NMR). Off-white solid; yield: see Tables; $[\alpha]_D^{14} = -40.0$ (c 0.01, CH$_3$OH); ν_{max} (KBr disc) 3356, 2972, 2360, 1723, 1621, 1473, 1180, 777 cm^{-1}; δ_H (400 MHz, DMSO-d_6) 10.20 (s, br, 1H, N–H), 7.22 (d, J = 7.2 Hz, 1H, H-3), 7.15 (t, J = 8.0 Hz, 1H, H-4), 6.88 (t, J = 7.6 Hz, 1H, H-5), 6.76 (d, J = 7.6 Hz, 1H, H-6), 5.96 (s, 1H, OH), 3.25 (d, J = 16.4 Hz, 1H, CH$_2$-a), 2.97 (d, J = 16.4 Hz, 1H, CH$_2$-a), 2.24–2.42 (m, 2H, CH$_2$-b), 0.74 (t, J = 7.2 Hz, 3H, CH$_3$); δ_C (100 MHz, DMSO-d_6) 207.4 (CH$_2$–CO–CH$_2$), 178.2 (amide C=O), 142.5 (C-7a), 131.5 (C-3a), 128.9 (C-6), 123.7 (C-4), 121.2 (C-5), 109.4 (C-7), 72.7 (C-3), 49.1 (C–CH$_2$-CO), 35.6 (CH$_3$CH$_2$–CO), 7.3 (CH$_3$); m/z 242 (MNa$^+$); HRMS (ESI): MNa$^+$, found 242.0797, C$_{12}$H$_{13}$NO$_3$Na requires 242.0793.

4.6. General procedure for aldol reaction of isatins with acetaldehyde followed by reduction[65]

To a solution of optimum catalyst 7 (30 mol %, 0.09 mmol, 17.2 mg), chloroacetic acid (60 mol %, 17 mg, 0.18 mmol) and isatin (0.3 mmol) in DMF (0.3 mL) was added acetaldehyde (84 μL, 1.50 mmol). This reaction mixture was stirred at room temperature under N$_2$ for 48 h, followed by the addition of methanol (0.5 mL) and NaBH$_4$ (56 mg, 1.5 mmol and the mixture was stirred for 1 h at −20 °C. The resulting mixture was quenched with pH 7.0 phosphate buffer solution, extracted with ethyl acetate (3 × 25 mL), dried over anhydrous Na$_2$SO$_4$, filtered and the solvent removed in

vacuo. The product was isolated by flash chromatography (80:20 ethyl acetate:petroleum ether for the isatin derivative and 50:50 ethyl acetate:petroleum ether for the benzylisatin product).

4.6.1. (*R*)-3-Hydroxy-3-(2-hydroxyethyl)indolin-2-one 23[36]

The ee was determined on the purified reaction mixture (flash chromatography) using chiral HPLC (Chiralpak IA column, 10:1 hexane:*i*-PrOH, flow rate 0.7 mL/min; t_R = 30.9 min (minor enantiomer); t_R = 44.1 min (major enantiomer), λ = 254 nm). White solid; yield: see Tables; $[\alpha]_D^{14}$ = +19.1 (*c* 0.01, CHCl$_3$); ν_{max} (KBr disc) 3379, 2963, 1664, 1529, 1269, 997, 750, 694 cm^{-1}; δ_H (400 MHz, CD$_3$CN) 8.35 (s, br, 1H, N–H), 7.30 (d, *J* = 6.87 Hz, 1H, Ar-H), 7.22 (t, *J* = 6.87, 1H, Ar-H), 7.0 (t, *J* = 7.63, 1H, Ar-H), 6.85 (d, *J* = 7.63 Hz, 1H, Ar-H), 4.30 (s, br, 1H, OH), 3.53–3.59 (m, 2H, C*H*$_2$OH), 2.98 (s, br, 1H, OH), 1.95–2.09 (m, 2H, C*H*$_2$CH$_2$OH); δ_C (100 MHz, CD$_3$CN) 180.0 (amide C=O), 142.0 (C-7a), 132.4 (C-3a), 130.3 (C-6), 125.1 (C-4), 123.2 (C-5), 110.8 (C-7), 76.2 (C-3), 58.3 (CH$_2$OH), 40.5 (C–CH$_2$); *m/z* 216 (MNa$^+$); HRMS (ESI): MNa$^+$, found 216.0638, C$_{10}$H$_{11}$NO$_3$Na requires 216.0637.

4.6.2. (*R*)-1-Benzyl-3-hydroxy-3-(2-hydroxyethyl)indolin-2-one 24[36]

The ee was determined on the purified reaction mixture (after flash chromatography) using chiral HPLC (Chiralpak IA column, 10:1 hexane:*i*-PrOH, flow rate 0.7 mL/min; t_R = 36.2 min (minor enantiomer); t_R = 40.2 min (major enantiomer), λ = 254 nm). Colourless oil; yield: see Tables; $[\alpha]_D^{14}$ = +14.0 (*c* 0.01, CHCl$_3$); ν_{max} (KBr disc) 3395, 2924, 1705, 1613, 1269, 1468, 1174, 753 cm^{-1}; δ_H (400 MHz, CDCl$_3$) 7.38–7.42 (m, 1H, H-5), 7.24–7.33 (m, 5H, Bz protons), 7.17–7.22 (m, 1H, H-4), 7.03–7.09 (m, 1H, H-3), 6.68–6.72 (m, 1H, H-6), 4.96 (d, *J* = 16.0 Hz, 1H, C*H*$_2$–Ph), 4.77 (d, *J* = 16.0 Hz, 1H, CH$_2$–Ph), 4.43 (s, br, 1H, OH), 3.92–4.04 (m, 2H, CH$_2$–OH), 2.99 (s, br, 1H, OH), 2.26–2.34 (m, 1H, C*H*$_2$–C(OH)), 2.03–2.12 (m, 1H, C*H*$_2$–C(OH)); δ_C (100 MHz, CDCl$_3$) 178.4 (amide C=O), 141.9 (C-7a), 135.3(C-1′), 130.6 (C-3a), 129.6 (C-3′), 128.8 (C-2′), 127.7 (C-4′), 127.2 (C-6), 123.9 (C-4), 123.3 (C-3), 109.6 (C-7), 58.6 (CH$_2$OH), 43.8 (N–CH$_2$-Ph), 39.3 (C–CH$_2$); *m/z* 306 (MNa$^+$); HRMS (ESI): MNa$^+$, found 306.1107, C$_{17}$H$_{17}$NO$_3$Na requires 306.1106.

Acknowledgements

References

1. Suzuki, H.; Morita, H.; Shiro, M.; Kobayashi, J. *Tetrahedron* **2004**, *60*, 2489–2495.
2. Kitajima, M.; Mori, I.; Arai, K.; Kogure, N.; Takayama, H. *Tetrahedron Lett.* **2006**, *47*, 3199–3202.
3. Suarez-Castillo, O. R.; Sanchez-Zavala, M.; Melendez-Rodriguez, M.; Castelan-Duarte, L. E.; Morales-Rios, M. S.; Joseph-Nathan, P. *Tetrahedron* **2006**, *62*, 3040–3051.
4. Kawasaki, T.; Nagaoka, M.; Satoh, T.; Okamoto, A.; Ukon, R.; Ogawa, A. *Tetrahedron* **2004**, *60*, 3493–3503.
5. Goehring, R. R.; Sachdeva, Y. P.; Pisipati, J. S.; Sleevi, M. C.; Wolfe, J. F. *J. Am. Chem. Soc.* **1985**, *107*, 435–443.
6. Labroo, R. B.; Cohen, L. A. *J. Org. Chem.* **1990**, *55*, 4901–4904.
7. Rasmussen, H. B.; MacLeod, J. K. *J. Nat. Prod.* **1997**, *60*, 1152–1154.
8. Kohno, J.; Koguchi, Y.; Niskio, M.; Nakao, K.; Kuroda, M.; Shimizu, R.; Ohnuki, T.; Komatsubara, S. *J. Org. Chem.* **2000**, *65*, 990–995.
9. Tang, Y. Q.; Sattler, I.; Thiericke, R.; Grabley, S.; Feng, X. Z. *Eur. J. Org. Chem.* **2001**, 261–267.
10. Tokunaga, T.; Hume, W. E.; Umezome, T.; Okazaki, K.; Ueki, Y.; Kumagai, K.; Hourai, S.; Nagamine, J.; Seki, H.; Taiji, M.; Noguchi, H.; Nagata, R. *J. Med. Chem.* **2001**, *44*, 4641–4649.
11. Albrecht, B. K.; Williams, R. M. *Org. Lett.* **2003**, *5*, 197–200.
12. Lee, S.; Hartwig, J. F. *J. Org. Chem.* **2001**, *66*, 3402–3415.
13. Shibata, N.; Tarui, T.; Doi, Y.; Kirk, K. L. *Angewandte Chemie-International Edition* **2001**, *40*, 4461.
14. Nakamura, T.; Shirokawa, S.; Hosokawa, S.; Nakazaki, A.; Kobayashi, S. *Org. Lett.* **2006**, *8*, 677–679.
15. Guo, X.; Huang, H. X.; Yang, L. P.; Hu, W. H. *Org. Lett.* **2007**, *9*, 4721–4723.
16. Malkov, A. V.; Kabeshov, M. A.; Bella, M.; Kysilka, O.; Malyshev, D. A.; Pluhackova, K.; Kocovsky, P. *Org. Lett.* **2007**, *9*, 5473–5476.
17. Adachi, S.; Harada, T. *Eur. J. Org. Chem.* **2009**, *2009*, 3661–3671.
18. Nakamura, H.; Hara, N.; Nakashima, H.; Kubo, K.; Shibata, N.; Toru, T. *Chem.-A European J.* **2008**, *14*, 8079–8081.
19. Luppi, G.; Monari, M.; Correa, R. J.; Violante, F. D.; Pinto, A. C.; Kaptein, B.; Broxterman, Q. B.; Garden, S. J.; Tomasini, C. *Tetrahedron* **2006**, *62*, 12017–12024.
20. Chen, G.; Wang, Y.; He, H. P.; Gao, S.; Yang, X. S.; Hao, X. J. *Heterocycles* **2006**, *68*, 2327–2333.
21. Chen, J. R.; Liu, X. P.; Zhu, X. Y.; Li, L.; Qiao, Y. F.; Zhang, J. M.; Xiao, W. J. *Tetrahedron* **2007**, *63*, 10437–10444.
22. Trost, B. M.; Brindle, C. S. *Chem. Soc. Rev.* **2010**, *39*, 1600–1632.
23. Pellissier, H. *Tetrahedron* **2007**, *63*, 9267–9331.
24. Guillena, G.; Najera, C.; Ramon, D. J. *Tetrahedron: Asymmetry* **2007**, *18*, 2249–2293.
25. Russo, A.; Botta, G.; Lattanzi, A. *Tetrahedron* **2007**, *63*, 11886–11892.
26. Chimni, S. S.; Singh, S.; Mahajan, D. *Tetrahedron: Asymmetry* **2008**, *19*, 2276–2284.
27. Chimni, S. S.; Mahajan, D. *Tetrahedron: Asymmetry* **2006**, *17*, 2108–2119.
28. List, B.; Lerner, R. A.; Barbas, C. F. *J. Am. Chem. Soc.* **2000**, *122*, 2395–2396.
29. List, B.; Pojarliev, P.; Castello, C. *Org. Lett.* **2001**, *3*, 573–575.
30. Sakthivel, K.; Notz, W.; Bui, T.; Barbas, C. F. *J. Am. Chem. Soc.* **2001**, *123*, 5260–5267.
31. Tang, Z.; Jiang, F.; Cui, X.; Gong, L. Z.; Mi, A. Q.; Jiang, Y. Z.; Wu, Y. D. *Proc. Natl. Acad. Sci. U.S.A.* **2004**, *101*, 5755–5760.
32. Raj, M.; Vishnumaya; Ginotra, S. K.; Singh, V. K. *Org. Lett.* **2006**, *8*, 4097–4099.
33. Guizzetti, S.; Benaglia, M.; Pignataro, L.; Puglisi, A. *Tetrahedron: Asymmetry* **2006**, *17*, 2754–2760.
34. Enders, D.; Gasperi, T. *Chem. Commun.* **2007**, 88–90.
35. Wiesner, M.; Revell, J. D.; Wennemers, H. *Angewandte Chemie-International Edition* **2008**, *47*, 1871–1874.
36. Chen, W. B.; Du, X. L.; Cun, L. F.; Zhang, X. M.; Yuan, W. C. *Tetrahedron* **2010**, *66*, 1441–1446.
37. Popp, F. D.; Donigan, B. E. *J. Pharm. Sci.* **1979**, *68*, 519–520.
38. Raj, M.; Veerasamy, N.; Singh, V. K. *Tetrahedron Lett.* **2010**, *51*, 2157–2159.
39. Luppi, G.; Cozzi, P. G.; Monari, M.; Kaptein, B.; Broxterman, Q. B.; Tomasini, C. *J. Org. Chem.* **2005**, *70*, 7418–7421.
40. Correa, R. J.; Garden, S. J.; Angelici, G.; Tomasini, C. *Eur. J. Org. Chem.* **2008**, *4*, 736–744.
41. Zhang, Z. G.; Schreiner, P. R. *Chem. Soc. Rev.* **2009**, *38*, 1187–1198.
42. Tang, Z.; Cun, L.-F.; Cui, X.; Mi, A.-Q.; Jiang, Y.-Z.; Gong, L.-Z. *Org. Lett.* **2006**, *8*, 1263–1266.
43. Tellado, F. G.; Goswami, S.; Chang, S. K.; Geib, S. J.; Hamilton, A. D. *J. Am. Chem. Soc.* **1990**, *112*, 7393–7394.
44. Cao, Y.-J.; Lai, Y.-Y.; Wang, X.; Li, Y.-J.; Xiao, W.-J. *Tetrahedron Lett.* **2007**, *48*, 21.
45. Brown, H. C.; Heim, P. *J. Am. Chem. Soc.* **1964**, *86*, 3566–3567.
46. Wang, J.; Li, H.; Lou, B.; Zu, L.; Guo, H.; Wang, W. *Chem.-A European J.* **2006**, *12*, 4321–4332.
47. Couturier, M.; Andresen, B. M.; Jorgensen, J. B.; Tucker, J. L.; Busch, F. R.; Brenek, S. J.; Dube, P.; am Ende, D. J.; Negri, J. T. *Org. Process Res. Dev.* **2002**, *6*, 42–48.
48. Geib, S. J.; Vicent, C.; Fan, E.; Hamilton, A. D. *Angew. Chem., Int. Ed.* **1993**, *32*, 119–121.
49. Gryko, D.; Lipinski, R. *Eur. J. Org. Chem.* **2006**, 3864–3876.
50. Gryko, D.; Saletra, W. J. *Org. Biomol. Chem.* **2007**, *5*, 2148–2153.
51. Gryko, D.; Zimnicka, M.; Lipinski, R. *J. Org. Chem.* **2007**, *72*, 964–970.
52. Angelici, G.; Corrêa, R. J.; Garden, S. J.; Tomasini, C. *Tetrahedron Lett.* **2009**, *50*, 814.
53. Fu, S. D.; Fu, X. K.; Zhang, S. P.; Zou, X. C.; Wu, X. J. *Tetrahedron: Asymmetry* **2009**, *20*, 2390–2396.
54. pK_a data compiled by Williams; http://research.chem.psu.edu/brpgroup/pK$_a$_compilation.pdf.
55. Chimni, S. S.; Singh, S.; Kumar, A. *Tetrahedron: Asymmetry* **2009**, *20*, 1722–1724.
56. See Ref. 47.
57. Shen, C.; Shen, F. Y.; Xia, H. J.; Zhang, P. F.; Chen, X. Z. *Tetrahedron: Asymmetry* **2011**, *22*, 708–712.
58. Moorthy, J. N.; Saha, S. *Eur. J. Org. Chem.* **2009**, 739–748.
59. He, L.; Tang, Z.; Cun, L. F.; Mi, A. Q.; Jiang, Y. Z.; Gong, L. Z. *Tetrahedron* **2006**, *62*, 346–351.
60. Kokotos, G.; Bellis, E.; Vasilatou, K. *Synthesis* **2005**, 2407–2413.
61. Kinsella, M.; Duggan, P. G.; Muldoon, J.; Eccles, K. S.; Lawrence, S. E.; Lennon, C. M. *Eur. J. Org. Chem.* **2011**, *2011*, 1125–1132.
62. Berkessel, A.; Koch, B.; Lex, J. *Adv. Synth. Catal.* **2004**, *346*, 1141–1146.
63. Yang, H.; Carter, R. G. *Synlett* **2010**, 2827–2838.
64. Determined by ^{1}H NMR spectroscopy.
65. Itoh, T.; Ishikawa, H.; Hayashi, Y. *Org. Lett.* **2009**, *11*, 3854–3857.
66. Luo, S.; Xu, H.; Li, J.; Zhang, L.; Mi, X.; Zheng, X.; Cheng, J. P. *Tetrahedron* **2007**, *63*, 11307–11314.
67. Xu, X.; Daka, P.; Budik, I.; Wang, H.; Bai, F. Q.; Zhang, H. X. *Eur. J. Org. Chem.* **2009**, 4581–4585.
68. de Arriba, A. L. F.; Simon, L.; Raposo, C.; Alcazar, V.; Moran, J. R. *Tetrahedron* **2009**, *65*, 4841–4845.